



Hashemite Kingdom of Jordan



Jordan Journal of



Biological Sciences

An International Peer-Reviewed Scientific Journal

Financed by the Scientific Research and Innovation Support Fund



<http://jjbs.hu.edu.jo/>

المجلة الأردنية للعلوم الحياتية Jordan Journal of Biological Sciences (JJBS)

<http://jjbs.hu.edu.jo>

Jordan Journal of Biological Sciences (JJBS) (ISSN: 1995–6673 (Print); 2307-7166 (Online)): An International Peer- Reviewed Open Access Research Journal financed by the Scientific Research and Innovation Support Fund, Ministry of Higher Education and Scientific Research, Jordan and published quarterly by the Deanship of Scientific Research , The Hashemite University, Jordan.

Editor-in-Chief

Professor Atoum, Manar F.

Molecular Biology and Genetics,
The Hashemite University

Assistant Editor

Dr. Muhammad, Massadeh I.

Microbial Biotechnology,
The Hashemite University

Editorial Board (Arranged alphabetically)

Professor Al-Eitan, Laith

Biotechnology and Genetic Engineering
Jordan University of Science and Technology

Professor Al-Khateeb , Wesam M.

Plant Genetics and Biotechnology
Yarmouk University

Professor Al-Ghzawi , Abdul Latief A.

Plant biotechnology
The Hashemite University

Professor Al-Najjar , Tariq Hasan Ahmad.

Marine Biology
The University of Jordan/ Aqaba

Professor Khleifat, Khaled M.

Microbiology and Biotechnology
Mutah University

Professor Odat , Nidal

Plant biodiversity
Al Balqa Applied University

Associate Editorial Board

Professor Al-Hindi, Adnan I.

Parasitology
The Islamic University of Gaza, Faculty of Health
Sciences, Palestine

Dr Gammoh, Noor

Tumor Virology
Cancer Research UK Edinburgh Centre, University of
Edinburgh, U.K.

Professor Kasperek, Max

Natural Sciences
Editor-in-Chief, Journal Zoology in the Middle East,
Germany

Professor Krystufek, Boris

Conservation Biology
Slovenian Museum of Natural History,
Slovenia

Dr Rabei, Sami H.

Plant Ecology and Taxonomy
Botany and Microbiology Department,
Faculty of Science, Damietta University, Egypt

Professor Simerly, Calvin R.

Reproductive Biology
Department of Obstetrics/Gynecology and
Reproductive Sciences, University of
Pittsburgh, USA

Editorial Board Support Team

Language Editor

Dr. Shadi Neimneh

Publishing Layout

Eng.Mohannad Oqdeh

Submission Address

Professor Atoum, Manar F

The Hashemite University
P.O. Box 330127, Zarqa, 13115, Jordan
Phone: +962-5-3903333 ext.4147
E-Mail: jjbs@hu.edu.jo

International Advisory Board (Arranged alphabetically)

Professor Ahmad M. Khalil

Department of Biological Sciences, Faculty of Science,
Yarmouk University, Jordan

Professor Anilava Kaviraj

Department of Zoology, University of Kalyani, India

Professor Bipul Kumar Das

Faculty of Fishery Sciences W. B. University of Animal &
Fishery Sciences, India

Professor Elias Baydoun

Department of Biology, American University of Beirut
Lebanon

Professor Hala Gali-Muhtasib

Department of Biology, American University of Beirut
Lebanon

Professor Ibrahim M. AlRawashdeh

Department of Biological Sciences, Faculty of Science, Al-
Hussein Bin Talal University, Jordan

Professor João Ramalho-Santos

Department of Life Sciences, University of Coimbra, Portugal

Professor Khaled M. Al-Qaoud

Department of Biological sciences, Faculty of Science,
Yarmouk University, Jordan

Professor Mahmoud A. Ghannoum

Center for Medical Mycology and Mycology Reference
Laboratory, Department of Dermatology, Case Western
Reserve University and University Hospitals Case Medical
Center, USA

Professor Mawieh Hamad

Department of Medical Lab Sciences, College of Health
Sciences , University of Sharjah, UAE

Professor Michael D Garrick

Department of Biochemistry, State University of New York at
Buffalo, USA

Professor Nabil. A. Bashir

Department of Physiology and Biochemistry, Faculty of
Medicine, Jordan University of Science and Technology,
Jordan

Professor Nizar M. Abuharfeil

Department of Biotechnology and Genetic Engineering, Jordan
University of Science and Technology, Jordan

Professor Samih M. Tamimi

Department of Biological Sciences, Faculty of Science, The
University of Jordan, Jordan

Professor Ulrich Joger

State Museum of Natural History Braunschweig, Germany

Professor Aida I. El Makawy

Division of Genetic Engineering and Biotechnology, National
Research Center. Giza, Egypt

Professor Bechan Sharma

Department of Biochemistry, Faculty of Science University of
Allahabad, India

Professor Boguslaw Buszewski

Chair of Environmental Chemistry and Bioanalytics, Faculty of
Chemistry, Nicolaus Copernicus University Poland

Professor Gerald Schatten

Pittsburgh Development Center, Division of Developmental
and Regenerative Medicine, University of Pittsburgh, School
of Medicine, USA

Professor Hala Khyami-Horani

Department of Biological Sciences, Faculty of Science, The
University of Jordan, Jordan

Professor James R. Bamburg

Department of Biochemistry and Molecular Biology, Colorado
State University, USA

Professor Jumah M. Shakhaneh

Department of Biological Sciences, Faculty of Science, Mutah
University, Jordan

Dr. Lukmanul Hakkim Faruck

Department of Mathematics and Sciences College of Arts and
Applied Sciences, Dhofar, Oman

Professor Md. Yeamin Hossain

Department of Fisheries, Faculty of Fisheries , University of
Rajshahi, Bangladesh

Professor Mazin B. Qumsiyeh

Palestine Museum of Natural History and Palestine Institute for
Biodiversity and Sustainability, Bethlehem University,
Palestine

Professor Mohamad S. Hamada

Genetics Department, Faculty of Agriculture, Damietta
University, Egypt

Professor Nawroz Abdul-razzak Tahir

Plant Molecular Biology and Phytochemistry, University of
Sulaimani, College of Agricultural Sciences, Iraq

Professor Ratib M. AL- Ouran

Department of Biological Sciences, Faculty of Science, Mutah
University, Jordan

Professor Shtaywy S. Abdalla Abbadi

Department of Biological Sciences, Faculty of Science, The
University of Jordan, Jordan

Professor Zihad Bouslama

Department of Biology, Faculty of Science Badji Mokhtar
University, Algeria

Instructions to Authors

Scopes

Study areas include cell biology, genomics, microbiology, immunology, molecular biology, biochemistry, embryology, immunogenetics, cell and tissue culture, molecular ecology, genetic engineering and biological engineering, bioremediation and biodegradation, bioinformatics, biotechnology regulations, gene therapy, organismal biology, microbial and environmental biotechnology, marine sciences. The JJBS welcomes the submission of manuscript that meets the general criteria of significance and academic excellence. All articles published in JJBS are peer-reviewed. Papers will be published approximately one to two months after acceptance.

Type of Papers

The journal publishes high-quality original scientific papers, short communications, correspondence and case studies. Review articles are usually by invitation only. However, Review articles of current interest and high standard will be considered.

Submission of Manuscript

Manuscript, or the essence of their content, must be previously unpublished and should not be under simultaneous consideration by another journal. The authors should also declare if any similar work has been submitted to or published by another journal. They should also declare that it has not been submitted/ published elsewhere in the same form, in English or in any other language, without the written consent of the Publisher. The authors should also declare that the paper is the original work of the author(s) and not copied (in whole or in part) from any other work. All papers will be automatically checked for duplicate publication and plagiarism. If detected, appropriate action will be taken in accordance with International Ethical Guideline. By virtue of the submitted manuscript, the corresponding author acknowledges that all the co-authors have seen and approved the final version of the manuscript. The corresponding author should provide all co-authors with information regarding the manuscript, and obtain their approval before submitting any revisions. Electronic submission of manuscripts is strongly recommended, provided that the text, tables and figures are included in a single Microsoft Word file. Submit manuscript as e-mail attachment to the Editorial Office at: JJBS@hu.edu.jo. After submission, a manuscript number will be communicated to the corresponding author within 48 hours.

Peer-review Process

It is requested to submit, with the manuscript, the names, addresses and e-mail addresses of at least 4 potential reviewers. It is the sole right of the editor to decide whether or not the suggested reviewers to be used. The reviewers' comments will be sent to authors within 6-8 weeks after submission. Manuscripts and figures for review will not be returned to authors whether the editorial decision is to accept, revise, or reject. All Case Reports and Short Communication must include at least one table and/ or one figure.

Preparation of Manuscript

The manuscript should be written in English with simple lay out. The text should be prepared in single column format. Bold face, italics, subscripts, superscripts etc. can be used. Pages should be numbered consecutively, beginning with the title page and continuing through the last page of typewritten material.

The text can be divided into numbered sections with brief headings. Starting from introduction with section 1. Subsections should be numbered (for example 2.1 (then 2.1.1, 2.1.2, 2.2, etc.), up to three levels. Manuscripts in general should be organized in the following manner:

Title Page

The title page should contain a brief title, correct first name, middle initial and family name of each author and name and address of the department(s) and institution(s) from where the research was carried out for each author. The title should be without any abbreviations and it should enlighten the contents of the paper. All affiliations should be provided with a lower-case superscript number just after the author's name and in front of the appropriate address.

The name of the corresponding author should be indicated along with telephone and fax numbers (with country and area code) along with full postal address and e-mail address.

Abstract

The abstract should be concise and informative. It should not exceed **350 words** in length for full manuscript and Review article and **150 words** in case of Case Report and/ or Short Communication. It should briefly describe the purpose of the work, techniques and methods used, major findings with important data and conclusions. No references should be cited in this part. Generally non-standard abbreviations should not be used, if necessary they should be clearly defined in the abstract, at first use.

Keywords

Immediately after the abstract, **about 4-8 keywords** should be given. Use of abbreviations should be avoided, only standard abbreviations, well known in the established area may be used, if appropriate. These keywords will be used for indexing.

Abbreviations

Non-standard abbreviations should be listed and full form of each abbreviation should be given in parentheses at first use in the text.

Introduction

Provide a factual background, clearly defined problem, proposed solution, a brief literature survey and the scope and justification of the work done.

Materials and Methods

Give adequate information to allow the experiment to be reproduced. Already published methods should be mentioned with references. Significant modifications of published methods and new methods should be described in detail. Capitalize trade names and include the manufacturer's name and address. Subheading should be used.

Results

Results should be clearly described in a concise manner. Results for different parameters should be described under subheadings or in separate paragraph. Results should be explained, but largely without referring to the literature. Table or figure numbers should be mentioned in parentheses for better understanding.

Discussion

The discussion should not repeat the results, but provide detailed interpretation of data. This should interpret the significance of the findings of the work. Citations should be given in support of the findings. The results and discussion part can also be described as separate, if appropriate. The Results and Discussion sections can include subheadings, and when appropriate, both sections can be combined

Conclusions

This should briefly state the major findings of the study.

Acknowledgment

A brief acknowledgment section may be given after the conclusion section just before the references. The acknowledgment of people who provided assistance in manuscript preparation, funding for research, etc. should be listed in this section.

Tables and Figures

Tables and figures should be presented as per their appearance in the text. It is suggested that the discussion about the tables and figures should appear in the text before the appearance of the respective tables and figures. No tables or figures should be given without discussion or reference inside the text.

Tables should be explanatory enough to be understandable without any text reference. Double spacing should be maintained throughout the table, including table headings and footnotes. Table headings should be placed above the table. Footnotes should be placed below the table with superscript lowercase letters. Each table should be on a separate page, numbered consecutively in Arabic numerals.

Each figure should have a caption. The caption should be concise and typed separately, not on the figure area. Figures should be self-explanatory. Information presented in the figure should not be repeated in the table. All symbols and abbreviations used in the illustrations should be defined clearly. Figure legends should be given below the figures.

References

References should be listed alphabetically at the end of the manuscript. Every reference referred in the text must be also present in the reference list and vice versa. In the text, a reference identified by means of an author's name should be followed by the year of publication in parentheses (e.g.(Brown,2009)). For two authors, both authors' names followed by the year of publication (e.g.(Nelson and Brown, 2007)). When there are more than two authors, only the first author's name followed by "*et al.*" and the year of publication (e.g. (Abu-Elteen *et al.*, 2010)). When two or more works of an author has been published during the same year, the reference should be identified by the letters "a", "b", "c", etc., placed after the year of publication. This should be followed both in the text and reference list. e.g., Hilly, (2002a, 2002b); Hilly, and Nelson, (2004). Articles in preparation or submitted for publication, unpublished observations, personal communications, etc. should not be included in the reference list but should only be mentioned in the article text (e.g., Shtyawy,A., University of Jordan, personal communication). Journal titles should be abbreviated according to the system adopted in Biological Abstract and Index Medicus, if not included in Biological Abstract or Index Medicus journal title should be given in full. The author is responsible for the scuracy and completeness of the references and for their correct textual citation. Failure to do so may result in the paper being withdraw from the evaluation process. Example of correct reference form is given as follows:-

Reference to a journal publication:

Bloch BK. 2002. Econazole nitrate in the treatment of *Candida vaginitis*. *S Afr Med J.* , **58**:314-323.

Ogunseitan OA and Ndoye IL. 2006. Protein method for investigating mercuric reductase gene expression in aquatic environments. *Appl Environ Microbiol.*, **64**: 695-702.

Hilly MO, Adams MN and Nelson SC. 2009. Potential fly-ash utilization in agriculture. *Progress in Natural Sci.*, **19**: 1173-1186.

Reference to a book:

Brown WY and White SR.1985. **The Elements of Style**, third ed. MacMillan, New York.

Reference to a chapter in an edited book:

Mettam GR and Adams LB. 2010. How to prepare an electronic version of your article. In: Jones BS and Smith RZ (Eds.), **Introduction to the Electronic Age**. Kluwer Academic Publishers, Netherlands, pp. 281–304.

Conferences and Meetings:

Embabi NS. 1990. Environmental aspects of distribution of mangrove in the United Arab Emirates. Proceedings of the First ASWAS Conference. University of the United Arab Emirates. Al-Ain, United Arab Emirates.

Theses and Dissertations:

El-Labadi SN. 2002. Intestinal digenetic trematodes of some marine fishes from the Gulf of Aqaba. MSc dissertation, The Hashemite University, Zarqa, Jordan.

Nomenclature and Units

Internationally accepted rules and the international system of units (SI) should be used. If other units are mentioned, please give their equivalent in SI.

For biological nomenclature, the conventions of the *International Code of Botanical Nomenclature*, the *International Code of Nomenclature of Bacteria*, and the *International Code of Zoological Nomenclature* should be followed.

Scientific names of all biological creatures (crops, plants, insects, birds, mammals, etc.) should be mentioned in parentheses at first use of their English term.

Chemical nomenclature, as laid down in the *International Union of Pure and Applied Chemistry* and the official recommendations of the *IUPAC-IUB Combined Commission on Biochemical Nomenclature* should be followed. All biocides and other organic compounds must be identified by their Geneva names when first used in the text. Active ingredients of all formulations should be likewise identified.

Math formulae

All equations referred to in the text should be numbered serially at the right-hand side in parentheses. Meaning of all symbols should be given immediately after the equation at first use. Instead of root signs fractional powers should be used. Subscripts and superscripts should be presented clearly. Variables should be presented in italics. Greek letters and non-Roman symbols should be described in the margin at their first use.

To avoid any misunderstanding zero (0) and the letter O, and one (1) and the letter l should be clearly differentiated. For simple fractions use of the solidus (/) instead of a horizontal line is recommended. Levels of statistical significance such as: * $P < 0.05$, ** $P < 0.01$ and *** $P < 0.001$ do not require any further explanation.

Copyright

Submission of a manuscript clearly indicates that: the study has not been published before or is not under consideration for publication elsewhere (except as an abstract or as part of a published lecture or academic thesis); its publication is permitted by all authors and after accepted for publication it will not be submitted for publication anywhere else, in English or in any other language, without the written approval of the copyright-holder. The journal may consider manuscripts that are translations of articles originally published in another language. In this case, the consent of the journal in which the article was originally published must be obtained and the fact that the article has already been published must be made clear on submission and stated in the abstract. It is compulsory for the authors to ensure that no material submitted as part of a manuscript infringes existing copyrights, or the rights of a third party.

Ethical Consent

All manuscripts reporting the results of experimental investigation involving human subjects should include a statement confirming that each subject or subject's guardian obtains an informed consent, after the approval of the experimental protocol by a local human ethics committee or IRB. When reporting experiments on animals, authors should indicate whether the institutional and national guide for the care and use of laboratory animals was followed.

Plagiarism

The JJBS hold no responsibility for plagiarism. If a published paper is found later to be extensively plagiarized and is found to be a duplicate or redundant publication, a note of retraction will be published, and copies of the correspondence will be sent to the authors' head of institute.

Galley Proofs

The Editorial Office will send proofs of the manuscript to the corresponding author as an e-mail attachment for final proof reading and it will be the responsibility of the corresponding author to return the galley proof materials appropriately corrected within the stipulated time. Authors will be asked to check any typographical or minor clerical errors in the manuscript at this stage. No other major alteration in the manuscript is allowed. After publication authors can freely access the full text of the article as well as can download and print the PDF file.

Publication Charges

There are no page charges for publication in Jordan Journal of Biological Sciences, except for color illustrations,

Reprints

Ten (10) reprints are provided to corresponding author free of charge within two weeks after the printed journal date. For orders of more reprints, a reprint order form and prices will be sent with article proofs, which should be returned directly to the Editor for processing.

Disclaimer

Articles, communication, or editorials published by JJBS represent the sole opinions of the authors. The publisher shoulders no responsibility or liability what so ever for the use or misuse of the information published by JJBS.

Indexing

JJBS is indexed and abstracted by:

DOAJ (Directory of Open Access Journals)

Google Scholar

Journal Seek

HINARI

Index Copernicus

NDL Japanese Periodicals Index

SCIRUS

OAJSE

ISC (Islamic World Science Citation Center)

Directory of Research Journal Indexing
(DRJI)

Ulrich's

CABI

EBSCO

CAS (Chemical Abstract Service)

ETH- Citations

Open J-Gat

SCImago

Clarivate Analytics (Zoological Abstract)

Scopus

AGORA (United Nation's FAO database)

SHERPA/RoMEO (UK)

المجلة الأردنية للعلوم الحياتية
Jordan Journal of Biological Sciences (JJBS)
ISSN 1995- 6673 (Print), 2307- 7166 (Online)

<http://jjbs.hu.edu.jo>

The Hashemite University
Deanship of Scientific Research
TRANSFER OF COPYRIGHT AGREEMENT

Journal publishers and authors share a common interest in the protection of copyright: authors principally because they want their creative works to be protected from plagiarism and other unlawful uses, publishers because they need to protect their work and investment in the production, marketing and distribution of the published version of the article. In order to do so effectively, publishers request a formal written transfer of copyright from the author(s) for each article published. Publishers and authors are also concerned that the integrity of the official record of publication of an article (once refereed and published) be maintained, and in order to protect that reference value and validation process, we ask that authors recognize that distribution (including through the Internet/WWW or other on-line means) of the authoritative version of the article as published is best administered by the Publisher.

To avoid any delay in the publication of your article, please read the terms of this agreement, sign in the space provided and return the complete form to us at the address below as quickly as possible.

Article entitled:-----

Corresponding author: -----

To be published in the journal: Jordan Journal of Biological Sciences (JJBS)

I hereby assign to the Hashemite University the copyright in the manuscript identified above and any supplemental tables, illustrations or other information submitted therewith (the "article") in all forms and media (whether now known or hereafter developed), throughout the world, in all languages, for the full term of copyright and all extensions and renewals thereof, effective when and if the article is accepted for publication. This transfer includes the right to adapt the presentation of the article for use in conjunction with computer systems and programs, including reproduction or publication in machine-readable form and incorporation in electronic retrieval systems.

Authors retain or are hereby granted (without the need to obtain further permission) rights to use the article for traditional scholarship communications, for teaching, and for distribution within their institution.

- I am the sole author of the manuscript
- I am signing on behalf of all co-authors of the manuscript
- The article is a 'work made for hire' and I am signing as an authorized representative of the employing company/institution

Please mark one or more of the above boxes (as appropriate) and then sign and date the document in black ink.

Signed: _____ Name printed: _____

Title and Company (if employer representative) : _____

Date: _____

Data Protection: By submitting this form you are consenting that the personal information provided herein may be used by the Hashemite University and its affiliated institutions worldwide to contact you concerning the publishing of your article.

Please return the completed and signed original of this form by mail or fax, or a scanned copy of the signed original by e-mail, retaining a copy for your files, to:

Hashemite University
Jordan Journal of Biological Sciences
Zarqa 13115 Jordan
Fax: +962 5 3903338
Email: jjbs@hu.edu.jo

EDITORIAL PREFACE

Jordan Journal of Biological Sciences (JJBS) is a refereed, quarterly international journal financed by the Scientific Research and Innovation Support Fund, Ministry of Higher Education and Scientific Research in cooperation with the Hashemite University, Jordan. JJBS celebrated its 12th commencement this past January, 2020. JJBS was founded in 2008 to create a peer-reviewed journal that publishes high-quality research articles, reviews and short communications on novel and innovative aspects of a wide variety of biological sciences such as cell biology, developmental biology, structural biology, microbiology, entomology, molecular biology, biochemistry, medical biotechnology, biodiversity, ecology, marine biology, plant and animal biology, plant and animal physiology, genomics and bioinformatics.

We have watched the growth and success of JJBS over the years. JJBS has published 11 volumes, 45 issues and 479 articles. JJBS has been indexed by SCOPUS, CABI's Full-Text Repository, EBSCO, Clarivate Analytics- Zoological Record and recently has been included in the UGC India approved journals. JJBS Cite Score has improved from 0.18 in 2015 to 0.7 in 2019 (Last updated on 1 March, 2021) and with Scimago Institution Ranking (SJR) 0.18 (Q3) in 2019.

A group of highly valuable scholars have agreed to serve on the editorial board and this places JJBS in a position of most authoritative on biological sciences. I am honored to have six eminent associate editors from various countries. I am also delighted with our group of international advisory board members coming from 15 countries worldwide for their continuous support of JJBS. With our editorial board's cumulative experience in various fields of biological sciences, this journal brings a substantial representation of biological sciences in different disciplines. Without the service and dedication of our editorial; associate editorial and international advisory board members, JJBS would have never existed.

In the coming year, we hope that JJBS will be indexed in Clarivate Analytics and MEDLINE (the U.S. National Library of Medicine database) and others. As you read throughout this volume of JJBS, I would like to remind you that the success of our journal depends on the number of quality articles submitted for review. Accordingly, I would like to request your participation and colleagues by submitting quality manuscripts for review. One of the great benefits we can provide to our prospective authors, regardless of acceptance of their manuscripts or not, is the feedback of our review process. JJBS provides authors with high quality, helpful reviews to improve their manuscripts.

Finally, JJBS would not have succeeded without the collaboration of authors and referees. Their work is greatly appreciated. Furthermore, my thanks are also extended to The Hashemite University and the Scientific Research and Innovation Support Fund, Ministry of Higher Education and Scientific Research for their continuous financial and administrative support to JJBS.

Professor Atoum, Manar F.
March, 2021

CONTENTS

Original Articles

- 159 – 164 Complications of COVID-19: Correlation between Arrhythmia, Acute Cardiac Injury and COVID-19 Severity
Lo'ai Alanagreh , Foad Alzoughool, Suhad Abumweis , Ali Atoom, Wajdy Al-Awaid, Hamzeh Al-Ameer
- 165 – 172 Polycyclic Aromatic Hydrocarbons (Pahs) in Some Plant Species at West Qurna-1 Oil Field in Basra, Southern Iraq
Hamzah A. Kadhim, Makia M. Al-Hejuje, Hamid T. Al-Saad
- 173 – 181 Effects of Biotic and Abiotic Factors on the Yield and Chemical Composition of Essential Oils from Four *Thymus* Species Wild-Growing in Northeastern Algeria
Nesrine Gherairia, Soumia Boukerche , Mohamed Abou Mustapha , Azzedine Chefrou
- 183 – 191 Enhanced Production of Organosulfur Bioactive Compounds in Cell Suspension Culture of Single Garlic (*Allium sativum* L.) Using Precursor Feeding
Frida K Setiowati , Wahyu Widoretno, Sasangka Prasetyawan and Betty Lukiati
- 193 – 197 Towards Food Security: Essential Oil Components as Protectants Against the Rice Weevil, *Sitophilus Oryzae*
Mobolade D. Akinbuluma, Olanike T. Okunlola, Olajumoke Y. Alabi, Modupe I. Timothy, David O. Omobusuyi
- 199 – 203 Expression of Recombinant Lipase from *Serratia marcescens* LII61 in *Escherichia coli*
Sri Sumarsih, Fatimah, Sofijan Hadi, Ni' matuzahroh, Almando Gerald, Rizka Diah Fitri, Gilva Illavi
- 205 – 208 Bioactivity of Moringa Oleifera and Albumin Formulation in Controlling TNF- α and IFN- γ Production by NK Cells in Mice Model Type 1 Diabetes
Noviana Dwi Lestari, Anita Chanisya Rahmah, Wahyu Isnia Adharini, Ruri Vivian Nilamsari, Yoga Dwi Jatmiko Nashi Widodo, Sri Rahayu, Muhaimin Rifa'i
- 209 – 217 An Overview of COVID-19 in Sub-Saharan Africa: the Transmissibility, Pathogenicity, Morbidity and Mortality so far
Chinyere Alope, Balasubramanian Ganesh, Nwogo A. Obasi, Patrick M. Aja, Emmanuel I. Ugwuja, Joseph O. Nwankwo
- 219 – 225 Bioremediation for the Decolorization of Textile Dyes by Bacterial Strains Isolated from Dyeing Wastewater
Fahimeh Firoozeh, Yousef Dadban Shahamat, Susana Rodríguez-Couto, Ebrahim Kouhsari, Farhad Niknejad
- 227 – 238 Phenotypic and Genotypic Diversity of Microsymbionts Nodulating *Medicago sativa* (L.) in the Algerian Sahara
Salim Azib, Hamid Cheloufi, Sara Attab, Noureddine Bouras and Michael D. Holtz
- 239 – 247 Prevalence of Some Pathogenic Bacteria in Caged- Nile Tilapia (*Oreochromis niloticus*) and their Possible Treatment
Ahmed Hammad Sherif and Rasmia Hanafy AbuLeila
- 249 – 255 Effect of Physico-Chemical Parameters in the Production of Hydrolytic Enzymes from Yeast *Candida Tropicalis* Isolated from the Mangrove Sediments of North Kerala, India
Vidya Pothayi, Sreedevi N. Kutty and Sebastian Chempakassery Devasia
- 257 – 261 The Effect of the Biologically Complex of a Medical Leech Active Substances on The Immunosuppressive State of Rats
Aminov Ruslan, Frolov Alexander, Aminova Alina
- 263 – 267 Comparison of the Folate and Homocysteine Levels with A80G -RFC1 Gene Polymorphism between the Sample of Iraqi Children with and without Down Syndrome
Shatha Qassim Jawad, Huda Musleh Mahmood, Gulboy Abdolmajeed Nasir
- 269 – 274 Synthesis of Calcium Oxide Nanoparticles from Waste Eggshell by Thermal Decomposition and their Applications
Yusra M. Alobaidi , Mahmood Mohammed Ali, Ahmed Mishaal Mohammed

- 275 – 287 BAX and P53 Over-Expression Mediated by the Marine Alga *Sargassum Myriocystum* leads to MCF-7, Hepg2 and Hela Cancer Cells Apoptosis and Induces In-Ovo Anti-Angiogenesis Effects
Shabana Parveen and Varalakshmi K.N
- 289 – 294 Optimization of Bioremediation Enhancement Factors in an Aged Crude Oil Polluted Soil.
Lawrence Edemhanria and Christopher Chijindu Osubor
- 295 – 302 Genetic Diversity Analysis Based on Retrotransposon Microsatellite Amplification Polymorphisms (REMAP) for Distinguishing the Ginger Chemotype of *Thua Thien Hue (Zingiber officinale Roscoe)* from other Vietnamese Ginger Types
An H. Nguyen, Nguyen T. T. Phan, Lan T. Tran, Quang T. Hoang, Phuong T. B. Truong
- 303 – 310 GC-MS Chemical Profile, Antioxidant Ability, Antibacterial Effect, A-Glucosidase, A-Amylase and Acetylcholinesterase Inhibitory Activity of Algerian Fir Essential Oil
Djamila Benouchene, Ines Bellil, Chawki Bensouici, Mustafa Abdullah Yilmaz, Salah Akkal, Hatice Banu Kesinkaya, Douadi Khelifi
- 311 – 337 Structural and Catalytical Features of Different Amylases and their Potential Applications
Saptadip Samanta
- 339 – 346 Molecular Docking and TLC Analysis of Candidate Compounds from Lesser used Medicinal Plants Against Diabetes Mellitus Targets
Bhavika Batra, Sukhvinder Singh Sudan, Manu Pant, Kumud Pant, Ankita Lal, Tushar Gusain

Complications of COVID-19: Correlation between Arrhythmia, Acute Cardiac Injury and COVID-19 severity

Lo'ai Alanagreh^{1,*}, Foad Alzoughool^{1,2}, Suhad Abumweis^{3,4}, AliAtoom⁵, Wajdy Al-Awaid⁶, Hamzeh Al-Ameer⁶

¹Department of Medical Laboratory Sciences, Faculty of Applied Medical Sciences, The Hashemite University, Zarqa, Jordan; ²Faculty of Health Sciences, Fujairah Women's College, Higher Colleges of Technology, UAE; ³Department of Clinical Nutrition and Dietetics, Faculty of Applied Medical Sciences, The Hashemite University, Zarqa, Jordan; ⁴College of Pharmacy, AL Ain University, Abu Dhabi, UAE;

⁵Department of Medical Laboratory Sciences, Faculty of Allied Medical Sciences, Al-Ahliyya Amman University, Amman, Jordan;

⁶Department of Biology and Biotechnology, Faculty of Science, American University of Madaba

Received: Dec 15, 2021; Revised: Feb 5, 2022; Accepted Feb, 9, 2022

Abstract:

Occurrence of cardiac arrhythmias in COVID-19 patients with myocardial injuries is common, and it is potentially a life-threatening complication. The current study presents the published literature on cardiac arrhythmia occurrence in COVID-19 patients during 2020. We aimed to evaluate the association among cardiac arrhythmias, acute cardiac injury, and disease severity. Databases, including PubMed, Science Direct, and Scopus, were searched to find studies describing subjects with cardiac arrhythmias and COVID-19. In this study, we recruited 4,355 patients with COVID-19, collected from 13 studies. Relevant data were manually extracted and compared among two groups: arrhythmia as a complication of COVID-19 and cardiac injury as a complication of COVID-19. The pooled prevalence of cardiac arrhythmia was 19% (95%CI: 12% to 29%), compared to 9% (95%CI: 5% to 18%) in acute cardiac injury. Compared to patients without arrhythmias, the probability of developing severe symptoms was increased by ten folds in patients with arrhythmias. In addition, acute cardiac injury significantly increased the severity of COVID-19 by nearly 15-folds. No significant publication bias was indicated by either the visual symmetry or the Egger's test. In conclusion, the incidence of cardiac arrhythmias and acute cardiac injury is highly associated with the severity and the mortality rate of COVID-19.

Keywords: COVID-19, Arrhythmia, Acute cardiac injury

1. Background

The ongoing COVID-19 pandemic poses a significant threat to the health care systems around the globe [1, 2]. As of February 2nd, 2022, the epidemic infected approximately 382,296,709 million people, including nearly 5,706,691 million patients who have died. And the numbers keep increasing globally, indicating that the pandemic is far from the end.

Cardiac manifestations in COVID-19 patients, including arrhythmia and acute cardiac injury, have been reported since the pandemic's beginning [3-5, 37, 38]. Epidemiological studies have reported different mortality rates for COVID-19 patients with cardiac manifestations [6].

Arrhythmias can be triggered by myocardial dysfunction that results from severe systematic inflammation. Severe inflammation conditions like sepsis and septic shock were associated with several types of cardiac arrhythmias [7, 8, 9][9]. Several studies reported that most inflammatory cytokines are associated with deadly arrhythmias [10, 11]. Although many case series studies have reported the occurrence of arrhythmia as a

cardiac manifestation of COVID-19 [12-14], fewer meta-analyses have quantified arrhythmia's pooled event rate in COVID-19 patients and its association with disease severity.

COVID-19 can induce acute cardiac injury through several suggested pathways: myocarditis which is caused by the cytokine storm mediated through the T cells and monocytes [15], the cardiac myocytes damage which is caused by hypoxemia and respiratory failure and the inhibition of the protective signaling pathways in cardiac myocytes as a result of the downregulation of Angiotensin-converting enzyme 2 (ACE2) expression [17].

Evaluating the contribution of cardiac manifestations to COVID-19 severity is essential to improve treatment protocols. Therefore, the present meta-analysis study was performed to evaluate the association of both cardiac arrhythmia and acute cardiac injury with the severity of COVID-19 in patients.

2. Methods:

2.1. Data search

The international web databases, including PubMed, Science Direct, and Scopus, were searched between

* Corresponding author e-mail: Loai-alanagreh@hu.edu.jo.

January 1, 2020, and August 18, 2020. Several combined keywords were used for searching the databases, including cardiac arrhythmias and COVID-19; arrhythmia and SAR-CoV-2; acute cardiac injury and SAR-CoV-2; and COVID-19. Besides, the lists of references of all relevant studies were also manually checked to identify further studies. The protocol for this meta-analysis is registered at PROSPERO CRD42020191768. The meta-analysis was also conducted following the Meta-analyses of Observational Studies in Epidemiology (MOOSE) [18].

2.2. Study selection

Studies that provided adequate details on cardiac arrhythmia and acute cardiac injury as outcomes complications in positively diagnosed COVID-19 were included. Case reports, review articles, and editorials were excluded from this analysis. Studies that did not provide enough details on the number of cases with severe or fatal outcomes were excluded. The selection of the studies was limited to articles in the English language.

2.3. Data abstraction

For studies that met the inclusion criteria, the following data were extracted from each one using a standardized form:

- The surname of the first author
- The design of the study
- Ratios of clinical characteristics of interest
- Sample size, country, data relevant to arrhythmia and acute cardiac injury as an outcome, the number of cases with severe and non-severe outcomes, and the number of survivors and non-survivors

As reported in the included studies, the severity of the disease validation was identified if patients needed to be admitted to the intensive care unit, needed vital life support, or required mechanical ventilation. Two investigators (FA and MA) extracted the relevant data,

2.4. Quality assessment

The Joanna Briggs Institute (JBI) critical appraisal checklist for the case series was used to assess the internal validity and the risk of bias [19]. The ten items in the JBI checklist deals with issues related to confounding, selection, and information bias to assess the internal validity of the case series. We presented the quality assessment results of the included studies in a table and not as a score [19]. SA carried out the quality assessment of the included studies in this meta-analysis.

2.5. Quantitative data synthesis and analysis

Data analysis was performed using Comprehensive Meta-Analysis V2 (Biostat, USA). A p-value of <0.05 was considered statistically significant. The pooled event rates of pre-existing cardiovascular disease comorbidities and the odds ratio (OR) with 95% confidence intervals (95%CI) of disease severity and mortality associated with the exposures of interest were estimated using a random-

effect model. Heterogeneity in any analysis was tested using the I² statistic (p-value of <0.1), which estimates the percentage of variation in study results explained by between-study heterogeneity rather than sampling error. Usually, an I² value $>50\%$ indicates considerable heterogeneity [20]. To assess the presence of publication bias, we used funnel plots as well as Egger's test.

3. Results

3.1. Search results and study characteristics

A total of 650 articles were identified from the three examined databases examined. After excluding duplicated or overlapping articles and removing reviews and editorials, 36 articles met the primary searched criteria. For the quantitative part of our study, eight studies were included in the meta-analysis that reported arrhythmia as disease complications. On the other hand, ten studies were included in this meta-analysis that reported acute cardiac injury as disease complications (Figure 1). Studies were conducted mainly in China (n=9) and the United States of America (n=4).

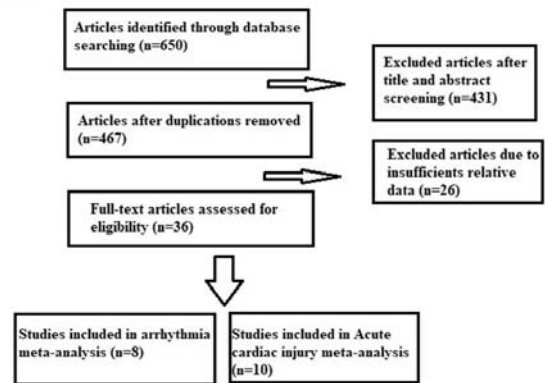


Figure 1. Flow chart of the literature search and study selection

3.2. The proportions of cardiac manifestations in COVID-19 patients.

Relevant data regarding the event rate of cardiac manifestations, particularly arrhythmia and acute cardiac injury in 4,355 patients with COVID-19, were collected from 13 studies; eight studies reported arrhythmia, and ten of them reported acute cardiac injury. The pooled prevalence of arrhythmia as a complication of COVID-19 among the eight included studies (Table 1) was 19% (95%CI: 12% to 29%), as shown in figure 2. Moreover, the pooled prevalence of acute cardiac injury as a complication of COVID-19 among the ten included studies (Table 2) was 9% (95%CI: 5% to 18%), as shown in figure 3.

Table 1. Arrhythmia outcomes complication in COVID-19 patients.

Study's Author	Country	Condition	Sample size	Events (n)	Non-events (n)	Severe cases ratio	Non-sever cases ratio
Wang D, et al [21]	China	Arrhythmia	138	23	115	16/36	7/102
Goyal P, et al [14]	USA	Arrhythmia	393	29	364	24/130	5/263
Zhang G, et al [22]	China	Arrhythmia	221	24	197	22/55	2/166
Hu L, et al [3]	USA	Arrhythmia	323	98	225	80/172	18/151
Du Y, et al [23]	China	Arrhythmia	85	51	34		
Rosenberg E, et al [24]	USA	Arrhythmia	1438	240	1198		
Lei S, et al [13]	China	Arrhythmia	34	8	26	5/15	3/19
Enzmann M, et al [25]	USA	Arrhythmia	150	14	136		

Table 2. Acute cardiac injury outcomes complication in COVID-19 patients.

Study's Author	Country	Condition	Sample size	Events (n)	Non-events (n)	Severe cases ratio	Non-sever cases ratio
Wang D, et al [21]	China	Acute cardiac injury	138	10	128	8/36	2/102
Zhang G, et al [22]	China	Acute Cardiac injury	221	17	204	16/55	1/166
Hu L, et al [3]	USA	Acute Cardiac injury	323	24	299	22/172	2/151
Du Y, et al [23]	China	Acute cardiac injury	85	38	47		
Lei S, et al [13]	China	Acute cardiac injury	34	5	29		
Guan W, et al [26]	China	Acute cardiac injury	1099	6	1093	5/926	1/962
Huang C, et al [9]	China	Acute cardiac injury	41	5	36	4/13	1/28
Wan S, et al [27]	China	Acute cardiac injury	135	10	125	2/40	8/95
Zhou F, et al [28]	China	Acute Cardiac injury	191	33	158	32/54	1/137
Wang D, et al [29]	China	Acute Cardiac injury	107	12	95	8/19	4/88

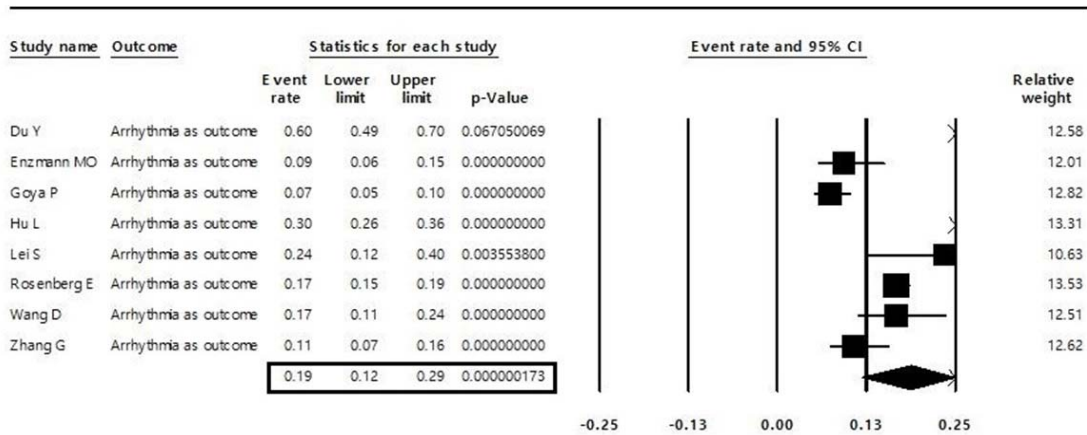


Figure 2: Pooled event rate of arrhythmia as a complication in patients with COVID-19.

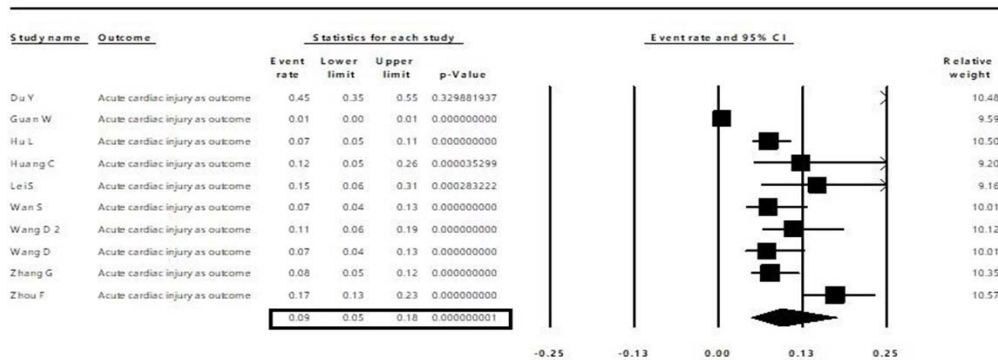


Figure 3: Pooled event rate of acute cardiac injury as a complication in patients with COVID-19.

3.3. Arrhythmia and the risk of severity outcomes in COVID-19

Relevant data regarding the association of arrhythmia with severity in 4,355 patients with COVID-19 were collected from five included studies. The OR of

arrhythmia in severe compared to non-severe cases of COVID-19 was significantly higher (OR= 9.9, 95% CI: 4.8 to 20.4), which means that arrhythmia increases the severity of COVID-19 about ten folds as shown in figure 4.

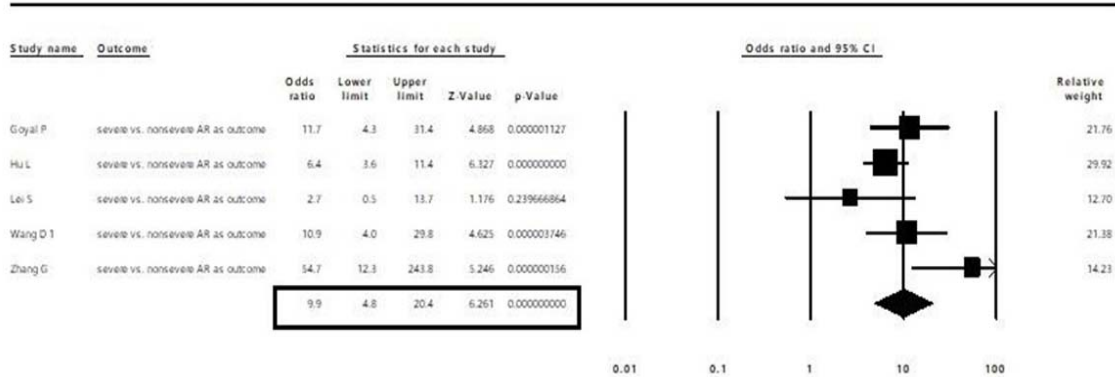


Figure 4: Forest plot of the odd ratios of arrhythmia in severe compared to non-severe COVID-19 cases.

3.4. Acute cardiac injury and the risk of severity outcomes in COVID-19

Relevant data regarding the association of acute cardiac injury severity rate in patients with COVID-19 were

collected from six studies. The OR of acute cardiac injury in severe compared to non-severe cases of COVID-19 was significantly higher with nearly 15-fold risk of poor outcomes (OR=14.6,95% CI: 2.9 to 73.7) as it is shown in figure 5.

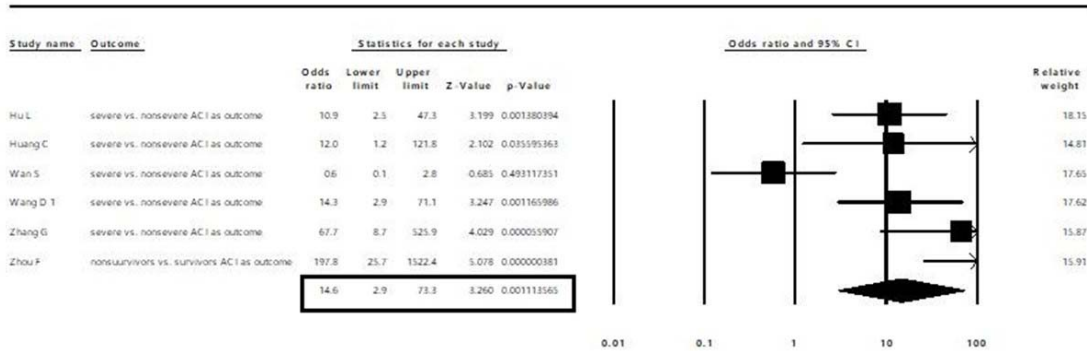


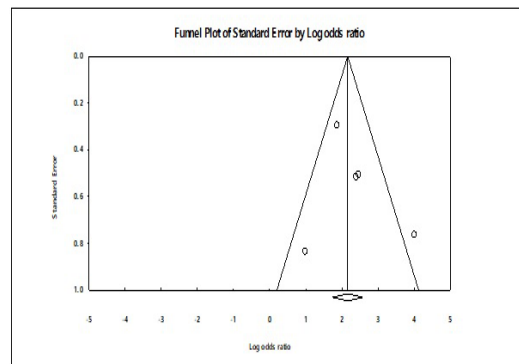
Figure 5: Forest plot of the odd ratios of acute cardiac injury in severe compared to non-severe COVID-19 cases.

3.5. Quality of the included studies

Supplementary Table S1 summarizes the quality assessment of the included studies. All included studies in this analysis reported the demographic and clinical characteristics and the outcomes of the participants. However, most of the studies did not have defined participants' eligibility criteria. In addition, it was unclear whether most of the studies had consecutive inclusion of the participants and whether it was a complete inclusion. Most of the studies diagnosed COVID-19 disease and outcome of interests using valid and reliable methods and used appropriate statistical analysis.

3.6. Assessment of publication bias

As shown, figures 6 and 7 evaluate publication bias using a funnel plot based on the event rate of arrhythmia and acute cardiac injury outcomes; a visual symmetry indicates the absence of publication bias. Also, the Egger's test revealed no significant publication bias (Egger's test: p =0.5124, and 0.30009 respectively).



No significant publication of bias (Egger's test: p=0.5124)

Figure 6: Funnel plot for publication bias based on arrhythmia

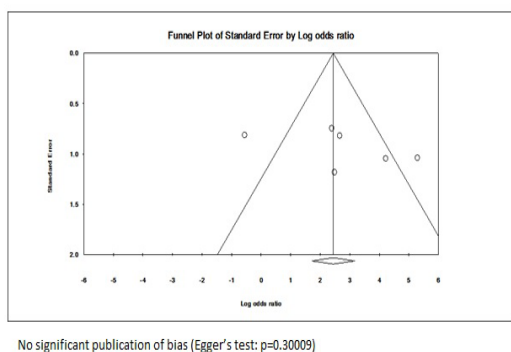


Figure 7: Funnel plot for publication bias based on acute cardiac injury

4. Discussion

In the present meta-analysis, we examined 18 independent studies. Eight of these studies discussed arrhythmia as a COVID-19 disease complication, and ten studies were included in this meta-analysis of acute cardiac injury as disease complications. Pooled studies were reporting clinical data on 4,355 COVID-19 patients. Results added value to the literature as it summarized the prevalence of arrhythmia and acute cardiac injury as a disease outcome among COVID-19 patients.

Our results showed that incidence of arrhythmia occurrence in COVID-19 patients was 19% compared to a study describing the outcomes in 138 Chinese patients with COVID-19 reported 16.7% incidence of arrhythmia [21]. A recent study reported the incidence of arrhythmia at 6.9% in hospitalized patients [38]. For acute cardiac injury, a meta-analysis of the Chinese studies reported an 8% incidence of acute cardiac injury, while our study indicates a 9% incidence of acute cardiac injury [30].

Severe systemic inflammation associated with COVID-19 can trigger myocardial dysfunction, which leads to arrhythmia [7, 8]. Many studies reported that pro-inflammatory cytokines are associated with arrhythmia [11, 31]. Pro-inflammatory cytokines like C-reactive protein (CRP), TNF- α , and IL6 played a role in inducing the synthesis of several coagulation markers, including tissue factor (TF) [31, 32]. Moreover, these markers have been extremely investigated in the association with atrial fibrillation (AF) [11].

COVID-19, as a viral infection, can trigger a hyper-inflammatory state with a fatal storm of cytokine and arrhythmogenic potential. Interleukin 1 (IL-1), interleukin 2 (IL-2), interleukin 1 β (IL-1 β), IL-7, granulocyte colony-stimulating factor (G-CSF), interferon- γ , inducible protein 10, monocyte chemoattractant protein 1 (mcp1), and tumor necrosis factor- α (TNF- α) are cytokines reported to increase in COVID-19 patients. One of the possible mechanisms of triggering arrhythmia by systematic inflammation is inducing ischemic heart disease. Many inflammatory markers are shown to be increased locally at ischemia, such as; IL-6 [33] and TNF- α [34]. Arrhythmias can also be triggered by myocardial dysfunction that results from severe systematic inflammation. Severe inflammation conditions like sepsis and septic shock were reported to be associated with several types of cardiac arrhythmias [7, 8]. Another important indirect potential

pathway of how systematic inflammation induces arrhythmia is the activation of systematic coagulation response. Even though there are not fully established clinical settings that prove the association between systemic inflammation and cardiac arrhythmias, several studies shed light on the potential association between atrial fibrillation and systemic inflammation due to its high incidence [11, 35, 36].

Our results showed that the incidence of arrhythmia was associated with ten folds increase in disease severity. Patients with the more severe systemic disease also had a higher probability of promoting cardiac arrhythmias, as evidenced by ICU admissions. Therefore, clinical protocols should pay attention to preventing and managing arrhythmia in COVID-19 patients. Future studies should investigate whether arrhythmia management in COVID-19 patients reduces disease severity.

The most common cardiovascular disease complication is acute cardiac injury. Our results reported that the incidence of acute cardiac injury was 14 folds higher in patients with severe complications than in non-severe patients. Early cardiac interventional protocols in COVID-19 patients may aid in reducing the disease severity and mortality. The myocarditis caused by the cytokine storm, cardiac myocytes damage, inhibition of the protective signaling pathways in cardiac myocyte, and increased hypercoagulability and microvascular thrombosis suggested mechanisms of induced acute cardiac injury among COVID-19 patients. Future studies should look at risk factors for developing cardiac injury in COVID-19 patients.

Our study rigorously analyzed the number of patients with arrhythmia outcomes and acute cardiac injury outcomes collected from a large sample of patients with COVID-19; advantageously, a visual symmetry indicates the absence of publication bias. Most studies did not report the eligibility criteria and whether participants were recruited consecutively. Therefore, selection bias is likely concern in the included studies. Other biases in the included studies are less likely since all studies address sufficiently other points in the JBI tool.

5. Conclusion

In summary, present evidence showed that cardiac arrhythmias and acute cardiac injury are highly associated with the severity and the mortality rate of COVID-19. Early cardiac arrhythmias and acute cardiac injury management may considerably improve COVID-19 prognosis.

Funding

This research received no external funding.

Conflicts of Interest

The authors declare no conflict of interest.

References

Alzoughool, F. and L. Alanagreh, *Coronavirus drugs: Using plasma from recovered patients as a treatment for COVID-19*. Int J Risk Saf Med, 2020. 31(2): p. 47-51.

- Alanagreh, L., F. Alzoughool, and M. Atoum, *The Human Coronavirus Disease COVID-19: Its Origin, Characteristics, and Insights into Potential Drugs and Its Mechanisms*. Pathogens, 2020. **9**(5).
- Hu, L., et al., *Risk Factors Associated With Clinical Outcomes in 323 Coronavirus Disease 2019 (COVID-19) Hospitalized Patients in Wuhan, China*. Clin Infect Dis, 2020. **71**(16): p. 2089-2098.
- Mehra, M.R., et al., *Cardiovascular Disease, Drug Therapy, and Mortality in Covid-19*. N Engl J Med, 2020. **382**(25): p. e102.
- Si, D., et al., *Death, discharge and arrhythmias among patients with COVID-19 and cardiac injury*. Cmaj, 2020. **192**(28): p. E791-e798.
- Mishra, A.K., et al., *A review of cardiac manifestations and predictors of outcome in patients with COVID - 19*. Heart Lung, 2020. **49**(6): p. 848-852.
- Okazaki, R., et al., *lipopolysaccharide induces atrial arrhythmogenesis via down-regulation of L-type Ca²⁺ channel genes in rats*. Int Heart J, 2009. **50**(3): p. 353-63.
- Court, O., et al., *Clinical review: Myocardial depression in sepsis and septic shock*. Crit Care, 2002. **6**(6): p. 500-8.
- Huang, C., et al., *Clinical features of patients infected with 2019 novel coronavirus in Wuhan, China*. Lancet, 2020. **395**(10223): p. 497-506.
- Fernández-Sada, E., et al., *Proinflammatory Cytokines Are Soluble Mediators Linked with Ventricular Arrhythmias and Contractile Dysfunction in a Rat Model of Metabolic Syndrome*. Oxid Med Cell Longev, 2017. **2017**: p. 7682569.
- Guo, Y., G.Y. Lip, and S. Apostolakis, *Inflammation in atrial fibrillation*. J Am Coll Cardiol, 2012. **60**(22): p. 2263-70.
- Zhang, J.J., et al., *Clinical characteristics of 140 patients infected with SARS-CoV-2 in Wuhan, China*. Allergy, 2020. **75**(7): p. 1730-1741.
- Lei, S., et al., *Clinical characteristics and outcomes of patients undergoing surgeries during the incubation period of COVID-19 infection*. EClinicalMedicine, 2020. **21**: p. 100331.
- Goyal, P., et al., *Clinical Characteristics of Covid-19 in New York City*. N Engl J Med, 2020. **382**(24): p. 2372-2374.
- Zhou, Y., et al., *Pathogenic T cells and inflammatory monocytes incite inflammatory storm in severe COVID-19 patients*. Natl Sci Rev. 2020 Mar 13:nwaa041. doi: 10.1093/nsr/nwaa041.
- Kubasiak, L.A., et al., *Hypoxia and acidosis activate cardiac myocyte death through the Bcl-2 family protein BNIP3*. Proc Natl Acad Sci U S A, 2002. **99**(20): p. 12825-30.
- Han, H., et al., *Prominent changes in blood coagulation of patients with SARS-CoV-2 infection*. Clin Chem Lab Med, 2020. **58**(7): p. 1116-1120.
- Stroup, D.F., et al., *Meta-analysis of observational studies in epidemiology: a proposal for reporting. Meta-analysis Of Observational Studies in Epidemiology (MOOSE) group*. Jama, 2000. **283**(15): p. 2008-12.
- Munn, Z., et al., *Methodological quality of case series studies: an introduction to the JBI critical appraisal tool*. JBI Database System Rev Implement Rep, 2019.
- Higgins, J.P. and S.G. Thompson, *Quantifying heterogeneity in a meta-analysis*. Stat Med, 2002. **21**(11): p. 1539-58.
- Wang, D., et al., *Clinical Characteristics of 138 Hospitalized Patients With 2019 Novel Coronavirus-Infected Pneumonia in Wuhan, China*. Jama, 2020. **323**(11): p. 1061-1069.
- Zhang, G., et al., *Clinical features and short-term outcomes of 221 patients with COVID-19 in Wuhan, China*. J Clin Virol, 2020. **127**: p. 104364.
- Du, Y., et al., *Clinical Features of 85 Fatal Cases of COVID-19 from Wuhan. A Retrospective Observational Study*. Am J Respir Crit Care Med, 2020. **201**(11): p. 1372-1379.
- Rosenberg, E.S., et al., *Association of Treatment With Hydroxychloroquine or Azithromycin With In-Hospital Mortality in Patients With COVID-19 in New York State*. Jama, 2020. **323**(24): p. 2493-2502.
- Enzmann, M.O., et al., *Treatment and preliminary outcomes of 150 acute care patients with COVID-19 in a rural health system in the Dakotas*. Epidemiol Infect, 2020. **148**: p. e124.
- Guan, W.J., et al., *Clinical Characteristics of Coronavirus Disease 2019 in China*. N Engl J Med, 2020. **382**(18): p. 1708-1720.
- Wan, S., et al., *Clinical features and treatment of COVID-19 patients in northeast Chongqing*. J Med Virol, 2020. **92**(7): p. 797-806.
- Zhou, F., et al., *Clinical course and risk factors for mortality of adult inpatients with COVID-19 in Wuhan, China: a retrospective cohort study*. Lancet, 2020. **395**(10229): p. 1054-1062.
- Wang, D., et al., *Clinical course and outcome of 107 patients infected with the novel coronavirus, SARS-CoV-2, discharged from two hospitals in Wuhan, China*. Crit Care, 2020. **24**(1): p. 188.
- Li, B., et al., *Prevalence and impact of cardiovascular metabolic diseases on COVID-19 in China*. Clin Res Cardiol, 2020. **109**(5): p. 531-538.
- van den Oever, I.A., N. Sattar, and M.T. Nurmohamed, *Thromboembolic and cardiovascular risk in rheumatoid arthritis: role of the haemostatic system*. Ann Rheum Dis, 2014. **73**(6): p. 954-7.
- McInnes, I.B., et al., *Effect of interleukin-6 receptor blockade on surrogates of vascular risk in rheumatoid arthritis: MEASURE, a randomised, placebo-controlled study*. Ann Rheum Dis, 2015. **74**(4): p. 694-702.
- Maier, W., et al., *Inflammatory markers at the site of ruptured plaque in acute myocardial infarction: locally increased interleukin-6 and serum amyloid A but decreased C-reactive protein*. Circulation, 2005. **111**(11): p. 1355-61.
- Satoh, M., et al., *The expression of TNF-alpha converting enzyme at the site of ruptured plaques in patients with acute myocardial infarction*. Eur J Clin Invest, 2008. **38**(2): p. 97-105.
- Liew, R., et al., *Role of tumor necrosis factor- α in the pathogenesis of atrial fibrosis and development of an arrhythmogenic substrate*. Circ J, 2013. **77**(5): p. 1171-9.
- Yalta, K., et al., *Meteorologic factors may trigger arrhythmogenesis through induction of systemic inflammation and coagulation response: potential antiarrhythmic benefits of mitigating this response in arrhythmia-prone subjects under poor meteorologic conditions?* Int J Cardiol, 2013. **168**(5): p. 4937-8.
- Duckheim M, Schreieck J. COVID-19 and Cardiac Arrhythmias. Hamostaseologie. 2021 Oct;41(5):372-378. doi: 10.1055/a-1581-6881. Epub 2021 Oct 25. PMID: 34695853.
- Malaty M, Kayes T, Amarasekera AT, Kods M, MacIntyre CR, Tan TC. Incidence and treatment of arrhythmias secondary to coronavirus infection in humans: A systematic review. Eur J Clin Invest. 2021 Feb;51(2):e13428. doi: 10.1111/eji.13428. Epub 2020 Nov 26. PMID: 33043453; PMCID: PMC7646010.

Polycyclic Aromatic Hydrocarbons (Pahs) in Some Plant Species at West Qurna-1 Oil Field in Basra, Southern Iraq

Hamzah A. Kadhim¹, Makia M. Al-Hejuje², Hamid T. Al-Saad^{3,*}

¹Department of Geology / college of Science –Basrah University, Basrah, Iraq; ²Department of Ecology / college of Science –Basrah University, Basrah, Iraq; ³College of Marine Science, University of Basrah, Basrah, Iraq.

Received: December 3, 2020; Revised: March 3, 2021; Accepted: March 28, 2021

Abstract

Concentrations and sources of Polycyclic aromatic hydrocarbons were determined seasonally in some terrestrial plant species (*Conocarpus lancifolius*, *Eucalyptus camaldulensis* and *Suaeda vermiculata*) at three stations in west Qurna-1 oil field, southern Iraq during the period from January 2018 to December 2018. The results showed that the highest mean concentration of PAHs in plant species at DS6 was (2.813 ng/g dry weight) in *E. camaldulensis* and the lowest was in *C. lancifolius* (2.106 ng/g dry weight). Seasonal variation of PAHs concentration showed that the highest mean concentration was recorded in spring (2.634 ng/g dry weight) in *E. camaldulensis* while the lowest mean concentration was recorded in winter (1.975 ng/g dry weight) in *Suaeda vermiculata*. According to the PAHs indices [(The Fluoranthene/Pyrene ratio, Phenanthrene/Anthracene ratio, LMW/HMW ratio, Ant/(Ant+Phen) ratio, BaA/(BaA+Chry) ratio and InP/(InP+BghiP) ratio)], the main sources of PAHs in these plants species were pyrogenic and petrogenic.

Keywords: PAHs, Plant species, Oil field, Iraq

1. Introduction

Polycyclic aromatic hydrocarbons (PAHs) exist in the environment, and they are distributed in both aquatic and terrestrial environments and both biogenic and anthropogenic origin. They can be formed by several pathways: biosynthesis, pyrogenic and petrogenic (Karem, 2016).

Petrogenic PAHs are derived from petroleum and other fossil fuels containing PAHs. Diagenetic PAHs refer to PAHs formation from biogenic precursors, like plant terpenes, leading to the formation of compounds, such as retene (methyl isopropyl phenanthrene or 1-methyl-7-isopropyl phenanthrene C₁₈H₁₈) and derivatives of phenanthrene and chrysene. A potential fourth source of PAHs is biogenic or purely from bacteria, fungi, plants or animals in sedimentary environments without any contributions from diagnostic processes; however, this source is not significant. Their presence in all environment compartments results from both natural processes, such as volcanic activity or forest fires, and predominantly anthropogenic activities, including waste incineration, burning wood, coal or garbage, and operation of gasoline and diesel engines (Bakhtiar *et al.*, 2009). PAHs are very dangerous substances because of their cariogenic properties. It is important to know the features of PAHs transport and accumulation in soils, especially on agricultural lands. The PAHs are produced by combustion

of fossil fuel (coal and petroleum) and as a natural source released to the environment (Zakaria *et al.*, 2002).

They can be transported over long distances in the atmosphere and deposited in faraway areas; hence, they are widely found in the environment (Wang *et al.*, 2015). There are a large number of PAH compounds in the environment, comprising of sixteen compounds of increasing environmental and health interests: naphthalene, acenaphthylene, acenaphene, phenanthrene, fluorene, anthracene, fluoranthene, pyrene, chrysene, benzo (a) anthracene, benzo (b) fluoranthene, benzo (k) fluoranthene, benzo (a) pyrene, benzo (ghi) perylene, dibenzo (ah) and anthracene, indeno[1,2,3(cd)] pyrene. The physical, chemical and toxicological properties for each of these compounds are different. Therefore, their evaluation in nature is required (Al-Hejuje *et al.*, 2015).

Long-term exposure to hydrocarbon compounds can negatively impact human life in terms of comfort and health (Al-Hejuje *et al.*, 2015). PAHs may largely contaminate all environmental matrices and raise toxicological, mutagenic, and carcinogenic concerns (Karem, 2016).

The aim of the present study is to determine the levels of PAH compounds in some plant species at west Qurna-1 oil field in Basra, southern Iraq by collecting, extracting and analysing the aromatic compounds in the plant samples.

Study Area

* Corresponding author e-mail: htalsaad@yahoo.com.

The super-giant west Qurna oil field in southern Iraq is located in Basra Governorate, around 65 km northwest of the city of Basra. The west Qurna field is situated in a long, sinuous North South trending structure. The field is comprised of two separate license areas, 1 and 2. The west Qurna field was discovered in August 1973 and a total of

early to late Cretaceous Sa'di, Khasib, Mishrif, Zubair, Ratawi and Yamama formations, and gas condensate was recovered from a tesin the late Jurassic Najmah formation.

West Qurna-1 oil field is located southwest of Basra city. The study area extended between latitudes (30° 45' 35'' E, 30° 52' 54'' N) and longitude (47° 19' 12'' E, 47°

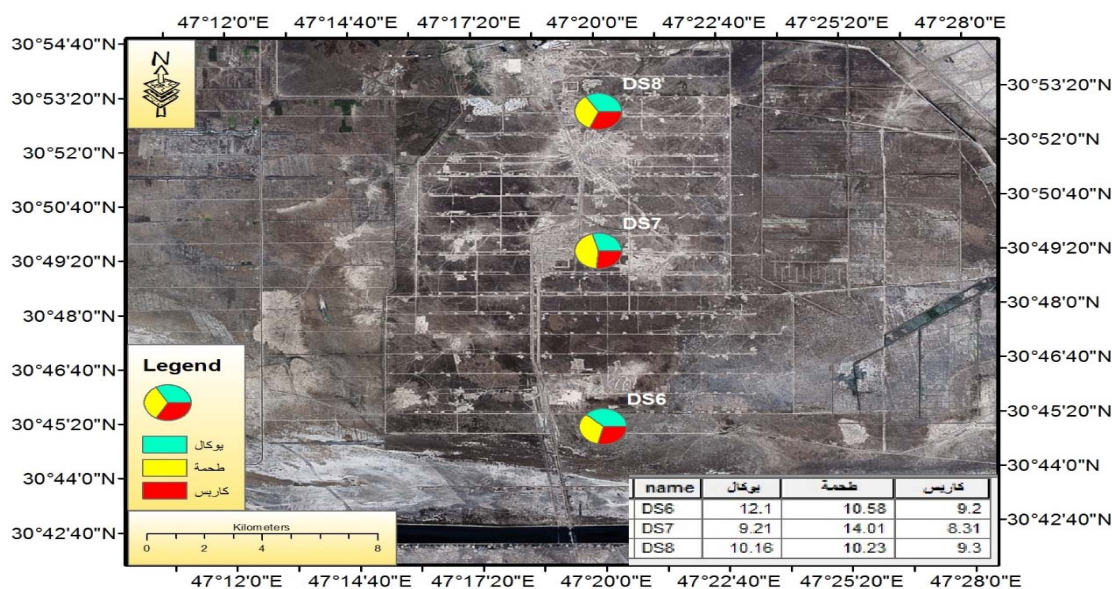


Figure 1. The study area in west Qurna-1 oil field.

13 wells have been drilled in the West Qurna-1 area. Significant oil accumulations have been discovered in the

19° 53'') as shown in Fig 1. The west Qurna oil field area is characterized by a flat topography, where the elevation of the overall study area ranges from 0.5 m to 2 m above sea level.

2. Materials and Methods

Three species of plants (*Conocarpus lancifolius*, *Eucalyptus camaldulensis* and *Suaeda vermiculata*) were chosen. The plants leaves samples were collected by hand from three stations (DS6, DA7 and DS8) seasonally during the period from January 2018 to December 2018. The plant samples were washed with distilled water, dried at room temperature, ground finely in an electrical mortar, and stored in glass containers until analysis. Five grams of each ground plant samples were placed separately in soxhlet using soxhlet intermittent extraction (Goutex and Saliot, 1980) with 120 ml mixed solvents methanol:benzene (1:1 v/v) for 24-36 hr at a temperature that did not exceed 40°C. At the end of this period, the combined extracts underwent saponification for 2 hr by adding 20 ml 4M MeOH(KOH) at the same temperature and cooled to room temperature, and the saponification matter with 40 ml n-hexane was extracted using a separator funnel. The extract was then concentrated to about 2 ml by a rotary evaporator for the following clean-up. The concentrated extract was fractionated by column chromatography on anhydrous sodium sulphate (1 g) over alumina (10 g) and silica gel (10 g). The aromatic hydrocarbons were obtained by successively eluting Benzen (25 ml). The aromatic fractions were concentrated again on a rotary evaporator and transferred to a vial, and the volume was adjusted to 1 ml exactly using a stream of

nitrogen gas. An aliquot of 1 ml of aromatic hydrocarbons extract was subjected to analysis. The determination of PAHs was done by using HPLC (Shimadzu LC). A standard (PAHs) was used to determine the qualities and quantities of these compounds in the plant samples. The condition operation for HPLC was as follows: the column was C18 (250mm, 25cm, 4.6mm), the mobile phase was acetonitrile:water (90:10 v/v), the flow rate was 0.5ml/min, the injection volume was 20µl, the wavelength of UV/visible was 254 nm (Al-Hejuje, 2014; Al-Hejuje *et al.*, 2015).

3. Statistical Analysis

Analysis of Variance (One-way ANOVA) was applied using Statistical Package for Social Science (SPSS) ver.17.0 software to identify the existence of significant temporal and spatial differences (Al-Hejuje, 2014).

4. Results

The PAHs concentration in plants are classified as shown in Table 1-3.

Table 1. Concentrations of Polycyclic Aromatic Hydrocarbons (ng/g dry weight) in *C. lancifolius*.

PAHs	Winter			Spring			Summer			Autumn		
	DS6	DS7	DS8									
Naphthalene	0.109	0.138	0.134	0.114	0.146	0.143	0.120	0.164	0.152	0.116	0.151	0.141
Acenaphthylene	0.126	0.142	0.125	0.132	0.166	0.130	0.141	0.173	0.126	0.135	0.162	0.117
Acenaphene	0.043	0.150	0.108	0.042	0.143	0.116	0.024	0.021	0.112	0.011	0.016	0.062
Fluorene	0.148	0.121	0.127	0.152	0.138	0.130	0.153	0.142	0.131	0.148	0.135	0.125
Phenanthrene	0.122	0.117	0.133	0.124	0.125	0.148	0.110	0.131	0.152	0.102	0.122	0.130
Anthracene	0.167	0.109	0.177	0.177	0.215	0.227	0.198	0.233	0.249	0.173	0.197	0.213
Fluoranthene	0.112	0.155	0.175	0.117	0.262	0.212	0.221	0.225	0.225	0.175	0.194	0.210
Pyrene	0.129	0.115	0.228	0.132	0.127	0.254	0.211	0.101	0.320	0.167	0.100	0.299
Benzo(a) anthracene	0.115	0.102	0.109	0.113	0.013	0.114	0.121	0.011	0.030	0.126	0.042	0.037
Chrysene	0.117	0.113	0.210	0.113	0.139	0.227	0.117	0.146	0.214	0.112	0.135	0.196
Benzo(b) fluoranthene	0.297	0.124	0.137	0.310	0.175	0.154	0.325	0.198	0.163	0.210	0.168	0.142
Benzo(k) fluoranthene	0.118	0.130	0.106	0.124	0.165	0.113	0.126	0.071	0.022	0.115	0.066	0.113
Benzo(a) pyrene	0.021	0.121	0.118	0.024	0.233	0.126	0.125	0.259	0.133	0.117	0.221	0.115
Indo(1,2,3-cd) pyrene	0.018	0.133	0.175	0.021	0.147	0.216	0.119	0.152	0.236	0.100	0.134	0.201
Dibenzo anthracene	0.177	0.123	0.137	0.185	0.131	0.132	0.194	0.130	0.136	0.166	0.120	0.121
Benzo(g,h,i) perylene	0.057	0.036	0.125	0.064	0.054	0.247	0.173	0.173	0.263	0.153	0.144	0.195
Total	1.876	1.929	2.319	1.944	2.283	2.680	2.478	2.330	2.664	2.126	2.107	2.457

Table 2. Concentrations of Polycyclic Aromatic Hydrocarbons (ng/g dry weight) in *E. camaldulensis*

PAHs	Winter			Spring			Summer			Autumn		
	DS6	DS7	DS8									
Naphthalene	0.134	0.107	0.170	0.114	0.190	0.032	0.116	0.036	0.036	0.107	0.027	0.138
Acenaphthylene	0.125	0.114	0.125	0.114	0.138	0.186	0.210	0.215	0.218	0.194	0.192	0.194
Acenaphene	0.108	0.165	0.134	0.202	0.143	0.043	0.027	0.150	0.036	0.022	0.143	0.027
Fluorene	0.127	0.124	0.102	0.140	0.033	0.139	0.141	0.024	0.140	0.127	0.015	0.152
Phenanthrene	0.133	0.132	0.103	0.158	0.116	0.127	0.164	0.129	0.139	0.148	0.114	0.142
Anthracene	0.177	0.167	0.095	0.198	0.112	0.156	0.260	0.115	0.164	0.244	0.104	0.152
Fluoranthene	0.175	0.211	0.197	0.262	0.220	0.318	0.362	0.236	0.320	0.226	0.218	0.312
Pyrene	0.228	0.164	0.195	0.211	0.231	0.211	0.201	0.252	0.209	0.191	0.247	0.194
Benzo(a) anthracene	0.109	0.310	0.100	0.348	0.102	0.148	0.357	0.063	0.164	0.341	0.041	0.013
Chrysene	0.210	0.027	0.102	0.032	0.112	0.110	0.124	0.131	0.012	0.115	0.124	0.015
Benzo(b) fluoranthene	0.137	0.102	0.020	0.119	0.021	0.113	0.123	0.063	0.115	0.113	0.048	0.172
Benzo(k) fluoranthene	0.106	0.105	0.047	0.113	0.275	0.063	0.121	0.311	0.030	0.116	0.290	0.035
Benzo(a) pyrene	0.118	0.221	0.201	0.274	0.221	0.057	0.281	0.210	0.069	0.255	0.201	0.061
Indo(1,2,3-cd) pyrene	0.175	0.148	0.326	0.326	0.376	0.125	0.312	0.456	0.146	0.289	0.397	0.138
Dibenzo anthracene	0.137	0.131	0.304	0.137	0.317	0.072	0.142	0.326	0.056	0.133	0.311	0.074
Benzo(g,h,i) perylene	0.125	0.142	0.026	0.214	0.032	0.114	0.217	0.053	0.124	0.199	0.034	0.133
Total	2.319	2.370	2.247	2.962	2.639	2.302	3.152	2.770	1.978	2.820	2.506	1.952

Table 3. Concentrations of Polycyclic Aromatic Hydrocarbons (ng/g dry weight) in *S. Vermiculata*

PAHs	Winter			Spring			Summer			Autumn		
	DS6	DS7	DS8									
Naphthalene	0.117	0.095	0.120	0.127	0.106	0.131	0.142	0.035	0.225	0.126	0.028	0.193
Acenaphthylene	0.119	0.100	0.117	0.125	0.116	0.125	0.140	0.132	0.093	0.134	0.125	0.081
Acenaphene	0.149	0.126	0.093	0.142	0.143	0.113	0.173	0.138	0.115	0.157	0.127	0.104
Fluorene	0.102	0.147	0.113	0.036	0.162	0.124	0.046	0.172	0.127	0.035	0.155	0.110
Phenanthrene	0.116	0.134	0.120	0.136	0.167	0.141	0.129	0.186	0.142	0.111	0.160	0.132
Anthracene	0.123	0.129	0.135	0.127	0.147	0.160	0.147	0.153	0.173	0.134	0.141	0.153
Fluoranthene	0.147	0.110	0.128	0.135	0.115	0.148	0.198	0.035	0.259	0.167	0.220	0.237
Pyrene	0.131	0.194	0.056	0.117	0.201	0.088	0.172	0.210	0.092	0.158	0.191	0.071
Benzo(a) anthracene	0.032	0.122	0.112	0.110	0.021	0.120	0.032	0.011	0.113	0.026	0.015	0.106
Chrysene	0.125	0.127	0.024	0.126	0.031	0.046	0.660	0.014	0.031	0.431	0.012	0.033
Benzo(b) fluoranthene	0.114	0.132	0.119	0.095	0.158	0.137	0.100	0.171	0.146	0.089	0.153	0.129
Benzo(k) fluoranthene	0.031	0.125	0.253	0.094	0.143	0.311	0.025	0.216	0.177	0.017	0.194	0.157
Benzo(a) pyrene	0.186	0.100	0.141	0.117	0.108	0.186	0.220	0.117	0.198	0.213	0.114	0.175
Indo(1,2,3-cd) pyrene	0.135	0.194	0.196	0.125	0.227	0.219	0.028	0.217	0.226	0.016	0.101	0.195
Dibenzo anthracene	0.195	0.189	0.104	0.104	0.310	0.113	0.032	0.320	0.116	0.021	0.302	0.103
Benzo(g,h,i) perylene	0.124	0.119	0.114	0.124	0.135	0.133	0.256	0.152	0.137	0.217	0.136	0.122
Total	1.946	2.033	1.945	1.840	2.290	2.275	2.500	2.279	2.334	2.052	2.174	2.101

C. lancifolius:

The highest mean concentration of total PAHs in this plant was recorded at DS8 (2.530 ng/g dry weight) while the lowest mean concentration (2.106 ng/g dry weight) was recorded at DS6 (Table 4). Signification differences ($p=0.041$) were found among locations.

The highest seasonal mean concentrations (2.490 ng/g dry weight) were detected during summer season while the lowest seasonal mean concentration (2.041 ng/g dry weight) was during winter season (Table 4). The differences among seasons were not significant ($p=0.267$).

E. camaldulensis:

The highest mean concentration of total PAHs in this plant was recorded at DS6 (2.813 ng/g dry weight) while the lowest mean concentration (2.119 ng/g dry weight) was recorded at DS8 (Table 4). Significant differences ($p=0.007$) were found among locations.

The total PAHs seasonal variations were observed in the present study. The highest seasonal mean concentration (2.634 ng/g dry weight) was detected during spring season while the lowest seasonal mean concentration (2.312 ng/g dry weight) was during winter (Table 4). The differences among seasons were not significant ($p=0.161$).

S. vermiculata:

The highest mean concentration of total PAHs in this plant was recorded at DS7 (2.194 ng/g dry weight) while the lowest mean concentration (2.128 ng/g dry weight) was recorded at DS6 (Table 4). The differences among locations were not significant ($p=0.403$).

The seasonal variations of total PAHs were observed in this study. The highest seasonal mean concentration (2.371 ng/g dry weight) was detected during summer season while lowest seasonal mean concentration (1.975 ng/g dry weight) was during winter (Table 4). Significant differences ($p=0.008$) were found among seasons.

Table 4. Spatial and Temporal variations of Polycyclic Aromatic Hydrocarbons concentrations (ng/g dry weight) in plants species.

locations	Winter	Spring	Summer	Autumn	Sp. Mean	± SD
DS6**	2.319	2.962	3.152	2.820	2.813	0.333
DS7**	2.370	2.639	2.770	2.506	2.571	0.223
DS8**	2.247	2.302	1.978	1.952	2.119	0.162
S. Mean**	2.312	2.634	2.633	2.426	-	-

Locations	Winter	Spring	Summer	Autumn	Sp. Mean	±SD
DS6*	1.876	1.944	2.478	2.126	2.106	0.269
DS7 *	1.929	2.283	2.330	2.107	2.162	0.182
DS8*	2.319	2.680	2.664	2.457	2.530	0.173
S. Mean *	2.041	2.302	2.490	2.230	-	-

Locations	Winter	Spring	Summer	Autumn	Sp. Mean	±SD
DS6***	1.946	2.014	2.500	2.052	2.128	0.251
DS7***	2.033	2.290	2.279	2.174	2.194	0.119
DS8***	1.945	2.275	2.334	2.101	2.163	0.176
S.Mean***	1.975	2.193	2.371	2.109	-	-

* *Conocarpus lancifolius* ** *Eucalyptus camaldulensis* *** *Suaeda vermiculata*

Polycyclic Aromatic Hydrocarbons (PAH) Indices in plants:

Fluoranthene/Pyrene Ratio:

The Fluoranthene/Pyrene Ratio ranged from 0.166 at DS7 in *S. vermiculata* in summer to 2.227 in *C. lancifolius* at DS7 in summer (Table 5).

Phenanthrene/Anthracene Ratio:

Phenanthrene/Anthracene ratio ranged from 0.561 at DS6 in *C. lancifolius* in summer to 1.215 at DS7 in *S. vermiculata* in summer (Table 5).

LMW/HMW Ratio:

LMW/HMW ratio ranged from 0.300 at DS7 in *E. camaldulensis* in autumn to 0.760 at DS7 in *C. lancifolius* in winter (Table 5).

Ant/(Ant+Phen) Ratio:

Ant/(Ant+Phen) ratio ranged from 0.441 at DS7 in *E. camaldulensis* during spring to 0.673 at DS7 in *C. lancifolius* during Summer (Table 6).

Benzo (A) Anthracene/Benzo (A) Anthracene+Chrysene Ratio

BaA/(BaA+Chry) ratio ranged from 0.056 at DS6 in *S. vermiculata* in autumn to 0.931 at DS8 in *Eucalyptus camaldulensis* in summer (Table 6).

InP/(InP+BghiP) Ratio:

InP/(InP+BghiP) ratio ranged from 0.068 at DS6 in *S. vermiculata* in autumn to 0.926 at DS7 in *E. camaldulensis* in winter (Table 6).

Table 5. Pollution indices values of PAHs and their origin source descriptions in the plant samples of the present study.

Locations	Seasons	Fl/Py	Description	Phen/Ant	Description	LMW /HMW	Description
DS 6 *	Winter	0.868	Petrogenic	0.730	Pyrogenic	0.615	Pyrogenic
	Spring	0.886	Petrogenic	0.700	Pyrogenic	0.615	Pyrogenic
	Summer	1.047	Pyrogenic	0.561	Pyrogenic	0.430	Pyrogenic
	Autumn	1.047	Pyrogenic	0.589	Pyrogenic	0.475	Pyrogenic
DS7*	Winter	1.347	Pyrogenic	1.073	Pyrogenic	0.760	Pyrogenic
	Spring	2.062	Pyrogenic	1.000	Pyrogenic	0.730	Pyrogenic
	Summer	2.227	Pyrogenic	0.562	Pyrogenic	0.589	Pyrogenic
	Autumn	1.940	Pyrogenic	0.619	Pyrogenic	0.612	Pyrogenic
DS 8 *	Winter	0.767	Petrogenic	0.751	Pyrogenic	0.528	Pyrogenic
	Spring	0.834	Petrogenic	0.651	Pyrogenic	0.498	Pyrogenic
	Summer	0.703	Petrogenic	0.610	Pyrogenic	0.534	Pyrogenic
	Autumn	0.702	Petrogenic	0.610	Pyrogenic	0.483	Pyrogenic
DS 6**	Winter	1.286	Pyrogenic	0.790	Pyrogenic	0.518	Pyrogenic
	Spring	1.241	Pyrogenic	0.797	Pyrogenic	0.454	Pyrogenic
	Summer	1.800	Pyrogenic	0.630	Pyrogenic	0.409	Pyrogenic
	Autumn	1.183	Pyrogenic	0.660	Pyrogenic	0.425	Pyrogenic
DS 7**	Winter	1.010	Pyrogenic	1.084	Pyrogenic	0.480	Pyrogenic
	Spring	0.952	Petrogenic	1.035	Pyrogenic	0.383	Pyrogenic
	Summer	0.936	Petrogenic	1.121	Pyrogenic	0.537	Pyrogenic
	Autumn	0.882	Petrogenic	1.096	Pyrogenic	0.300	Pyrogenic
DS 8**	Winter	1.480	Pyrogenic	0.914	Pyrogenic	0.416	Pyrogenic
	Spring	1.507	Pyrogenic	0.814	Pyrogenic	0.663	Pyrogenic
	Summer	1.531	Pyrogenic	0.847	Pyrogenic	0.514	Pyrogenic
	Autumn	1.608	Pyrogenic	0.934	Pyrogenic	0.700	Pyrogenic
DS 6 ***	Winter	1.122	Pyrogenic	0.943	Pyrogenic	0.595	Pyrogenic
	Spring	1.085	Pyrogenic	0.887	Pyrogenic	0.544	Pyrogenic
	Summer	1.151	Pyrogenic	0.877	Pyrogenic	0.450	Pyrogenic
	Autumn	1.056	Pyrogenic	0.828	Pyrogenic	0.514	Pyrogenic
DS 7***	Winter	0.567	Petrogenic	1.038	Pyrogenic	0.496	Pyrogenic
	Spring	0.572	Petrogenic	1.136	Pyrogenic	0.485	Pyrogenic
	Summer	0.166	Petrogenic	1.215	Pyrogenic	0.557	Pyrogenic
	Autumn	0.868	Petrogenic	1.134	Pyrogenic	0.516	Pyrogenic
DS 8***	Winter	0.437	Petrogenic	0.888	Pyrogenic	0.559	Pyrogenic
	Spring	1.681	Pyrogenic	0.881	Pyrogenic	0.618	Pyrogenic
	Summer	0.355	Petrogenic	0.820	Pyrogenic	0.585	Pyrogenic
	Autumn	0.299	Petrogenic	0.862	Pyrogenic	0.581	Pyrogenic

* Conocarpus lancifolius ** Eucalyptus camaldulensis *** Suaeda vermiculata

Table 6. Another PAHs pollution indices values and their origin source descriptions in the plant samples of the present study.

Locations	Season	Ant/(Ant+ Phen)	Description	BaA/(BaA+ Chry	Description	InP/(InP+ BghiP)	Description
DS 6*	Winter	0.577	Pyrolytic	0.495	Pyrogenic	0.240	Petrogenic or Pyrogenic
	Spring	0.588	Pyrolytic	0.575	Pyrogenic	0.250	Petrogenic or Pyrogenic
	Summer	0.642	Pyrolytic	0.508	Pyrogenic	0.407	Petrogenic or Pyrogenic
	Autumn	0.629	Pyrolytic	0.529	Pyrogenic	0.395	Petrogenic or Pyrogenic
DS 7*	Winter	0.482	Pyrolytic	0.474	Pyrogenic	0.786	Petrogenic
	Spring	0.632	Pyrolytic	0.085	Pyrogenic	0.731	Petrogenic
	Summer	0.673	Pyrolytic	0.070	Petrogenic	0.467	Petrogenic or Pyrogenic
	Autumn	0.617	Pyrolytic	0.237	Petrogenic or Pyrogenic	0.482	Petrogenic or Pyrogenic
DS 8*	Winter	0.570	Pyrolytic	0.341	Petrogenic or Pyrogenic	0.583	Pyrogenic
	Spring	0.605	Pyrolytic	0.334	Petrogenic or Pyrogenic	0.466	Petrogenic or Pyrogenic
	Summer	0.620	Pyrolytic	0.140	Petrogenic	0.472	
	Autumn	0.620	Pyrolytic	0.158	Petrogenic	0.507	Pyrogenic
DS 6**	Winter	0.558	Pyrolytic	0.919	Pyrogenic	0.510	Pyrogenic
	Spring	0.556	Pyrolytic	0.915	Pyrogenic	0.603	Pyrogenic
	Summer	0.613	Pyrolytic	0.779	Pyrogenic	0.612	Pyrogenic
	Autumn	0.622	Pyrolytic	0.747	Pyrogenic	0.592	Pyrogenic
DS 7**	Winter	0.479	Pyrolytic	0.495	Pyrogenic	0.926	Pyrogenic
	Spring	0.441	Pyrolytic	0.476	Pyrogenic	0.921	Pyrogenic
	Summer	0.471	Pyrolytic	0.324	Petrogenic or Pyrogenic	0.895	Pyrogenic
	Autumn	0.477	Pyrolytic	0.248	Petrogenic or Pyrogenic	0.560	Pyrogenic
DS 8**	Winter	0.501	Pyrolytic	0.580	Pyrogenic	0.569	Pyrogenic
	Spring	0.551	Pyrolytic	0.573	Pyrogenic	0.523	Pyrogenic
	Summer	0.541	Pyrolytic	0.931	Pyrogenic	0.540	Pyrogenic
	Autumn	0.517	Pyrolytic	0.464	Pyrogenic	0.509	Pyrogenic
DS 6***	Winter	0.514	Pyrolytic	0.203	Petrogenic or Pyrogenic	0.521	Pyrogenic
	Spring	0.529	Pyrolytic	0.190	Petrogenic	0.626	Pyrogenic
	Summer	0.532	Pyrolytic	0.460	Pyrogenic	0.098	Petrogenic
	Autumn	0.546	Pyrolytic	0.056	Petrogenic	0.068	Petrogenic
DS 7***	Winter	0.490	Pyrolytic	0.489	Pyrogenic	0.619	Pyrogenic
	Spring	0.468	Pyrolytic	0.403	Pyrogenic	0.627	Pyrogenic
	Summer	0.458	Pyrolytic	0.440	Pyrogenic	0.588	Pyrogenic
	Autumn	0.468	Pyrolytic	0.555	Pyrogenic	0.426	
DS 8***	Winter	0.529	Pyrolytic	0.823	Pyrogenic	0.632	Pyrogenic
	Spring	0.531	Pyrolytic	0.722	Pyrogenic	0.622	Pyrogenic
	Summer	0.549	Pyrolytic	0.784	Pyrogenic	0.622	Pyrogenic
	Autumn	0.536	Pyrolytic	0.762	Pyrogenic	0.615	Pyrogenic

* *Conocarpus lancifolius* ** *Eucalyptus camaldulensis* *** *Suaeda vermiculata*

5. Discussion

Plants are the most important components of the ecosystem because they are the main source of energy on land, in marine or in fresh water. Plants accumulate chemical compounds such as hydrocarbons; hence, they are used as bio-indicators to identify environmental changes in the region (USEPA, 2011).

The predominant light PAHs compounds are Acenaphthylene, Acenaphthene, Fluorene, Phenanthrene, and Anthracene while the dominant heavy PAHs

compounds are Floranthene, Pyrene, Benzo(a)Pyrene, Benzo(a)anthracene, Benzo(k) flouranthene (Patel *et al.*, 2015).

The highest levels of PAHs compounds in plants were recorded during summer whereas the lowest levels were found during spring or winter. The seasonal variations may be due to the high temperature during the summer season which is considered as a growth period for these plants due to the long period of solar radiation and the abundance of

nutrients as compared with other seasons. This will lead to an increase in the photosynthesis processes and absorption of the PAHs compounds (Jazza, 2015).

There are differences in the concentration of PAHs compounds among the studied plants. These variations may be attributed to the lipid compounds of each plant species, the nature of growth substrate for each plant, the tolerance of each species to the environmental conditions, and the surface area that affects the rate of accumulation of plants (Hassan *et al.*, 2016). To determine the origin of PAHs according to ratios, the results revealed that LMW-PAHs/HMW-PAHs ratio was less than one during all seasons, indicating that the sources of PAHs in these species were pyrogenic. This finding was in agreement with other studies (Vrana *et al.*, 2001; Al-Hejuje, 2014; Sander *et al.*, 2002).

From the presented results, we can conclude that the source of PAHs compounds in the studied plants is a mix of petrogenic and pyrogenic.

References

- Al-Hejuje MM. 2014. Application of water quality and pollution Indices to evaluate the water and sediments status in the middle part of Shatt Al-Arab river. Ph.D. Thesis. University of Basrah, Iraq.
- Al- Hejuje MM, Al-Saad HT and Hussain NA. 2015. Total Petroleum Hydrocarbons (TPHs), n-alkanes and Polynuclear Aromatic Hydrocarbons (PAHs) in sediments of Shatt Al-Arab river – part 2. *Glob J Agric Health Sci*, **4(1)**: 95-100
- Bakhtiari AR, Zakaria MP, Yaziz MI, Lajis MNH and Bi X. 2009. Polycyclic aromatic hydrocarbons and n-alkanes in suspended particulate matter and sediments from the Langat river, Peninsular Malaysia. *Environm Asia*, **2**: 1-10.
- Goutex MA and Saliot A.1980. Relationship between dissolved and particulate fatty acids, hydrocarbons, chlorophyll a and zooplankton biomass in Ville franche bay, Mediterranean Sea. *Mar. Chem.*, **8**:299-318.
- Hassan FM, Salman JM, Douabul AA and Naji AS. 2016. Polycyclic aromatic hydrocarbon (PAHs) concentrations in some aquatic macrophytes in Hilla river, Iraq. *Eart and Environ Sci.*, **7(2)**: 198-211.
- Jazza SH .2015. The state of hydrocarbon compounds pollution of water, sediments and some aquatic biota in Al-Kahlaa river-Missan Province/Iraq. Ph.D. Thesis, University of Basrah, Iraq.
- Karem DSA. 2016.Environmental Impact Assessment of air, noise and petroleum hydrocarbons pollution in soil of west qurna-2 oil field at Basrah city ,southern Iraq. MSc dissertation University of Basrah,Iraq.
- Patel KS, Ramteke S, NaikY, Sahu BL, Sharma S, Lintelmann J and Georg M.2015. Contamination of environment with polycyclic aromatic hydrocarbons in India. *J Environ Protect*, **6**: 1268-1278.
- Sander M, Sivertsen S and Scott G.2002.Origin and distribution of polycyclic aromatic hydrocarbon in surficial sediment from the Savanah river. *Arch. Environ. Contam. Toxicol.*, **43**: 438-448.
- United States Environmental Protection Agency (UNEP, 2011) .National ambient air quality standards (NAAQS),Available on :<http://www.epa.gov/ttn/naaqs/>.
- Vrana B, Pasch A and Popp P.2001. Polycyclic aromatic hydrocarbon concentration and patterns in sediments and surface water of Mansfed region, Saxony. Anhalt, Germany.*J Environ Monit.*,**3(6)**:602-609
- Wang Z, Liu M and Yang Y.2015. Characterization and sources analysis of polycyclic aromatic hydrocarbons in surface sediments in the Yangtze river Estuary. *Environ Earth Sci.*,**73**: 2453-2462.
- Zakaria MP, Takada H, Tsutsumi S, Ohno K, Yamada J, Kouno E and Kumata H.2002. Distribution of polycyclic aromatic hydrocarbons (PAHs) in rivers and estuaries in Malaysia: A widespread input of petrogenic PAHs. *Environ Sci Technol*, **36**: 1907-1918.

Effects of Biotic and Abiotic Factors on the Yield and Chemical Composition of Essential Oils from Four *Thymus* Species Wild-Growing in Northeastern Algeria

Nesrine Gherairia^{1,*}, Soumia Boukerche¹, Mohamed Abou Mustapha², Azzedine Chefrou^{3,4}.

¹Laboratory of Science and Techniques for Living, Institute of Agronomic and Veterinary, Institute of Agronomic and Veterinary Sciences, Taoura, Souk Ahras University, Souk Ahras, 41000, Algeria; ²Centre of Scientific Research and technology in Physico-chemical Analysis (CRAPC), Tipaza, 42000, Algeria; ³Departement of biology, Faculty of Natural and Life Sciences, Souk Ahras University, Souk Ahras, 41000, Algeria; ⁴Laboratory Development and Control of Hospital Pharmaceutical Preparations, Annaba University, Annaba, 23000, Algeria.

Received: December 6, 2020; Revised: March 25, 2020; Accepted: May 18, 2021

Abstract

In order to evaluate the appropriate factors for producing better quality and quantity essential oils (EOs), we performed a comparative study between the yields and the chemical compositions of the EOs of four *Thymus* species, spontaneously growing in six different locations in northeastern Algeria. EOs hydrodistillation gave yields that ranged from 0.9% to 2.35%. The highest yield (2.35%) was obtained from Dekma's *Thymus algeriensis* oils. GC/MS analyses revealed the presence of 61 compounds, representing 93.6 to 98.23% of the total EOs composition. The hierarchical cluster analysis allowed the six EOs populations to be grouped into two chemotypes: one with thymol and the other with α -pinene. The ANOVA test showed significant differences between the yields and chemical compositions of essential oils; the plant species factor had no significant effect on the variability of these two parameters. Therefore, the variability highlighted was related to the significant impact of abiotic factors. Altitude and soil type were the most influential factors in the secretion of EOs and the emergence of various chemical profiles.

Keywords: *Thymus*, essential oils, yields, chemical compositions, abiotic factors

1. Introduction

As the entire Algerian national territory, the flora of the Souk Ahras region enjoys tremendous biodiversity; it includes several aromatic and medicinal plants rich in secondary metabolites endowed with many therapeutic and pharmacological activities, including plants of the genus *Thymus*.

Such plants are commonly referred to as "*Zaitra*" and include twelve national species, nine of which are endemic (Quezel and Santa, 1963). They are spread throughout most coastal and inland regions, and also in arid areas (Saidj, 2006).

Some plants' essential oils (EOs) are ranked among the most bioactive and common oils in the world. This bioactivity is demonstrated by the unique excess of certain essences in phenolic compounds such as thymol and carvacrol (Cosentino *et al.*, 1999; Trombetta *et al.*, 2002; Amarti *et al.*, 2011). *Thymus* EOs are characterized by a high degree of polymorphism and exceptional chemical heterogeneity which leads to several chemotypes being identified. This variability depends on several factors which are typically ecological, i.e. soil type, altitude,

climatic conditions, adjacent plants populations (Baydar *et al.*, 2004; Colombo *et al.*, 2013), but can also be genetic and seasonal (Ložienė *et al.*, 2007).

In this context, we carried out a comparative study in this research between the EOs of four species of the genus *Thymus* (*Thymus hirtus*, *Thymus capitatus*, *Thymus ciliatus* and *Thymus algeriensis*), growing spontaneously in different areas for northeastern Algeria in order to check the possible impact of biotic (plant species) and abiotic (climate, soil, altitude) factors on the quantity and quality of these essential oils.

2. Materials and Methods

2.1. Plant collection and identification

Aerial parts of spontaneous *Thymus* spp plants were collected from six different locations for Souk Ahras region (northeastern Algeria) during full flowering in June and July 2016. Clumps of adjacent young plants were chosen at each collection site to achieve a homogeneous sample of plants with the same morphology and development stage. The geographical coordinates of the sampling areas are available as supplemental material (Table S).

* Corresponding author e-mail: nesrine.gherairia@univ-soukahras.dz.

Table S. Geographical coordinates of study stations

Collection sites	Geographical coordinates		
	Latitude (N)	Longitude (E)	Altitude (m)
Dekma	36° 14' 43,8''	007° 54' 26,5''	695
Sedrata	36° 10' 33,7''	007° 30' 11,9''	1277
Zouabi	36° 05' 32,8''	007° 26' 31,3''	882
Ain Scynour	36° 18' 24,0''	007° 50' 43,0''	1151
Boukabech	36° 17' 08,3''	008° 02' 36,5''	772
Ouled Driss	36° 23' 24,3''	008° 01' 52,6''	1228

The harvested plants were identified by Professor Azzedine Chefrour, Faculty of Natural and Life Sciences, Department of Biology, Souk Ahras university, Souk Ahras, Algeria.

2.2. Climatic and edaphic characterization of collection sites

Climate data (average annual temperatures and rainfall) were taken from the website (Climate-data.org, (2019).

The edaphic analyses were carried out at the level of the National Institute of Irrigation and Drainage Soils (INSID) of Oum El Bouaghi (Algeria). Soil samples were collected at the rhizosphere level (30 cm) of the thyme tussocks, which presents an essential interface between the plant and the soil. They are air-dried and then passed through a 2 mm mesh sieve (AFNOR, 1987). Soil texture was determined using the Robinson's pipette method. pH meter and conductivity meter were used to measure the pH and electrical conductivity of the soil, respectively. Organic matter was determined using the Walkley and Black method. Limestone was determined by a volumetric method using Bernard's Calcimeter.

2.3. Essential oil isolation

Clevenger-type apparatus was used to separate the EOs from 50 g of dry plant matter (leaves and flowers). The samples obtained were stored at 4°C in hermetically sealed brown glass vials until analysis. The yield obtained for the essential oil was expressed as a percentage (w/w).

2.4. GC-MS characterization of EOs

The GC-MS analyses were performed via a Hewlett-Packard Agilent 6890 plus series GC system (Agilent Technologies) coupled with a quadrupole mass spectrometer (HP Agilent 5973), using an HP-5MS non-polar fused-silica capillary column (30 m × 0.32 mm, 0.25

µm film thicknesses). The oven temperature programme was initially held for 8 min at 60°C then increased by 2°C/min until 250°C and held at 250°C for 10 min. Helium was used as the carrier gas with a flow rate of 0.5 ml/min. EO was injected with a volume of 0.2 µl in split mode 1:80. Injector and detector transfer line temperatures were set at 250°C and 270 °C, respectively. The ion source temperature was set at 230°C. Ionization of the sample components was performed in the electron impact mode (70 eV) over a scan range of 30–550 m/z. The ion source temperature was set at 230°C.

Essential oils compounds were identified by comparing of their mass spectra data with those stored from MS databank (NIST02.L and WILEY7n.L), and confirmed by comparing of their Kovat retention index (KI), determined referring to a standards series of n-alkanes (C5–C29) injected under the same conditions with those previously reported in the literature (Hazzit *et al.*, 2009; Zouari *et al.*, 2012; Amiri *et al.*, 2011; Benchabane, 2014; Helmi *et al.*, 2014; Bendif *et al.*, 2016; Mahboubi *et al.*, 2017 and Guesmi *et al.*, 2019)

2.5. Statistical study

The data processing has been performed using the XLSTAT statistical software (Version: 2019.1.3, Addinsoft). One-way statistical analysis (ANOVA) was used to compare the averages obtained at the 5% significance level. Correlations between variations in yields and chemical compositions with exogenous factors were calculated using the Spearman coefficient. A hierarchical ascending classification (HAC) was performed to determine the level of similarity between *Thymus* spp populations based on the percentages of seven major components. Principal Component Analysis (PCA) was conducted to study the variability in the chemical composition of EOs as a function of environmental factors.

3. Results

3.1. Yields of essential oils

The yields of essential oils obtained by hydrodistillation of the aerial parts of six populations of *Thymus* spp collected from six different localities of Souk Ahras, as well as the environmental characteristics and the physico-chemical properties of the soils of the collection sites have been established in Table (1).

Variance analysis (ANOVA) at the 5 % level of significance revealed the existence of a significant difference between the EO yields of six *Thymus* spp populations. EO yields varied between 0.9% and 2.35%. The highest yield was obtained from Dekma's *Thymus algeriensis* EO (TR₁) and the lowest (0.9%) from Oued Driss's *Thymus ciliatus* EO (TR₆).

Table 1. Essential oils yields, environmental characteristics and soils physico-chemical properties of *Thymus* spp. collection sites.

Codes	Collection sites	Texture and soil characteristics						Climate			Yield (%)*
		Altitude (m)	Clay (%)	Silt (%)	CaCO ₃ (%)	pH	EC (dS/m)	OM (%)	P (mm)	T (C°)	
TR ₁	Dekma	695	33.3	22.2	30.8	7.4	0.4	2.1	661	14.4	2.3 ± 0.8
TR ₂	Sedrata	1277	34.3	0.6	nd	6.8	0.3	5.5	523	14.2	1.3 ± 0.2
TR ₃	Zouabi	882	24	20	35.6	7.5	0.2	2.1	478	14.1	1.7 ± 0.2
TR ₄	Ain Seynour	1151	7.4	2.1	nd	6.3	0.2	7.6	763	13.7	1.0 ± 0.2
TR ₅	Boukabech	772	31.9	26.5	41.7	7.3	0.3	8.5	726	13.4	1.2 ± 0.6
TR ₆	Ouled Driss	1228	20	4.0	nd	6.6	0.2	3.8	868	13.5	0.9 ± 0.2

EC: Electrical conductivity (dS/m); OM: Organic matter (%); P: Mean annual precipitation (mm); T: Mean annual temperature (°C); *p-value = 0.04 at a significance level of 0.05; nd: not detected; TR₁: *Thymus algeriensis* Boiss. & Reut. of Dekma; TR₂: *Thymus capitatus* (L.) Hoffmanns & Link of Sedrata; TR₃: *Thymus capitatus* (L.) Hoffmanns & Link of Zouabi; TR₄: *Thymus hirtus* willd subsp. *algeriensis* (Boiss. & Reut.) Of Ain Seynour; TR₅: *Thymus hirtus* willd of Boukabech; TR₆: *Thymus ciliatus* subsp. *mumbyanus* (Boiss. & Reut.) Batt. of Ouled Driss.

3.1.1. Variability of extraction yields between species

Using multivariate analysis of variance (MANOVA), the effect of the species on the essential oil extraction yields of six *Thymus* spp populations was calculated by Wilks' test at a significance level of 5%. The plant species was chosen as an explanatory qualitative variable (Table 2).

Based on the Wilks test table, we note that Lambda value is associated with a p-value (0.095) higher than the risk-alpha threshold (0.05). Therefore, we cannot reject the null hypothesis (H0), and it is assumed that the qualitative variable (species) has no significant impact on the EO yield of the different species of the *Thymus* genus studied.

Table 2. p-value of Wilks test (Rao approximation)

Wilks test	species
Lambda	0.065
F (Observed values)	9.646
DDL1	3
DDL2	2
F (Critical value)	19.164
p-value	0.095

3.1.2. Variability of extraction yields as a function of environmental factors

The correlation between environmental factors and essential oil yield was calculated by the Spearman correlation coefficient (Fig. 1). A positive correlation was found between essential oil yield and pH (ρ=0.83), average annual temperatures and electrical conductivity of the soil (ρ=0.77) and with clay content (ρ= 0.66). A negative relationship was found with average annual rainfall (ρ= - 0.83), organic matter and sand content (ρ= - 0.60) and with altitude (ρ= - 0.54). Therefore, it can be deduced that environmental factors could significantly affect the essential oil yields of *Thymus* spp. populations.

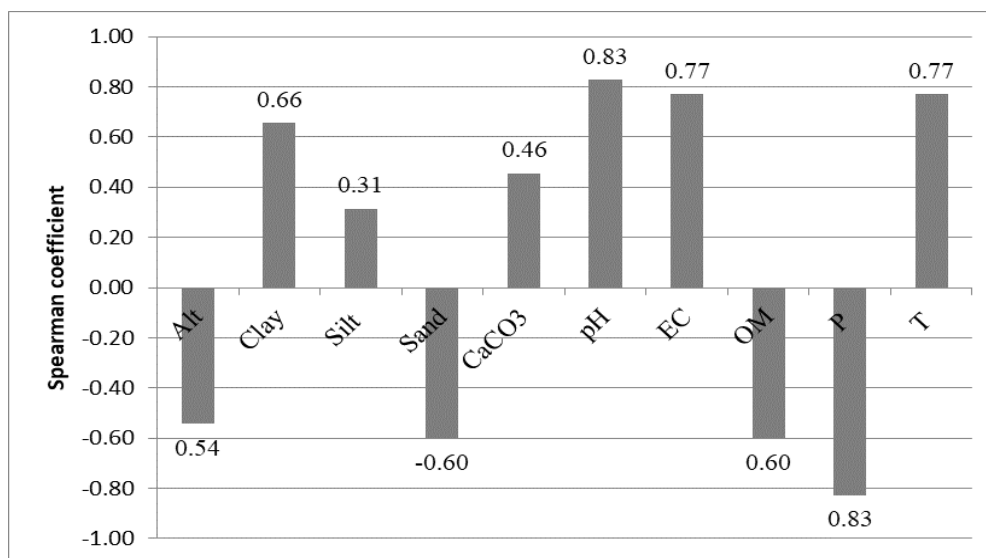


Figure 1. Correlation between the essential oil yield of *Thymus* spp populations and environmental factors.

3.2. Chemical composition of EOs

Chemical analyses of EOs were carried out by GC/MS. The percentages, times, and retention indices of the identified EO compounds were listed in Table (3) in the order of their elution on the HP-5MS column. Chromatographic profiles of volatile fractions are available as supplemental material (Figure S).

Chromatographic analyses of *Thymus* spp EOs have identified 61 compounds, representing 93.6 to 98.23% of the total EOs composition. These constituents were grouped into four chemical classes: hydrocarbon

monoterpenes (24.6-60.6%), oxygenated monoterpenes (8.0-68.1%), hydrocarbon sesquiterpenes (1-15%) and oxygenated sesquiterpenes (0.6-9.4%).

Analysis of variance showed that thirty-six out of sixty-one compounds differed significantly among the six EOs *Thymus* spp populations including: α -Pinene ($p < 0.05$), Camphene ($p < 0.001$), β -Pinene ($p < 0.001$), β -Myrcene ($p < 0.001$), Limonene ($p < 0.05$), Linalool ($p < 0.05$), Thymol ($p < 0.05$), (E)-Caryophyllene ($p < 0.05$), Borneol ($p < 0.001$), Caryophyllene oxide ($p < 0.05$).

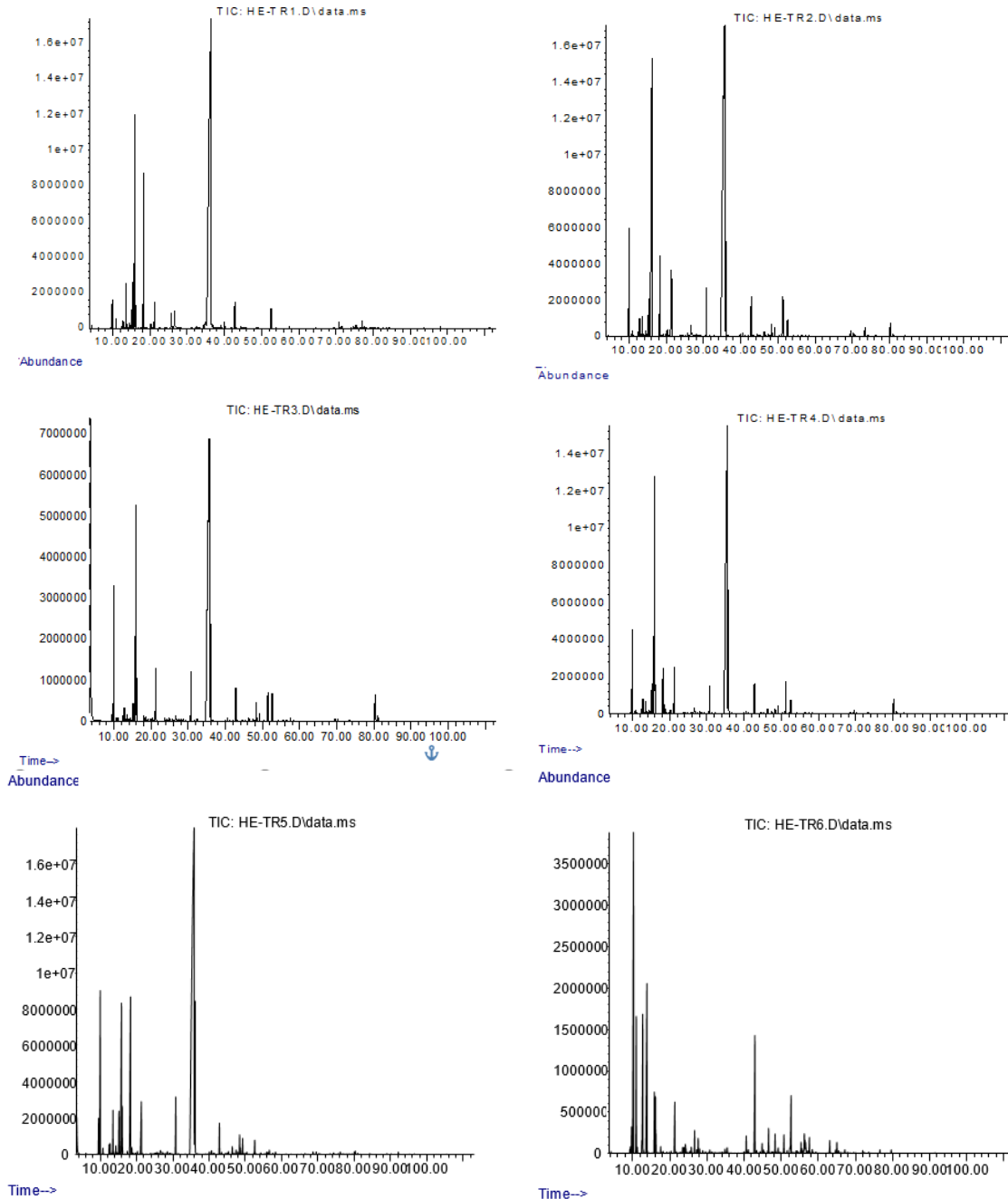


Figure S. Chromatographic profile of volatile fractions of six *Thymus* spp population

Table 3. Chemical composition of the volatile fractions of six samples of *Thymus* species

N°	Compound	KI	KIL	Relative peak areas (%)						Anova
				TR ₁	TR ₂	TR ₃	TR ₄	TR ₅	TR ₆	
1	Tricyclene	921	923 ^H	0.01	0.01	0.02	0.01	0.01	0.31	**
2	α -Thujene	925	925 ^H	0.6	0.65	0.55	0.71	0.87	1.45	*
3	α -Pinene	932	935 ^H	0.75	2.82	5.18	2.65	5.32	23.07	*
4	Camphene	945	948 ^H	0.27	0.13	0.12	0.11	0.14	6.45	**
5	Verbenene	951	953 ^H	-	0.03	0.08	0.03	0.01	0.25	*
6	β -Pinene	974	976 ^H	0.12	0.17	0.19	0.18	0.24	8.7	**
7	1-Octen-3-ol	978	982 ^H	0.24	0.54	0.51	0.56	0.29	0.13	<i>nls</i>
8	β -Myrcene	992	992 ^Z	1.41	0.51	0.21	0.37	1.14	13.12	*
9	n-Octan-3-ol	996	1001 ^H	0.12	0.07	0.09	0.06	0.05	0.08	<i>nls</i>
10	α -Phellandrene	1004	1005 ^H	0.18	0.16	0.12	0.12	0.23	-	<i>nls</i>
11	α -Terpinene	1016	1017 ^H	1.66	1.49	0.8	1.31	1.2	-	<i>nls</i>
12	p-Cymene	1027	1027 ^Z	13.48	23.14	17.37	19.8	6.25	3.19	<i>nls</i>
13	β -Phellandrene	1029	1030 ^H	0.55	-	-	-	-	-	**
14	Limonene	1030	1030 ^Z	-	0.85	1.09	0.72	1.24	3.56	*
15	1,8-Cineole	1031	1033 ^H	-	-	-	-	0.11	-	**
16	(E)- β -Ocimene	1048	1048 ^H	0.05	0	0.01	-	0.09	0.29	<i>nls</i>
17	γ -Terpinene	1061	1061 ^H	8.44	2.68	0.21	1.65	7.79	0.08	<i>nls</i>
18	<i>cis</i> -Sabinene hydrate	1066	1069 ^H	0.02	0.04	0.19	0.37	0.17	-	<i>nls</i>
19	<i>trans</i> -Linalool oxide	1071	1072 ^H	0.01	0.08	0.12	0.08	-	0.06	<i>nls</i>
20	α -terpinolene	1087	1089 ^Z	0.18	0.23	0.19	0.19	0.1	0.13	<i>nls</i>
21	Linalool	1101	1104 ^H	0.94	3.53	3.36	2.41	2.21	3.43	*
22	<i>trans</i> -Pinocarveol	1136	1036 ^Z	-	0.1	0.19	0.11	0.04	0.34	<i>nls</i>
23	Camphor	1148	1044 ^H	0.03	-	-	0.01	0.2	0.78	<i>nls</i>
24	Verbenol	1152	1146 ^H	-	-	0.27	0.13	-	-	<i>nls</i>
25	Borneol	1163	1164 ^Z	0.81	0.21	0.2	0.17	0.17	0.4	**
26	Terpinen-4-ol	1176	1177 ^Z	0.92	0.78	0.54	0.6	0.44	1.21	<i>nls</i>
27	p-Cymen-8-ol	1184	1184 ^Z	-	-	0.25	0.15	0.05	0.22	<i>nls</i>
28	α -Terpineol	1189	1189 ^Z	0.01	0.14	0.19	0.13	0.14	0.78	*
29	Myrtenol	1203	1198 ^H	-	0.04	0.09	-	-	0.37	*
30	Dihydrocarvone	1207	1203 ^H	-	0.13	0.11	0.06	0.06	0.16	*
31	Thymol methyl ether	1234	1235 ^H	0.01	1.45	1.99	0.98	1.7	0.25	<i>nls</i>
32	Thymoquinone	1258	1260 ^H	-	-	0.14	0.05	-	-	<i>nls</i>
33	Thymol	1306	1302 ^Z	59.79	48.85	49.69	52.96	59.25	0.27	*
34	Carvacrol	1311	1312 ^Z	5.3	3.85	4.28	6.51	5.31	0.34	<i>nls</i>
35	Carvacrol Acetate	1374	1372 ^Z	0.22	-	-	-	-	-	**
36	β -Bourbonene	1383	1380 ^H	-	0.1	0.13	0.08	0.11	0.98	*
37	β -Elemene	1391	1393 ^Z	-	-	-	-	-	0.2	**
38	(E)-Caryophyllene	1418	1409 ^B	0.92	1.28	1.33	1.15	0.91	8.42	*
39	β -Copaene	1427	1420 ^B	-	0.04	0.06	0.04	0.06	0.15	*

40	α -Humulene	1451	1450 ^Z	0.05	0.05	0.08	0.06	0.05	0.52	*
41	Allo-Aromadendrene	1458	1456 ^H	-	0.02	0.04	0.03	0.09	0.18	ns
42	α -Amorphene	1475	1475 ^C	-	0.16	0.18	0.19	0.21	0.12	*
43	Germacrene-D	1479	1477 ^H	-	-	-	-	-	1.33	**
44	Valencene	1493	1491 ^A	0.01	0.07	0.11	0.12	0.15	0.2	ns
45	β -Bisabolene	1508	1505 ^H	-	0.35	0.7	0.16	0.52	0.96	ns
46	γ -Cadinene	1512	1511 ^Z	-	0.11	0.16	0.16	0.21	0.1	ns
47	δ -Cadinene	1522	1518 ^Z	0.01	0.29	0.34	0.33	0.45	0.36	ns
48	Elemol	1555	1546 ^Z	-	-	-	-	-	1.06	**
49	Thymohydroquinone	1560	1567 ^M	-	1.86	1.73	1.76	-	-	ns
50	Nerolidol	1565	1563 ^{Bc}	-	-	-	-	-	0.14	**
51	Spathulenol	1575	1578 ^Z	0.02	-	-	0.04	0.02	0.35	*
52	Caryophyllene oxide	1581	1583^Z	0.72	0.57	1.24	0.56	0.43	3.8	*
53	p-1-Menthene	1607	/	-	-	-	-	-	0.19	**
54	δ -Selinene	1631	1590 ^G	-	-	0.03	-	-	0.75	*
55	α -Caryophylladienol	1635	1628 ^H	-	-	-	-	-	0.25	**
56	Calarene	1641	/	-	-	-	-	-	0.2	**
57	β -Caryophyllene epoxide	1643	/	-	-	-	-	-	1.21	**
58	β -Eudesmol	1646	1644 ^H	-	0.05	0.1	0.03	0.06	1.52	*
59	α -Cadinol	1650	1650 ^H	-	-	-	0.02	0.14	0.1	ns
60	Germacrene A	1661	/	-	-	-	-	-	0.17	**
61	(Z)- α -Bisabolene epoxide	1669	1680 ^H	-	-	0.16	-	-	0.98	*
Number of identified compounds				32	40	46	45	43	52	
Identification rate (%)				97.85	97.63	94.74	97.92	98.23	93.66	
Hydrocarbon monoterpenes				27.7	32.9	26.1	27.9	24.6	60.6	
Oxygenated monoterpenes				67.8	59.6	61.4	65.5	68.1	8.0	
Hydrocarbon sesquiterpenes				1.0	2.5	3.2	2.4	2.8	15.0	
Oxygenated sesquiterpenes				0.7	0.6	1.5	0.6	0.7	9.41	
Other Compounds				0.4	2.1	2.6	1.6	2.1	0.1	

RT: retention times; IK: kovat index calculated against C9-C29 n-alkanes on the apolar HP-5MS column; IKL: literature kovat index; TR₁: *Thymus algeriensis* Boiss. & Reut. of Dekma; TR₂: *Thymus capitatus* of Sedrata; TR₃: *Thymus capitatus* of Zouabi; TR₄: *Thymus hirtus* ssp. *algeriensis* Boiss. & Reut. Of Ain Seynour; TR₅: *Thymus hirtus* of Boukabech; TR₆: *Thymus ciliatus* ssp. *mumbyanus* of Ouled Driss, -: not detected; ^H: (Hazzit *et al.*, 2009); ^Z: (Zouari *et al.*, 2012); ^A: (Amiri *et al.*, 2011); ^{Bc}: (Benchabane, 2014); ^H: (Helmi *et al.*, 2014); ^B: (Bendif *et al.*, 2016); ^M: (Mahboubi *et al.*, 2017); ^G: (Guesmi *et al.*, 2019). The analysis of variance (ANOVA) is highly significant (**) at p < 0.001, significant (*) at p < 0.05 and non-significant (ns) at p > 0.05.

3.2.1. Variability of chemical composition as a function of species

To evaluate the effect of the species on the chemical composition of EOs of the *Thymus* spp populations studied, a hierarchical cluster analysis (HCA) was performed using Euclidean distances between major components of the *Thymus* EOs populations (Fig. 2).

The general structure of the dendrogram shows a Euclidean distance greater than thirty-six (36) units, which demonstrates explicitly the existence of two groups, one at thymol majority comprised five populations (TR₁, TR₅, TR₄, TR₂, TR₃), the other at α -pinene majority represented by the (TR₆) population. Further, the Thymol group is broken down into two subgroups (dissimilarity < 10), one

with Thymol/p-Cymene (TR₂, TR₃, TR₄) and the other with Thymol/ γ -Terpinene (TR₁, TR₅).

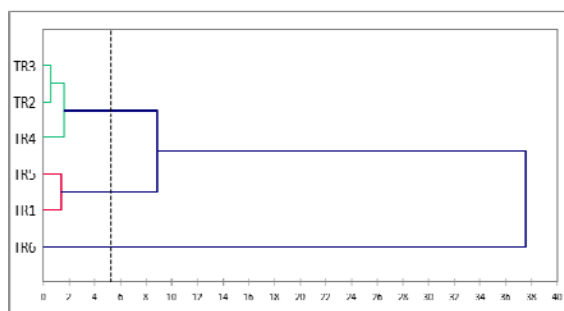


Figure 2. Dendrograms of the major constituents of six EO populations of *Thymus* spp.

3.2.2. Chemical variability of the composition of EOs as a function of environmental factors

The Spearman's test showed the presence of significant correlations between the chemical composition of the *Thymus* spp populations' EOs and environmental factors (altitude and soil physico-chemical parameters) at 5% significance level.

a. Impact of altitude

The PCA (Fig.3) carried out from the cumulative data of the four main classes of chemical components of EOs from six *Thymus* spp populations shows that hydrocarbon monoterpenes are positively correlated with altitude (0.771), while oxygenated monoterpenes are negatively correlated with this factor (-0.886). There was no correlation between altitude and the other two chemical classes sesquiterpenes (hydrocarbons and oxygenated sesquiterpenes).

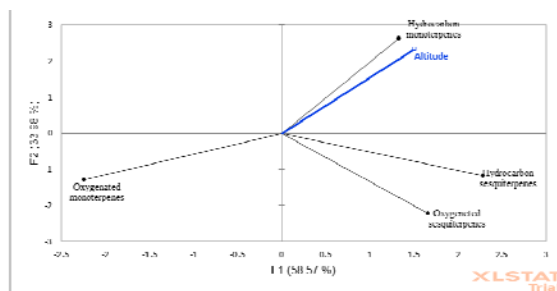


Figure 3. Arrangement of the EOs chemical families as a function of altitude

b. Impact of soil nature

Based on the PCA results (Fig. 4), we find that hydrocarbon monoterpenes versus oxygenated monoterpenes correlate positively with sand content and negatively with pH, electrical conductivity, and limestone and silt content. Hydrocarbon and oxygenated sesquiterpenes have no significant correlation with soil physico-chemical parameters.

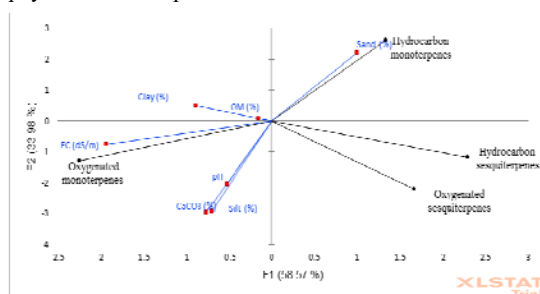


Figure 4. Arrangements of the EOs chemical families as a function of the soil samples' physico-chemical parameters.

4. Discussion

Based on the results of the statistical analyzes performed in this study, the species diversity factor had no significant impact on the variability of the yield and chemical composition between the EOs of six *Thymus* spp populations. Accordingly, the observed variations can be due to the influence of environmental factors.

TR1 population corresponding to Dekma's *Thymus algeriensis* recoded the highest EO yield. Its collection site was relatively characterized by low elevation, low mean annual precipitation and maximum annual temperatures. The soil of this site was classified as silty-clay, non-saline, calcareous, neutral with an alkaline tendency and not humus-bearing. Similar experiments on the impact of environmental factors on the rate of extraction of aromatic plant EOs affirm the negative relationship between altitude and extraction yield (Baydar *et al.*, 2004; Avci, 2010; El-Jalel *et al.*, 2018).

Hierarchical cluster analysis (Fig. 2) revealed that our EO samples are divided into two chemotypes: one at Thymol and the other at α -Pinene, and this distribution is independent of the plant species. The Thymol chemotype found in the five *Thymus* spp populations belonging to three different species (*Thymus algeriensis*, *Thymus capitatus* and *Thymus hirtus*) confirms the increase of this phenol in *Thymus* genus plants. Our findings are similar to those already reported by Giordani *et al.*, (2008) for the essences of *Thymus numidicus* from Khedara (Souk ahras) and Berrahal (Annaba) and *Thymus ciliatus* from Jebel Ansel (Guelma)-Algeria region which noted that thymol was the main component of these plants. Guedri Mkaddem and collaborators (2010) also confirmed that thymol was the key constituent of the Matamata region's *Thymus capitatus*, constituting 89.0% of the essential oil. Thymol with a 44.2% similarly characterized the EO of *Thymus ciliatus* from the Azrou-Maroc region (Amarti *et al.*, 2010). The α -Pinene chemotype found in the TR6 population would correspond to *Thymus ciliatus* subsp. *munbyanus* from the Ouled Driss region, is different from that found in most previous work on EOs of the same species. Carvacrol was the main constituent of *Thymus ciliatus* from eight localities in Tlemcen-Algeria (Bousmaha-Marroki *et al.*, 2007), *Thymus munbyanus* from Azzazga-Algeria (Benchabane *et al.*, 2012) and *Thymus munbyanus* from the Hennaia-Tlemcen-Algeria region (Tefiani *et al.*, 2015). The key constituent of *Thymus ciliatus* EOs from area of Jebel Ansel (Giordani *et al.*, 2008) and that Moroccan *Thymus ciliatus* (Amarti *et al.*, 2011) was Thymol, whereas chemotype α -Pinene characterized the EOs of *Thymus algeriensis* from the Khedara and Fatoum Souda regions of Algeria (Giordani *et al.*, 2008) and of *Thymus algeriensis* from different regions of Tunisia (Zouari *et al.*, 2012).

The high chemical diversity observed between various *Thymus* populations studied has been noted by several authors, including Ben El Hadj Ali *et al.*, (2012) and Zouari *et al.*, (2012), who attributed the high chemical polymorphism discovered in *Thymus algeriensis* Tunisian populations to the influence of geographical location.

The PCA results showed the presence of significant correlations between the chemical composition of the *Thymus* spp populations' EOs and abiotic factors (altitude and soil physico-chemical parameters). The altitude factor has an important impact on the biosynthesis of terpenoids, the anabolism of hydrocarbon monoterpenes is favoured at high altitude a, while that of oxygenated monoterpenes is favoured at low altitude. These findings are in line with those reported by Sanli and Karadogan (2017) who assert the impact of altitude on the terpenoid biosynthesis of EOs terpenoids from *Kundmannia anatolica* Hub. -Mor. fruits spontaneously growing at different altitudes in the lake

region (Turkey). El-Jalel *et al.*, (2018), showed that the altitudinal variance may clarify the heterogeneity in the composition of the *Thymus capitatus* EOs from Libya. The soil type seems to have a major effect on the chemical composition of *Thymus* EOs by promoting compound biosynthesis and inhibiting others. Ben El Hadj Ali *et al.*, (2012) suggested that local abiotic factors (humidity, temperature, topography and edaphic factors) and/or biotic selection factors (associated fauna and flora) acting on the biosynthesis pathways of terpene compounds and leading to the emergence of different chemical profiles may be explanatory factors.

5. Conclusion

As a result of this research, it was found that the species diversity factor had no significant effect on the extraction rate and chemical composition variability of *Thymus* spp Eos; therefore, the variability highlighted was due to the impact of abiotic factors. Altitude and soil physico-chemical characteristics were the most prominent factors affecting terpene compounds biosynthesis pathways and contributing to the emergence of various chemical profiles. Through this approach, we can carefully select thyme collection areas with the appropriate ecological conditions allowing these plants to produce EOs of better quality and quantity.

Acknowledgements

The authors gratefully thank Mr. Redouane Chebout, Chairman of the CRAPC Research Center's Board of Directors, for his assistance in performing EO's GC / MS studies.

References

- Amarti F, Satrani B, Ghanmi M and Aafi A. 2010. Composition chimique et activité antimicrobienne des huiles essentielles de *Thymus Algeriensis* Boiss. & Reut. et *Thymus ciliatus* (Desf.) Benth. du Maroc. *Biotechnol. agron. soc. Environ*, **14**(1): 141-148.
- Amarti F, Satrani B, Ghanmi M, Aafi A, Farah A, Aarab L, El Ajjouri M, Guedira A and Chaouch A. 2011. Activité antioxydante et composition chimique des huiles essentielles de quatre espèces de thym du Maroc. *Acta Bot. Gall*, **158**(4): 513-523.
- Amiri H, Yazdi H L, Dehshiri M, Eghbali D, Mohammadi A, & Zarei A. 2011. Essential oils composition and antioxidant properties of three *Thymus* species. *Planta Med*, **77**(12), PE3.
- Association française de normalisation (AFNOR).1987. **Qualité des sols. Méthodes d'analyses**. Recueil des normes françaises. AFNOR, Paris,135p.
- Avcı A B. 2010. Chemical Variation on the Essential Oil of *Thymus praecox* ssp. *scorpilii* var. *laniger*. *Int J Agric Biol*, **13**(4): 607-610.
- Baydar H, Sağdıç O, Özkan G and Karadoğan T. 2004. Antibacterial activity and composition of essential oils from *Origanum*, *Thymbra* and *Satureja* species with commercial importance in Turkey. *Food Control*, **15**(3): 169-172.
- Ben El Hadj Ali I, Guetat A and Boussaid M. 2012. Chemical and genetic variability of *Thymus algeriensis* Boiss. Et Reut. (Lamiaceae), a North African endemic species. *Ind. Crops. Prod.* **40**: 277-284.
- Benchabane O, Hazzit M, Baaliouamer A and Mouhouche F. 2012. Analysis and Antioxidant Activity of the Essential Oils of *Ferula vesceritensis* Coss. Et Dur. And *Thymus munbyanus* Desf. *J. Essent. Oil-Bear. Plants*, **15**(5): 774-781.
- Benchabane O. 2014. Chemical composition and insecticidal activities of essential oils of two Algerian endemic plants: *Ferula vesceritensis* Coss. et Dur. and *Thymus pallescens* de Noe. *Int J Agric Sci Res*, **4**(6): 185-191.
- Bendif H, Adouni K, Miara M D, Baranauskienė R, Kraujalis P, Venskutonis P R, Nabavi S M, & Maggi F. 2018. Essential oils (EOs), pressurized liquid extracts (PLE) and carbon dioxide supercritical fluid extracts (SFE-CO2) from Algerian *Thymus munbyanus* as valuable sources of antioxidants to be used on an industrial level. *Food Chem*, **260**: 289-298.
- Bousmaha-Marroki L, Atik-Bekkara F, Tomi F and Casanova J.2007. Chemical Composition and Antibacterial Activity of the Essential Oil of *Thymus ciliatus* (Desf.) Benth. ssp. *Eu-ciliatus* Maire from Algeria. *J. Essent. Oil Res*, **19**(5): 490-493.
- Chemat S, Cherfouh R, Meklati B Y & Belanteur K. 2012. Composition and microbial activity of thyme (*Thymus algeriensis genuinus*) essential oil. *J. Essent. Oil Res*, **24**(1): 5-11.
- Colombo R P, Martínez A F, di Pardo A F, Ridondo I F, Van Baren C, Lira P I and Godeas A M. 2013. **Differential effects of two strains of *Rhizoglyphus intraradices* on dry biomass and essential oil yield and composition in *Calamintha nepeta***. *Rev. Argent. Microbiol*, **45**(2):114-118.
- Cosentino S, Tuberoso C I, Pisano B, Satta M, Mascia V, Arzedi E and Palmas F. 1999. In-vitro antimicrobial activity and chemical composition of Sardinian *Thymus* essential oils. *Lett Appl Microbiol*, **29**(2): 130-135.
- El-Jalel L F A, Elkady W M, Gonaid M H and El-Gareeb K A. 2018. Difference in chemical composition and antimicrobial activity of *Thymus capitatus* L. essential oil at different altitudes. *Future J. Pharm. Sci*, **4**(2):156-160.
- Giordani, R., Hadeif, Y., Kaloustian, J., (2008). Compositions and antifungal activities of essential oils of some Algerian aromatic plants. *Fitoterapia*, **79**(3): 199-203.
- Guedri Mkaddem M, Romdhane M, Ibrahim H, Ennajar M, Lebrihi A, Mathieu F and Bouajila J. 2010. Essential Oil of *Thymus capitatus* Hoff. et Link. from Matmata, Tunisia: Gas Chromatography-Mass Spectrometry Analysis and Antimicrobial and Antioxidant Activities. *J. of Med. Food*, **13**(6): 1500-1504.
- Guesmi F, Saidi I, Bouzenna H, Hfaiedh N, & Landoulsi A. 2019. Phytochemical variability, antioxidant and antibacterial activities, anatomical features of glandular and aglandular hairs of *Thymus hirtus* Willd. Ssp. *algeriensis* Boiss. and Reut. over developmental stages. *South African Journal of Botany*, **127**: 234-243.
- Hazzit M, Baaliouamer A, Veríssimo A R, Faleiro M L, & Miguel M G. 2009. Chemical composition and biological activities of Algerian *Thymus* oils. *Food Chem*, **116**: 714-721.
- Helmi Z, Al Azzam K M, Tsymbalista Y, Ghazleh R A, Shaibah H, & Aboul-Enein H. 2014. Analysis of Essential Oil in Jerusalem Artichoke (*Helianthus tuberosus* L.) Leaves and Tubers by Gas Chromatography-Mass Spectrometry. *Adv Pharm Bull*, **4**(Suppl 2): 521-526.
- Ložienė K, Venskutonis P R, Šipailienė A, and Labokas J. 2007. Radical scavenging and antibacterial properties of the extracts from different *Thymus pulegioides* L. chemotypes. *Food Chem*, **103**(2): 546-559.
- Mahboubi M, Heidarytabar R, Mahdizadeh E, & Hosseini H. 2017. Antimicrobial activity and chemical composition of *Thymus* species and *Zataria multiflora* essential oils. *Agric. Nat. Resour*, **51**(5): 395-401.

- Quezel P and Santa S. 1963. **Nouvelle flore de l'Algérie et des régions désertiques méridionales**. Tome I, C.N.R.S, Paris, 558 p.
- Russo M, Suraci F, Postorino S, Serra D, Roccotelli A and Agosteo G E. 2013. Essential oil chemical composition and antifungal effects on *Sclerotium cepivorum* of *Thymus capitatus* wild populations from Calabria, southern Italy. *Rev. Bras. Farmacogn*, **23(2)**: 239-248.
- Saidj F.2006. Extraction de l'huile essentielle de thym : *Thymus numidicus* kabylica. Thèse de magistère en Technologie des hydrocarbures, Département génie des procédés chimiques et pharmaceutiques, Université M'Hamed Bougara-Boumerdes, Algérie.
- Sanli A and Karadoğan T. 2017. Geographical Impact On Essential Oil Composition Of Endemic *Kundmannia Anatolica* Hub.-Mor. (Apiaceae). *J. Tradit. Complement. Med*, **14(1)**: 131-137.
- Tefiani C, Riazi A, Youcefi F, Aazza S, Gago C, Faleiro M L, Pedro L G, Barroso J G, Figueiredo A C, Megias C, Cortés-Giraldo I, Vioque J and Miguel M G. 2015. *Ammoides pusilla* (Apiaceae) and *Thymus munbyanus* (Lamiaceae) from Algeria essential oils: Chemical composition, antimicrobial, antioxidant and antiproliferative activities. *J. Essent. Oil Res*, **27(2)**: 131-139.
- Trombetta D, Saija A, Bisignano G, Arena S, Caruso S, Mazzanti G, Uccella N and Castelli F. 2002. Study on the mechanisms of the antibacterial action of some plant α , β -unsaturated aldehydes. *Lett Appl Microbio*, **35(4)**: 285-290.
- Zouari N, Ayadi I, Fakhfakh N, Rebai A and Zouari S. 2012. Variation of chemical composition of essential oils in wild populations of *Thymus algeriensis* Boiss. et Reut., a North African endemic species. *Lipids in Health and Disease*, **11**:28.

Enhanced Production of Organosulfur Bioactive Compounds in Cell Suspension Culture of Single Garlic (*Allium sativum* L.) Using Precursor Feeding

Frida K Setiowati^{1,3,*}, Wahyu Widoretno¹, Sasangka Prasetyawan² and Betty Lukiati³

¹Department of Biology, Faculty of Mathematics and Natural Sciences, Universitas Brawijaya, Malang 65145, East Java, Indonesia,

²Department of Chemistry, Faculty of Mathematics and Natural Sciences, Universitas Brawijaya, Malang 65145, East Java, Indonesia,

³Department of Biology, Faculty of Mathematics and Natural Sciences, Universitas Negeri Malang, Malang 65145, East Java, Indonesia

Received: December 29, 2020; Revised: April 20, 2021; Accepted: June 5, 2021

Abstract

Precursor feeding in cell suspension culture is one of the effective strategies used to induce plant bioactive compounds. The effect of feeding different glutathione precursors on cell suspension growth and organosulfur production in cell suspension of single garlic (*Allium sativum* L.) was investigated. The establishment of suspension culture was carried out by transferring callus to liquid MS media supplemented with 0.3 mg/L 2,4-D and 0.5 mg/L kinetin. The addition of glutathione precursor up to 15 mM on the culture media increased the cell suspension biomass and the accumulation of organosulfur compounds. The highest fresh weight (2.691 ± 0.006 g), dry weight (1.738 ± 0.007 g), settled cell volume ($15\% \pm 0.0$), and growth index (1.69 ± 0.006) were obtained from a media with 10 mM glutathione addition. HPLC analysis revealed 30 types of organosulfur compounds in the cell suspension culture of single garlic. The highest 12 essential organosulfur bioactive compound was detected from the media augmented by 12.5 mM glutathione (3 to 4 fold than the control). The docking molecular visualization results toward the ligands acting as a substrate with the targeted protein in the alliin biosynthesis through glutathione pathway showed interactions in the ligand-protein complex. Feeding glutathione is an effective means to increase the production of organosulfur bioactive compounds in single garlic cell suspension.

Keywords: Cell suspension, Precursor feeding, Organosulfur compound, Single garlic

1. Introduction

Single garlic (*Allium sativum* L.) is garlic with only one clove in each bulb. Compared to the garlic with many cloves, single garlic is frequently used to solve different health issues due to its robust therapeutic properties (Bharat, 2014; Subramanian *et al.*, 2020). Its unique smell and organosulfur compound content have carried various biological functions of garlic, such as being antioxidant (Sankaran *et al.*, 2010; Rahman, 2012; Jang *et al.*, 2017), antimicrobial (Nakamoto *et al.*, 2020), anti-inflammatory (Tavakoli-Far *et al.*, 2021) and immunity within COVID-19 infection (Donma and Donma, 2020). Besides, it can also inhibit diabetes (Habtemariam, 2019), atherosclerosis (Lindstedt *et al.*, 2021), hypertension (Ugwu and Suru, 2016; Saljoughian *et al.*, 2017), and cancer (Pourzand *et al.*, 2016; Zhang *et al.*, 2020).

The essential organosulfur compounds within garlic include alliin, allicin, allyl sulfide group, sulfide, vinyl dithiin, ajoene (Ramirez, 2017). Alliin is the parent in the forming of other groups of organosulfur compounds. Alliin is produced through the reaction between glutathione and allyl sources. The biosynthesis of the organosulfur compounds begins with the conjugation among glutathione

and methacrylyl-CoA, resulting in S-(2-carboxypropyl) glutathione, an intermediate compound in the formation of alliin. After that, the glycyl group is eliminated from S-(2-carboxypropyl)glutathione, become S-(2-carboxypropyl) cysteine; meanwhile, the S-2-carboxypropyl group is transformed into S-2-propenyl group through an oxidative decarboxylation become γ -glutamyl-S-2-propenylcysteine (γ -glutamyl-S-allyl cysteine). The γ -glutamyl-S-allylcysteine experiences γ -glutamyl group omission, become S-allylcysteine. Oxygenation toward S-allylcysteine results in S-allyl cysteine sulfoxide or alliin (Yoshimoto *et al.*, 2019). Hydrolysis of alliin by the alliinase enzyme will produce an intermediate compound of allyl sulfenic acid which then undergoes condensation to produce allicin (Borlinghaus, 2014). Allicin is an unstable compound and can quickly be degraded into allyl disulfide, ajoene, dithiin, and other sulfur compounds (Gruhlke, 2010).

In the pharmaceutical field, the plant cell and tissue culture can be an alternative source to attain bioactive compounds (Murthy, 2014; Espinosa-Leal *et al.*, 2018). One of the effective means and strategies to increase bioactive compound production is through the plant tissue culture with the precursor feeding (Gaosheng and Jingming, 2012; Isah *et al.*, 2018; Guerriero *et al.*, 2018).

* Corresponding author e-mail: frida.fmipa@um.ac.id.

The precursor is an exogenous or endogenous compound converted by the plant cells into secondary metabolites through biosynthetic pathways. The addition of precursor can be carried out based on the inclusion of intermediate compounds in the biosynthesis pathway of the bioactive molecule during the culture period as an additional substrate to enhance the production of the bioactive compounds within the cell culture (Isah *et al.*, 2018; Singh and Sharma, 2020). Most of the intermediary substances can be selected as the precursor. The upstream precursor is transformed into a downstream compound using the specific enzyme catalysis. The precursor concentration determines the reaction speed; a high concentration frequently results in a more significant reaction pace than a lower concentration (Gaosheng and Jingming, 2012).

A number of studies discovered that the use of precursor expand the bioactive compounds on some plants, such as 200 mg/L concentration of tryptophan improves the alkaloid production on the callus culture of god's crown (*Phaleria macrocarpa* [Scheff.]Boerl.) (Gusni *et al.*, 2015), 150 mg/L concentration of tryptophan increases the thymol and proline production, while its 150 mg/L concentration multiply the coumarin production on callus culture of *Verbascum thapsus* L (Al- Jibouri *et al.*, 2016). Simultaneously, 100 μ M L-phenylalanine concentration increases the scopoletin production on the cell culture of *Spilanthes acmella* Murr (Abyari *et al.*, 2016). This study aims to investigate the growth of cell suspension and production of organosulfur bioactive compound with the addition of various concentrations of glutathione, as a precursor, in the suspension culture of single garlic (*Allium sativum* L.).

This study aims to analyze the growth of cell biomass and the production of bioactive organosulfur compounds

in cell suspension cultures of single garlic (*Allium sativum* L.) with the addition of glutathione as a precursor feeding at different concentrations. The results of this study were expected to obtain alternative methods to increase the production of organosulfur bioactive compounds in single garlic, which can help the availability of organosulfur bioactive compounds that have important benefits in the health field.

2. Materials and Methods

2.1. Establishment of cell suspension culture

The callus was induced from crown explant of single garlic variety Tawangmangu Baru, obtained from Magelang, Central Java. The explant was cultured on solid MS media with the addition of 0.3 mg/L 2,4-D and 0.5 mg/L kinetin. The cell suspension was initiated by inoculating 1 g of friable callus in 25 ml of liquid MS media, with the same growth regulator as callus induction media. The cell suspension was incubated at 25°C under continuous fluorescent white light (approx. 13.5 μ mol/m².s) and agitated on a shaker at 100 rpm. It was routinely subcultured every two weeks by transferring 1 g of cell mass from the previous culture into 25 mL new liquid MS medium. The cell biomass was weighted using the SCV method every three days for three weeks to obtain the optimum growth rate. The optimum growth rate is considered to be a medium from which maximum cell mass and organosulfur compound production was obtained within the single garlic cell culture. The initiation and establishment of single garlic cell suspension cultures were presented in Figure 1.

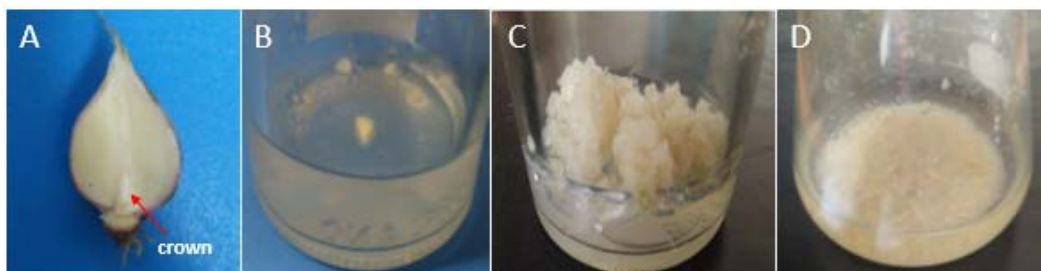


Figure 1 Initiation and establishment of single garlic cell suspension: (A) Single garlic crown explant (B) Inoculation of explant in the MS media (C) Single garlic callus (D) Single garlic cell suspension.

2.2. Feeding of glutathione precursor to cell suspension culture

In the precursor feeding, glutathione with variations of 0, 5, 7.5, 10, 12.5, 15 mM was added to the suspension culture media. The liquid MS media with no glutathione addition was used as a control. The cell suspension was harvested and analyzed after two weeks to attain cell suspension kinetics growth and accumulation of organosulfur bioactive compound. The effect of precursor feeding on the cell suspension culture was evaluated based on the culture growth and the production of organosulfur compounds. Evaluation of cell suspension growth was carried out on the growth parameters, including the fresh weight, the dry weight, settled cell volume, and growth index. Measurement of fresh weight was carried out by weighing the cells that have been previously settled, while the dry weight was done by weighing the cells that have

been previously dried in an oven (50°C, 12 h). Measurement of settled cell volume was done by pouring the cell suspension into a measuring glass and leaving it for 1 hour until all cells were settled. The volume fraction of cells precipitated was expressed as settled cell volume. The growth index is calculated based on the difference between the final weight and the initial weight divided by the initial weight of the cell (Loyola-Vargas and Ochoa-Alejo, 2012).

2.3. Analysis of organosulfur content

The analysis of the organosulfur compound on the cell suspension was carried out using the HPLC method. Extraction of the single garlic cell suspension was carried out with a slight modification of the method described by Al-Jibouri *et al.* (2016). A 100 mg of cells were taken and crushed using pestle and mortar. The crushed cells were extracted with 95%

methanol. The solution was stirred until homogenized and incubated overnight at cold temperature. The collected extracts were centrifuged and filtered out using Whatman No.1. The aliquots from the filtrate were filtered again using 0.22 µm syringe filters. Organosulfur content in the extract was estimated by high-performance liquid chromatography (HPLC). The instrument used was HPLC Shimadzu with Shim-pack VP ODS (5 µm 150 x 4,6 mm) column type as the stationary phase. A detector type SPD 20-A UV-Vis with 210 nm wavelength was used. The mobile step used was 10 mM Potassium dihydrogen phosphate: Acetonitrile (1:1)(v/v), isocratically, with a flow speed of 1mL/minute.

2.4. Statistical Analysis

The experiment was analyzed using one-way ANOVA. The average score was compared using Duncan's Multiple Range Test, at a 5% significance level ($p < 0.05$), using SPSS software version 25.

2.5. Molecular docking in the biosynthesis of organosulfur compounds

The ligand preparation was completed by examining the compound activities using Pass Server (<http://www.pharmaexpert.ru/passonline/>) database. The potential effect of a compound on the targeted protein as its interaction partner was analyzed and predicted using the STITCH (<http://stitch.embl.de>) database. The ligand's three-dimension structure collection was obtained from PubChem (<https://pubchem.ncbi.nlm.nih.gov/>) database. The protein preparation was carried out using the protein with a role in the alliin biosynthesis path. It was analyzed and predicted using the Plant Metabolic Pathway (<https://plantcyc.org/>) and STITCH (<http://stitch.embl.de>) database to discover its interaction with other compounds. The three-dimension structure collection for the targeted protein was completed by modelling it into the SWISS-MODEL Repository database (<https://swissmodel.expasy.org/>). After that, molecular docking was completed using PyRx 0.8 software to gain the best binding affinity. The compound with the lowest binding affinity was saved in the PDB format. The interaction of that compound was visualized in three dimensions using PyMol software. The two-dimension scheme and type of receptor interaction with formulated ligand were visualized using Discovery Studio software.

3. Results

3.1. The effects of glutathione precursor feeding on cell suspension growth

The addition of glutathione as a precursor in the culture medium showed a significant effect on the suspension culture growth of single garlic. As compared to control, the addition of glutathione with a 5 to 15 mM concentration range can enhance the fresh weight, dry weight, settled cell volume, and growth index. The fresh weight, dry weight, settled cell volume, and growth index increased from 5 mM to 10 mM and subsequently decreased at 12.5 mM and 15 mM glutathione concentration, as presented in Figure 2.

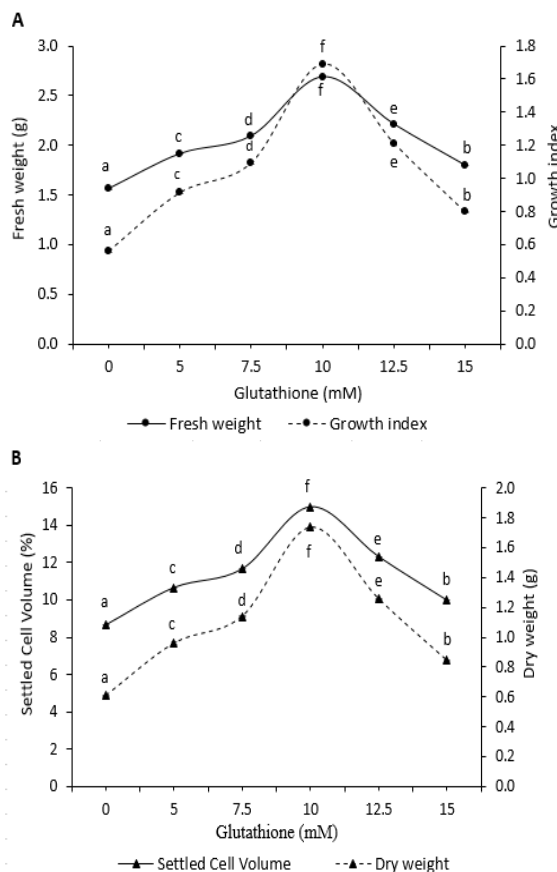


Figure 2. The effect of glutathione precursor feeding in cell suspension culture of single garlic: (A) Fresh weight and growth index (B) Settled cell volume and dry weight. The different letters show significant differences in the Duncan's Multiple Range Test ($p < 0.05$) on each parameter.

The cell mass, including fresh weight, dry weight, and settled cell volume without the addition of glutathione to the culture medium, were 1.562 ± 0.006 g, 0.608 ± 0.007 g, 8.7 ± 0.0 %, respectively. The highest cell suspension growth was produced at the addition of 10 mM glutathione for all growth parameters, of about 2.691 ± 0.006 g on fresh weight, 1.738 ± 0.007 g on dry weight, and 15 ± 0.0 % on settled cell volume. The growth index represents the same increases and decreases in the cell fresh weight at each glutathione concentration added to the culture medium. The maximum growth index (1.692 ± 0.006) was achieved at the addition of 10 mM glutathione, which showed the occurrence of faster growth compared to control (0.562 ± 0.006).

3.2. The effects of glutathione precursor feeding on organosulfur production

The HPLC chromatogram analysis demonstrated that the single garlic cell suspensions, with or without precursor, identified 30 types of organosulfur compounds. The different peak area of each compound represents the organosulfur bioactive compound level difference in each glutathione concentration. From those 30 compound types, 12 essential organosulfur compounds for human health, namely alliin, allicin, ajoene, dithiin groups (2-vinyl 1,3-

dithiin; 3-vinyl 1,2-dithiin) and allyl sulfide group (2-propenyls 1-propenyl disulfide; 1-propenyl allyl disulfide; allyl methyl disulfide; allyl propyl disulfide; allyl trisulfide; allyl methyl trisulfide; diallyl heptasulfide) (**Figure 3**). However, among those 12 compounds, alliin, allicin, and ajoene are responsible for the characteristic taste and odor of single garlic.

The addition of glutathione on the culture media significantly affected the increase of 12 organosulfur bioactive compound levels. The organosulfur bioactive compound level improves from the 5 mM to 15 mM glutathione addition. Meanwhile, the highest level was detected at 12.5 mM precursor addition (**Figure 4**). In the suspension culture, alliin, allicin, and ajoene levels were found to have more considerable than the other organosulfur compounds. These three compounds experience a significant increase in cell suspension due to the provision of the glutathione precursor. Their higher increase was detected at 12.5 mM precursor concentration. Additionally, on the control, the alliin, allicin, and ajoene compounds were 9.88, 4.81, and 3.70 mg/g, respectively.

The compounds level increased three times higher (30.90, 13.90, and 11.64 mg/g, respectively) at the 12.5 mM precursor concentration. The same pattern of increase in levels was also showed in other organosulfur compounds, such as 2-propenyl 1-propenyl disulfide, allyl propyl disulfide, allyl methyl disulfide, 2-vinyl 1,3-dithiin, 3-vinyl 1,2-dithiin, E1-propenyl allyl disulfide, allyl methyl trisulfide, allyl trisulfide, and diallyl heptasulfide. The compounds level of allyl propyl disulfide, allyl methyl trisulfide, allyl trisulfide, and diallyl heptasulfide before treatment were 0.98, 0.99, 0.78, and 1.35 mg/g respectively, and increased three times higher after the administration of glutathione (2.93, 2.94, 2.36, and 3.52 mg/g, respectively). Meanwhile, the compounds level of 2-propenyl 1-propenyl disulfide, allyl methyl disulfide, 2-vinyl-1,3-dithiin, 3-vinyl-1,2-dithiin, and E1-propenyl allyl disulfide before treatment were 0.36, 0.83, 0.42, 0.46, 0.58 mg/g respectively, and also increased four times higher after the administration of glutathione (1.47, 3.68, 1.62, 1.90, and 2.35 mg/g, respectively).

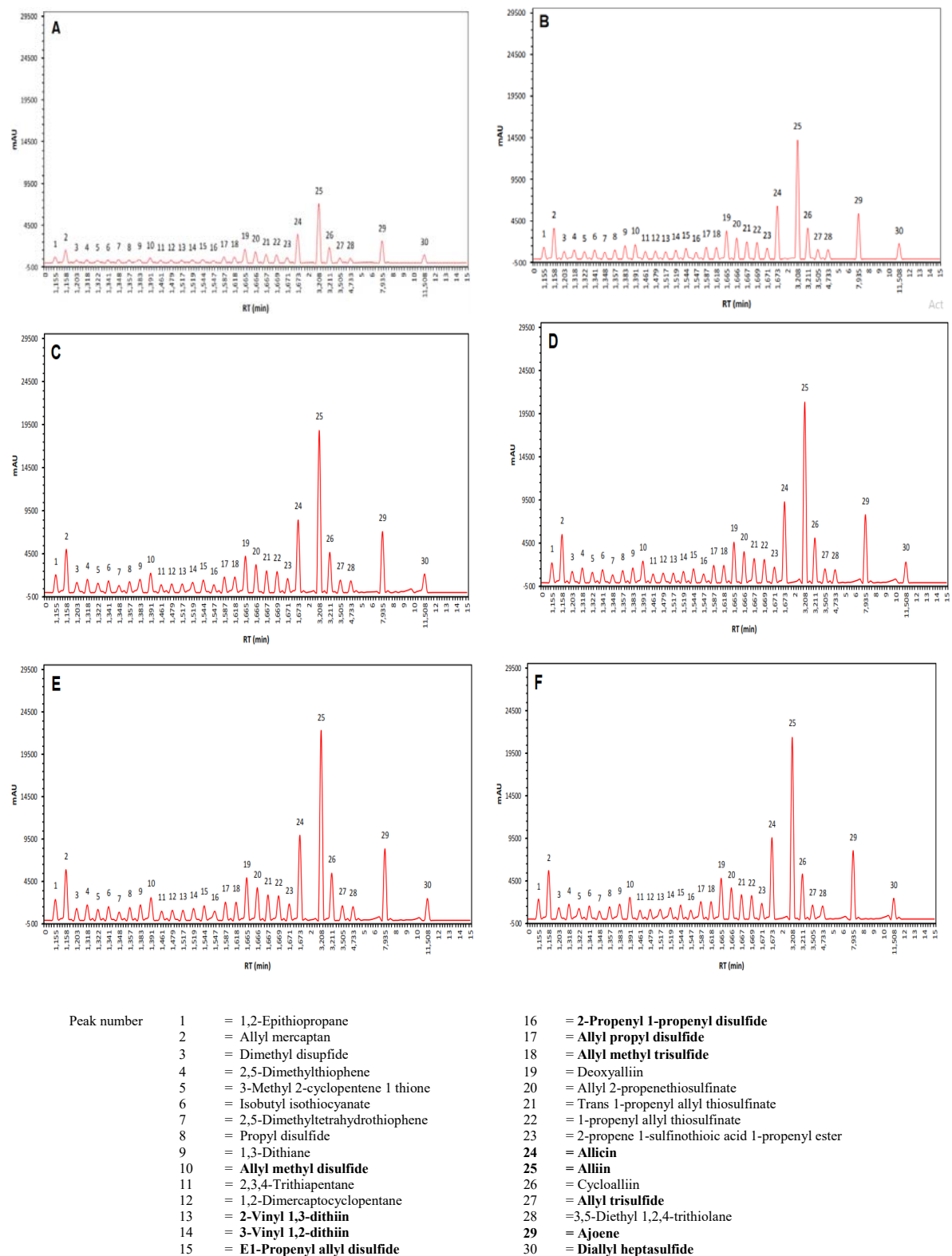


Figure 3. Chromatogram of organosulfur bioactive compounds in cell suspension of single garlic with differences in glutathione concentration (A) 0mM. (B) 5mM. (C) 7.5mM. (D) 10mM. (E) 12.5mM (F) 15mM.

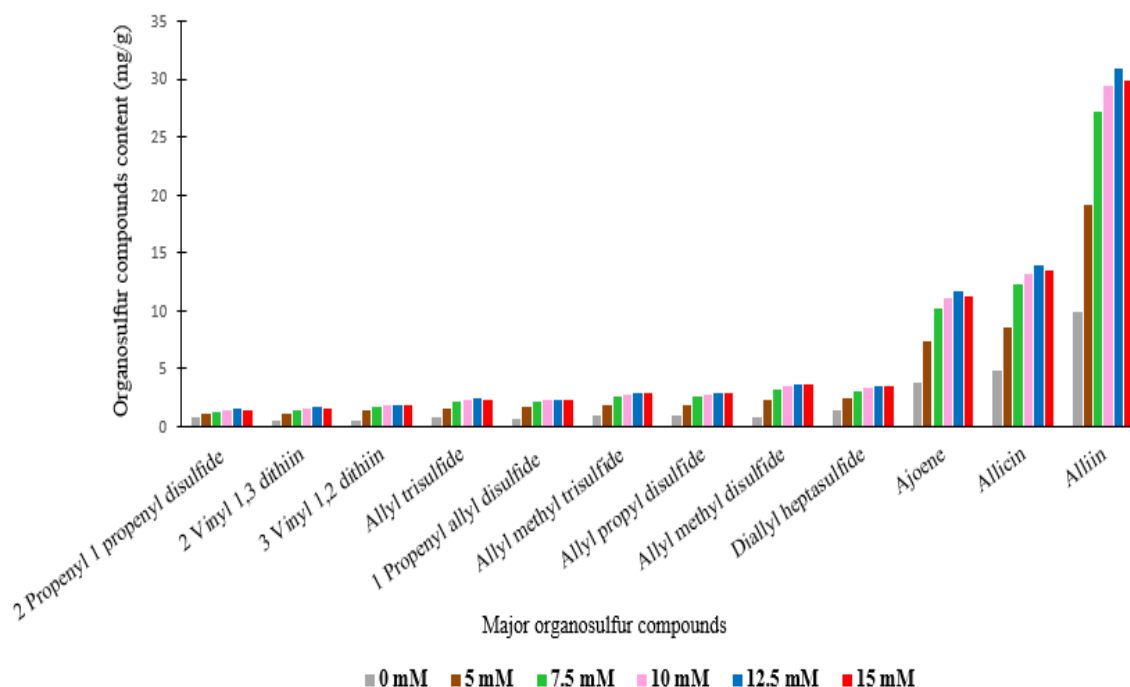


Figure 4. Differences in concentration of glutathione on organosulfur bioactive compounds content in single garlic suspension culture

3.3. The molecular docking visualization in the biosynthesis of organosulfur compounds

As a precursor, glutathione role that improves the organosulfur bioactive compound on the suspension culture can be predicted from the molecular docking between the ligands and enzymes that catalyze the reaction as a targeted protein. The biosynthetic pathways that are possible in the biosynthesis of alliin (as the parental of other organosulfur compounds) from the glutathione include some reaction stages, namely conjugation glutathione, the glycyl group removal, the S-alk(en)yl group modification, γ -glutamyl group removal, and S-oxygenation catalyzed by a specific enzyme. Glutathione transferase U24 (GSTU24) is predicted to catalyze glutathione conjugation and methacrylic acid into S-2 carboxypropyl glutathione. The release of glycyl group on S-2 carboxypropyl glutathione into γ -glutamyl-S-allylcysteine is presumed to be catalyzed by glutathione- γ -glutamylcysteinyltransferase (AT5G4407). Simultaneously, the discharge of the glutamyl group on γ -glutamyl-S-allylcysteine is possibly catalyzed by γ -glutamyltranspeptidase (AsGGT1). AsFMO1, which is a

coding gene of garlic, is forecasted to catalyze S-allylcysteine, generating alliin. Besides, alliin conversion to be allyl sulfonate and amino acrylate is predicted to be catalyzed by alliin lyase.

The presence of glutathione precursors interaction as a ligand, GSTU24 as the targeted protein, through in silico method, is illustrated by the complex formulated those two (Figure 5). The molecular docking results reveal that interaction that formulates the complex among glutathione, and GSTU24 is observed in the initial reaction. The interaction can be seen from the bonds glutathione on the active side of GSTU24. That interaction emerges because of the hydrogen bond and van der Waals on the amino acid residues that bind the glutathione on the active bond side (Figure 5A). The docking results on the different reactions also indicate interactions with the formation of the complex between ligand and the targeted protein, such as between methacrylic acid-GSTU24, S-2 carboxypropyl glutathione-AT5G4407, γ -glutamyl S allylcysteine-AsGGT1, S-allylcysteine-AsFMO1, and alliin-alliin lyase1 (Figure. 5B-F).

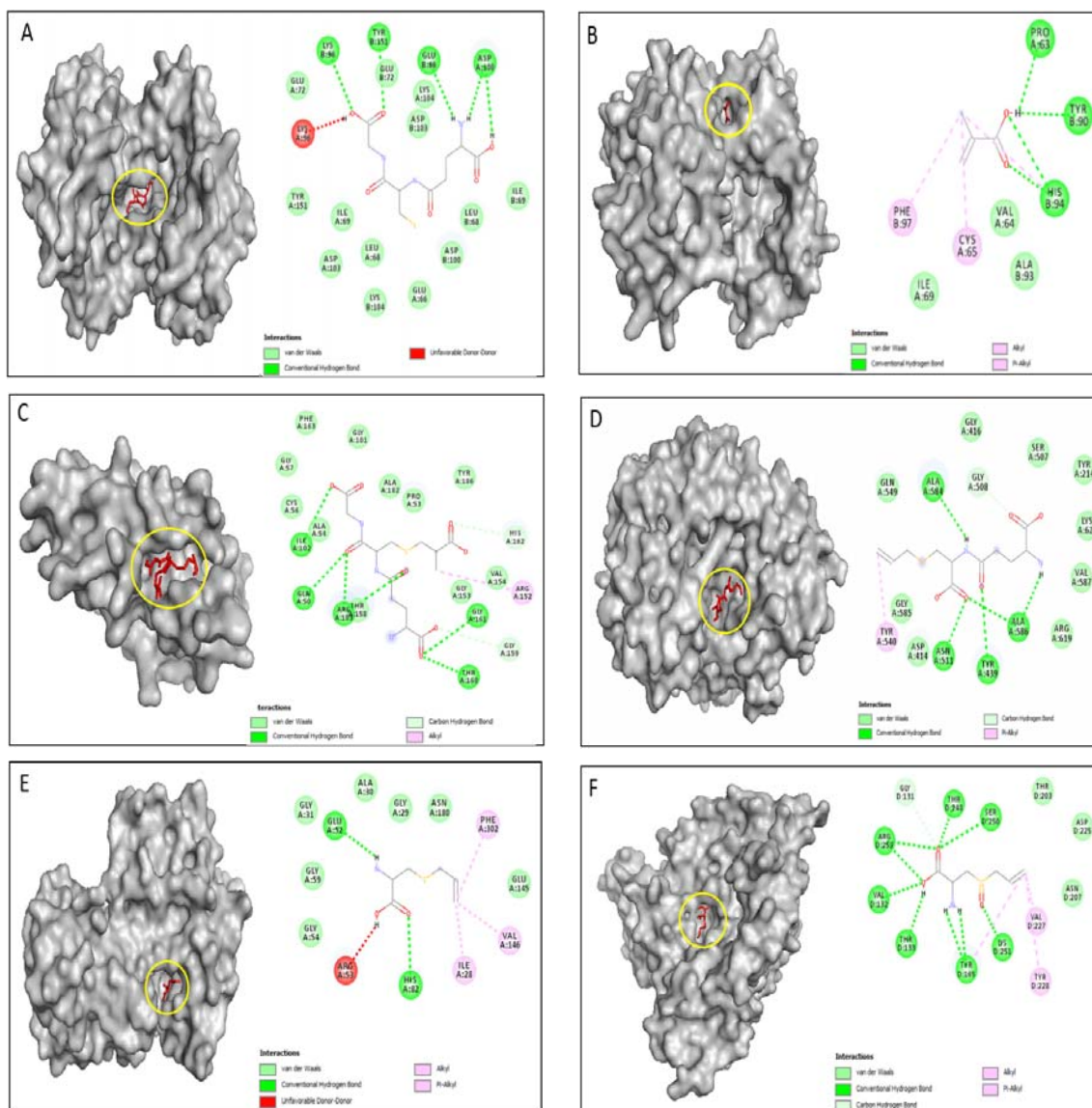


Figure. 5 Formed complex between ligand (red) - receptor (grey) and the bound appears in the interactions between ligand-receptor (the yellow circle): (A) Complex of glutathione and GSTU24 (B) Complex of methacrylic acid with GSTU24 (C) Complex of S-2 carboxypropyl glutathione and AT5G4407 (D) Complex of γ -glutamyl S-allylcysteine and AsGGT1 (E) Complex of S-allylcysteine and AsFMO1 (F) Complex of alliin with alliin lyase1.

4. Discussion

Feeding precursor in cell suspension cultures increased the growth of cultures and the content of organosulfur compounds. Glutathione is a tripeptide (γ -glutamyl-cysteine-glycine) with a thiol group, which has a role as the main regulator of cellular redox. Cellular redox potential is important mediator of several cell processes such as cell growth, proliferation, and differentiation. According to Ogawa (2005), Maher (2011), and Nahar *et al.* (2015), glutathione plays a role in modulating cell proliferation, growth, development, cell cycle, gene expression, and protein activation. Kerk *et al.* (1995) further stated that in the early stage of the cell cycle (G1), cells have a low glutathione content. The lack of glutathione availability at this stage can cause the cell cycle to stop (Potter *et al.*, 2004). In the regulation of cell

proliferation, glutathione is involved in the continuation of the cell cycle. Sequestering of glutathione in the nucleus occurs in the early stage of the cell proliferation cycle, where glutathione in the nucleus affects the gene transcription process, including cell division, redox regulation and regulation of transcription factors. Distributed glutathione into the nucleus causes a reduction in the accumulation of glutathione in the cytoplasm, whereas the availability of glutathione in the nucleus and cytoplasm in a balanced state is needed during the cell cycle (Diaz Vivancos *et al.*, 2010; Diaz Vivancos *et al.*, 2015; Schnaubelt *et al.*, 2015). By feeding the glutathione, there will be an increase in the amount of glutathione needed by cells to be able to develop from the initial stage (G1) to the synthesis stage (S) (Kerk and Feldman, 1995). The glutathione also affects the production of endogenous cytokinin, growth regulators that play a role in promoting cell division in meristematic tissue. As reported by

Synkova *et al.* (2004), overproducing of cytokinins was detected in plants with high glutathione and ascorbate enzyme activity. Glutathione added to culture media contributes to stimulating growth when applied at levels appropriate to physiological levels. Precursor feeding with a too high concentration can inhibit cell growth and enzyme activity, which can be toxic to cells (Gaosheng and Jingming, 2012). A number of studies reported that the use of glutathione was able to increase callus multiplication in *Phoenix dactylifera* L (Al-Mayahi *et al.*, 2020).

The increase in organosulfur compounds in single garlic cell suspension culture cannot be separated from the involvement of glutathione in the biosynthesis of alliin organosulfur compounds, which are parental to other organosulfur compounds. The administration of glutathione involved in the biosynthetic pathway into the culture media can increase the alliin organosulfur compound. It is based on the fact that any intermediate compounds present at the beginning or in the secondary metabolite biosynthetic pathway can increase the end product. In the biosynthetic pathway of alliin organosulfur compounds, glutathione is upstream and involved in the reaction's initial stage. According to Gaosheng (2012), upstream precursors can be converted into downstream compounds after being catalyzed by specific enzymes. The precursors added at the beginning or during the culture period can serve as additional substrates for increasing the high production of metabolites in cultivated plant cells, tissue, or organ cultures (Isah *et al.*, 2018). In the conjugation reaction between glutathione and methacrylic acid to produce S-2 carboxypropyl glutathione, the enzyme glutathione transferase (GSTU24) is predicted to catalyze the reaction. The increase in S-2 carboxypropyl glutathione produced at the initial stage of the reaction will increase a product in the next reaction stage and increase the organosulfur compound as the end product. The stimulation given to the metabolic pathways in plant cell culture can produce bioactive compounds with a significant increase (Wang *et al.*, 2001).

Glutathione as a precursor feeding can be seen in the visualization of molecular docking between glutathione and GSTU24. Glutathione and methacrylic acid can bind to the active site of GSTU24 by hydrogen bonding and van der Waals interactions, with a binding affinity of -6.5 and -4.6 kcal/mol, respectively. This interaction is dominated by hydrogen bonds, which are stronger than the other bonds. The formation of glutathione and methacrylic acid complexes on GSTU24 macromolecules, then glutathione has the potential to become a GSTU24 substrate to produce S-2 carboxypropyl glutathione. Plant glutathione S-transferase enzyme has various roles in endogenous metabolism; one of them is an enzyme that catalyzes glutathione conjugation (Dixon *et al.*, 2010; Obeidat *et al.*, 2017). The next reaction stage reveals an interaction formulating complex between the ligand and the target protein, namely S-2 carboxypropyl glutathione and AT5G4407, γ -glutamyl S allylcysteine and AsGGT1, S-allylcysteine and AsFMO1, alliin and alliin lyase1. The formation of the complex between the substrates as a ligand, and the enzymes that catalyze it as target protein at each reaction stage of the metabolic pathway, shows that organosulfur bioactive compound can be produced and increased by the addition of glutathione precursor.

5. Conclusion

The results of this study showed that glutathione as precursor feeding added to the culture medium is an effective method to increase the suspension cell growth and production of bioactive organosulfur compounds in single garlic cell suspension culture, which can enhance the availability of organosulfur compounds with important health benefits. Cell suspension culture of single garlic with glutathione precursor has the potential for scale-up studies at the commercial level by the pharmaceutical industry to further enhance the medicinally important bioactive organosulfur compounds. The molecular docking visualization on every reaction stage in the alliin biosynthesis through the glutathione pathway showed the presence of interaction between ligands as a substrate and enzymes as the target protein.

Acknowledgements

The authors of this study would like to express gratitude to the Ministry of Research, Technology, and Higher Education, Republic of Indonesia (KEMENRISTEKDIKTI) for the funding support of research and publication of this paper.

References

- Abyari M, Nasr N, Soorni J and Sadhu D. 2016. Enhanced accumulation of scopoletin in cell suspension culture of *Spilanthes acmella* Murr. using precursor feeding. *Braz Arch Biol Technol*, **59**: e1615053.
- Al-Jibouri JM, Abed SA, Ali AJ and Mejeed MD. 2016. Improvement of phenols production by amino acids in callus cultures of *Verbascum thapsus* L. *Am. J Plant Sci*, **7(7)**:84-91.
- Al-Mayahi AMW, Jafar ON and Mohsen KA. 2020. Effect of glutathione (GSH) on Date palm (*Phoenix dactylifera* L.) micropropagation. *Folia Oecol*, **47(1)**:64-69.
- Bharat P. 2014. Comparative analytical study of single bulb and multi bulb garlic (*Allium sativum* Linn.). *Int J Ayurveda Med*, **2(4)**:86-91.
- Borlinghaus J, Albrecht F, Gruhlke H, Nwachukwu DI and Slusarenko JA. 2014. Allicin : chemistry and biological properties. *J Mol*, **19(8)**:12591-12618.
- Diaz-Vivancos P, De-Simone A, Kiddle G and Foyer CH. 2015. Glutathione-linking cell proliferation to oxidative stress. *Free Rad Biol Med*, **89**:1154-1164.
- Diaz-Vivancos P, Dong Y, Ziegler K, Markovic J, Pallardo FV, Pellny TK, Verrier PJ and Foyer CH. 2010. Recruitment of glutathione into the nucleus during cell proliferation adjusts whole-cell redox homeostasis in *Arabidopsis thaliana* and lowers the oxidative defence shield. *Plant J*, **64(5)**:825-838.
- Dixon DP, Skipsey M and Edwards R. 2010. Roles for glutathione transferases in plant secondary metabolism. *Phytochemistry*, **71**:338-350.
- Donma MM, Donma O. 2020. The effects of allium sativum on immunity within the scope of COVID-19 infection. *Med Hypotheses*, **144**:109934.
- Espinosa-Leal CA, Puente-Garza CA, and Garcia-Lara S. 2018. In vitro plant tissue culture : Mean for production of biological active compounds. *Planta*, **248(1)**: 1-18.
- Gaosheng H and Jingming J. 2012. Production of the useful secondary metabolites through the regulation of biosynthetic pathway in the cell & tissue suspension culture of medicinal

- plants. In: Gaosheng H and Jingming J (Eds.), **Recent Advances in Plant in Vitro Culture**. Intech Open, United Kingdom, pp. 197-210.
- Gruhlke MCH, Portz D, Stitz M, Anwar A, Schneider T, Jacob C, Schlaich NL and Slusarenko AJ. 2010. Allicin Disrupts the Cell's Electrochemical Potential and Induces Apoptosis in Yeast. *Free Rad Biol Med*, **49(12)**:1916-1924.
- Guerriero G, Berni R, Muñoz-Sanchez JA, Apone F, Abdel-Salam EM, Qahtan AA, Alatar AA, Cantini C, Cai G, Hausman JF, Siddiqui KS, Hernández-Sotomayor SMT and Faisal M. 2018. Production of plant secondary metabolites: Examples, tips and suggestions for biotechnologists. *Genes*, **9(6)**:309.
- Gusni WR, Suwirman, Noli ZA. 2015. Increasing alkaloid-contained callus of gods crown (*Phaleria macrocarpa* [Scheff.]Boerl.) using tryptophan as precursor in Murashige & Skoog media. *Jurnal Biologi Universitas Andalas*, **4(1)**:4-8.
- Habtemariam S. 2019. The chemical and pharmacological basis of garlic (*Allium sativum* L.) as potential therapy for type 2 diabetes and metabolic syndrome. **Medicinal Foods as Potential Therapies for Type-2 Diabetes and Associated Diseases**, Academic Press, United Kingdom, pp.689-749.
- Isah T, Umar S, Mujib A, Sharma MP, Rajasekharan PE, Zafar N and Frukh A. 2018. Secondary metabolism of pharmaceuticals in the plant in vitro cultures: strategies, approaches, and limitations to achieving higher yield. *Plant Cell Tissue Organ Cult*, **132(2)**:239-265.
- Jang HJ, Lee HJ, Yoon DK, Ji DS, Kim JH and Lee CH. 2017. Antioxidant and antimicrobial activities of fresh garlic and aged garlic by-products extracted with different solvents. *Food Sci Biotechnol*, **27(1)**:219-225.
- Kerk NM and Feldman LJ. 1995. A biochemical model for the initiation and maintenance of the quiescent centre: implications for organization of root meristem. *Dev*, **121**:2825-2833.
- Lindstedt S, Wlosinska M, Nilsson AC, Hlebowicz J, Fakhro M and Sheikh R. 2021. Successful improved peripheral tissue perfusion was seen in patients with atherosclerosis after 12 months of treatment with aged garlic extract. *Int Wound J*, 1-11.
- Loyola-Vargas VM and Ochoa-Alejo N. 2012. **Plant Cell Culture Protocols**. third ed. Totowa, New Jersey.
- Maher YA. 2011. Glutathione as potential target for cancer therapy; more or less is good? (Mini-Review). *Jordan J Biol Sci*, **4(3)**:119-124.
- Murthy HN, Lee EJ and Paek KY. 2014. Production of secondary metabolites from cell and organ cultures: Strategies and approaches for biomass improvement and metabolite accumulation. *Plant Cell Tissue Org Cult*, **118(1)**: 1-16.
- Nahar K, Hasanuzzaman M, Alam MM and Fujita M. 2015. Glutathione-induced drought stress tolerance in mung bean: coordinated roles of the antioxidant defence and methylglyoxal detoxification systems. *AoB Plants*, **7**: plv069.
- Nakamoto M, Kunimura K, Suzuki JI and Kodera Y. 2020. Antimicrobial properties of hydrophobic compounds in garlic: Allicin, vinylidithiin, ajoene and diallyl polysulfides (Review). *Exp Ther Med*, **19(2)**: 1550-1553.
- Naniou-Obeidat I, Madesis P, Kissoudis C, Voulgari G, Chronopoulou E, Tsaftaris A and Labrou NE. 2017. Plant glutathione transferase-mediated stress tolerance: functions and biotechnological applications. *Plant Cell Rep*, **36(6)**:791-805.
- Ogawa K. 2005. Glutathione-associated regulation of plant growth and stress responses. *Antioxid Redox Signal*, **7**:973-981.
- Potters G, Horemans N, Bellone S, Caubergs RJ, Trost P, Guisez Y and Asard H. 2004. Dehydroascorbate influences the plant cell cycle through a glutathione-independent reduction mechanism. *Plant Physiol*, **134**:1479-1487.
- Pourzand A, Tajaddini A, Pirouzpanah S, Asghari-Jafarabadi M, Ostadrahimi AR and Sanaat Z. 2016. Associations between dietary allium vegetables and risk of breast cancer: A hospital-based matched case-control study. *J Breast Cancer*, **19(3)**: 292-300.
- Rahman MM, Fazlic V and Saad NW. 2012. Antioxidant properties of raw garlic (*Allium sativum*) extract. *Int Food Res J*, **19(2)**:589-591.
- Ramirez DA, Locatelli DA, Torres-Palazzolo CA, Altamirano JC and Camargo AB. 2017. Development of garlic bioactive compounds analytical methodology based on liquid phase microextraction using response surface design. Implications for dual analysis: Cooked and biological fluids samples. *Food Chem*, **215**:493-500.
- Saljoughian S, Roohinejad S, Bekhit AEDA, Greiner R, Omidzadeh A, Nikmaram N and Khaneghah AM. 2017. The effects of food essential oils on cardiovascular diseases: A review. *Crit Rev Food Sci Nutr*, **8(10)**:1688-1705.
- Sankaran M, Vadivel A and Thangam A. 2010. Curative effect of garlic on alcoholic liver diseased patients. *Jordan J Biol Sci*, **3(4)**:147-152.
- Schnaubelt D, Queval G, Dong Y, Diaz-Vivancos P, Makgopa ME, Howell G, De Simone A, Bai J, Hannah MA and Foyer CH. 2015. Low glutathione regulates gene expression and the redox potentials of the nucleus and cytosol in *Arabidopsis thaliana*. *Plant Cell Environ*, **38(2)**:266-279.
- Singh B and Sharma RA. 2020. **Secondary Metabolites of Medicinal Plants**, first ed. Weinheim, Germany.
- Subramanian MS, Nandagopal MSG, Nordin SA, Thilakavathy K and Joseph N. 2020. Prevailing knowledge on the bioavailability and biological activities of sulphur compounds from Alliums: A potential drug candidate. *Molecules*, **25**:4111.
- Synkova H, Semoradova S, Schnablova R, Witters E, Husak M and Valcke R. 2006. Cytokinin-induced activity of antioxidant enzymes in transgenic Pssu-ipt tobacco during plant ontogeny. *Biol Plant*, **50**: 31-41.
- Ugwu CE and Suru SM. 2016. The functional role of garlic and bioactive components in cardiovascular and cerebrovascular health : What we do know. *J Biosci Med*, **4**:28-42.
- Wang C, Wu J and Mei X. 2001. Enhancement of taxol production and excretion in *Taxus chinensis* cell culture by fungal elicitation and medium renewal. *Appl Microbiol Biotechnol*, **55(4)**:404-410.
- Yoshimoto N and Saito K. 2019. S-Alk(en)ylcysteine sulfoxides in the genus *Allium*: Proposed biosynthesis, chemical conversion, and bioactivities. *J Exp Bot*, **70(16)**:4123-4137.
- Zhang Y, Liu X, Ruan J, Zhuang X, Zhang X and Li Z. 2020. Phytochemicals of garlic: Promising candidates for cancer therapy. *Biomed Pharmacother*, **123**:109730.

Towards Food Security: Essential Oil Components as Protectants Against the Rice Weevil, *Sitophilus Oryzae*

Mobolade D. Akinbuluma*, Olanike T. Okunlola, Olajumoke Y. Alabi, Modupe I. Timothy, David O. Omobusuyi

Department of Crop Protection and Environmental Biology, University of Ibadan, Nigeria

Received: January 20, 2021; Revised: May 13, 2021; Accepted: July 5, 2021

Abstract

Rice (*Oryza sativa*) is an important staple with high food value for a large part of the world population, but damage caused by rice weevil, *Sitophilus oryzae* (Coleoptera: Curculionidae) is a major constraint to its production. Synthetic chemicals are effective in managing stored produce insect pests, but they leave residues on food substances. Although botanical essential oils have potential in managing insect pests, information is scanty on the use of their constituents against the rice weevil.

Therefore, this study was conducted to evaluate the efficacy of two essential oil constituents: linalool and nerolidol against *Sitophilus oryzae*. Each of the constituents was formulated at 1, 5 and 25 $\mu\text{L/mL}$, relative to the actellic dust, pirimiphos-methyl (0.015 g) and ethanol-treated control. Treatments were evaluated on rice grains (FARO 60, an Indian variety) infested with *Sitophilus oryzae* under laboratory conditions ($27\pm 2^{\circ}\text{C}$ temperature; $78\pm 5\%$ relative humidity). The median lethal concentration (LC_{50}) of the oil components was evaluated using probit analysis while mortality was assessed following standard procedure. Repellent effect of the oil constituents on *S. oryzae* was determined in an olfactometer bioassay. Data were analysed using Analysis of Variance (ANOVA) and *t*-test analysis while means were compared with the Least Significant Difference at 5% significant level.

Linalool and nerolidol gave LC_{50} values of 3.98 $\mu\text{L/mL}$ and 5.01 $\mu\text{L/mL}$, respectively, while mortality ranged from 0.00% in the control to 79.72% in treatment with linalool and 58% in nerolidol. Linalool and nerolidol at concentrations 5 and 25 $\mu\text{L/mL}$ were highly repellent ($P < 0.05$) to adult *S. oryzae* in olfactometry test. The use of linalool and nerolidol as essential oil components could be included in design of Integrated Pest Management approach of *Sitophilus oryzae*, thereby reducing the problems caused by synthetic insecticides to human and environmental health.

Keywords : Bio-insecticides; Linalool; Adult mortality; Olfactometry test; Repellent effects

1. Introduction

Many biotic factors including diseases, bacteria, virus, nematodes, weeds, vertebrate pests and insects, are constraints to production of rice (*Oryza sativa* L.), an important staple with high food value for a large part of the world population (Okpale *et al.*, 2021). Field insects such as the rice gall midge, *Orseola oryzivora* (Wood-Mason) and the rice stem borer, *Scirpophaga incertus* (Walker) (Paul, 2007) as well as storage insect pests like *Sitotroga cerealella* (Olivier) and *Sitophilus oryzae* L. (Okpale *et al.*, 2021) are responsible for yield reduction in cultivated and stored rice. The rice weevil, *Sitophilus oryzae* (L.) is a major insect pest damaging rice grains in storage (Nwaubani *et al.*, 2014; Akhtar *et al.*, 2015) with a cosmopolitan distribution, occurring in several agro-ecologies of the world as well.

In Nigeria, towards reducing importation of rice, farmers are currently empowered to increase production of rice grains to feed the teeming population but being damaged by insects such as *S. oryzae* remains a challenge. The damage of stored rice, which usually occurred under

both larvae and adult stages, lead to loss in nutritive value, grain weight and inducing secondary contamination by fungi and mites (Ashamo and Ogungbite, 2014). Synthetic insecticides and fumigants are commonly used to control pests due to their availability and rapid actions; however, their overuse, misuse and abuse have resulted in serious environmental consequences thus warranting widespread criticisms. In addition to the risks associated with the use of chemicals on human and environmental health, a number of insect pests has been reported to be resistant to them.

Use of botanicals as pest control agents have constituted alternative strategies to the use of chemical insecticides as plants constitute a rich and cheap source of bioactivities (Wink, 2008; Akinbuluma *et al.*, 2017). Given that many of the plant part powders and their extracts are specific to target insects, have low mammalian toxicity and are eco-friendly, their exploration should be an eloquent indicator towards the development of novel classes of biopesticides for a resilient pest management. Botanical essential oils are among the products that have been used to mitigate the effects of both field and storage insect pests (Marimuth *et al.*, 1997; Isman, 2000; Isman

* Corresponding author e-mail: delebuluma@yahoo.com.

and Ahkar, 2007; Aboaba *et al.*, 2019; Akinbuluma 2020) as a potential alternative to synthetic pesticides (Al Dawsari, 2020). Although efforts are directed at investigating plant-derived constituents as useful products in insect-control practices, only little progress is made in the determination of actual compounds responsible for insecticidal activities. There was no recent report on the effects of individual constituents of plant essential oils as biopesticides against *S. oryzae*. So, this study aims to assess the potential of two essential oil components, linalool and nerolidol, relative to a synthetic compound, pirimiphos-methyl on *Sitophilus oryzae*.

2. Materials and Methods

2.1. Study location

This study was conducted between January and April, 2020. All experiments were carried out at the Entomology Research Laboratory and the PEARL Laboratory, Department of Crop Protection and Environmental Biology, University of Ibadan, at 27±2°C (temperature) and 78±5% (relative humidity).

2.2. Insects

Infested rice grains were bought from the market and kept in Kilner jars with mesh lids. Emerged adults were sieved out and used to infest clean grains in 3 Kilner jars (200 g/jar). Old insects were removed after 7 days of mating and oviposition and newly emerged adults were used for the experiments (Akinbuluma and Ewete, 2014).

2.3. Insecticidal materials and rice variety

Linalool and nerolidol were obtained from the Behavioural and Chemical Ecology unit of International Centre of Insect Physiology and Ecology, Nairobi, Kenya. Rice grains (FARO 60, japonica indica variety) were purchased from the International Institute for Tropical Agriculture, Ibadan, Nigeria. The grains were parboiled, dried and subsequently dehusked.

2.4. Biological assays

2.4.1. Median Lethal Concentration (LC₅₀)

Each of linalool and nerolidol was diluted in 95% ethanol to obtain ten concentrations, 1, 2, 3, 4, 5, 6, 7, 8, 9 and 10 microliter/millilitre (µL/mL) with a control 0 (µL/mL) containing only ethanol. The concentrations were applied topically on the ventral sides of five pairs of adult *S. oryzae* with a micro-syringe. Mortality was recorded after 24 hours and converted to probits, while the logarithms of the concentrations were taken. Probits were plotted against the logarithmic values to obtain a regression line, using Microsoft Excel (DAASTAT version 1.101). The LC₅₀ for each of linalool and nerolidol was determined where the log-dose at the median point was changed to antilogarithm (Finney, 1971; Akinbuluma and Ewete, 2014).

2.4.2. Insect mortality

Thirty grammes (30 g) of rice grains was weighed in each of five 1-L kilner jar, and 0.5 mL of three selected concentrations (1, 5 and 25 µL/mL) of linalool was added to the grains inside each jar and the jars were shaken for about 3 minutes to allow effective coverage of the grain surface with the oils (Aboaba *et al.*, 2019). The set-up

included a jar containing ethanol only (negative control) and another jar containing 0.015 g of synthetic chemical, pirimiphos-methyl as the positive control. Thereafter, each jar received five pairs (1♀: 1♂) of 1-2 day-old adult *S. oryzae* and were covered with lid wire mesh. The five treatments were arranged in a Completely Randomised Design (CRD) with 4 replications. The number of adult *S. oryzae* that died was recorded every other day for 7 days (an insect was taken as dead when it does not respond when probed with a camel hair brush). Mortality data obtained were converted to percentage and transformed before analysis. Another set-up was repeated with nerolidol at the same concentrations and experimental conditions as above.

2.4.3. Repellent effects of oils

Behavioural response of adult *S. oryzae* to linalool and nerolidol was evaluated on a Y-tube olfactometer (internal diameter 0.5 cm, stem length 4 cm, arm length 5.5 cm). Each of linalool and nerolidol at concentrations; 1, 5 and 25 µL/mL was applied to a filter paper strip (No. 1 Whatman, Int Ltd. Maidstone, England) and placed at one arm of the tube, while the control (ethanol only) was placed on the other arm. Compressed clean air from a pump was drawn through two flow metres (at 60 ml/min rate) and later passed through two polyester (Nalophan) bags (38 x 25) cm. The bags contained the odour sources, and each was connected to each arm of the olfactometer with Teflon tubes. With the aid of a soft hairbrush, six adult female *S. oryzae* were placed at the stem inlet of the Y-tube and were observed for 5 minutes. Each concentration of the compounds was assayed in five replications with new batch of insects in each case. The number of entries from treated and control sides of the tubes was recorded and compared using a *t*-test analysis (Akinbuluma, 2017).

3. Results

3.1. Median lethal concentration (LC₅₀) and insect mortality

The LC₅₀ of linalool and nerolidol on adult *S. oryzae* were 3.98 µL/mL and 5.01 µL/mL, respectively, as shown in Figs 1 and 2). Percentage mortality of adult *S. oryzae* treated with the concentrations of linalool and nerolidol relative to pirimiphos-methyl and ethanol-treated control are presented in Tables 1 and 2). All concentrations of linalool were significantly higher ($P < 0.05$) than the ethanol-control in causing mortality to *S. oryzae* in all the days of the trials. Although percentage mortality values were highest on jars treated with pirimiphos-methyl, they were not significantly different ($P > 0.05$) from percentage mortality on grains treated with linalool (at 25 µL/mL) under days 3, 5 and 7 of the trials (Table 1). At higher concentrations of nerolidol and in later days of trials, percentage mortality was significantly higher than those in ethanol-treated control (Table 2).

3.2. Repellent effect

Significant difference ($P < 0.05$) was observed between repellence of adult *S. oryzae* caused by the concentrations of linalool at 5 µL/ml and 25 µL/mL and the ethanol control. Linalool at 25 µL/mL exhibited the highest repellent effect on *S. oryzae* (Table 3), even though

nerolidol at 25 µL/mL also exhibited repellent effect that was significantly higher than the control.

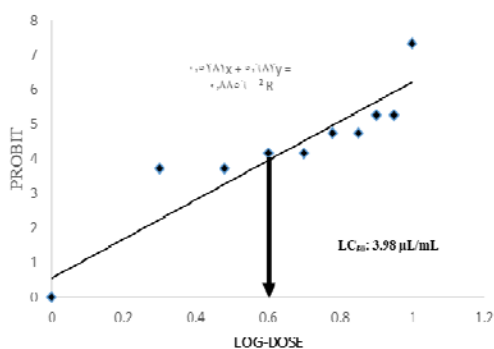


Figure 1. Median Lethal Concentration (LC₅₀) of Linalool on adult *Sitophilus oryzae*

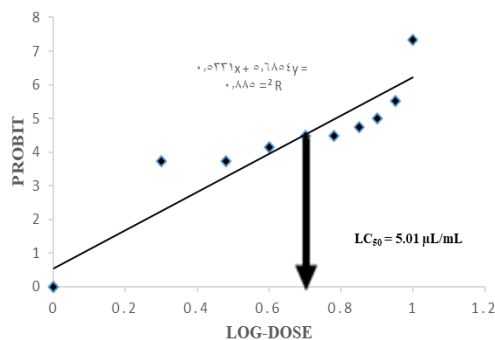


Figure 2. Median Lethal Concentration (LC₅₀) of Nerolidol on adult *Sitophilus oryzae*

Table 1. Mortality of adult *S. oryzae* treated with Linalool in the University of Ibadan, Nigeria in January, 2020

Conc. (µL/mL)	Mortality (± SE) of <i>Sitophilus oryzae</i> over 1-7 days infestation			
	1	3	5	7
0 (Ethanol)	0.00±0.00	0.00±0.00	0.00±0.00	0.00±0.00
1	13.83±4.61	20.47±2.03	25.83±4.26	25.83±4.26
5	20.47±2.03	22.13±3.69	27.70±4.29	30.87±5.11
25	54.00±3.96	68.94±12.21	75.89±10.53	79.72±7.67
Pirimiphos-methyl (0.015g)	18.44±0.00	72.11±6.26	90.00±0.00	90.00±0.00
LSD (0.05)	8.63	19.35	16.37	13.68

Means whose differences are greater than LSD (0.05) within a column are significantly different

Table 2. Mortality of adult *S. oryzae* treated with Nerolidol in the University of Ibadan, Nigeria in January, 2020

Conc. (µl/ml)	Mortality (± SE) of <i>Sitophilus oryzae</i> over 1-7 days infestation			
	1	3	5	7
0 (Ethanol)	0.00±0.00	0.00±0.00	0.00±0.00	0.00±0.00
1	0.00±0.00	4.61±4.61	11.25±6.70	15.86±5.62
5	4.61±4.61	14.61±4.61	23.83±4.61	40.47±2.03
25	9.22±5.83	19.22±5.32	42.50±2.34	58.22±1.66
Pirimiphos-methyl (0.015g)	20.47±2.03	78.75±6.70	90.00±0.00	90.00±0.00
LSD (0.05)	9.88	14.50	11.41	8.36

Means whose differences are greater than LSD (0.05) within a column are significantly different

Table 3. Repellent effect of linalool and nerolidol on adult *S. oryzae* in the University of Ibadan, Nigeria in January, 2020

Essential oil constituents	Conc (µL/mL)	Control	Test	t stat	t critical
Linalool	1	3.25	2.75	1.00	3.18
	5	5.00	1.00	4.90	3.18
	25	5.25	0.75	9.00	3.18
Nerolidol	1	3.25	2.75	0.52	3.18
	5	3.75	2.25	1.00	3.18
	25	4.75	1.25	9.00	3.18
-	-	-	-	-	(df: 3, at 5%)

Mean values are significant where *t*-stat is greater than *t*-critical within the same row

4. Discussions

Botanical essential oils and their constituents do not only exhibit activities including fumigant and contact toxicity, antifeedant and repellence on stored product insect pests, but they also possess some advantages like low mammalian toxicity, biodegradation and availability in developing countries (Isman 2000; El-Bakry, 2016).

The low LC₅₀ values of linalool and nerolidol shows that both oil constituents possess contact toxicity against adult *Sitophilus oryzae*. Ayvaz *et al.* (2010) also reported LC₅₀ value as low as 12.74 µL/L from the essential oils of oregano, *Origanum onites* L. on *Acanthoscelides obtectus* on stored beans. A more recent study revealed that the essential oils from *Syzygium aromaticum* and *Aegle marmelos* gave an LC₅₀ of 15.34 and 16.133 µL, respectively, on *S. oryzae* adults at 48 h exposure (Mishra *et al.*, 2012).

Although the mortality of *S. oryzae* increased with increasing concentration of the essential oil components and with exposure period, linalool and nerolidol were generally toxic to the insects. This might be due to the presence of terpenes in them, agreeing with the reports of Garcia *et al.* (2005) that the several monoterpenes and some sesquiterpenes were toxic to insects of stored produce. Earlier reports have shown that crude essential oils and their components are effective against insect pests of stored produce. Akinbuluma (2020) reported that the essential oil constituents from stem bark of *Cedrela odorata* caused high mortality and reduced egg-laying capacity of maize weevil. Similarly, oil from flowers of *Hyptis spicigera* elicited high insecticidal activity against *S. oryzae* (L.) and its toxicity was attributed to the presence of 1,8 cineole, carvacrol, α-pinene and β-pinene, in the crude oil (Ngamo *et al.*, 2007c). Specifically, linalool and nerolidol have been effective against some insect pests. Insecticidal properties of linalool are implicated as being a reversible inhibitor of acetylcholinesterase (Weaver *et al.*, 1991). Chang *et al.* (2009) have shown that linalool is a major component in basil oil active against tephritid fruit flies, *Ceratitis capitata*, *Bactrocera dorsalis* and *Bactrocera cucurbitae*, while Lapczynski *et al.* (2008) and Ferreira *et al.* (2012) reported that nerolidol is a naturally occurring compound present in the oil of many plants with a floral odour. A recent study also revealed the presence of linalool and nerolidol and other compounds as constituents of essential oils in *Piper guineense* fruits (Akinbuluma, 2017).

In this study, linalool and nerolidol were highly repellent to *S. oryzae*, indicating that these compounds can actually exhibit a 'sniff and run' property on the insect. Olfactometry test, however, showed that linalool was more repellent than nerolidol to the insects. Muller *et al.* (2009) reported that linalool, among other compounds tested, significantly repelled more mosquitoes than untreated control, and Kim *et al.* (2010) also reported that linalool from origanum, produced 85% repellence to *Tribolium castaneum*.

5. Conclusions

This study concludes that linalool at 25 µL/mL was very effective in causing mortality and was highly repellent to adult *Sitophilus oryzae*. Therefore, the use of essential oils, especially their main components could be applicable to the management of *Sitophilus oryzae* and as a valid alternative to synthetic insecticides.

Acknowledgements

The authors are grateful to Dr. O. S. Olubode of the Department of Crop Protection and Environmental Biology, for his technical assistance during the course of this work. We also acknowledge the efforts of Dr. Olatunbosun Odu for assisting to conduct plagiarism test.

References

- Aboaba SA, Okunlola IO and Akinbuluma MD. 2019. Chemical constituents and insecticidal activity of the essential oils from *Cardiospermum grandiflorum* (Sweet) Sapindaceae on *Sitophilus zeamais*. *J Entomol. Zool*, 7: 1565-1569.
- Akhtar M, Raza AM, Iram N, Chaudhry MI and Azeem W. 2015. Effect of infestation of *Sitophilus oryzae* L. (Coleoptera: Curculionidae) on protein quality of rice under storage conditions. *Int J Agric Appl Sci*, 7:43-45.
- Akinbuluma MD and Ewete FK. 2014. Comparative efficacy of extracts of *Azadirachta indica* and *Piper guineense* with pirimiphos - methyl in the control of *Sitophilus zeamais* on stored maize. *J Biol Agric Health care*, 4: 327 - 335.
- Akinbuluma MD, Ewete FK and Torto B. 2017. Isolation and identification of compounds from *Piper guineense* seed extract for the management of *Sitophilus zeamais* on stored maize. Proceedings of the 1st All Africa Postharvest Congress and Exhibition, University of Nairobi, Kenya.

- Akinbuluma MD. 2017. Bioecology of *Sitophilus zeamais* on maize and its management with resistant varieties and bioactive compounds of *Piper guineense*. Ph.D Thesis, University of Ibadan, Nigeria.
- Akinbuluma MD. 2020. Volatile oils from *Cedrela odorata* L. as protectants against *Sitophilus zeamais* (Coleoptera: Curculionidae). *Am. J. Essent. Oil*, **8**: 20-29.
- Al Dawsari MM. 2020. Insecticidal potential of cardamom and clove extracts on adult red palm weevil *Rhynchophorus ferrugineus*. *Saudi J. Biol Sci*, **27**: 195–201.
- Ashamo MO and Ogungbite OC. 2014. Extracts of medicinal plants as entomocide against *Sitotroga cerealella* (Olivier) infestation on paddy rice. *J Med Plant Res*, **4**:1–7.
- Ayvaz A, Sagdic O, Karaborklu S, Ozturk I. 2010. Insecticidal activity of the essential oils from different plants against three stored-product insects. *J. Insect Sci*, **10**: 1-13
- Chang CL, Cho IK and Li QX. 2009. Insecticidal Activity of Basil Oil, trans-Anethole, Estragole, and Linalool to adult Fruit Flies of *Ceratitis capitata*, *Bactrocera dorsalis* and *Bactrocera cucurbitae*. *J Econ Entomol*, **102**: 203-209.
- El-Bakry AM, Abdel-Aziz NF, Sammour EA and Abdelgaleil SAM. 2016. Insecticidal Activity of Natural Plant Essential Oils against Some Stored Product Insects and Their Side Effects on Wheat Seed Germination. *Egypt J Biol Pest Control*, **26**: 83-88.
- Ferreira FM, Palmeira CM, Oliveira MM, Santos D, Simoes AM, Rocha SM, Coimbra MA and Peixoto F. 2012. Nerolidol effects on mitochondrial and cellular energetics. *Toxicol In Vitro*, **26**:189–196.
- Finney DJ. 1971. Probit Analysis. 3rd ed. Cambridge University Press, London.
- Garcia M, Donadel OJ, Ardanaz C.E, Tonn CE and Sosa ME. 2005. Toxic and repellent effects of *Baccharis salicifolia* essential oil on *Tribolium castaneum*. *Pest Manage Sci*, **61**: 612-618.
- Isman MB 2000. Plant essential oils for pest and disease management. *Crop Prot*, **19**: 603–608.
- Isman MB and Akhtar Y. 2007. Plant natural products as a source for developing environmentally acceptable insecticides. In: Ishaaya RN and Rami H (Eds)., *Insecticides design using advanced technologies*. Springer-Verlag, pp. 235-258.
- Khan HR, Halder PK. 2012. Susceptibility of six varieties of rice to the infestation of rice weevil, *Sitophilus oryzae* (L.) (Coleoptera: Curculionidae). *Dhaka Univ J Biol Sci*, **21**:163–168.
- Kim S, Yoon J, Jung JW, Hong K, Ahn Y and Kwon HW. 2010. Toxicity and repellency of origanum essential oil and its components against *Tribolium castaneum* (Coleoptera: Tenebrionidae) adults. *J Asia Pac Entomol*, **13**: 369–373.
- Lapczynski A, Letizia CS and Api AM. 2008. Fragrance material review on cis-nerolidol. *Food Chem Toxicol*. **46**: 245 - 246.
- Marimuth S, Gurusubramanian G and Krishna SS. 1997. Effect of exposure of eggs to vapours from essential oils on egg mortality, development and adult emergence in *Earias vittella* (F.) (Lepidoptera: Noctuidae). *Biol. Agric. Hortic*. **14**: 303-307.
- Mishra BB, Tripathi SP, Tripathi CPM 2012. Bioactivity of Two Plant Derived Essential Oils Against the Rice Weevils *Sitophilus oryzae* (L.) Coleoptera: Curculionidae). *Biol Sci*, **83**:171-175.
- Muller GC, Jummila A, Butler J, Kravchenko VD, Revay EE, Weiss RW, Schlein Y. 2009. Efficacy of the Botanical Repellents Geraniol, Linalool and Citronella Against Mosquitoes. *J Vector Ecol*, **34**: 2-8
- Ngamo TSL, Ngatanko I, Ngassoum MB, Mapongmestsem PM and Hance T, 2007c. Persistence of insecticidal activities of crude essential oils of three aromatic plants towards four major stored product insect pests. *Afr J Agric Res* **2**: 173-177.
- Nwaubani SI, Opit GP, Otitodun GO and Adesida MA. 2014. Efficacy of two Nigeria derived diatomaceous earths against *Sitophilus oryzae* (Coleoptera: Curculionidae) and *Rhyzopertha dominica* (Coleoptera: Bostrichidae) on wheat. *J Stored Prod Res* **59**: 9-16.
- Okpale C, Zakka U and Nwosu LC. 2021. Susceptibility of ten rice brands to weevil, *Sitophilus oryzae* L. (Coleoptera: Curculionidae), and their influence on the insect and infestation rate. *Bull Natl Res Cent*, **45**: 1-10.
- Paul A.V.N. 2007. 'Insect pests and their management'. Indian Agricultural Research Institute, New Delhi. <https://www.nsdlnisair.res.in> (April 29, 2007).
- Weaver DK, Dunkel FV, Ntezurubanza L, Jackson LL and Stock DT. 1991. The efficacy of linalool, a major component of freshly-milled *Ocimum canum* Sims (Lamiaceae), for protection against postharvest damage by certain stored product Coleoptera. *J Stored Prod Res*, **27**:213–220
- Wink M. 2008. Plant Secondary Metabolism: Diversity, Function and its Evolution. *Nat. Prod. Commun*, **3**:1205-1216.

Expression of Recombinant Lipase from *Serratia marcescens* LII61 in *Escherichia coli*

Sri Sumarsih^{1,*}, Fatimah^{2, 3}, Sofijan Hadi¹, Ni'matuzahroh^{2, 3}, Almando Gerald^{2, 3},
Rizka Diah Fitri², Gilva Illavi²

¹ Department of Chemistry, Universitas Airlangga, Surabaya, Indonesia; ² Department of Biology, Universitas Airlangga, Surabaya, Indonesia; ³ University Center of Excellence Research Center for Bio-molecule Engineering, Universitas Airlangga, Surabaya, Indonesia

Received: January 27, 2021; Revised: May 8, 2021; Accepted: June 15, 2021

Abstract

Recombinant lipase encoding gene of *Serratia marcescens* LII61 has been successfully expressed in *Escherichia coli*. The gene was amplified from genomic DNA of *S. marcescens* LII61 by PCR method using lipase specific primers. The amplified DNA was then subsequently inserted in pGEM®-T easy vector and transformed into *E. coli* JM109. The inserted DNA fragment in the plasmid was analyzed for studying the lipase gene sequence. The recombinant gene was subcloned in pET-28b(+) vector/ *E. coli* BL21(DE3) system. The positive clones were selected by growing *E. coli* cells in antibiotic medium and lipase-specific medium. The analysis of recombinant DNA showed that the lipase gene of *S. marcescens* LII61 was 1845 bp in size. The inserted gene in the pGEM-T easy vector was composed of 1842 bp lipase gene and flanked by several restriction enzyme as stated on the map vector. The recombinant *E. coli* BL21 (DE3) showed a fluorescent orange color on LB-IPTG-rhodamine B-olive oil agar plate, indicated that the recombinant bacteria were able to express the lipase gene from *S. marcescens* LII61. This report is the first endeavor on cloning and expression of lipase from Indonesian isolate of *S. marcescens*.

Keywords: Lipase, Recombinant Protein, *Serratia marcescens*, *Escherichia coli*,

1. Introduction

Microbial lipases have received special attention from biotechnology industries and been widely used in synthesis of organic compounds because the enzymes are selective, substrate-specific, stable to organic solvents, and due to regio/stereo-selectivity (Sharma et al., 2001; Hasan et al., 2006; Thakur, 2012; Andualema and Gessesse, 2012; Borrelli and Trono, 2015). Microbial lipase has been widely studied by researchers, both in terms of structure, characteristic, production, increasing productivity, development, and exploration of producing microorganisms as a new source for lipase production. Several bacteria and fungi isolated from various sources were potential lipase producers; for example, *Micrococcus luteus* L69 Microbial lipase has been widely studied by researchers, both in terms of structure, characteristic, production, increasing productivity, development, and exploration of producing microorganisms as a new source for lipase production. Several bacteria and fungi isolated from various sources were potential lipase producers; for example, *Micrococcus luteus* L69 isolated from POME-contaminated soil (Sumarsih et al., 2020), *Mycobacterium* sp. isolated from pulp and paper mill effluent (Tripathi et al., 2014), *Sporobolomyces salmonicolor* OVS8 from oil mill spillage (Thabet et al., 2012). Several genera of bacteria and fungi have been screened as sources of lipase

in large-scale production, including *Bacillus*, *Achromobacter*, *Alcaligenes*, *Arthrobacter*, *Pseudomonas*, *Penicillium*, *Fusarium*, *Aspergillus* (Chandra et al., 2020). Microbial enzymes are easy to produce in large quantities, easily manipulated genetically, have high activity in various environmental conditions and are very useful in a variety of industrial applications (Andualema and Gessesse, 2012). However, native microbial enzymes have many disadvantages, including non-reproducibility, low yield for certain bio-catalytic processes and requiring optimization of conditions. This disadvantage can be overcome by using molecular technology for recombinant proteins production, which allows the catalytic improvement, protein over-expression and production (Borrelli and Trono, 2015).

The Gram-negative enteric bacterium *Serratia marcescens* represent as one of best lipase producers, in particular Family I.3 lipase (Borrelli and Trono, 2015, Lee et al., 2007). Several strains *S. marcescens* had been explored for lipase production (Mohanasrinivasan et al., 2018; Nwachukwu et al., 2017). The extracellular lipases are widely used as biocatalyst in enantioselective hydrolysis and synthesis of many chiral drug precursors. *S. marcescens* ES-2 showed high enantioselectivity for (S)-flurbiprofen (Lee et al., 2007). Lipase from *S. marcescens* ECU1010 used in asymmetric synthesis of trans-3-(4-methoxyphenyl) glycidic acid methyl ester] (Shibatani et al., 2000; Zhao et al., 2010).

* Corresponding author e-mail: sri-sumarsih@fst.unair.ac.id.

Serratia marcescens strain LII61 was isolated from slaughterhouse waste in North Surabaya Indonesia, was a good lipase and biosurfactant producer (Ni'matuzahroh et al., 2017; Renjana et al., 2017). The bacterium was a potent bacterial for oil sludge cleaning agent, showed oil sludge dissolving activity by $86.38 \pm 2.39\%$ (Ni'matuzahroh et al., 2017). The bacteria isolate LII61 showed unique character, had variable gram characters, indicated by the change in color of the cell wall resulting from gram staining at the observed age of the culture (Fatimah et al., 2019). The isolate was similar (99%) to *S. marcescens* based on its 16S ribosomal RNA gene sequence (Renjana et al., 2017; Fatimah et al., 2019).

Serratia marcescens is human opportunistic pathogen (Haddix and Shanks, 2017; Takayama and Kato, 2020). Therefore, a recombinant production in relatively safer bacterial strain is needed for future mass production and industrial application, especially in foods, pharmaceutical, and cosmetic industries. In this first effort on constructing recombinant *E. coli* strain expressing lipase from Indonesia *S. marcescens* isolate, lipase-encoding gene was amplified from *S. marcescens* LII61 genome, then inserted in plasmid pGEM[®]-T easy and expressed in pET-28b(+)/*Escherichia coli* system.

2. Materials and Methods

2.1. Bacteria, Plasmid and Media

The bacteria *S. marcescens* LII61 (GenBank accession number of 16S ribosomal RNA gene: MK702080.1) was used as a source of lipase gene, was grown on nutrient agar medium. The bacteria used as host cells in the cloning process, *E. coli* JM109 and *E. coli* BL21 (DE3), were grown in Luria Bertani (LB) medium (1% NaCl, 1% tripton and 0.5% yeast extract). The plasmids used as vectors for construction of recombinant DNAs were pGEM[®]-T Easy (Promega) and pET-28b(+) (Novagen). Medium used for selection of recombinant *E. coli* strain was LB agar supplemented with 50 mg/mL X-gal (5-bromo-4-chloro-3-indolyl-beta-D-galacto-pyranoside), 100mM IPTG (isopropyl-β-D-thiogalacto-pyranoside) and suitable antibiotics. The medium used in the lipase expression test was LB agar supplemented 100mM IPTG and 50 µg/mL kanamycin, olive oil and rhodamin-B.

2.2. Lipase gene amplification

Lipase gene was amplified from genomic DNA of *S. marcescens* LII61 using forward primer (lip-F) 5'-GGCCAGGCGGCATAATTC-3' and reverse primer (lip-R) 5'-GGCCAACACCACCTGATCG-3' (Lee et al., 2007). The components in the PCRmix consisted of Go Taq[®] Green Master Mix (Promega), primers, genomic DNA, Nuclease-Free Water. The thermal cycling process was initiated by pre-denaturation for 2 minutes at 95 °C. The PCR process was carried out in 35 cycles with the conditions of each cycle: 95 °C-denaturation for 30 seconds, 49.4 °C- annealing for 45 seconds, 72 °C-extension for 1 minute. The PCR product was then purified using GenElute™ Gel Extraction Kit (Sigma Aldrich) and sent to 1st Base Laboratories, Malaysia for sequencing.

2.3. Cloning and nucleotide sequence analysis of lipase gene

The purified PCR product was inserted into pGEM[®]-T easy vector, then transformed into *E. coli* JM109 host cells (Promega). The mixture containing recombinant DNA was spread on solid LB media supplemented with Ampicillin (100 µg/mL), IPTG (100 mM) and X-gal (20 µg/mL) followed by incubation at 37 °C for overnight. The presence of recombinant pGEM[®]-T plasmid (pGEM-lip) in the white colonies were verified using colony PCR method (Woodman, 2008).

pGEM-lip were isolated from the positive clones using The Wizard[®] Plus SV Minipreps DNA Purification System (Promega) and sent to 1st Base Laboratories, Malaysia for sequencing. The analysis of DNA sequences was performed using BioEdit (version 7.2.5) software. The translated amino acid sequence of the lipase gene of *S. marcescens* LII61 was then aligned with other sequences of *S. marcescens* strains lipase using BLASTp (<https://blast.ncbi.nlm.nih.gov/Blast.cgi>).

2.4. Subcloning of recombinant lipase

The recombinant plasmid pGEM-lip was digested out using restriction enzyme *Eco*RI. The digested-lipase gene was ligated using T4 DNA ligase into *Eco*RI digested-pET28b(+) plasmid, then transformed into *E. coli* BL21 (DE3). The transformant then was inoculated onto LB agar containing kanamycin (50 µg/ml) and incubated at 37°C for 18 hours. The bacterial clones were picked and inoculated onto lipolytic specific medium, LB agar containing kanamycin (50 µg/ml), 100 mM IPTG, olive oil, and rhodamine B. Recombinant *E. coli* BL21 (DE3) that produced and excreted recombinant lipase showed a fluorescent orange color under UV light. This condition proved recombinant *E. coli* BL21 harboring recombinant plasmid with *S. marcescens* LII61 lipase (pET28b-lip.)

3. Results

3.1. Construction of recombinant gene

Lipase gene of *S. marcescens* LII61 was successfully amplified. Single band of approximately 1800 bp was observed in the electropherogram shown in Figure 1.

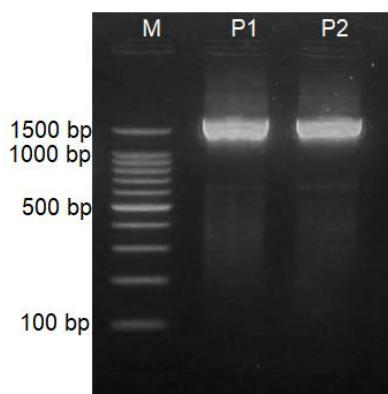


Figure 1. Agarose electropherogram of lipase gene from *S. marcescens* LII61 (P1 and P2).M: DNA ladder 100 bp

The analysis of PCR product, showed a coding sequence of 1845 bp has been amplified from *S. marcescens* LII61 genome. The sequence of the PCR product showed highly similarities to sequence of *S. marcescens* strain ECU1010 extracellular lipase lipA gene (99.73%) (GenBank Acc. No. DQ884880.1) and lipase lipB gene (99.46%) (GenBank Acc. No. HM440338.1).

The PCR product was successfully inserted into the pGEM[®]-T easy/ *E. coli* JM109 system, which was shown by the presence of white colonies on LB medium containing ampicillin, IPTG and X-gal after incubation for 20 hours. The presence of target gene in the recombinant plasmids was confirmed by colony PCR using the lipase-specific primers (Lee *et al.*, 2007). The presence of PCR product of approximately 1800 bp indicated that the picked

recombinant *E. coli* JM109 colonies carried the target lipase gene.

The sequencing of recombinant plasmid was performed using universal primers T7 and SP6, as well as a pair of lipase-specific primers, lip-F and lip-R, for the determining the entire nucleotide inserted in the recombinant pGEM[®]-T easy. Nucleotide sequence analysis revealed the cloned insert in the pGEM[®]-T easy plasmid was 1874 bp containing lipase gene starting at 32th nucleotide. The sequence of inserted gene was identical to the sequence gene encoding lipase of *S. marcescens* LII61. According to the pGEM-T easy vector map, the cloned insert is flanked by several restriction enzyme sequences, as shown in the schematic in Figure 2.

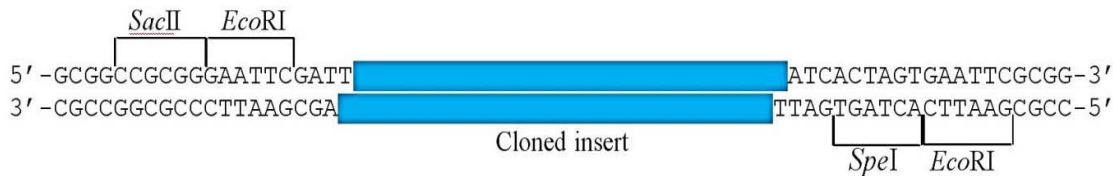


Figure 2. Scheme of cloned insert in pGEM[®]-T easy vector

Based on sequence analysis, the lipase gene inserted in the pGEM(R)-T plasmid consisted of 1842 bp nucleotides which encode a protein composed of 614 amino acids which was predicted to have a molecular weight of 64.8 KDa. Protein analysis using Basic Local Alignment Search Tool (<https://blast.ncbi.nlm.nih.gov/Blast.cgi>) revealed that the recombinant lipase have high similarity to

extracellular lipase of *S. marcescens* GenBank Accession no. ABI83633.1 (99.67%) and ADI77082.1 (99.02%). Based on amino acids sequence, the relationships of recombinant lipase to the other deposited lipase in GenBank shown in Figure 3. The phylogenetic tree was constructed using MEGA X program.

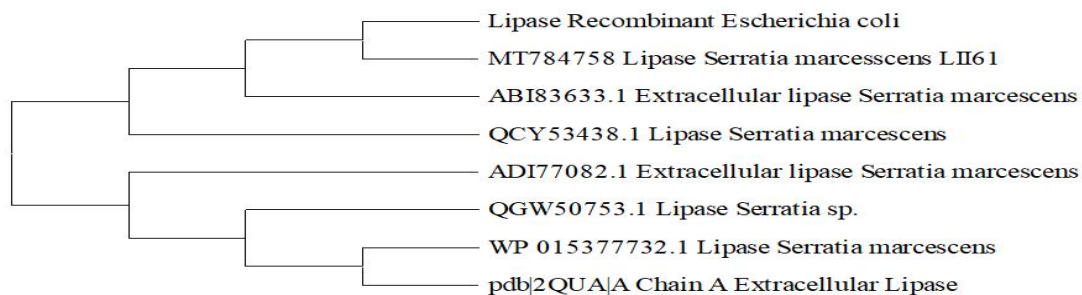


Figure 3. Relationships of recombinant lipase to the other deposited lipase in GenBank

3.2. Expression of lipase in *E. coli* BL21

The lipase gene constructed into *EcoRI* site in pET28b(+) vector. The constructed recombinant plasmid pET28b-lip is shown in Figure 4.

The recombinant plasmid pET28b-lip was transformed in competent cells of *E. coli* BL21(DE3). The positive cloned bacteria were collected from solid antibiotic-LB media. Lipase expression was detected by cultivating the recombinant *E. coli* cells in the lipolytic specific medium containing IPTG as an inducer. The presence of IPTG in the LB medium induced recombinant bacteria to express the lipase gene. The positive clone, harboring pET-28b-lip capable expressed the lipase gene, gives an orange fluorescent at bacterial culture.

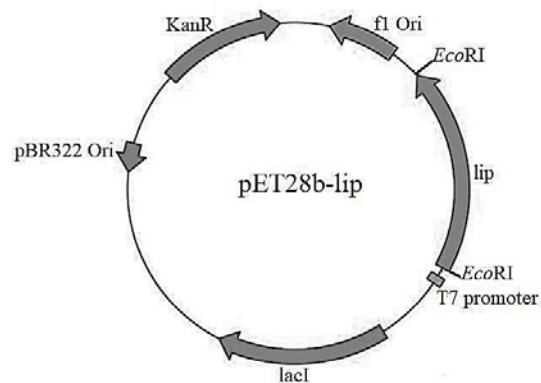


Figure 4. The map of recombinant plasmid pET28b-lip

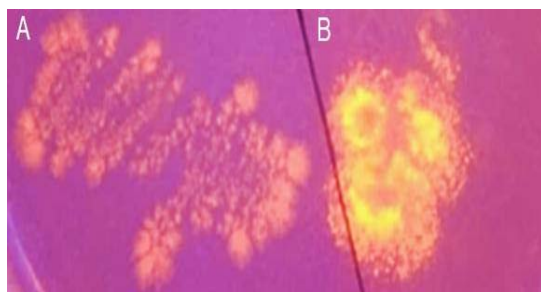


Figure 5. Recombinant *E. coli* BL21 (DE3) (A), and *S. marcescens* LII61 (B) cells grown on LB-olive oil-rhodamine B agar plate

Figure 5. showed recombinant *E. coli* BL21 (DE3) and *S. marcescens* LII61 cells appeared grown well on lipase-specific medium. The production of extracellular lipase is indicated by the presence of a fluorescent orange color around the colony that is visible under UV light. The cationic form of indicator dyes reacts with free fatty acids to form complex orange fluorescent compounds which excite at 350 nm (Lanka and Latha, 2015). The recombinant bacteria colonies showed a fluorescent orange color under UV light indicated that the lipase gene from *S. marcescens* LII61 produced extracellularly. Meanwhile, *S. marcescens* LII61 cells as the source of the lipase gene showed mixed color (yellow and orange), because bacteria produce Prodigiosin which gives bacteria a red color, which appears yellow under UV light as shown at Figure 5.

4. Discussion

Here, the first endeavors to clone and express recombinant lipase from Indonesian isolate of *S. marcescens* (strain LII61) were presented. The lipase-encoding gene from *S. marcescens* LII61 was successfully constructed in pET-28(+) vector and transformed into *E. coli* BL21(DE3) for further expression and mass production studies. The amino acid sequence of the recombinant lipase from *S. marcescens* strain LII61 showed high similarity to extracellular lipase of *S. marcescens* ECU1010, which was utilized to produce anti-inflammatory drug (S)-ketoprofen (Long *et al.*, 2007).

Furthermore, the lipase expression test using LB-IPTG-rhodamine B-olive oil agar plate indicated that the recombinant lipase produced extracellularly in *E. coli* BL21(DE3). This result is interesting due to the fact that recombinant proteins are usually expressed intracellularly in *E. coli* (Fakruddin *et al.*, 2013; Ma *et al.*, 2020). Moreover, in various studies, recombinant *S. marcescens* lipase in *E. coli* were reported to be expressed intracellularly (Su *et al.*, 2014; Mohammadi *et al.*, 2016; Chen *et al.*, 2017; Yin *et al.*, 2020)

As previously reported, *S. marcescens* LII61 lipase exhibited high activity (Ni'matuzahroh *et al.*, 2017; Renjana *et al.*, 2017). However, the industrial application of the lipase is hampered by the pathogenicity of *S. marcescens*. Recombinant production *S. marcescens* LII61 lipase in *E. coli* BL21(DE3) and other Generally Recognized as Safe (GRAS) microorganisms is critical for the development of the lipase as industrial enzyme. In the future study, the mass production, purification, kinetics study, and substrate conversion using recombinant *S. marcescens* LII61 lipase need to be conducted.

5. Conclusion

Lipase encoding gene from *S. marcescens* LII61, which was isolated from slaughterhouse waste in Indonesia, was successfully cloned and constructed into pET-28(a) plasmid. The extracellular expression of the lipase gene was observed based on assay on LB-IPTG-rhodamine B-olive oil agar plate.

Acknowledgment

The authors would like to thank Direktorat Riset dan Pengabdian kepada Masyarakat, Deputi Penguatan Riset dan Pengembangan, Kementerian Riset dan Teknologi / Badan Riset dan Inovasi Nasional Indonesia for funding this research.

References

- Andualema B and Gessesse A. 2012. Microbial lipases and their industrial applications: review. *Biotechnology.*, **11**(3):100-118.
- Borrelli GM and Trono D. 2015. Recombinant lipases and phospholipases and their use as biocatalysts for industrial applications. *Int. J. Mol. Sci.*, **16**:20774-20840. doi:10.3390/ijms160920774.
- Chandra P, Singh R, and Arora PK. 2020. Microbial lipases and their industrial applications: a comprehensive review. *Microb Cell Fact.*, **19**:169. doi:10.1186/s12934-020-01428-8.
- Chen KC, Zheng MM, Pan J, Li CX, and Xu JH. 2017. Protein engineering and homologous expression of *Serratia marcescens* lipase for efficient synthesis of a pharmaceutically relevant chiral epoxyester. *Appl Biochem Biotechnol.*, **183**(2):543-54. doi:10.1007/s12010-017-2543-z.
- Fakruddin M, Mohammad Mazumdar R, Bin Mannan KS, Chowdhury A, and Hossain M. 2013. Critical factors affecting the success of cloning, expression, and mass production of enzymes by recombinant *E. coli*. *Int Sch Res Notices.*, **2013**:1-7. doi:https://doi.org/10.5402/2013/590587
- Fatimah, Fitri RD, Illavi G, Renjana E, Pratiwi IA, Ni'matuzahroh, and Sumarsih S. 2019. Cell wall response of bacteria *Serratia marcescens* LII61-lipase and protease producer-in gram staining. *Ecol Environ Conserv.*, **25**(Suppl. Issue):S76-S80.
- Haddix PL and Shanks RMQ. 2018. Prodigiosin pigment of *Serratia marcescens* is associated with increased biomass production. *Arch Microbiol.*, **200**:989-999. doi:10.1007/s00203-018-1508-0.
- Hasan F, Shah AA, and Hameed A. 2006. Industrial applications of microbial lipases. *Enzyme Microb Technol.*, **39**:235-251. doi:10.1016/j.enzmictec.2005.10.016
- Lanka S and Latha NL. 2015. A short review on various screening methods to isolate potential lipase producers: lipase the present and future enzymes of biotech industry. *Int J Biol Chem.*, **9**(5):207-219. doi:10.3923/ijbc.2015.207.219.
- Lee KW, Bae HA, and Lee YH. 2007. Molecular cloning and functional expression of *esf* gene encoding enantioselective lipase from *Serratia marcescens* ES-2 for kinetic resolution of optically active (S)-flurbiprofen. *J Microbiol Biotechnol.*, **17**(1):74-80.
- Long ZD, Xu JH, Zhao LL, Pan J, Yang S, and Hua L. 2007. Overexpression of *Serratia marcescens* lipase in *Escherichia coli* for efficient biorevolution of racemic ketoprofen. *J Mol Catal B Enzym.*, **47**(3-4):105-10. doi:10.1016/j.molcatb.2007.04.004.

- Ma Y, Lee CJ, and Park JS. 2020. Strategies for optimizing the production of proteins and peptides with multiple disulfide bonds. *Antibiotics*, **9(9)**:541. doi:10.3390/antibiotics9090541.
- Mohammadi M, Sepchrizadeh Z, Ebrahim-Habibi A, Shahverdi AR, Faramarzi MA, and Setayesh N. 2016. Enhancing activity and thermostability of lipase A from *Serratia marcescens* by site-directed mutagenesis. *Enzyme Microb Technol.*, **93**:18-28. doi: 10.1016/j.enzmictec.2016.07.006.
- Mohanasinivasan V, Devi CS, Jayasmita D, Subathra C, Selvarajan E, and Naine SJ. 2018. Purification and characterization of extracellular lipase from *Serratia marcescens* VITS2. *Proc Natl Acad Sci India B.*, **88**:373–381.
- Ni'matuzahroh, Pratiwi IA, Surtiningsih T, Fatimah, and Sumarsih S. 2017. The potency of *Micrococcus* sp. LII61 bacteria as oil sludge cleaning agent. *J Biol Res.*, **22(2)**:38-42.
- Nwachukwu E, Ejike EN, Ejike BU, Onyeonula EO, Chikezie-Abba RO, Okorocho NA, and Onukaogu. 2017. Characterization and optimization of lipase production from soil microorganism (*Serratia marcescens*). *Int J Curr Microbio. App Sci.*, **6(12)**:1215-1231.
- Renjana E, Helga L, Fatimah, Sumarsih S, and Ni'matuzahroh. 2017. Co-Utilization of molasse and glycerol as carbon sources on the production of biosurfactant by isolate bacteria LII61. *J Appl Environ Biol Sci.*, **7(11)**:174-180.
- Sharma R, Christi Y, and Banerjee UC. 2001. Production, purification, characterization, and applications of lipases. *Biotechnol. Adv.*, **19(8)**:627-662. doi:10.1016/S0734-9750(01)00086-6.
- Shibatani T, Omori K, Akatsuka H, Kawai E, and Matsumae H. 2000. Enzymatic resolution of diltiazem intermediate by *Serratia marcescens* lipase: molecular mechanism of lipase secretion and its industrial application. *J. Mol. Catal. B Enzym.*, **10(1)**:141-149. doi: 10.1016/S1381-1177(00)00122-3.
- Su E, Xu J, and You P. 2014. Functional expression of *Serratia marcescens* H30 lipase in *Escherichia coli* for efficient kinetic resolution of racemic alcohols in organic solvents. *J Mol Catal B Enzym.*, **106**:11-6. doi:10.1016/j.molcatb.2014.04.012.
- Sumarsih S, Fatimah, Hadi S, Adhiningsih RT, and Prasetyo FE. 2020. Characterization and lipase production of *Micrococcus* sp. L69 isolated from palm oil-contaminated. *Asian J. Water, Environ. Pollut.*, **17(3)**:77-80. doi:10.3233/AJW200040.
- Takayama Y and Kato N. 2020. Inhibition of quorum sensing in opportunistic pathogen, *Serratia marcescens*, using cyclodextrin-immobilized, multiple parallel gel filaments fabricated with dynamic flow of polymer blend solution. *Mater Sci Eng C*. **107**:110331. doi:10.1016/j.msec.2019.110331.
- Thabet HM, Pasha C, Ahmed MM, and Linga VR. 2012. Isolation of novel lipase producing *Sporobolomyces salmonicolor* OVS8 from oil mill spillage and enhancement of lipase production. *Jordan J Biol Sci.*, **5(4)**:301-306.
- Thakur S. 2012. Lipase, its sources, properties and applications: a review. *Int J Sci Eng Res.*, **3(7)**:1-21.
- Tripathi R, Singh J, Bharti RK, and Thakur IS. 2014. Isolation, purification and characterization of lipase from *Microbacterium* sp. and its application in biodiesel production. *Energy Procedia.*, **54**:518 – 529. doi:10.1016/j.egypro.2014.07.293.
- Woodman ME. 2008. Direct PCR of intact bacteria (colony PCR). *Curr Protoc Microbiol.*, **9**: A.3D.1-A.3D.6. doi: 10.1002/9780471729259.mca03ds9.
- Yin YC, Li HQ, and Wu XS. 2020. Refolding with simultaneous purification of recombinant *Serratia marcescens* lipase by one-step ultrasonication process. *Appl Biochem Biotechnol.*, **21**:1-4. doi:10.1007/s12010-019-03172-1.
- Zhao LL, Pan J, and Xu JH. 2010. Efficient production of diltiazem chiral intermediate using immobilized lipase from *Serratia marcescens*. *Biotechnol Bioprocess Eng.*, **15**:199-207. doi:10.1007/s12257-009-0173-1.

Bioactivity of *Moringa oleifera* and Albumin Formulation in Controlling TNF- α and IFN- γ Production by NK Cells in Mice Model Type 1 Diabetes

Noviana Dwi Lestari, Anita Chanisya Rahmah, Wahyu Isnia Adharini, Ruri Vivian Nilamsari, Yoga Dwi Jatmiko Nashi Widodo, Sri Rahayu, Muhaimin Rifa'i*

¹Biology Department, Faculty of Mathematics and Natural Sciences, Brawijaya University, Jl. Veteran Malang, 65145, Malang, Jawa Timur, Indonesia.

Received: February 1, 2021; Revised: May 9, 2021; Accepted: May 31, 2021

Abstract

Type 1 diabetes (T1D) is a disease caused by pancreatic beta-cell injury due to high pro-inflammatory cytokines. TNF- α and IFN- γ are pro-inflammatory cytokines that play a role in T1D progression. *Moringa oleifera* (MO) and albumin (A) have anti-inflammatory and antidiabetic effects. The combination of both can work synergistically in suppressing the production of pro-inflammatory molecules. This study was conducted using five different groups (healthy mice, T1D, D1, D2, and D3). A dose of 145 mg/kg BW streptozotocin was used to induce T1D in mice. *Moringa oleifera* and albumin formulation (MOA) were orally administered for 14 days. Dose 1 (800 mg/kg MO:800 mg/kg A), dose 2 (615 mg/kg MO:615 mg/kg A), and dose 3 (800 mg/kg MO:615 mg/kg A). On day 15, hepatic cells from mice were isolated post-treatment, and the profile of NK⁺TNF- α ⁺ and NK⁺IFN- γ ⁺ were analyzed by flow cytometry. This study reports that MOA administered in D3 more effectively suppresses TNF- α and IFN- γ produced by NK cells. MOA could be synergies work to decrease or suppress the level TNF- α and IFN- γ in T1D. So, administered MOA had the potential to be used as an alternative medicine for DM.

Keyword: *Moringa oleifera*, pro-inflammatory, T1D, TNF- α , IFN- γ

1. Introduction

Type 1 diabetes (T1D) is a disease caused by the destruction of pancreatic beta cells resulting in an absolute or relative deficiency in insulin production. The poverty of insulin leads to hyperglycemia (Simmons and Michels, 2015). The failure of pancreatic beta cells to produce insulin is closely related to NK and regulatory T cell function loss (Graham *et al.*, 2012). Infiltration of autoreactive T cells and Natural Killer (NK) cells in Langerhans islets lead to the progression of diabetes because of the increased secretion of pro-inflammatory cytokines (Nekoua *et al.*, 2020). *Tumor Necrosis Factor-Alpha* (TNF- α) dan *Interferon-Gamma* (IFN- γ) are pro-inflammatory cytokines most prominent produced by NK cells (Fauriat *et al.*, 2010). NK cells are one of the immunocompetent cells that increased inflammatory progression in diabetes mellitus (DM) by producing TNF- α and IFN- γ . Increased pro-inflammatory cytokines can cause chronic inflammation in the tissue (Abel *et al.*, 2018).

The high levels of TNF- α could induce dendritic cell activation that causes activation of T cells, which are

mediators of damage to pancreatic β cells (Lee *et al.*, 2005). TNF- α can activate the transcription factor nuclear factor kappa-light-chain-enhancer of activated B cells (NF- κ B) which plays a role in the secretion of pro-inflammatory cytokines (Patel and Santani, 2009). IFN- γ and TNF- α play a role in autoimmunity in DM and apoptosis of pancreatic β cells. The increase in IFN- γ causes activation of macrophages and CD8 T cells, which causes damage to pancreatic β cells through TNF- α and interleukin (IL)-1 β secretion (Tsiavou *et al.*, 2004). T1D is disease-related with numerous factors such as genetic, environmental, low insulin production due to pancreatic B cell damage, and uncontrolled secretion of pro-inflammatory cytokines (Marrack *et al.*, 2001; Cerf, 2013). Based on these factors, an effective treatment is needed in treating DM. Currently, treatment focuses on managing blood sugar levels with insulin and synthetic drug consumption to prevent complications. However, as we know, long-term use of synthetic drug lead to harmful side effects. Natural treatment is considered due to having many benefits without causing harmful side effects.

In this experiment, we have the purpose of investigating the effect of MOA on the T1D mice model

* Corresponding author e-mail: immunobiology@ub.ac.id.

** **Abbreviations:** ANOVA: analysis of variance; BW: body weight; DM: diabetes mellitus; H₂O₂: hydrogen peroxide; IFN- γ : Interferon-Gamma; IL: interleukin; MO: *Moringa oleifera*; NF- κ B: transcription factor nuclear factor kappa-light-chain-enhancer of activated B cells; NK: Natural Killer; PB: peripheral blood; PBS: phosphate buffer saline; SH: sulfhydryl; STAT4: signal transducer and activator of transcription 4; STZ: streptozotocin; T1D: Type 1 diabetes; TACE: tumor necrosis factor-alpha converting enzyme; TNF- α : Tumor Necrosis Factor-Alpha

through to control the TNF- α and IFN- γ production by NK cells. MOA consists of a combination of *Moringa oleifera* and Toman fish albumin (*Channa micropeltes*). Combining natural ingredients is expected to form a complex that works synergistically to maximize the natural compound's efficacy. *Moringa oleifera* has been known as a traditional medicine in various kinds of diseases. The effectiveness of *Moringa oleifera* was attributed to bioactive compounds such as phenol, flavonoid, alkaloid, glucosinolate, β -sitosterol-3-O- β -D-glucoside, isothiocyanate, tannin, terpenoid, and saponin (Lopez *et al.*, 2018). In addition, MO has many beneficial properties such as anti-inflammatory, antimicrobial, antioxidant, anticancer, cardiovascular, antidiabetic, and diuretic effects (Osman *et al.*, 2012; Bhattacharya *et al.*, 2018). Albumin from fish can serve as an alternative to fulfill albumin in the body. Moreover, albumin has a group sulfhydryl (-SH), which plays a role and functions as a free-radical scavenger (Quilan *et al.*, 2005).

2. Materials and Methods

2.1. Experimental animals protocol

Animals used in this experiment were male BALB/c mice, obtained from Malang Murine Farm, Singosari, Malang, East Java, Indonesia. A total of 25 normal BALB/c male mice were 8-10 weeks with body weight (BW) around 25-30 g maintained in a pathogen-free chamber with controlled conditions. They had free access to standard pellet feed and water daily during the experiment period. Experimental mice were divided into five treatment groups: healthy mice, T1D mice model, and T1D mice model administered with three different doses (D1, D2, and D3). These experiments' protocols were carried out and internationally accepted and permitted by the Ethical Committee of Brawijaya University, Malang, Indonesia (Reg. No. 1180-KEP-UB).

2.2. Animal models type 1 diabetes

The induction of T1D was conducted by DiaComp Protocols (Brosius, 2015) with modification. T1D was induced by a single intraperitoneal (i.p.) injection of freshly prepared streptozotocin (STZ) (Bioworld, USA) at a dose of 145 mg/kg BW in 0.1 M citrate buffer (pH 4.5). The mice fasted for 4-6 hours before injection. The blood glucose levels were measured at six days post-injection of STZ with a glucometer. Mice were considered to suffer from diabetes if blood glucose level ≥ 200 mg dL⁻¹.

2.3. Preparation and oral treatment of *Moringa oleifera*-Albumin combination

MOA consists of a combination of *Moringa oleifera* and albumin from Toman fish (*Channa micropeltes*). *Moringa oleifera* (MO) leaves were collected from the Materia Medica Batu, Malang, Indonesia. A total of 50 g of MO powder were boiled in 500 mL of water for 5 minutes and filtered to obtain MO extract before stored in a freezer at -80°C for 24 hours. The frozen extract was then evaporated with a freeze dryer. Albumin was obtained from IFALMIN[®] manufactured by Ismut Fitomedika,

Makassar, Indonesia. IFALMIN[®] is a product derived from Toman fish extract. MOA combination was given orally to T1D mice for 14 days with three different doses. All doses we showed here are adjusted to mg/kg BW. Dose 1 (800 mg/kg BW MO:800 mg/kg BW A), dose 2 (615 mg/kg BW MO:615 mg/kg BW A), and dose 3 (800 mg/kg BW MO:615 mg/kg BW A). On day 15, all of the mice were sacrificed post-treatment for flow cytometry analysis.

2.4. Isolation of liver organ and Flow cytometry analysis

On day 15 of this experiment, the mice were sacrificed by dislocation and then dissected for liver isolation. In our study, we used the liver for analysis of the NK cell that produces TNF- α and IFN- γ . According to Sun *et al.* (2013), the percentage of NK cells in the liver is higher than in the spleen and peripheral blood (PB). The liver was isolated and washed in a petri dish containing sterile phosphate buffer saline (PBS). Cells from mice's liver were isolated by crushing liver in PBS. The cell suspension was removed to the polypropylene tube, and added with PBS. Homogenates of the cell were centrifuged at 2500 rpm, 10 °C, for 5 min. Pellet was resuspended in 1 mL of PBS and divided into 1 mL microtube. Intracellular cytokine staining was performed with a Cytotfix/Cytoperm kit (Biolegend BD Sciences) according to the protocol presented by the manufacturer. Cells were incubated with anti-TNF- α and anti-IFN- γ antibodies. Before intracellular staining, cells were subjected to surface molecules staining with anti-NK. The antibodies were applied at a concentration of 0.005 mg/100 μ L. The cells stained with extracellular and intracellular antibodies were added with PBS of 300-500 μ L and transferred to cuvettes to be analyzed with flow cytometry.

2.5. Data Analysis

The data from flow cytometry were analyzed by BD. cell quest PRO[™] software, then tabulated using Microsoft Excel for statistical analysis. The statistical analysis was executed by SPSS version 16 for windows. Data were analyzed using a one-way analysis of variance (ANOVA) ($p \leq 0.05$) followed by the Tukey test to decide the significant difference among treatments.

3. Results

T1D mouse groups models had the highest profile of cytokine pro-inflammatory than the normal groups ($p \leq 0.05$), including the relative number of TNF- α and IFN- γ production by NK cells (NK⁺TNF- α ⁺ and NK⁺IFN- γ ⁺). T1D mouse groups were treated using three different doses of MOA. All of the doses giving various effects after post-treatment in suppressing TNF- α and IFN- γ production by NK cells. D1 and D3 have a significant impact on decreasing the relative number of NK⁺TNF- α ⁺ (figure 1). Meanwhile, D2 does not have a significant impact. Furthermore, D2 and D3 were significantly able to reduce the relative number of NK⁺IFN- γ ⁺ compared to D1 (figure 2). Thus, in this study, D3 as a whole affected suppressing TNF- α and IFN- γ expressed by NK cells.

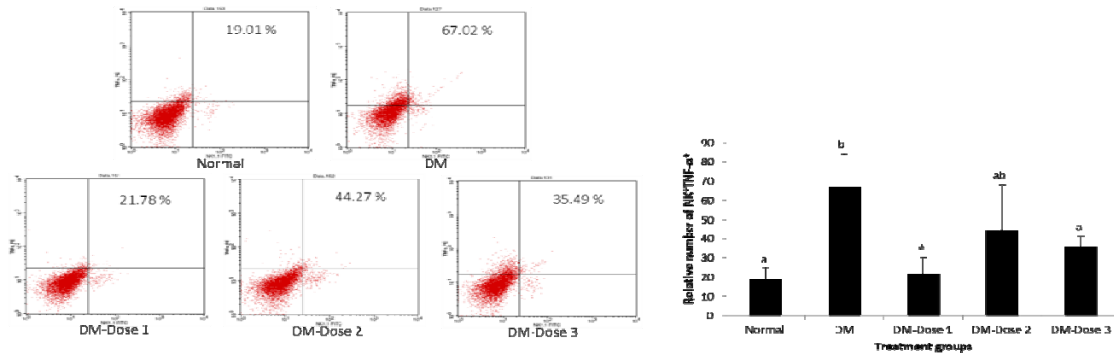


Figure 1. The administration of MOA in T1D mice model can suppress the relative number of NK⁺TNF- α ⁺. Normal = healthy mice; T1D = mice STZ induced; D1 = T1D + dose 1 (800 mg/kg BW (MOL) : 800 mg/kg BW (I)); D2 = T1D + dose 2 (615 mg/kg BW (MOL) : 615 mg/kg BW (I)); D3 = T1D + D3 (800 mg/kg BW (MOL) : 615 mg/kg BW (I)). Mice were sacrificed and analyzed using flow cytometry (left) on day 15 and tabulated into Microsoft Excel (right). The data are mean+SD in each group with p value ≤ 0.05 .

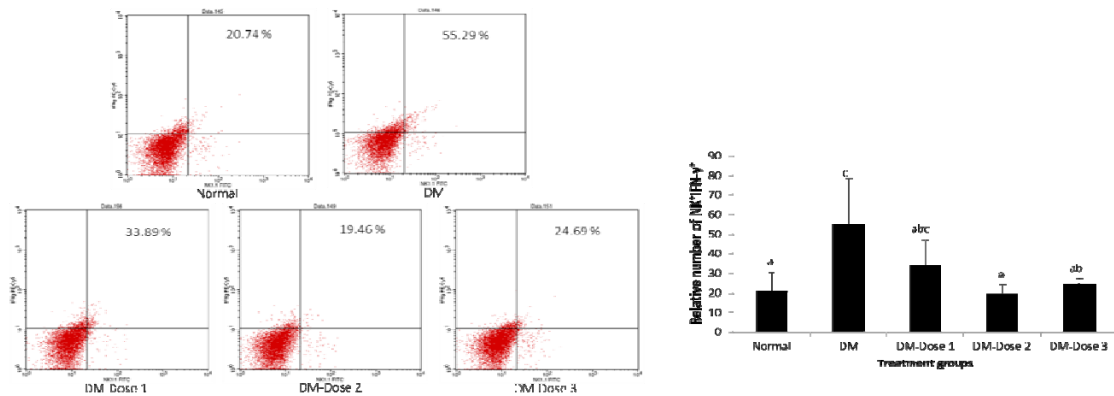


Figure 2. The administration of MOA in T1D mice model can suppress the relative number of NK⁺IFN- γ ⁺. Normal = healthy mice; T1D = mice STZ induced; D1 = T1D + dose 1 (800 mg/kg BW (MOL) : 800 mg/kg BW (I)); D2 = T1D + dose 2 (615 mg/kg BW (MOL) : 615 mg/kg BW (I)); D3 = T1D + D3 (800 mg/kg BW (MOL) : 615 mg/kg BW (I)). Mice were sacrificed and analyzed using flow cytometry (left) on day 15 and tabulated into Microsoft Excel (right). The data are mean+SD in each group with p value ≤ 0.05 .

4. Discussion

T1D is also known as insulin-dependent diabetes mellitus (IDDM) (Arora *et al.*, 2009). People with T1D generally rely on insulin injections to regulate their sugar metabolism. Type I diabetes resulted from deficiency or failure of the pancreatic islet to secrete insulin. Insulin is a hormone with a pivotal role that served the body to make blood glucose available to cells (Rifa'i *et al.*, 2018). If the levels of insulin are low in the long term, it will cause hyperglycemia. Hyperglycemia is a condition of high blood glucose levels exceeding normal limits (Balakrishnan *et al.*, 2012; Mohamed *et al.*, 2016), resulting in oxidative stress that causes tissue damage in the liver. Tissue damage in the liver causes further disruption of glucose metabolism, resulting in increased ROS and pro-inflammatory cytokines production, such as TNF- α (Zwirner and Ziblat, 2017). NK cells can produce TNF- α . The high level of TNF- α in DM causes an inflammatory response that worsening health in DM. In addition to TNF- α , IFN- γ is also known to play a role in the inflammatory response. According to Zwirner and Ziblat (2017), the high levels of secretion of IFN- γ by NK cells were mediated by the activation of signal transducer and activator of transcription4 (STAT4) promoted by IL-12.

MOA consists of *Moringa oleifera* and Toman fish albumin. The administration of MOA in T1D mice can decrease inflammatory responses. The combination of bioactive compounds from MOA can work synergistically to reduce the level of TNF- α and IFN- γ produced by NK cells. The previous study showed that MO and albumin have a role as an antioxidant that suppresses ROS production. The high level of oxidative stress will trigger inflammatory factors such as the transcription factor Nf- κ B and various cytokines such as IFN- γ and TNF- α . In this study, the MOA's high antioxidant content was able to work synergistically to prevent oxidative stress. Albumin has the amino acid cysteine (cyst 34), which acts as a ROS scavenger such as hydrogen peroxide (H₂O₂) and inhibits lipid peroxidation. Albumin also inhibits the activation of the transcription factor NF- κ B and modulate intracellular GSH levels. Albumin has many sulfhydryl (-SH) groups that can bind free radicals that cause oxidative stress (Taverna *et al.*, 2013).

MOA administration of various doses has yielded varying results. The MOA administration at D3 was able to vary significantly suppress the level of TNF- α and IFN- γ produced by NK cells (Figures 1 and 2). Actually, administration of MOA at D1 and D2 was able to suppress, but not significantly. In figure 1, at D1 MOA could suppress the level of TNF- α , but the administration at D2 was increased and decreased in administration at D3, whereas, in figure 2, D2 and D3 significantly could

decrease the level of IFN- γ . Administration at D1 is still not able to significantly reduce IFN levels. Based on these results, it can be assumed that MOA is an immunomodulator. This is because MOA can control the production of cytokine by NK cells, wherein certain doses of MOA can suppress, but on the other hand MOA also increase the level of cytokine.

The decline production of TNF- α and IFN- γ by NK cells post-treatment indicates a reduction in inflammation and improved homeostasis in T1D model mice. The presence of flavonoids in MOA plays a role in the mechanism of inhibiting the activation of the transcription factor NF- κ B and the activity of tumor necrosis factor- α converting enzyme (TACE) in the synthesis of TNF- α . One of the receptors that regulate the activation of NK cells is the NKG2D receptor. Generally, the NKG2D ligand is expressed by stress cells. The binding between NKG2D and NKG2D ligands causes an increase in TACE activity and TNF- α secretion (Sharma *et al.*, 2017). Inhibition of TACE by flavonoids can reduce the production of TNF- α by NK cells (Gesso *et al.*, 2015). MOA is also known to contain β -sitosterol-3-O- β -D-glucoside, which suppresses IL-12 production by dendritic cell or macrophage, which activates STAT4 in NK cells, resulting in a decrease of IFN- γ production (Jimenez *et al.*, 2017; Ma *et al.*, 2018).

5. Conclusions

MOA has a potential role as an anti-inflammatory agent in mice models of T1D by controlling TNF- α and IFN- γ production in NK cells. Administration of MOA decreases the number of NK⁺ IFN- γ ⁺ and NK⁺ TNF- α ⁺ cell expression and is close to normal control.

Acknowledgement

The authors would like to gratefully thank all the colleagues in the Laboratory of Animal Anatomy and Physiology, Biology Department, Brawijaya University for participation in this research.

References

- Abel AM, Chao Y, Thakar MS, Malarkannan S. 2018. Natural killer cells: Development, maturation, and clinical utilization. *Front Immunol.*, **9**: 1869-1888.
- Arora S, Ojha SK and Vohora D. 2009. Characterization of streptozotocin-induced diabetes mellitus in swiss albino mice. *Glob J Pharmacol.*, **3**(2): 81-84.
- Balakrishnan S, Singh B, Gill GS, Kaliappan I and Dubey GP. 2012. Evaluation of antihyperglycemic and other complication effects of extracts of *Thespesia lampas* dalz and gibs on streptozotocin induced diabetic rats. *Jordan J Biol Sci.*, **5**(3): 161-166.
- Bhattacharya A, Tiwari P, Sahu PK and Kumar S. 2018. A review of the phytochemical and pharmacological characteristics of *Moringa oleifera*. *J Pharm Bioallied Sci.*, **10**(4): 181-191.
- Brosius, F (2015). "High-Dose Streptozotocin Induction Protocol (Mouse)." Diabetic Complications Consortium, <https://www.diacomp.org/> (Jul. 3, 2020).
- Cerf ME. 2013. Beta-cell dysfunction and insulin resistance. *Front Endocrinol.*, **4**: 37.
- Fauriat C, Long EO, Ljunggren HG and Bryceson YT. 2010. Regulation of human NK-cell cytokine and chemokine production by target cell recognition. *Blood.*, **115**(11): 2167-2176.

Gesso GL, Kerr JS, Zhang Q, Raheem S, Yalamanchili SK, O'Hagan D, Kay CD and O'Connell MA. 2015. Flavonoid metabolites reduce tumor necrosis factor- α secretion to a greater extent than their precursor compounds in human THP-1 monocytes. *Mol Nutr Food Res.*, **59**(6): 1143-1154.

Graham KL, Sutherland RM, Mannering SI, Zhao Y, Chee J, Krishnamurthy B, Thomas HE, Lew AM and Kay TWH. 2012. Pathogenic mechanisms in type 1 diabetes: the islet is both target and driver of disease. *Rev Diabet Stud.*, **9**(4): 148-168.

Jimenez MV, Almatrafi MM and Fernandez ML. 2017 Bioactive components in *Moringa oleifera* leaves protect against chronic disease. *Antioxidants.*, **6**(4): 34-47.

Lee LF, Xu B, Michie SA, Beilhack GF, Warganich T, Turley S and Mcdevitt HO. 2005. The role of TNF- α in the pathogenesis of type 1 diabetes in the nonobese diabetic mouse: Analysis of dendritic cell maturation. *Proc Natl Acad Sci USA.*, **102**(44): 595-600.

Lopez AV, Mora DA, Paulino OD, Mora AG, Vitela MR, Quiroz LA and Nuno K. 2018. Effect of *Moringa oleifera* consumption on diabetic rats. *BMC Complement Altern Med.*, **18**(1): 127.

Ma N, Tang Q, Wu WT, Hu XA and Hu Q. 2018. Three constituents of *Moringa oleifera* seeds regulate the expression of Th17-relevant cytokines and ameliorate TPA-induced psoriasis-like skin lesions in mice. *Molecules.*, **23**(12): 32-56.

Marrack P, Kappler J and Kotzin BL. 2001. Autoimmune disease: Why and where it occurs. *Nat Med.*, **7**(8): 899-905.

Mohamed J, Nafizah AHN, Zariyantey AH and Budin SB. 2016. Mechanisms of diabetes-induced liver damage the role of oxidative stress and inflammation. *Sultan Qaboos Univ Med J.*, **16**(2): 132-141.

Nekoua MP, Dechaumes A, Sane F, Alidjinou EK, Moutairou K, Yessoufou A and Hober D. 2020. Enteroviral pathogenesis of type 1 diabetes: The role of natural killer cells. *Microorganisms.*, **8**(7): 989.

Osman HM, Shayoub ME and Babiker EM. 2012. The effect of *Moringa oleifera* leaves on blood parameters and body weights of albino rats and rabbits. *Jordan J Biol Sci.*, **5**(3): 147-150

Patel S and Santani D. 2009. Role of NF- κ B in the pathogenesis of diabetes and its associated complication. *Pharmacol Reports.*, **61**(4): 595-561.

Quilan GJ, Martin GS and Evans TW. 2005. Albumin: Biochemical properties and therapeutic potential. *Hepatology.*, **41**(6): 1211-1219.

Rifa'i M, Wahyuningsih MD, Lestari ND, Mansur I, Aris S and Hideo T. 2018. Bioactivity of cherry (*Muntingia calabura* L.) leaves extract for IL-6 production and NF-B activity in hyperglycemic BALB/c mice. *Med Plants.*, **10**(4): 305-311.

Sharma N, Trinidad CV, Trembath AP and Markiewicz MA. 2017. NKG2D signaling between human NK cells enhances TACE-mediated TNF- α release. *J Immunol.*, **199**(8): 2865-2872.

Simmons KM and Michels AW. 2015. Type 1 diabetes: A predictable disease. *World J Diabetes.*, **6**(3): 380-390.

Sun H, Sun C, Tian Z and Xiao W. 2013. NK cells in immunotolerant organs. *Cell Mol Immunol.*, **10**(3): 202-212.

Taverna M, Mariel AL, Mira JP and Guidet B. 2013. Specific antioxidant properties of human serum albumin. *Ann Intensive Care.*, **3**(1): 21-33.

Tsiavou A, Degiannis D, Hatziazgelaki E, Koniavitou K and Raptis SA. 2004. Intracellular IFN- γ production and IL-12 serum levels in latent autoimmune diabetes of adults (LADA) and type 2 diabetes. *J Interf Cytokine Res.*, **24**(7): 381-387.

Zwirner NW and Ziblat A. 2017. Regulation of NK cell activation and effector functions by the IL-12 family of cytokines: The case of IL-27. *Front Immunol.*, **8**: 56-68.

An Overview of COVID-19 in Sub-Saharan Africa: the Transmissibility, Pathogenicity, Morbidity and Mortality so far

Chinyere Alope^{1,4*}, Balasubramanian Ganesh², Nwogo A. Obasi¹, Patrick M. Aja³, Emmanuel I. Ugwuja³, Joseph O. Nwankwo¹

¹ Department of Medical Biochemistry, Faculty of Basic Medical Sciences, Alex Ekwueme Federal University Ndufu-Alike, P.M.B 1010 Abakaliki, Ebonyi State, Nigeria.; ² ICMR-National Institute of Epidemiology, R-127, Second Main Road, TNHB, Ayapakkam, Chennai-600 077, Tamil Nadu, India.; ³ Department of Biochemistry, Faculty of Sciences, Ebonyi State University, P.M.B. 053 Abakaliki, Ebonyi State, Nigeria.; ⁴ Protein Structure-Function and Research Unit, School of Molecular and Cell Biology, Faculty of Science, University of the Witwatersrand, Braamfontein, Johannesburg 2050, South Africa

Received: February 2, 2021; Revised: April 15, 2021; Accepted: June 15, 2021

Abstract

This narrative review documented the available knowledge on the transmissibility, pathogenicity, morbidity and mortality of COVID-19 in sub-Saharan African region in order to inform recommendations of future containment of the virus. Internet search for studies on COVID-19 transmission, pathogenicity, morbidity and mortality in Africa was conducted from February to July 2020. Although Africa was classified among the high-risk continents due to high volume of human air traffic occasioned by international trade relations and poor health facilities, available data showed that most sub-Saharan African countries were prepared with strategies to reduce and manage the disease beyond expectations. However, despite health guidelines, which include but are not limited to personal hygiene, maintaining social and physical distancing, avoiding crowded places, use of nose and mouth or face masks that will limit its spread, the high burden of other diseases in Africa, such as malaria, diabetes mellitus, cancer, and asthma among others coupled with poor health facilities have been attributed to contribute significantly to the cause of coronavirus mortality in Africa. While information on the pathogenicity and therapeutic management of coronavirus continue to evolve, medicinal plants with potent metabolites are reported to be effective in early treatment of the virus abound in African countries, thus bringing a positive development with futuristic hope for cheaper and effective medication. A potentially significant contribution to reduced severity of the severe acute respiratory syndrome coronavirus 2 (SARS-CoV-2) pandemic in sub-Saharan Africa may be due to the elevated temperatures of climate in this part of the world.

Keywords: COVID-19, world pandemic, Africa, pathogenicity, health guidelines, mortality.

1. Introduction

The last several decades have been faced with emerging novel strains of coronaviruses which cause severe respiratory disease (Alfaraj *et al.*, 2019). In December 2019, another outbreak of unusual respiratory disease was recorded in Wuhan, China. This reported unusual disease was later found to be caused by an unfamiliar coronavirus named 2019-nCoV by the World Health Organization (WHO, 2020a; CDC, 2019). On 30th January, 2020, this disease outbreak was declared an emergency of international concern on public health as the virus and its infectivity rapidly expanded to many other countries of the world. On March 11, 2020, WHO renamed the disease and called it 'coronavirus disease 2019 (COVID-19)' and declared it a global pandemic (WHO, 2020b). COVID-19 was later identified based on a phylogenetic analysis as severe acute respiratory syndrome coronavirus 2 (SARS-CoV-2) by the Coronavirus Study Group (CSG) of the International Committee on Virus Taxonomy. COVID-19 caused by coronavirus is the first

ever pandemic associated with the virus (Coronaviridae Study Group, 2020; WHOc, 2020). Today, COVID-19 is known to affect people of all ages with higher severity in the elderly especially those above 60 years and those with compromised health status such as those living with heart disease, chronic respiratory disease or cancer (Chen *et al.*, 2020).

Some health experts arguably suggest that minimal records of SARS-CoV-2 cases experienced in African continent were probably due to low flight patronage to the region, which made it easier for identification and isolation of initial cases and limit its transmission (Njenga *et al.*, 2020). Besides, the rate of introduction of imported cases was further mitigated by the initial implementation of partial or complete travel restriction which facilitated identification and isolation of initial cases, tracing of their contacts and thereby limit its transmission. Compelling evidence has shown that sub-Saharan Africa demonstrated strong resolve in carrying out preventive protocols for SARS-CoV-2 transmission, mainly via the structures adopted by the WHO aided Integrated Disease Surveillance and Response (IDSR) and the knowledge

* Corresponding author e-mail: alokec2002@yahoo.com; chinyere.aloke@funai.edu.ng.

acquired from reoccurring episodes of Ebola viral infections in the region (Ihekweazu and Agogo, 2020). However, the preventive and control protocols for COVID-19 epidemics in African region were grossly inadequate when compared to that obtainable in most European countries and countries in the United States of America due to poor standard of living occasioned by poor income status of majority of people in the region, poor healthcare system, and lack of adherence to rules that reduce virus spread (<https://www.worldbank.org/en/region/afr/publication/for-sub-saharanafrica-coronavirus-crisis-calls-for-policies-for-greater-resilience>). Literature has revealed that the low numbers of severe COVID-19 cases and deaths in sub-Saharan Africa may be due to the fact that majority of them are at their youthful stage of life with mean age bracket of 20 years compared to those in most European countries and countries in the United States of America with mean age bracket of 38 years and above (<https://population.un.org/wpp/>. Accessed May 3, 2020) Dowd *et al.*, 2020). This notion is plausible; nevertheless, other causative factors such as malnutrition, cultural factors and overcrowding within urban settlements may have contributed substantially to it (Njenga *et al.*, 2020).

2. Transmission of SARS-COV-2 in sub-Sahara Africa

The wet animal market located at the Wuhan city of Hubei Province where animals were regularly sold was suspected as the point of human–animal transmissible origin of COVID-19 as many people exposed to this wet animal market were infected with the virus. Researchers have made several efforts in a bid to look for a reservoir or intermediate host where the virus infection was transmitted to humans. Two species of snake have been recognized to be probable primary host of COVID-19 in an earlier study. At present, there is no reliable or scientific evidence of coronavirus reservoirs other than mammals and birds (Bassetti *et al.*, 2020). However, genome analysis has revealed a strong link between human COVID-19 and two bat-derived severe acute respiratory syndromes (SARS)-like coronaviruses, which showed 88 % similarity (Lu *et al.*, 2020). Accumulating pieces of evidence have shown that COVID-19 infection could be spread from person-to-person. This was corroborated by cases that took place within families and among people who did not visit the wet animal market in Wuhan (Wu *et al.*, 2020). Transmission from individual to individual occurs mainly through direct contact or via droplets released by coughing or sneezing from infected person (Rothan and Byrareddy, 2020). Previous study has shown no evidence of the virus transmission from COVID-19 positive mothers to child, but it is still uncertain whether transmission can occur during vaginal birth (Chen *et al.*, 2020).

The transmission from individual to individual is mainly from symptomatic infected individuals. However, in Germany, transmission of coronavirus infection from SARS-CoV-2 patients not displaying any symptoms has been reported which has generated debate on the elucidation of present transmission dynamics of the virus (Rothe *et al.*, 2020). The transmissibility of the pandemic is greatly influenced by the presence of asymptomatic or mildly symptomatic persons.

In an imported case, the methods of transmission are via spread of droplet, fecal-oral route, conjunctiva and fomites (Xu *et al.*, 2020; Ong *et al.*, 2020). Besides, the transmission and infectivity of the virus locally could be by infected person's bodily fluids like respiratory droplets, saliva, feces, and urine (Ong *et al.*, 2020). The virion has high survival rate at lower temperature, i.e 4°C in comparison with 22°C (Kampf *et al.*, 2020). Previous study by van Doremalen *et al.* (2020), revealed a resemblance for SARS-CoV-1 and SARS-CoV-2 stability under similar experimental conditions. This was an indication that the variance in the epidemiologic features of these viruses most likely stem from other factors, besides elevated high viral loads in the upper respiratory tract and the capability of SARS-CoV-2 patients to shed and spread the virus while not displaying any symptom of the disease (asymptomatic) (Bai *et al.*, 2020). From their result, there was strong indication that SARS-CoV-2 could be spread via aerosol and fomite transmission since the virus can stay alive and be transmissible in aerosols for hours and on surfaces up to days. Similar findings were reported for SARS-CoV-1, where transmission patterns were linked with some forms of nosocomial spread and super-spreading events and they provide facts on the alleviation of the pandemic. The residence time of SARS-CoV-2 virion on surfaces varies. The SARS-CoV-2 half-life in copper, aerosols, stainless steel, plastic and cardboard are 1 hour, 1.5 hours, 5.6 hours, 6.8 hours and 3.4 hours, respectively while the active life span of SARS-CoV-1 in similar media are 4 hours, 3 hours, 48 hours, 72 hours and 24 hours, respectively (van Doremalen *et al.*, 2020)

Speculations have projected that Sub-Sahara Africa may have a higher risk index in terms of transmission and contacting of COVID-19 epidemics due to high volume of air traffic and trade between China and African countries (Nkengasong and Mankoula, 2020). Public health experts were worried about COVID-19 becoming all year-round viral pandemic with continued transmission similar to influenza, as seen in several countries now (<http://outbreaknewstoday.com/italy-covid-19-case-count-now-79-government-introduces-urgentmeasures-37376/>. accessed Feb 23, 2020). They were concerned about the fate of most African countries with poor health-care systems, insufficient tracing and laboratory facilities, and inadequate skilled public health labour force and inadequate or no finances peradventure there are reoccurring episodes of the pandemic. In addition, without vaccination or treatment and in the absence of pre-existing immunity, the impact would be catastrophic following many health challenges bedeviling the continent already such as endemic diseases like human immunodeficiency virus, tuberculosis, malaria, Ebola virus disease, Lassa fever, higher non-communicable diseases in existence, in addition to rising population growth and increased movement of people. Incidentally, on the 11th of March, 2020, the WHO declared COVID-19 a global pandemic due to its acceleration and spread globally (Bedford *et al.*, 2020). In Africa, the first index case reported for COVID-19 was in Egypt. It was reported and recorded on February 14, 2020. This was followed by Algeria which confirmed her first case on February 25, 2020 while Nigeria confirmed her first index case on February 27, 2020. The first country in the southern African region to report

confirmed case of COVID-19 on the 5th March 2020 was South Africa. All these cases were mainly imported from Europe (Anjorin, 2020). The disease has virtually spread to all African countries with South Africa having the highest number of cases.

3. Pathogenicity of SARS-COV-2

Coronavirus is known to cause human respiratory tract infection or animal intestinal infection. The host cell membrane surface receptors are involved in the course of virus invasion of the body. The surface of coronavirus contains the S-protein which can detect and become attached to the receptor and consequently have access into the human host cell via clathrin-mediated endocytosis (Wang *et al.*, 2008). For this invasion, disparate coronaviruses make use of different receptors. For instance, aminopeptidase N (referred to as CD13) is the human coronavirus 229E (HCoV-229E) receptor, severe acute respiratory syndrome coronavirus (SARS-CoV) has angiotensin-converting enzyme 2 (ACE2) receptor (Kuba *et al.*, 2005) while Middle East respiratory syndrome coronavirus MERS-CoV has dipeptidyl peptidase 4 (DPP4) also known as CD26 receptor (Lu *et al.*, 2013). Recent report has shown that ACE2 can be employed by SARS-CoV-2 receptors unlike aminopeptidase N and DPP4 (Zhou *et al.*, 2020).

Every coronavirus has genes particularly in open reading frames (ORF1) at the downstream regions that produce proteins which the viruses use to replicate and develop nucleocapsid and spikes (van Boheemen *et al.*, 2012). On the periphery of coronaviruses lies the glycoprotein spikes which facilitates its entrance to host cells. The virus could perhaps infect many hosts because the receptor-binding domain (RBD) is not firmly bound within the virus (Raj *et al.*, 2013). For invasion of human cells, the main receptor mostly recognized by other coronaviruses are aminopeptidases or carbohydrates but in the case of SARS-CoV and MERS-CoV, the key receptor primarily recognized is exopeptidases (Wang *et al.*, 2013).

The mode of invasion of COVID-19 virus is dependent on proteases such as human airway trypsin-like protease (HAT), cathepsins and transmembrane protease serine 2 (TMPRSS2) that process the spike proteins and then modify the cellular components allowing the viruses to gain access (Glowacka *et al.*, 2011)

SARS-CoV-2 has spike protein and equally possesses other polyproteins in its structures typical of coronaviruses. Such polyproteins include nucleoproteins and membrane proteins such as RNA polymerase, 3-chymotrypsin-like protease, papain-like protease, helicase, glycoprotein, and accessory proteins (Wu *et al.*, 2020; Zhou *et al.*, 2020). Like other coronaviruses, SARS-CoV-2 is an enclosed single-strand, positive sense RNA virus. The spike protein that regulates the host cell tropism and infectivity equally facilitates receptor binding and membrane fusion (Li, 2016). For cell invasion, SARS-CoV and SARS-CoV-2 make use of human angiotensin-converting enzyme II receptor. The receptor-binding domain structure of SARS-CoV-2 is akin to that of SARS-CoV in spite of the fact that some differences exist in amino acids at key residues (Lu *et al.*, 2020). Despite the fact that SARS-CoV-2 genome encodes an exonuclease enzyme, it also has a fairly high mutation rate per genome replication. Hence, it may comfortably adjust to its new host and become infectious from one individual to another. The 3-D structural configuration in the receptor-binding domain (RBD) region of the SARS-CoV-2 spike protein functions to conserve the van der Waals forces (Xu *et al.*, 2020).

The lysine 31 residue on the human angiotensin-converting enzyme 2 (ACE2) receptors facilitates the recognition of the 394-glutamine residue in the RBD region of SARS-CoV-2 (Wan *et al.*, 2020). Thus, SARS-CoV-2 mode of pathogenicity in human is briefly elucidated from its attachment to human host and replication within the host (Figure 1).

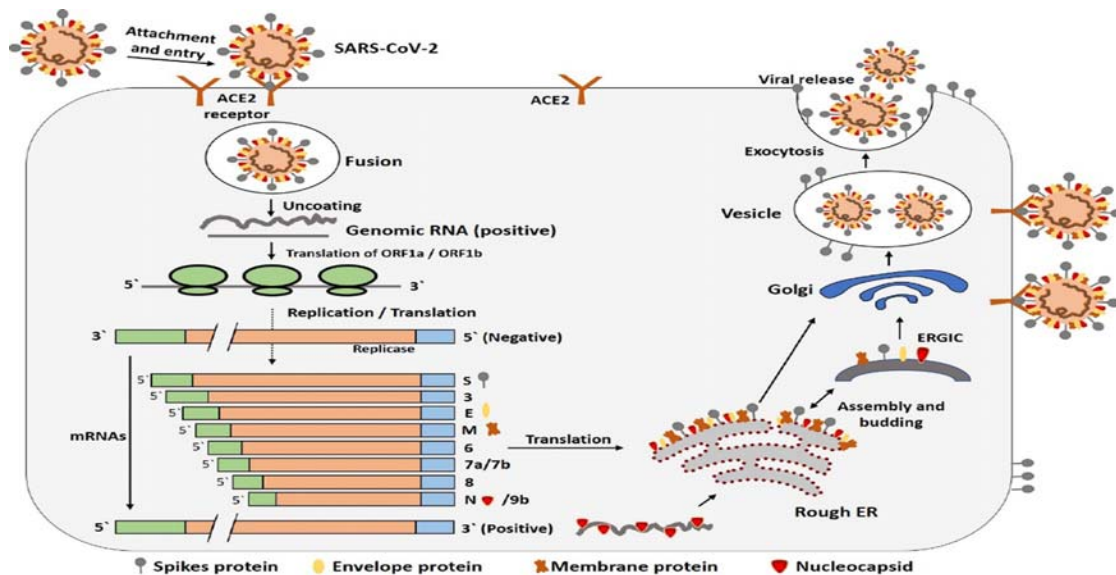


Figure 1. The life cycle of SARS-CoV-2 in host cells. ACE2 = angiotensin-converting enzyme 2; ER = endoplasmic reticulum; ERGIC= ER-Golgi intermediate compartment. (Source: Shereen *et al.* (2020).

The SARS-CoV-2 begins its infectivity of the host when its S-protein becomes attached to ACE2 receptor. Upon binding with ACE2 receptor, there is alteration in the shape of the S-protein which promotes the integration of the viral envelope with the host cell membrane via the endosomal pathway. Thereafter, RNA is liberated by SARS-CoV-2 into cell hosting it. The viral replicase polyproteins pp1a and 1ab produced from the translation of the RNA genome are thereafter degraded into miniature products by proteinases. Through discontinuous transcription, the polymerase enzyme catalyzes the production of a string of sub-genomic mRNAs which are ultimately converted to relevant viral proteins by the processes of translation. Later on, the viral proteins and RNA genome are congregated into virions in the endoplasmic reticulum and Golgi and subsequently conveyed through vesicles and liberated out of the cell (Shereen *et al.*, 2020).

4. Morbidity, Comorbidity and Mortality in Africa

Reports have argued that the minimal incidences of COVID-19 in Africa may not be attributed to decreased inspection and fewer testing because shooting up of the number of COVID-19 cases may be observed via reports of high incidences of pneumonia cases at local hospitals and these have not been observed. Assuming that the COVID-19 monitoring and testing are low in Africa due to scarce resources, the high viral incidence witnessed in Asia, Europe, and North America would implicate that local transmission in highly populated metropolis in continent of Africa such as Lagos or Nairobi would culminate in high incidences of pneumonia cases at local hospitals (Pan *et al.*, 2020). A differing notion that SARS-CoV-2 transmission in the continent may be comparable to that elsewhere but that its development to clinical disease outcomes is significantly lower may be acceptable (Yang *et al.*, 2020). Many public health professionals are amazed that the case fatality rate (CFR) in Africa has not escalated despite her high burden of chronic diseases such as tuberculosis, HIV/AIDS, malaria and other infections, including the prevalence of other underlying situations, for instance malnutrition and unorganized settlement with high population density in urban areas with dirty environment. For instance, in Nigeria, the CFR based on the Nigeria Centre for Disease Control (NCDC) is only 1.8%. Nevertheless, it is worthy noting that comorbidities linked with severe COVID-19 disease like diabetes mellitus and asthma are not much prevalent in the region (Yang *et al.*, 2020; Saeedi *et al.*, 2019). In spite of the profound poor health systems in sub-Sahara Africa, the CFR has been below the average in global records compared to that of European countries and those in the United States of America as at 31st July, 2020. It is therefore highly probable that the elevated temperatures of the climate in sub-Saharan Africa may contribute significantly to the decreased survivability of the virus in the environment and consequent decreased disease severity and mortality in the population. This may be evidenced in the graphs of Figures 2 and 3 where death rates are

relatively less in countries around the equator compared to geographical extremes of Africa in the North and South such as Egypt, Algeria and South Africa.

Respiratory failure has been identified as the principal cause of human death in COVID-19 cases and it is similar to those caused by flu infection. Recently, recovery from respiratory failure caused by this COVID-19 incidence has been promoted through the use of invasive mechanical ventilation until the lung's injury heals (Zhou *et al.*, 2020). Extra-corporeal membrane oxygenation could be employed if the situation gets worse (Tao *et al.*, 2017). Septic Shock and multiple organ failure have been strongly implicated as other causes of high mortality rate experienced in COVID-19 infection. The role of reoccurring bacterial infections in increased incidences of mortality due to COVID-19 is not well-documented in literature (Meo *et al.*, 2020). Others causes associated with increased mortality due to COVID-19 include acute kidney injury and cardiogenic shock resulting from acute myocardial injury or myocarditis (Paudel, 2020). This era of the global pandemic, deaths due to COVID-19 are hardly differentiated from others caused by overload of cases in hospitals. Critically ill persons infected and associated mortalities with COVID-19 for now do not have access to adequate medical attention because of limited resources in terms of personnel, funds and inadequate hospital facilities (Tao *et al.*, 2017).

In Africa, the daily cases of COVID-19 have been on the increase and the number of deaths reported daily has also increased drastically. As at 31 July 2020, the ten most hit countries with COVID-19 in Africa is as shown in Figure 2. Data from African Centre for Disease Control reveals increasing cases of death resulting from COVID-19 in the last three months and experts' project that the cases may not have reached peak due to poor health facilities and increased community transmission in these African countries. The rise in the death rates from March to July in five most affected countries are shown in Figure 3.

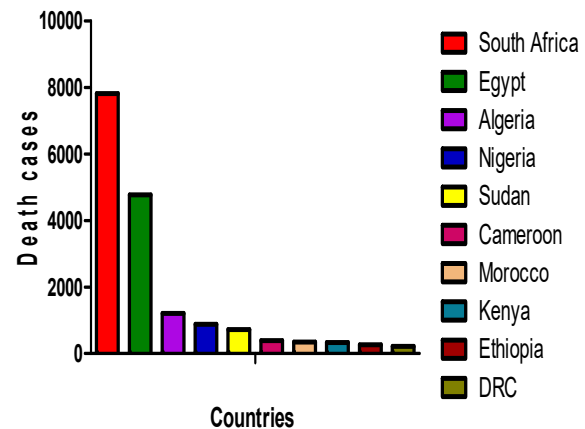


Figure 2. COVID-19 Total Death Counts in ten most affected Countries in Africa as at July 31, 2020.

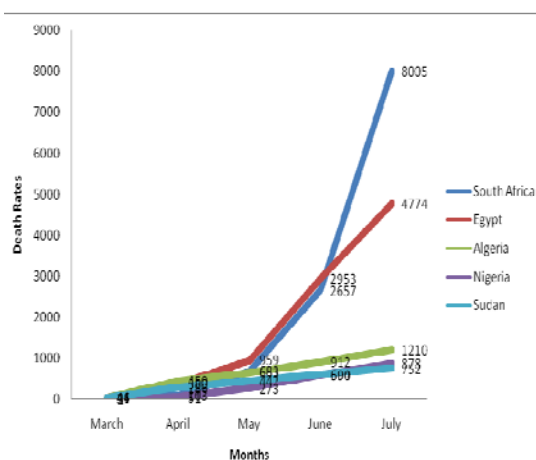


Figure 3. COVID-19 Total Death Counts as at July 2020 in five most affected Countries in Africa.

COVID-19 pandemic is a relatively new and understudied disease and as such, there is limited available data. In Africa individuals having comorbidities such as diabetes mellitus, hypertension and malignancy had low recovery performance following COVID-19 infection treatment (Saeedi, 2019). However, from the cases reported to have emerged from Africa, it was observed that infections were increased by comorbidities. Recent health information and clinical experience indicate that the elderly, particularly those with protracted health problems and any other persons irrespective of age with serious underlying health conditions are prone to getting COVID-19 (Paudel, 2020). Reports have shown that vulnerable population with chronic medical conditions like diabetes and cardiovascular or lung disease and the aged are not only prone to developing severe illness but are also at greater risk of death if they develop ill (Saeedi, 2019). Individuals with underlying unchecked medical conditions like diabetes, hypertension, lung, liver, and kidney disease, cancer patients on chemotherapy. Reports have also shown that transplant recipients, smokers and patients on steroids are more prone to COVID-19 infection (Paudel, 2020).

5. Sub-Sahara African Mitigation Measures and Challenges in Tackling COVID-19

Africa is better ready and equipped than before for any outbreak of any infectious viral disease like COVID-19. There has been significant improvement since the Ebola outbreak of 2014-2016 and the lessons garnered previously and ongoing outbreaks in addition to marked investment in surveillance and preparedness (WHO, 2020d; Hoffman and Silverberg, 2018). African countries have thus far intensified effort and have been on the alert for detection and isolation of any imported case of COVID-19. Prior to the reported case of COVID-19 from Africa, there has been a very quick response to the COVID-19 epidemic by the **sub-Sahara** public health systems of Africa. The re-organization of WHO as well as the establishment of the World Health Emergencies Programme, the setting up of Africa CDC, (<http://www.africacdc.org/>, accessed 17 February, 2020) the establishment and funding of

development partners like ONE-HUMAN-ANIMAL-HEALTH Africa- Europe research, training and capacity development network (PANDORA-ID-NET) (PANDORA-ID-NET, 2020) for handling emerging and re-occurring infections with epidemic potential facilitated the rapid response. This ONE-HEALTH network will work in all the regions in Africa continent alongside locally approved disease control authorities and public health institutes, such as Nigeria CDC, Africa CDC and other African and global public health agencies to effectively and efficiently tackle health problems such as the coronavirus pandemic (NCDC, 2020).

Concerted efforts were made by the Africa CDC, country specific CDC like Nigeria CDC, African Union, PANDORA-ID-NET and other research and capacity development and training consortia in preparation to deal with any imported case or in the wake of local outbreaks of COVID-19. Screening for COVID-19 patients on arrival at airports and at some seaports was launched by several African countries. There was a meeting of public health emergency responders from Africa in early February, 2020 in Senegal to keep themselves abreast of newest advances in COVID-19 diagnostics, (Corman *et al.*, 2020) prevention and healthcare knowledge. Many countries in Africa have set up isolation and quarantine centers, swiftly attending to suspected cases by carrying out laboratory test and in some cases quarantining them while laboratory tests were being performed (Kapata *et al.*, 2020).

In Africa, Nigeria was among the first to acknowledge the danger and commenced strategic planning to contain the COVID-19 pandemic. In preparedness, the National Coronavirus Preparedness Group was set up by Nigeria CDC on 7th January, 2020, seven days after the republic of China announced the first confirmed case and twenty-one days prior to the declaration of the COVID-19 as disease of international concern. Nigeria under one month established three diagnostic laboratories for COVID-19. In the same vein, the National Coronavirus Preparedness Group was set up by the Nigeria CDC that meets on daily basis for the assessment of the risk posed by the coronavirus pandemic and review of her response to it (Kapata *et al.*, 2020).

Many countries in African have put up thermal body scanners at all ports of entry to detect travelers displaying the symptoms of the virus. In south Africa, the national and provincial response teams were put in place, while 300 health personnel were stationed at ports of entry to enable them screen all travelers from China. Several participants from different countries in Africa have been trained by the Africa CDC to facilitate COVID-19 detection at points-of-entry in partnership with US-CDC, WHO, and the International Civil Aviation Authority (WHO, 2020). Different bodies and unions such as the Africa Union, West African Health Organization (WAHO) and external donors have been swift in the provision of assistance to the Africa CDC. There have been many consortia sending in applications for research grants and capacity development in response to the containment of COVID-19 emergency grant calls.

Sequel to the confirmation of first case of COVID-19 in Africa, the Africa CDC, Nigeria CDC and other national public health institutes in collaboration with the World

Health Organization were putting up concerted effort in African region to help countries in carrying out the recommendations as provided by WHO International Health Regulations Emergency Committee. The WHO emergency committee proposed that all countries by prepared for containment, surveillance and contact tracing, early detection and isolation, case management, and preventive measures to forestall transmission of SARS-CoV-2. Besides, diagnostic kits reagents and positive controls were sent to 29 laboratories in Africa by the WHO through PANDORA-ID- NET partner in Germany, Charité-Universitätsmedizin Berlin Institute of Virology to facilitate the capacity to screen and test while some African countries including DRC leveraged on the facilities, they have set up for Ebola screening, to screen for COVID-19 (WHO, 2020f).

In a bid to checkmate the transmission of the virus, different precautionary and preventive measures as recommended by the WHO were adopted. There was serious public enlightenment campaign both in radio, television and other print media on the need for regular washing of hands with water and soap at least 30 seconds, the use of nose and mouth masks, use of hand sanitizers when water and soap are not readily available, discouragement from touching eyes, nose, and mouth, social and physical distancing. Additionally, people were advised to distance themselves from people, to cover their mouth and nose while coughing or sneezing with a tissue and thereafter cast the tissue in the dustbin for quick disposal (Sandaradura *et al.*, 2020). Likewise, people were advised to always wash and sterilize objects and surfaces mostly touched employing household cleaning spray or wipe (NCDC, 2020). There was an embargo on social gatherings like burials, wedding ceremonies, birthday party and religious activities in most African countries. People were encouraged to seek medical attention when they have a fever, cough and difficulty in breathing or call in advance the local health authority and were warned to avoid unneeded visits to medical facilities to protect themselves and their loved ones. Other measures taken include border closures and screening at airports and checkpoints. In Nigeria, there was initial total lockdown of Lagos and Ogun states including the nation's capital territory, Abuja. Subsequently there was interstate lockdown while curfew was imposed in areas where cases were reported in some states.

Despite so many efforts being made by several Africa countries in the fight against COVID-19 pandemic, they were confronted with a lot of challenges. The majority of the African countries are low-middle income countries (LMICs) that lack the capacity to test in a large scale. Thus, they faced several problems ranging from diagnosis of suspected cases, contact tracing of suspected carriers for confirmatory tests and plans on active surveillance testing. There have been reported cases of test kit shortages in different African countries (VOA, 2020) owing to high global demand. The COVID-19 RT-PCR test kits are exorbitant, making it difficult for LMICs to embark on large-scale testing. In addition, the PCR machines and adequately equipped BSL-2 labs are expensive to come by and this required highly skilled manpower which limit the testing capacity for COVID-19 by many African countries (Kobia and Gitaka, 2020).

In Africa, social coherence and social gatherings are highly valued. For instance, attendance of weekly religious activities is reported highest in most Africa countries with reported rates of about 82% in Uganda and Ethiopia. Consequently, mitigation measures based on social and physical distancing as in health guidelines may be more difficult to achieve, as attested by the Senegalese protest on 20 March 2020 after public gatherings, including gatherings at mosques were banned as cases of COVID-19 rose. The high prevalence of malnutrition, anemia, malaria, HIV/AIDs, and tuberculosis in African population is a critical challenge in containing the escalation of the pandemic. For instance, Liberia has the highest rate of stunting globally, one out every three children under the age five years are stunted. Increase in the incidence of malnutrition has been witnessed recently. Besides, there is early onset of rainy season this year, which implies rapid increment in malaria cases in 2020 which its peak coincided with the present COVID-19 pandemic being experienced. All these factors wear out the immune system and make the population more vulnerable (<https://www.weforum.org/agenda/2020/03/why-sub-saharan-africa-needs-a-unique-response-to-covid-19/>, accessed March 30, 2020).

Even though, the lock-down imposed in most **sub-Saharan** African countries will have the benefit of reducing spread, fatality and disability from the virus but the aftermath on the Africa's economy is worrisome. In the continent, many countries are already in economic dips, the lockdown and decrease in economic activities due to the pandemic will further diminish the economic growth of many African countries. In addition, the decline in oil prices and international commodities which most African countries are dependent upon will further worsen the situation and will probably occasion grave economic recession for the continent. This will culminate to increment in poverty rate which many may view as bad for the African continent as the COVID-19 pandemic itself (Okonofua *et al.*, 2020).

6. Conclusion

Sub-Saharan African countries like other countries of the world have been negatively impacted by COVID-19 with comorbidities worsening its progression and outcomes. There is, therefore, a need to take all the precautions rolled out by approved health guidelines to avoid contacting SARS CoV-2 infections. Precautionary measures recommended include regular hand washing using detergents and soap in running water, regular application of safe alcohol-based hand sanitizer, reduction in the number of person-to-person contact, maintenance of social distancing, covering of nose and mouth or face with approved mask in public places, and generally reducing public activities involving physical contacts with as many persons as possible. Also, there is urgent need for increased public health campaign to create more awareness on the need to reduce the burden of comorbid illnesses capable of causing increase in the numbers of deaths in patients infected with COVID-19.

Since reports have shown that a combination of health guidelines is likely to contribute to reduction in the incidences of transmission and disease severity in Africa,

contrasting reports linked to the pandemic in different countries herein presented are grounds for further studies. From this review, it can be inferred that warmer weather and large population mostly in the youthful age contribute to low transmission incidences of COVID-19 disease and severity in Africa.

Although acquired immunity as a result of earlier exposure to cross-reacting corona viruses is a novel area, more research studies are needed for better understanding. It is pertinent to note that the WHO has forewarned that Africa may experience increased cases and deaths as reported in Brazil and so need all hands-on deck to avert the danger of the dreaded COVID-19 virus.

Again, although reports have shown that some African countries have deployed medicinal plants products (herbal remedies) such as COVID-19 organics used in Madagascar and other phytochemicals-rich-compounds for the earlier treatment of the disease, research is on-going for validation of these claims and if successful, then African countries will make rapid progress as medicinal plants with these potent bioactive compounds abound in the continent. In the final analysis, it may well be that the elevated temperatures of sub-Saharan climates may be a major contributing factor to the reduced severity of the COVID-19 pandemic in this part of the world.

References

- Alfaraj SH, Al-Tawfiq JA and Memish ZA. 2019. Middle East Respiratory Syndrome Coronavirus (MERS-CoV) infection during pregnancy: Report of two cases & review of the literature. *J Microbiol Immunol Infect.*, **52(3)**: 501-503.
- Anjorin AA. 2020. The coronavirus disease 2019 (COVID-19) pandemic: A review and an update on cases in Africa. *Asian Pac J Trop Med.*, **13**: 99-203.
- Bai Y, Yao L, Wei T, Tian F, Jin DY, Chen L and Wang M. 2020. Presumed asymptomatic carrier transmission of COVID-19. *JAMA.*, **323(14)**: 1406-1407.
- Bassetti M, Vena A and Giacobbe DR. 2020. The Novel Chinese Coronavirus (2019- nCoV) Infections: challenges for fighting the storm. *Eur J Clin Invest.*,:13209.
- Bedford J, Enria D, Giesecke J, Heymann DL, Ihekweazu C, Kobinger G, Lane HC, Memish Z, Oh M-D, Sall AA, Schuchat A, Ungchusak K and Wieler LH. 2020. COVID-19: towards controlling of a pandemic. *Lancet. Lancet.*, **395(10229)**: 1015–1018.
- Centre for Disease Control. 2019 Novel Coronavirus, Wuhan, China. CDC. Available at <https://www.cdc.gov/coronavirus/2019-ncov/about/index.html>. (Accessed: January 27, 2020)
- Chen H, Guo J, Wang C, Luo F, Yu X, Zhang W, Li J, Zhao D, Xu D, Gong Q, Liao J, Yang H, Hou W and Zhang Y. 2020. Clinical characteristics and intrauterine vertical transmission potential of COVID-19 infection in nine pregnant women: a retrospective review of medical records. *Lancet.*, **395(10226)**: 809-815.
- Chen N, Zhou M, Dong X, QO J, Gong F, Han Y, Qiu, Y, Wang J, Liu Y, Wei Y, Xia J, Yu T, Zhang X and Zhang L. 2020. Epidemiological and clinical characteristics of 99 cases of 2019 novel coronavirus pneumonia in Wuhan, China: a descriptive study. *Lancet.*, **395**: 507-13.
- Corman VM, Landt O, Kaiser M, Molenkamp R, Meijer A, Chu DKW, Bleicker T, Brünink S, Schneider J, Schmidt ML, Mulders DGJC, Haagmans BL, van der Veer B, van den Brink S, Wijsman L, Goderski G, Romette J-L, Ellis J, Zambon M, Peiris M, Goossens H, Reusken C, Koopmans MPG and Drosten C. 2020. Detection of 2019 novel coronavirus (2019- nCoV) by real-time RT-PCR. *Euro Surveill.*, **25(3)** 2020.
- Coronaviridae Study Group of the International Committee on Taxonomy of Viruses. 2020. The species severe acute respiratory syndrome-related coronavirus: classifying 2019-nCoV and naming it SARS-CoV-2. *Nat Microbiol.*, **5(4)**: 536-544.
- Dowd JB, Andriano L, Brazel DM, Rotondi V, Ding X, Liu Y and Mills MC. 2020. Demographic science aids in understanding the spread and fatality rates of COVID-19. *Proc Natl Acad Sci.*, **117**: 9696–9698.
- Glowacka I, Bertram S, Müller MA, Allen P, Soilleux E, Pfefferle S, Steffen I, Tsegaye TS, He Y, Gnirss K, Niemeyer D, Schneider H, Drosten C and Pöhlmann S. 2011. Evidence that TMPRSS2 activates the severe acute respiratory syndrome coronavirus spike protein for membrane fusion and reduces viral control by the humoral immune response. *J Virol.*, **85(9)**: 4122–34.
- Hoffman SJ and Silverberg SL. 2018. Delays in global disease outbreak responses: lessons from H1N1, Ebola, and Zika. *Am J Public Health.*, **108(3)**: 329–33.
- http://www.africacdc.org/_Africa centers for disease control and prevention. (Accessed 17 February, 2020).
- <https://www.weforum.org/agenda/2020/03/why-sub-saharan-africa-needs-a-unique-response-to-covid-19/>. Why Sub-Saharan Africa needs a unique response to COVID-19. May 20
- Ihekweazu C and Agogo E. 2020. Africa's response to COVID-19. *BMC Med.*, **18**: 151.
- Kampf G, Todt D, Pfaender S and Steinmann E. 2020. Persistence of coronaviruses on inanimate surfaces and their inactivation with biocidal agents. *J Hosp Infect.*, **104**: 246-251.
- Kapata N, Ihekweazu C, Ntounia F, Raji T, Chanda-Kapata P, Mwaba P, Mukonka V, Bates M, Tembo J, Corman V, Mfinanga S, Asogun D, Elton L, Arruda LB, Thomason MJ, Mboera L, Yavilinsky A, Haider N, Simons D, Hollmann L, Lule SA, Veas F, Hamid MMA, Dar O, Edwards S, Vairo F, McHugh TD, Drosten C, Kock R and Ippolito G. 2020. Is Africa prepared for tackling the COVID-19 (SARS-CoV-2) epidemic. Lessons from past outbreaks, ongoing pan-African public health efforts, and implications for the future. *Int J Infect Dis.*, **93**: 233–236.
- Kobia F and Gitaka J. 2020. COVID-19: Are Africa's diagnostic challenges blunting response effectiveness? [version 1; peer review: 1 approved] *AAS Open Research.*, **3**: 4
- Kuba K, Imai Y, Rao S, Gao H, Guo F, Guan B, Huan Y, Yang P, Zhang Y, Deng W, Bao L, Zhang B, Liu G, Wang Z, Chappell M, Liu Y, Zheng D, Leibbrandt A, Wada T, Slutsky AS, Liu D, Qin C, Jiang C and Penninger JM. 2005. A crucial role of angiotensin converting enzyme 2 (ACE2) in SARS coronavirus-induced lung injury. *Nat Med.*, **11**: 875–879.
- Li F. 2016. Structure, function, and evolution of coronavirus spike proteins. *Annu Rev Virol.*, **3(1)**: 237–261.
- Lu G, Hu Y, Wang Q, Qj J, Gao F, Li Y, Zhang, Y, Zhang, W, Yuan, Y, Bao, J, Zhang, B, Shi, Y, Yan, J and Ga GF. 2013. Molecular basis of binding between novel human coronavirus MERSCoV and its receptor CD26. *Nature.*, **500**: 227–231.

- Lu R, Zhao X, Li J, Niu P, Yang B, Wu H, Wang W, Song H, Huang B, Zhu N, Bi Y, Ma X, Zhan F, Wang L, Hu T, Zhou H, Hu Z, Zhou W, Zhao L, Chen J, Meng Y, Wang J, Lin Y, Yuan J, Xie Z, Ma J, Liu WJ, Wang D, Xu W, Holmes EC, Gao GF, Wu G, Chen W, Shi W and Tan W. 2020. Genomic characterisation and epidemiology of 2019 novel coronavirus: implications for virus origins and receptor binding. *Lancet.*, **395(10224)**: 565–574.
- Meo SA, Alhowikan AM, Al-Khlaiwi T, Meo IM, Halepoto DM, Iqbal M, Usmani AM, Hajjar W and Ahmed N. 2020. Novel coronavirus 2019-nCoV: prevalence, biological and clinical characteristics comparison with SARS-CoV and MERS-CoV. *Eur Rev Med Pharmacol Sci.*, **24(4)**: 2012-2019.
- NCDC Coronavirus diseases (COVID-19) prevention. https://ncdc.gov.ng/themes/common/docs/protocols/183_1584444646.pdf. (accessed 18th May, 2020)
- Njenga MK, Dawa J, Nanyingi M, Gachohi J, Ngere I, Letko M, Otieno CF, Gunn BM and Osoro E. 2020. Why is There Low Morbidity and Mortality of COVID-19 in Africa?. *Am J Trop Med Hyg.*, **103(2)**: 564–569.
- Nkengasong JN and Mankoula W. 2020. Looming threat of COVID-19 infection in Africa: act collectively, and fast. *Lancet.*, **395(10227)**: 841-842.
- Okonofua FE, Eimuhi KE and Akhere A. 2020. COVID-19: Perspectives and Reflections from Africa. *Afr J Reprod Health.*, **24(1)**: 10-13.
- Ong SWX, Tan YK, Chia PY, Lee TH, Ng OT, Wong MSY and Marimuthu K. 2020. Air, surface environmental, and personal protective equipment contamination by severe acute respiratory syndrome coronavirus 2 (SARS-CoV-2) from a symptomatic patient. *JAMA.*, **323(16)**: 1610-1612.
- Outbreak News Today. Italy COVID-19 case count now 79, government introduces urgent measures. Feb 23, 2020. <http://outbreaknewstoday.com/italy-covid-19-case-count-now-79-government-introduces-urgentmeasures-37376/> (accessed Feb 23, 2020).
- Pan A, Liu I, Wang C, Guo H, Hao X and Wang QT. 2020. Association of public health interventions with the epidemiology of the COVID-19 outbreak in Wuhan, China. *JAMA.*, **323(19)**: 1915-1923.
- PANDORA-ID-NET: Pan-African Network for rapid research and response and preparedness for infectious diseases epidemics. <https://www.pandora-id.net/>. [Accessed 17 February 2020].
- Paudel SS. 2020. A meta-analysis of 2019 novel coronavirus patient clinical characteristics and comorbidities. *Research Square.*, **3**: 12-23.
- Raj VS, Mou H, Smits SL, Dekkers DHW, Muller MA, Dijkman R, Muth D, Demmers JAAA, Zaki A, Fouchier RAM, Thiel V, Drosten C, Rottier PJM, Osterhaus ADME, Bosch BJ and Haagmans BL. 2013. Dipeptidyl peptidase 4 is a functional receptor for the emerging human coronavirus-EMC. *Nature.*, **495(7440)**: 251–4.
- Rothan HA and Byrareddy SN. 2020. Review article. The epidemiology and pathogenesis of coronavirus disease (COVID-19) outbreak. *J Autoimmun.* **109**:102433.
- Rothe C, Schunk M, Sothmann P, Bretzel G, Froeschl G, Wallrauch C, Zimmer T, Thiel V, Janke C, Guggemos W, Seilmaier M, Drosten C, Vollmar P, Zwirgmaier K, Zange S, Wölfel R and Hoelscher M. 2020. Transmission of 2019-nCoV Infection from an Asymptomatic Contact in Germany. *N Engl J Med.*, **382(10)**: 970-971.
- Saeedi P, Petersohn I, Salpea P, Malanda B, Karuranga S, Unwin N, Colagiuri S, Guariguata L, Motala AA, Ogurtsova K, Shaw JE, Bright D and Williams R. 2019. Global and regional diabetes prevalence estimates for 2019 and projections for 2030 and 2045: results from the International Diabetes Federation Diabetes Atlas, 9th edition. *Diabetes Res Clin Pract.*, **157**: 107843.
- Saeedi P. 2019. Global and regional diabetes prevalence estimates for 2019 and projections. *Diabetes Res Clin Pract.*, **157**: 107-843.
- Sandaradura I, Goeman E, Pontivivo G, Fine E, Gray H, Kerr S, Marriott D, Harkness J and Andresen D. 2020. A close shave? Performance of P2/N95 respirators in health care workers with facial hair: Results of the BEARDS (Adequate Respiratory DefenceS) study. *J Hosp Infect.*, **104(4)**: 529-533.
- Shereen MA, Khan S, Kazmi A, Bashir N and Siddique R. 2020. COVID-19 infection: Origin, transmission, and characteristics of human Coronaviruses. *J Adv Res.*, **24**: 91–98.
- Tao Y, Shi M, Chommanard C, Queen K, Zhang J, Markotter W, Kuzmin IV, Holmes EC and Tong S. 2017. Surveillance of bat corona viruses in Kenya identifies relatives of human corona viruses. *J Virol.*, **91**: 53-60.
- United Nations 2019. Population Dynamics, World Population Prospectus. Available at: <https://population.un.org/wpp/>. (Accessed May 3, 2020).
- van Boheemen S, de Graaf M, Lauber C, Bestebroer TM, Raj VS, Zaki AM, Osterhaus ADME, Haagmans BL, Gorbalenya AE, Snijder EJ and Fouchier RAM. 2012. Genomic characterization of a newly discovered coronavirus associated with acute respiratory distress syndrome in humans. *MBio.*, **3(6)**: e00473–e512.
- van Doremalen N, Bushmaker T, Morris DH, Holbrook MG, Gamble A, Williamson BN, Tamin A, Harcourt JL, Thornburg NJ, Gerber SI, Lloyd-Smith JO, de Wit, E and Munster, VJ. 2020. Aerosol and surface stability of SARS-CoV-2 as compared with SARS-CoV-1. *N Engl J Med.*, **382(16)**: 1564-1567.
- VOA: African Nations Try to Overcome Shortage of COVID-19 Test Kits | Voice of America - English. 2020; (Accessed: 4 April, 2020).
- Wan Y, Shang J, Graham R, Baric RS and Li F. 2020. Receptor recognition by novel coronavirus from Wuhan: an analysis based on decade-long structural studies of SARS. *J Virol.*, **94(7)**: e00127-20
- Wang H, Yang P, Liu K, Guo F, Zhang Y, Zhang G and Jiang C. 2008. SARS coronavirus entry into host cells through a novel clathrin and caveolae-independent endocytic pathway. *Cell Res.*, **18(2)**: 290–301.
- Wang N, Shi X, Jiang L, Zhang S, Wang D, Tong P, Guo D, Fu L, Cui Y, Liu X, Arledge KC, Chen Y-H, Zhang L and Wang X. 2013. Structure of MERS-CoV spike receptor-binding domain complexed with human receptor DPP4. *Cell Res.*, **23(8)**: 986-993
- WHOa. Pneumonia of unknown cause- China. Emergencies, preparedness, response, disease outbreak news, World health organization (WHO) 2020.
- WHOb. Director-General’s remarks at the media briefing on 2019-nCoV on 11 February 2020 <https://www.who.int/dg/speeches/detail/who-director-general-remarks-at-the-media-briefing-on-2019-ncov-on-11-february-2020>
- WHOc. Director-General’s opening remarks at the media briefing on COVID-19 - 11 March 2020 <https://www.who.int/dg/speeches/detail/who-director-general-s-opening-remarks-at-the-media-briefing-on-covid-19---11-march-2020>.

- WHOd. Ebola virus disease. 2020. <https://www.afro.who.int/health-topics/ebola-virus-disease>.
- WHOe. Management of ill travellers at Points of Entry–international airports, seaports and ground crossings – in the context of COVID -19 outbreak. 2020. <https://www.who.int/publications-detail/management-of-ill-travellers-at-points-of-entry-international-airports-seaports-and-ground-crossings-in-the-context-of-covid-19-outbreak>
- WHOf. Emergency ministerial meeting on COVID-19 organized by the African union and the Africa centres for disease control and prevention. 2020. <https://www.who.int/dg/speeches/detail/emergency-ministerial-meeting-on-covid-19-organized-by-the-african-union-and-the-africa-centres-for-disease-control-and-prevention>.
- World Bank. For Sub-Saharan Africa, Coronavirus Crisis Calls for Policies for Greater Resilience. 2020 Available at: <https://www.worldbank.org/en/region/afr/publication/for-sub-saharanafrica-coronavirus-crisis-calls-for-policies-for-greater-resilience>.
- Wu F, Zhao S, Yu B, Chen YM, Wang W, Song ZG, Hu Y, Tao Z-W, Tian J-H, Yuan PeiY-Y, Yuan M-L, Zhang Y-L, Dai F-H, Liu Y, Wang Q-M, Zheng J-J, Xu L, Holmes, EC and Zhang Y-Z. 2020. A new coronavirus associated with human respiratory disease in China. *Nature.*, **579(7798)**: 265-269.
- Wu P, Hao X, Lau EHY, Wong JY, Leung KSM, Wu JT, Cowling BJ and Leung GM. 2020. Real-time tentative assessment of the epidemiological characteristics of novel coronavirus infections in Wuhan, China, as at 22 January 2020, *Euro Surveill.*, **25(3)**:2000044.
- Xu I, Zhang X, Song W, Sun B, Mu J, Wang B, Wang, Z, Cao, Y and Dong, X. 2020. Conjunctival polymerase chain reaction-tests of 2019 novel coronavirus in patients in Shenyang, *China Med Rxiv* 2020. [Published online ahead of print]
- Xu X, Chen P, Wang J, Feng J, Zhou H, Li X, Zhong W and Pei HP. 2020. Evolution of the novel coronavirus from the ongoing Wuhan outbreak and modeling of its spike protein for risk of human transmission. *Sci China Life Sci.*, **63(3)**: 457–60.
- Yang J, Zheng Y, Gou X, Pu K, Chen Z, Guo Q, Ji R, Wang H, Wang Y and Zhou Y. 2020. Prevalence of comorbidities and its effects in patients infected with SARS-CoV-2: a systematic review and meta-analysis. *Int J Infect Dis.*, **94**: 91–95.
- Zhou F, Yu T, Du R, Fan G, Liu Y, Liu Z, Xiang J, Wang Y, Song B, Gu X, Guan L, Wei Y, Li H, Wu X, Xu J, Tu S, Zhang Y, Chen H and Cao B. 2020. Clinical course and risk factors for mortality of adult in patients with COVID-19 in Wuhan, China: a retrospective cohort study. *Lancet.*, **395(10229)**: 1054–1062.
- Zhou P, Yang X, Wang X, Hu B, Zhang L, Zhang W, Si H-R, Zhu Y, Li B, Huang C-L, Chen H-D, Chen J, Luo Y, Guo H, Jiang R-D, Liu M-Q, Chen Y, Shen X-R, Wang X, Zheng X-S, Zhao K, Chen Q-J, Deng F, Liu L-L, Yan B, Zhan F-X, Wang Y-Y, Xiao G-F and Shi Z-L. 2020. A pneumonia outbreak associated with a new coronavirus of probable bat origin. *Nature.*, **579(7798)**: 270-273.

Bioremediation for the Decolorization of Textile Dyes by Bacterial Strains Isolated from Dyeing Wastewater

Fahimeh Firoozeh¹, Yousef Dadban Shahamat², Susana Rodríguez-Couto³, Ebrahim Kouhsari⁴, Farhad Niknejad^{4,*}

¹Department of Microbiology, Islamic Azad University of Damghan, Damghan, Iran; ²Environmental Health Research Center; Department of Environmental Health Engineering, Faculty of Health, Golestan University of Medical Sciences, Gorgan, Iran; ³ Department of Separation Science, LUT School of Engineering Science, LUT University, Sammonkatu 12, 50130 Mikkeli, Finland; ⁴Laboratory Sciences Research Center, Golestan University of Medical Sciences, Gorgan, Iran.

Received: February 16, 2021; Revised: April 12, 2021; Accepted: May 23, 2021

Abstract

Background: The major concern to meet environmental regulations is related with the decolorization and detoxification of industrial dyes contaminated wastewater. So, this study was undertaken to examine the use of bacteria isolated from wastewater of textile factories in the removal of the synthetic textile dyes (Sudan Black, Methyl Red, Malachite Green, Rhodamine B and Brilliant Cresyl Blue). **Methods:** Dye contaminated wastewater was collected from some synthetic textile factories in Gorgan and Gonbad, Iran, and evaluated for the screening and isolation of bacteria capable of decolorizing textile dyes. The effect of function of operational parameters includes temperature (25, 37 and 50 °C), pH (4, 6 and 8) and initial dye concentration (100, 200 and 300 mg/mL) on the efficiency and rate of discoloration was assessed. **Results:** Totally, out of the 19 bacterial isolates from textile wastewater: Five bacterial isolates showed dye discoloration ability and the most efficient bacterial isolates were *Enterococcus faecium* and *Pantoea* spp. that decolorized Methyl Red, Sudan Black and Malachite Green dyes at 25-37°C, concentration of 200-300 mg/mL and slightly acidic to neutral pH. *Enterococcus* bacterium was able to decolorize Sudan Black to the 19.79% in the concentration of 100 mg/ml and pH=8 and temperature of 50°C. The highest amount of decolorizing was observed by *Pantoea* on Malachite Green to the amount of 73%. *Enterococcus* had the highest decolorizing on Methyl Red to the 65.7%. The amount of decolorizing on Sudan Black by *Enterococcus* (49.9%) was also higher than *Pantoea* (39.7%). **Conclusion:** Isolated bacteria had a significant reduction in toxicity and cationic malachite green dye and azo dye- methyl red. Thus, bacteria can be used in full-scale industrial wastewater treatment with the bio-synergy and its application in discoloration.

Key words: Textile Effluent, Dye, Bio-synergy, *Pantoea*, *Enterococcus faecium*

1. Introduction

Since 1856 when the first synthetic dye Mauveine was obtained, 100000 synthetic dyes in the world with an annual volume of a 0.7 million tons have been produced so far (Zollinger, 2005). Textile industry consumes two-thirds of this amount of dye (Gita *et al.*, 2017; Lakshmanan and Raghavendran, 2017; Singleton, 2013). Synthetic dyes are macromolecules that are not easily degraded, and some of them are toxic to plants and animals (Varjani *et al.*, 2020). Synthetic azo dyes are known with nitrogen-nitrogen double bond attached to the aromatic groups, and are as the most widely used dyes in the textile industry (Kannan *et al.*, 2013; Chaturvedi *et al.*, 2019). Inefficiency in the dyeing processes makes the 10-15% of the used dyes enters the wastewater (Nikhil *et al.*, 2012; Natarajan *et al.*, 2018; Samsami *et al.*, 2020). Declining water quality, lack of penetration into the lower layers of water, the impact on the gases solubility and toxicity of the dyes or materials resulting from their degradation are such factors threatening the environment (Boyd, 2019). Therefore,

elimination of dyes from textile dyeing effluents currently represents a major ecological concern. Chemical methods of wastewater treatment are generally expensive and have limited effectiveness with creating a lot of waste materials, eliminating of which is a new problem (Wu *et al.*, 2011; Crini and Lichtfouse, 2019). Microorganisms are a good alternative for treating contaminants such as synthetic dyes due to genetic and metabolic diversity because many of them, such as a variety of gram positive and negative bacteria, fungi, etc., are capable to decolorize synthetic dyes (Dangi *et al.*, 2019; Lellis *et al.*, 2019). Thus, bioremediation is very important because of low cost, no damage to the nature and small amount of waste products (Alalewi and Jiang, 2012; Vikrant *et al.*, 2018). Effluents of many textile mills of Iran are discarded to the deserts and saline lands because of their geographical location. The structure of many dyes contains toxic metals such as chromium that are released to the wastewater during dyeing and soluble salts such as sodium chloride and potassium chloride are also used in the process of dyeing. Thus, bioremediation in saline soils is associated with many problems due to the harsh conditions in these areas

* Corresponding author e-mail: fniknejad@yahoo.com.

and the only microorganisms are capable of solving it that can withstand the harsh conditions and grow and operate in which. Therefore, the use of halophilic and halotolerant bacteria is considered as a good choice for treating such effluents because halophilic and halotolerant bacteria show high tolerance in harsh environmental conditions such as high content of salt and pollutants such as heavy metals and oxyanions. Halophilic and halotolerant bacteria have shown great success in bioremediation of contaminants from oil and toxic oxyanions (Solís *et al.*, 2012; Ghodake *et al.*, 2011; Romano-Armada *et al.*, 2020). Thus, the aim of this study was to evaluate the use of microorganisms isolated from industrial textile effluents in the Gorgan and Gonbad cities in Golestan province, Iran for the removal of different synthetic dyes.

2. Materials and methods

2.1. Bacteria isolation and identification

In this study, 86 samples from different devices and final effluent of textile factories in Gorgan and Gonbad, Iran were collected and transported to the laboratory under sterile conditions. Then, 10 mL of each sample was added to 100 mL of Tryptic Soy Broth medium (Merck, Germany) and were incubated for 24 h at 37°C. Then, the bacteria were identified as conventional microbiological methods (Mahon *et al.*, 2018; Murray *et al.*, 2020).

2.2. PCR-Based-Sequencing

After the extracted purified genomic DNA, PCR was performed to amplify *tuf* gene using forward primer of 5'-GCCAGTTGAGGACGTATTCT-3' and reverse primer of 5'-CCATTTTCAGTACCTTCTGGTAA-3'.

The amplification reaction was done in 25 µL containing 10 pmol of each primer, dNTP in 2.5 mM, 0.6 U of Taq polymerase, 2.5 µL of the DNA template and 15 mM MgCl₂ buffer. The time and temperature cycle of thermocycler was as 15 minutes at 95 °C, then 35 cycles as 30 seconds at 95°C, 30 seconds at 56 °C and 45 seconds at 72 °C; and finally, 72 °C for 10 minutes (MyCycler Thermal Cycler, Bio-Rad, Munich, Germany) (Hwang *et al.*, 2011). Amplified products were pooled and purified were purified from agarose gel, and then they sequenced by a national instrumentation center for environmental management, South Korea (NICEM). Sequenced alignments were analyzed by the Basic Local Alignment Search Tool (BLAST) program and submitted to National Center Biotechnology Information (NCBI).

2.3. Dye discoloration

Dyes were sterilized by 0.45 micro-filter and then were added to Tryptic Soy Broth medium. Then, the purified strains were added to the culture medium tubes containing 10 mL of decolorizing medium (containing 0.5 g of glucose, 2.5 g yeast extract and 5 mg dye in 100 mL). The tubes were inoculated with 1% bacteria (opacity of 0.5

McFarland) and incubated at 37°C. Five different dyes (Sudan Black, Methyl Red, Malachite Green, Rhodamine B and Brilliant Cresyl Blue) were used (R Rohban *et al.*, 2009). Sudan Black (C₂₉H₂₄N₆) is a non-fluorescent, fat-soluble and thermostable azo dye that is used for staining neutral triglycerides, lipids and some lipoproteins. It seems as a dark brown to black powder with the maximum absorption at 596-605 nm and melting point of 120-124 °C. Methyl Red (2-(N,N-dimethyl-4-aminophenyl) azobenzenecarboxylic acid) that is also called as C.I. Acid Red 2 is an indicator dye that turns red in acidic solutions. Methyl Red is an azo dye as dark red crystalline powder. Methyl Red is a pH indicator. Malachite Green is an organic compound that is used as a pigment and is used as an antimicrobial agent in aquaculture controversially. It is commercially used for staining materials such as silk, leather and paper. Among the 19 isolated strains, the 5 strains were able to decolorize that were selected based on the degree of decolorizing. All strains were investigated separately at the effect of different temperature (25, 37 and 50°C), different initial dye concentration (100, 200 and 300 mg/L) and different pH (4, 6 and 8) on dye discoloration was assessed. All experiments were performed two times and mediums with dyes and non-inoculated mediums with dyes used as a blank. Due to the lack of decolorizing on Rhodamine B and Brilliant Cresyl Blue, these two dyes were deleted, and the process was continued with three other dyes (Rohban *et al.*, 2009).

2.4. Determination of dye discoloration

The maximum absorption wavelength of each dye determines by the spectrophotometer in the range of 200 to 800 nm. Then it was plotted the chart of each dye according to the amount of absorption in the wavelength of maximum absorbance and concentration of dye in the medium. Absorption of each dye in the wavelength of maximum absorption was measured, and the percentage of discoloration was calculated in accordance with the following formula (Pathak *et al.*, 2014; Rahimi *et al.*, 2016).

Percentage of discoloration: (The obtained OD - The initial OD)/ initial OD × 100

3. Results

Based on biochemical tests and molecular methods, some species of *Pantoea* genus and Gram-positive cocci, *Enterococcus faecium* were identified (Table 1).

The percentages of discoloration in samples of Methyl Red, Sudan Black and Malachite Green dyes based on the absorption at 340 nm for different initial dye concentrations, temperatures and pHs are shown in Tables 2, 3 and 4, respectively. The highest discoloration percentages for all the tested dyes were attained for acidic to neutral pH values and room temperature (25°C) and 37°C.

Table 1. Identification of species of *Pantoea* genus and Gram-positive cocci, *Enterococcus faecium*

No.	Sequencing Result	BLAST
1	CCATCCAAACCCACGCCACAAAAAGCACCTTGCCCGGAGTATAAGAAAGCCTT CGGGTTGTAAGTACTTTCACCGGGAGGAAAGCGATGGGGTTAATAGCCCCTTT TATTGACGTGACCCGCAAATAATCCACGCTAACTCCGCTGCCTACAACCTCGGT AACTTTTATAAGGTGCCGGCTGTTCTTGACAACCTTCGGCGGGGTCGTGCACGCTC GTGCTCCTGCTTCGATTCAATCTACACTTCCCAATCTAAACGTAAGTTTACCTTTT ACTTTAGACTAGGGTGGACCTCCACCCATTCTTCAATACTACCGCCACACTCCT ATCTTCATACTACTCACGTAACCTCGTGTTTTAACTTACTACAGGACTTGATGAT GGATCTTTAACTTACTAGACCTAATCGCAACCTCAAGTTTAAATTTAAATTCATCAT ATCCTTCTCTTTAAAATTTCTTCTGTCTCTTCAATTTCCACCGTCATTCCTTCTT TCA	<i>Pantoea</i> sp.
2	AAATTGGCGGGACTGTTGCTACAGGTCGTGTTGACGTGGACAAGTTCGCGTTGGT GACGAAGTTGAAGTTGTTGGTATTGCTGAAGAAACTTCAAAAACAACAGTTACTG GTGTTGAAATGTTCCGTAATGTTAGACTACGCTGAAGCTGGAGACAACATTGG TGCTTTACTACGTGGTGTGCACGTGAAGACATCCAACGTGGACAAGTTTGTAGCTA AACCAGGTACAATCACACCTCATAAAAATTCTCTGCAGAAGTATACGTGTTGAC AAAAGAAGAAGGTGGACGTCATACTCCATTCTTCAACTACCGTCCACAATTC TACTTCCGTACAACGTGACGTAACAGGTGTTGTTGAATTACCAGAAGGTACTGAAA TGGAAGGAGAAAAATTAGGGAAAAAGATTTTTTTTTTTAATTATAA	<i>Enterococcus faecium</i>
3	AATTGGGGGGTCTGTTGCTACGGTCGTGTTGACGTGGACAAGTTCGCGTTGGTG ACGAAGTTGAAGTTGTTGGTATTGCTGAAGAAACTTCAAAAACAACAGTTACTGG TGTTGAAATGTTCCGTAATGTTAGACTACGCTGAAGCTGGAGACAACATTGGT GCTTTACTACGTGGTGTGCACGTGAAGACATCCAACGTGGACAAGTTTGTAGCTA AACCAGGTACAATCACACCTCATAAAAATTCTCTGCAGAAGTATACGTGTTGAC AAAAGAAGAAGGTGGACGTCATACTCCATTCTTCAACTACCGTCCACAATTC TACTTCCGTACAACGTGACGTAACAGGTGTTGTTGAATTACCAGAAGGTACTGAAA TGGAAGGAGTTGTTAACTTATCAGGAGGGCCCGTGAGTGGAAC	<i>Enterococcus faecium</i>

Table 2. Discoloration percentage of Methyl Red at different initial dye concentrations, temperatures and pH values by *E. faecium* and *Pantoea* sp.

Dye	The initial concentration (mg/L)	pH	25 °C		37 °C		50 °C	
			<i>Enterococcus</i>	<i>Pantoea</i>	<i>Enterococcus</i>	<i>Pantoea</i>	<i>Enterococcus</i>	<i>Pantoea</i>
Methyl Red	100	4	4.3%	12.06%	4.3%	9.04%	0.00%	2.51%
		6	9.1%	26.02%	7.3%	28.31%	0.00%	0.00%
		8	43.99%	9.02%	1.34%	11.45%	0.00%	0.00%
	200	4	14.33%	16.57%	13.16%	26.28%	0.00	18.85%
		6	54.43%	49.22%	12.11%	45.87%	0.00	15.93%
		8	65.78%	49.74%	28.62%	42.21%	28.22%	0.00%
	300	4	0.00%	14.09%	0.00%	14.09%	0.00%	0.00%
		6	0.00%	9.55%	0.00%	9.55%	0.00%	0.00%
		8	0.00%	0.00%	0.00%	0.00%	0.00%	0.00%

Table 3. Discoloration percentage of Sudan Black at different initial dye concentrations, temperatures and pH values by *E. faecium* and *Pantoea* sp.

Dye	The initial concentration (mg/L)	pH	25 °C		37 °C		50 °C	
			<i>Enterococcus</i>	<i>Pantoea</i>	<i>Enterococcus</i>	<i>Pantoea</i>	<i>Enterococcus</i>	<i>Pantoea</i>
Sudan Black	100	4	26.08%	0.00%	29.34%	0.00%	5.34%	0.00%
		6	28.88%	18.85%	37.03%	22.13%	0.00%	0.00%
		8	44.67%	35.29%	46.19%	39.70 %	19.79%	8.08%
	200	4	24.21%	0.00%	0.00%	0.00%	24.21%	0.00%
		6	49.96%	28.99%	0.00%	34.31%	32.10%	0.00%
		8	43.60%	13.18%	0.00%	18.13%	43.12%	0.00%
	300	4	7.3%	0.00%	7.3%	0.00%	7.1%	0.00%
		6	0.00%	0.00%	0.00%	0.00%	0.00%	0.00%
		8	43.25%	0.00%	23.41%	0.00%	0.00%	0.00%

Table 4. Discoloration percentage of Malachite Green at different initial dye concentrations, temperatures and pH values by *E. faecium* and *Pantoea* sp.

Dye	The initial concentration (mg/L)	pH	25 °C		37 °C		50 °C	
			Enterococcus	<i>Pantoea</i>	Enterococcus	<i>Pantoea</i>	Enterococcus	<i>Pantoea</i>
Malachite Green	100	4	5.6%	0.00%	0.00%	0.00%	0.00%	0.00%
		6	22.33%	0.00%	26.21%	0.00%	2.9%	0.00%
		8	41.84%	0.00%	42.55%	0.00%	41.84%	0.00%
	200	4	2.81%	8.6%	0.00%	10.75%	0.00%	7.52%
		6	0.00%	8.8%	0.00%	12%	0.00%	8.8%
		8	25.73%	71.53%	44.85%	18.13%	25%	0.00%
	300	4	0.00%	7.05%	0.00%	9.4%	0.00%	9.4%
		6	0.00%	0.00%	0.00%	0.00%	0.00%	0.00%
		8	28.08%	73.87%	32.87%	73.87%	32.19%	0.00%

3.1. Effect of pH on dye discoloration

The highest decolorizing percentage of Methyl Red and Malachite Green for both bacteria (i.e. *Pantoea* sp. and *E. faecium*) was attained at pH 8. As for Sudan Black, the highest discoloration was achieved at pH 8 for *Pantoea* sp. and at pH 6 for *E. faecium*.

3.2. Effect of temperature on dye discoloration

The highest decolorizing percentage of Methyl Red for both bacteria was attained at 25°C, whereas for Sudan Black it occurred at 37°C for *Pantoea* sp. and at 25°C for *E. faecium*. As for Malachite Green, highest discoloration was achieved at 37 °C for *E. faecium* and at 25 °C and 37 °C for *Pantoea* sp.

3.3. Effect of initial dye concentration on dye discoloration

Both bacteria showed the highest Methyl Red discoloration at a concentration of 200 mg/L. The highest Sudan Black discoloration was attained at 100 mg/L for *Pantoea* sp and at 200 mg/L for *E. faecium* whereas Malachite Green was highest decolorized at the concentrations of 200 mg/L and 300 mg/L for *E. faecium* and *Pantoea* sp., respectively.

3.4. Effect of bacteria type on dye discoloration

According to the results obtained, both *E. faecium* and *Pantoea* spp. showed high ability in dye discoloration at 25 and 37 °C, initial dye concentrations of 200-300 mg/L, and pH values from slightly acidic to neutral. But *E. faecium* decolorized Sudan Black by 19.79% at an initial dye concentration of 100 mg/L, pH=8 and 50 °C. It also had discoloration ability in the concentration of 200 mg/L at 50 °C and pH of 4, 6 and 8 to the extent of 24.21%, 32.10% and 43.12%, respectively. Methyl Red was decolorized at a temperature of 50 °C and pH=8 by 28.22% and Malachite Green was decolorized at three initial dye concentrations (100, 200 and 300 mg/L) at pH=8 and a temperature of 50 °C by 41.84%, 25% and 32.19%.

4. Discussion

Azo dyes are the largest group of synthetic dyes that are about 60-70% of all organic dyes in the world. These dyes have a great performance and are used in various industries such as textile, pharmaceutical and cosmetics

industries, as well as food, paper, leather and painting industries. However, the negative aspects of these dyes and the risks may have for human health and the environment are not considered more and this may cause the disorder in nature in the not-too-distant future. Based on the findings of this study, the highest amount of discoloration was observed by *Pantoea* sp. bacterium on Malachite Green (73.87%) followed by *E. faecium* on Methyl Red (65.78%). The amount of discoloration on Sudan Black by *E. faecium* (49.96%) was higher than by *Pantoea* sp. (39.7%).

Enterococcus bacteria had the highest discoloration of Methyl Red at the concentration of 200 mg/L, the pH of 8 and 6, as the 65.78% and 54.43%, respectively. It had the highest discoloration on Sudan Black at the concentration of 200 mg/L, pH=6 to the 49.96%; and so, the discoloration of 44.85% was for Malachite Green at the concentration of 200 mg/L and pH=8. Overall, this study is consistent with other studies more closely and found that the experimental conditions of discoloration are almost identical for the isolated strains. The five dyes used in this study were isolated from the 19 strains, and two strains were not capable of decolorizing at experimental conditions including Rhodamine B and Brilliant Cresyl Blue in comparison with remaining three dyes of Methyl Red, Sudan Black and Malachite Green.

Adsorption and/or degradation are the two mechanisms responsible for dye decolorization by microorganisms (Ohadi *et al.*, 2020; Ghazvini *et al.*, 2016).

Due to the fact that the studies so far had wide variation in the type of dyes used for discoloration, the varying metabolic functions of the different bacterial isolates, and diversity of microbial species in the process of discoloration, so the model described by other researchers may be different from each other, but all showed a positive trend for these activities in laboratory and research scale processes. Mujtaba Ali and her colleague in 2014 revealed that the ability of discoloration on crystal violet occurred with better percentage by *Pseudomonas aeruginosa*, *Clostridium perfringens* and *Proteus vulgaris* in the presence of organic compounds compared with inorganic compounds (Ali and Akthar, 2014).

In the present study, the presence of organic compounds was considered in the wastewater by default. Despite the difference in the type of dyes used and the type of decolorizer microorganisms, the decolorizing capability of bacterial strains will not be inevitable. Aftab *et al.*

performed a research in Pakistan in 2011 to study the ability of *Corynebacterium* sp. for discoloration and degradation of Reactive Black 5 and Yellow 15 dyes to the concentration of higher than 10 mg/ml and observed the growth of bacteria at 37 °C and pH=7. *Corynebacterium* indicated high azoreductase activity against Reactive Black 5 (68%) and Reactive Yellow 15 (80%) (Aftab *et al.*, 2011).

The amount of discoloration in any of the microorganisms tested during both studies reached 80 percent in special circumstances, which shows high degradation power on dyestuff by some microbes.

Discoloration performed at lower concentrations follows first-order kinetics and high concentrations have second-order kinetics. The calculated rate constants for lower concentrations show higher values. Evaluation of different results shows that different strains of *Pseudomonas* have various abilities for degradation of azo dyes in different concentrations which can be used based on the components and concentration of colors.

It is also the results of discoloration of azo dye of Acid Orange by *Staphylococcus hominis* RMLRT03 in the soil around the textile factories in Bushnell Haas medium (BHM) were showed that the bacterial strains were found by 16S rDNA sequence as *Staphylococcus hominis*. This strain of bacteria along with glucose supplement and yeast extract as an ancillary substrate shows good discoloration in terms of stillness. Optimal conditions for discoloration of Acid Orange by *Staphylococcus hominis* RMLRT03 was pH=7.0 and temperature of 35 °C in 60 hours' incubation. This bacterial strain can withstand high concentrations of Acid Orange dye to more than 600 mg/L. High discoloration activity under natural environmental conditions shows that bacterial strains have practical application in the treatment of wastewater containing dyes (Singh *et al.*, 2014).

In the other study in India isolated *Pseudomonas* bacteria from soil contaminated quickly was decolorized the Methyl Orange azo dye solution. This bacterium has a remarkable discoloration in a wide range of concentrations of dye (50 to 200 mg/L) and pH (6-10) and temperature (30-40 °C). In addition, *Pseudomonas* spp. demonstrated discoloration of Methyl Orange for more than four cycles with high discoloration (10-94%) (Shah *et al.*, 2013).

Another study has performed to discoloration and decomposition of azo dye of Remazol Black B by new strains of *Pseudomonas putida* in India. Results showed that the pH=7.0 and temperature of 35 °C was optimal conditions for discoloration because the maximum discoloration has been observed only in these conditions. The amount of 5 g/L glucose in the culture medium also showed maximum discoloration. The new isolate has grown well in high concentrations of dye (300 mg/L) and has had 97.12% discoloration during 48 hours, and it also withstands concentrations over 1000 mg/L dye. *P. putida* colorless cells and UV-visible spectroscopy analysis suggested that discoloration activity of bio-decomposition is not just through disabling adsorption. The above results showed that this bacterial strain can be used in biological treatment of textile wastewater under optimal conditions (Kannan *et al.*, 2013). Haidari-kashl *et al.* (2013) had performed a kinetic and comparative study on microbial degradation of azo dyes by *P. aeruginosa* and *P. putida*. In this study, four azo dyes including Acid Blue 113 (AB-

113), Basic Red 46 (BR-46), Direct Blue 151 (DB- 151), Direct Brown (DB-2) and a mixture of these four colors (Mix) were investigated for biodegradation by *P. aeruginosa* and *P. putida* at pH=7.2 and temperature of 30 °C. *P. aeruginosa* has fully decomposed AB-113 dye at all concentrations, BR-46 dye at concentrations of 0.1 and 0.2 g/L and DB-2 dye at concentrations of 0.1, 0.2 and 0.5 g/L. *P. putida* has completely decomposed the AB-113 dye at concentrations of 0.1 and 0.2 g/L and DB-2 dye in concentrations of 0.1 and 0.2 g/L. Also, a mixture of four dyes was degraded at a concentration of 0.1 g/L by *P. putida*. Discolorations performed at lower concentrations follow first-order kinetics and high concentrations follow second-order kinetics. The calculated rate constants for lower concentrations show higher values. Evaluation of different results showed that different of *Pseudomonas* strains have various abilities in decomposition of azo dyes in different concentrations which could be used based on components and concentrations of dyes (Haidari kashl *et al.*, 2013).

Kumar *et al.* (2012) have examined discoloration of Red 3BN azo dyes by *Bacillus cereus* and *Bacillus megaterium* in ZZ Medium in India. Physico-chemical parameters such as carbon sources, nitrogen sources, temperature, pH and volume of injection for discoloration process were optimized by changing one of these parameters at a time. Optimal conditions for *B. cereus* was 1% sucrose, 25% peptone, pH=7, 37 °C and 8% inoculation and for *B. megaterium* was 1% glucose, 0.25% yeast extract, pH=6, 37 °C and 10% inoculation. Enhancement of discoloration under the above conditions was 93.64% for *B. cereus* and 96.88% for *B. megaterium* (Kumar and Bhat Sumangala, 2012).

Regarding the wide range of dyes with different structures, wastewater can mainly contain highly variable combinations. Currently, conventional treatment systems to remove dyes are available which are primarily dependent on the chemical and physical principles. In these ways, a large amount of sludge is produced due to the use of high levels of chemicals, so dyes do not disappear completely, and this is administratively difficult and costly. Thus, new approaches of microbial discoloration are economically efficient; they are also very valuable in terms of contribution to the health of the environment. In the past two decades, it has been performed considerable works aimed at using microorganisms as cleaning agents for environmental pollutants from dyeing wastewater of textile mills. According to the results obtained and the ability of bacteria isolated from decomposition of dyestuff in wastewater, optimization of conditions for the use of these microorganisms or the same microorganisms in biological purification in wastewater containing industrial dyes can be an effective help in this process and reuse of reversible waters. Therefore, applicable and targeted studies on strains such as *Enterococcus*, *Pantoea* or other microbial species can help in achieving this importance in the long run. Therefore, these studies highlight prospect for the authorities of economically feasible, environmental-friendly, effective and worthwhile approaches for treatment of textile industry waste waters. The principal benefit to use of bacteria is that they are easy to culture and can grow more rapidly as compared to other microbes. Future study is expected to focus in this significant area of

microbial sciences to solve industry's environmental problems.

5. Conclusion

Our observations emphasize that *Enterococcus* and *Pantoea* as bioremediation have a good efficiency to remove toxic and cationic Malachite Green and azo dye of Methyl Red. Bacteria can be used in the full-scale textile wastewater treatments as bioaugmentation, decolorization, degradation and effectively and economically treat non-biodegradable and toxic wastewaters. Nevertheless, more investigation is required to authenticate the process with particular interest.

Acknowledgments

This study was a part of M. Sc. thesis entitled "Discoloration of dyes wastewater from industrial park of Gorgan by selected microorganism (fungi-bacteria) and identification with molecular methods"; which was submitted at Islamic Azad University of Damghan. The authors thank the members of microbial laboratory of Golestan University of Medical Sciences for their cooperation.

Reference to a journal publication:

Ogunseitan OA. 1998. Protein method for investigating mercuric reductase gene expression in aquatic environments. *Appl Environ Microbiol.*, 64 (2): 695-702.

Reference to a book:

Brown WY and White SR. 1985. **The Elements of Style**, third ed. MacMillan, New York.

References

- Aftab U, Khan MR, Mahfooz M, Ali M, Aslam SH and Rehman A. 2011. Decolorization and degradation of textile azo dyes by *Corynebacterium* sp. isolated from industrial effluent. *Pakistan J. Zool.*, 43 (1):1-8.
- Alalewi A and Jiang C. 2012. Bacterial influence on textile wastewater decolorization. *J. Environ. Prot.*, 3 (08): 889-991.
- Ali SM and Akthar N. 2014. A study on bacterial decolorization of crystal violet dye by *Clostridium perfringens*, *Pseudomonas aeruginosa* and *Proteus vulgaris*. *Biol Sci.*, 4 (2): 89-96.
- Boyd CE. 2019. **Water quality: an introduction**, third ed, Springer International Publishing, Switzerland.
- Chaturvedi S. 2019. Azo Dyes Decolorization Using White Rot Fungi. *Res Rev J Microbiol Biotechnol.*, 8 (2): 9-19.
- Crini G, Lichtfouse E. 2019. Advantages and disadvantages of techniques used for wastewater treatment. *Environmental Chemistry Letters*, Springer Verlag., 17 (1):145-155.
- Dangi A, Sharma B, Hill R and Shukla P. 2019. Bioremediation through microbes: systems biology and metabolic engineering approach. *Crit Rev Biotechnol.*, 39 (1): 79-98.
- Ghazvini RD, Kouhsari E, Zibafar E, Hashemi SJ, Amini A and Niknejad F. 2016. Antifungal activity and aflatoxin degradation of *Bifidobacterium bifidum* and *Lactobacillus fermentum* against toxigenic *Aspergillus parasiticus*. *Open Microbiol J.*, 10:197-201.
- Ghodake G, Jadhav U, Tamboli D, Kagalkar A and Govindwar S. 2011. Decolorization of textile dyes and degradation of mono-azo dye amaranth by *Acinetobacter calcoaceticus* NCIM 2890. *Indian J Microbiol.*, 51 (4): 501-508.
- Gita S, Hussan A and Choudhury T. 2017. Impact of textile dyes waste on aquatic environments and its treatment. *Environ. Ecol.*, 35 (3C): 2349-2353.
- Haidari Kashi S, Rezaee Tavirani M, Khorasani A, Falavarjani I, Pakzad I and Nourmoradi H. 2013. Comparative and Kinetic Studies on Microbial Decolorization of Azo Dyes By *Pseudomonas Aeruginosa* and *Pseudomonas Putida*. *J Ilam Uni Med Sci.*, 21 (4): 159-170.
- Hwang SM, Kim MS, Park KU, Song J and Kim E. 2011. Tuf gene sequence analysis has greater discriminatory power than 16S rRNA sequence analysis in identification of clinical isolates of coagulase-negative staphylococci. *J Clin Microbiol.*, 49 (12): 4142-4149.
- Kannan S, Dhandayuthapani K and Sultana M. 2013. Original Research Article Decolorization and degradation of Azo dye-Remazol Black B by newly isolated *Pseudomonas putida*. *Int. J. Curr. Microbiol. App. Sci.* 2 (4): 108-116.
- Lakshmanan S and Raghavendran G. 2017. Low water-consumption technologies for textile production. **Sustainable fibres and textiles**. Elsevier.
- Lellis B, Fávaro-Polonio C, Pamphile JA and Polonio J, Innovation. 2019. Effects of textile dyes on health and the environment and bioremediation potential of living organisms. *Biotechnol. Res. Innov.*, 3(2):275-90.
- Mahon C, Lehman D, Manuvelis G. 2018. **Textbook of diagnostic microbiology-e-book**, Elsevier Health Sciences.
- Murray P, Rosenthal K and Pfaller M. 2020. **Medical Microbiology E-Book**, Elsevier Health Sciences.
- Natarajan S, Bajaj H and Tayade R. 2018. Recent advances based on the synergetic effect of adsorption for removal of dyes from waste water using photocatalytic process. *J Environ Sci (China)*, 65: 201-222.
- Nikhil B, Sapna T and Kshama B. 2012. Biodegradation of reactive red M8B by bacterial consortium SpNb1. *Indian J Sci Technol.*, 5 (7): 3047-3053.
- Ohadi E, Lotfali E, Ahmadi A and Ghafouri Z. 2020. Microbiological detoxification of mycotoxins: Focus on Mechanisms and Advances. *Infect Disord Drug Targets.*, 20: 1-19.
- Pathak H, Soni D and Chauhan K. 2014. Evaluation of in vitro efficacy for decolorization and degradation of commercial azo dye RB-B by *Morganella* sp. HK-1 isolated from dye contaminated industrial landfill. *Chemosphere*. 105: 126-132.
- Kumar G and Sumangala K. 2012. Decolorization of azo dye Red 3BN by bacteria. *Int. res. j. biol. Sci.*, 1 (5): 46-52.
- Rahimi E, Shahamat Y, Atabi F and Khezri S. 2016. Mineralization and Decolorization of Fermentation Industry Wastewater by Catalytic Ozonation Process: Kinetics and Mechanism. *J-Mazand-Univ-Med-Sci.* 26 (140): 115-126.
- Rohban R, Amoozegar M and Ventosa A. 2009. Screening and isolation of halophilic bacteria producing extracellular hydrolyses from Howz Soltan Lake, Iran. *J. Ind. Microbiol. Biotechnol. J IND MICROBIOL BIOT.*, 36 (3): 333-340.
- Romano-Armada N, Yañez-Yazlle M, Irazusta V, Rajal V and Moraga N. 2020. Potential of bioremediation and pgp traits in streptomycetes as strategies for bio-reclamation of salt-affected soils for agriculture. *Pathogens.*, 9 (2): 117.
- Samsami S, Mohamadi M, Sarrafzadeh M, Rene E, Firoozbahr M, and Protection E. 2020. Recent advances in the treatment of dye-containing wastewater from textile industries: Overview and perspectives. *Process Saf Environ Prot.*, 143: 138-163.

- Shah M, Patel K, Nair S and Darji A. 2013. Microbial decolorization of methyl orange dye by *Pseudomonas* spp. *Int. J. Environ. Bioenergy*. **1**: 54-59.
- Singh R, Singh P, Singh R. 2014. Bacterial decolorization of textile azo dye acid orange by *Staphylococcus hominis* RMLRT03. *Toxicol. Int.* **21** (2): 160.
- Singleton J. 2013. **World textile industry**, Routledge.
- Solis M, Solis A, Pérez H, Manjarrez N, and Flores M. 2012. Microbial decolouration of azo dyes: a review. *Process Biochem.* **47** (12): 1723-1748.
- Varjani S, Rakholiya P, Ng H, You S and Teixeira J. 2020. Microbial degradation of dyes: An overview. *Bioresour Technol.*, **314**:123728.
- Vikrant K, Giri B, Raza N, Roy K, Kim K and Rai B. 2018. Recent advancements in bioremediation of dye: current status and challenges. *Bioresour Technol.*, **253**: 355-367.
- Wu Y, Hu Y, Xie Z, Feng S, Li B and Mi X. 2011. Characterization of biosorption process of acid orange 7 on waste brewery's yeast. *Appl. Biochem. Biotechnol.*, **163** (7): 882-894.
- Zollinger H. 2005. Color Chemistry: Synthesis, Properties, and Applications of Organic Dyes and Pigments, 3rd revised edition. *Color Res Appl.*, **30** (4): 313-314.

Phenotypic and Genotypic Diversity of Microsymbionts Nodulating *Medicago sativa* (L.) in the Algerian Sahara

Salim Azib^{1,*}, Hamid Cheloufi², Sara Attab¹, Nouredine Bouras^{3,4} and Michael D. Holtz⁵

¹ Laboratoire des Bioressources Sahariennes. Préservation et Valorisation, Université de Ouargla, BP 511, Ouargla 30000, Algeria; ² Laboratoire de Recherche en Phœniciculture, Université de Ouargla, BP 511, Ouargla 30000, Algeria; ³ Laboratoire de Biologie des Systèmes Microbiens (LBSM), Ecole Normale Supérieure de Kouba, Alger, Algeria; ⁴ Département de Biologie, Faculté des Sciences de la Nature et de la Vie et Sciences de la Terre, Université de Ghardaïa, BP 455, Ghardaïa 47000, Algeria; ⁵ Field Crop Development Centre, Alberta Agriculture and Forestry, 5030 – 50 Street, Lacombe, Alberta T4L1W8, Canada.

Received: February 16, 2021; Revised: June 2, 2021; Accepted: July 1, 2021

Abstract

This work was conducted to evaluate the phenotypic and phylogenetic diversity of 48 rhizobial strains. All rhizobial strains exhibited a broad tolerance to salinity and pH. In general, they grew well at 28°C and 37°C but poorly at 4°C and 45°C. The rhizobial strains showed an array of antibiotic sensitivity patterns. The numerical (UPGMA) analysis of phenotypic traits and the phylogenetic tree of concatenated housekeeping genes produced highly similar results. Phylogenetic analysis of *recA* and *glnII* showed that all the isolates were affiliated to the genus *Sinorhizobium*, but belong to two distinct groups: Group I, originating in Ghardaïa, was close to the species *S. meliloti* and *S. kummerowiae*. Group II, originating in Ouargla and El Oued, clustered separately from sequences of known *Sinorhizobium* species, which suggests they could be a new lineage. The classifications resulting from the *nodC* gene reflect host specificity, while phylogeny based on chromosomal genes is independent of the host plant. Based on the studies documented in the literature, the genetically characterized rhizobial strains can be used as an effective inoculant for the improvement of forage yields in Saharan regions.

Keywords: Abiotic stress, phylogeny, alfalfa, rhizobia, arid environment.

1. Introduction

Alfalfa (*Medicago sativa*) is one of the oldest forage crops and contributes immensely to world food production (Massimi et al., 2017). It is vital due to its high protein content, high biomass yield, excellent nutritive value and high digestibility. It is widely planted throughout the world, especially in the arid and semi-arid areas (Zhang and Wang, 2015). This forage crop provides fixed nitrogen to agricultural ecosystems and reduces dependence on synthetic N fertilizers (Mouradi, 2016; Ahmad et al., 2016). However, in adverse conditions such as high salinity and drought, the survival of rhizobia is greatly affected (Domínguez-Ferreras et al., 2006) and therefore, nodulation and effectiveness in alfalfa can be significantly reduced (Brigido et al., 2013; del Pozo et al., 2017; Azib et al., 2020).

Very little is known about the diversity of rhizobial strains nodulating Saharan varieties of alfalfa, despite the alfalfa-sinorhizobia symbiosis being one of the best studied plant-microorganism interactions. So far, only two closely related species are known to be able to nodulate alfalfa: *Sinorhizobium meliloti* and *S. medicae* (Tabares-Rosa et al., 2019).

The development of polyphasic taxonomy (phenotypic, genotypic and phylogenetic characteristics) and the use of

16S rRNA as a taxonomic marker has led to many changes in the taxonomy of rhizobia (Zakhia and de Lajudie, 2006). A highly conserved gene like *16S rRNA* is not suitable for the discrimination of closely related *Sinorhizobium* (or *Ensifer*) species (Martens et al., 2007). To overcome these limitations, the multilocus sequence analysis (MLSA) of several protein encoding housekeeping genes (*atpD*, *recA* and *glnII*, etc.) has been suggested as alternative phylogenetic markers (Stackebrandt et al., 2002).

The aim of this study was to investigate phenotypic and genotypic diversity of 48 strains nodulating alfalfa in 14 Algerian Saharan sites affected by salt and drought. Firstly, phenotypic characterization for tolerance to salinity, temperature, pH and antibiotics was assessed; secondly, housekeeping genes *recA* and *glnII*, and symbiotic gene *nodC* were used to establish phylogeny of these strains.

2. Materials and methods

2.1. Nodule collection and isolation of rhizobia

During the period from February to March of 2014, root nodules of alfalfa plants were collected from 14 sites (Table 1) and rapidly dried and kept in tubes containing desiccant according to the method described by Somasegaran and Hoben (1985).

* Corresponding author e-mail: s_azib@hotmail.com.

Desiccated nodules were rehydrated before sterilization. Nodules were placed in small beakers with clean cool water and left in the refrigerator to soak overnight. Then, they were surface sterilized with 95% ethanol for 10 seconds, and transferred to 3% (v/v) solution of sodium hypo-chlorate for 3-4 minutes. The surface sterilized nodules were then rinsed in five changes of sterile distilled water to completely rinse the sterilizing chemicals (Somasegaran and Hoben, 1985).

The rhizobia were isolated following the standard method on yeast extract mannitol medium (YEM) (Vincent, 1970). Each nodule was crushed in a drop of sterile distilled water and suspension was streaked onto YEM Agar. Bacterial colonies appeared after incubation at 28°C for 3-5 days. A single representative colony, for each sample, was restreaked on freshly prepared YEM plates in order to obtain pure cultures.

Table 1. Site description, and strain names, location, type of climate, soil type, salinity of irrigation water and year of sampling.

Site	Station	Strains	Geographical position	Soil texture	Salinity of irrigation water (g/l)*	Period of sampling
Ouargla	Hassi Ben Abdallah	O114, O144, O152, O172	Lat. 32°00'77''N Long. 5°46'27''E	Sandy	2 to 42 to 4	February 2014
	Oum Erraneb	O211, O213, O223	Lat. 32°05'03''N Long. 5°34'46''E		2 to 4	February 2014
	ITAS	O313, O321, O344	Lat. 31°94'11''N Long. 5°29'54''E			March 2014
	Chott Ain Beida	O413, O422, O434, O442, O452, O461	Lat. 31°97'76''N Long. 5°38'96''E			March 2014
Ghardaia	Daya Ben Dahoua	G131, G132, G122, G124	Lat. 32°53'53''N Long. 4°40'35''E		1 to 41 to 1.5	March 2014
	Mansoura	G211, G241, G242	Lat. 31°98'25''N Long. 3°57'52''E	Sandy	1 to 1.5	March 2014
	Oued Laroui	G312, G315, G321	Lat. 32°57'01''N Long. 3°62'86''E			March 2014
	Sebseb	G42, G422, G424, G431, G432	Lat. 32°17'01''N Long. 3°57'52''E			March 2014
	Guerrara	G514, G522	Lat. 32°67'89''N Long. 4°73'77''E			March 2014
El Oued	Tenedla	E114, E131, E141	Lat. 33°67'58''N Long. 6°03'72''E	Sandy	2 to 62.5 to 6	April 2014
	El-Meghaier	E213, E222, E251	Lat. 33°56'25''N Long. 5°92'71''E		2 to 4	April 2014
	Djamaa	E353	Lat. 33°52'30''N Long. 6°02'32''E		2 to 4	April 2014
	Guemmar	E414, E421, E432, E441, E452	Lat. 33°51'07''N Long. 6°78'26''E			April 2014
	Reguiba	E52, E532, E543	Lat. 33°56'25''N Long. 6°71'74''E			April 2014

*: values taken from OSS (2003).

2.2. Nodulation tests

All the cultures obtained were tested for nodulation in the host plant *Medicago sativa* (Alfalfa). Isolates were used to inoculate surface sterilized alfalfa seeds growing in tubes containing Jensen's N-free agar medium (Jensen and Hauggaard-Nielsen, 2003) and evaluated after six weeks according to presence or absence of nodules (Gibson, 1980). The experiment was conducted in a plant growth chamber with 16/8 h day/night and 22°C.

Two day old seedlings were transferred into test tubes (15 cm × 2 cm) with one seedling per tube, containing 10 ml of agar slant medium and inoculated with 1 ml of standardized bacterial suspension (OD_{600nm} of 0.9).

2.3. Phenotypic characterization

Isolates that induced nodulation in alfalfa were used in this study. Two closely related *Sinorhizobium meliloti* strains, Sm1021 and Sm2011 received from Dr. Helene Berges, Plant Genomic Center (CNRGV, INRA-France), were used as reference strains.

The tolerance of isolates to NaCl was tested by using YEM supplemented with 1.7, 40, 80, 160, 320, 640 and 1280 mM NaCl. The tolerance to pH was assessed by adjusting the pH to 4.0, 5.0, 6.0, 6.8, 8.0 and 9.0 through the addition of acid or base to the YEM (Vincent, 1970). Isolates were examined for tolerance to temperature by

incubating at 4, 28, 37 and 45°C as described by Niste *et al.* (2015).

The resistance to ten antibiotics ($\mu\text{g}/\text{disc}$): fusidic acid: 10 μg (FA), amikacin: 30 μg (AK), amoxicillin: 25 μg (AMX), chloramphenicol: 30 μg (C), colistin: 10 μg (CS), erythromycin: 15 μg (E), kanamycin: 30 μg (K), penicillin: 6 μg (P), spiramycin: 100 μg (SP) and vancomycin: 30 μg (VA), was tested on YEM plates by adding antibiotic discs on the surface of the agar.

The growth was recorded after 72 h of incubation at 28°C in liquid YEM by measuring the OD at 600 nm (Wei *et al.*, 2004) and on solid YEM by counting the colonies appearing on the plates. Tests tubes containing 10 ml of liquid YEM were inoculated with 0.1 ml of a fresh culture of each isolate and incubated under shaking (200 rpm). On solid YEM, supplemented with 1.5% agar, inoculation is carried out by streaking on Petri plates (Vincent, 1970; Somasegaran and Hoben, 1985).

2.4. DNA extraction and PCR amplification and purification

Total genomic DNA of the isolates was extracted using DNeasy® Blood and Tissue Kit columns in accordance with the manufacturer's protocol (QIAGEN Ltd.) from cells grown for 3 days in yeast extract mannitol broth (YMB) at 28°C under shaking (200 rpm). After extraction, the DNA was quantified to determine its approximate quantity and relevance for further analysis using agarose gel electrophoresis.

Housekeeping genes *glnII* and *recA*, and symbiotic gene *nodC* were amplified by PCR using the following primers: GSII-1F (5'-AACGCAGATCAAGGAATTCG-3') and GSII-4R (5'-GCGACGATCTGGTAGGGGT-3') (Turner and Young, 2000); *recA*_41F (5'-TTCGGCAAGGGMTCGRTSATG-3') and *recA*_640R (5'-ACATSACRCCGATCTTCATGC-3') (Vinuesa *et al.*, 2005); *nodC*_for540 (5'-TGATYGAYATGGARTAYTGGCT-3') and *nodC*_rev1160 (5'-CGYGACARCCARTCGCTRITG-3') (Sarita *et al.*, 2005). The quantity of DNA was determined by using a NanoDrop spectrophotometer (NanoDrop ND1000). The PCR reaction was carried out in a 25 μl volume containing 2.5 μl 10 \times Standard Reaction Buffer with MgCl₂ (Biotools), 2 μl DNA, 1 μl *Taq* DNA polymerase (Biotools), 0.5 μl dNTP, 1 μl of each primer and 17 μl of distilled water.

The thermal program for PCR reactions of *glnII* and *recA* was carried out at 95°C for 90s; 35 cycling times at 95°C for 45s, 55°C for 45s and 72°C for 2min and a final cycle was 72°C for 7min. For *nodC*, it was at 95°C for 3min; 35 cycling times at 94°C for 1min, 55°C for 1min and 72°C for 2min and a final cycle was 72°C for 7min. Unincorporated primers and dNTPs were removed from PCR mixes with PCR Clean-up (Macherey-Nagel). PCR products were verified by electrophoresis in 1% agarose gel submerged in TBE buffer (Del Papa *et al.*, 1999) and visualized with a Gel Doc EZ system (Bio-Rad).

Sequencing reactions were outsourced to Stabvida (Lisbon, Portugal).

2.5. Phylogenetic analysis

The quality of the sequences was checked and edited manually using BioEdit 7.2.5 (Hall, 1999) and automatically using DNA Baser Assembler v4.36.0 (2013) (Heraclio BioSoft, <http://www.DnaBaser.com>).

Initially, a blast search (Altschul *et al.*, 1990) conducted using the National Center of Biotechnological Information (NCBI) website was carried out for preliminary identification and *recA*, *glnII* and *nodC* gene sequences of the reference species related to our strains were downloaded. The phylogenetic analyses were performed using MEGA 6.06 software (Tamura *et al.*, 2013). A neighbor-joining tree was constructed using the Kimura two-parameter model of evolution (Kimura, 1980) and support of internal branches was assessed using 1000 bootstrap replications.

2.6. Statistical analysis

The phenotypic characters results were analyzed by utilizing XLSTAT software (version 2016.02.28451). Bacterial growth in liquid medium was subjected to analyses of variance (ANOVA) and treatment means compared using Tukey's HSD (honest significant different) test. Numerical analysis of phenotypic traits was evaluated by UPGMA algorithm to infer a dendrogram on the basis of growth (+) or no growth (-) for each of the isolate in solid medium.

3. Results

3.1. Morphologic characterization and authentication

After 3 days of incubation at 28°C, all isolates formed visible colonies on YEM Agar medium. Colonies were whitish and translucent, varying in diameter from 1 to 3 mm, circular, convex, with a regular outline and a smooth surface. Furthermore, the isolates formed nodules on the roots of alfalfa plants six weeks after inoculation.

3.2. Phenotypic characterization

The results show that all strains exhibited a broad spectrum of tolerance to salinity. All strains were able to grow in the presence of 1.7 mM to 640 mM NaCl (Table 2). In contrast, no strain grew at 1280 mM NaCl. It is worth mentioning that tolerance to a given concentration of NaCl does not necessarily mean good growth of the strains. Analysis of variance shows significant differences between the salt concentrations of 80, 160, 320 and 640 mM with the average growth of the strains decreased with increasing salt concentrations (Figure 1a).

At low salinities (1.7 and 40 mM), strains G132 and G424, from Ghardaïa, had the best growth. At 80 and 160 mM, strains O152, O211 and E141 from Ouargla and El Oued were the most resistant. At the highest concentrations, the E543 and E452 strains from the El Oued region performed the best (Table 3).

Table 2. Results of strains tolerance to some environmental stress factors and antibiotics.

Strains	Temperature (C°)			pH			NaCl (mM)		Antibiotic									
	4	28 and 37	45	4	5	6 to 9	1.7 to 640	1280	FA	AK	AMX	C	CS	E	K	P	SP	VA
O114	-	+	-	-	+	+	+	-	-	+	-	-	+	-	-	-	-	+
O144	-	+	+	-	-	+	+	-	-	+	-	-	+	-	-	-	-	-
O152	-	+	+	+	+	+	+	-	-	-	-	-	+	-	-	-	+	-
O172	-	+	-	-	+	+	+	-	-	+	-	+	+	-	+	-	+	+
O211	-	+	-	-	+	+	+	-	-	+	-	+	+	-	+	-	+	+
O213	-	+	-	-	+	+	+	-	-	+	-	+	+	-	+	-	+	+
O223	-	+	-	-	+	+	+	-	+	+	-	+	+	-	-	-	+	-
O313	-	+	-	-	+	+	+	-	-	-	-	+	+	-	-	-	+	+
O321	-	+	-	-	+	+	+	-	-	-	-	+	+	-	+	-	+	+
O344	-	+	-	-	+	+	+	-	-	-	-	+	+	-	+	-	+	+
O413	-	+	-	+	+	+	+	-	-	+	-	+	+	-	+	-	+	+
O422	-	+	-	+	+	+	+	-	-	-	-	-	-	-	-	-	-	-
O442	-	+	-	+	+	+	+	-	-	-	-	+	+	-	-	-	-	+
O452	-	+	-	+	+	+	+	-	-	-	+	+	+	-	+	-	+	+
O461	-	+	-	-	+	+	+	-	-	-	-	+	+	-	+	-	+	-
E114	-	+	-	-	+	+	+	-	-	+	-	+	+	-	+	-	+	+
E131	-	+	-	-	-	+	+	-	+	+	-	+	+	-	+	-	+	+
E141	-	+	-	-	-	+	+	-	+	+	-	+	+	-	+	-	+	+
E213	-	+	-	-	+	+	+	-	+	-	-	+	+	-	+	-	+	+
E222	-	+	-	-	+	+	+	-	-	+	-	+	+	-	-	-	+	+
E251	-	+	+	-	+	+	+	-	-	-	-	+	+	-	-	-	-	-
E353	-	+	-	-	+	+	+	-	-	+	-	+	+	-	-	-	-	+
E421	-	+	-	-	-	+	+	-	-	+	-	+	+	-	+	-	-	+
E432	-	+	-	-	+	+	+	-	+	+	-	+	+	-	+	-	+	+
E441	-	+	-	-	+	+	+	-	+	+	-	-	-	-	+	-	-	+
E452	-	+	-	-	+	+	+	-	-	-	-	-	-	-	-	-	-	-
E521	-	+	+	-	+	+	+	-	-	+	-	+	+	-	+	-	+	+
E532	-	+	+	-	+	+	+	-	-	-	-	+	+	-	+	-	+	+
E543	-	+	-	-	+	+	+	-	+	+	-	+	+	+	+	-	+	+
G131	-	+	-	-	+	+	+	-	+	-	+	+	-	+	-	+	-	+
G132	-	+	-	-	+	+	+	-	-	-	+	+	+	+	-	+	+	-
G241	-	+	-	+	+	+	+	-	+	-	+	-	-	-	+	+	+	-
G242	-	+	+	-	+	+	+	-	+	-	+	+	-	+	+	+	+	+
G122	-	+	-	-	+	+	+	-	+	-	+	-	-	-	+	+	+	+
G124	-	+	+	+	+	+	+	-	+	-	+	-	-	-	+	+	+	+
G211	-	+	-	-	+	+	+	-	-	-	+	+	-	+	-	+	-	+
G312	-	+	+	-	+	+	+	-	-	-	+	+	-	+	-	+	+	-
G315	-	+	-	-	+	+	+	-	+	-	+	-	+	-	+	+	+	+
G321	-	+	-	+	+	+	+	-	+	-	+	+	-	+	-	+	+	+
G421	-	+	+	-	-	+	+	-	+	-	+	+	-	+	-	+	+	+
G422	-	+	+	-	+	+	+	-	+	-	+	+	-	+	-	+	+	+
G424	-	+	-	+	+	+	+	-	-	-	+	-	-	-	+	+	+	+
G431	-	+	-	+	+	+	+	-	+	-	+	-	+	-	+	+	+	+
G432	-	+	+	+	+	+	+	-	+	-	+	-	+	-	+	+	+	+
G514	-	+	+	+	+	+	+	-	+	-	+	+	+	+	+	+	+	+
G522	-	+	+	-	-	+	+	-	-	-	+	+	+	+	-	+	+	+
Sm1021	+	+	+	-	-	+	+	-	+	-	+	-	+	+	+	-	-	+
Sm2011	+	+	+	-	-	+	+	-	-	-	+	+	+	+	+	-	-	+

The resistant strains for the different factors were coded as “+” and the sensitive strains as “-”.

Growth of rhizobial strains differed with differences in pH values. They tolerated alkaline and neutral pH better than acidic pH (Figure 1c). The strains were affected by excessively acidic pHs and registered growth rates of 32.43% and 81.63% at pH 4 and 5, respectively. At slightly acidic, neutral and alkaline pH, all rhizobial strains

grew well. The ANOVA test showed significant differences between the growths of strains at different pH (Figure 1d). Eleven strains (O152, O413, O422, O452, G241, G124, G321, G424, G431, G4311 and G514), from Ouargla and Ghardaïa, were resistant to pH 4.

Table 3. Selection of strains tolerant to different NaCl concentrations.

Strains	NaCl Concentrations						
	1.7 mM	40 Mm	80 mM	160 mM	320 mM	640 Mm	1280 mM
G132 ^a	G132 ^a	O152 ^a	E141 ^a	G241 ^a	E543 ^a	-	
O211 ^{ab}	G424 ^{ab}	O211 ^a	O223 ^{ab}	E521 ^a	E452 ^a	-	
O114 ^{abc}	E222 ^{abc}	O172 ^{ab}	O172 ^{abc}	E141 ^a	O461 ^{ab}	-	
O452 ^{abc}	G122 ^{abc}	O223 ^{ab}	O321 ^{abcd}	E114 ^{ab}	O442 ^{abc}	-	
G321 ^{abcd}	O152 ^{abcd}	E222 ^{ab}	E114 ^{abcd}	G124 ^{ab}	E251 ^{abcd}	-	
O144 ^{abcde}	O172 ^{abcde}	E521 ^{ab}	O313 ^{abcd}	O313 ^{ab}	E213 ^{abcde}	-	
O313 ^{abcde}	E131 ^{abcde}	E131 ^{ab}	G422 ^{abcde}	O211 ^{abc}	O144 ^{abcdef}	-	

For each parameter, the means in the same column followed by the same letter are not significantly different, as determined by Tukey's HSD test at P = 0.05.

At 28 and 37°C, all strains showed good growth, produced visible colonies on solid medium (Figure 1e) and high optical densities (OD) (Figures 1f). At 4°C, only the two reference strains, Sm2011 and Sm1021, were able to grow. Increasing the temperature to 45°C significantly reduced growth and only 15 isolates (O144, O152, E251, E521, E532, G242, G321, G421, G422, G431, G432, G514, G522, Sm2011 and Sm1021) were thermotolerant (Table 2).

The strains showed different resistance profiles to antibiotics. They exhibited strong resistance to spiramycin 100 µg (SP), vancomycin 30 µg (VA) and colistin 10 µg (CS), while their resistance was low, but comparable, for the other antibiotics (Figure 1b). Strains from Ghardaïa and reference strains are, generally, more tolerant to antibiotics (61.17% and 65% respectively) than those from Ouargla and El Oued that show low levels of resistance (around 35% and 43.5%), apart from a few that are resistant to a single antibiotic.

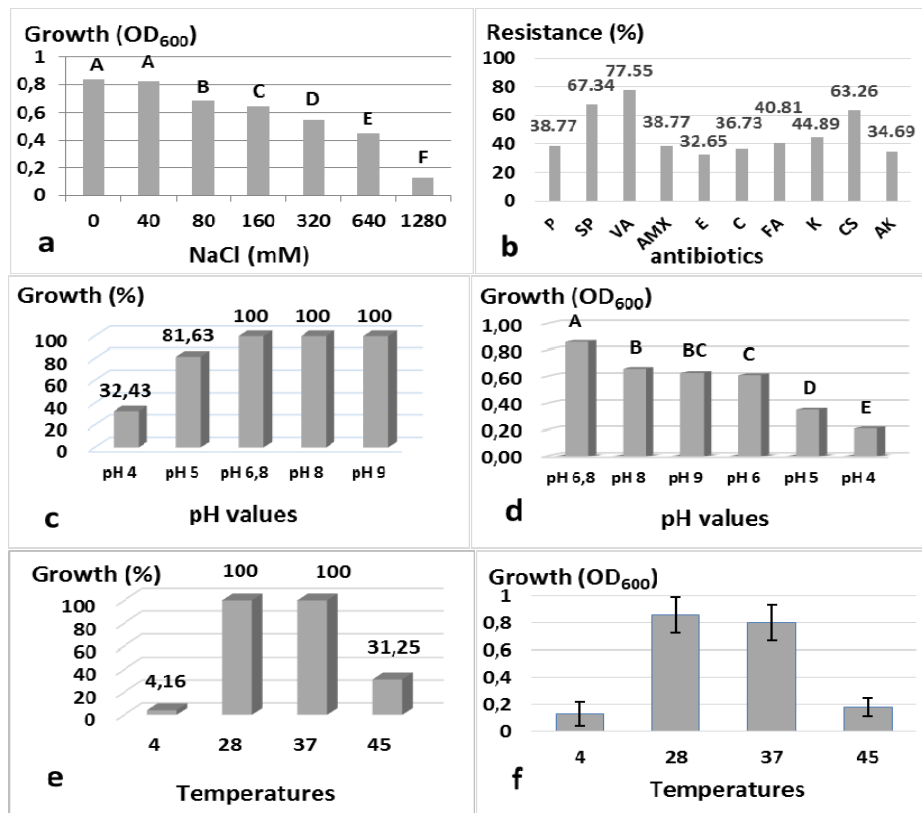


Figure 1. Growth of strains under: salinity (a), antibiotics (b), different pH (c, d) and temperatures (e, f) (done at the Saharan Bioresources Laboratory of the University of Ouargla, in 2017).

3.3. Numerical analysis of phenotypic traits

The 27 phenotypic characters of the strains were used to construct a dendrogram using the UPMGA method (Figure 2). At about 60% dissimilarity, rhizobial strains have been classified into three phenotypic groups. Group 3 has 29 strains, all from the Ouargla and El Oued regions. Group 1 consists of 17 strains exclusively from the Ghardaïa region. The two reference strains Sm1021 and Sm2011 were in a separate group (group 2), closer to group 1 than to group 3.

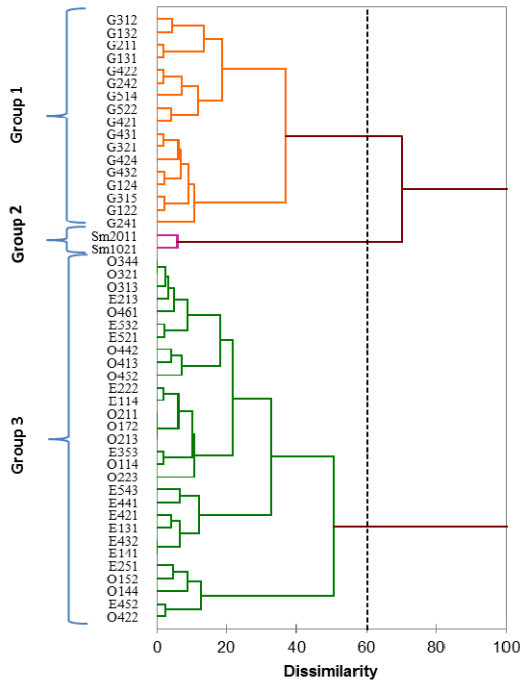


Figure 2. Dendrogram showing the phenotypic diversity of 48 strains constructed using the UPGMA method, based on a binary matrix of 27 physiological characters.

3.4. Phylogenetic analysis

Forty-eight strains were chosen for the phylogenetic examination of housekeeping genes (*recA* and *glnII*) and the symbiotic gene *nodC*. Phylogenetic trees were constructed for each gene utilizing the Neighbor-joining method and Kimura's two-parameter model. Bootstrap analysis was based on 1000 replications.

3.4.1. Housekeeping gene phylogenies

Strains were more closely related to *S. meliloti* and *S. kummerowiae* (De Lajudie *et al.*, 1994; Wei *et al.*, 2002) than to other species according to the housekeeping gene phylogenies (Table 4). Sequence analysis of *recA* and *glnII* respectively revealed 98–100% and 97–99% similarities with type strains *S. meliloti* USDA 1002^T, 98–99% and 97–100% with type strains *S. kummerowiae* CCBAU 71714^T and 91% and 91–93% with type strains *S. medicae* A321^T (Rome *et al.*, 1996).

Table 4. Sequence similarities for *recA*, *glnII* and *nodC* genes relatedness among the 48 strains and related type strains.

Type strain	Gene marker and sequence similarity with type strains %							
	<i>glnII</i> Similarity %	Stains number	<i>recA</i> Similarity %	Isolate numbers	<i>glnII+recA</i> Similarity %	Isolate numbers	<i>nodC</i> Similarity %	Isolate Numbers
<i>S. meliloti</i> USDA 1002 ^T	99%	14	100%	05	99%	14	99%	18
	98%	10	99%	06	98%	27	97%	08
	97%	24	98%	37	97%	07	96%	18
<i>S. kummerowiae</i> CCBAU 71714 ^T	100%	04	99%	04	99%	13	89%	04
	99%	10	98%	44	98%	35	96%	02
	98%	33					95%	13
<i>S. medicae</i> A321 ^T	97%	01					94%	29
	91%	01	91%	48	92%	47	90%	04
<i>S. medicae</i> USDA 1037	92%	46			91%	01		
	93%	01					100%	02
							99%	13
							96%	29
							90%	04

***glnII* gene phylogeny**

The phlogenetic tree corresponding to *glnII* (Figure 3) showed that the strains clustered into two groups with high bootstrap support (99 for group I and 72 for group II).

Group I consisted of 14 strains, originating exclusively from Ghardaïa, closely related to reference strains *S. kummerowiae* CCBAU 71714^T and *S. meliloti* USDA 1002^T. There were 13 strains (G421, G422, G242, G424, G431, G432, G514, G211, G242, G315, G321, G122

and G124) clustered with *S. kummerowiae* CCBAU 71714^T at sequence similarities of 99.82 to 100% and one strain (G312) clustered only with *S. meliloti* USDA 1002^T at sequence similarity of 99.52%. Group II contained 34 strains, coming from the El Oued and Ouargla (except G131, G132 and G522), which were separated from the

reference strains. Similarities between the strains in this group and type strains *S. kummerowiae* CCBAU 71714^T and *S. meliloti* USDA 1002^T were 97.69 to 98.58% and 97.46 to 98.19%, respectively.

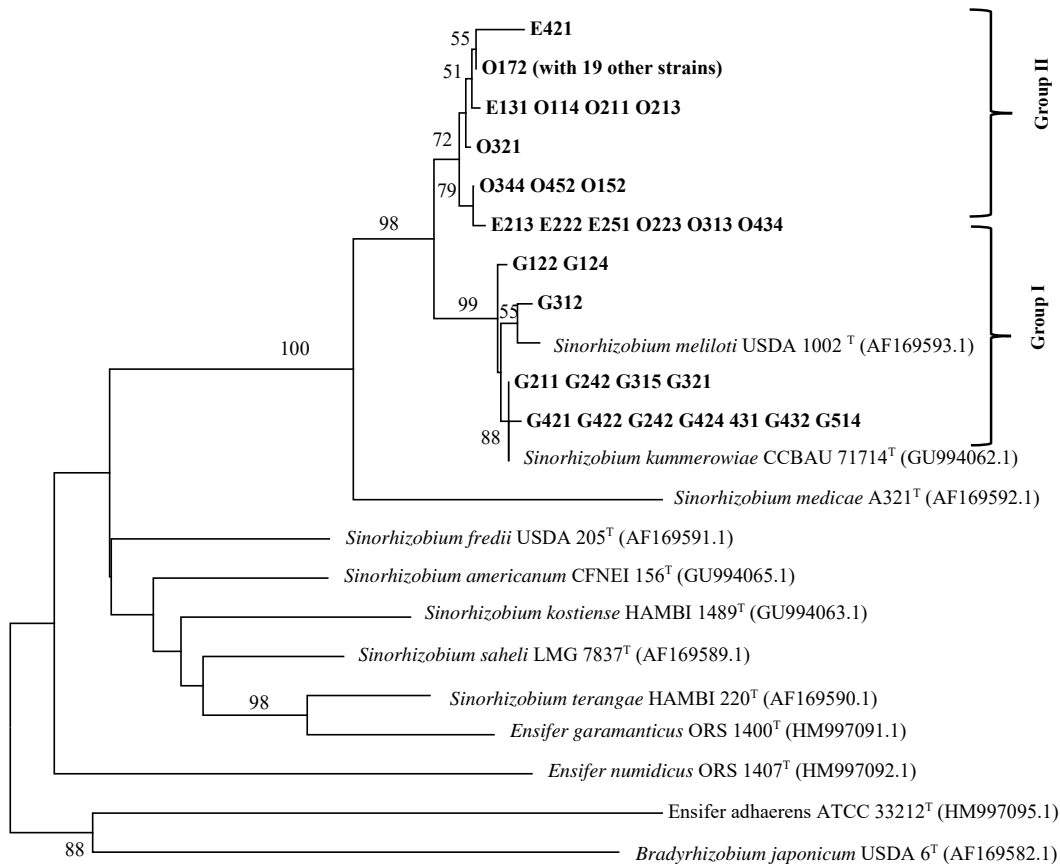


Figure 3. Neighbor-joining phylogenetic tree constructed from *glnII* gene (555 bp) showing the relationship among strains nodulating alfalfa and related species of the *Sinorhizobium*–*Ensifer* group. Bootstrap values (1000 replicates; only values over 50 % are given) are indicated above the branches. *Bradyrhizobium japonicum* USDA6^T was used as an outgroup. Type strains are indicated with a superscript^T.

recA gene phylogeny

The strains clustered into 2 groups with very high bootstrap values (97 for group I and 93 for group II) (Figure 4). There were 14 strains from Ghardaïa in group I, and they were closely related to type strains *S. meliloti* USDA 1002^T and *S. kummerowiae* CCBAU 71714^T. There were 10 strains (G122, G124, G211, G241, G242, G312, G315, G32, G421 and G422) clustered with *S. meliloti* USDA 1002^T at sequence similarities of 100% and 4

strains clustered with the reference strain *S. kummerowiae* CCBAU 71714^T at sequence similarity of 99.24%. Thirty-four strains in group II from the El Oued and Ouargla regions (except G131, G132 and G522) are not grouped with any of the known reference strains and form an individualized clade on the tree. The similarities between these strains and *S. meliloti* USDA 1002^T and *S. kummerowiae* CCBAU 71714^T were 98.22 to 98.67%.

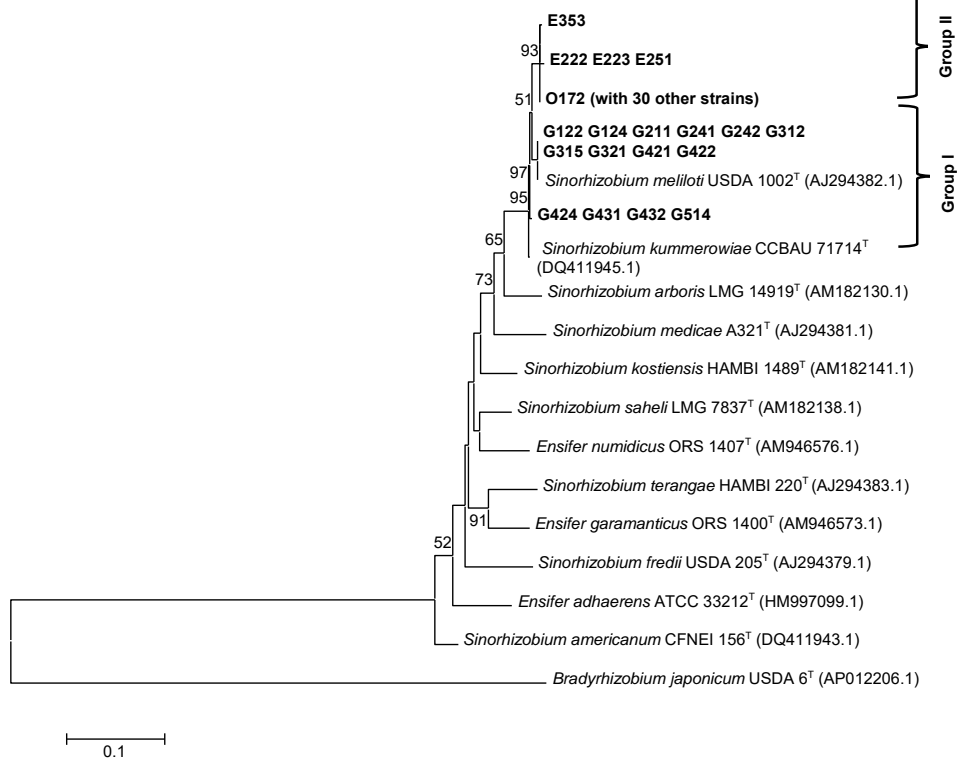


Figure 4. Neighbor-joining tree constructed from *recA* gene (430 bp) showing phylogenetic relationships of strains nodulating alfalfa and related species of the *Sinorhizobium-Ensifer* group. Only values over 50 % are indicated above the branches.

Concatenated housekeeping gene phylogeny

In order to refine the phylogeny of the studied strains, a phylogenetic tree was constructed from concatenated *glnII* and *recA* gene sequences (Figure 5). The grouping results were similar to those of the individual gene trees. The 48 strains clustered into 2 different groups. Fourteen strains belong to group I with a bootstrap value of 98. Seven strains (G122, G124, G211, G242, G315, G321 and G312) were grouped with the *S. meliloti* USDA 1002^T at sequence similarity of 99.48 to 99.69% and seven others (G431, G432, G514, G424, G241, G421 and G422) were linked with *S. kummerowiae* CCBAU 71714^T at similarity

rates of 99.38 to 99.69%. It should be noted that all the strains composing group I came from the region of Ghardaïa. Group II, composed of 34 strains coming exclusively from the El Oued and Ouargla regions (except G131, G132 and G522), formed a clearly separated group from the reference strains with 97 bootstrap support and suggested that these novel strains may represent a distinct lineage from defined species. Similarities between the group 2 strains and the closest reference strains are 97.73–98.25% with *S. meliloti* USDA 1002^T and 98.04–98.56% with *S. kummerowiae* CCBAU 71714^T, respectively.

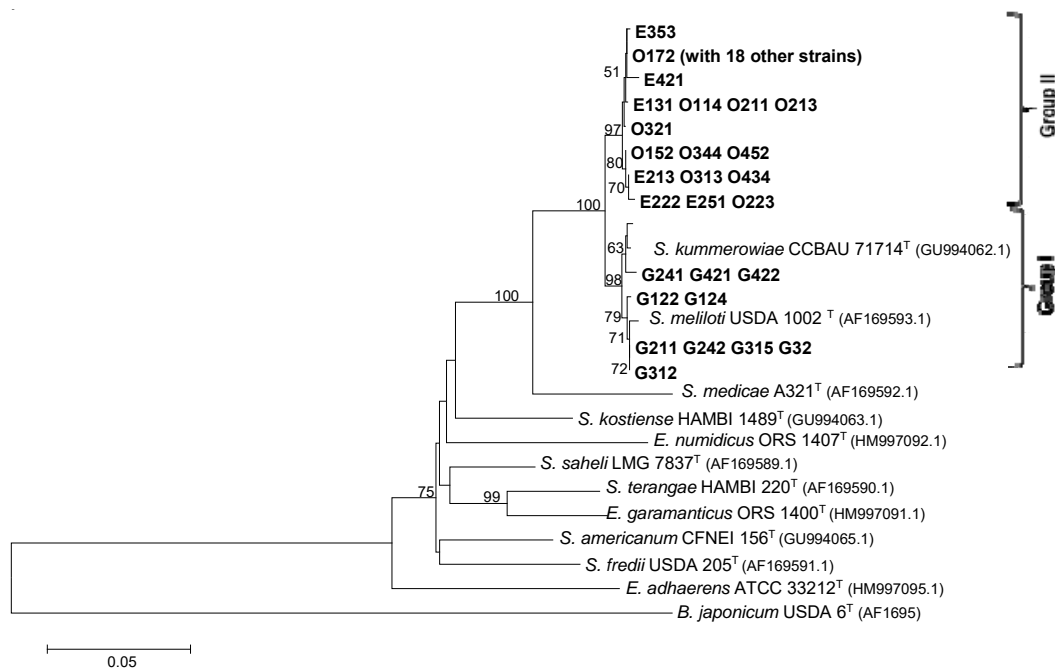


Figure 5. Neighbor-joining tree constructed from concatenated housekeeping genes *glnII* and *recA* (985 bp) showing phylogenetic relationships of strains nodulating alfalfa and related species of the *Sinorhizobium-Ensifer* group. Bootstrap values (1000 replicates; only values over 50 % are given) are indicated above the branches.

3.4.2. *nodC* gene phylogeny

The *nodC* phylogenetic tree showed three well-supported distinct groups, at bootstrap value of 100 for groups I and II, and 99 for group III, as presented in Figure 6. The group I and II strains from different areas were clustered with type strains *S. meliloti* USDA 1002^T at similarity of 97.05 to 99.66% and *S. medicae* A321^T at

similarity of 99.65 to 100%, respectively. The strains G424, G431, G432 and G514 composing group III displayed high sequence identities with *S. meliloti* LAIII42 (99.66% similarity) and came from the region of Ghardaïa. Thus, the strains used in this study belong to two types of symbiovars: *meliloti* (groups I and II) and *medicaginis* (group III) described by Villegas *et al.* (2006).

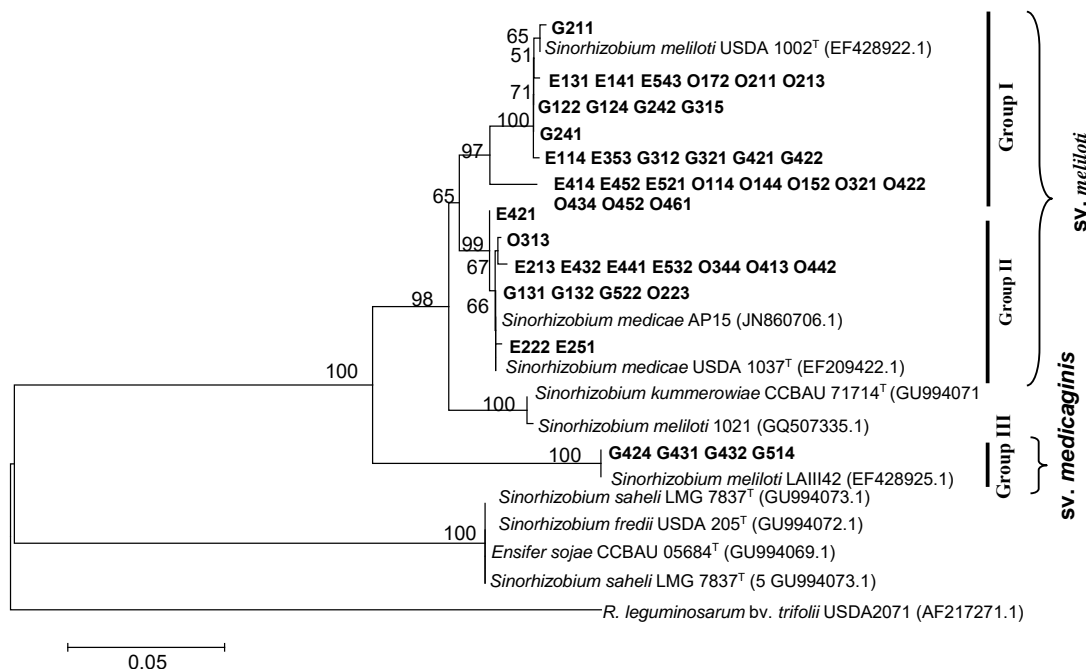


Figure 6. Neighbor-joining tree constructed from *nodC* genes showing phylogenetic relationships of strains nodulating alfalfa and related species of the *Sinorhizobium-Ensifer* group. Bootstrap values (1000 replicates; only values over 50 % are given) are indicated above the branches.

4. Discussion

In this study, we analyzed for the first time a collection of 48 strains obtained from *Medicago sativa* root nodules collected from three different regions in the North eastern Algerian Sahara. This study included both phenotypic and phylogenetic analyses and was the first time such an investigation was conducted on rhizobial isolates from this region.

The phenotypic characterization showed that morphological and growth characteristics of the strains were in agreement with those already described in the literature (Vincent, 1970; Latrache *et al.*, 2017). The results of the plant nodulation tests showed that all strains could produce nodules.

Salinity is an important stress factor for rhizobia, as it inhibits their growth and development (Graham, 1998; Farissi *et al.*, 2014). In the present study, all strains were able to tolerate salt concentrations from 1.7 mM to 640 mM (Table 2). In contrast, no strains were able to grow at 1280 mM. Our results are in agreement with those of Mohammad *et al.* (1991), Embalomatis *et al.* (1994) and Jebara *et al.* (2000) who indicated that strains of *S. meliloti* were tolerant of NaCl concentrations between 300–700 mM in American, Greek and Tunisian soils respectively. Likewise, a tolerance of up to 800 mM of NaCl was observed in rhizobia collected in the Sebkhia of Misserghine (north-western Algeria) (Merabet *et al.*, 2006). Elboutahiri *et al.* (2010) were able to isolate strains of *S. meliloti* capable of growing at 1711 mM NaCl. These were sampled in areas heavily affected by salinity in southern Morocco.

At 80 and 160 mM, the most resistant strains were O152, O211 and E141 and at the highest concentrations, strains E543 and E452 performed best. Adaptation to salinity in a few *Rhizobium* species is the result of intracellular accumulation of low molecular weight organic solutes called osmolytes, as described by Boscari *et al.* (2002)

At pH of 4.0 and 5.0, strains were sensitive thus confirming the results of Elboutahiri *et al.* (2010) and Thami-Alami *et al.* (2010) that strains tolerated acidic pH of 5.5 to 6.0 where most isolates grow (Latrache *et al.*, 2017). Our results are also in agreement with those of Abolhasani *et al.* (2010), Thami-Alami *et al.* (2010) and Hameed *et al.* (2014) who indicate that the strains of *S. meliloti* nodulating alfalfa were all resistant to the alkaline pH 8.0 and 9.0. At pH 6.8, all strains showed maximum growth, which is in agreement with Rodrigues *et al.* (2006) and Shetta *et al.* (2011) who stated that the optimum pH for rhizobia multiplication is between 6.5 and 7.0.

At temperatures 28°C and 37°C, we recorded 100% growth. Our results agree with those of Zahran (1999) and Dekak (2018) who found that rhizobia are mesophilic bacteria and optimum growth of most strains is between 28°C and 31°C. At 4°C and 45°C, the strains that were able to grow only produced a few small colonies on solid medium and low OD's in liquid medium. High and low temperatures have been reported to be among the main factors limiting growth and nitrogen fixation by rhizobia (Niste *et al.*, 2015).

We found that the strains show different antibiotic resistance profiles. The sensitivity to antibiotics, which is higher in some strains, can be attributed to the less

abundant microbial biomass in the rhizosphere (Grego *et al.* 1995). The more pronounced resistance in Ghardaïa strains can be explained by the use of large amounts of intensive livestock manure in this region as noted by Guessoum *et al.* (2014), where antibiotics are commonly added to animal feed to treat diseases and promote growth (McManus, 1997).

Many studies have described *S. meliloti* and *S. medicae* as the only rhizobia capable of nodulating alfalfa. Phylogenetic analysis of *recA* and *glnII* showed that instead it is *S. meliloti* and *S. kummerowiae*, which are the microsymbionts of *M. sativa* in the Saharan regions of Algeria. The strains were more closely related to *S. meliloti* and *S. kummerowiae* than to other species. Sequence analysis of *recA* and *glnII* revealed high similarities with type strains *S. meliloti* USDA1002^T and *S. kummerowiae* CCBAU71714^T. Our results converge with those of Wei *et al.* (2002) and Toularoud *et al.* (2016) who mentioned that alfalfa could be efficiently nodulated by *S. kummerowiae* in Chinese and Turkish soils. The presence of *S. kummerowiae* in the study areas was reported recently by Arbi *et al.* (2015) and Chaïch *et al.* (2017) as dominant microsymbiont, with *S. meliloti*, of the spontaneous legumes *Medicago littoralis*, *Melilotus indicus* and *Genista saharae*.

The concatenated housekeeping gene phylogeny showed that the strains were grouped into 2 different groups. Group I comprises strains from Ghardaïa, strongly related to type strains *S. kummerowiae* CCBAU 71714^T and *S. meliloti* USDA 1002^T. The thirty four strains composing group II were separated from the reference strains, and this suggested that these novel strains may represent a distinct lineage from defined species. As suggested by Toularoud *et al.* (2016), housekeeping gene phylogenetic analyses may help to further resolve the taxonomic relationship between *S. kummerowiae* and *S. meliloti*, which may belong to a single species. The grouping results were, generally, similar to those of the individual gene (Figures 3 and 4).

The results obtained were very similar to those of the concatenated housekeeping gene phylogenetic tree (Figure 5). The strains originating from the region of Ghardaïa are phylogenetically and phenotypically linked to the species *S. kummerowiae* and *S. meliloti* and separated from those of the regions of Ouargla and El Oued. These results revealed geographic variation in the rhizobial population composition as shown in many works (Fierer and Jackson, 2006; Talebi *et al.*, 2008).

Neighbor-joining phylogenetic tree of *nodC* gene sequences revealed three distinct well-supported clusters (Figure 6). Twenty-four strains were in group I that consisted of strains related to *S. meliloti* USDA 1002^T. Group II consisted of thirteen strains related to the type strain *S. medicae* A321^T. Four separate strains forming group III showed 100% similarity to *S. meliloti* LAIII42. To label resulting groups, we used the system of symbiovars proposed by Rogel *et al.* (2011) and De Meyer *et al.* (2011). So, the *Sinorhizobium* isolates used in this study belonged to two symbiovar types, *meliloti* (group I and II) and *medicaginis* (group III) as described by Villegas *et al.* (2006). These results are explained by the fact that the tested strains and *S. meliloti* and *S. medicae* have the same host plant.

Several studies have shown that the evolutionary history of chromosomal genes may be different from that of symbiotic genes. Our results are in agreement with those of Laguerre *et al.* (2001) who indicated that the classification resulting from the analysis of the symbiotic *nodC* gene reflects host specificity, while the phylogeny based on chromosomal genes is independent of the host plant. Symbiovars can be shared by different species due to lateral transfer of symbiotic genes (Rogel *et al.*, 2011).

5. Conclusion

This study showed that the bacteria isolated from the root nodules of *Medicago sativa*, cultivated in the Algerian Sahara, are genetically and phenotypically diverse. Phenotypic analysis showed that many strains have interesting characteristics. This may allow them to be used as an effective inoculum for Saharan soils, which are subjected to many edaphoclimatic stress conditions. Phylogenetic analysis showed that our strains are strongly related to *S. meliloti* and *S. kummerowiae*, which are the effective symbiotic partners of alfalfa in the study area. There was a similarity between the genotypic and phenotypic profiles suggesting the existence of a relationship between the groups of strains and their geographic distribution.

Acknowledgements

The authors would like to thank M. Juan Imperial and all the members of the GEBIOPAD laboratory, of the Centre for Plant Biotechnology and Genomics (UPM-INIA) in Madrid, for their invaluable help during the realization of the molecular part of this study.

References

- Abolhasani M, Lakzian A, Tajabadipour A and Haghnia G. 2010. The study salt and drought tolerance of *Sinorhizobium* bacteria to the adaptation to alkaline condition. *Aust J Basic & Appl Sc*, **4**: 882-886.
- Ahmad E, Zaidi A, Khan MS (2016) Effects of plant growth promoting rhizobacteria on the performance of greengram under field conditions. *Jordan J Biol Sci* **9**: 79-88.
- Altschul SF, Gish W, Miller W, Myers EW and Lipman DJ. 1990. Basic local alignment search tool. *J Mol Biol*, **215**: 403-410.
- Arbi SB, Chekireb D, Quatrini P, Catania V, Cheriet D and Ouarts A. 2015. Phenotypic and genotypic characterization of root nodules rhizobia of *Medicago littoralis* Rhode and *Melilotus indicus* (L.) All. growing in the Oasis of Touggourt, Oued Righ Valley, in the Algerian Sahara. *Symbiosis*, **66**: 75-87.
- Azib S, Chelouf H, Attab S and Bouras N. 2019. Improvement of alfalfa growth under water stress by inoculation with *Sinorhizobium meliloti* strains from the Algerian Sahara. *International Journal*, **75**(7): 35-43.
- Boscari A, Mandon K, Dupont L, Poggi MC and Le Rudulier D. 2002. BetS is a major glycine betaine/proline betaine transporter required for early osmotic adjustment in *Sinorhizobium meliloti*. *J Bacteriol*, **184**: 2654-2663.
- Brígido C, Nascimento FX, Duan J, Glick BR and Oliveira S. 2013. Expression of an exogenous 1-aminocyclopropane-1-carboxylate deaminase gene in *Mesorhizobium* spp. reduces the negative effects of salt stress in chickpea. *FEMS Microbiol Lett*, **349**(1): 46-53.
- Chatch K, Bekki A, Bouras N, Holtz MD, Soussou S, Mauré L, Brunel B, De Lajudie P and Cleyet-Marel JC. 2017. Rhizobial diversity associated with the spontaneous legume *Genista saharae* in the northeastern Algerian Sahara. *Symbiosis*, **71**: 111-120.
- Dekak A, Chabi R, Menasria T and Benhizia Y. 2018. Phenotypic characterization of rhizobia nodulating legumes *Genista microcephala* and *Argyrolobium uniflorum* growing under arid conditions. *J. Adv. Res*, **14**:35-42.
- De Lajudie P, Willems A, Pot B, Dewettinck D, Maestrojuan G, Neyra M, Collins DM, Dreyfus B, Kersters K and Gillis M. 1994. Polyphasic Taxonomy of Rhizobia: Emendation of the genus *Sinorhizobium* and description of *Sinorhizobium meliloti* comb. nov., *Sinorhizobium sahari* sp. nov., and *Sinorhizobium teranga* sp. nov. *Int J Syst Evol Microbiol*, **44**: 715-733.
- De Meyer SE, Van Hoorde K, Vekeman B, Braeckman T and Willems A. 2011. Genetic diversity of rhizobia associated with indigenous legumes in different regions of Flanders (Belgium). *Soil Sci Am J*, **43**: 2384-2396.
- Del Papa MF, Balagué LJ, Sowinski SC, Wegener C, Segundo E, Abarca FM, Toro N, Niehaus K, Pühler A, Aguilar OM, Martínez-Drets G and Lagares A. Isolation and characterization of alfalfa-nodulating rhizobia present in acidic soils of central Argentina and Uruguay. *Appl Environ Microbiol*, **65**: 1420-1427.
- del Pozo A, Ovalle C, Espinoza S, Barahona V, Gerding M and Humphries A. 2017. Water relations and use-efficiency, plant survival and productivity of nine alfalfa (*Medicago sativa* L.) cultivars in dryland Mediterranean conditions. *Eur J Agron*, **84**: 16-22.
- Domínguez-Ferreras A, Pérez-Arnedo R, Becker A, Olivares J, Soto MJ and Sanjuán J. 2006. Transcriptome profiling reveals the importance of plasmid *pSymB* for osmoadaptation of *Sinorhizobium meliloti*. *J Bacteriol*, **188**(21): 7617-7625.
- Elbouthairi N, Thami-Alami I and Udupa SM. 2010. Phenotypic and genetic diversity in *Sinorhizobium meliloti* and *S. medicae* from drought and salt affected regions of Morocco. *BMC Microbiol*, **10**: 1-13.
- Embalomatis A, Papaxosta D and Katinakis P. 1994. Evaluation of *Rhizobium mloti* strains isolated from indigenous populations in Northern Greece. *J Agron Crop Sci*, **172**: 73-80.
- Farissi M, Ghoulam C and Bouizgaren A. 2014. The effect of salinity on yield and forage quality of alfalfa populations in the Marrakech region (Morocco). *Fourrages*, **219**: 271-275.
- Fierer N and Jackson RB. 2006. The diversity and biogeography of soil bacterial communities. *Proc Natl Acad Sci*, **103**: 626-631.
- Gibson A. 1980. Methods for legumes in glasshouses and controlled environment cabinets. In: Bergersen F.J. (Eds.), **Methods for Evaluating Biological Nitrogen Fixation**. John Wiley and Sons Ltd., Chichester, UK, pp. 139-184.
- Graham PH. 1998. Biological dinitrogen fixation: symbiotic. Principles and applications of soil microbiology, **2**: 222-241.
- Grego S, Quatrini P, Badalucco L, De Cesare F, Zanotti C and Cacciari I. 1995. Souches résistantes de *Rhizobium* dans une rhizosphère caractérisée d'Acacia au nord et au sud du Sahara. In : Ed. Pontanier R., M'Hiri A., Akrimi N., Aronson J., Le Floc'h E. (Eds.), **L'homme peut-il refaire ce qu'il a défait ?**. John Libbey Eurotext, Paris, 201-210.
- Guessoum H, Benbrahim F, Halilat M, Laouar F, Bensalama M and Darem S. 2014. Pollution biologique des eaux phréatiques de la région de Ghardaïa (Cas de Sebseb). *Int J Adv Sci Technol*, **3**: 35-43.
- Hall TA.1999. BioEdit: a user-friendly biological sequence alignment editor and analysis program for Windows 95/98/NT. *Nucleic Acids Symp Ser*, **81**: 95-98.
- Hameed RA, Hussain NN and Aljibouri AM. 2014. Phenotypic Characterization of Indigenous Iraqi *Sinorhizobium meliloti* Isolates for Abiotic Stress Performance. *J Life Sci*, **8**(1): 1-9.

- Jebara M, Aouani ME, Mhamdi R, Ghir R and Mars M. 2000. Effet du sel sur des isolats de *Sinorhizobium* sp. de Tunisie *in vitro* ou en association avec *Medicago* sp. *Cah Agric*, **9**: 99-102.
- Kimura M. 1980. A simple method for estimating evolutionary rates of base substitutions through comparative studies of nucleotide sequences. *J Mol Evol*, **16**: 111-120.
- Laguerre G, Nour SM, Macheret V, Sanjuan J, Drouin P and Amarger N. 2001. Classification of rhizobia based on nodC and nifH gene analysis reveals a close phylogenetic relationship among *Phaseolus vulgaris* symbionts. *Microbiology*, **147**: 981-993.
- Latrach L, Mouradi M, Farissi M, Bouzigaren A and Ghoulam C. 2017. Physiological characterization of rhizobial strains nodulating alfalfa (*Medicago sativa*) isolated from soils of Southeastern Morocco. *Appl J Envir Eng Sci*, **3**(4):353-364.
- Martens M, Delaere M, Coopman R, De Vos P, Gillis M and Willems A. 2007. Multilocus sequence analysis of *Ensifer* and related taxa. *Int J Syst Evol Microbiol*, **57**: 489-503.
- Massimi M, Haseeb M, Kanga L and Legaspi J. 2017. Enhancement of silage sorghum and corn production using best management practices. In: Proceeding, Association of 1890 Research Directors Symposium, Georgia, Atlanta, United States of America.
- McManus MC. 1997. Mechanisms of bacterial resistance to antimicrobial agents. *Am J Health-Syst Pharm*, **54**: 1420-1433.
- Merabet C, Bekki A, Benrabah N, Baba-Hamed Bey M, Bouchentouf L, Ameziane H, Rezki MA, Domergue O, Cleyet-Marel JC, Avarre JC, Béna G, Bailly X and De Lajudie P. 2006. Distribution of *Medicago* species and their microsymbionts in a saline region of Algeria. *Arid Land Res Manag*, **20**: 219-231.
- Mohammad R, Akhavan-Kharazian M, Campbell W and Rumbaugh M. 1991. Identification of salt-and drought-tolerant *Rhizobium meliloti* L. strains. *Plant Soil*, **134**: 271-276.
- Mouradi M, Bouzigaren A, Farissi M, Latrach L, Qaddoury A and Ghoulam C. 2016. Seed osmopriming improves plant growth, nodulation, chlorophyll fluorescence and nutrient uptake in alfalfa (*Medicago sativa* L.) rhizobia symbiosis under drought stress. *Sci Hortic*, **213**: 232-242.
- Niste M, Vidican R, Rotar I and Pop R. 2015. The Effect of temperature stress on *Rhizobium trifolii* and *Sinorhizobium meliloti* strains *in vitro*. *Bull Univ Agric Sci Vet Med Cluj Napoca*, **72**(1): 297-298.
- OSS. 2003. **Système aquifère du Sahara septentrional: gestion commune d'un bassin transfrontière**. Rapport de synthèse, Observatoire du Sahara et du Sahel, Tunisie.
- Rodrigues CS, Laranjo M and Oliveira S. 2006. Effect of heat and pH stress in the growth of chickpea mesorhizobia. *Curr Microbiol*, **53**: 1-7.
- Rogel MA, Ormeno-Orrillo E and Romero EM. 2011. Symbiovars in rhizobia reflect bacterial adaptation to legumes. *Syst Appl Microbiol*, **34**: 96-104.
- Rome S, Fernandez MP, Brunel B, Normand P and Cleyet-Marel JC. 1996. *Sinorhizobium medicae* sp. nov., isolated from annual *Medicago* spp. *Int J Syst Evol Microbiol*, **46**: 972-980.
- Sarita S, Sharma PK, Priefer UB and Prell J. 2005. Direct amplification of rhizobial *nodC* sequences from soil total DNA and comparison to *nodC* diversity of root nodule isolates. *FEMS Microbiol Ecol*, **54**: 1-11.
- Shetta N, Al-Shaharani T and Abdel-Aal M. 2011. Identification and characterization of *Rhizobium* associated with woody legume trees grown under Saudi Arabia condition. *Am Eurasian J Agric Environ Sci*, **10**: 410-418.
- Somasegaran P and Hoben HJ. 1985. **Methods in legume-Rhizobium technology**. University of Hawaii NifTAL Project and MIRCEN, Department of Agronomy And Soil Science Hawaii Institute Tropical Agriculture Human research.
- Stackebrandt E, Frederiksen W, Garrity GM, Grimont PAD, Kämpfer P, Maiden MCJ ... and Whitman WB. 2002. Report of the ad hoc committee for the re-evaluation of the species definition in bacteriology. *Int J Syst Evol Microbiol*, **52**: 1043-1047.
- Tabares-da Rosa S, Signorelli S, Del Papa M, Sabatini O, Reyno R, Lattanzi F, Rebuffo M, Sanjuán J and Monza Galetti J. 2019. *Rhizobium* inoculants for alfalfa in acid soils. *Agrocienc Urug*, **23**(2): 1-13.
- Talebi MB, Bahar M, Saeidi G, Mengoni A and Bazzicalupo M. 2008. Diversity of *Sinorhizobium* strains nodulating *Medicago sativa* from different Iranian regions. *FEMS Microbiol Lett*, **288**: 40-46.
- Tamura K, Stecher G, Peterson D, Filipski A and Kumar S. 2013. MEGA6: molecular evolutionary genetics analysis version 6.0. *Mol Biol Evol*, **30**: 2725-2729.
- Thami-Alami I, Elbouthhiri N and Udupa S. 2010. Variability in natural populations of *Sinorhizobium meliloti* in Morocco. *Options Mediterr, Série A. Séminaires Méditerranéens*, **92**: 265-269.
- Toularoud AS, Asersec AA, Alikhanian HA, Jouzanid GRS, Rahmanid HA, Khavazid K, Räsänene LA and Lindström K. 2016. Taxonomic diversity and symbiotic efficiency of rhizobial strains obtained from nodules of *Medicago sativa* growing in Iran. *Ann Biol Res*, **7**: 29-38.
- Turner SL and Young JPW. 2000. The glutamine synthetases of rhizobia: phylogenetics and evolutionary implications. *Mol Biol Evol*, **17**: 309-319.
- Villegas MDC, Rome S, Mauré L, Domergue O, Gardan L, Bailly X, Cleyet-Marel JC and Brunel B. 2006. Nitrogen-fixing sinorhizobia with *Medicago laciniata* constitute a novel biovar *medicaginis* of *S. meliloti*. *Syst Appl Microbiol*, **29**: 526-538.
- Vincent JM. 1970. **A manual for the practical study of the root-nodule bacteria**. Blackwell Science Ltd., UK.
- Vinuesa P, Silva C, Werner D and Martínez-Romero E. 2005. Population genetics and phylogenetic inference in bacterial molecular systematics: the roles of migration and recombination in *Bradyrhizobium* species cohesion and delineation. *Mol Phylogenetics Evol* **34**: 29-54.
- Wei GH, Wang ET, Tan ZY, Zhu ME and Chen WX. 2002. *Rhizobium indigoferae* sp. nov. and *Sinorhizobium kummerowiae* sp. nov., respectively isolated from *Indigofera* spp. and *Kummerowia stipulacea*. *Int J Syst Evol Microbiol*, **52**: 2231-2239.
- Wei W, Jiang J, Li X, Wang L and Yang S. 2004. Isolation of salt-sensitive mutants from *Sinorhizobium meliloti* and characterization of genes involved in salt tolerance. *Lett Appl Microbiol*, **39**: 278-283.
- Zahrán HH. 1999. *Rhizobium*-legume symbiosis and nitrogen fixation under severe conditions and in an arid climate. *Microbiol Mol Biol Rev*, **63**: 968-989.
- Zakhia F and De Lajudie P. 2006. La taxonomie bactérienne moderne: revue des techniques-application à la caractérisation des bactéries nodulant les légumineuses BNL. *Can J Microbiol*, **52**: 169-181
- Zhang F and Smith DL. 1996. Inoculation of soybean *Glycine max*.L. Merr. with genistein-preincubated *Bradyrhizobium japonicum* or genistein directly applied into soil increases soybean protein and dry matter yield under short season conditions. *Plant Soil*, **179**: 233-241.
- Zhang WJ and Wang T. 2015. Enhanced salt tolerance of alfalfa (*Medicago sativa*) by *rstB* gene transformation. *Plant Sci*, **234**: 110-118.

Prevalence of Some Pathogenic Bacteria in Caged- Nile Tilapia (*Oreochromis Niloticus*) and their Possible Treatment

Ahmed Hammad Sherif^{1,*} and Rasmia Hanafy AbuLeila²

¹ Fish Disease Department, Animal Health Research Institute AHRI, Agriculture Research Center ARC, Kafrelsheikh, Egypt, ² Fish Diseases Department, Animal Health Research Institute AHRI Agriculture Research Center ARC, Egypt

Received: February 25, 2021; Revised: June 5, 2021; Accepted: June 26, 2021

Abstract

Bacteria are the primary cause of fatal disease outbreaks in aquaculture. Nine fish cages located at three different sites (3 cages/site) in the north Rosetta branch of the Nile River have exhibited high mortality rates. A total of 220 moribund *Oreochromis niloticus* and fish feed and water samples were examined for pathogenic bacteria in this study. Fish infected with *Vibrio parahaemolyticus* were located at only site 1 (62.5% infection rate), and *Streptococcus agalactiae* was isolated from fish at sites 1 and 3 (25% and 37.5% infection rates, respectively). Fish infected with *V. parahaemolyticus* or *S. agalactiae* were coinfecting with *Aeromonas hydrophila*. Further investigation revealed that *V. parahaemolyticus* infection at site 1 may occur via a fish feed that was contaminated with *V. parahaemolyticus* (the fish feed was containing improperly manufactured marine fish meal). The median lethal dose (LD₅₀) 96h of *A. hydrophila*, *V. parahaemolyticus*, and *S. agalactiae* was 2.4×10^5 , 1.9×10^5 , and 5.2×10^3 colony-forming unit / ml, respectively for *O. niloticus* (50 ± 2.5 g b.w.) at a water temperature of 25.1 °C ± 1.5 °C. In an indoor experiment, *O. niloticus* were injected with the LD₅₀ of the isolated bacteria. Florfenicol was found to be superior to ciprofloxacin in treating *A. hydrophila* and *V. parahaemolyticus* infection (mortality 13.3 % and 16.7 %, respectively), and ciprofloxacin was found to be more efficient in treating *S. agalactiae* infection (mortality 13.3%). In conclusion, inappropriately manufactured marine fishmeal was the source of *V. parahaemolyticus* infection in caged fish. *V. parahaemolyticus* or *S. agalactiae* infection co-occurred with *A. hydrophila* in fish cages containing low-quality water (high unionized ammonia content).

Keywords: *Aeromonas hydrophila*; *Vibrio parahaemolyticus*; *Streptococcus agalactiae*; fish cages; *Oreochromis niloticus*.

1. Introduction

Tilapia species come after carp species as the second major cultured fish around the world. In 2018, the production of *O. niloticus* in Egypt was 1.2 million tonnes, which, formed 65.15%, of total production which was 1.5 million tonnes (FAO, 2020). High market demands have led to intensive fish culture, wherein fish are exposed to infectious diseases, which have been considered one of the main obstacles facing aquaculture industries due to severe economic losses (Plant and LaPatra, 2011; Hamidan and Shobrak, 2019). In recent years in Egypt, the high mortality and morbidity rates recorded in freshwater fish farms were due to the prevalence of bacterial diseases that are concomitant with water temperature in summer (Enany *et al.*, 2019). In Egypt, Osman *et al.* (2021) reported that *Pseudomonas* sp. Isolated from Nile tilapia farmed or wild captured (River Nile) were carried antibiotic resistance, Quorum sensing, and virulence genes. In Bangladesh, Hamom *et al.* (2020) found that farmed diseased tilapia harboured *Edwardsiella tarda* *Streptococcus agalactiae*, and *Flavobacterium columnare* while live fish carried *Streptococcus iniae* and *Aeromonas salmonicida*. They also added that *columnare* and *E. tarda* caused a coinfection status in tilapia. *Aeromonas* is considered the

most important pathogen in the aquatic environment that results in significant economic losses. This bacterium could be considered as a specific primary pathogen in freshwater, and it also acts as a secondary opportunistic pathogen attacking immunocompromised or stressed freshwater fish where it normally inhabits in the gut of *O. niloticus* (Sherif *et al.*, 2020). *Vibrio* spp. are bacteria that are ubiquitous in marine and brackish waters and are typical examples of opportunistic bacteria that cause diseases. These bacteria cause disease not only in fish but also in humans and shrimp. Vibriosis, a disease caused by *Vibrio* spp., is highly dependent on water quality deterioration, which results in severe immunosuppression and initiates bacterial infection outbreaks (Amal *et al.*, 2015). *Streptococcus* spp. are gram-positive bacteria that normally present in the aquatic environment causing a haemorrhagic disease in fish (Chang and Plumb, 1996). They caused a condition called by streptococcosis predominantly in *O. niloticus*. This disease is considered one of the worst diseases in *O. niloticus* worldwide (Yang *et al.*, 2018).

Several fish cages in the Nile River exhibit severe mortalities due to common bacteria that infect freshwater fish, and no uncommon species have been observed through classic bacterial investigation. Coinfection in fish is common, as indicated by the fact that a single fish could

* Corresponding author e-mail: ahsherif77@yahoo.com.

harbour more than one species of bacteria; such coinfection could be explained by the kind of the fish diet, sampling sites, human activities and water parameters at the fish culture sites (Abdelsalam *et al.*, 2017). Comparison of 16S rRNA sequences is a reliable approach to distinguish between the different species of pathogenic bacteria (Woo and Bruno, 2014).

One of the common ways to control bacterial infections in fish culture is through the use of antibiotics. A bacterial outbreak is considered as a major threat for farming, due to which a large number of antibiotics are used not only for treatment but also for prophylaxis (Noga, 2010). In the Vietnam aquaculture sector, 82% of lobster farmers and 28% of fish farmers used antibiotics at an average rate of 5 and 0.6 kg per produced ton of lobster and fish respectively (Hedberg *et al.*, 2018). In the United States of America (USA), fish treatment with florfenicol and ciprofloxacin was recommended by the food and drug administration (FDA) under the veterinary feed directive and the investigational new animal drug (INAD) to combat fish diseases in aquaculture (Noga, 2010). Some antibiotics were approved for aquacultures such as florfenicol, ciprofloxacin, enrofloxacin, difloxacin, sarafloxacin, chlortetracycline, oxytetracycline, doxycycline, and erythromycin by the authority of veterinarian pharmaceuticals in highly producing countries (Noga, 2010).

Therefore, the aim of this investigation was to highlight the possible treatment and to enhance the understanding of the circumstances of the massive mortality of fish reared in cages. Therefore, we conducted this study to investigate the bacteria associated with caged fish mortality outbreaks in the northern Nile River and the treatment prospects.

2. Materials and Methods

2.1. The sites of the investigated Cages

This study focused on nine fish cages located at three different sites (3 cages/site) north of the Edfina Barrage in the Rosetta branch of the Nile River, Egypt. The fish cages (3 × 2 × 2 m) were stocked with the freshwater fish *O. niloticus*. A total of 220 moribund *O. niloticus* (80, 60, and 80 fish at sites 1–3, respectively) were collected along with fish feed and water samples. The moribund *O. niloticus* were immediately transported alive to the Animal Health Research Institute (AHRI), Fish Diseases Department, Kafrelsheikh Provincial Laboratory, Egypt, in the summer of 2017. All applicable international, national, and/or institutional guidelines for the care and use of animals were followed by the authors.

2.2. Bacterial Analyses

2.2.1. Primary bacterial isolation

The *O. niloticus*, feed, and water samples were examined for the presence of bacteria. Bacterial culture was attempted from hepatopancreas, spleen and kidney tissues according to previously described methods (Woo and Bruno, 2014). Water samples (3 replicate/site) were aseptically collected at 0.5 m depth in glass containers.

Samples of fish feed (3 replicate/site) were randomly and aseptically collected in sterile plastic bags at different cage sites, each sample of 1 g aseptically dissolved in 9 ml distilled water. The tubes containing tryptic soy broth (TSB) were inoculated with samples of fish tissue, water, and dissolved fish feed then the tubes were incubated for 24 h at 26 ± 1 °C. In addition, samples were inoculated into TSB with 1.5% NaCl then incubated for 24 h at 26 °C ± 1 °C.

2.2.2. Biochemical profiles

Phenotypic characterization of the bacterial isolates was demonstrated according to (Madigan and Martinko, 2005). Biochemical analyses (in triplicates) were conducted using API20 E following guidelines of (BioMerieux, Marcy l'Etoile, France).

2.2.3. Selective isolation of bacterial strains

For *Aeromonas hydrophila* isolation, the inoculum was spread onto Rimler-Shotts agar then incubated for 24 h at 26 °C ± 1 °C. For *Streptococcus agalactiae* isolation, the inoculum was streaked onto tryptic soy agar (TSA) with 5% sterile sheep blood then incubated for 72 h at 26 °C ± 1 °C, according to previously described methods (Facklam and Carey, 1985), and then spread onto brain heart infusion (BHI) agar then incubated for 24 h at 26 °C ± 1 °C. For *Vibrio parahaemolyticus* isolation, inoculates were streaked onto thiosulfate citrate bile salt (TCBS) agar (to produce green colonies) and incubated at 26 °C ± 1 °C for 24 h.

2.2.4. Determination of bacterial strains and their virulence genes

Further identification of the recovered bacteria was done using the technique of polymerase chain reaction (PCR), the bacterial DNA was extracted by means of a QIAamp DNA Mini Kits (Qiagen GmbH, Germany) following to the manufacturer's guidelines, then the products of PCR were analyzed using gel electrophoresis (AppliChem GmbH, Germany) and a documentation system (Alpha Innotech, Biometra), and then the results were evaluated using the Chip PCR computer software (Rodiger and Burdukiewicz, 2013).

Molecular identification (sequencing) of the isolated strains was performed using a universal primer specific for 16S rRNA (F: AGA GTT TGA TCC TGG CTC AG and R: GGT TAC CTT GTT ACG ACT T) with a PCR product size of 1500 bp (Weisburg *et al.*, 1991). The sequencing process was conducted using ABI 3730xl DNA sequencer. To identify the bacterial strains, the obtained sequences were matched with the other related ones that were registered in GenBank by using the Blastn program.

In Table 1, the primers of virulence genes were cytotoxic enterotoxin (act and alt) for *A. hydrophila*; regulatory gene of toxin (toxR) and haemolysin genes (tdh and trh) for *V. parahaemolyticus*; and a CAMP factor (cfb) that enhances the haemolysis processes and C-b protein (bac), a protein serving as an IgA-binding protein for *S. agalactiae*. All primers were manufactured by Metabion, Germany.

Table 1. The sequences of primers, virulence genes, sizes and annealing temperature.

Gene name	Sequences 5'-3'	Size (bp)	Annealing temperature	References
<i>A. hydrophila</i>				
act	F:AGAAGGTGACCACCACCAAGAACA R:AACTGACATCGGCCTTGAAGCTC	232	55°C	Nawaz <i>et al.</i> , 2010
alt	F:TGACCCAGTCCTGGCACGGC R:GGTGATCGATCACCACCAGC	442	55°C	Nawaz <i>et al.</i> , 2010
<i>V. parahaemolyticus</i>				
toxR	F:GTCTTCTGACGCAATCGTTG R:ATACGAGTGGTTGCTGT CATG	368	57 °C	Kim <i>et al.</i> , 1999
tdh	F:CCATTCTGGCAAAGTTATT R:TTCATATGCTTCTACATTAAC	534	48	Cai <i>et al.</i> , 2007
trh	F:TTGGCTTCGATATTTTCAGTATCT R:CATAACAAACATATGCCCATTTCCG	500	52	Cai <i>et al.</i> , 2007
<i>S. agalactiae</i>				
cfb	F:GGATTCAACTGAACTCCAAC R:GACAACTCCACAAGTGGTAA	600	72°C	Kannika <i>et al.</i> , 2017
bac	F:CTCCAAGCTCTCACTCATAG R:GAAACATCTGCCACTGATAC	750	47°C	Kannika <i>et al.</i> , 2017

2.3. Antimicrobial Sensitivity Analyses

The activity of different antimicrobial drugs against the isolated bacteria was analyzed following the procedures described by Finegold and Martin (1982). Pure cultures of the strains were cultivated in TSB (Oxoid) then incubated for 24 h at 26 °C ± 1 °C. Subcultures were spread with a sterile cotton stick onto Mueller–Hinton agar plates (Oxoid). Results were recorded after incubation at 26 °C ± 1 °C for 24 h, by disc diffusion including florfenicol (KF 10 µg), ciprofloxacin (CIP 5 µg), clindamycin (DA 2 µg), amoxy-clavulanic AMC (30 µg), amoxicillin AML (10 µg), doxycycline (DO 30 µg), streptomycin (S 10 µg), spiramycin (SP 100 µg), sulphamethazol +trimethoprim (SXT 25 µg), lincomycin (MY 10 µg), cefotaxime (CTX 30 µg), and cepharadin (CE 30 µg) manufactured by Oxoid, Waltham, MA, USA. According to the standards provided by the manufacturer and guidelines of NCCLS (1999), the isolated bacteria could be classified into three categories: resistant, intermediate, and sensitive depending on the diameters of inhibition zones.

2.4. Antibiotics Treatment Trial

Florfenicol: Floricol® 100 mg/g reg. No. 2533/2015 (Pharma Swede Company, Egypt) and ciprofloxacin: Ciprofar® (tablet) 500 mg/g reg. No. 21515/2012 (Pharco Pharmaceutical Company, Egypt) were used. Antibiotics were coated onto the surface of the pellets using capelin oil to prevent antibiotic dissociation, heat oil to 40 °C and antibiotics were added then mixtures of oil-antibiotic were evenly spread on the fish feed. The dosages of antibiotics were 10 mg/kg b.w./day for 10 successive days and capelin oil was 20 g/kg fish feed. The dosages and application methods of the antibiotics were implemented according to the methods described by (Noga, 2010).

2.5. Examination of Water Parameters

The water samples were analyzed at cages sites for temperature and salinity, (model YSI environmental, EC300) as well as dissolved oxygen (DO) (Aqualytic, OX 24) and pH (Thermo Orion, model 420A). Samples of 1 L were placed in a polyethylene bottle and transferred on ice

to the laboratory to analyze the total ammonia nitrogen (TAN), unionized ammonia (NH₃), nitrite (NO₂), and nitrate (NO₃) using a UV/Visible spectrophotometer (Thermo-Spectronic 300) as described by Rice and Bridgewater (2012).

2.6. Median Lethal Dose (LD₅₀)

The LD₅₀ values of *A. hydrophila*, *V. parahaemolyticus*, and *S. agalactiae* in *O. niloticus* (mean body weight = 50±2.5 g) were estimated following the method described by (Reed and Muench, 1938). Fish were acclimated in indoor tanks for 2 weeks at a water temperature of 25°C ±1.5 °C. Serial 10-fold dilutions were made of the bacteria cultured in BHI broth for 24 h at 30 °C and then adjusted to 1 × 10², 1 × 10³, 1 × 10⁴, 1 × 10⁵, 1 × 10⁶ or 1 × 10⁷ (CFU/ml) in normal saline. Then, 100 µl of the bacterial suspension was intraperitoneally injected into duplicate groups of five *O. niloticus*. Each bacterial dose (CFU/ml) was based on a standard curve generated by performing plate counts. Mortality rates were recorded for 96 h; however, accidental mortalities occurring in the first 24 h were excluded. All bacterial strains were re-isolated from the dead fish (liver, spleen, and kidneys) and confirmed by PCR using specific primers (Table 1).

2.7. Treatment Trial with Antibiotics

A total of 360 healthy *O. niloticus* fish with a mean body weight of 40 ±0.5 g were collected from a local fish farm and acclimated for 2 weeks at a water temperature of 25°C ±1.5 °C. *O. niloticus* were subdivided into four groups G1-4 (90 fish/ group) and then infected with *A. hydrophila* (G1), *V. parahaemolyticus* (G2), and *S. agalactiae* (G3), whereas un-challenged (G4) fish were considered as the control negative group. Each group was subdivided into three treatments, viz., T1–3, each consisting of three replicates (10 fish/replicate) as follows: control-untreated (T1), ciprofloxacin-treated (T2), and florfenicol -treated (T3). The antibiotics were applied for 10 days before and after bacterial infection. *O. niloticus* were injected i.p. with the LD₅₀ of bacteria as described by Alcaide *et al.*, (1999). *A. hydrophila*, and *S. agalactiae* isolates were grown overnight on TSA and TSA

containing 3% NaCl for *V. parahaemolyticus* at 30 °C, one of each resulted colonies was subcultured TSB for another 16 h. The mortality rate (MR %) was calculated as follows:

$$\text{MR \%} = \frac{\text{number of dead fish at the end}}{\text{number of fish in the same group at the start}} \times 100$$

2.8. Statistical Analyses

Data analyses were performed by determining the variance (ANOVA) using the SPSS software for windows, SPSS Inc., Chicago, IL, USA (SPSS, 2004). The obtained data are presented as mean \pm SE (standard error). The significant difference among treatments is determined at a level of 0.05 using Duncan's multiple range test (Duncan, 1955).

3. Results

3.1. Clinical Signs and Gross Lesions

Moribund *O. niloticus* exhibited a lack of appetite, lethargy, skin petechiae, detached scales and exophthalmia (Figure. 1). Postmortem examination of the fish revealed intestinal inflammation, visceral adhesion, hepatomegaly, splenomegaly, and gall bladder distension (Figure. 2).

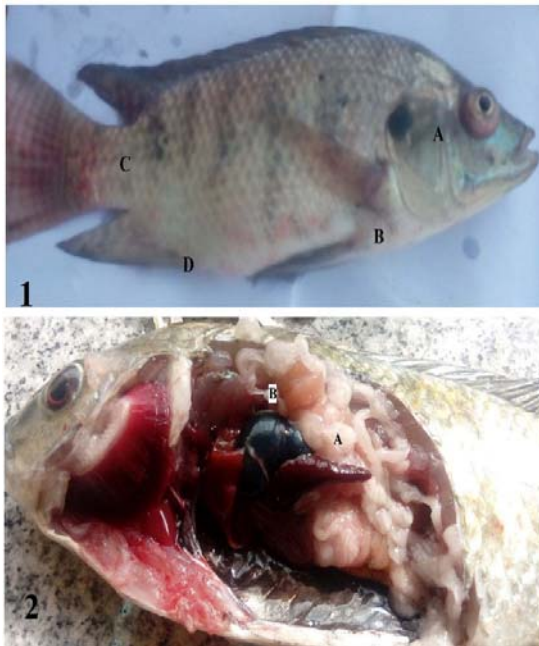


Figure 1. (1) *O. niloticus* collected from fish cages suffered from exophthalmia (A), haemorrhages on base of pectoral fin (B) and tail (C), and slightly distended abdomen. (2) *O. niloticus* collected from fish cages suffered from splenomegaly (A) and distended gallbladder (B).

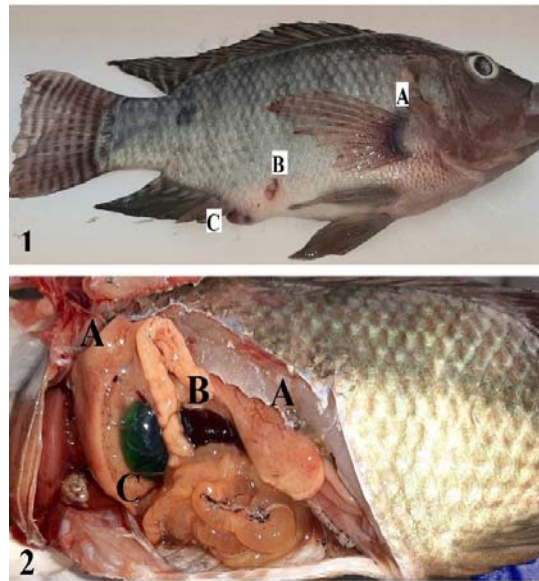


Figure 2. (1) *O. niloticus* experimentally infected with *Aeromonas hydrophila* suffered from pectoral haemorrhages (A), site of injection (B), and protruded inflamed-intestine (C). (2) *O. niloticus* experimentally infected with *A. hydrophila* with haemorrhages on hepatopancreatic tissue (A), splenomegaly (B), distended gall bladder (C).

3.2. Microbiological Examination

Bacteriological analyses (Table 2) using classical methods and PCR technique showed that the moribund *O. niloticus* were mostly infected with virulent strains of *Aeromonas hydrophila* (78.18%), followed by *Vibrio parahaemolyticus*, and *S. agalactiae* (22.73% each). The identification numbers obtained with API20 E were 107126, 4046107, and 1463410 for *A. hydrophila*, *V. parahaemolyticus*, and *S. agalactiae*, respectively. The blast results of the obtained isolates revealed 100% homology with *A. hydrophila*, *V. parahaemolyticus*, and *S. agalactiae*, in the GenBank database. The isolated strains (*A. hydrophila* AHRAS2, *V. parahaemolyticus* AHRAS44, and *S. agalactiae* AHRAS33) were deposited to the GenBank under the accession numbers of MW092007, MW092008, and MW092091, respectively. Phylogenetic trees were generated for the three strains (Figures. 3, 4, and 5). No other bacterial species were isolated from the collected samples.

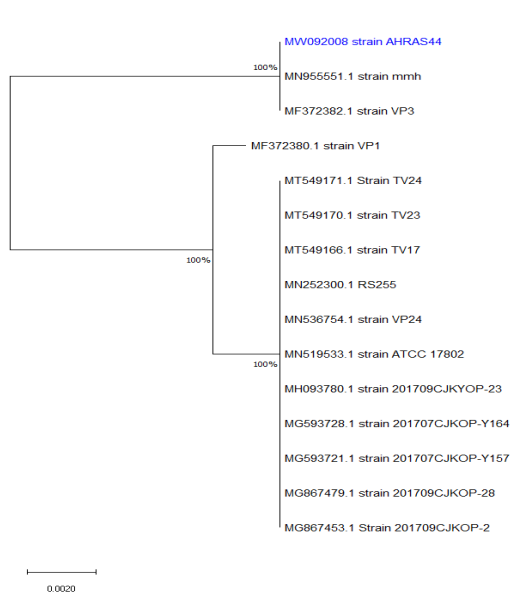


Figure 3. Phylogenetic analyses of *Aeromonas hydrophila*;

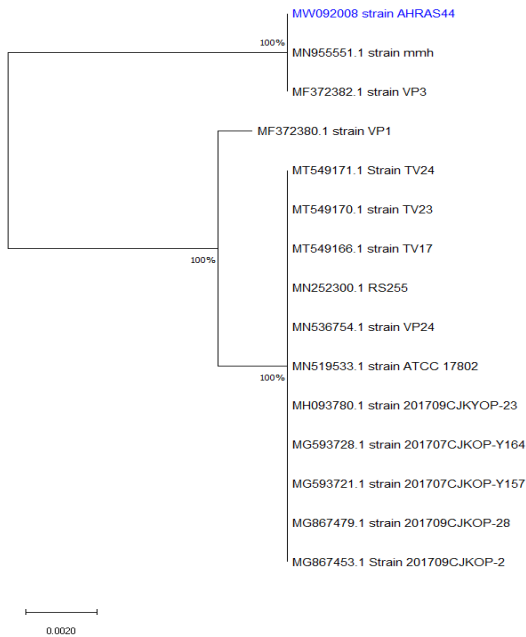


Figure 4. Phylogenetic analyses of *Vibrio parahaemolyticus*;

Table 2. Infection rates by bacterial isolate in *O. niloticus* collected from fish cages.

Items	No.	<i>A. hydrophila</i>		<i>V. parahaemolyticus</i>		<i>S. agalactiae</i>		Co-infection	
		No.	%	No.	%	No.	%	No.	%
Site 1	80	70	87.5	50	62.5	20	25	50	62.5
Site 2	60	52	86.7	0	0	0	0	0	0
Site 3	80	50	62.5	0	0	30	37.5	30	37.5
Overall	220	172	78.18	50	22.73	50	22.73	100	45.45

No.= number of fish.

3.3. Water Parameters of the Examined Cages

The physicochemical parameters of the water (Table 3), including temperature, DO, salinity, pH, TAN, NH₃, NO₂ and NO₃, were insignificantly differed in the three sites.

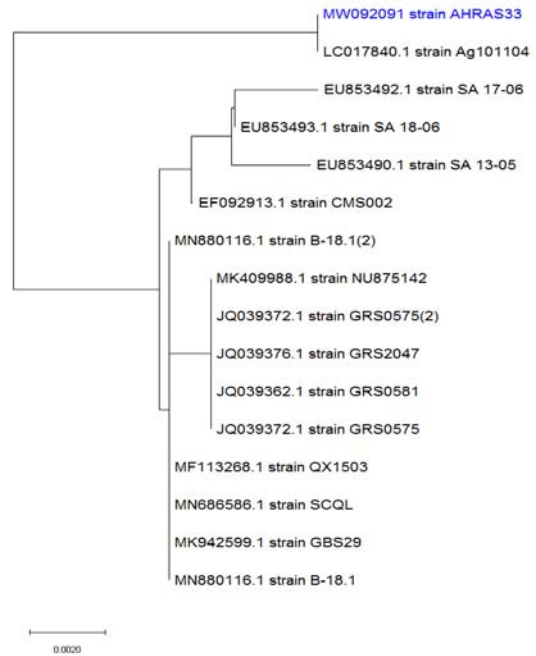


Figure 5. Phylogenetic analyses of *Streptococcus agalactiae*

At site 1, only *V. parahaemolyticus* infection occurred concurrently with *A. hydrophila* infection, with an infection rate of 62.5% (Table 2), whereas at site 3, all the *S. agalactiae* isolates were concurrently present with *A. hydrophila* and *V. parahaemolyticus*. Although *V. parahaemolyticus* is a classic pathogen of marine and brackish water fish, it was isolated from caged *O. niloticus* at site 1. *V. parahaemolyticus* was isolated only from caged fish that were fed a diet formulated with locally produced fish meal. The caged *O. niloticus* exhibited obvious infection through contaminated feed as *V. parahaemolyticus* was isolated from water and feed in site 1. The infection rates of *S. agalactiae* in *O. niloticus* 25% and 37.5% at sites 1 and 3, respectively, and the infection occurred concurrently only with *A. hydrophila* infection. *A. hydrophila* and *S. agalactiae* were isolated from water samples at (all three sites, and sites 1 and 3, respectively, and both organisms were not isolated from fish feed.

The water parameters were suitable range for *O. niloticus* culture; however, NH₃ content was high at 0.2 mg/l, resulting in stress conditions.

Table 3. Physicochemical parameters and ammonia compounds of the water samples.

Item*	S 1	S 2	S 3
Temperature (°C)	27±0.5	28±1.5	28±1.5
DO (mg/l), mid-day	5.4±0.5	5.3±0.7	5.13±0.3
Salinity (ppt)	1.5±0.05	1.6±0.1	1.5±0.2
pH	7.9±0.2	8±0.2	8.2±0.1
TAN (mg/l)	2.1±0.5	2.4±0.25	2.5±0.4
NH ₃ (mg/l)	0.3±0.1	0.28±0.12	0.27±0.1
NO ₂ (mg/l)	0.01±0.0	0.01±0.0	0.01±0.0
NO ₃ (mg/l)	1.65±0.2	1.6±0.1	1.7±0.2

S, cage site; water DO, dissolved oxygen; pH, hydrogen ions; TAN, total ammonia nitrogen; NH₃; unionized ammonia; NO₂, nitrite; NO₃, nitrate. * Significant difference ($P \leq 0.05$) indicates by different letters in the same row.

3.4. LD₅₀ of the Isolated Bacteria

The LD₅₀ 96h of values *A. hydrophila*, *V. parahaemolyticus*, and *S. agalactiae* were 2.4×10^5 , 1.9×10^5 , and 5.2×10^3 CFU/ml, respectively, for *O. niloticus* with a body weight of 50 ± 2.5 g at a water temperature of $25^\circ\text{C} \pm 1.5^\circ\text{C}$.

3.5. Antibacterial Profile

The bacterial isolates were highly sensitive to ciprofloxacin and florfenicol, confirming that these antibiotics would be suitable for treatment, whereas the bacteria exhibited intermediate resistance to clindamycin, amoxicillin clavulanate, and sulfamethoxazole-trimethoprim and full resistance to amoxicillin, lincomycin, cefotaxime, streptomycin, doxycycline, spiramycin, and cephradine.

3.6. Treatment Trial

The three groups of *O. niloticus* injected with the LD₅₀ of the isolated bacteria exhibited mortality, and gross lesions were eye opacity, haemorrhages at the base of the pectoral fin, inflamed intestines, haemorrhages on hepatopancrease, splenomegaly and gall-bladder distension (Figure. 5). The two different treatment regimens decreased the mortality compared with the control regimen. The florfenicol-treated (T2) group had the lowest mortality rates (13.3 % and 16.7 %) among groups challenged with *A. hydrophila* (G1) and *V. parahaemolyticus* (G2), respectively, whereas the ciprofloxacin-treated (T3) group showed 13.3 % mortality among fish challenged with *S. agalactiae* (G3) compared with the control positive treatment (T1) group (Figure. 6). The antibiotic treatments had no effect on the mortality rate (3.33 %) in the unchallenged *O. niloticus* (G4) group.

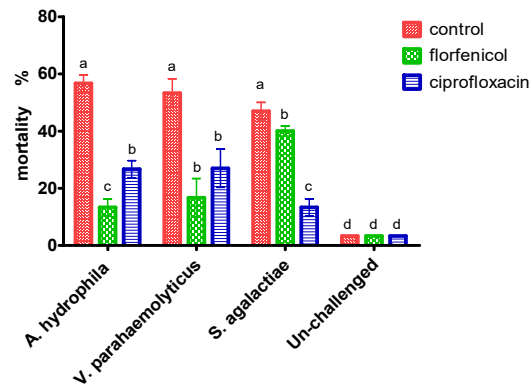


Figure 6. Mortality percentages of the different groups of *O. niloticus* experimentally infected with the three bacterial isolates and unchallenged group. Significant difference ($P \leq 0.05$) indicates by different letters.

4. Discussion

Aeromonas hydrophila, *Vibrio parahaemolyticus*, and *Streptococcus agalactiae* produced common symptoms of bacterial diseases. Similar to the clinical signs observed in this study, previous researchers have also reported the most common clinical and postmortem signs of *V. parahaemolyticus* infection as external haemorrhages, white nodular skin lesions, necrotic eyes, sudden death with haemorrhages in the skeletal muscles, deep ulcers, liver haemorrhage, pale kidneys and splenomegaly in studies on *Dicentrarchus labrax* (Rahman *et al.*, 2010), Iberian toothcarp (*Aphanius iberus*) (Alcaide *et al.*, 1999), and *Amphiprion sebae* (Marudhupandi *et al.*, 2017). Similarly, *Streptococcus* infection in *Oreochromis niloticus* was manifested by behavioural disorders, pop eye, and haemorrhagic dots on the body surface and bases of the fins in naturally infected tilapias (Figueiredo *et al.*, 2006). Consistently, the post mortem investigation of *O. niloticus*, experimentally infected with *A. hydrophila*, showed hepatomegaly and splenomegaly (Sherif *et al.*, 2015) and *S. agalactiae* in red tilapia (Abdelsalam *et al.*, 2017).

To confirm the identification of *Aeromonas* spp., some genes such as *gyrB*, *rpoD*, *dnaJ*, *gyrA*, *dnaX*, *recA*, and *atpD* are commonly used (Zhou *et al.*, 2019). Moreover, *V. parahaemolyticus* strains have been previously identified through PCR-based methods similar to those in our study (Kim *et al.*, 1999). The 16S rRNA sequencing approach (Figures. 3, 4, and 5) along with virulence genes (Table 1) were used to confirm the accuracy of bacterial identification of the isolated bacteria. Several researchers have identified bacterial species using PCR (16S-23S rDNA intergenic spacers) such as *Aeromonas* spp., and *Streptococcus* spp. (Sebastiao *et al.*, 2015).

In the examined cages, *A. hydrophila* was the most prevalent bacterium at a rate of 78.18% irrespective of the site. The most important diseases affecting fish in Egypt are *A. hydrophila* infection, Saprolegniasis, Aflatoxicosis, *Ichthyophonus* infection, *Trichodina* infestation, Costiasis, and *A. hydrophila* and *Saprolegnia* coinfection (Aly, 2013). In the Nile River, *A. hydrophila* and *Pseudomonas fluorescens* have been isolated from both *O. niloticus* and *Clarias gariepinus* (Mohamed *et al.*, 2006). *V. parahaemolyticus* is a classic pathogen of marine and brackish water fish; however, it was isolated from caged *O. niloticus* (62.5% infection rate). At site 1, *V. parahaemolyticus* infection co-occurred with *Aeromonas* spp infection in caged *O. niloticus* (infection rate: 62.5%) and the fish feed and water samples were contaminated with *V. parahaemolyticus*. Supporting the obtained findings, *V. parahaemolyticus* has been isolated from tilapia cultured in freshwater cages (Amal *et al.*, 2010) and fish cultured in low-salinity water (5–30 ppt NaCl) (Iwamoto *et al.*, 2010). Moreover, infection rates of 52.11%, 29.5%, and 18.4% have been recorded in the Terengganu River, Pedu Lake, and Kenyir Lake, respectively (Ismail *et al.*, 2016). *S. agalactiae* was concurrently isolated from caged-*O. niloticus* with *A. hydrophila* at sites 1 and 3 with infection rates of 25% and 37.5%, respectively. *S. agalactiae* has been reported to cause large-scale outbreaks in cultured tilapia Thailand and Latin America (Marcusso *et al.*, 2015). Furthermore, similar to the obtained findings regarding coinfection, Abdelsalam *et al.*, (2017) reported that *S. agalactiae* concurrently infected red hybrid tilapia reared in cement ponds in north coast, Egypt.

Conversely, *Aeromonas* spp., *Streptococcus* spp., *Vibrio* spp., and *Flavobacterium* spp., coinfecting cultured *O. niloticus*, water, and sediment (Al-Harbi and Uddin, 2006). Moreover, *A. hydrophila*, *A. sobria*, *P. fluorescens* and *P. aeruginosa* were concurrently isolated from *O. niloticus* (Sherif *et al.*, 2015). In our findings, *A. hydrophila*, *V. parahaemolyticus*, and *S. agalactiae* were isolated from water samples. Supporting this finding, it has been reported that infected fish released bacteria through feces, which survive in water and spread infection (Apun *et al.*, 1999).

The suitable water parameters are an important part of aquaculture systems. The parameters of water samples (temperature, DO, salinity, and pH) in the fish cages were suitable for fish culture (Table.3). Maintaining optimal water quality conditions or parameters is a vital part of fish for optimal performance (FAO, 2020). Caged-*O. niloticus* suffer from stressful conditions that predispose them to bacterial infection. Although most of the water parameters in this study were suitable for fish culture, high levels of ammonia were observed with the levels of TAN and NH₃ being 2.1, 2.4 and 2.5; 0.3, 0.28, and 0.27 mg/l, respectively. Accordingly, Noga (2010) mentioned that NH₃ level > 1.00 mg/l are lethal whereas those > 0.05 mg/l are sublethal concentrations for freshwater fish. The outbreaks of *Aeromonas* infection in fish farms were due to the limited knowledge and awareness of fish farmers regarding appropriate management (Sherif *et al.*, 2015; Mzula *et al.*, 2019).

Based on antibiogram findings, ciprofloxacin (despite being illegal for veterinary use in Egypt, some farmers and paramedics use ciprofloxacin unintentionally and

erratically for treating bacterial fish diseases) and florfenicol are the optimal antibacterial substances for bacterial isolates. As shown in Figure. 6, the mortality rates of fish infected with *A. hydrophila* (G1) and *V. parahaemolyticus* (G2) and then treated with florfenicol were significantly lower (13.3% and 16.7, respectively) than those of control fish (56.7 and 53.3 %, respectively). In *S. agalactiae* infection (G3), ciprofloxacin-treatment (T3) resulted in significantly lowest mortality (13.3%) compared with florfenicol-treatment (T2) (40%) and control (47 %). Similarly, Ashiru *et al.*, (2011) found that pefloxacin, ofloxacin, and ciprofloxacin are suitable drugs for controlling *Aeromonas* infection, although, oxytetracycline, nitrofurans, potentiated sulfonamides, and oxolinic acid have been successfully used, bacteria, especially *V. anguillarum* and *V. salmonicida*, can exhibit resistance to these drugs. Despite the alleviated mortality (14.4%) resulting from ciprofloxacin treatment, immunosuppression has been detected in *A. sebae* infected with *V. parahaemolyticus* (Marudhupandi *et al.*, 2017), whereas *S. agalactiae*, which was isolated from cultured yellowtail (*Seriola quinqueradiata*) in Japan, was resistant to these antibiotics (Kitao and Aoki, 1979).

5. Conclusion

This study highlighted the presence of unusual pathogens that cause mortality in caged fish in the north Rosetta branch of the Nile River. *V. parahaemolyticus* or *S. agalactiae* infection co-occurred with *A. hydrophila* infection. The source of *V. parahaemolyticus* infection in cage-cultured *O. niloticus* would be fish feeds containing inappropriately manufactured marine fishmeal so that this classical marine bacterial pathogen causes fish mortality in the freshwater environment. The infections caused by the bacteria *A. hydrophila*, *S. agalactiae*, and *V. parahaemolyticus* correlated with high unionized ammonia content in cage-water. In such cases, florfenicol was the most effective antibacterial agent along with the maintenance of water quality.

Conflicts of interest

None of the authors has any conflict of interests to declare.

References

- Abdelsalam M, Shaalan M and Moustafa M. 2017. Rapid identification of pathogenic streptococci isolated from moribund red tilapia (*Oreochromis* spp.). *Acta Vet Hun*, **65**: 50-59.
- Alcaide E, Amaro C, Todoli R and Oltra R. 1999. Isolation and characterization of *Vibrio parahaemolyticus* causing infection in Iberian tooth carp *Aphanius iberus*. *Dis Aquat Org*, **35**: 77-80.
- Al-Harbi AH and Uddin MN. 2006. Seasonal changes in bacterial flora of fish pond sediments in Saudi Arabia. *J Appl aquac*, **18**: 35-45.
- Aly SM. 2013. A Review of fish diseases in the Egyptian aquaculture sector. Working report. Research program on livestock and fish. CGIAR, pp. 1-41.
- Amal MNA, Zamri-Saad M, Siti-Zahrah S and Zulkafli AR. 2015. Water quality influences the presence of *Streptococcus agalactiae* in cage cultured red hybrid tilapia, *Oreochromis niloticus* × *Oreochromis mossambicus*. *Aquac Res*, **46**: 313-323.

- Amal, MNA, Zamri-Saad, M., Siti-Zahrah, A, Zulkafli, R, Misri, S, Nur-Nazifah, M and Shahidan, H. 2010. Prevalence of *Streptococcus agalactiae* in tilapia kept indifferent water bodies. *Online J Vet Res*, **14**: 153-162.
- Apun K, Yusof AM and Jugang K. 1999. Distribution of bacteria in tropical freshwater fish and ponds. *Int J Environ Health Res*, **9**: 285-292. <https://doi.org/10.1080/09603129973083>
- Ashiru AW, Uaboi-Egbeni PO, Oguntowo JE and Idika CN. 2011. Isolation and antibiotic profile of *Aeromonas* species from tilapia fish (*Tilapia nilotica*) and catfish (*Clarias betrachus*). *Pak J Nutr*, **10**: 982-986.
- Cai SH, Wu ZH, Jian JC and Lu YS. 2007. Cloning and expression of the gene encoding an extracellular alkaline serine protease from *Vibrio alginolyticus* strain hy9901, the causative agent of Vibriosis in *Lutjanus erythropterus* (Bloch). *J Fish Dis*, **30**: 493-500. <https://doi.org/10.1111/j.1365-2761.2007.00835.x>
- Chang PA and Plumb JA. 1996. Histopathology of experimental *Streptococcus* sp. infection in tilapia, *Oreochromis niloticus* (L.), and channel catfish, *Ictalurus punctatus* (Rafinesque). *J Fish Dis*, **19**: 235-241. <https://doi.org/10.1111/j.1365-2761.1996.tb00130.x>
- Duncan DB. 1955. Multiple ranges and multiple "F" test. *Biometrics*, pp10-11
- Enany M, Eidaroos N and Eltamimy N. 2019. Microbial causes of summer mortality in farmed fish in Egypt. *SCVMJ*, **24**: 45-56. <https://doi.org/10.21608/scvmj.2019.59198>.
- Facklam RR and Carey RB. 1985. *Streptococci and Aerococci*. In "Manual of clinical microbiology" 4th Ed. Lennette, Hauser, Shadomy (Eds). American Society for Microbiology, Washington DC, pp. 154-175.
- FAO. (2020). Fishery and aquaculture statistics. Global production by production source 1950-2018 (FishstatJ). Retrieved from FAO Fisheries and Aquaculture Department [online] website: www.fao.org/fishery/statistics/software/fishstatj/en.
- Figueiredo HC, Carneiro DO, Faria FC and Costa GM. 2006. *Streptococcus agalactiae* associado à meningoencefalite e infecção sistêmica em tilápia-do-nylo (*Oreochromis niloticus*) no Brasil. *Arq Bras Med Vet Zoo*, **58**: 678-680. <https://doi.org/10.1590/S0102-09352006000400036>
- Finegold, SM and Martin WJ. 1982. Bailey and Scott's Diagnostic microbiology. (Eds.) Mosby, Philadelphia.
- Hamidan NAF and Shobrak M. 2019. An Update on Freshwater Fishes of Saudi Arabia. *Jordan J Biol Sci*, **12**: 495-502.
- Hamom A, Alam MM, Iqbal MM, Khalil SM, Parven M, Sumon TA and Mamun MA. 2020. Identification of pathogenic bacteria from diseased Nile tilapia *Oreochromis niloticus* with their sensitivity to antibiotics. *Int J Curr Microbiol Appl Sci*, **9**: 716-1738. <https://doi.org/10.20546/ijemas.2020.903.200>
- Hedberg N, Stenson I, Nitz Pettersson M, Warshan D, Nguyen-Kim H, Tedengren M and Kautsky N. 2018. Antibiotic use in Vietnamese fish and lobster sea cage farms; implications for coral reefs and human health. *Aquaculture*, **495**: 366-375.
- Ismail NIA, Amal MNA, Shohaimi S, Saad MZ and Abdullah SZ. 2016. Associations of water quality and bacteria presence in cage cultured red hybrid tilapia, *Oreochromis niloticus* × *O. mossambicus*. *Aquacult Rep*, **8**: 39-44. <https://doi.org/10.1016/j.aqrep.2016.06.004>
- Iwamoto M, Ayers T, Mahon BE and Swerdlow DL. 2010. Epidemiology of seafood-associated infections in the United States. *Clin Microbiol Rev*, **23**: 399-411.
- Kannika K, Pisuttharachai D, Srisapoom P, Wongtavatchai J, Kondo H, Hirono I, Unajak S and Areechon N. 2017. Molecular serotyping, virulence gene profiling and pathogenicity of *Streptococcus agalactiae* isolated from tilapia farms in Thailand by multiplex PCR. *J Appl Microbiol*, **122**: 1497-1507. <https://doi.org/10.1111/jam.13447>
- Kim YB, Okuda J, Matsumoto C, Takahashi N, Hashimoto S and Nishibuchi M. 1999. Identification of *Vibrio parahaemolyticus* strains at the species level by PCR targeted to the toxR gene. *J Clin Microbiol*, **37**:1173-1177.
- Kitao T and Aoki T. 1979. Therapeutic studies of doxycycline of Streptococcosis of cultured yellow tail (*Seriola Quinqueradiata*). *Bull Fac Agric Univ Miyazaki*, **26**: 357-63.
- Madigan MT and Martinko J. 2005. Brock Biology of Microorganisms, 11th Ed. Prentice Hall.
- Marcusso PF, Eto SF, Claudiano GD, Vieira FC, Salvador R, Moraes JR and Moraes FR. 2015. Isolamento de *Streptococcus agalactiae* em diferentes órgãos de tilápias do nylo (*Oreochromis niloticus*) criadas em tanques-rede. *Biosci J*, 549-554.
- Marudhupandi T, Kumar TTA, Prakash S, Balamurugan J and Dhayanithi NB. 2017. *Vibrio parahaemolyticus* a causative bacterium for tail rot disease in ornamental fish, *Amphiprion sebae*. *Aquacult Rep*, **8**: 39-44. <https://doi.org/10.1016/j.aqrep.2017.09.004>
- Mohamed LA, Osman KM, El-Seedy S and Soliman W. 2006. Isolation and characterization of *Aeromonas* species and *Pseudomonas fluorescens* from freshwater fishes. International Conference, Research Division, NRC, 219-229.
- Mzula A, Wambura PN, Mdegela RH and Shirima GM. 2019. Phenotypic and molecular detection of *Aeromonads* infection in farmed Nile tilapia in Southern highland and Northern Tanzania. *Heliyon*, **5**: e02220. <https://doi.org/10.1016/j.heliyon.2019.e02220>
- Nawaz M, Khan SA, Khan AA, Sung, K, Tran Q, Kerdahi K and Steele R. 2010. Detection and characterization of virulence genes and integrons in *Aeromonas veronii* isolated from catfish. *Food Microbiol*, **27**: 327-331. <https://doi.org/10.1016/j.fm.2009.11.007>
- NCCLS (National Committee for Clinical Laboratory Standards). 1999. Performance standard for antimicrobial disk and dilution susceptibility tests for bacteria isolated from animals. Approved Standard M 31A19 (11). NCCLS, Wayne, Pennsylvania.
- Noga EJ. 2010. Fish diseases: Diagnosis and treatment 2nd Ed, Wiley-Blackwell
- Osman KM, da Silva Pires Á, Franco OL, Saad A, Hamed M, Naim H, Ali AH and Elbehiry A. 2021. Nile tilapia (*Oreochromis niloticus*) as an aquatic vector for *Pseudomonas* species of medical importance: Antibiotic Resistance Association with Biofilm Formation, Quorum Sensing and Virulence. *Aquaculture*, **532**:736068. <https://doi.org/10.1016/j.aquaculture.2020.736068>
- Plant KP and LaPatra SE. 2011. Advances in fish vaccine delivery. *Dev Comp Immunol*, **35**: 1256-1262. <https://doi.org/10.1016/j.dci.2011.03.007>
- Rahman MM, Ferdowsy H, Kashem MA and Foyals MJ. 2010. Tail and fin rot disease of Indian major carp and climbing perch in Bangladesh. *J Biol Sci*, **10**: 800-804. <https://scialert.net/abstract/?doi=jbs.2010.800.804>
- Reed LJ and Muench H. 1938. A simple method of estimating fifty percent endpoints. *Am J Epidemiol*, **27**: 493-497. <https://doi.org/10.1093/oxfordjournals.aje.a118408>
- Rice EW and Bridgewater L. 2012. A.P.H. Association, standard methods for the examination of water and wastewater, American public health association, Washington, DC.
- Rodiger S and Burdukiewicz M. 2013. ChipPCR: toolkit of helper functions to pre-process amplification data Available from: <https://github.com/michbur/chipPCR>
- Sebastiao FD, Lemos EG and Pilarski F. 2015. Validation of absolute quantitative real-time PCR for the diagnosis of

- Streptococcus agalactiae* in fish. *J Microbiol Methods*, **119**: 168-175. <https://doi.org/10.1016/j.mimet.2015.10.021>
- Sherif AH, Elgamel A and Amin HA. 2015. Investigation of mass mortality of some fresh water fish in late summer in some fish farms at Kafr El Shiekh governorate. *J Arabaqs*, **10**: 33-44. <https://doi.org/10.12816/0026660>
- Sherif AH, Gouda MY, Naena NA and Ali AH. 2020. Alternate weekly exchanges of feeding regime affect the diversity of intestinal microbiota and immune status of Nile tilapia *Oreochromis niloticus*. *Aquac Res*, **51**: 4327-4339. <https://doi.org/10.1111/are.14778>
- SPSS 2004. "Statistical and package for social science, SPSS for windows release14.0.0, 19 June, 2004." Standard version, copyright SPSS Inc., 1989- 2004.
- Weisburg WG, Barns SM, Pelletier DA and Lane DJ. 1991. 16S Ribosomal DNA Amplification for Phylogenetic study. *J Bacteriol*, **173**: 697-703.
- Woo P and Bruno D. 2014. Diseases and Disorders of Finfish in Cage Culture. 2nd Ed. CABI Pub, pp. 159-160.
- Yang Q, Liu JX, Wang KY, Liu T, Zhu L, He SY, Geng Y, Chen DF, Huang XL, and Ouyang P. 2018. Evaluation of immunogenicity and protective efficacy of the elongation factor Tu against *Streptococcus agalactiae* in tilapia. *Aquaculture*, **492**: 184-189. <https://doi.org/10.1016/j.aquaculture.2018.03.056>
- Zhou Y, Yu L, Nan Z, Zhang P, Kan B, Yan D and Su J. 2019. Taxonomy, virulence genes and antimicrobial resistance of *Aeromonas* isolated from extra-intestinal and intestinal infections. *BMC Infect Dis*, **19**: 158.

Effect of Physico-Chemical Parameters in the Production of Hydrolytic Enzymes from Yeast *Candida Tropicalis* Isolated from the Mangrove Sediments of North Kerala, India

Vidya Pothayi¹, Sreedevi N. Kutty² and Sebastian Chempakassery Devasia^{1,*}

¹Division of Molecular Biology, Department of Zoology, University of Calicut, Kerala 673 635;

²Department of Zoology, N. S. S. College, Nemmara, Palakkad, Kerala 678508

Received: February 25, 2021; Revised: May 4, 2021; Accepted: June 5, 2021

Abstract

The extracellular enzymes produced by yeasts present in mangrove sediments were found to have wide range of biotechnological and industrial applications. Large scale production of these enzymes by bioprocess techniques needs proper optimization of culture conditions for high enzyme yield in a cost-effective manner. In the present study, we investigated the effect of different growth conditions like pH, salinity, substrate concentration and temperature on the growth and production of enzymes protease, amylase, lipase and ligninase by selected strains of *Candida tropicalis*. The optimum conditions for the maximum growth and enzyme production for protease, amylase, lipase and ligninase producing strains were found to be at pH 8.5-9; salinity 5-10 ppt and temperature 35 – 40°C with 2% casein, 1% starch, 1% tributyrin, 0.5% tannic acid as substrate concentrations respectively. The results suggest the use of yeast *C. tropicalis* from mangrove sediments as potent and promising strain for the large-scale production of hydrolytic enzymes when compared to the previous studies done on marine counter parts.

Keywords: Mangrove sediments, yeasts, *Candida tropicalis*, extracellular enzymes, optimization, culture conditions

1. Introduction

Benthic yeasts from mangroves have wide ecological significance as they are involved in various transformation processes. This is attributed by the extracellular enzymes produced as a result of different metabolic reactions that take place inside their cell (Kutty *et al.*, 2014). Yeast enzymes were found to be actively involved in nutrient recycling, decomposition of litter, mineralization of organic compounds and degradation of oil and recalcitrant substances (Kutty *et al.*, 2012; Pothayi and Devasia, 2020). Moreover, the benthic fauna of mangroves survives in extreme conditions such as high salinity variation, fluctuating temperature, low oxygen concentrations, high UV exposure and varying nutrient compositions. The secondary metabolites from mangroves which are toxic to microorganisms are detoxified or degraded by them as a part of their metabolic activities. These factors act as driving force for the microbes to compete with each other and evolve to produce novel bioactive compounds (Solntsev *et al.*, 2019). So, the enzymes produced by them possess unique properties like salt tolerance, thermostability, anaerobic tolerance, substrate flexibility etc. (Sengupta *et al.*, 2015). Altogether, these characteristics of yeast enzymes make them potential candidates for various industrial applications.

Yeast enzymes (due to their industrial, medical and food applications) have been produced in large scale

recently by bioprocess technology. In comparison to other microbes, yeasts are preferred as better sources for the large scale enzyme production due to their ease in generation by environmental and genetic manipulation, simplicity of extraction, economic cost, stability, non-toxicity and quality of the metabolites (Elsanhoty *et al.*, 2017). Moreover, large scale production of yeasts can be done using different types of culture media using cheap industrial by-products and wastes as nutrient sources (Cheng and Yang, 2016).

One of the most important yeast extracellular enzymes is lipase which is found to be produced by almost all the strains (Paskevicius, 2001). Lipases have wide catalytic activity including hydrolysis, acidolysis, esterification, alcoholysis and aminolysis (Kutty *et al.*, 2014) and are used in the production of detergents, cosmetics, chemicals and pharmaceutical agents (Choudhury and Bhunia, 2015); also they have applications in bioremediation of environments contaminated with inorganic and organic pollutants, hydrocarbons and metals (Vakhlu and Kour, 2006). Yeast proteases have many significant applications in manufacture of detergents and chemicals, food and feed processing, leather and chemical industries, also in medical sector and waste treatment (Bessadok *et al.*, 2015; Shahat, 2017).

Amylases that hydrolyze starch molecules are of great biotechnological importance and constitute 25% of world enzyme market. They are largely used in bread and baking industries, textile, paper, medical and detergent industries

* Corresponding author e-mail: drcdsebastian@gmail.com.

apart from their use in clinical biochemistry (Yalsein and Corbaci, 2013). Their ability to convert starchy biomass into single cell proteins and ethanol has received much attention during recent years (Kachiprath *et al.*, 2018). Ligninases from yeast, though least studied, are found to have applications in feed, fuel, food, agricultural, paper, textile and cosmetics industries (Bonugli-Santos *et al.*, 2012).

The production of extracellular enzymes by yeasts is greatly influenced by several physico-chemical factors like temperature, pH, substrate concentration and composition, salinity, oxygen availability etc. Proper optimization of the factors affecting the growth of yeast in culture medium is of great importance for maximum enzyme production (Rahman *et al.*, 2013). It would help in the large-scale production of yeast enzymes by fermentation technology in a very cost effective manner.

The main objective of the present study was to screen benthic yeast isolates from mangroves for production of lipase, protease, amylase and ligninase enzymes. Study was also focused on evaluating the effect of various physico-chemical parameters on selected strains for maximum biomass yield and enzyme production.

2. Materials and Methods

Sediment samples were collected from the mangroves of the 5 districts from 8 sites along North Kerala coast during the period 2018-2019. The sites were Chandragiri (KGD), 12°05'32" N 75°13'39" E (Kasaragod Dt), Edat (EDT), 12°05'3" N 75°13'39" E; Pazhayangadi (PYD), 12°02' 72" N 75°29'31" E; Valapattanam(VPT), 11°93'45" N 75°35'35" E (Kannur Dt), Elathur (ELR), 11°19'43" N 75°45'2" E; Kadalundi(KDI), 11°07'43" N 75°49'48" E (Kozhikode Dt), Ponnani (PON), 10°47'10" N 75°55'30" E (Malappuram Dt) and Chettuva (CTV), 11°1'41" N 75°52'62" E (Thrissur Dt).

2.1. Isolation of yeasts

Approximately, 10-20g of sub surface sediment was collected using sterile plastic corer and was transferred aseptically into sterile polythene bags. The collected samples were transported in ice boxes and processed within 2 hours of collection. For the isolation of yeasts, spread-plate method was employed using Wickerham's agar supplemented with 200 mg/L chloramphenicol (Wickerham, 1951) in duplicates. The plates were incubated at $18 \pm 2^\circ \text{C}$ for 7 days, and the colonies developed were purified by quadrant streaking and transferred to malt extract agar slants for further studies.

2.2. Screening for enzyme activity and Identification of potent isolates

All the isolates obtained were tested for the production of extracellular hydrolytic enzymes viz., protease, amylase, lipase, urease, ligninase, cellulase, DNase, pectinase and chitinase. Since the enzymes protease, amylase, lipase and ligninase were found to be produced by majority of the isolates, they were selected for further studies. Nutrient agar medium supplemented with casein (2%), starch (1%) and tributyrin (1%) were used for the detection of hydrolytic activities of protease, amylase and lipase, respectively. Crawford's agar supplemented with 0.5% tannic acid was used for the detection of ligninase activity. The plates were spot-inoculated and incubated at

$28 \pm 2^\circ \text{C}$ for 7 days. Formation of clearance / halo zone around the colonies was considered as positive result for lipase. Plates were flooded with 1M HCl and Gram's iodine solution after incubation for protease and amylase, respectively and the appearance of clearance zone was noted as positive result. Formation of brown colour around the colonies was considered as positive result for ligninase. The isolates which showed maximum enzyme activity on plates at 24 – 48 hours with significant increase in their activity by 72 hours were selected for growth optimization studies.

The selected potent isolates were then characterized using morphological, biochemical and molecular methods. For morphological characterization, colony characteristics on malt extract agar and microscopic appearance of methyl blue stained smear, under 40x and oil immersion (100x) were observed. For biochemical characterization, urea hydrolysis, sugar fermentation (MOF – Microbial Oxidation Fermentation test), fatty acid hydrolysis, nitrate assimilation, starch like substance production, citric acid production, Diazonium Blue B reaction (DBB) and growth at 37°C were performed (Barnett *et al.*, 2000). Finally, species identification of the isolates was performed by sequencing of ITS region as per Harju *et al.* (2004) with ITS primers (Forward ITS 1: 5' -TCC GTA GGT GAA CCT GCG G- 3' and Reverse ITS 4 - 5' -TCC TCC GCT TAT TGA TAT GC- 3') (White *et al.*, 1990). The amplified fragments of approximately 580 bp containing the ITS 1, 5.8 S and ITS 2 regions were used for the sequence similarity search using NCBI BLAST.

2.3. Effect of physico-chemical parameters for extracellular enzyme production

Different yeast isolates showing highest activity on plates for each of the four enzymes were selected for optimizing growth conditions. PON5-7, CTV3-1, KDI4-17 and KDI5-8 were the strain numbers given for the isolates studied for optimization of growth for the maximum production of protease, amylase, lipase and ligninase, respectively.

Various growth parameters like pH, salinity, substrate concentration and temperature were optimized for the production of enzymes under study (Kutty *et al.*, 2012). Selected yeast strains were inoculated into malt extract broth, grown at $28 \pm 2^\circ \text{C}$ for 48 hours and the optical density of the culture suspension was taken at 540 nm with the help of a UV-VIS spectrophotometer. Later, the OD was adjusted to 1 by dilution with sterile water and 10 μl of this cell suspension was used as inoculum. The experiment was performed in triplicates and incubated at $28 \pm 2^\circ \text{C}$ for 5 days except for temperature optimization. The optical density/absorbance was measured using UV-VIS spectrophotometer at 540 nm and was used for further calculations. The mean absorbance value of the triplicate samples and their standard deviation were calculated.

Malt extract broth supplemented with casein, starch and tributyrin were used for the production of protease, amylase and lipase, respectively. Crawford's broth supplemented with tannic acid was used for testing ligninase production.

pH: Malt extract broth with respective substrates for protease, amylase, lipase and ligninase were prepared at pH 5, 6, 7, 8 and 9 in triplicates, inoculated with selected strains and incubated as mentioned.

Salinity: Malt extract broth with respective substrates for protease, amylase, lipase and ligninase of different salinities 5ppt, 10 ppt, 15 ppt, and 20 ppt at optimized pH were prepared in triplicates, inoculated with selected strain and incubated as mentioned.

Substrate concentration: Malt extract broth with respective substrates for protease, amylase, lipase and ligninase at optimized pH and salinity and varying substrate concentrations viz 0.5%, 1%, 1.5%, 2%, 2.5% for protease, 0.25%, 0.5%, 1%, 1.5%, 2% for amylase and lipase, 0.1%, 0.25%, 0.5%, 0.75%, 1% for ligninase was prepared in triplicates, inoculated with selected strain and incubated as mentioned.

Temperature: Malt extract broth with respective substrates for protease, amylase, lipase and ligninase at optimized pH, salinity and substrate concentrations were prepared in triplicates, inoculated and incubated at temperatures 20° C, 25° C, 30° C, 35° C and 40° C.

3. Results

3.1. Screening for enzyme activity and Identification of potent isolates

A total of 486 yeast isolates from the mangrove sediments were screened for the presence of different extracellular enzymes, out of which 429 isolates showed hydrolytic activities for one or more enzymes under study. Plates with medium containing respective substrates showing hydrolytic activities for the enzymes under study were shown as Figure 1. Clearance zone was formed by precipitation after the addition of 1M HCl for protease while clearance zone was formed after flooding with Gram's iodine for amylase. Lipase and ligninase activity were determined by the formation of clearance and halo/brown zones respectively. The isolates which showed maximum activity at 72 hours of incubation as measured by the increase in zone of clearance every 24 hours were selected and identified. PON5-7, CTV3-1, KDI4-17 and KDI5-8 were the potent isolates selected for protease, amylase, lipase and ligninase activity, respectively. The colony characteristics of the isolates on malt extract agar showed mucoid and glossy appearance with irregular margins. Microscopic examination showed oval shaped, hyphated / pseudohyphated cells which asexually reproduced by budding (Fig. 2). The biochemical characteristics of the 4 strains were studied (Table 1). The amplification and sequencing of the ITS region of the yeast DNA confirmed that all the selected strains belong to *Candida tropicalis* when compared with the NCBI GenBank database, with 100% sequence homology. The GenBank accession numbers obtained were MW 617308, MW 617310, MT 149215 and MW 617305 for isolates PON5-7, CTV3-1, KDI4-17 and KDI5-8, respectively.

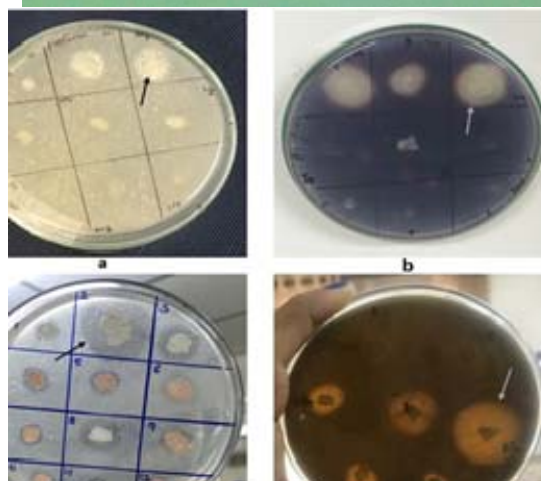
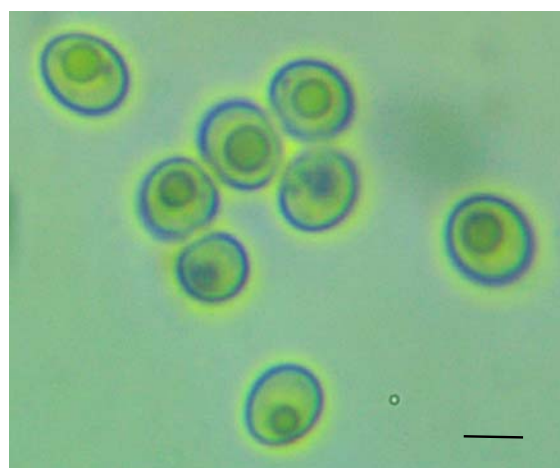


Figure 1: Plates showing hydrolytic activities of enzymes. Arrows indicate the clearance / halo zones formed due to the hydrolysis of substrates. **a)** Protease – clearance zone formed by precipitation after the addition of 1M HCl. **b)** Amylase – clearance zone after Gram's iodine treatment **c)** Lipase – clearance/ halo zone. **d)** Ligninase – formation of halo zone

Figure 2: Microscopic appearance of methylene blue stained *C. tropicalis* under 100x (oil immersion) magnification.

Table 1: Biochemical characterization of different *C. tropicalis* isolates in the present study

Sl. No.	Tests	Results			
		PON5-7	CTV3-1	KDI4-17	KDI5-8
	Urea hydrolysis	-	-	-	-
	Glucose fermentation (MOF test)	+	+	+	+
	Fatty acid hydrolysis	+	+	+	+
	Nitrate assimilation	-	-	-	-
	Starch like substance production	-	+	-	+
	Citric acid production	-	-	-	+
	Diazonium Blue B reaction (DBB)	-	-	-	-
	Growth at 37° C	+	+	+	+

3.2. Study of growth parameters for extracellular enzyme production

Study of various parameters for efficient growth and maximum biomass yield which result in maximum extracellular enzyme production was determined for the enzymes protease, amylase, lipase and ligninase. The growth/biomass in the culture media was measured on the basis of turbidity obtained by measuring the absorbance at 540nm wavelength. Growth parameters of isolates PON5-7, CTV3-1, KDI4-17 and KDI5-8 (all identified as *C. tropicalis*) were studied for the maximal production of its protease, amylase, lipase and ligninase enzymes, respectively.

3.2.1. Effect of pH: The effect of the pH on the growth of yeast strains under study is graphically summarized as Fig. 3.

Protease: Maximum growth / absorbance at 540 nm was observed at pH 8, when the pH of the media was pre-adjusted from 5-9. At acidic pH, the growth was very low but increased as the media became basic. The optimum pH 8 was maintained for the culture media for further procedures.

Amylase: Maximum growth / absorbance at 540 nm was observed at acidic media of pH 5 and the growth decreased as the media became basic. The optimum pH 5 was maintained for the culture media for further procedures.

Lipase: The isolate showed increased growth / maximum absorbance at 540 nm as the pH of the media became basic and maximum growth was observed in media with pH 9. The optimum pH 9 was maintained for the culture media for further procedures.

Ligninase: Maximum growth/ absorbance at 540 nm was observed in basic media with pH 9 and no much significant growth was seen in acidic media. The optimum pH 9 was maintained for the culture media for further procedures.

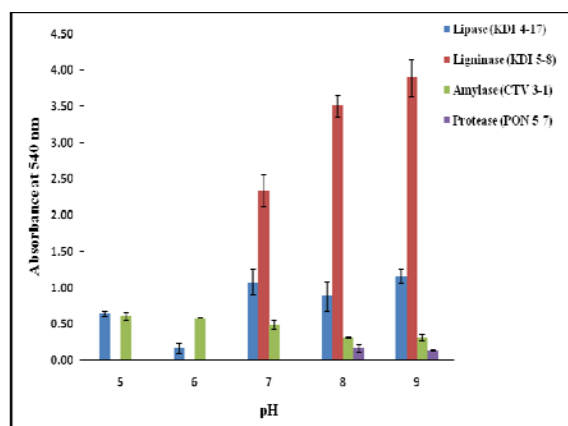


Figure 3: Effect of different pH in media on the growth and enzyme production potential of selected strains of *C. tropicalis* in the present study

3.2.2. Effect of salinity: The effect of the salinity of media on the growth of yeast strains under study is graphically summarized as Figure 4.

Protease: Maximum growth / absorbance at 540 nm was observed when the salinity of the media was adjusted

to 5 ppt and decreased as the salinity increased. The optimum salinity of 5 ppt was maintained in the culture for further procedures.

Amylase: The culture showed maximum growth/ absorbance at 540 nm in media with salinity of 5 ppt and gradually decreased as the salinity increased. The optimum salinity of 5 ppt was maintained in the culture for further procedures.

Lipase: Maximum growth/ absorbance at 540 nm was observed in media with salinity of 10 ppt and reduced at other concentrations. The optimum salinity of 10 ppt was maintained in the culture for further procedures.

Ligninase: The media with salinity of 5 ppt showed maximum growth/ absorbance at 540 nm and it decreased in higher salinities. The optimum salinity of 5 ppt was maintained in the culture for further procedures.

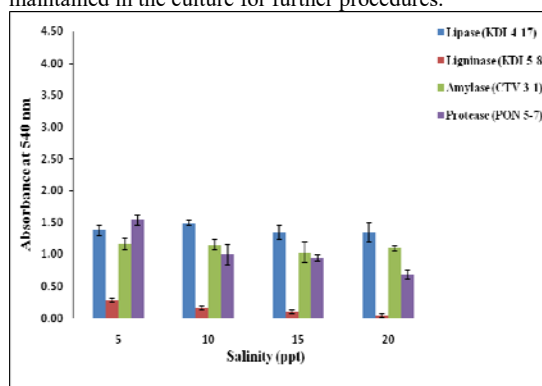


Figure 4: Effect of different salt concentrations in media on the growth and enzyme production potential of selected strains of *C. tropicalis* in the present study

3.2.3. Effect of substrate concentration: The effect of the salinity of media on the growth of yeast strains under study is graphically summarized as Figure 5.

Protease: The media with substrate concentration of 2% casein showed maximum growth/ absorbance at 540 nm while it decreased in lower and higher substrate concentrations. The optimum substrate concentration of 2% casein was maintained in the culture for further procedures.

Amylase: Maximum growth / absorbance at 540 nm was observed in media with substrate concentration 1% starch and the growth decreased at lower and higher concentrations. The optimum substrate concentration of 1% starch was maintained in the culture for further procedures.

Lipase: The media with substrate concentration of 1% tributyrin showed maximum growth/ absorbance at 540 nm while it decreased in lower and higher substrate concentrations. The optimum substrate concentration of 1% tributyrin was maintained in the culture for further procedures.

Ligninase: Maximum growth/ absorbance at 540 nm was observed in media with substrate concentration 0.5% tannic acid and the growth decreased at lower and higher concentrations. The optimum substrate concentration of 0.5% tannic acid was maintained in the culture for further procedures.

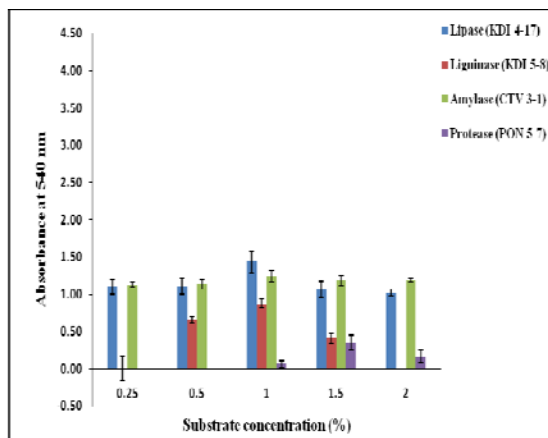


Figure 5. Effect of various substrate concentrations in media on the growth and enzyme production potential of selected strains of *C. tropicalis* in the present study

3.2.4. Effect of temperature: The effect of various incubation temperatures on the growth of yeast isolates cultured under optimized media conditions under study is graphically summarized as Figure 6.

Protease: Maximum growth / absorbance at 540 nm was obtained when the culture was incubated at 40°C and below that temperature there was reduction in growth of the culture

Amylase: Maximum growth / absorbance at 540 nm was obtained when the culture was incubated at 35°C but above and below that temperature the growth showed a decreasing pattern.

Lipase: Maximum growth / absorbance at 540 nm was obtained when the culture was incubated at 35°C but above and below that temperature the growth showed a decreasing pattern.

Ligninase: Maximum growth / absorbance at 540 nm was obtained when the culture was incubated at 40°C and below that temperature there was reduction in growth of the culture.

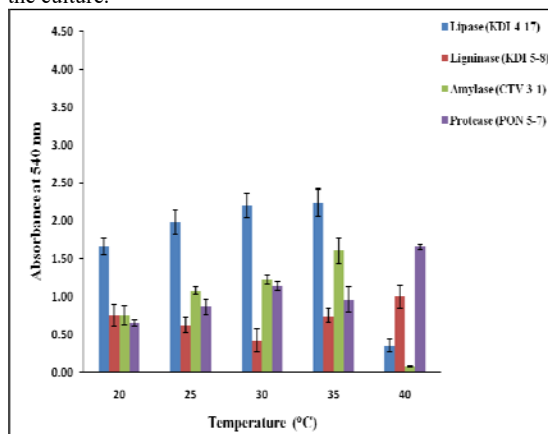


Figure 6. Effect of various incubation temperatures on the growth and enzyme production potential of selected strains of *C. tropicalis* in the present study

4. Discussion

In the present study, the effects of various growth parameters including pH and salinity of the media, substrate concentration and incubation temperature were

determined to obtain maximum growth and enzyme production from selected yeast strains. Though many of the yeast isolates showed significant extra cellular enzyme activities, those potent strains which showed maximum activity for particular enzymes as determined by the measurement of clearance zones on enzyme plates with respective substrates were screened and studied. All the four isolates selected for the study of enzymes protease, amylase, lipase and ligninase were identified as *C. tropicalis*. *C. tropicalis* is considered as a biological and biotechnological important yeast strain due to its applications in agricultural, fermentation and chemical industries (Kuiran *et al.*, 2010). Still, there are less studies conducted on the hydrolytic enzyme potential of *Candida* species, especially *C. tropicalis* isolated from marine and mangrove samples.

The phenotypic characteristics expressed by microorganisms are greatly influenced by the environment they exist in, and it acts as their adaptation strategy. Yeasts, like *C. tropicalis* that can produce extracellular enzymes, have specific genes to express particular enzymes (Yan *et al.*, 2005). The ability of these genes to express enzymes in turn are impacted by their environment as well as the nutrients present there (Amadi *et al.*, 2020). Hence, understanding and proper optimization of the factors affecting the growth of yeast to achieve maximum biomass and enzyme production in culture is necessary.

C. tropicalis has a wide distribution and has been isolated from different marine habitats including mangrove ecosystem (Kuiran *et al.*, 2010). A study conducted in marine oil degrading yeast strain *C. tropicalis* SD 302 shows maximum growth at pH 7, 15 ppt salinity and 30°C temperature (Kutty *et al.*, 2012). The optimum culture conditions for maximum biomass yield and increased production of protease from *C. tropicalis* in our study was found to be pH 8, 5 ppt salinity, 2% casein as substrate concentration at 40°C temperature. This reveals the potency of the isolated strain in present study compared to the marine counterpart, due to its maximum production at high pH, high temperature and medium salinity. Studies on genus other than *Candida* have also shown that the optimum culture conditions for the high productivity of yeast protease obtained *Metschnikovia pulcherrima* and *Wickerhamomyces anomalus* was at basic pH at temperature ranging from 40-45° C, with salinity between 5-10ppt (Schlander *et al.*, 2017). Research on yeast amylases showed that higher enzyme production was seen normally at acidic pH ranging from 5-6 at 1% substrate concentration with 5-10 ppt salt concentrations at temperature ranging from 30-35° C (Nahas and Waldemarin, 2002; Souza and Magalhaes, 2010). In our study, the optimum culture conditions for large scale production of yeast amylase from *C. tropicalis* were found to be at an acidic pH of 5, with 5% salt concentration and 1% starch as substrate at incubation temperature of 35° C. Lipases hydrolyze acylglycerides and are highly valuable enzymes in detergent industry and also in biodegradation of oil residues (Hasan *et al.*, 2006). Recently yeast lipases have been widely used in developing novel techniques like biosensing, organic synthesis of drugs and synthesis of optically active compounds in pesticide industries (Vakhlu and Kour, 2006). Previous studies on yeast lipases mainly, those from *C. tropicalis*, showed that the optimal pH, temperature and salinity for their production were between

6.0-8.5, 35-40° C, 5-10 ppt, respectively at 1% substrate concentration (Abu *et al.*, 2017; Alamia *et al.*, 2017). The culture conditions for the production of lipases from *C. tropicalis* in our study were optimized as pH 9, 10 ppt salinity, 1% tributyrin as substrate at an incubation temperature of 35°C. Though yeast ligninase have not been studied much, interest has been recently increased due to its applications in wood, paper and cosmetic industries (Malgas *et al.*, 2017). Optimization of the culture conditions required for the high yield and enzyme production of ligninase producing yeasts would be of great help in the development of its fermentation process. In our study, the optimum culture conditions for the large scale production of ligninase from *C. tropicalis* was found to be at pH 9, 5 ppt salinity, with 2% tannic acid as substrate at an incubation temperature of 40°C.

During the large-scale fermentation of enzymes, especially in detergent and chemical industries, the alkalinity and temperature of the culture media tend to increase as the procedure progresses. So, it is advisable to use strains which can survive, grow and produce enzymes at higher temperatures, increased pH and saline conditions (Gurung *et al.*, 2013; Arnau *et al.*, 2019). Since mangrove sediments experience extreme environmental alterations, the microbes including yeasts isolated from it will be adapted to such variations and they use this property to survive in different cultural conditions. Also, the biomolecules like extracellular enzymes produced by them would be able to withstand such extreme parameters (Thatoi *et al.*, 2013; Capdeville *et al.*, 2019). This helps in performing hassle free scaling up process for the mass production of these biomolecules from yeasts. The optimum culture conditions needed by yeast *C. tropicalis* for the maximum biomass and enzyme production in the present study were in accordance with the requirements for the large scale production of enzymes. Hence, *C. tropicalis* can be exploited as a suitable candidate for the industrial and biotechnological production of hydrolytic enzymes.

5. Conclusion

The quest for novel and improved microbial strains that can produce industrially important enzymes is a continuous process. Since, yeasts are one of the most active extracellular enzyme producers and can be fermented using cheap substrates; they have gained massive attention during recent years. We have studied the effect of various culture parameters including pH, substrate concentration, salinity and incubation temperature on the growth of selected strains of *C. tropicalis* for the production of hydrolytic enzymes protease, amylase, lipase and ligninase. The results showed that the optimum growth conditions required for this strain would be favorable in the large- scale fermentation process for producing extracellular enzymes. Hence, the present study suggests that the yeast *C. tropicalis* isolated from mangrove sediments effectively produce extracellular hydrolytic enzymes and can be utilized for various biotechnological and industrial applications.

Acknowledgements

Financial support from Back to Lab Projects, Women Scientist Division (BLP-WSD), Kerala State Council for

Science, Technology and Environment (KSCSTE) is gratefully acknowledged. The authors thank Central Sophisticated Instrumentation Facility (CSIF), University of Calicut for the technical support.

References

- Abu ML, Nooh HM, Oslan SN and Salleh AB. 2017. Optimization of physical conditions for the production of thermostable T1 lipase in *Pichia guilliermondii* strain SO using response surface methodology. *BMC Biotechnol*, **17**: 78 – 83.
- Alamia NH, Nasihah L, Umar RLA, Kuswytasari N, Zulaika E and Shovitri, M. 2017. Lipase production in lipolytic yeast from Wonorejo mangrove area. Proceeding of International Biology Conference. AIP Conference Proceedings, 1854.
- Amadi OC, Egong EJ, Nwagu TN, Okpala G, Onwosi CO, Chukwu GC, Okolo BN, Agu RC and Moneke AN. 2020. Process optimization for simultaneous production of cellulase, xylanase and ligninase by *Saccharomyces cerevisiae* SCPW 17 under solid state fermentation using Box-Behnken experimental design. *Heliyon*, **7**: 1-12.
- Arnau J, Yaver Dand Hjort CJ. 2019. Strategies and challenges for the development of industrial enzymes using fungal cell factories. *Grand Chall Fungal Biotechnol*, **1**: 179–210
- Barnett JA, Payne RW and Yarrow D. 1990. Yeasts: characteristics and identification, second ed. Cambridge University Press, Cambridge.
- Bessadok B, Masri M, Breuck T and Sadok S. 2015. Isolation and screening for protease activity by marine micro-organisms. *Bull Inst Nat Sci Tech*, **42**: 21- 24.
- Bonugli-Santos RC, Durrant LR and Sette LD. 2012. The production of lignolytic enzymes by marine-derived basidiomycetes and their biotechnological potential in the biodegradation of recalcitrant pollutants and the treatment of textile effluents. *Water Air Soil Pollut*, **223**: 2333–2345.
- Capdeville C, Pommier T, Gervais J, Fromard F, Rols J and Leflaive J. 2019. Mangrove facies drives resistance and resilience of sediment microbes exposed to anthropogenic disturbance. *Front Microbiol*. **9**: 1-17.
- Cheng YT and Yang CF. 2016. Using strain *Rhodotorulamucilaginosa* to produce carotenoids using food wastes. *J Taiwan Inst ChemEng*, **61**: 270–275.
- Choudhury P and Bhunia B. 2015. Industrial application of lipase: a review. *Biopharm J*, **11**: 2454-1397.
- Elsanhoty RM, Al-Turki AI and El-Razik MMA. 2017. Production of carotenoids from *Rhodotorula mucilaginosa* and their applications as colorant agent in sweet candy. *J Food Agri Env*, **15**: 21-26.
- Gurung N, Ray S, Bose S and Rai V. 2013. A broader view: microbial enzymes and their relevance in industries, medicine, and beyond. *Bio Med Res Int*, **5**: 1-18.
- Harju S, Fedosyuk H and Peterson KR. 2004. Rapid isolation of yeast genomic DNA. Bust n'Grab. *BMC Biotech*, **4**: 8 – 12.
- Kachiprath B, Solomon S, Jayanath G and Philip R. 2018. Mangrove microflora as potential source of hydrolytic enzymes for commercial applications. *Indian J Geo Mar Sci*, **48**: 678-684.
- Kuiran Y, Ying Z and Zhenming C. 2010. Distribution and diversity of *C. tropicalis* strains in different marine environments. *J Ocean Univ China*, **9**: 139-144.
- Kutty SN, Damodaran R and Philip R. 2012. Degradation of petroleum hydrocarbons by marine yeasts *C. tropicalis* SD 302 and *Pichia guilliermondii* SD 337. *Blue Biotech*, **1**: 423- 431.

- Kutty SN, Damodaran R and Philip R. 2014. Yeast isolates from the slope sediments of Arabian Sea and Bay of Bengal: Physiological characterization. *Adv Appl Sci Res*, **5**: 177–87.
- Malgas S, Thoresen M, van Dyk JS and Pletschke BI. 2017. Time dependence of enzyme synergism during the degradation of model and natural lignocellulosic substrates. *Enzyme Microb Technol*, **103**:1-11.
- Nahas E and Waldemarin HM. 2002. Control of amylase production and growth characteristics of *Aspergillus ochraceus*. *Rev Latin Microbiol*, **44**: 5-10.
- Paskevicius A. 2001. Lipase activity of yeasts and yeast like fungi functioning under natural conditions. *Biologija*, **4**: 16- 18.
- Pothayi V and Devasia SC. 2020. A study on the distribution and hydrolytic enzyme potential of yeasts in the mangrove sediments of Northern Kerala. *Indian J Microbiol Res*, **7**: 161–167.
- Rahman SS, Hossain MM and Choudhury N. 2013. Effect of various parameters on the growth and ethanol production by yeasts isolated from natural sources. *Bangladesh J Microbiol*, **30**: 49-54.
- Schlender M, Distler U, Tenzer S, Thines E and Claus H. 2017. Purification and properties of yeast proteases secreted by *Wickerhamomyces anomalus* 227 and *Metschnikovia pulcherrima* 446 during growth in a white grape Juice. *Fermentation*, **3**: 1-12.
- Sengupta S, Pramanik A, Ghosh A and Bhattacharyya M. 2015. Antimicrobial activities of actinomycetes isolated from unexplored regions of Sundarbans mangrove ecosystem. *BMC Microbiol*, **15**: 1-16.
- Shahat AS. 2017. Production of extracellular hydrolytic enzymes by yeast extracts on some commercial media. *Ann Biol Res*, **8**: 6-11.
- Solntsev KM, Schram S, Kremb S, Gunsalus KC and Amin SA. 2019. Isolation of biologically active compounds from mangrove sediments. *Anal Bioanal Chem*, **411**: 6521-6529.
- Souza PM and Magalhaes PO. 2010. Application of microbial amylase in industry. *Brazilian J Microbiol*, **41**: 850-861.
- Thatoi H, Behera BC, Mishra RR and Dutta SK. 2013. Biodiversity and biotechnological potential of microorganisms from mangrove ecosystems: A review. *Ann Microbiol*, **63**: 1-19.
- Vakhlu J and Kour A. 2006. Yeast lipases: Enzyme purification, biochemical properties and gene cloning. *Electron. J. Biotechnol*, **9**: 69- 85.
- White TJ, Bruns T, Lee S and Taylor J. 1990. Amplification and direct sequencing of fungal ribosomal RNA genes for phylogenetics. In Innis MA, Gelfand DH, Sninsky JJ, White TJ (eds), PCR Protocols, A guide to methods and applications, Academic Press: San Diego, CA, pp 315–324.
- Wickerham LJ. 1951. Taxonomy of yeasts. *U.S. Dept Agric Tech Bull*, **1029**: 1-19.
- Yalsein HT and Çorbac C. 2013. Isolation and characterization of amylase producing yeasts and improvement of amylase production. *Turk J Biochem*, **38**: 101–108.
- Yan J, Jianping W, Hongmei L, Suliang Y and Zongding H. 2005. The Biodegradation of Phenol at High Initial Concentration by the Yeast *Candida tropicalis*. *Biochem Eng J*, **24**: 243-247.

The Effect of the Biologically Complex of a Medical Leech Active Substances on the Immunosuppressive State of Rats

Aminov Ruslan*, Frolov Alexander, Aminova Alina

Zaporizhzhya National University, Ukraine 69600, Zaporozhye, 66 Zhukovskogo str.

Received: March 3, 2021; Revised: June 15, 2021; Accepted: August 5, 2021

Abstract

The course of all infectious diseases largely depends on immunity. An organism with a weak immune system gives up faster before diseases. Also, the number of immunodeficiencies with various etiologies has increased. Therefore, scientists are looking for various methods of dealing with these diseases. One such method is hirudotherapy using medicinal leeches, which has many therapeutic effects. As a result, the study of animals with a chemically immunosuppressive state has become relevant. The experiment was carried out on 45 mature male nonlinear rats with a body weight of 360-370 g. To simulate immunosuppression in experimental groups of animals, we used "Endoxan". It was administered intraperitoneally to mature rats after the formation of 3 study groups: 1) control - without intervention; 2) "Endoxan" at a dose of 100 mg / kg; 3) "Endoxan" at a dose of 100 mg / kg + water-salt extract of *Hirudo verbana*. After 3 weeks, the animals were measured for weight and body length, and were decapitated. Blood was taken with the addition of an anticoagulant. Then the total number of erythrocytes and leukocytes, the relative blood leukocyte formula, the mass and morphology of the thymus, the weight of the spleen and liver were examined. As a result, in the second and third groups, all indicators decreased, which indicates the immunosuppressive effect of the drug. After the introduction of the water-salt extract in the third group, the indicators increased (in some respects, even more) in comparison with the control group.

Keywords: medical leeches, infectious diseases, immunosuppressive, hirudotherapy

1. Introduction

A significant number of infectious and non-infectious diseases has grown in the world. The most common infectious diseases include: influenza, tonsillitis, pneumonia, tuberculosis, rabies, herpes, hepatitis, salmonellosis, dysentery, acquired immunodeficiency syndrome, as well as the number of coronavirus infections has increased significantly. All these diseases can occur at different times of the year, especially during the cold season. The most common non-communicable diseases include hypertension, coronary heart disease, heart attack, stroke, malignant neoplasms, diabetes, chronic obstructive pulmonary disease, and bronchial asthma. The course of all these infectious and non-infectious diseases is largely dependent on the immune system. Diseases of various etiologies often develop with weak immunity. Therefore, scientists are looking for various methods of dealing with these diseases with natural and synthetic methods (Pejin *et al.*, 2014; Tešanović *et al.*, 2017; Pejin *et al.*, 2019; Zouaghi *et al.*, 2021; Girgis *et al.*, 2021; Rawung *et al.*, 2021). And they are also looking for different ways to stimulate the immune system, because it is known, as we described earlier in our work, that the balanced immune system is already a great chance for recovery.

One of these methods is naturo-therapeutic - the use of medicinal leeches. Many scientists have already proven that their biologically active substances have a positive

effect on the links of immunity: they normalize the cytokine profile, increase local and systemic immunity, reduce cytolysis and the absolute number of neutrophils, increase the content of lysosomal cationic proteins in neutrophils, and stimulate lymphopoiesis (Deniskina, 2003; Spitsina, 2005; Borovaya, 2008; Zolonyi *et al.*, 2010) and negatively affect various infections caused by different pathogens: *Escherichia coli* MG1655, *Botrytis cinerea*, *Verticillium Lateriticum*, *Candida guillermoudii*, *Shizosaccharomyces pombe*, *Pseudomonas fluorescens*, *Pseudomonas aeruginosa* (Yudina *et al.*, 2012; Pavlova *et al.*, 2015) and others. This mainly depends on the ingestion of a medicinal leech substance - destabilase. Among the world's major diseases, their positive effect on cancer cells and cancer therapy has been proven now, which may be due to the effect on them of biologically active substances of eglin, which prevent division and destroy cancer pain and cancer cells (Kalender *et al.*, 2010; Shakouri *et al.*, 2018), *Mycobacterium tuberculosis* (Ojo *et al.*, 2018). Their action has also been proven in various diseases of a non-infectious nature. Among them: treatment of chronic dermatoses (Karadag *et al.*, 2011; Zhulebina, 2017); psoriasis, in which the antielastase substance plays an important role (Kumar, 2012; Senchukova, 2012); in the treatment of heart failure (Kuznetsova, 2008), radiculopathy (Belyakov, 2008), arthritis (Mikhalsen, 2003; Abduvaliev, 2017). Factor Xa inhibitors are anticoagulants, which include antistasin and gilant, which have the same effects. Also, a trypsin inhibitor is involved

* Corresponding author: e-mail: 91_amin_91@ukr.net, aminovruslan947@gmail.com, alina.evlach@gmail.com.

in the treatment of these diseases. In case of endometriosis, uterine myoma, chronic inflammation of the appendages, the main active ingredient is bdelins that relieve inflammation (Dobrynina *et al.*, 2005, Sorokina, 2008). In the treatment of thrombophlebitis (Tashiro *et al.*, 2016), varicose veins and other vascular diseases (Porshinsky *et al.*, 2011; Nikar and Alam, 2011; Prakash *et al.*, 2013; Makhova, 2015), plastic and reconstructive surgery (Hackenberger and Janis, 2019) hirudin and kalin play an important role. Male and female infertility (Lyalina, 2016; Stokoz and Bystritskaya, 2016) and male priapism (Sayed, 2017) are treated with destabilase. In experiments on rats: an increase in body mass and organs, hemoglobin (Babai *et al.*, 2018), improved liver performance (Praise *et al.*, 2019), improves wound healing (Kaveh *et al.*, 2014). Hirudological influence in veterinary medicine is used in various diseases of cats, dogs, horses (Popov *et al.*, 2008; Canpolat and Sağlam, 2004; Sobczak and Kantyka, 2014; Rychapova, 2017), for example, for the treatment of mastitis and increase reproductive capacity in cows (Kondratieva *et al.*, 2015; Glazunova and Anodina, 2013). And this is only a large part of the complex therapeutic effects of a medical leech *Hirudo verbana*. As a result of its enormous positive effect in many pathological conditions, which mainly arise due to a violation of the immune system, it has become urgent to analyze animals with an artificial immunosuppressive state under the influence of a complex of biologically active substances obtained from a medicinal leech.

2. Material and methods

The research was performed in the laboratory of cell and organism biotechnology of Zaporizhzhya National University. All experimental research with animals was carried out in compliance with the Law of Ukraine - On the Protection of Animals from Abuse, the European Convention for the Protection of Vertebrate Animals used for experimental and other scientific purposes. National Health and Medical Research Council of Australia, 'Australian Code for the Care and Use of Animals for Scientific Purposes, 8th Edition' (National Health and Medical Research Council; Canberra, 2013). The experiment was conducted on 45 male non-linear adult rats weighing 360-370 g. "Endoxan" was used to simulate immunosuppression in experimental groups of animals, in the form of a powder for injection of 200 mg/kg, manufactured by Baxter Oncology GmbH (Germany), which was prepared in saline. This drug was used because a conventional chemical model can cause prolonged immunodeficiency in animals without significant destructive effects on cells and tissues. Saline was made from NaCl powder with a final concentration of 0.9%.

It was administered intraperitoneally to sexually mature male rats after the formation of 3 research groups of 15 animals each: 1) control-without intervention; 2) "Endoxan" in a dose of 100 mg / kg; 3) "Endoxan" at a dose of 100 mg / kg + water-salt extract of medicinal leech *Hirudo verbana*. The extract was administered on the third day with a final concentration of water-salt extract of 5 µg / g in animals (1 time in 3 days). The total amount of injection of the extract 5 times. After 3 weeks, the animals, after measuring body weight and length, were decapitated using the method of dislocation of the cervical vertebrae.

Blood was taken with the addition of the anticoagulant - 2% heparin (9/1). The total number of erythrocytes and white blood cells, the relative amount of blood leukocytes, the weight and morphology of the thymus, and the weight of the spleen and liver were then examined.

Determination of hematological and immunological parameters was performed by standard methods (Higgins, 2017). Organ weights were measured on analytical scales. Removed lymphoid organs after weighing were fixed in 10% formalin solution in a glass-darkened glassware, stored at room temperature for 3 days before histological examination. Next, the thymus was poured into paraffin blocks using standard histological techniques, from which 6 micron thick sections were made. Serial sections were made using a Thermo Scientific HM 325 microtome and stained with hematoxylin-eosin according to the standard procedure (Zolotarev *et al.*, 2013). Morphometric and cytological studies were performed directly on histological specimens using a Carl Zeiss Primo Star microscope. The micrographs were prepared using a PrimoStar iLED microscope and Axio CamERc5s (ZEISS, Germany), which were analyzed using the ZEISS ZEN 2011 microscopy program.

Statistical data processing was performed using the computer program SPSS v.21.0. (IBM SPSS Statistics., USA). The selected parameters indicated in the table below have the following notation: X - sample mean, SE - standard error of the mean. The significance of differences between the mean values was evaluated by the Student criterion after checking the normal distribution. Differences were considered significant at $p < 0.05$.

3. Results and discussion

In the second group of animals, which were injected only with the cytotoxic drug "Endoxan", a significant decrease in the total number of leukocytes was observed as compared to the control group of animals (Table 1). In the analysis of the third group, which was administered five times more water-salt extract, there was a significant increase in the total number of leukocytes in comparison with the control group table 1.

Table 1. The state of the indicators of blood, body mass and organs

Indicators	Group of animals		
	I Control	II Endoxan in the dose 100 mg / kg	III Endoxan at a dose of 100 mg / kg + water-salt extract of 5 µg / g <i>Hirudo verbana</i>
The total number of leukocytes ($\times 10^9$)	11,9±0,49	9,5±0,37*	16,6±0,66*
The total number of erythrocytes ($\times 10^{12}$)	7,7±0,36	3,4±0,19*	9,5±0,45*
Body weight (g)	373,5±15,4	342±13,2*	366±14,2
Body length (cm)	22±0,9	21,5±0,7	23,3±0,8
Thymus weight (mg)	119±4,2	89±3,5*	211±5,1*
Spleen weight (mg)	1213±50,1	1103±44,3*	1227±48,6
Liver weight (g)	17,8±0,73	13±0,56*	17,3±0,68

Note: * - $p < 0,05$ in comparison with the control group

The decrease in the number of leukocytes in the second group may be associated with a decrease in the total number of lymphocytes. We see this by analyzing the leukocyte blood count. An increase in neutrophils occurs due to a decrease in lymphocytes. It is also known fact that "Endoxan" inhibits the lymphoid row of cells to a greater extent. In the third group, all types of leukocytes were equated to the control group with a slight increase in lymphocytes due to a decrease in neutrophils. This dynamic indicates the stimulation of cell proliferation from the complex influence of biologically active substances of the water-salt extract. Analysis of the total number of erythrocytes showed their significant decrease in the second group and their significant increase in the third group as compared to the control group accelerated cell proliferation. When analyzing body weight, there was a significant decrease in the second group compared to the control of table 1. When analyzing the thymus weight,

growth in the third group and a decrease in the second compared with the control group of animals, table 1. A decrease in weight in the second group can indirectly confirm the suppression of lymphoid cells, and in the third, on the contrary, increased proliferation. The study of the weight of the liver and spleen showed a significant decrease in the second group compared with the control. The weight of the spleen and liver of the third group within the control group table 1. An increase in blood counts, body weight and the studied organs in the third group compared with the control indicates a compensating and then immune-stimulating effect of the water-salt extract of the medicinal leech. The complex of biologically active substances corrected the lymphotoxic effect of endoxan. This is evidenced by a slight increase in lymphocytes in the leukocyte blood count, even in comparison with the control table 2.

Table 2. White blood cell condition

Group of animals	Leukocyte blood formula, %				
	Neutrophils		Lymphocytes	Monocytes	Eosinophils
	Segmentonuclear	Palichkonuclear			
I Control	8,11±0,25	3,75±0,12	87,14±1,2	0,75±0,12	0,25±0,02
II Endoxanin the dose 100 mg / kg	16,51±0,11*	15,16±0,10*	67,23±2,9*	0,81±0,06	0,29±0,03
Experiment III Endoxan at a dose of 100 mg / kg + water-salt extract of 5 µg / g <i>Hirudo verbana</i>	7,50±0,27*	2,86±0,11*	89,56±1,1*	0,80±0,23	0,28±0,05

Note: * - $p < 0,05$ in comparison with the control group

The complex of biologically active substances corrected the lymphotoxic effect of "Endoxan". This is evidenced by an insignificant increase in lymphocytes in the leukocyte blood count even in comparison with the control group table 2. Our theory stated above is confirmed by the results of a histological study of the cytological composition of the thymus gland, which were analyzed in all groups of animals 3 weeks after the start of the experiment Fig. 1.

We visually observed in the third group that the number of cells is close to the control group. This is not the case for the second group, where normal cells are replaced by adipose and connective tissue.

The devastation of cells in the thymus in the second group is associated with the action of cytostatic, as described previously. "Endoxan" primarily affects cytotoxicity on lymphocytes. Visually, the third group is no different from the control. Firstly, this may be due to

the compensatory effect of the second immune-modulating properties of leeches. In our previous experiments, we showed an immune-stimulating effect on the immune system of females and their offspring (Aminov and Frolov, 2017, 2018, 2020). But immune-deficient animals under hirudological influence were studied for the first time. Other scientists have shown that the body recovers after cytostatics when its dose is not toxic. Therefore, it can be used as a drug that can cause a measurable immune-deficiency state (Akhter *et al.*, 2008; Ukpo, 2013; Mohamed, 2014; Lee *et al.*, 2019). Therefore, we chose it to obtain an immunodeficiency model that is being corrected. The results we obtained can be useful for worldwide viewing and in future applications for increasing and modulating immunity in various diseases of an infectious and non-infectious nature. As we said above, all diseases mainly arise due to weak immunity, which is not able to cope with the disease.

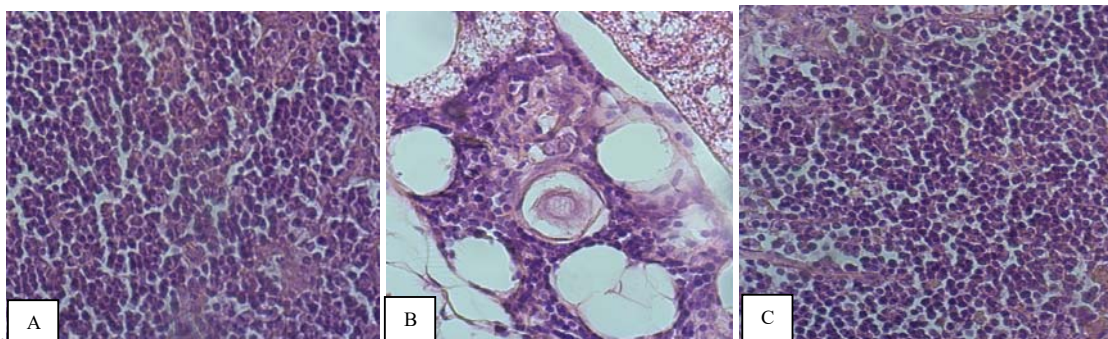


Figure 1. Morphology of animal thymus: A) control; B) endoxan in a dose of 100 mg / kg; C) endoxan at a dose of 100 mg / kg + water-salt extract of 5 µg / g *Hirudo verbana*

4. Conclusions

As a result of our research, the biologically active substances of a medicinal leech *Hirudo verbana* can modulate the immune system, which has failed, to a normal physiological state, and even more. This was manifested by an increase in hematological and immunological parameters, as well as an increase in body weight and major organs: spleen, thymus and liver, positive changes in the morphological structure of the central lymphoid organ. In the future, our research is aimed at a deeper study of this effect on immunity. So, the obtained results show the immune-modulating effect from the introduction of the extract.

References

- Abduvaliev AA and Daurekhanov AM. 2017. Hirudotherapy in the complex treatment of patients with reactive arthritis. *Bulletin of KazNMU.*, **1**: 250-252.
- Akhter J, Yao P, Johnson LA, Riordan SM and Morris DL. 2008. A New Peritoneal Carcinomatosis Model in Cyclosporine Immunosuppressed Rats. *Anticancer Res.*, **28(1A)**: 105-109.
- Aminov RF and Frolov AK. 2017. Influence of ectoparasite - *Hirudo verbana* on morphogenetic reactions of the host organism - *rattus*. *Current trends in immunology*, **18**: 107-117.
- Aminov RF and Frolov AK. 2018. The impact of fetal load of *Hirudo verbana* saline extract antigens morphometrical, hematological and immunological parameters of rats in the early stages of post-embryonic development. *Annals of parasitology*, **64(1)**: 13-20.
- Aminov RF, Frolov AK and Fedotov YeR. 2020. Rat peripheral blood leukocyte subset composition, hemogram, lymphoid organ and body morphometry after exposure to biologically active substances derived from *Hirudo verbana* saliva. *Russian Journal of Infection and Immunity*, **10(1)**: 167-174.
- Babayi H et al. 2018. Evaluation of the effects of Leech Salivary Extract (LSE) on Haematological parameters in Rats. *J Hematol Clin Res.*, **2**: 006-014.
- Belyakov KM, Veliichko LA, Profyev AL and Smirnov AA. 2008. Experience with the combined use of manual and hirudotherapy for discogenic lumbosacral radiculopathies. *Manual therapy*, **4**: 47-50.
- Borovaya EP. 2008. Hirudotherapy and endoecological rehabilitation in the complex spa treatment of patients with coronary heart disease of middle and old age. MSc dissertation, Roszdrav, Moscow.
- Canpolat İ and Sağlam N. 2004. Treatment of aural hematomas in dog with the medicinal leech, *Hirudo medicinalis*. *Doğu Anadolu Bölgesi Araştırmaları*, **2 (2)**: 67-69.
- Deniskina EV. 2003. Clinical and laboratory substantiation of hirudotherapy in the complex treatment of chronic apical periodontitis. MSc dissertation, Moscow State Medical and Dental University, Moscow.
- Dobrynya UJ, Zhivoglyad RN, Khadartseva KA and Shipilova TN. 2005. Hirudotherapeutic management of human homeostasis in gynecological pathologies in the North. *Bulletin of new medical technologies*, **12(2)**: 25-27.
- Hackenberger P and Janis JE. 2019. A Comprehensive Review of Medicinal Leeches in Plastic and Reconstructive Surgery. *Plast Reconstr Surg - Global Open*, **7(12)**: e2555.
- Higgins K. 2017. Deciphering clinical laboratory tests. Binom. Knowledge Laboratory M. Karadag AS, Calka O and Akdeniz NA. 2011. Case of irritant contact dermatitis with leech. *Cecen I Cutan Ocul Toxicol.*, **30**: 234-235.
- Kumar SA. 2012. Anti inflammatory effect of leech therapy in the patients of psoriasis (ek kustha). *J. Pharmaceut and Sci. Innovat.*, **1(1)**: 71-74
- Kuznetsova LP, Lyusov VA, Volov NA, Smirnova NA and Bogdanova LS. 2008. The place of hirudotherapy in the complex treatment of chronic heart failure. *Russian Journal of Cardiology*, **2**: 28-30.
- Kalender ME et al. 2010. Leech therapy for symptomatic relief of cancer pain. *Pain Med.*, **11**: 443-445.
- Kaveh DD et al. 2014. Leech therapy for linear incisional skin-wound healing in rats. *Journal of Acupuncture and Meridian Studies*, **7(4)**:194e201
- Kondratieva MM, Sidorova KA and Glazunova LA. 2015. Influence of hirudin on hematological parameters in cows with subclinical mastitis. *Agricultural sciences*, **3(30)**: 58-63.
- Lyalina EG. 2016. The combined use of hirudotherapy, reflexology and homeopathy in the treatment of female infertility. *Psychosomatic and integrative research*, **2**: 0207.
- Lee HY et al. 2019. *Orostachys Japonicus* A. Berger Extracts Induce Immunity-Enhancing Effects on Cyclophosphamide-Treated Immunosuppressed Rats. *Biomed Res. Int.*, **1**: 1-9.
- Makhova EV. 2015. Features of the treatment of varicose veins with leeches. *Scientific almanac*, **11-4(13)**: 107-109.
- Michalsen A, Klotz S, Lütke R, Moebus S, Spahn G and Dobos GJ. 2003. Effectiveness of leech therapy in osteoarthritis of the knee: A randomized, controlled trial. *Ann. Intern. Med.*, **139**: 724-725.
- Mohamed WA. 2014. Can Lactoferrin Modulate the Immunostimulant Activity of Levamisole in Rats Immunosuppressed by Cyclophosphamide? *J. Clin. Exp. Investig.*, **5(1)**: 48-53.
- Niqar Z and Alam MA. 2011. Effect of taleeq (leech therapy) in dawali (varicose veins). *Anc. Sci. Life*, **30**: 84-91.
- Ojo PO et al. 2018. Anti-Tubercular Activities and Molecular Characterization of Salivary Extract of Leech (*Hirudo medicinalis*) against *Mycobacterium tuberculosis*. *Journal of Tuberculosis Research*, **6**: 1-9.
- Pavlova IB, Yudina TG and Baskova IP. 2015. Studying of prospects of use of the secret of salivary cages of the medical bloodsucker of *Hirudo medicinalis* and preparation «Piyavit» as the antimicrobial complexes which aren t causing resistance in microorganisms. Modern problems of science and education. **2**.
- Pejin B et al. 2019. The polysaccharide extracts from the fungi *Coprinus comatus* and *Coprinellus truncorum* do exhibit AChE inhibitory activity. *Natural Product Research*, **33(5)**: 750-754.
- Pejin B et al. 2014. Further in vitro evaluation of antimicrobial activity of the marine sesquiterpene hydroquinone avarol. *Current Pharmaceutical Biotechnology*. **15(6)**: 583-588.
- Praise OO et al. 2018. Effects of leech salivary extract (lse) on indices of liver function in rats. *Clin. Diagn. Pathol.*, **2**.
- Porshinsky BS et al. 2011. Clinical uses of the medicinal leech: a practical review *J. Postgrad. Med.*, **57**: 65-71.
- Popov LK, Dolgova SA and Popova IS. 2008. Hirudopuncture with endometritis in dogs. *Veterinary medicine*, **10**: 55-56.
- Prakash A et al. 2013. A review on the role of jalaukavacharana (hirudotherapy) in the management of the venous ulcer. *Universal Journal of Pharmacy*, **2(4)**: 38-43.

- Rawung LD et al. 2021. Effectivity of Curcumin and Thyroxine Supplementations for Improving Liver Functions to Support Reproduction of African Catfish (*Clarias gariepinus*). *Jordan Journal of Biological Sciences*, **14(1)**: 121-128.
- Rychapova LS. 2017. Experience of using hirudotherapy for endometritis in cats and a postgraduate dog. *The successes of modern science and education*, **6(3)**: 182-185.
- Sayed AA, Sadeq R and Mojtaba T. 2017. Leech Therapy for Treating Priapism: Case Report Iran. *J. Public. Health.*, **46(7)**: 985-988.
- Senchukova SR and Zhuravleva TA. 2012. The dynamics of the PASI index of psoriasis patients with complex treatment using hirudotherapy. *Basic research*, **8(1)**: 149-152.
- Sorokina AB. 2008. Hirudotherapy in gynecological practice. *Nurse*, **7**: 19-20.
- Stokoz KYu and Bystritskaya TS. 2016. Leech therapy in women with a history of primary oligomenorrhea. *Amur Medical Journal*, **3 - 4 (15 - 16)**: 106-108.
- Sobczak N and Kantyka M. 2014. Hirudotherapy in veterinary medicine. *Annals of Parasitology*, **60(2)**: 89-92.
- Shakouri A, Adljouy N and Abdolizadeh J. 2018. Anti-Cancer Activity of liposomal Medical leech saliva extract (LSE). Proceedings of the 3rd World Congress on Recent Advances in Nanotechnology (RAN'18), April, Budapest, Hungary.
- Spitsyna VI. 2005. Immune disorders and the pathogenetic substantiation of their correction in patients with chronic diseases of the oral mucosa. MSc dissertation, State Enterprise State Scientific Center "Institute for Advanced Studies of the Federal Administration of Biomedical and Extreme Problems", Moscow.
- Tashiro K, Fujiki M, Arikawa M, Kagaya Y, Miyamoto S. 2016. Free Flap Salvage after Recurrent Venous Thrombosis by Means of Large-Scale Treatment with Medical Leeches. *Plast Reconstr Surg Glob Open*, **4**: e1157.
- Tešanović K et al. 2017. A comparative overview of antioxidative properties and phenolic profiles of different fungal origins: fruiting bodies and submerged cultures of *Coprinus comatus* and *Coprinellus truncorum*. *Journal of Food Science and Technology*, **54(2)**: 430-438.
- Glazunova LA and Anodina MM. 2013. Hirudotherapy in the treatment of subclinical mastitis in cows. *Modern problems of science and education*, **6**: 1060.
- Girgis SM, ElRaouf AA and Abdou HS. 2021. Protective effect of Ferula hermonis root extract against cycraminduced DNA, biochemical and testicular damage in rats. *Jordan Journal of Biological Sciences*, **14(1)**: 105-110.
- Ukpo G. 2013. Evaluation of the Haematological and Biochemical Effects of Averno®, a Herbal Formulation, against Cyclophosphamide-Induced Immunomodulated Male Rats. *Int. J. Pharm. Sci. Res.*, **4(9)**: 3556-3562.
- Yu G et al. 2016. Combination Effects of Antimicrobial Peptides. *Antimicrob Agents Chemother*, **60(3)**: 1717 - 1724.
- Yudina TG et al. 2012. Antifungal and antibacterial functions of medicinal leech recombinant destabilase-lysozyme and its heated-up derivative. *Frontiers of Chemical Science and Engineering*, **6(2)**: 203-209.
- Zolotarev AG, Pimenov EV and Devrishov DA. 2013. **Light Microscopy of Microorganisms**. Agrovvet, Moscow, pp.277-288.
- Zolonyi II, Kuznetsova LV, Frolov VM and Peresadin MO. 2010. Influence of hirudotherapy on indicators of a cytokine blood profile in ailments for relapsing beshihu on aphids of varicose veins of a homilka. *Ukrainian medical almanac*, **1(13)**: 52-55.
- Zouaghi N et al. 2021. Antimicrobial Activities of Natural Volatiles Organic Compounds Extracted from *Dittrichia viscosa* (L.) by Hydrodistillation. *Jordan Journal of Biological Sciences*, **14(1)**: 41-49.
- Zhulebin NN. 2017. Hirudotherapy in dermatology. *Bulletin of Medical Internet Conferences*, **7**: 972.

Comparison of the Folate and Homocysteine Levels with A80G - RFC1 Gene Polymorphism between the Sample of Iraqi Children with and without Down Syndrome

Shatha Qassim Jawad¹, Huda Musleh Mahmood^{2,*}, Gulboy Abdolmajeed Nasir³

¹Assist. Prof. Department of Basic Science, College of Dentistry, University of Baghdad, Baghdad, Iraq; ²Assist. Prof. Department of Biotechnology, College of Science, University of Anbar, Anbar, Iraq; ³ Assist. Prof at Division of Basic Sciences, College of Agricultural Engineering Sciences, University of Baghdad, Baghdad, Iraq.

Received: March 12, 2021; Revised: June 26, 2021; Accepted: July 24, 2021

Abstract

Many international studies indicated that the polymorphisms of some genes disturbed the folate homocysteine (Hcy) metabolism and increased the vulnerability to Down syndrome (DS). We aimed to measure the serum levels of folate and Hcy in DS children and compare the levels with age and sex-matched apparently normal healthy children. We also aimed to study the A80G polymorphism of the gene reduced folate carrier (RFC1) in the DS children as a risk factor. Forty children with DS (24 were boys, and 16 were girls) with the age range between 5-13 years, and 26 normal healthy children (16 boys and ten girls) were included in this study. The results show that the highest genotype in the control group was AG (53.85%) followed by AA and GG (30.77% and 15.38%) respectively. The genotype percentages in children with DS were (50, 35, and 15) for AG, AA, and GG respectively. There was no statistically significant Down syndrome risk RAC-1A80G polymorphic genotype and DS in the Iraqi children sample (A/A Vs. G/G, OR= 1.13, 95%CI = 0.48-2.68) (A/A Vs. A/G, OR= 1.2, 95%CI = 0.66-2.26) (G/G vs. A/G, OR=1.08, 95%CI = 0.48-2.43) respectively. Significant decrease in the concentrations of Hcy and folate in the serum of DS children 5.54 ± 0.94 and 6.99 ± 1.16 , then in the control group 7.14 ± 1.46 , 7.86 ± 1.78 , respectively. We did not detect a significant difference between male and female DS subjects. There was no correlation between the Hcy concentration and folate level of the DS group. The results showed that the frequency of RFC1 alleles and A80G genotypes (GG Vs AA, AA Vs AG, GG Vs AG) had no risk with down syndrome in a sample of Iraqi children. Thus, we need further studies with a large sample of children in comparison with mothers of DS birth.

Keywords: RFC1 80A-G Polymorphism, Down Syndrome, Serum Folate, Homocysteine Levels, Iraqi patients

1. Introduction

Trisomy 21, known as Down Syndrome (DS), is the most common human chromosomal disorders in born children (1 in 800–1000) (Capone, 2004; Sadiq *et al.*, 2014). It has been assumed that the interactive role of various genetic and environmental factors is associated with DS (Sadiq *et al.*, 2019). Folic acid (globolotamic acid), as a dietary factor, plays a vital function in the progress of distribution of genetic materials during cell division due to its role in cellular methylation reactions. Folic acid is implicated in epigenetic regulation and other processes in the synthesis and repair of DNA (Argellati *et al.*, 2006; Sadiq *et al.*, 2019). The loss of chromosomal balance and the disturbed gene expression of extra chromosome 21 are products of mitotic error in the embryo development. The gene expression of extra chromosome 21 is a result of the failure of normal chromosomal segregation during maternal meiosis. Alternatively, oxidative stress caused by DNA damage plays a crucial role in clinical manifestation of DS (Biselli *et al.*, 2008; Zitnanova *et al.*, 2006), due to over-expression of antioxidant enzyme present in chromosome 21-

associated with many other clinical traits including mental retardation and congenital heart disease (Carratelli *et al.*, 2005).

Chromosome 21 contains 225 genes, some of which are believed to be located in the critical area of Down syndrome (DSCR), implicated in the pathogenesis of DS. However, the functions of most of the encoded proteins are still unknown. DSCR contains genes coding for Folate is significantly implicated in cellular methylation reactions (Fenech, 2005). Folic acid acts primarily as a single carbon unit donor involved in many essential body processes, including DNA and RNA synthesis and repair. Its metabolism is associated with the primary methyl group donor for methylation reactions of DNA, lipid, and proteins. Proteins that carry folic acid are also crucial in sustaining DNA methylation because they determine the level of folate present in the cells (Yates, Z., and Lucock, 2005; Chango *et al.*, 2000). Recent evidence indicates that up to ninety percent of children with psychological and DS are born from young mothers, and have other risk factors than maternal age (Hobbs *et al.*, 2000 & 2002).

Some studies have suggested a relationship is found in the presence of DS and some mutations or polymorphism in genes of mother implicated in the mechanism of the

* Corresponding author e-mail: huda.mahmood@uoanbar.edu.iq.

metabolism during folate acid transport and synthesis (Scala *et al.*, 2006; Santos-Reboucas *et al.*, 2008).

Homocysteine (Hcy) is a sulphuric amino acid produced via folate metabolism and could undergo reconstitution to methionine or conversion to cysteine in the transsulfuration pathway. Hcy concentration is affected by modifiable and non-modifiable factors such as vitamin status, sex, and genetic factors (Yelina *et al.*, 2012).

Among the genes involved in the folic acid metabolism, reduced folate carrier 1 (RFC1) also known as SLC19A1 is by implication involved in neural tube defects, Down syndrome, and leukemia. RFC1 is found in the intestinal mucosa membrane. According to Nguyen *et al.* (1997), RFC1 is involved in folic acid absorption by conveying 5-methyltetrahydrofolate into the cells. The A80G variant of the RFC1 gene could also be linked to the changes in products got in this metabolic pathway (Coppedè *et al.*, 2006; Coppedè *et al.*, 2013).

Different research works have shown the pathogenicity of folate or the function of folate in preventing neural tube defects. Abnormal Folate and homocysteine metabolism lead to DNA strand breaks, chromosomal instability, impede DNA repair capability, DNA hypomethylation, and abnormal gene expression (Moustafa *et al.*, 2016; Kazemi *et al.*, 2016). Consequently, the current work aims to evaluate the serum levels of folate and homocysteine in children with DS and compare them with normal controls. For the first time, the RFC1 gene A80 G polymorphism was evaluated in Iraqi children with DS.

Subjects, Materials, and Methods

The study included a patient group of 40 children with DS from Baghdad Teaching Hospital –Medical City-Ministry of Health, and from Al-Safa center in Zayoonah city, Baghdad, Iraq. This study was performed from April 2019 to the end of September 2020.

The control group included 26 (16 boys and ten girls) Iraqi pupils from 5 and sixth class Zamzam primary schools in Baghdad city, with the age range between 10 to 14 years.

All pupils who were involved in this study were interviewed to allow for case-control design by comparing serum folate and homocysteine levels as well as RFC1.

1.1. Samples collection

We collected five milliliters of the venous blood sample from each child in the two study groups carried out. Two ml- serum was used for biochemical analysis and two ml of the blood sample was transferred to EDTA tubes for molecular analysis to detect RFC1-A80G Polymorphism.

1.2. RFC-1 Gene Polymorphism

The genomic DNA was isolated from 66 blood samples collected in EDTA anticoagulant tubes from the two study groups, according to the protocol of the Relia Prep TM Blood gDNAMiniprep System Kit (Promega, USA). Polymorphism analyses by using PCR-RFLP, the amplification of primers were as reported by Neagos *et al.* (2010): forward of primer: 5'-AG TGT CAC CTT CGT

CCC-3' and the sequence for reverse 5'-TCC CGC GTG AAG TTC TTG-3'.

The polymerase chain reaction for RFC - 1 gene A80G polymorphism was performed in a total volume of 25 µl, with PCR conditions as follow: one cycle of 94°C for 2 minutes as a preliminary DNA denaturation step, followed by 44 cycles of 94°C for 30 seconds, 52°C for 30 seconds, and 72°C for 55 seconds, which is followed by 1 cycle at 72°C for 7 minutes for a final extension. Five µl from each sample PCR product were electrophoresed to ensure the positive reaction of amplification. The PCR products were digested with *Cfo I* (Sigma, USA) with 0.5 µl restriction enzyme, which was added to 20 µl of PCR products for 3 hr. The incubation period generated three parts of 125, 68, and 37 bp, with the G allele, while the A allele generated two parts of 162 and 68 bp. Amplicons were electrophoresed, and visualization was done by gel 2 % agarose which contains the ethidium stain bromide; after that, we reached the results from comparison to the ladder of 100- base pair.

Serum Hcy and folate levels were measured according to the principle of immunoassay kits using Immulite analyzer –Siemens-Germany in teaching laboratory-hormonal and biochemical assay for the ministry of the health-medical city.

1.3. Statistical Analysis:

The Statistical Analysis System- SAS (2012) method was adopted for the detection of the impact of various indicators in study parameters. T-test was utilized for a substantial comparison between means. The estimate of correlation coefficient-r in this study and the chi-square test were utilized in comparing allele and genotype frequenters between the two study groups. Odds ratio with 95% confidence interval in the DS group. P<0.05 was regarded as statistically significant (SAS. Version 9, 2012).

2. Results

Table 1 illustrates the allele numbers and RFC1 genotype frequencies for control and Down syndrome children by using Hardy-Weinberg equilibrium. The percentages of genotypes involved in this polymorphism for healthy normal children were the A-G (53.85%), A/A (30.77%), 15.38% ,and G/G genotypes respectively.

The children with DS group have a higher percentage of the genotype A/G (50%) followed by A/A (35%), then G/G genotypes (15%), without any statically significant differences about the polymorphism A-G in the RFC1 gene when compared Down syndrome to healthy control children.

Table 1. RFC1 rs 1051266, A/G genotypes and allele frequencies among study groups

Group	Genotype (%)			Allele frequency		Persons chi-square X ² (df=2)	P
	AA	GG	AG	A	G		
	N (%)	N (%)	N (%)				
Control N=26	8(30.77)	4(15.38)	14(53.85)	0.58	0.42	0.15	0.93
Patients N=40	14(35)	6(15)	20(50)	0.6	0.4		

From the odds ratios calculation (table 2), the study subjects who carried the A/A or A/G genotypes of RFC1 gene have a non-significant effect ($p > 0.05$) Down syndrome risk (OR= 1.2, 95% CI=0.66-2.26), (OR= 1.08, 95% CI= 0.48-2.43) in comparison to individuals who carried A/G genotype.

The results showed that there was non-significant Down syndrome risk (OR= 1.13, 95% CI=0.48-2.68) when compared the subjects who carried the A/A genotype of RFC1 gene versus individuals who carried the G/G genotype.

Table 2. RFC1 A and G allele polymorphism in Down syndrome group

	Genotypes	OR	95%CI	P
Down syndrome	A/A Vs. G/G	1.13	0.48-2.68	0.78
	A/A Vs. A/G	1.2	0.66-2.26	0.53
	G/G Vs. A/G	1.08	0.48-2.43	0.85

The mean Homocysteine concentration in DS children showed a significant decrease (5.54 ± 0.94), compared to the control group (7.14 ± 1.46) ($P = 0.01$). The serum levels of folate were significantly lower in the DS group (6.99 ± 1.16) when compared to the control group (7.86 ± 1.78) as presented in table 3. However, there were no statistically significant differences between the concentration of Hcy and folate with gender in DS or normal healthy children (Table 4). There was no significant correlation between the Hcy concentration and folate level of the DS group and controls, as shown in table 5.

Table 3. Comparison between DS and control in Homocysteine and Folate

Group	Mean \pm SD	
	Homocysteine	Folate
DS	5.54 ± 0.94	6.99 ± 1.16
Control	7.14 ± 1.46	7.86 ± 1.78
T-Test	0.591 **	0.725 *
P-value	0.0001	0.0206

* ($P < 0.05$), ** ($P < 0.01$)

Table 4. Comparison between DS and control in Homocysteine and Folate

Group	Sex	Mean \pm SD	
		Homocysteine	Folate
DS	Male	5.83 ± 0.82	7.11 ± 1.34
	Female	5.10 ± 0.95	6.82 ± 0.85
	T-Test	0.575 NS	0.768 NS
Control	Male	7.34 ± 1.52	7.90 ± 1.88
	Female	6.84 ± 1.40	7.79 ± 1.72
	T-Test	1.228 NS	1.515 NS

** ($P < 0.01$), NS: Non-Significant

Table 5. The correlation coefficient between Homocysteine and Folate in patients and control

Group	Parameters	Correlation coefficient-r	Level of sig.
DS	Homocyst and Folate	0.19	NS
Control	Homocyst and Folate	0.13	NS

NS: Non-Significant

3. Discussion

Folic acid is a coenzyme in the folate metabolism that works by transferring the active form of folic acid to cells, which can affect the activity of enzymes that take a critical function as a risk factor for homocysteine level and many other diseases such as defects in neural senses and cardiovascular diseases (Zampieria et al., 2012).

The gene included in the metabolism of folic acid and folate is RFC1, also named SLC19A1; the purpose of our work is to compare the presence of RFC1 rs1051266, A80G polymorphism in DS children and healthy (Locke et al., 2010). In the present study, as appearing by chi-square test, it was found the allele A was more frequent than allele G in both DS and control children groups. No significant difference was detected in A80G polymorphism between the two groups.

Also, Neagos et al. (2010) indicate that the G allele may alter and increase the risk and probability to born child with DS from mothers over 34 in southern Italy. However, Saghadzadeh et al. (2017) considered the presence of the G allele as a risk factor for nsCLP in Iranian infants but considered the result to be commendable due to other conditions such as gene-environment interaction and amount of folic acid that play a role in the etiology. Similarly, in the Indian population, Lakkakula et al. (2015) demonstrated the association of allele G with nsCLP, and they consider the allele G to be associated with the Asian population.

Additionally, it was found that the AA is the most common genotype in DS children (35%) than the control group (30%). However, this was not a statistically significant difference. In recent years, due to the increased

occurrence of children with DS from mothers at an early age, it indicates that other factors are acting, as DS mainly occurs at older age, leading to the study of physiological conditions and mechanisms that are best to grow DS fetuses. The studies on cell cultures demonstrated the folate deficiency is eligible to stimulate chromosome 21 aneuploidy, and the results assumed DS has many causes linked to genetic and acquired factors such as epigenetic or environmental and random origin. Therefore, it is difficult to establish and identify the effect of the first contribution to each of these factors (Varga *et al.*, 2006).

The variation in the allele and genotype distribution maybe due to the differences in the sample of this study and genetic background differences of children adding to the impact of complicated environmental factors.

In our study, mean folate level in DS children was substantially lower than in the control group; this result agrees with study by Fillon-Emery *et al.* (2004) and Varga *et al.* (2008). However, this result disagrees with the results of Gueant *et al.* (2005) who did not observe the significant differences between DS and healthy individuals in the folate level while the level in this study let down than the folate concentration in the study of Kumar and his group (2014) in Indian children with DS, who proved active folate deficiency despite normal plasma amount of folate.

The folic acid level in this study was found to be below the biological range value in healthy children and DS children, and this can be explained by the fact that all cases and the control group were children with poor conditions, malnutrition, and wars with shelling. Essential sources of dietary folates are fruits, beans, cereals, green vegetables, and calf liver which is referred to as single carbon metabolism, to produce the main intracellular methylating like the S-adenosylmethionine (SAM). At the same time, DNA is also producing the precursor of the RNA (Pogribna *et al.*, 2001). Folate is considered one of the molecules having the hydrophilic characters which were not able to pass the membrane of biological object through promulgation alone unless by using various transport system to get in the cells.

In this study, the mean of serum Hcy concentration was significantly decreased ($p < 0.01$) among children from control, and the current result of lowering the Hcy concentration of children with DS agrees with the study of Pogribna *et al.* (2001) and Meguid *et al.* (2010).

Similarly, Nandha Kumar *et al.* (2014) observed hyperhomocysteinemia in DS. They explained that it could be as a result of the elevation in the transsulfuration for the Hcy pathway, which originates from the increase in the expression of cystathionine B synthase on chromosome number 21 which leads to deficiency and decrease in the functional folate. Also explained that decreasing and increasing folate concentration and Hcy with the advancement in the children's age, which was described by the increased requirement for folate in the early stage of the growth and development of infants. The results of the present study about gender variations in the concentration of folate and Hcy between boys and girls of DS children or in normal healthy were statistically not significant, and this may be caused by that in our study all samples of children were at the stages of growth and development, in Iraq.

Gueant *et al.* (2005) and Laraqui *et al.* (2006) revealed that a high Hcy level may be harmful and is particularly

linked to the elevated risk for heart diseases and psychiatric with neurodegenerative disorders. According to the Hobbs *et al.* (2000 and 2002) study, the presence of genetic variants in genes implicated in the folate metabolism among individuals with DS may lead to a survival advantage. Hcy is responsible for a critical role in folate-dependent DNA synthesis. Hcy plays an essential part in the reactions of cellular methylation that are essential for the growth of the fetus and the interaction of fetal and maternal genotypes.

The preferable recognition of folate transporter was expressed reduced RFC-1 which takes part in the regulation and function of the cofactor of the folate involved in the blood (Stanger, 2002). Also, guide work of RFC-1 functions of specialized tissue like assimilation of the luminal layer of the intestine and the uptake for folate through the process as barriers between blood and the brain organ transplacental transmission of folate and travel through some tubules and membranes in the kidney. Decreasing of folate in cells outcome from disequilibrium in the DNA methylation process, chromosome breakage, point mutations, aneuploidy, and chromosome recombination defect while related to various diseases of humans such as cardiovascular diseases and congenital diseases, neuropsychiatric disorders, and cancer (Santos-Reboucas *et al.*, 2008).

4. Conclusion

The results of our work revealed a substantial decline in the Hcy and folate levels in DS children when compared to the control group, but not significant with the gender. There was no correlation between the Hcy concentration and folate level of the DS group.

The results showed that the frequencies of RFC-1 alleles and A80G genotypes (GG Vs AA, AA Vs AG, GG Vs AG) had no risk with Down syndrome in a sample of Iraqi children. Thus, we need further studies with a large sample of children in comparison with mothers of DS birth.

Acknowledgments

We thank all the staff members of Al-Safa center, Baghdad teaching hospital, and primary Zamzam school in Baghdad city, all managers, the teachers, and children involved in this study. We acknowledge all the staff of the Genetic Engineering and Biotechnology Institute for postgraduate studies at the University of Baghdad. Also, our thanks go to the staff of a teaching laboratory in the Medical City-Ministry of Health. We express our thanks to those who contributed directly or indirectly to this study.

References

- Argellati F, Massone S, Abramo C, Marinari UM, Pronzato MA, Domenicotti C and Ricciarelli R. 2006. Evidence against the overexpression of APP in Down Syndrome. *IUBMB Life*. **58**(2): 103–106.
- Bailey LB & Gregory JF. 1999. Folate metabolism and requirements. *J. Nutr.*, **129**: 779–782.
- Biselli JM, Goloni-Bertollo EM, Zampieri BL, Haddad R, Eberlin MN and Pavarino-Bertelli EC. 2008. Genetic polymorphisms involved in folate metabolism and elevated plasma concentrations of homocysteine: maternal risk factors for Down syndrome in Brazil. *Genet. Mol. Res.* **7**(1): 33–42.

- Capone GT. 2004. Down Syndrome: Genetic insights and thoughts on early intervention. *Infants and Young Children*, **17(1)**:45-58.
- Carratelli M, Porcaro L, Ruscica M, De Simone E, Bertelli AA, Corsi MM. 2001. Reactive oxygen metabolites and prooxidant status in children with Down's syndrome. *Int J Clin Pharmacol Res.*, **21**:79-84.
- Chango A, Emery-Fillon N, de Courcy GP, et al. 2000. A polymorphism (80GA) in the reduced folate carrier gene and its associations with folate status and homocysteinemia. *Mol. Genet. Metab.*, **70**: 310-315.
- Copped'e F. 2009. The complex relationship between folate/homocysteine metabolism and risk of Down syndrome. *Mutat Res.*, **682(1)**, 54-70.
- Coppedè F, Lorenzoni V. and Migliore L. 2013. The Reduced Folate Carrier (RFC-1) 80AG Polymorphism and Maternal Risk of Having a Child with Down Syndrome: A Meta-Analysis *Nutrients*, **5**: 2551-2563.
- Coppedè F, Marini G, Bargagna SM Stuppia LM, Minichilli F, Fontana I, Colognato RM, Astrea G, Palka G, Migliore L. 2006. Folate gene polymorphisms and the risk of Down syndrome pregnancies in young Italian women. *Am. J. Med. Genet.*, **140**: 1083-1091.
- Eskes TK. 2006. Abnormal folate metabolism in mothers with Down syndrome offspring: Review of the literature, *Eur. J Obstet. Gynecol. Reprod. Biol.*, **124**:130-133.
- Fenech M. 2001. The role of folic acid and vitamin B12 in genomic stability of human cells. *Mutat. Res.*, **475**: 57-67.
- Fillon-Emery N, Chango A, Marcher C. 2004. Homocysteine concentrations in adults with trisomy 21: Effect of B vitamins and genetic polymorphisms. *Am J Clin Nutr.*, **80**: 1551-1557.
- Gueant JL, Anello G, Bosco PM Rodriguez RMG, Romano AM, Barone C, Gerard P, Romano C. 2005. Homocysteine and related genetic polymorphisms in Down's syndrome IQ. *J Neurol Neurosurg Psychiatry.*, **76**:706-709.
- Hobbs CA, Cleves MA, Lauer RM, Burns TL, et al. 2002. **Preferential transmission of the MTHF**. Oxford University.
- Hobbs CA, Sherman SL, Yi P, Hopkins SE, et al. 2000. Polymorphisms in genes involved in folate metabolism as maternal risk factors for Down syndrome. *Am. J. Hum. Genet.*, **67**: 623-630.
- Kazemi M, Salehi M, Kheirollahi M. 2016. Down Syndrome: current status, challenges, and future perspectives. *IJMCM.*, **5(3)**.
- Kumar S N, Bahubali Gane B, Rao RK, Bhat VB. 2014. Folate and Homocysteine metabolism in Indian children with Down syndrome. *CurrPediatr Res.*, **18 (1)**: 11-14.
- Lakkakula B, Murthy J, Gurramkonda VB. 2015. Relationship between reduced folate carrier gene polymorphism and non-syndromic cleft lip and palate in the Indian population. *J Matern Fetal Neonatal Med.*, **28(3)**: 329-32.
- Laraqui A, Allami A, Carrie A, Coiffard AS, et al. 2006. Influence of methionine synthase (A2756G) and methionine synthase reductase (A66G) polymorphisms on plasma homocysteine levels and relation to risk of coronary artery disease. *Acta Cardiol.*, **61**:51-61.
- Locke AE, Dooley KJ, Tinker SW, Cheong SY, Feingold E, Allen EG Freeman SB, Torfs CP, Cua CL, Epstein MP, et al. 2010. Variation in folate pathway genes contribute to the risk of congenital heart defects among individuals with Down syndrome. *Genet. Epidemiol.*, **34**: 613-623.
- Megarbane A, Ravel A, Marcher C, et al. 2009. The 50th anniversary of the discovery of trisomy 21: the past, present, and future of research and treatment of Down syndrome. *Genet Med*, **11**:611-6.
- Meguid NA, Dardir AA, El-Sayed EM, Ahmed HH, Hashish AF, Ezzat A. 2010. Homocysteine and oxidative stress in Egyptian children with Down syndrome. *Clin. Biochem.*, **43**: 963-967.
- Moustafa M, Gaber E and Abo El Fath G. 2016. Methionine synthase A2756G and reduced folate carrier1 A80G gene polymorphisms as maternal risk factors for Down syndrome in Egypt. *The Egyptian Journal of Medical Human Genetics*, **17**: 217-221.
- Neagos D, Cretu R, Tutulan-Cuneta A, Stoian VM, Bohiltea LC. 2010. RFC - 1 Gene Polymorphism and the Risk of Down Syndrome in Romanian Population. *Medica A Journal of Clinical Medicine*, **5(4)**.
- Pogribna M, Melnyk S, Pogribny I, Chango A, Yi P, James J. 2001. Homocysteine metabolism in children with Down syndrome in vitro modulation. *Am J Hum Genet.*, **69(1)**: 88-95.
- Sadiq MF, Hunaiti AA, Alkaraki AK, Alfassed RA.(2015). The association between anti-oxidant/Redox Status and sister chromatid exchanges in down syndrome individuals. *Jordan Journal of Biological Sciences*.**8(1)**: 11-15.
- Sadiq MF, Abu Issa NM, Alhakim MO, Alkaraki AK, Khabour OF, Yaghan RJ, and Gharaibeh MY.(2019). Association of Genetic Variants of Enzymes Involved in Folate / One-Carbon Metabolism with Female Breast Cancer in Jordan. *Jordan Journal of Biological Sciences*. **12(1)**: 89-97.
- Saghazadeh A, Mahmoudi M, Dehghani Ashkezari A, Olliaie Rezaie N, Rezaei N (2017). Systematic review and meta-analysis shows a specific micronutrient profile in people with Down Syndrome: Lower blood calcium, selenium and zinc, higher red blood cell copper and zinc, and higher salivary calcium and sodium. *PLoS ONE*, **12(4)**: 1-20.
- Santos-Reboucas CB, Corrêa CJ, Bonomo, A. et al. 2008. The impact of folate pathway polymorphisms combined to nutritional deficiency as a maternal predisposition factor for Down syndrome. *Dis. Markers*, **25**:149.
- SAS. Statistical Analysis System, User's Guide. 2012. Statistical Version 9.1th ed. SAS. Inst. Inc. Cary. N.C. The USA.
- Scala I, Granese B, Sellitto M. et al. 2006. Analysis of seven maternal polymorphisms of genes involved in homocysteine/folate metabolism and risk of Down syndrome offspring, *Genet. Med.*, **8**: 409-416.
- Stanger O. 2002. Physiology of folic acid in health and disease. *Curr. Drug Metab.*, **3**: 211-223.
- Varga P, V Oláh A, Oláh E. 2008. Biochemical alterations in patients with Down syndrome. *Orv Hetil.*, **149**:1203-1213.
- Yates Z, and Lucock M. 2005. G80A. reduced folate carrier SNP modulates cellular uptake of folate and affords protection against thrombosis via a non homocysteine related mechanism. *Life. Sci.*, **77**:2735-2742.
- 34- Yelina NE, Choi K, Chelysheva L, Macaulay M, de Snoo B, Wijnker E, Miller N, Drouaud J, Green M, Copenhagen GP, et al. 2012. Epigenetic remodeling of meiotic crossover frequency in Arabidopsis thaliana DNA methyltransferase mutants. *PLoS Genet.*, **8(8)**: e1002844.
- Zampieria BL, Bisellia JM, Goloni-Bertollo EM, Vannucchi H, Carvalhoc VM Cordeirod JA and Pavarino EC. 2012. Maternal risk for Down syndrome is modulated by genes involved in folate metabolism. *Disease Markers*. **32**: 73-81.
- Zhao R, Matherly LH, Goldman ID. 2009. Membrane transporters and folate homeostasis: intestinal absorption and transport into systemic compartments and tissues. *Expert Rev. Mol. Med.*, **11(4)**:1-32.
- Zitanova I, Korytar P, Sobotova H, Horakova L, Sustrova M, Pueschel S and Durackova Z. 2006. Markers of oxidative stress in children with Down syndrome. *Clin Chim Lab Med.*, **44(3)**:306-310.

Synthesis of Calcium Oxide Nanoparticles from Waste Eggshell by Thermal Decomposition and their Applications

Yusra M. Alobaidi¹, Mahmood Mohammed Ali², Ahmed Mishaal Mohammed^{1,*}

¹ Department of Chemistry, College of Science, University of Anbar, Ramadi, Iraq; ² Iraqi Ministry of Education, General Directorate of Education in Anbar, Anbar, Iraq

Received: March 24, 2021; Revised: June 28, 2021; Accepted: July 4, 2021

Abstract

This study used the physical method to synthesize calcium oxide nanoparticles (CaO NPs) from eggshell. The method provided a new and improved approach with the advantage of being low cost as it uses eggshell waste as a synthesis precursor. Calcium oxide is an important inorganic compound with many biomedical applications because of its antimicrobial activities against gram negative *Escherichia coli* and the gram positive *Staphylococcus aureus*. Results showed that the mean inhibition increased with increased concentration of calcium oxide particles (70, 140, 280, and 560) µg/ml. The obtained particles were characterised by scanning electron microscopy, energy dispersive X-ray spectroscopy, and X-ray diffraction. The images showed that the calcium oxide NPs were nearly spherical granules. The annotated SEM images that produced the CaO NPs had a mean size of 20-70 nm.

Keyword: Calcium oxide, Nanoparticles, Thermal decomposition, *Staphylococcus aureus*, *Escherichia coli*

1. Introduction

Scientists confirm that nanotechnology has revolutionized science in recent years. This development is clearly due to the unique general properties of nanoparticles (NPs) in terms of surface area (increased surface to volume ratio), particle size, charge, shape, and magnetic properties compared with its bulk counterparts which give nanomaterials improved and unique properties that enable their wide-ranging applications, such as in space, electronics, and energy (Kanude and Jain, 2017; Sorbiun et al., 2018) where NPs are more effective chemically and feasible at low temperatures (Bundschuh et al., 2018). The nanotechnology field has achieved extensive progress (Bano and Pillai, 2020). Thus, they are included in optical applications and catalysis applications (Zhang and Wang, 2017).

The importance of metal oxide NPs is attributed to their numerous applications, including medical ones such as drug delivery (Anderson et al., 2019), bio-imaging (McNamara et al., 2020), biosensors (Fathi et al., 2019), hyperthermia (Salem et al., 2020), gene mapping, and gene delivery (Zhang et al., 2015). Apart from their biological importance owing to their low toxicity, chemical stability, and biocompatibility (Karimi et al., 2013), metal oxide nanoparticles are also involved in catalysis applications (Yang et al., 2017) and environmental treatment (Zhang et al., 2017).

Calcium oxide (CaO) is an alkali-earth metal oxide considered as a promising oxide because of its many applications. One of the most important advantages of CaO NPs is its easy and low-cost production (Bano and

Pillai, 2020). CaO has been used as a catalyst in many reactions (Kumar et al., 2016). The reaction of CaO with CO₂, SO₂, and NO_x may increase the use of calcium oxide as an excellent absorbent (Bharathiraja et al., 2018). It is also considered a narcotic to modify the optical properties (Mirghiasi et al., 2014), for the purification of vehicle exhaust gas (Habte et al., 2019), removal of sulfur from flue gas, and control of pollutant emissions (Liu et al., 2010), and it can serve as a treatment agent for toxic waste (Safaei-Ghomi et al., 2013) and an additive in refractory materials (Mirghiasi et al., 2014). In the medical field, CaO NPs have applications in drug delivery (Butt et al., 2015), where the above research mentioned studied the toxicity of CaO nanoparticles in rats using manual hematoxylin and eosin staining protocols and acute tubular and hepatic degenerations were observed in the kidneys and liver respectively. CaO NPs are used as a synaptic factor of chemotherapeutic agents, and in phototherapy (Aseel et al., 2018). Calcium oxide and calcium hydroxide Ca(OH)₂ NPs have proven efficacy in human root dentin by the elimination of *Enterococcus faecalis* (Louwakul et al., 2017).

The synthesis processes for calcium oxide NPs vary and always preferred the process which gives the best performance in terms of surface area (Habte et al., 2019). Synthesis methods are generally divided into physical, chemical, and Biological. Physical methods include thermal decomposition (Sadeghi and Husseini, 2013), sono-chemical method (Amin and Morsali, 2010), and microwave processing (Roy et al., 2013), whereas chemical ones include co-precipitation (Ghiasi and Malekzadeh, 2012) and sol-gel method (Darcanova et al., 2015). Biological or green methods may include the use of

* Corresponding author. e-mail: sc.dr.ahmedm.mohammed@uoanbar.edu.iq.

some plant extracts such as *Mentha piperita* (Ijaz et al., 2017), benign papaya leaf extract and green tea extract (Anantharaman et al., 2016), and rhododendron arboretum extracts (Ramola et al., 2019). These plant extracts contain many bioactive compounds such as antioxidants, phenolic, enzymes, amino acids, and sterols that act as a reducing agent (Aljabali et al., 2018; Vani et al., 2017; Some et al., 2018).

Eggshells contain about 85-95 % of calcium carbonate (Awogbemi et al., 2020), and the rest consists of protein and minerals (Mustapha et al., 2020). Each gram of eggshell contains 381-401 mg of calcium (Brun et al., 2013). In the industry, eggshells have many applications (Cree and Rutter, 2015). Eggshells contain large amounts of calcite or calcium carbonate (CaCO_3), which are the basic material for the manufacture of limestone and lime. The limestone produced by eggshells is characterized by its purity, unlike the quarried limestone, which contains minerals, clay, and sand. Limestone is used as a filler in plastics, cement, and rubber. calcium carbonate can be transformed into calcium oxide by heating. CaO is known as lime or quicklime, which used to remove the acidity of agricultural soils and gardens. Lime is considered an ingredient in Portland cement. The overall calcination reaction of the eggshell powder is the conversion of CaCO_3 to CaO and CO_2 , as follows (Nuryantini et al., 2019).



Researchers have demonstrated the importance of the particulate size of metal oxides in anti-microorganism activity as it is characterised by high bacterial resistance and great thermal stability (Nirmala et al., 2013). In addition to the histocompatibility of calcium oxide and its anti-microbial potential (Mohammadi and Dummer, 2011), CaO NPs also have a strong anti-bacterial activity related to active oxygen species and alkalinity owing to increased pH by hydrating CaO with water and the superoxide generated on its surface, Figure 1 shows characterization of CaO NPs as anti-microbial agent (Yamamoto et al., 2010).

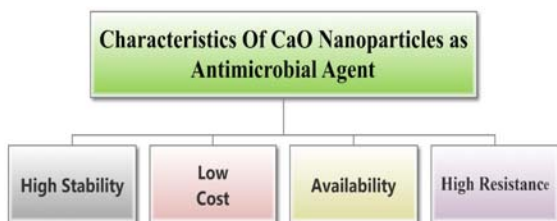


Figure1. Characteristics of calcium oxide as anti-Microbial agent.

Staphylococcus aureus is one of the most common microorganisms that cause human and animal infections alike (Foster and Geoghegan, 2015). The risk of infection increases in cases of immune deficiency. It is treated with penicillin anti-biotics, but the process became difficult owing to the development of resistance against most common anti-biotics because it carries multiple resistance to wide ranging antibiotics bearing the beta-lactam ring (Lee et al., 2018).

Escherichia coli is a Gram negative bacillus that is widespread in nature and lives in the intestines of humans and mammals. It is found in soil and surface waters contaminated with human and animal feces. Most of its types are not pathogenic, but they do become pathogenic after acquiring virulence factors (Roth et al., 2019).

The present study aimed to examine the synthesis of calcium oxide NPs through calcination of eggshells after grinding and burning them at 900 °C. The calcium oxide NPs formed were analysed by scanning electron microscopy (SEM), X-ray diffraction (XRD), and energy-dispersive X-ray spectroscopy (EDX) techniques. The effects of these particles on inhibiting the growth of *S. aureus* and *E. coli* bacteria were also investigated. It can be concluded from this study that the preparation of calcium oxide NPs gave good and encouraging preliminary results for future work as an anti-microbial agent.

2. Materials and methods

2.1. Materials

Local waste eggshell. Muller-Hinton (M-H) agar from Hi-Media (India), and “Riedel-de Haen” (Germany), Deionized water (H_2O) from Chem-Lab (Belgium).

2.2. Preparation of CaO NPs

Eggshells were collected from some houses after using the eggs. The shells were washed, and the internal membranes attached onto the eggshell were removed. The shells were dried at room temperature after breaking them into small pieces. The dried shells were ground using an electrical milling machine for 5 min, after which the fine powder was calcined at 900 °C for 1 h, as shown in Figure 2. The resulting nano-calcium oxide was characterised by SEM, XRD, and EDX techniques.

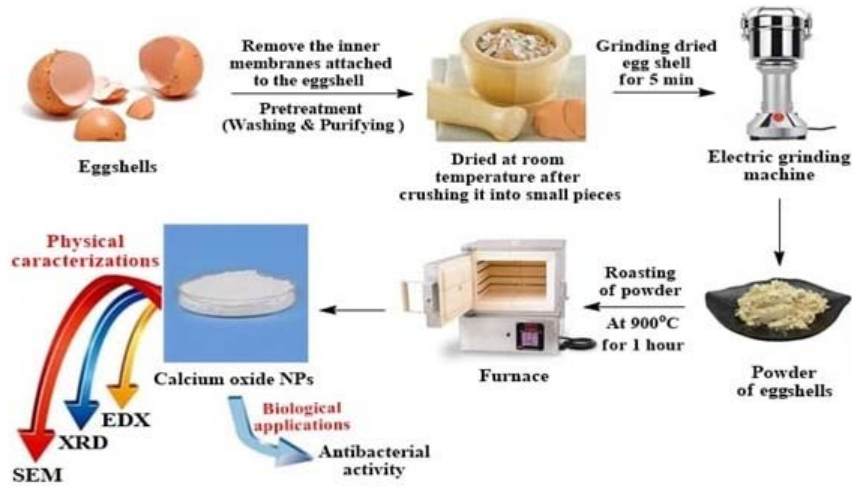


Figure 2. Diagram of preparation and applications of CaO NPs

2.3. Characterization of CaO NPs

Calcium oxide NPs size was measured by SEM to identify morphology. The content of all materials present in the composite CaO was determined by EDX. The crystalline size and structure of NPs were determined by XRD using an automated diffractometer (Shimadzu 6000 XRD) with Cu-K α radiation ($\lambda = 1.5418 \text{ \AA}$).

2.4. Anti-bacterial activity of CaO NPs

The anti-bacterial activity of the CaO NPs was tested against the Gram negative *E. coli* and the Gram positive *S. aureus* through an agar-well diffusion technique (Kadhim et al., 2019). After culturing the organisms into the bored wells, different concentrations of CaO NPs (70, 140, 280, and 560) $\mu\text{g/ml}$ were used. CaO NPs and the test organisms in cultured plates were incubated for 24 hours at 37 °C. Afterwards, the average diameter of the generated zones of bacterial inhibition by the respective CaO NPs concentrations was measured and recorded. The

experiments were performed in triplicate (Mohammed et al., 2020).

2.5. Statistical analysis

The obtained data were statically analyzed using an unpaired t-test. (Ali et al., 2018). The values are presented as the mean \pm SD of triplicate measurements (Younus et al., 2019).

3. Result and discussion

3.1. SEM

Figure 3 shows the morphology and size of spherical calcium oxide NPs prepared by the thermal decomposition of waste eggshell at 900 °C with a scanning electron microscope. The images showed particle diameters ranging from (20-70) nm as demonstrated in the SEM images.

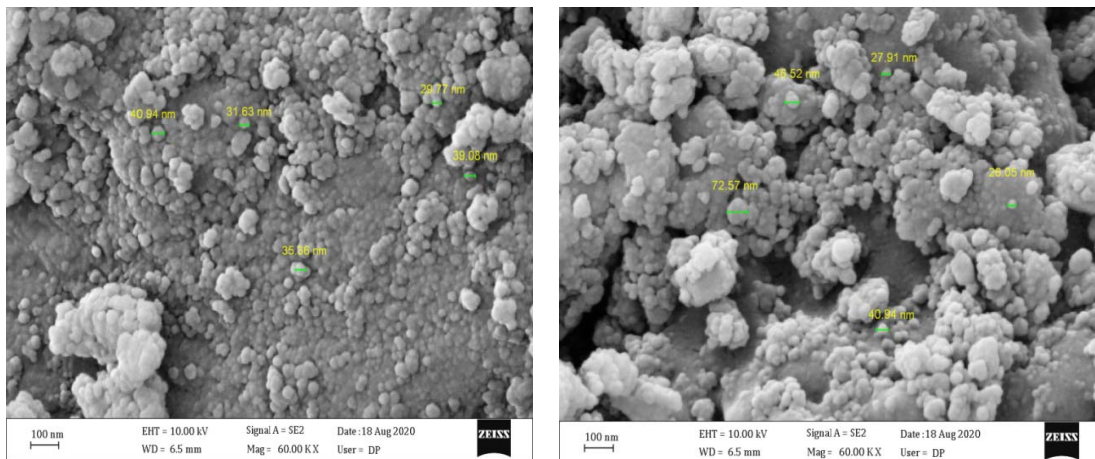


Figure 3: SEM micrograph of CaO NPs

3.2. XRD analysis

Figure 4 shows the XRD patterns of CaO NPs prepared by thermal decomposition compared with those of ICDD card No. 00-004-0784, which is the standard reference for CaO NPs. The diffraction peaks indexed to (111), (200), (220), (311), and (222) corresponded to the peaks at $2\theta = 38.12^\circ$, 44.28° , 64.47° , 77.73° , and 80.10° , respectively, all these peaks confirmed the face-centered cubic structure of CaO as indicated in ICDD card No. JCPDS No. 00-033-0664.

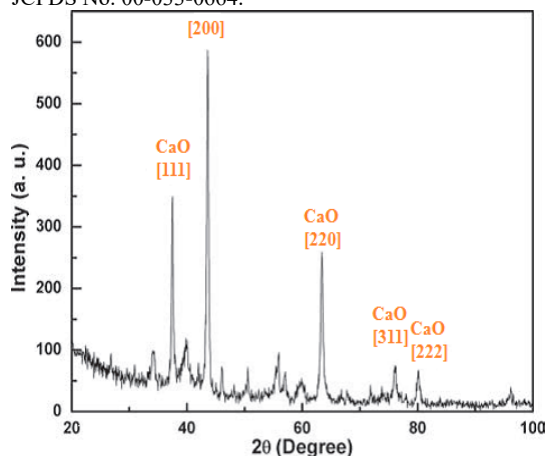


Figure 4: X-ray diffractions of CaO NPs powders after calcination at 900 °C temperatures

3.3. EDX analysis

To emphasize the presence and formation of CaO NPs, EDX analysis was performed with focus on different regions. Identical peaks are shown in Fig. 5. CaO NPs can be seen in the composite nanostructure in the EDX spectrum. As shown in the bottom spectrum, the weight percentages of Ca and O were 71.4% and 28.6% respectively, and σ was 0.9 for both. Energy-dispersive X-ray analysis showed the main peaks of calcium and oxygen. No other peaks related to impurities have been assigned in the spectra which confirm the purity of the CaO NPs.

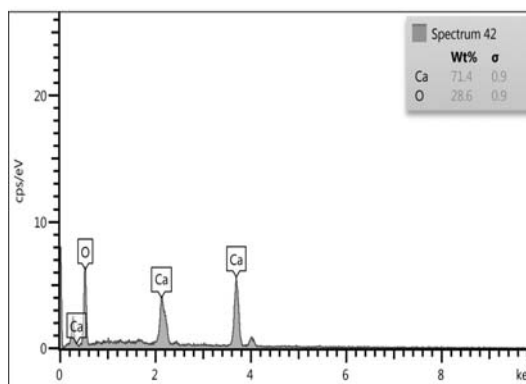


Figure 5: Energy dispersive X-ray analysis of CaO NPs powders after calcination at 900 °C temperature

3.4. Anti-microbial activity

Owing to the large surface area and small particle size of CaO NPs, they exhibited good anti-bacterial reactivity. Conversely, owing to the small size of the particles, they can easily enter the bacterial cells, and inhibition occurred inside the bacterial cells. CaO NPs destroyed and distorted the cell membrane, leading to bacterial cell death (Ramola et al., 2019). Figures 6 and 7 show the mean diameter of inhibition of calcium oxide NPs against *E. coli* and *S. aureus*. With increased concentration of calcium oxide NPs, the mean diameters of inhibition increased. The effect of inhibition appeared from the concentration 70 $\mu\text{g/ml}$, and it increased directly with increased concentration. The highest mean diameter of inhibition appeared at a concentration of 560 $\mu\text{g/ml}$ against *E. coli* and *S. aureus*. These results were consistent with previous studies (Jeong et al., 2007; Anantharaman et al., 2016) in terms of the effectiveness of calcium oxide against *E. coli* and *S. aureus*. The effects of concentration and pH, considered as the main factors affecting anti-microbial activity, also agreed with previous results (Yamamoto et al., 2010).

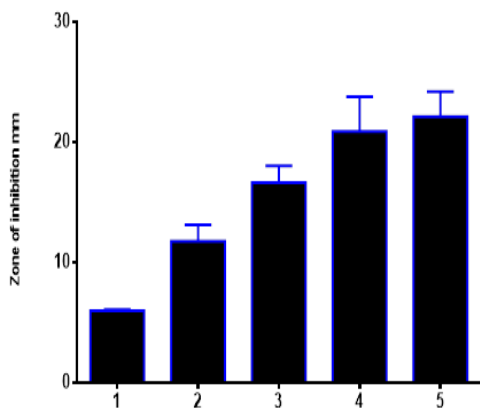


Figure 6: Anti-bacterial activity of CaO NPs against *Staphylococcus aureus*. 1. Represented control untreated bacterial strain. 2. Bacterial strain treated with CaO NPs at concentration 70 $\mu\text{g/ml}$ 3. Bacterial strain treated with CaO NPs at concentration 140 $\mu\text{g/ml}$ 4. Bacterial strain treated with CaO NPs at concentration 280 $\mu\text{g/ml}$ 5. Bacterial strain treated with CaO NPs at concentration 560 $\mu\text{g/ml}$

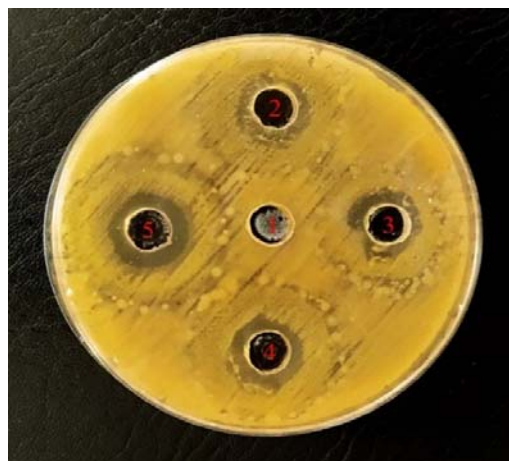
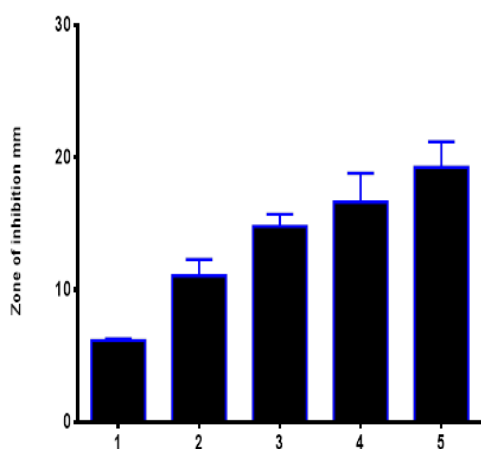


Figure 7: Anti-bacterial activity of CaO NPs against *Escherichia coli* ,1. Represented control untreated bacterial strain 2. Bacterial strain treated with CaO NPs at concentration 70 µg/ml 3. Bacterial strain treated with CaO NPs at concentration 140 µg/ml 4. Bacterial strain treated with CaO NPs at concentration 280 µg/ml 5. Bacterial strain treated with CaO NPs at concentration 560 µg/ml

4. Conclusion

We proposed a method that was economical, simple, and did not require expensive equipment to synthesize calcium oxide particles from eggshells containing a high percentage of calcium carbonate. The NPs formed were characterised by SEM, EDX, and XRD analyses. SEM images showed the formation of spherical granules with sizes ranging from (20 – 70) nm. Studies on the synthesis of calcium oxide particles confirmed the effectiveness of these particles against the Gram negative *E. coli* and the Gram positive *S. aureus*. Furthermore, increased concentration was found to directly affect the mean diameters of inhibition.

Acknowledgement

The authors would like to acknowledge the contribution of the University Of Anbar (www.uoanbar.edu.iq) via their prestigious academic staff in supporting this research with all required technical and academic support.

References

- Ali IH, Jabir MS, Al-Shmgani HSA, Sulaiman GM and Sadoon AH. 2018. Pathological And immunological study on infection with escherichia coli in ale balb/c mice. In: *J Phys Conf Ser.*, IOP Publishing., **1003(1)**: 012009.
- Aljabali AAA, Akkam Y, Zoubi MS Al, Al-Batayneh KM, Al-Trad B, Abo Alrob O, Alkilany AM, Benamara M and Evans DJ. 2018. Synthesis of gold nanoparticles using leaf extract of *Ziziphus zizyphus* and their antimicrobial activity. *Nanomaterials.*, **8**: 174.
- Amin Alavi M and Morsali A. 2010. Ultrasonic-assisted synthesis of Ca (OH)₂ and CaO nanostructures. *J Exp Nanosci.*, **5**: 93–105.
- Anantharaman A, Ramalakshmi S and George M. 2016. Green synthesis of calcium oxide nanoparticles and its applications. *Int J Eng Res Appl.*, **6**: 27–31.
- Anderson SD, Gwenin V V and Gwenin CD. 2019. Magnetic functionalized nanoparticles for biomedical, drug delivery and imaging applications. *Nanoscale Res Lett.*, **14**: 1–16.

Asael MA, Itab FH and Ahmed FM. 2018. Producing high purity of metal oxide nano structural using simple chemical method. In *J Phys Conf Ser.*, IOP Publishing, **1032(1)**: 012036.

Awogbemi O, Inambao F, and Onuh EI. (2020). Modification and characterization of chicken eggshell for possible catalytic applications. *Heliyon.*, **6(10)**: e05283.

Bano S and Pillai S. 2020. Green synthesis of calcium oxide nanoparticles at different calcination temperatures. *World J Sci Technol Sustain Dev.*, **17**: 283–295.

Bharathiraja DB, Sutha M, Krishnamoorthy S, Masi C, Dinakarkumar Y, Ramanujam PK. 2018. Calcium oxide nanoparticles as an effective filtration aid for purification of vehicle gas exhaust. In: *Advances in internal combustion engine research*. Springer, Singapore, pp. 181–192. https://doi.org/10.1007/978-981-10-7575-9_9

Brun LR, Lupo M, Delorenzi DA, Loreto VE Di and Rigalli A. 2013. Chicken eggshell as suitable calcium source at home. *Int J Food Sci Nutr.*, **64**: 740–743.

Bundschuh M, Filser J, Lüderwald S, McKee MS, Metreveli G, Schaumann GE, Schulz R and Wagner S. 2018. Nanoparticles in the environment: where do we come from, where do we go to? *Environ. Sci. Eur.* **30(6)**: 1-17

Butt AR, Ejaz S, Baron JC, Ikram M and Ali S. 2015. CaO Nanoparticles As A Potential Drug Delivery Agent For Biomedical Applications. *Dig J Nanomater Biostructures.*, **10(3)**: 799 - 809

Cree D and Rutter A. 2015. Sustainable bio-inspired limestone eggshell powder for potential industrialized applications. *ACS Sustain. Chem. Eng.*, **3**: 941–949.

Darcanova O, Beganskiene A and Kareiva A. 2015. Sol-gel synthesis of calcium nanomaterial for paper conservation. *Chemija.*, **26**: 25–31.

Fathi F, Rashidi M-R and Omid Y. 2019. Ultra-sensitive detection by metal nanoparticles-mediated enhanced SPR biosensors. *Talanta.*, **192**: 118–127.

Foster TJ and Geoghegan JA. 2015. *Staphylococcus aureus*. Mol Med Microbiol. Academic Press, pp. 655–674.

Ghiasi M and Malekzadeh A. 2012. Synthesis of CaCO₃ nanoparticles via citrate method and sequential preparation of CaO and Ca (OH)₂ nanoparticles. *Cryst Res Technol.*, **47**: 471–478.

- Habte L, Shiferaw N, Mulatu D, Thenepalli T, Chilakala R and Ahn JW. 2019. Synthesis of nano-calcium oxide from waste eggshell by sol-gel method. *Sustainability*, **11**: 3196.
- Ijaz U, Bhatti IA, Mirza S and Ashar A. 2017. Characterization and evaluation of antibacterial activity of plant mediated calcium oxide (CaO) nanoparticles by employing Mentha pipertia extract. *Mater Res Express*, **4**: 105402.
- Jeong MS, Park JS, Song SH and Jang SB. 2007. Characterization of antibacterial nanoparticles from the scallop, *Ptinopecten yessoensis*. *Biosci Biotechnol Biochem*, **71**: 2242–2247.
- Kadhim WKA, Nayef UM and Jabir MS. 2019. Polyethylene glycol-functionalized magnetic (Fe₃O₄) nanoparticles: a good method for a successful antibacterial therapeutic agent via damage DNA molecule. *Surf Rev Lett*, **26**: 1950079.
- Kanude KR and Jain P. 2017. Biosynthesis of CdS nanoparticles using Murraya Koenigii leaf extract and their biological studies. *Int J Sci Res Multidiscip Stud*, **3**: 5–10.
- Karimi Z, Karimi L and Shokrollahi H. 2013. Nano-magnetic particles used in biomedicine: Core and coating materials. *Mater Sci Eng C*, **33**(5): 2465–2475.
- Kumar D, Kuk H and Ali A. 2016. One-pot solvent-free synthesis of fatty acid alkanamides from natural oil triglycerides using alkali metal doped CaO nanoparticles as heterogeneous catalyst. *J Ind Eng Chem*, **38**: 43–49.
- Lee AS, Lencastre H de, Garau J, Kluytmans J, Malhotra-Kumar S, Peschel A and Harbarth S. 2018. Methicillin-resistant *Staphylococcus aureus*. *Nat Rev Dis Prim*, **4**: 1–23.
- Liu T, Zhu Y, Zhang X, Zhang T, Zhang T and Li X. 2010. Synthesis and characterization of calcium hydroxide nanoparticles by hydrogen plasma-metal reaction method. *Mater Lett*, **64**: 2575–2577.
- Louwakul P, Saelo A and Khemaleelakul S. 2017. Efficacy of calcium oxide and calcium hydroxide nanoparticles on the elimination of *Enterococcus faecalis* in human root dentin. *Clin Oral Investig*, **21**: 865–871.
- McNamara K, Tofail SAM, Thorat ND, Bauer J and Mulvihill JJE. 2020. Biomedical applications of nanoalloys. *Nanoalloys*, p. 381–432.
- Mirghiasi Z, Bakhtiari F, Darezereshki E and Esmaeilzadeh E. 2014. Preparation and characterization of CaO nanoparticles from Ca (OH)₂ by direct thermal decomposition method. *J Ind Eng Chem*, **20**: 113–117.
- Mohammadi Z and Dummer PMH. 2011. Properties and applications of calcium hydroxide in endodontics and dental traumatology. *Int Endod J*, **44**: 697–730.
- Mohammed MKA, Mohammad MR, Jabir MS and Ahmed DS. 2020. Functionalization, characterization, and antibacterial activity of single wall and multi wall carbon nanotubes. In: *IOP Conf. Ser. Mater. Sci. Eng.*, IOP Publishing, **757**(1): 12028.
- Mustapha K, Ayinla R, Ottan AS and Owoseni TA. 2020. Mechanical properties of calcium carbonate/eggshell particle filled polypropylene Composites. *MRS Adv*, **5**: 2783–2792.
- Nirmala PN, Suresh G and Karunakaramoorthy K. 2013. Influence of annealing temperature on optical properties of cao thin films. *Int J Recent Sci Res*, **4**: 425–427.
- Nuryantini AY, Sundari CDD, Halimahtussa'diah H and Nuryadin BW. 2019. Synthesis and Characterization of Calcium Oxide Nanoparticles from Duck Eggshells using Ball Milling Methods. *J kim Valensi*, **5**: 232–235.
- Ramola B, Joshi NC, Ramola M, Chhabra J and Singh A. 2019. Green synthesis, characterisations and antimicrobial activities of CaO nanoparticles. *Orient J Chem*, **35**: 1154.
- Roth N, Käsbohrer A, Mayrhofer S, Zitz U, Hofacre C and Domig KJ. 2019. The application of antibiotics in broiler production and the resulting antibiotic resistance in *Escherichia coli*: A global overview. *Poult Sci*, **98**: 1791–1804.
- Roy A, Gauri SS, Bhattacharya M and Bhattacharya J. 2013. Antimicrobial activity of CaO nanoparticles. *J Biomed Nanotechnol*, **9**: 1570–1578.
- Sadeghi M and Husseini MH. 2013. A novel method for the synthesis of CaO nanoparticle for the decomposition of sulfurous pollutant. *J Appl Chem Res*, **7**: 39–49.
- Safaei-Ghomi J, Ghasemzadeh MA and Mehrabi M. 2013. Calcium oxide nanoparticles catalyzed one-step multicomponent synthesis of highly substituted pyridines in aqueous ethanol media. *Sci Iran*, **20**: 549–554.
- Salem NFA, Abouelkheir SS, Yousif AM, Meneses-Brassee BP, Sabry SA, Ghazlan HA and El-Gendy AA. 2020. Large scale production of superparamagnetic iron oxide nanoparticles by the haloarchaeon *Halobiforma* sp. N1 and their potential in localized hyperthermia cancer therapy. *Nanotechnology*, **32**: 09LT01.
- Sorbiun M, Shayegan ME and Ramazani A. 2018. Biosynthesis of metallic nanoparticles using plant extracts and evaluation of their antibacterial properties. *Nanochemistry Res*, **3**: 1–16.
- Some S, Sen IK, Mandal A, Aslan T, Ustun Y, Yilmaz EŞ, Katı A, Demirbas A, Mandal AK and Ocoy I. 2018. Biosynthesis of silver nanoparticles and their versatile antimicrobial properties. *Mater Res Express*, **6**: 12001.
- Vani P, Manikandan N and Vinitha G. 2017. A green strategy to synthesize environment friendly metal oxide nanoparticles for potential applications: a review. *Asian J Pharm Clin Res*: 337–343.
- Wang L, Hu C and Shao L. 2017. The antimicrobial activity of nanoparticles: present situation and prospects for the future. *Int J Nanomedicine*, **12**: 1227.
- Yamamoto O, Ohira T, Alvarez K and Fukuda M. 2010. Antibacterial characteristics of CaCO₃-MgO composites. *Mater Sci Eng B*, **173**: 208–212.
- Yang Q, Xu Q and Jiang H-L. 2017. Metal-organic frameworks meet metal nanoparticles: synergistic effect for enhanced catalysis. *Chem Soc Rev*, **46**: 4774–4808.
- Younus A, Al-Ahmer S and Jabir M. 2019. Evaluation of some immunological markers in children with bacterial meningitis caused by *Streptococcus pneumoniae*. *Res J Biotechnol*, **14**: 131–133.
- Zhang H, Nai J, Yu L and Lou XWD. 2017. Metal-organic-framework-based materials as platforms for renewable energy and environmental applications. *Joule*, **1**: 77–107.
- Zhang Y and Wang Y. 2017. Nonlinear optical properties of metal nanoparticles: a review. *RSC Adv*, **7**(71): 45129–45144.
- Zhang D, Wang J, Wang Z, Wang R, Song L, Zhang T, Lin X, Shi P, Xin H and Pang X. 2015. Polyethyleneimine-coated Fe₃O₄ nanoparticles for efficient siRNA delivery to human mesenchymal stem cells derived from different tissues. *Sci Adv Mater*, **7**: 1058–1064.

BAX and P53 Over-Expression Mediated by the Marine Alga *Sargassum Myriocystum* leads to MCF-7, Hepg2 and Hela Cancer Cells Apoptosis and Induces *In-Ovo* Anti-Angiogenesis Effects

Shabana Parveen and Varalakshmi K.N*

Department of Biotechnology, School of Sciences, Jain (Deemed to be University), #18/3, 9th Main, 3rd Block, Jayanagar, Bengaluru 560011, Karnataka, India;

Received: April 1, 2021; Revised: May 31, 2021; Accepted: June 10, 2021

Abstract

As marine algae are well known for their biological activities, in the present work, the brown marine alga *Sargassum myriocystum* was analysed for its anti-cancer potentials on *in-vitro* cancer cell lines. MTT assay was performed to screen for its cytotoxicity in HepG2, MCF-7 and HeLa cancer cells, followed by bioactivity guided fractionation through thin layer chromatography (TLC). The mechanism of anti-cancer action of the bioactive fraction (SF6) was evaluated by DNA fragmentation analysis, LDH activity, caspase 3, 7, 10 assay, cell cycle study by flow cytometry and study of gene expression by qRT-PCR methods. The anti-angiogenic potential was checked on chick embryos by CAM assay. The characterization of bioactive compound was carried out by HPLC, ESI-MS and GC-MS studies. Significant cytotoxicity and apoptosis induction in HepG2, MCF-7 and HeLa cancer cells by SF6 were confirmed as per MTT assay results, while no toxicity was observed on normal lymphocytes. The up regulation of apoptosis regulatory genes, p53 and Bax in cancer cells by SF6 was indicated by qRT-PCR results. The anti-angiogenesis property was clearly evidenced on chick embryos through CAM assay, with significant inhibition of blood vessel formation (66%) and branching growth. Characterization of SF6 through HPLC, ESI-MS, followed by GC-MS analysis indicated the presence of imidazole carboxamide and ellagic acid, which are listed in the anti-cancer database. These compounds along with some unidentified compounds in the partially purified *S. myriocystum* fraction appear to be majorly responsible for the anti-cancer activity of this brown alga. It can be concluded from the study results that *S. myriocystum* has potent antiproliferative, apoptogenic and angiogenesis inhibitory properties towards cancer cells and has the potential towards the development of anti-cancer drug molecule, after complete characterization of the bioactive compound and *in-vivo* validation studies.

Keywords: Anti-angiogenesis, BAX, Brown algae, Caspase, DNA fragmentation, p53, *Sargassum myriocystum*

1. Introduction

Cancer is a complex disease characterized by uncontrolled proliferation of affected cells that invade the cells around and metastasize to other tissues; it is the second major cause of death worldwide. It is one of the major health problems of people at the global level (Rashan *et al.*, 2018). Cancer can be a result of inherited genes or can result from mutations in the chromosome of a healthy cell; otherwise, it can be triggered by external factors such as chemicals, alcohol, infectious agents, tobacco and radiation (Zong *et al.*, 2012). Cancer cells grow by evading one's immune responses, cell cycle regulatory mechanisms, suppressing pro-apoptotic genes and by neo-angiogenesis (Hanahan and Weinberg, 2011). The advancements in the technology for its diagnosis and treatment have miserably failed to reduce the mortality rate. Chemotherapeutic drugs of synthetic origin come with their own set of side effects. Hence, compounds from natural sources which can upregulate the pro-apoptotic genes, have anti-angiogenesis properties and do not have

any side effects to the normal cells are most sought-after goals in cancer therapy research.

Marine environment constitutes 71% of the earth's surface. Among the marine organisms, Algae have gained special interest owing to their diverse application potential, being rich in minerals, vitamins, fatty acids, amino acids, fibers and bioactive metabolites comprising sulfated polysaccharides, alginates, phlorotannins and carotenoids (Mac Artain and Gill, 2007; Chandini *et al.*, 2008; Cerna, 2011; Misurcova *et al.*, 2012). Compounds from macro algae have a variety of biological, therapeutic activities including anti-cancer, antifouling, antibiotics, anti-inflammatory, antiviral, antimutagenic and cytotoxic (Kim and Ta, 2011; Smit, 2004; Gupta and Ghannam, 2011). However, only a smaller fraction of algae has been analysed for their anti-cancer activity.

Sargassum is a brown alga, normally seen in the intertidal region at the bottom of the sea water. *Sargassum* group of brown algae are found in tropical areas of the world and are most obviously found near coral reefs. *Sargassum* is the largest brown seaweed and mainly grows on coral bubbles and the rocky shores (Agardh, 1848). The brown colour of algae is due to the presence of

* Corresponding author. e-mail: shabanaparveen2784@gmail.com, kn.varalakshmi@jainuniversity.ac.in.

fucoxanthin (Willstatter and Page, 1914). Mostly, *Sargassum* is used as food, animal feed, fertilizer for plants and for commercial production of alginate in industries. Many species of *Sargassum* are used for medicinal purposes also (Gade *et al.*, 2013). *Sargassum* can be consumed as food, either cooked or raw, and has diverse therapeutic applications. It has high iodine content that prevents goitre. It additionally contains algin, laminarin and fucoidan, compounds that can prevent stroke and heart diseases. Algin has the capability to remove toxic components like radioactivity and lead from human body. Tea prepared from *Sargassum* promotes weight loss. The basal part of this seaweed, which contains high amount of algin, can be used to dress wounds and skin burns, after drying (Novaczek, 2001). *S. latifolium* has E1–E4 (Polysaccharides), that inhibit cytochrome P450 1A, which is a carcinogen activator, while selective cytotoxicity was exhibited by E3 towards lymphoblastic leukemia cells (Gamal-Eldeen *et al.*, 2009). An extract from the brown seaweed *S. thunbergii* has shown antitumor activity (Zhuang *et al.*, 1995) and inhibited rat mammary adenocarcinoma cell metastasis (Coombe *et al.*, 1987). The brown marine macroalga, *S. myriocystum*, was reported to have potential radical scavenging activity but has not been explored for its anticancer and anti angiogenesis properties (Badrinathan *et al.*, 2012). Hence, the present research work was mainly focused to evaluate the cytotoxic potential of *S. myriocystum* against different cancer cell lines and also to identify the bioactive compound(s) responsible for this activity, mainly to find a natural anti-cancer compound that would be highly efficient in combating cancer.

2. Materials and Methods

2.1. Collection of the algal sample and extraction of the metabolites

The brown marine macroalga, *Sargassum myriocystum*, was picked up from the Gulf of Mannar, south east coast of India, Rameshwaram district in Tamilnadu. The sample was authenticated by the scientist (Dr. Karuppanan Eswaran), at the Marine Algal Research Station (MARS). The collected samples were rinsed 3- 5 times with water and dried under the shade for 7 days. The dried sample was powdered in a mixer and was extracted using methanol in a Soxhlet apparatus. The methanol extract of *S. myriocystum* was filtered and concentrated in a rotary evaporator at 40 °C. The concentrated extracts were evaporated to dryness (methanol was completely evaporated) and the dried extract was stored in a refrigerator at 4°C until use. A stock solution of 1 mg/ml in DMSO was used for the assays.

2.2. Cancer cell lines used

The cell lines for the current research were procured from NCCS (National Center for Cell sciences), Pune in India. The HepG2 (liver), HeLa (cervical) and MCF-7 (breast) cancer cell lines, authenticated and mycoplasma free, were used, which were maintained under controlled conditions in a humidified CO₂ incubator (with 5%CO₂) and at 37°C temperature. The media used for culturing the cells was MEM (from HIMEDIA) augmented with 10% Serum (Fetal Bovine), streptomycin (100µg/ml) and Penicillin (1000 U/ ml).

2.3. Screening for cytotoxicity

After subculturing the cells at suitable concentrations (1 x 10⁶ cells/mL) to 96 well plates for 24 h, various concentrations (200, 100, 50, 10 and 1 µg/mL) of the dried methanol extracts of the algae, dissolved in DMSO, were added for different time intervals (24h, 48h, 72h and 96 h). Diluted DMSO served as the vehicle control. Each experiment was performed in triplicates. After the treatment period, 10 µL of MTT dye was added and the 96 well plates were kept at 37°C in a CO₂ incubator for 3 hrs under dark conditions. Following this, DMSO was added (100 µL) to all the cells in the multiwell plates and the optical density was taken in an ELISA reader at a wavelength of 540 nm. The percentage viability was calculated by the following formula:

$$\% \text{ viability} = \frac{\text{Absorbance value of treated samples}}{\text{Absorbance value of control sample}} \times 100$$

(Mosmann, 1983).

2.4. Purification by thin layer chromatography (TLC) and bioassay

S. myriocystum extract was purified partially, by performing TLC fractionation using thin layer chromatography sheets (silica 50×20 cm size, Merck), as per standard protocols (Kirchner, 1974). The TLC sheets were cut into pieces of appropriate sizes (6 cm x 7 cm) and placed in the TLC chamber inside the hot air oven at 110° C for 45 min to activation of TLC sheets. The sample diluted with methanol was prepared for spotting the samples on TLC sheet. The sheet was kept inside the beaker containing a prepared solvent combination of Acetonitrile: Chloroform: Dichloromethane: Toluene in at 1:2:2:1 ratio. The beaker was covered with a lid to prevent solvent evaporation. Once the samples reached the top, the sheet was removed using forceps and immediately the solvent line was marked with a pencil. The fractions were marked by viewing under day light and under UV light (254 nm and 366 nm). Preparative TLC was carried out by scraping each band separately and dissolving in methanol. Six fractions (SF1, SF2, SF3, SF4, SF5 and SF6) were obtained. These samples were centrifuged at 5000 rpm for 15 min. The supernatant was carefully decanted to a vial, and the methanol was allowed to evaporate at room temperature, and the dry powder representing each fraction was weighed separately. These fractions were tested for anti-cancer activity using MTT assay in order to select the best fraction for further experiments.

2.5. HPLC and ESI-MS analysis

Further purification of *S. myriocystum* fraction was carried out by allowing the sample to run in a semi-preparative HPLC (Shimadzu make) LC-20. The C18 analytical column was injected with 2 µL of the TLC-purified SF6 fraction at 0.5 mL/min flow rate and the resultant fractions were eluted out at different retention times. By default, water was used in pump A and methanol in pump B to pass the pressurized liquid solvent carrying the sample. Afterwards, C18 preparatory column was used to collect the different fractions separated out. 100 microlitres of sample was injected into the preparatory column, the flow rate being 1.2 mL/min and was run for about 25 minutes. The fractions eluted from HPLC column were analyzed through the Mass spectrometer (Impact HD QTOF Mass spectrometer, Bruker, USA).

2.6. GC MS analysis

At the GC MS facility of SITRA (South Indian Textile Research Association), Coimbatore, the fraction (SF6) was analyzed to identify the compounds. The system (Thermo Scientific Trace DSQ GC-MS) uses Helium as the carrier gas. The SF6 fraction of *S. myriocystum* was injected to the GC-MS system (1 µl), the initial temperature was 70°C for 3 min, which was gradually increased to 260°C at 6°C /min. The sample gets vaporised and separated into different components, based on the mass-to-charge ratio (m/z). The components produce different peaks at different retention times. With the help of library search and search in anticancer compound database (<http://data-analysis.charite.de/care/>), we identified and quantified the unknown compounds present in the sample.

2.7. Trypan blue dye exclusion assay

The cell concentration and viability were measured by trypan blue staining method. Cancer cells (1x 10⁶ cells/ml) were treated at the IC₅₀ concentration of SF6 for 48 hrs, while the control cells received DMSO (0.4%). After 48 hrs, the cells from both control and treated flasks were treated with trypsin, detached cells were collected and centrifuged for 10 min (1000rpm). The cells thus collected were suspended in phosphate buffer, mixed with trypan blue dye (0.4% in PBS) and the viability of the cells was determined by manually counting the cells in a haemocytometer and observing under the microscope. The cell viability and cell count were calculated (Strober, 2001).

2.8. Lactate dehydrogenase (LDH) cytotoxicity assay

The cytotoxicity mediated by *S. myriocystum* fraction (SF6) on the HepG2, MCF-7 and HeLa cancer cell lines was analysed by LDH assay using a commercially available kit (G-Biosciences, India) as per the standard methodology provided by the manufacturer of the kit (Weyermann *et al.*, 2005). To the cultured cells, 50 µg/mL of SF6 was added and the cells were incubated for 48 hours. After this, the supernatant was collected from the treated flasks, where LDH would have been released from damaged cells. As a negative control, medium containing serum was used. The DMSO treated (control) cells were treated with 150 µL of lysis buffer. The cells were frozen and thawed for 3-4 times until the cells got lysed. The cells were centrifuged for 30 min at 10,000rpm. The supernatant was collected by aspiration and was the positive control used in this assay.

In a micro-titre plate, 50 µL of treated sample, positive and negative controls were added to different wells in triplicates. The LDH substrate (50 µL) was treated to all the samples and the reaction mixture was incubated in a CO₂ incubator at 37° C for 20 min. To stop the reaction, stop solution (200 µL) was added, and the optical density was recorded in an Elisa reader at 490 nm.

The cytotoxicity was calculated as a percentage as follows:

$$\text{Cytotoxicity (\%)} = \frac{\text{Experimental OD}_{490} - \text{Blank OD}_{490}}{\text{Control OD}_{490}} \times 100$$

2.9. DNA fragmentation

Treated (48 h) cancer cells (MCF-7, HeLa and HepG2), growing exponentially in 25 cm² tissue culture flasks were

harvested, and genomic DNA was isolated. The assay was performed as per the instructions given in the mammalian genomic DNA isolation kit manual (Bangalore Genei). Cells (2 x 10⁶ cells/mL) were sub-cultured and allowed to adhere for 24 h. The most effective concentration (50 µg/mL) of SF6 was added to adherent cancer cells and incubated at 37 °C for 48 hours in a CO₂ incubator. Trypsinization and centrifugation were used to collect the extract-treated or untreated cells. The cells were processed with RNase (20 mg/mL), 20 µL of proteinase K (20 mg/mL), followed by lysis buffer. Finally, 200 µL of chilled ethanol was added to the sample mix and stored overnight at -20 °C. The precipitated DNA was collected by centrifugation, discarding the supernatant and drying. The completely dry DNA was stored at -20° C until further use in TE buffer (Tris-EDTA buffer). The DNA samples were visualized after gel electrophoresis in a 0.8% agarose gel (Sambrook *et al.*, 1989).

2.10. Caspase enzyme activity

Caspase enzyme (caspase-3,7,10) activity was checked using the Caspase Assay Kit procured from G Biosciences (kit 786-205A) in MCF-7, HeLa and HepG2 cancer cells treated with SF6 fraction (50 µg /mL) for a duration 48 h, while the control cells were treated with DMSO (0.4%) for the same duration. All these cells were processed (as per the instructions in kit manual), and the collected cells were treated with 150 µL of lysis buffer. The cells were frozen and thawed for 3-4times, centrifuged (10,000rpm for 30 min), and the supernatant thus obtained from the treated and untreated samples were used for the caspase assay. 50 µL of treated and untreated samples were taken in different wells of a microtitre plate. The samples were treated with 50 µL of 5mM DTT in 1 ml of 2X caspase assay buffer and 50 µL of AFC-conjugated substrate mix. The wells where only reagents were added served as the blank. At 0 minute (t=0), the optical density of the samples was noted down in an ELISA reader at 405 nm. The samples were kept at 37 °C in a CO₂ incubator for about 90-120 minutes, and at every 15 minutes the optical density was measured until a significant difference in the readings were recorded.

2.11. Flow cytometry

The bioactive fraction SF6 (50 µg/mL) was treated to MCF-7, HepG2 and HeLa cancer cells (2 x 10⁶ cells/mL) for 48 h and after this duration, flow cytometry was used to quantify DNA in the treated cells to analyse the cell cycle stages (G2/M, S and G0/G1 phases) (Pazaroski and Darzynkiewicz, 2004). The treated cells were harvested after trypsinizing and to these cells, 2 mL of ice-cold buffer (PBS) was added to make a uniform cell suspension. The cell suspension was transferred to tubes pre-coated with 2% FBS (Fetal bovine serum) and kept overnight. The cells were fixed with 9 mL of 70% chilled ethanol and stored at -20°C until further use. The cell suspension was centrifuged at 4°C for 10 min at 1000 rpm and the pellet was washed with 3mL of ice-cold PBS (two times) and at 4°C for 10 minutes centrifuged at 1000 rpm. The cells were stained with 500 µ L of PI/Triton X -100 staining solution (1 mg Rnase, 0.02 mg/mL PI and 0.1% Triton X-100) in a dark condition and incubated at 37°C in a CO₂ incubator for 15 min. The cells were scored by a BD FACS verse (488 nm, at IISC Bengaluru) flow

cytometer and the data was analysed by BD FACS Diva™ software (v 6.0)

2.12. p53 and Bax mRNA levels through qRT-PCR

After treating the breast cancer (MCF-7) cells (wild type p53) with 50 µg/mL concentration of SF6 fraction for a period of 48 h, RNA was extracted with the help of RNAiso Plus (Takara, Japan), from the treated MCF-7 cells, as per the methodology given in the instruction manual of the kit for extraction of total RNA (Cat. #9108/9109). Following RNA isolation, cDNA was synthesized as per the instruction in the manual of the cDNA synthesizer kit (Thermo Scientific, #K1622). Real

time PCR (RT-PCR) was carried out for the isolated RNA sample using SYBR Green Chemistry kit from Bioline, USA (Vapo-protect PCR system, Eppendorf). The endogenous control was β-actin gene to compare the levels of expression of p53 and Bax. The condition for the PCR to run the sample was as follows i) 10 min denaturation at 95°C, ii) 30 s annealing at 60°C and iii) 30 s extension at 72°C. The primers used for the genes are shown in Table 1. The results were analysed with the help of gene expression formula. The results are expressed as relative fold changes in the sample treated cell gene expression as compared to that of the control cell.

Table 1 Sequences of Reverse and Forward Primers used for the assay

Genes	Forward Primer (5'-3')	Reverse Primer (5'-3')
p53	AGAGTCTATAGGCCACCCC	GCTCGACGCTAGGATCTGAC
Bax	TTTGCTTCAGGGTTTCATCC	CAGTTGAAGTTGCCGTGACA
β - actin	GGACTTCGAGCAAGAGATGG	AGCACTGTGTTGGCGTACAG

2.13. Anti-angiogenesis assay on chick embryos

Anti-angiogenic property of the bioactive fraction SF6 was analysed by following a modified method of the chick embryo assay (Hardeep *et al.*, 2014). The study was performed at the Institute of Animal Health and Veterinary Biologicals (IAH &VB), Bengaluru. Fertilized chicken eggs were purchased from the department of poultry sciences, Veterinary College and maintained at 37°C in an incubator at 60% humidity. Egg candler was used to mark on the eggs where the extract needs to be injected. On 8th day after fertilization, the eggs were pricked on the mark made on the Chorioallantoic membrane (CAM) layer using the egg puncher. Under aseptic conditions, 100 µl of *S. myriocystum* extract at different concentrations (2.0, 1.0 and 0.5 mg /mL) was injected to the CAM layer. 100 µl of DMSO diluted using phosphate buffer (1:9) and eggs without injection were used as controls. The eggs were then sealed with parafilm wax to prevent contamination and returned to the incubator for 72 hrs. After 72 hrs of incubation, the eggs were opened and the blood vessels (bv) were counted manually in the treated and control groups. The anti-angiogenesis effect of the algal sample was calculated as follows:

$$\text{Inhibition (\%)} = \frac{\text{Number of bv (C)} - \text{Number of bv (T)}}{\text{Number of blood vessels formation (C)}} \times 100$$

bv - blood vessel; C-control; T-treated

2.14. Histopathological examination (HPE) of the blood vessels

From chick embryos treated with varying concentrations (2.0, 1.0 and 0.5 mg /mL) of *S. myriocystum* extract for 72 hrs, as well as from DMSO treated control embryos, slides for histopathological

examination (HPE) were prepared from various layers of the embryos. Hematoxylin and Eosin stain were used for this purpose. The stained slides were observed under an Olympus microscope (binocular, 5X 541). Slides were screened for: (1) Structure of blood vessel, mainly endothelial cells (2) Blood vessel number and frequency (3) Integrity of the membrane.

2.15. Statistical analysis

All the experimental procedures were performed in triplicate samples and the results being expressed in terms of mean ± standard error. One-way analysis of variance (ANOVA) and Duncan's multiple range test (DMRT) were performed to analyse the experimental data with Graph Pad Prism 6.0 software. A p value of < 0.05 was considered as significant.

3. Results

3.1. Anti-proliferative effect of the methanol extract of *S. myriocystum* as per MTT assay

As shown in Figure 1, the results of MTT assay revealed significant cytotoxicity caused by *S. myriocystum* extract to MCF-7, HeLa and HepG2 cells with the most effective response being observed at 200µg/mL concentration of treatment. The viability of 100 µg/mL of extract treated HeLa cells was 50.14%, HepG2 cells was 47.03 % and MCF-7 was 45.76% and that of 200 µg/mL treated HeLa cells was 44.67%, HepG2 was 39.7% and MCF-7 cells was 35.4 %, for the treatment period of 96 h. The IC₅₀ value of *S. myriocystum* was calculated from the dose response as, 115µg/mL for HeLa, 80 µg/mL for MCF-7 and 60 µg/mL for HepG2 cells for 96h.

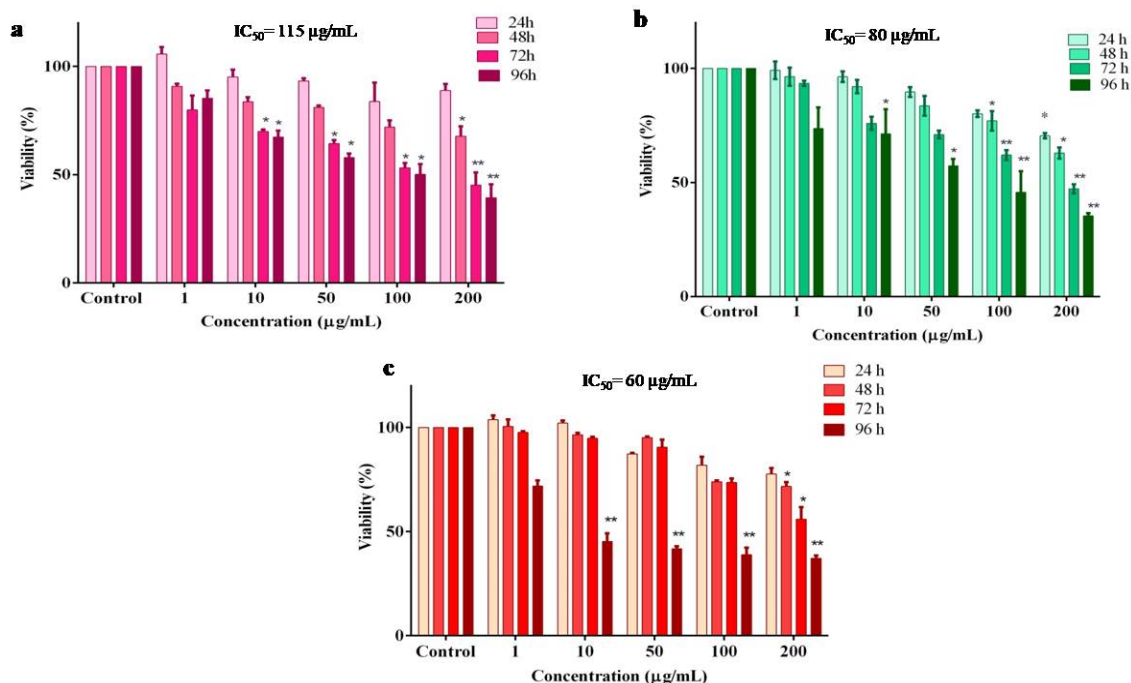


Figure 1. Effect of *S. myriocystum* methanol extract as per MTT assay. a) HeLa; b) MCF-7; c) HepG2 cancer cells post treatment with *S. myriocystum* for 24, 48, 72 and 96h. The values are expressed as mean \pm SE, with n=4. * p<0.05 and ** p<0.01.

3.2. Identification of SF6 as the bioactive fraction by TLC and bioassay

The methanol extract of *S. myriocystum* was fractionated by thin layer chromatography using different combinations of polar and non-polar solvents. Out of the several solvent combinations used on the TLC sheets, the solvent combination of Acetonitrile: Chloroform: Dichloromethane: Toluene in 1:2:2:1 ratio gave best separation of the components with six different fractions (Figure 2).

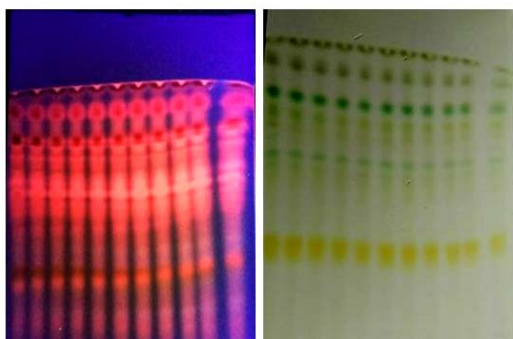
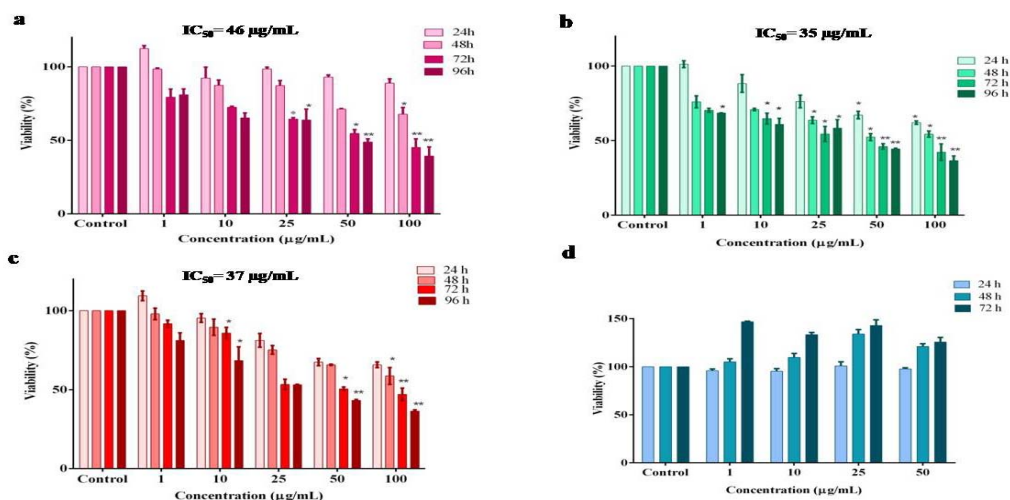


Figure 2. TLC fractionation of the methanol extract of SM under visible and UV light

These fractions were again tested on cancer cells through MTT assay to determine their cytotoxicity. Promising anti-proliferative effects were demonstrated by fraction 6 (SF6) as compared to other fractions against MCF-7 cancer cell line at all treatment concentrations (1, 10, 25 & 50 $\mu\text{g/mL}$) and at 48 h of treatment (Table 2). This SF6 fraction was considered as the bioactive fraction and was tested on HepG2, MCF-7 and HeLa cancer cells for 24, 48, 72 and 96 h. The results (Figure 3) were found to be highly significant at all treatment concentrations (p<0.05) with 39.34 % viability in HeLa, 39.76 % viability in HepG2 and 40.22 % in MCF-7 cells at 100 $\mu\text{g/mL}$ concentration of SF6 and at 96 h of treatment. The cytotoxicity to the cancer cells was directly proportional to the dose and time of treatments. No cytotoxicity was observed on the treated normal lymphocytes at the tested concentrations.

Table 2 Screening different fractions of *S. myriocystum* on MCF-7 cell line by MTT assay at 48h. Values are represented as mean \pm SE. n=3.

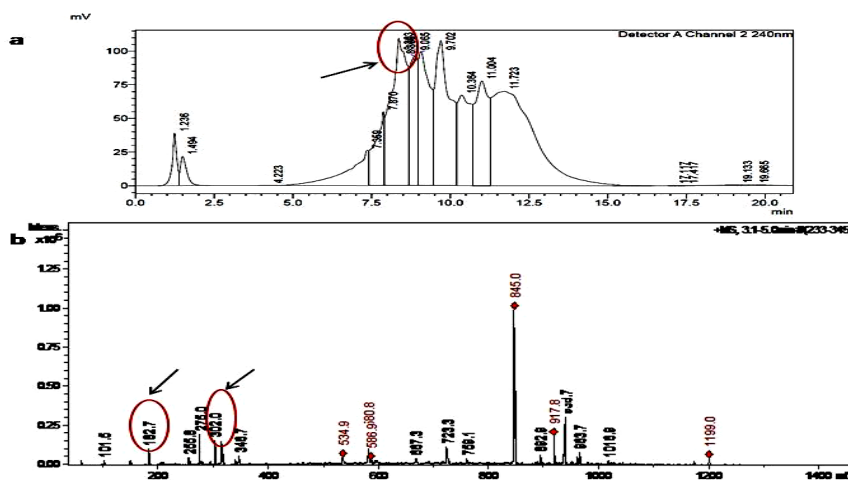
<i>S. myriocystum</i> fractions	Concentration ($\mu\text{g/mL}$)			
	1	10	25	50
	Cell Viability (%)			
SF1	100.68 \pm 1.11	95.89 \pm 1.30	66.13 \pm 1.41	74.21 \pm 0.96
SF2	119.69 \pm 1.93	97.60 \pm 1.40	73.39 \pm 1.49	65.58 \pm 1.48
SF3	127.32 \pm 0.88	118.32 \pm 1.79	81.26 \pm 1.11	60.30 \pm 0.71
SF4	82.05 \pm 0.67	99.31 \pm 1.94	71.43 \pm 1.07	51.74 \pm 0.44
SF5	85.75 \pm 0.88	76.67 \pm 1.69	62.91 \pm 1.34	57.26 \pm 0.52
SF6	67.12 \pm 0.86	62.08 \pm 1.22	51.30 \pm 1.08	47.84 \pm 0.83

**Figure 3.** Effect of SF6 extract as per MTT assay on a) HeLa b) MCF-7 c) HepG2 d) Normal Lymphocytes post treatment with fraction SF6 for 24, 48, 72 and 96h. The values are expressed as mean \pm SE, and n=4. * p<0.05 and ** p<0.01. IC₅₀ values are shown in the graphs for each cancer cell line.

3.3. HPLC and ESI-MS analysis of SF6 indicates molecular fragments of 182.1 and 302.1 m/z values

The partially purified fraction (SF6) obtained from TLC was again purified by the HPLC method. The fractions were eluted at different retention times (RT). The

fraction eluted at 8.8 RT (largest peak) was collected and ESI-MS analysis was carried out. The obtained mass spectra revealed presence of a fragment having an m/z value of 182.1 and another one with 302.1 which were taken and compared with the GC-MS result (Figure 4).

**Figure 4.** HPLC analysis of SF6 fraction (a) Chromatogram after HPLC of SF6 (b) ESI-MS of the fraction eluted at RT 8.8 min, showing spectral intensity of 182.7 and 302.1 Arrows indicate the peaks which resulted in showing m/z values of significant anti-cancer compounds.

3.4. GC-MS analysis indicates presence of dacarbazine and ellagic acid in SF6

The bioactive fraction SF6 was analysed by GC -MS method for characterizing the compounds in it. Through the library search (provided by SITRA in Coimbatore),

dacarbazine (m/z 182.19) (Chen *et al.*, 2008) and ellagic acid (302.19) reported as anti-cancer compounds in the anti-cancer database (<http://data-analysis.charite.de/care/>) were found to be present in SF6 through GC-MS results (Figure 5).

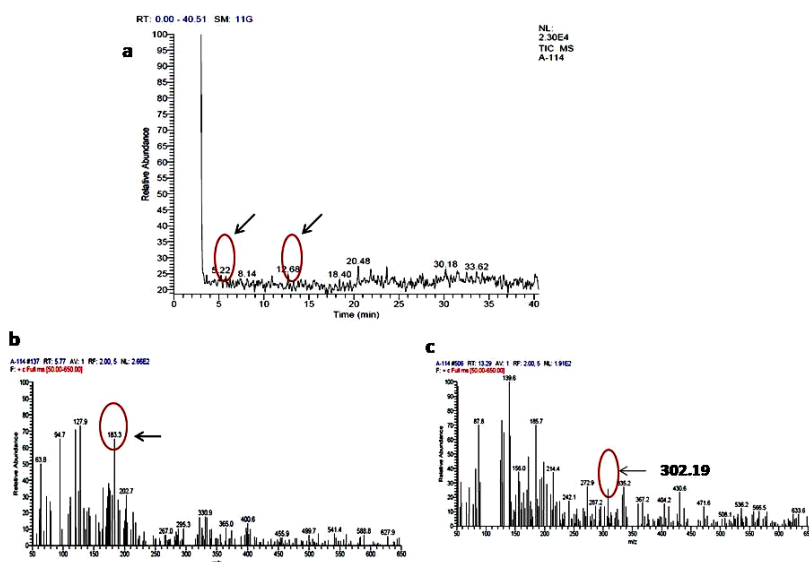


Figure 5. GC MS results of SF6 fraction (a). Chromatogram of SF6 (b) Mass spectrum showing a fragment of 183 m/z (peak of RT 5.77 min) c) Mass spectrum showing a fragment of 302.19 m/z (peak of RT 13. 29 min).

3.5. SF6 treatment decreases cell viability as tested by trypan blue assay

Through trypan blue assay, we found that the number of dead cells increased along with a decrease in viable cell

count, in the SF6 (50 µg/mL) treated HepG2, MCF-7 and HeLa cancer cells after 48 h, while majority of them were viable (97- 99%) in the control group (Table 3).

Table 3 Assessment of total cell count and viability by trypan blue method.

Cell lines	Cell count (1x10 ⁶ cells/ml)					
	Control			SF6 (50 µg/mL) Treated		
	Viable Cells	Non-viable Cells	Viability (%)	Viable cells	Non-viable cells	Viability (%)
HeLa	5.76	0.07	98.79	2.83	2.22	56.03
MCF-7	2.53	0.07	97.30	1.48	1.59	48.20
HepG2	3.12	0.02	99.36	1.60	1.14	58.39
Lymphocytes	1.32	0.03	97.77	0.99	0.02	98.01

3.6. Direct cytotoxicity caused by SF6 as per LDH assay

LDH assay is used to determine the release of LDH enzyme into the medium when the cells are undergoing lysis. The percentage cytotoxicity of HeLa, Hep G2 and MCF-7 cells treated for 48 h with 50 µg/mL of SF6 are 27.1%, 18% and 35% respectively, while no cytotoxic effect was seen on normal lymphocytes (Figure 6)

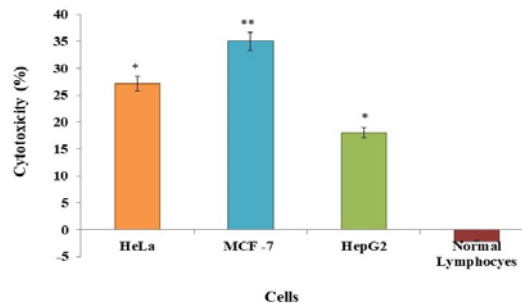


Figure 6. Cytotoxicity as per LDH assay on HeLa, MCF-7 cells, HepG2 cells and Normal Lymphocytes treated with SF6. * p<0.05, ** p<0.01.

3.7. SF6 induces caspase-3, 7, 10 activation in cancer cells

To evaluate the apoptogenic property of the algal fraction, caspase activity assay was performed on HepG2, MCF-7 and HeLa cancer cells after treating with SF6 at 50 µg/mL concentration for 48 h duration. In our analysis, we found an increase in caspase-3, 7, 10 activity of the SF6 treated cancer cells as compared to the negative controls. The increase in the caspase activity from initial (0 min) to final (90 min) was 23.11% in HepG2 cells, 15.53% in HeLa and 23.0% in MCF -7 cells, whereas in the control cells there was hardly any increase (Table 4).

Table 4. Activity (%) of caspase in HepG2, MCF-7 and HeLa cells treated with SF6

Time (min)	MCF-7		HeLa		HepG2	
	Control	Treated	Control	Treated	Control	Treated
0	7.17	17.92	1.36	6.84	2.19	13.73
30	7.21	13.18	1.06	7.32	2.1	24.7
60	6.04	25.27	1.71	15.15	2.9	37.08
90	7.96	41.03	1.82	22.37	3.02	37.45

3.8. DNA fragmentation mediated by SF6

DNA fragmentation is an indication of ongoing apoptotic process in cells. From Figure 7, it is clear that DNA was smeared in HepG2, MCF-7 and HeLa cancer cells treated with SF6, suggesting that treated cells were undergoing apoptosis as compared to control cells which are viable.

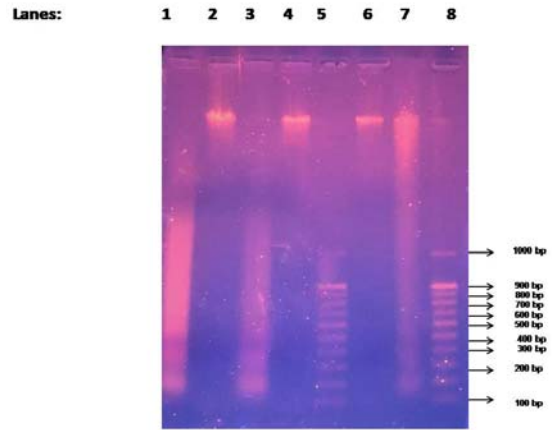


Figure 7. Photographs of agarose gel showing DNA isolated from SF6 treated and control cancer cells. Lanes: 1- treated HeLa; 2- control HeLa; 3- treated MCF-7; 4-control MCF-7; 5-Ladder DNA; 6-treated HepG2; 7-control HepG2; 8-ladder DNA.

3.9. SF6 induces altered cell populations in different phases of the cell cycle

Cell cycle stages of SF6 treated (48 h duration) cancer cells were analysed by flow cytometry with Propidium Iodide staining method. Propidium iodide stains the dead cells and emits fluorescence. The distribution of DNA in each of the phases (G0/G1, G2, S, M) of cell cycle in the treated and control groups was analysed with BD bioscience software. As shown in Figure 8, more cells were accumulated in the sub G1 phase with about 33.9% in HeLa, 56% in HepG2 and 66% in MCF-7 cells. Sub-G1 phase represents the apoptotic cells. Simultaneous to these changes, there was a decline in the percentage of cells in other phases such as G1, S and M, as shown in the DNA histogram.

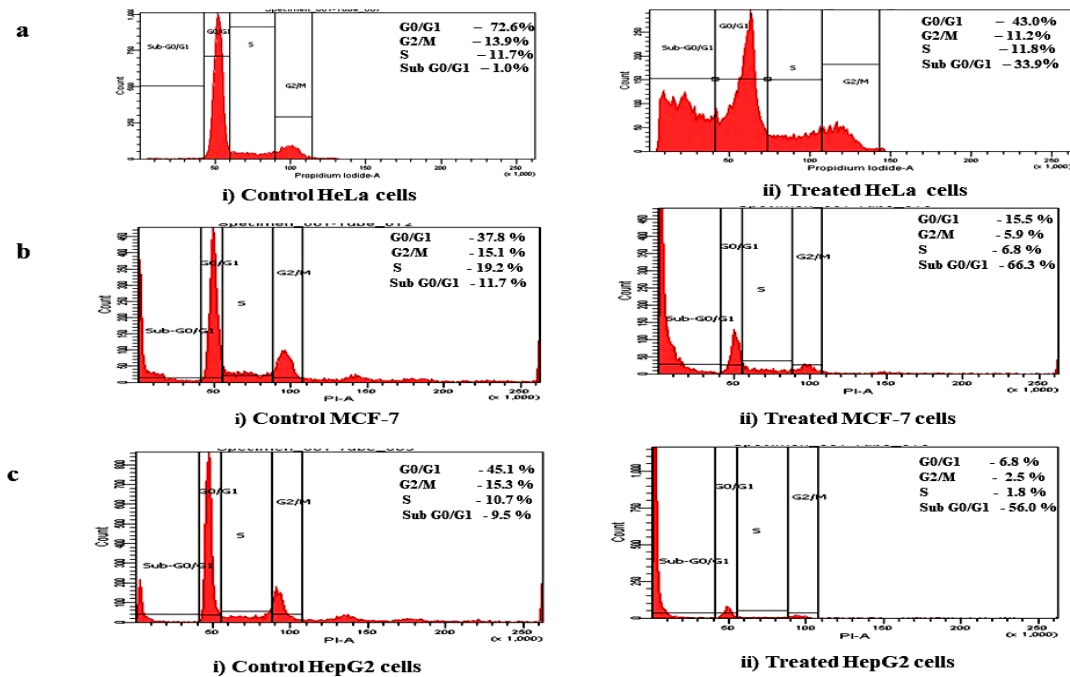


Figure 8. Cell cycle analysis of SF6 treated cancer cell lines through flow cytometry

3.10. Enhanced p53 and Bax gene expressions mediated by SF6 in MCF-7 cancer cells

The level of p53 and Bax gene expressions in MCF-7 cells was measured after 48 hrs of administration of SF6 fraction through qRT PCR. The levels of p53 and Bax genes were set to 1 in untreated control MCF-7 cancer cells and their relative expression is shown in Figure 9. Both p53 and Bax mRNAs were increased in the cells treated with SF6 in comparison with their levels in the negative controls (baseline).

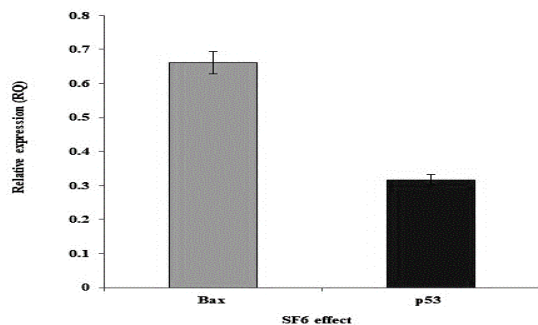


Figure 9. Expression of genes regulating apoptosis in the cells treated with SF6

3.11. S. myriocystum induces anti- angiogenesis effects in chick embryos

Various doses (2.0, 1.0 and 0.5 mg/mL) of extract from *S. myriocystum* were chosen for injecting into the 8th day fertilized chicken eggs for CAM assay. Blood vessel formation was checked after 72hrs of treatment. The main indication of anti-angiogenesis process is the inhibition of secondary and tertiary blood vessel branching regions along with lesser number of blood vessels, which were prominently observed in our experiments (Figure10). Significant inhibition of blood vessel formation and branching growth were observed at all treatment concentrations, with the effect being directly proportional to the increasing dosages of the algal extract. At 0.5 mg/mL concentration 43%, 1.0mg/mL 46% and at 2 mg/mL of treatment concentration 66% of inhibition in blood vessels was seen in comparison with the control eggs (Table 5).

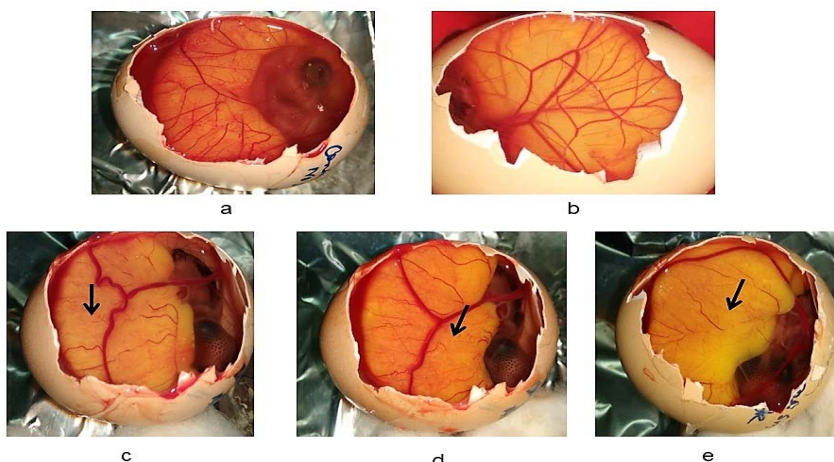


Figure 10. Angiogenesis inhibition by *S. myriocystum* on 8-day old embryos of chicken (a) CAM in control eggs (b) Controls with DMSO treatment (c) 0.5 mg/mL (d) 1.0 mg/mL and (e) 2.0 mg/mL of SF6 treatment. Inhibition of blood vessel branching is indicated by the arrows.

Table 5 Inhibition (%) of blood vessels in chick embryos injected with different concentrations of SF6 as per CAM assay.

Concentration of SF6 (mg/mL)	Blood vessels (Number) in control group	Blood vessels (Number) in treated group	Inhibition in blood vessel formation (%)
0.5	30 ± 5	17 ± 1	43
1.0	30 ± 5	16 ± 1	46
2.0	30 ± 5	10 ± 1.5	66.66

control embryos, more endothelial cells and higher number of large and small blood vessels were seen, while in the treated embryos lesser number of large and small blood vessels were observed, and the effect was dose dependent. Obliteration of endothelial lining of large blood vessel was clearly seen on embryos treated with 2 mg/mL of algal extract. Loss of ectodermal and mesodermal integrity was also noted (Figure11).

3.12. Obliteration of endothelial lining of blood vessels mediated by SF6 as per histopathological observations

The effects of *S. myriocystum* on angiogenesis were analyzed by histochemistry after staining with H&E. In

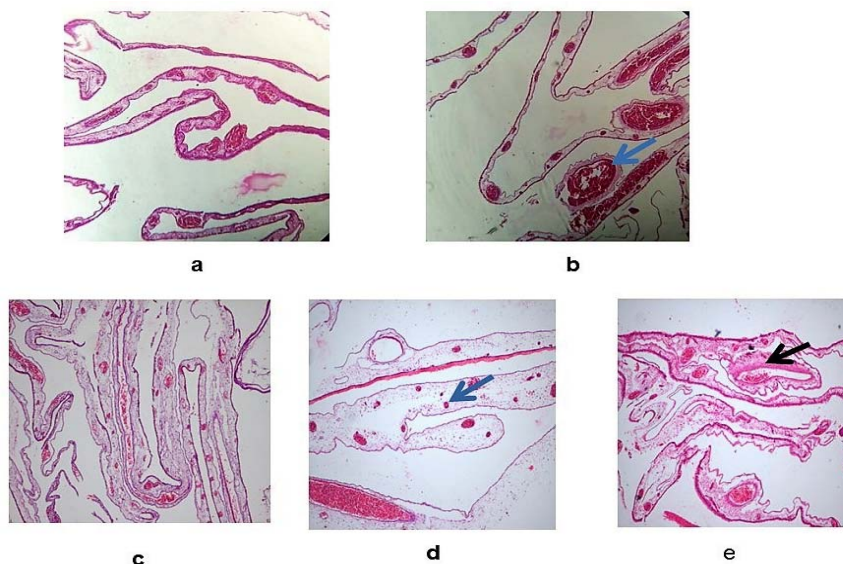


Figure 11. Histopathological examination of CAM layer in chick embryos (40 X) (a) Untreated control (b) DMSO-vehicle control (c) 0.5 mg/mL of SF6 (d) 1.0 mg/mL of SF6 (e) 2.0 mg/mL of SF6 treated groups. Blue arrow shows large and small blood vessels. Black arrows show the destruction of endothelial wall lining of large blood vessels. Scale bar (A- E) - 160X

4. Discussion

Natural compounds show promise towards the treatment of multiple diseases such as cancer. Since ancient times, many countries including India and China have used medicinal plants, microorganisms and marine resources for healing purposes (Liu *et al.*, 2012). Marine macroalgae were found to possess innumerable structurally diverse secondary metabolites with various bioactivities, which are under exploited for therapeutic purposes (Hong *et al.*, 2009). In this regard, the present work was initiated to explore the marine sea weeds, which are unreported for any economic significance, for finding their anti-cancer properties. The focus of the current research was to analyse the marine brown alga *Sargassum myriocystum* for anti-cancer activity, to identify the bioactive compound and analyse its mechanism of action on cancer cells.

The methanol extract of *S. myriocystum* (SM) and the bioactive fraction (SF6) were checked for their anti-cancer effects through MTT assay on cervical, breast and liver cancer cell lines. The results demonstrated that both crude and the SF6 fraction have anti-proliferative activity against cancer cells and the effect was dose and time dependent, with increasing concentrations causing decreased cell viabilities of all cancer cell lines. The IC_{50} value of the TLC purified fraction SF6 was 35 μ g/mL for MCF-7, 46 μ g/mL for HeLa and 37 μ g/mL for HepG2 cells. A similar study on another species, *S. oligocystum*, reported its anti-cancer effects with IC_{50} values as 500 and 400 μ g/mL against Daudi and K562 cell lines, respectively (Zandi *et al.*, 2010). The IC_{50} value of *S. myriocystum* in the present work is lower when compared to this report. Trypan blue assay results showed higher number of non-viable cells in SF6-treated (50 μ g/mL) cancer cells (Table 3), with 1.60x10⁶ cells/mL, 1.48x10⁶ cells/mL and 2.83x10⁶ cells/mL for HepG2, MCF-7 and HeLa cells respectively (control cell concentrations were 3.12x10⁶, 2.53 x10⁶ and 5.76 x10⁶ cells/mL respectively in HepG2, MCF-7 and HeLa). The anticancer activity of a fucoidan

from *Sargassum* sp. was reported as at 1000 μ g/ml concentration (Ale *et al.*, 2011) and the viability of Lewis Lung Carcinoma cells (LLC) was 40 \pm 7% and that of melanoma B16 cells (MC) was 56% at 100 and 200 μ g/mL treatment concentrations. Compared to these reports, the treatment of bioactive fraction SF6 from *S. myriocystum* in the present study (Figure 3) has resulted in lower cell viabilities of 48% in HeLa, 43% in MCF-7 and 44% in HepG2 cells at much lesser concentration (50 μ g/mL), thus proving its higher cytotoxicity towards the cancer cells. The same concentration of SF6 indicated its safety to normal healthy lymphocytes, with their viability being 99-100% at all of the time intervals.

Further evidence for the direct cytotoxicity caused by SF6 to cancer cells was provided by LDH assay. LDH release is used to assess the extent of toxicity and damage in cells and tissues due to traumatic exposures (Stoddart, 2011). The assay is based on the principle that, an increase in the production of formazan in the culture supernatant is directly proportional to the extent of cytotoxicity caused to the cells by any external agent. The current study results showed 18%, 35% and 27.1% cytotoxicity to HepG2, MCF-7 and HeLa cells treated with SF6 respectively, thus indicating the direct cytotoxic effect of SF6, apart from its anti-proliferative effects. The LDH mediated cytotoxicity was negative on normal lymphocytes (Figure 6), indicating the safety of SF6 to non-cancerous cells.

Apoptosis is a key indicator of programmed cell death resulting in changes in the morphological features such as chromatin condensation, membrane blebbing, DNA fragmentation, poly (ADPribose) polymerase (PARP) cleavage and increased caspase enzyme activity (Smyth *et al.*, 2002). The mechanism of cell death in the SF6-treated cancer cells in the current study was indeed due to apoptosis, as proven by the results of DNA fragmentation pattern on agarose gel (Figure 7) and increased caspase 3,7,10 activities (Table 4) in HepG2, MCF-7 and HeLa cancer cells (caspases being the key enzymes regulating apoptosis in cells). Apoptosis induction in the SF6-treated cancer cells was further supported by the gene expression

studies through qRT-PCR method in MCF-7 cells. As MCF-7 cancer cell line was found to be highly susceptible to SF6 treatment by most of the assay results such as higher caspase activation, greater fragmentation of DNA, higher LDH cytotoxicity, higher percentage of apoptotic cells (66%) in subG1 phase than both HeLa and HepG2 cells, we chose to perform gene expression studies in this cell line. Both p53 and Bax mRNA levels were elevated in MCF-7 cells in comparison with the untreated control cells (Figure 9). It is well known that p53 is mutated in more than 50% of all cancers in humans, and p53 tightly regulates the progression of cells through the DNA replication phase (Bell et al., 2002). Elevated p53 in the present study might be triggering the death of the SF6-treated cancer cells. Bax is a pro-apoptotic gene, which was reported to be down regulated in tumour cells, by which they escape apoptosis and are able to grow (Finucane et al., 1999). The enhanced expression of Bax by SF6 treatment in the current study proves the apoptotic and anticancer potential of *S. myriocystum* fraction.

Analysis of cell cycle stages is an important approach for understanding the effect of drug treatment to cancer cells. In the present study, when the cell cycle stages of MCF-7, HepG2 and HeLa cells were assessed by flow cytometry, it was observed that higher percentage of cells were accumulated in the sub-G1 phase in MCF-7 and HepG2 cells and thereby lead to the death of these cells (Figure 8). Sub-G1 phase indicates that the population of cells accumulated in the apoptotic phase (Grana and Reddy, 1995). In HeLa cells, higher percentage of cells were found in G0/G1 phase, and thereby suggesting that G0/G1 phase arrest led to the apoptosis of HeLa cells. Thus, the results confirm SF6 to be a strong inducer of apoptosis in cancer cells.

Cancer cells get nourishment for their uncontrolled growth by neo- angiogenesis. An ideal anti-cancer agent should be able to inhibit the formation of new blood vessels under *in-vivo* conditions. Chick embryos grow by forming newer blood vessels every day and could be considered suitable for demonstrating anti-angiogenesis experiments. In the present study, the fraction SF6 from *S. myriocystum* demonstrated potent anti-angiogenesis effects on chick embryos (Figures 10 & 11), proving to be efficient anti-cancer compound.

The promising anti-cancer traits of SF6 prompted us to characterize this fraction through GC-MS. As per this GC-MS study, it was found that dacarbazine (imidazole carboxamide) and ellagic acid are present in *S. myriocystum* fraction. Dacarbazine (imidazole carboxamide organic compound) is used as an anti-tumor drug for metastatic melanoma, sarcoma, Hodgkin lymphoma and effectively killing the cancer cells by adding alkyl groups to the DNA (Chen et al 2008; Sarkar et al., 2013). Imidazole compounds are widely found in marine resources especially marine sponges (Ahond et al., 1988; Dunbar et al., 2000). Imidazole based anti-cancer drugs have special properties to destroy the cancer cells by first inhibiting DNA synthesis and stopping cell growth and division. Apart from dacarbazine, ellagic acid is also one of the compounds observed in the bioactive fraction SF6. Ellagic acid is a polyphenol compound, belonging to the ellagitannin family and derivative of gallic acid (Milivojevic et al., 2011; Ribeiro et al., 2007; Cai et al., 2017). Ellagic acid is reported mainly from fruits and

vegetables and has been reported as antioxidant, antimicrobial and anti-cancer compound (Shahidi et al., 1992; Sanchez et al., 1999). Polyphenol group of compounds are abundantly found in seaweeds (Arguelles, 2020).

Molecular ion fragments related to dacarbazine and ellagic acid found from the ESI-MS results were observed even among the compounds obtained from GC-MS results. Further we found that neither the extract nor the bioactive fraction (SF6) from *S. myriocystum* have any toxicity to normal blood lymphocytes. We assume that the presence of dacarbazine and ellagic acid in *S. myriocystum* along with other unidentified compounds might be responsible for its anti-cancer activity and they might be acting synergistically towards inhibiting cancer cell proliferation.

S. myriocystum can be used for edible purposes also, as per reports (Kaliaperumal et al., 1995; Ogawa, et al., 2004; Shynu et al., 2013), and has the potential for the development of an anti-cancer therapeutic in the future, as shown through the results of the current study. Other species of *Sargassum* were earlier reported for various biological activities including anti-cancer activity (Khanavi et al., 2010; Ye et al., 2008; Chen et al., 2012). But with respect to *S. myriocystum*, the current research work reports for the first time, as far as our knowledge and available literature, its anti-cancer potential along with its mechanism of anti-cancer activity. As *Sargassum* group of marine algae are edible with nutritional and medicinal properties, through the current study results it can be concluded that *S. myriocystum* shows great promise towards anti-cancer drug developmental studies in the future.

5. Conclusions

Based on the current study results, it can be concluded that the brown marine alga, *S. myriocystum*, has promising anti-cancer potential as demonstrated by anti-angiogenesis and apoptogenic properties and hence can be taken up for further characterization, pre-clinical and clinical studies towards drug development. The therapeutic potential of this edible sea weed opens up further avenues for its commercial exploitation towards a safer alternative therapy for cancer through future research in this regard.

6. Declarations

Funding

Not applicable

Conflicts of interest/Competing interests

The authors disclose that they do not have any conflicts of interest

Ethics approval

Not applicable

Consent to participate

The written consent from healthy human volunteers was documented for isolation of lymphocytes.

Consent for publication

Not applicable

Availability of data and material

All data generated during this study are either included in this published article or available from the corresponding author on request.

Code availability

Not applicable

Authors' contributions

SP and VKN designed the experiments. SP performed all experiments and interpreted the data and wrote the first draft of the manuscript. SP and VKN contributed substantially to the revisions. Both authors read and approved the final manuscript.

Acknowledgements

The authors are grateful to Jain (Deemed to be University) for providing the fellowship and for the infrastructural facilities to carry out the work. The authors are grateful to Dr. Karuppanan Eswaran, Senior Principal Scientist in Marine Algal Research Station (CSMCRIMARS), Mandapam camp, Ramanathapuram, for helping in identification of algal samples. The authors are grateful to Dr. Byregowda, Director of Institute of Animal Health and Veterinary medicine, Bangalore for providing facilities to carry out chick embryo assay in his laboratory. The authors would also like to thank Dr. Sugana Rao, Professor in the Department of Veterinary Pathology, Veterinary College, Hebbal, Bangalore for helping to interpret the Histopathology slides.

References

- Agardh, JG. 1848. Species genera et ordines Algarum: Vol. I.
- Ahond A, Bedoya ZM, Colin M, Laboute P, Lavelle F, Laurent D, Poupat C, Pusset J, Pusset M and Thoison O. 1988. Girolline, a new anti-tumor substance extracted from the sponge, *Pseudaxinyssacantharella* n. sp. (Axinellidae). *Reports from the Academy of Sciences. Series 2: Mechanics*, **302**: 145–148.
- Ale MT, Maruyama H, Tamauchi H, Mikkelsen JD, Meyer AS. 2011. Fucoidan from *Sargassum* sp. and *Fucusvesiculosus* reduces cell viability of lung carcinoma and melanoma cells in vitro and activates natural killer cells in mice in vivo. *Int J Biol Macromol*, **49**: 331-336.
- Arguelles EDLR. 2020. Evaluation of Nutritional Composition and In vitro Antioxidant and Antibacterial Activities of *Codium intricatum* Okamura from Ilocos Norte (Philippines). *Jordan J Biol Sci*, **13**: 375-382.
- Badrinathan S, Shiju TM, Suneevasharonchrista A, Arya R and Pragasam V. 2012. Purification and structural characterization of sulfated polysaccharide from *Sargassum myriocystum* and its efficacy in scavenging free radicals. *Indian J Pharm Sci*, **74**: 549-555.
- Bell S, Klein C, Müller L, Hansen S and Buchner J. 2002. p53 contains large unstructured regions in its native state. *J mol Biol*, **322**: 917-927.
- Cai Y, Zhang J, Chen NG, Shi Z, Qiu J, He C and Chen M. 2017. Recent advances in anticancer activities and drug delivery systems of tannins. *Med Res Rev*, **37**: 665-701.
- Cerna M. 2011. Seaweed proteins and amino acids as nutraceuticals. *Adv Food Nutr Res*, **64**: 297-312.
- Chandini SK, Ganesan P, Suresh P and Bhaskar N. 2008. Seaweeds as a source of nutritionally beneficial compounds—a review. *J Food Sci Technol*, **45**: 1–13.
- Chen J, Wang Z, Lu Y, Dalton JT, Miller DD and Li W. 2008. Synthesis and antiproliferative activity of imidazole and imidazoline analogs for melanoma. *Bioorg Med Chem Lett*, **18**: 3183-3187.
- Chen X, Nie W, Yu G, Li Y, Hu Y, Lu J, et al. 2012. Antitumor and immunomodulatory activity of polysaccharides from *Sargassum fusiforme*. *Food Chem Toxicol*, **50**: 695–700.
- Coombe DR, Parish CR, Ramshaw IA and Snowden JM. 1987. Analysis of the inhibition of tumour metastasis by sulphated polysaccharides. *Int J Cancer*, **39**: 82-88.
- Dunbar DC, Rimoldi JM, Clark AM, Kelly M and Hamann MT. 2000. Anti-cryptococcal and nitric oxide synthase inhibitory imidazole alkaloids from the calcareous sponge *Leucetta cf. chagosensis*. *Tetrahedron*, **56**: 8795–8798.
- Finucane DM, Waterhouse NJ, Amarante-Mendes GP, Cotter TG, Green DR. 1999. Collapse of the inner mitochondrial transmembrane potential is not required for apoptosis of HL60 cells. *Exp Cell Res*, **251**: 166-174.
- Gade R, Tulasi MS and Bhai VA. 2013. Seaweeds: a novel biomaterial. *J Food Sci Technol*, **5**: 975-1491.
- Gamal-Eldeen AM, Ahmed EF, Abo-Zeid MA. 2009. In vitro cancer chemopreventive properties of polysaccharide extract from the brown alga, *Sargassum latifolium*. *Food Chem Toxicol*, **47**: 1378–1384.
- Graña X and Reddy EP. 1995. Cell cycle control in mammalian cells: role of cyclins, cyclin dependent kinases (CDKs), growth suppressor genes and cyclin-dependent kinase inhibitors (CKIs). *Oncogene*, **11**: 211-220.
- Gupta S and Abu-Ghannam N. 2011. Bioactive potential and possible health effects of edible brown seaweeds. *Trends Food Sci Technol*, **22**: 315-326.
- Hanahan D and Weinberg RA. 2011. Hallmarks of cancer: the next generation. *Cell*, **144**: 646-674.
- Hardeep S, Tuli S, Sandhu, Anil KS and Puneet G. 2014. Anti-angiogenic activity of the extracted fermentation broth of an entomopathogenic fungus *Cordyceps millitaris*. *Int J Pharm Pharm Sci*, **6**: 581-583.
- Hong DD, Hien HM, Son PN. 2007. Seaweeds from Vietnam used for functional food, medicine and biofertilizer. *J Appl Phycol*, **19**: 817-826
- Kaliaperumal NS and Kaliamuthu RJR. 1995. Economically important seaweeds. *CMFRI special publication*, **62**: 1-35.
- Khanavi M, Nabavi M, Sadati N, Shams AM, Sohrabipour J, Nabavi SM, et al. 2010. Cytotoxic activity of some marine brown algae against cancer cell lines. *Biol Res*, **43**: 31–7.
- Kim SK and Van Ta Q. 2011. Potential beneficial effects of marine algal sterols on human health. *Adv Food Nutr Res*, **64**: 191-198
- Kirchner JG. 1973. Thin-layer chromatographic quantitative analysis. *Journal of Chromatography A*, **82**: 101-115.
- Liu L, Heinrich M, Myers SP and Dworjanyn SA. 2012. Towards a better understanding of medicinal uses of the brown seaweed *Sargassum* in Traditional Chinese Medicine: A phytochemical and pharmacological review. *J Ethnopharmacol*, **142**: 591-619.
- MacArtain P, Gill CI, Brooks M, Campbell R and Rowland IR. 2007. Nutritional value of edible seaweeds. *Nutrition reviews*, **65**: 535-543.

- Milivojević J, Maksimović V, Nikolić M, Bogdanović J, Maletić R and Milatović D. 2011. Chemical and antioxidant properties of cultivated and wild *Fragaria* and *Rubus* berries. *J Food Qual*, **34**: 1-9.
- Misurcova L, Skrovankova S, Samek D, Ambrozova J and Machu L. 2012. Health benefits of algal polysaccharides in human nutrition *Adv Food Nutr Res*, **66**: 75-145.
- Mosmann T. 1983. Rapid colorimetric assay for cellular growth and survival: application to proliferation and cytotoxicity assays. *J Immunol Methods*, **1**: 55-63.
- Novaczek I. 2001. A Guide to the Common Edible and Medicinal Sea Plants of the Pacific Islands. Community Fisheries Training Pacific Series 3A. Supplementary Guide to Sea Plants: Pacific Series 3.
- Ogawa A, Murakami C, Kamisuki S, Kuriyama I, Yoshida H, Sugawara F and Mizushima Y. 2004. Pseudodefectusin, a novel isochroman derivative from *Aspergillus pseudodefectus*, a parasite of the sea weed, *Sargassum fusiform*, as a selective human cancer cytotoxin. *Bioorg Med Chem*, **14**: 3539-3543.
- Pazarowski P and Darzynkiewicz Z. 2004. Analysis of cell cycle by flow cytometry. *Methods Mol Bio*, **281**: 301-311.
- Rashan L, Hakkim FL, Fiebig HH, Kelter G, Merfort I, Al-Buloshi M and Hasson SSAA. 2018. *In vitro* Anti-Proliferative Activity of the *Rubia tinctorum* and *Alkanna tinctoria* Root Extracts in Panel of Human Tumor Cell Lines. *Jordan J Biol Sci*, **11**: 489 - 494.
- Ribeiro B, Valentão P, Baptista P, Seabra RM and Andrade PB. 2007. Phenolic compounds, organic acids profiles and antioxidative properties of beefsteak fungus (*Fistulina hepatica*). *Food Chem Toxicol*, **45**: 1805-1813.
- Sambrook J, Fritschi EF and Maniatis T. 1989. Molecular cloning: a laboratory manual, Cold Spring Harbor Laboratory Press, New York.
- Sánchez-Moreno C, Larrauri JA and Saura-Calixto F. 1999. Free radical scavenging capacity and inhibition of lipid oxidation of wines, grape juices and related polyphenolic constituents. *Food Res Int*, **32**: 407-412.
- Sarkarzadeh H, Miri R, Firuzi O, Amini M, Razzaghi-Asl N, Edraki N and Shafiee A. 2013. Synthesis and antiproliferative activity evaluation of imidazole-based indeno [1, 2-b] quinoline-9, 11-dione derivatives. *Arch Pharm Res*, **36**: 436-447.
- Shahidi F, Janitha PK and Wanasundara PD. 1992. Phenolic antioxidants. *Crit Rev Food Sci Nutr*, **32**:67-103.
- Shynu SP, Shibu S and Jayaprakash V. 2013. The economically valuable seaweeds of Thirumullavaram, south west coast of Kerala. *Journal of Aquatic Biology & Fisheries*, **2**: 133- 237.
- Smit AJ. 2004. Medicinal and pharmaceutical uses of seaweed natural products: a review. *J Appl phycol*, **16**: 245-262.
- Smyth PG, Berman SA and Bursztajn S. 2002. Markers of apoptosis: methods for elucidating the mechanism of apoptotic cell death from the nervous system. *Biotechniques*, **32**: 648-665.
- Stoddart MJ. 2011. Cell viability assays: introduction. In Mammalian cell viability Humana Press: 1-6.
- Strober W. 2001. Trypan blue exclusion test of cell viability. Current protocols in immunology, John Wiley & Sons **1**:77.
- Weyermann J, Lochmann D and Zimmer A. 2005. A practical note on the use of cytotoxicity assays. *Int J Pharm*, **288**: 369- 376.
- Willstätter R and Page HJ. 1914. Untersuchungenüber Chlorophyll. XXIV. Über die Pigmente der Braunalgen. *Justus Liebigs Annalen Der Chemie*, **404**: 237-271.
- Ye H, Wang K, Zhou C, Liu J and Zeng X. 2008. Purification, antitumor and antioxidant activities *in vitro* of polysaccharides from the brown seaweed *Sargassum pallidum*. *Food Chem*, **111**:428-432.
- Zandi K, Ahmadzadeh S, Tajbakhsh S, Rastian Z, Yousefi F, Farshadpour F, et al. 2010. Anticancer activity of *Sargassum oligocystum* water extract against human cancer cell lines. *Eur Rev Med Pharmacol Sci*, **14**: 669-673.
- Zhuang C, Itoh H, Mizuno T and Ito H. 1995. Antitumor active fucoidan from the brown seaweed, umitoranoo (*Sargassum thunbergii*). *Biosci Biotechnol Biochem*, **59**: 563-567.
- Zong A, Cao H and Wang F. 2012. Anticancer polysaccharides from natural resources: a review of recent research. *Carbohydr Polym*, **90**:1395-1410.

Optimization of Bioremediation Enhancement Factors in an Aged Crude Oil Polluted Soil.

Lawrence Edemhanria^{1,*} and Christopher Chijindu Osubor²

¹Chemical Sciences Department, Samuel Adegboyega University, Ogwa, Nigeria; ²Department of Biochemistry, University of Benin, Benin City, Nigeria

Received: April 7, 2021; Revised: July 8, 2021; Accepted: July 15, 2021

Abstract

Bioremediation as an environmentally friendly method of restoration of crude oil polluted soil is influenced by several conditions. This study was designed to optimize some bioremediation enhancement factors including soil moisture content, agitation or mixing and nutrient ratio. Baseline properties of the soil samples were determined using standard analytical procedures. The crude oil polluted soil studied was seeded with mixed microbial consortium and differentially supplemented with inorganic nitrogen and phosphorus using carbon, nitrogen and phosphorus ratios 100:10:1 and 100:2:0.2. The initial sample moisture content was adjusted to 80% of its water holding capacity. Subsequently, moisture content adjustment and mixing were done at different intervals while the experiment lasted. Residual total petroleum hydrocarbon was measured every 6 days. Mixing the set-up every three days and moisture content adjustment every six days resulted in more efficient crude oil attenuation in the contaminated soil while carbon, nitrogen and phosphorus ratio 100:2:0.2 yielded statistically significant ($p < 0.05$) higher crude oil degradation ($90.99 \pm 0.02\%$) over 100:10:1 ratio ($78.15 \pm 0.03\%$) after 36 days of remediation. The results obtained suggest that use of optimized site-specific conditions would enhance the microbial driven process of soil attenuation.

Keywords: Bioremediation, crude oil, moisture content, nutrient ratio, optimization, polluted soil.

1. Introduction

Oil exploration and other related activities remain a global concern because of the attendant environmental degradation and negative effect on the ecosystem (Ugochukwu and Ertel, 2008; Sam *et al.*, 2017; Ite *et al.*, 2018). Several approaches including physical, chemical and biological techniques are in place to manage this associated pollution (Siles and Margesin, 2018). However, biological remediation or bioremediation is preferred as it is reliable, cheap, efficient and eco-compatible (Azubuike *et al.*, 2016; Speight and El-Gendy, 2018). Indigenous microbes with potential to transform pollutants play an important role in this natural process of soil restoration (Azubuike *et al.*, 2016; Chauhan *et al.*, 2017).

A number of factors influence the optimum functioning of these microbes with effect on the rate of the bioremediation process. Some of these conditions include the nature of the pollutants, pH, temperature, nutrients, aeration, moisture, the impacted soil type and appropriate density of oleophilic microbes (Macaulay, 2015; Azubuike *et al.*, 2016; Varjani, 2017; Speight and El-Gendy, 2018). Microbes require nutrients like carbon, nitrogen and phosphorus to support their metabolic activities (Bamforth and Singleton, 2005; Ghaly *et al.*, 2013). Crude oil pollution leads to depletion of available nitrogen and phosphorus in impacted soil (Ghaly *et al.*, 2013). The introduction of the depleted nutrients stimulates the

activity of soil microbes during bioremediation (Walworth *et al.*, 2007; Varjani, 2017). These limiting nutrients must be introduced to the soil at optimum levels to enhance biodegradation; nitrogen supplied at high concentration can be inhibitory to microbial activity (Huesemann, 1994; Walworth *et al.*, 2007, Onwosi *et al.*, 2018).

Since the biotransformation of crude oil in polluted soil occurs mainly by aerobic process with molecular oxygen playing important role, oxygen deficiency reduces the rate of bioremediation (Jain *et al.*, 2011). Periodic tilling of the impacted soil helps to increase microbial activity due to enhanced aeration, uniform distribution of nutrients and also the pollutants (Azubuike *et al.*, 2016). Water in soil promotes microbial metabolism, diffusion of oxygen, nutrients and degradation products (Tibbett *et al.*, 2011). Very high moisture content in soils with low permeability is limiting to bioremediation as it reduces availability of oxygen (Tibbett *et al.*, 2011). Soil pH influences the ability of microbes to degrade crude oil (Varjani, 2017). Extremes of pH inhibit microbial activity with negative impact on the rate of bioremediation (Leahy and Colwell, 1990). A soil pH range of 6-8 is reported to be optimum for microbial crude oil degradation (Macaulay, 2015). Fungi are reported to tolerate acidic conditions better than bacteria (Leahy and Colwell, 1990). Soil permeability also affects the process of bioremediation; this is determined by the size of soil particles (Atlas, 1995; Macaulay, 2015). Soil with low permeability such as clay retains the crude oil at the surface resulting in low rate of biodegradation

* Corresponding author. e-mail: ledemhanria@gmail.com.

while highly permeable soil such as sand is more susceptible to leaching of the pollutant to low oxygen region of the soil (Macaulay, 2015).

Within the limits of our literature surveyed, there are no reports of specified optimal conditions for bioremediation in the Niger Delta region of Nigeria; consequently, some factors including aeration (mixing), moisture content and nutrients were investigated in this study to establish site-specific conditions that would enhance the potentials of indigenous microbes in the attenuation of aged crude oil polluted soil in this area.

2. Materials and Methods

2.1. Soil Sample Collection and Preparation

Soil samples were collected from Koko in Warri North Local Government Area of Delta State. The community is potentially exposed to environmental pollution arising from the industrial activities of a number of companies operating in the oil sector. Crude oil polluted soil sample was collected at a depth of 0-50 cm from a crude oil waste handling area while uncontaminated soil sample was collected from a fallow area without any history of crude oil pollution. The composite soil samples were aggregated, taken in sterile polythene bags, kept in ice packs and taken to the laboratory for use within twenty-four hours. The contaminated and uncontaminated soil samples were air-dried for five days and sieved using a 2 mm sieve.

2.2. Baseline Characterization of Soil Samples

Standard analytical procedures were used to determine the following physicochemical properties of the soil samples. Soil temperature was measured on-site and in the laboratory using a digital probe thermometer: H-9283 Multi-Thermometer (Almaw *et al.*, 2017), gravimetric method of Reynolds (1970) was used for moisture content (MC), particle size analysis by hydrometer method (Bouyoucos, 1962), pH by method of McLean (1982), electrical conductivity by method of Richards (1954), porosity and bulk density by weighing bottle method (FAO, 1980), water holding capacity (WHC) by gravimetric method (FAO, 1980), total organic carbon by wet oxidation method (Walkley and Black, 1934), total nitrogen by modified Kjeldahl method (FAO, 1980) and available phosphorus by modified sodium bicarbonate extraction (Wantanabe and Olsen, 1965; Olsen and Sommers, 1982).

2.3. Determination of Total Petroleum Hydrocarbon in Contaminated Soil

Spectrophotometric method with n-hexane as the extraction solvent was used (USEPA, 2000; Urum *et al.*, 2005, Akpe *et al.*, 2015). Five grams contaminated soil sample was weighed into a Nalgene bottle with 5 g sodium sulphate and shaken vigorously to mix. Thereafter, 10 ml n-hexane was added; the bottle was covered and shaken vigorously for 5 min. The soil extract was carefully decanted into a conical flask and covered with foil paper. The extraction process was repeated three times with addition of 10 ml n-hexane to the Nalgene bottle containing the contaminated soil and shaken vigorously for 5 minutes. All extracts were pooled together and transferred to a 50 ml volumetric flask. The volume of the extract in the volumetric flask was adjusted to 50 ml with

n-hexane. An aliquot of 10 ml soil extract was centrifuged at 3000 rpm for 10 minutes. Absorbance of supernatant was estimated at 400 nm using a spectrophotometer. The concentration of crude oil in the extract was estimated from n-hexane/crude oil standard curve using the absorbance obtained according to Equation 1.

$$\text{TPH (mg/kg)} = \frac{C \times V \times \text{DF}}{W} \quad (1)$$

Where: C = concentration of crude oil in the extract estimated from the standard curve. V = Total volume of the n-hexane/crude oil extract. DF = Dilution factor. W = Mass of soil used

2.4. Daily Moisture Content Monitoring

Three (3) kilograms each of contaminated soil was weighed into 7 plastic containers. The MC of the soil was adjusted to 60 – 80% of WHC. The containers were kept in the laboratory under ambient condition and subjected to agitation daily. A container was used to estimate MC daily by gravimetric method (Reynolds, 1970) till MC was ≤ 60% of sample WHC.

2.5. Evaluation of Effect of Agitation and Moisture Content on Crude Oil Degradation in the Contaminated Soil

Three (3) kilograms each of polluted soil was weighed into 4 plastic containers per group (5 groups) and control. Each container was amended with microbial consortium, composed of all microbial isolates with >50% crude oil degradation potential from our previous work (Edemhanria *et al.*, 2020), and nutrient at carbon, nitrogen, phosphorus ratio 100:2:0.2. Urea was used as source of nitrogen while potassium dihydrogen phosphate supplied phosphorus. Sample MC was adjusted to 80% of WHC. Each group was subjected to the following treatment at the specified interval indicated in Table 1. Crude oil degradation was measured as residual total petroleum hydrocarbon at 6 days interval for 24 days following the procedure described earlier.

Table 1. Treatment groups and intervals investigated

Group	Treatment Interval (days)	
	Agitation	Moisture Adjustment
A1	Daily	3
A2	3	3
A3	Daily	6
A4	6	6
A5	3	6
Control	None	None

2.6. Effect of Carbon, Nitrogen and Phosphorus Ratio on Crude Oil Degradation in Soil

Three (3) kilograms each of crude oil polluted soil was weighed into 7 plastic containers per group (2 groups) and subjected to the following treatment: Group one was treated with microbial consortium and supplemented with nutrient at carbon, nitrogen and phosphorus ratio 100:10:1 while Group two had microbial consortium with nutrient supplementation at ratio 100:2:0.2. The MC of the contaminated soil sample was adjusted to 60 – 80% field WHC for both groups. Each container was agitated every 3 days and moisture adjustment done every 6 days in both groups. The experiment lasted for 36 days with residual TPH evaluated every 6 days.

2.7. Data Analysis

All experiments were performed in triplicates, and data were analyzed using International Business Machines (IBM) Statistical Package for the Social Sciences (SPSS) Statistics 23 software for Windows. The data were presented as mean \pm standard error (SE). One-way Analysis of Variance (ANOVA) was used in comparing the means followed by Duncan's Multiple Range (DMRT) Post Hoc test. Student's *t* test was used to compare means for the nutrient ratios studied. $P < 0.05$ was taken as statistically significant.

3. Results and Discussion

The soil is a key natural resource and part of the terrestrial ecosystem; it serves as habitat to an enormous diversity of organisms such as microorganisms, insects, earthworms and other invertebrates while also supporting plant growth and other agricultural practices (Dominati *et al.*, 2010; Blum, 2013). However, the sustainable use of the soil as a key natural resource and its ability to function can be affected by a number of activities including pollution (Polyak *et al.*, 2018). This is particularly true of Nigeria's Niger Delta where soil pollution from crude oil exploration and utilization is a major issue (Sam *et al.*, 2017; Ite *et al.*, 2018). Baseline site characterization is useful in the identification of pollutants and establishing their effect on the properties of the impacted soil (Azubuike *et al.*, 2016). In this study, the baseline data presented in Table 2 confirmed crude oil pollution with TPH level higher than the regulatory intervention limit of 5000 mg/kg in Nigeria (DPR, 2002). Some soil properties are affected by crude oil in an impacted-soil (Bosma *et al.*, 1997; Michel and Fingas, 2016). This possibly explains the higher values for electrical conductivity, bulk density and WHC in the polluted soil compared to the uncontaminated soil (Barua *et al.*, 2011). Other properties like pH, porosity, total nitrogen and available phosphorus were higher in the uncontaminated soil compared to the contaminated sample. The sandy nature, porosity and the pH of the contaminated soil supports leaching and possible contamination of the ground water (Blum, 2013; Michel and Fingas, 2016). However, the low silt and clay content of the soil is suitable for microbial activity that drives bioremediation (Vidali, 2001). The acidic nature of the soil in Koko area due to petroleum hydrocarbon contamination corroborates report by Imasuen *et al.* (2014). The leaching of the basic cations due to heavy annual rainfall in the area (Imasuen *et al.*, 2014) and production of organic acid intermediates from microbial action on the oil contributed to the acidic pH (Nwachukwu and Ugoji, 1995; Barua *et al.*, 2011).

Table 2: Physicochemical properties of soil samples

Parameter	Contaminated	Uncontaminated
Particle size distribution		
Clay (%)	4.23 \pm 0.14	4.26 \pm 0.15
Silt (%)	1.78 \pm 0.19	1.64 \pm 0.26
Sand (%)	94.00 \pm 0.30	94.47 \pm 0.34
pH	5.55 \pm 0.05	6.68 \pm 0.31
Temperature (°C)	28.70 \pm 0.12	28.93 \pm 0.30
Electrical Conductivity (μ S/cm)	133.00 \pm 3.61	74.53 \pm 2.85
Bulk Density (g/cm ³)	1.31 \pm 0.02	1.24 \pm 0.02
Moisture Content (%)	9.44 \pm 0.09	7.15 \pm 0.37
Porosity (%)	50.72 \pm 0.76	53.21 \pm 0.65
Water Holding Capacity (%)	24.26 \pm 0.63	9.47 \pm 0.44
Total Organic Carbon (%)	2.87 \pm 0.49	0.61 \pm 0.16
Total Nitrogen (mg/kg)	265.87 \pm 3.41	289.18 \pm 1.73
Available Phosphorus (mg/kg)	40.47 \pm 2.38	48.07 \pm 2.09
Total Petroleum Hydrocarbon (mg/kg)	9906.40 \pm 1.48	ND

Values are mean \pm SE. ND is not determined.

3.1. Effect of Agitation and Moisture Content on Crude Oil Degradation in Polluted Soil

The various combinations of mixing or agitation and moisture content replenishment studied yielded different results for residual total petroleum hydrocarbon performed every 6 days. The results are presented in Figure 1. All treatment groups evaluated were significantly different from the control ($p < 0.05$) with higher crude oil degradation. However, A5 with 79.34 \pm 0.03% crude oil degradation following sample agitation every 3 days and moisture adjustment every 6 days for 24 days was more efficient, and so it was used in further experiments in the study. The daily monitoring of the MC of the contaminated soil sample after adjustment to about 80% of field WHC revealed that this reduced to 57.34 \pm 0.72% on day 5 at room temperature (Table 3). The minimum benchmark WHC for optimum bioremediation used in this study was 60% (Bahmani *et al.*, 2018).

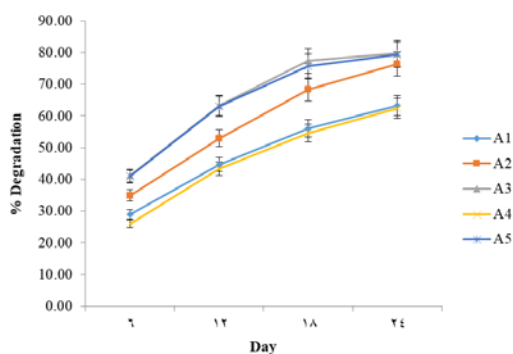
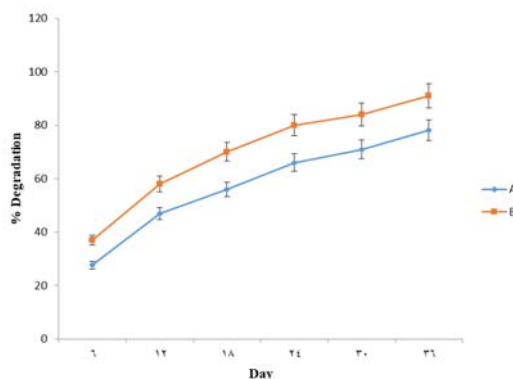
3.2. Effect of CNP Ratio on Crude Oil Degradation in Polluted Soil

The CNP ratio 100:10:1 that is widely reported in literature to be the optimum nutrient ratio for microbial transformation of crude oil in soil was compared with CNP ratio 100:2:0.2. The later resulted in 90.99 \pm 0.02% against 78.15 \pm 0.03% of the former (Figure 2) after 36 days. This difference was significant ($p < 0.05$).

Table 3. Daily moisture content monitoring in contaminated soil sample after moisture adjustment

Day	Moisture Content (%)	Water Holding Capacity (%)
	9.44 ± 0.09*	38.91 ± 0.38
0	19.49 ± 0.10	80.33 ± 0.42
1	19.01 ± 0.19	78.34 ± 0.78
2	18.46 ± 0.10	76.09 ± 0.42
3	16.96 ± 0.30	69.92 ± 1.26
4	15.05 ± 0.10	62.03 ± 0.41
5	13.91 ± 0.17	57.34 ± 0.72
6	12.48 ± 0.21	51.42 ± 0.85

Values are mean ± SE of triplicate determinations. *Moisture content of sample before adjustment to 80% of water holding capacity. Baseline water holding capacity = 24.26 ± 0.63%.

**Figure 1.** Effect of agitation and moisture adjustment on crude oil degradation. A1 (daily agitation with moisture adjustment every 3 days), A2 (agitation and moisture adjustment every 3 days), A3 (daily agitation and moisture adjustment every 6 days), A4 (agitation and moisture adjustment every 6 days), A5 (agitation every 3 days and moisture adjustment every 6 days).**Figure 2:** Effect of carbon, nitrogen and phosphorus ratio on crude oil degradation in polluted soil. A (100:10:1) and B (100:2:0.2).

Agitation (mixing) every 3 days and moisture content adjustment every 6 days resulted in more efficient crude oil degradation in this research. These strategies have been reported to enhance oil degradation (Azubuike *et al.*, 2016). Periodic tilling or agitation of soil increases microbial activity during bioremediation through improved aeration, increased nutrient availability and also pollutants (Tibbett *et al.*, 2011; Azubuike *et al.*, 2016). Adequate water is needed for growth and mobility of microbes as well as movement of nutrients, oxygen and waste products

(Bahmani *et al.*, 2018). The addition of water at regular intervals helps to compensate for moisture loss due to evaporation and maintain optimum level of moisture content in the soil during bioremediation (Bahmani *et al.*, 2018).

Microbes in soil require nutrients like carbon, nitrogen and phosphorus to support their metabolic activities (Bamforth and Singleton, 2005; Ghaly *et al.*, 2013). The indigenous oleophilic microbes in a crude oil polluted soil mineralize the pollutant as source of carbon to bring about a distortion of the nutrient ratio following depletion of available nitrogen and phosphorus in the impacted soil with time (Ghaly *et al.*, 2013). This is responsible for the lower values of total nitrogen and available phosphorus obtained in this study for the polluted soil (Table 2). The addition of the limiting nutrients (nitrogen and phosphorus) to the crude oil polluted soil stimulates microbial metabolic activities during the remediation process (Walworth *et al.*, 2007; Jiang *et al.*, 2016; Safdari *et al.*, 2018).

Several nutrient sources that may be organic or inorganic have been used to enhance bioremediation (Koshlaf *et al.*, 2016; Kumari *et al.*, 2016). Quantification of required nutrient level in bioremediation studies is easier when inorganic nutrients are used (Suja *et al.*, 2014; Shahi *et al.*, 2016). Achieving the desired CNP ratio is an important consideration in bioremediation optimization (Huesseman, 1994; Onwosi *et al.*, 2018). Urea containing 46.6% of nitrogen and potassium dihydrogen phosphate composed of 22.8% phosphorus were used in this study. Again, the limiting nutrients when supplied at high concentration to the bioremediation system can inhibit microbial activity hence the need for optimum CNP ratio (Huesemann, 1994; Walworth *et al.*, 2007). Although the CNP ratio 100:10:1 has been reported to be the optimum ratio for oil bioremediation in soil (Wu *et al.*, 2016), in this study, 90.99 ± 0.02% degradation with CNP ratio of 100:2:0.2 after 36 days remediation was significantly different from 78.15 ± 0.03% obtained with CNP ratio 100:10:1.

4. Conclusion

The widespread crude oil pollution with the associated negative impact on the environment in oil producing regions of Nigeria requires an enhanced strategy for bioremediation, which is the preferred cleanup approach. Such a plan will benefit from site-specific characterization to identify its peculiarity that will be factored into the design of an effective restoration approach. In this study, the optimization of parameters including agitation, moisture level and nutrient ratio enhanced the rate of bioremediation of aged crude oil polluted soil.

Acknowledgement

The authors acknowledge the facilities provided by the Department of Chemical Sciences, Samuel Adgboyega University, Ogwa, Edo State, Nigeria. No funding was received for this research.

References

- Akpe AR, Esumeh FI, Aigere SP, Umanu G and Obiazi H. 2015. Efficiency of plantain peels and guinea corn shaft for bioremediation of crude oil polluted soil. *J Microbiol Res*, **5**(1): 31-40.
- Almaw AA, Naveen KSK and Akshaya KA. 2017. Soil temperature sensors in agriculture and the role of nanomaterials in temperature sensors preparation. *Int J Eng Manuf Sci*, **7**(2): 363-372.
- Atlas RM. (1995). Petroleum biodegradation and oil spill bioremediation. *Mar Pollut Bull*, **31**: 178-182.
- Azubuikwe CC, Chikere CB and Okpokwasili GC. 2016. Bioremediation techniques - classification based on site of application: principles, advantages, limitations and prospects. *World J Microbiol Biotechnol*, **32**: 180.
- Bahmani F, Ataei SA and Mikaili MA. 2018. The effect of moisture content variation on the bioremediation of hydrocarbon contaminated soils: modelling and experimental investigation. *J Environ Anal Chem*, **5**: 236-242.
- Bamforth SM and Singleton I. 2005. Bioremediation of polycyclic aromatic hydrocarbons: Current knowledge and future directions. *J Chem Technol Biotechnol*, **80**: 723-736.
- Barua D, Buragohain J and Sarma SK. 2011. Certain physico-chemical changes in the soil brought about by contamination of crude oil in two oil fields of Assam, NE India. *Eur J Exp Biol*, **1**(3): 154-161.
- Blum WEH. 2013. Soil and land resources for agricultural production: general trends and future scenarios – a worldwide perspective. *Int Soil Water Conserv Res*, **1**(3): 1-14.
- Bosma TNP, Middeldorp PJM, Schraa G and Zehnder AJB. 1997. Mass transfer limitation of biotransformation: quantifying bioavailability. *Environ Sci Technol*, **31**: 248–252.
- Bouyoucos GJ. 1962. Hydrometer method improved for making particle-size analysis of soils. *Agron J*, **53**: 464-465.
- Chauhan M, Solanki M and Nehra K. 2017. Putative mechanism of cadmium bioremediation employed by resistant bacteria. *Jordan J Biol Sci*, **10**(2): 101-107
- Department of Petroleum Resources 2002. Environmental guidelines and standards for the petroleum industry in Nigeria (EGASPIN), DPR, Lagos, Nigeria.
- Dominati E, Patterson M and Mackay A. 2010. A frame work for classifying and quantifying national capital and ecosystem services of soils. *Ecol Econ*, **69**:1858-1868.
- Edemhanria L, Daodu AA, Ebhohimen IE and Osubor CC. 2020. Crude oil utilization and degradation potential of microbes isolated from aged crude oil polluted soil in Niger Delta, Nigeria. *Nat Resour Sustainable Dev*, **10**(2): 262-271.
- Food and Agriculture Organization - FAO. 1980. Soil testing and plant analysis a basis for fertilizer recommendations. FAO Soils Bulletin 38/2, FAO, Rome, Italy.
- Ghaly AE, Yusran A and Dave DF. 2013. Effects of biostimulation and bioaugmentation on the degradation of pyrene in soil. *J Bioremediat Biodegrad*, **55**: 001.
- Huesemann MH 1994. Guidelines for land – treating petroleum hydrocarbon – contaminated soils. *J Soil Contam*, **3**(3): 299-318.
- Imasuen OI, Galasi DT and Omorogieva OM. 2014. Impact assessment and bioremediation of oil contaminated soil: a case study of Koko and Ajoki communities, Niger Delta Nigeria. *J Appl Sci Environ Manage*, **18**(1): 55-60.
- Ite AE, Harry TA, Obadimu CO, Asuaiko ER and Inim IJ. 2018. Petroleum hydrocarbon contamination of surface water and groundwater in the Niger Delta region of Nigeria. *J Environ Pollut Human Health*, **6**(2): 51-61.
- Jain PK, Gupta VK, Gaur RK, Lowry M, Jaroli DP and Chauhan UK. 2011. Bioremediation of petroleum contaminated soil and water. *Res J Environ Toxicol*, **5**:1 – 26.
- Jiang Y, Brassington KJ, Prpich G, Paton GI, Semple KT, Pollard SJT and Coulon F. 2016. Insights into the biodegradation of weathered hydrocarbons in contaminated soils by bioaugmentation and nutrient stimulation. *Chemosphere*, **161**: 300–307.
- Koshlaf E, Shahsavari E, Aburto-Medina A, Taha M, Haleyr N, Makadia TH, Morrison PD and Ball AS. 2016. Bioremediation potential of diesel-contaminated Libyan soil. *Ecotoxicol Environ Saf*, **133**: 297–305.
- Kumari B, Singh SN and Singh DP. 2016. Induced degradation of crude oil mediated by microbial augmentation and bulking agents. *Int J Environ Sci Technol*, **13**: 1029-1042.
- Leahy JG and Colwell RR. 1990. Microbial degradation of hydrocarbons in the environment. *Microbiol Mol Biol Rev*, **54**: 305–315.
- Macaulay BM. 2015. Understanding the behavior of oil – degrading microorganisms to enhance the microbial remediation of spilled petroleum. *Appl Ecol Environ Res*, **13**(1): 247-262.
- McLean EO 1982. Soil pH and lime requirement. In: Page AL (Ed). Methods of soil analysis. Agron. No 9, Part 2: Chemical and microbiological properties, second ed. American Society of Agronomy Madison, WI, USA, pp 199 - 223.
- Michel J and Fingas M. 2016. Oil spill causes, consequences, prevention and countermeasures. In: Crawley GM (Ed.), **Fossil Fuels**, World Scientific, pp 159-201.
- Nwachukwu SU and Ugoji EO. 1995. Impacts of crude petroleum spills on microbial communities of tropical soils. *Int J Ecol Environ Sci*, **21**: 169-176.
- Olsen SR and Sommers LE. 1982. Phosphorus. In: Page AL (Ed). Methods of soil analysis. Agron. No 9, Part 2: Chemical and microbiological properties, second ed. American Society of Agronomy Madison, WI, USA, pp 403-430.
- Onwosi CO, Nwankwegu AS, Enebechi CK, Odimba JN, Nwuche CO and Igbokwe VC. 2018. Bioremediation of Soil Contaminated with Diesel Using Inorganic Nitrogen Sources: Incorporating nth-Order Algorithm in the Evaluation of Process Kinetics. *Soil Sediment Contam*, **27**:1-19.
- Polyak YM, Bakina LG, Chugunova MV, Mayachkina NV, Gerasimov AO, and Bure VM. 2018. Effect of remediation strategies on biological activity of oil-contaminated soil- A field study. *Int Biodeterior Biodegradation*, **126**:57-68.
- Reynolds SG. 1970. The gravimetric method of soil moisture determination. *J Hydrol*, **11**:258-273.
- Richards LA. 1954. Diagnosis and improvement of Saline and Alkaline soils. USDA Agricultural Handbook, Washington, D.C.
- Safdari MS, Kariminia HR, Rahmati M, Fazlollahi F, Polasko A, Mahendra S, Wilding WV and Fletcher TH. 2018. Development of bioreactors for comparative study of natural attenuation, biostimulation, and bioaugmentation of petroleum-hydrocarbon contaminated soil. *J Hazard Mater*, **342**: 270–278.
- Sam K, Coulon F and Prpich G. 2017. Management of petroleum hydrocarbon contaminated sites in Nigeria: Current challenges and future direction. *Land Use Policy*, **64**: 133-144.

- Shahi A, Aydin S, Ince B and Ince O. 2016. Evaluation of microbial population and functional genes during the bioremediation of petroleum-contaminated soil as an effective monitoring approach. *Ecotoxicol Environ Saf*, **125**: 153–160
- Siles JA and Margesin R. 2018. Insights into microbial communities mediating the bioremediation of hydrocarbon-contaminated soil from an alpine former military site. *Appl Microbiol Biotechnol*, **102**(10): 4409-4421.
- Speight JG and El-Gendy NS. 2018. Bioremediation of contaminated soil. In: **Introduction to Petroleum Biotechnology**. Gulf Professional Publishing. Cambridge, MA, USA, pp 361-417.
- Suja F, Rahim F, Taha MR, Hambali N, Razali MR, Khalid A and Hamzah A. 2014. Effects of local microbial bioaugmentation and biostimulation on the bioremediation of total petroleum hydrocarbons (TPH) in crude oil contaminated soil based on laboratory and field observations. *Int Biodeterior Biodegradation*, **90**: 115–122.
- Tibbett M, George SJ, Davie A, Barron A, Milton N and Greenwood PF. 2011. Just add water and salts: the optimization of petrogenic hydrocarbon biodegradation in soils from semi – arid Barrow Island, Western Australia. *Water Air Soil Pollut*, **216**: 513-525.
- Ugochukwu CNC and Ertel J. 2008. Negative impacts of oil exploration on biodiversity management in the Niger Delta area of Nigeria. *Impact Assess Proj Apprais*, **26**(2): 139-147.
- United States Environmental Protection Agency – USEPA. 2000. Demonstration plan. Field measurement technologies for total petroleum hydrocarbons in soil (EPA/600/R-01/060). Washington, DC.
- Urum K, Pekdemir T and Copur M. 2005. Screening of biosurfactants for crude oil contaminated soil weighing. *J Environ Eng Sci*, **4**: 487-496.
- Varjani SJ. 2017. Microbial degradation of petroleum hydrocarbons. *Bioresour Technol*, **223**: 277-286.
- Vidali M. 2001. Bioremediation: An overview. *Pure Appl Chem*, **73**: 1163-1172.
- Walkley A and Black IA. 1934. An examination of Degtjareff method for determining soil organic matter and a proposed modification of the chromic acid titration method. *Soil Sci*, **37**: 29-37.
- Walworth JL, Woolard CR and Harris KC. 2007. Nitrogen requirements for maximizing petroleum bioremediation in a sub – Antarctic soil. *Cold Reg Sci Technol*, **48**: 84–91.
- Watanabe FS and Olsen SR. 1965. Test of an ascorbic acid method for determining phosphorus in water and NaHCO₃ extracts from soil. *Soil Sci Soc of Am J*, **29**: 677-678.
- Wu ML, Dick WA, Li W, Wang XC, Yang Q, Wang TT, Xu LM, Zhang MH and Chen LM. 2016. Bioaugmentation and biostimulation of hydrocarbon degradation and the microbial community in a petroleum–contaminated soil. *Int Biodeterior Biodegradation*, **107**: 158 – 164.

Genetic Diversity Analysis Based on Retrotransposon Microsatellite Amplification Polymorphisms (REMAP) for Distinguishing the Ginger Chemotype of Thua Thien Hue (*Zingiber Officinale* Roscoe) from other Vietnamese Ginger Types

An H. Nguyen¹, Nguyen T. T. Phan¹, Lan T. Tran², Quang T. Hoang²,
Phuong T. B. Truong^{1,*}

¹Hue University of Sciences, Hue University, 77 Nguyen Hue St., Hue city, Thua Thien Hue, Vietnam; ²Institute of Biotechnology, Hue University, Provincial Highway 10, Phu Thuong, Phu Vang District, Thua Thien Hue, Vietnam.

Received: April 11, 2021; Revised: June 20, 2021; Accepted: July 4, 2021

Abstract

The ginger of Thua Thien Hue (“Hue” for short) is considered by local people as a chemotype that is different from other Vietnamese ginger populations. However, there is no molecular evidence supporting this statement. Thus, our purpose is to find whether there is a genetic difference between Hue’s ginger and other ginger types by using Retrotransposon Microsatellite Amplification Polymorphisms (REMAP). The results of our two cluster analyses (Unweighted Pair Group Method with Arithmetic mean (UPGMA) and Principal Coordinates Analysis (PCoA)) proved that they could separate Hue’s ginger samples (in Thuy Bieu Ward, Hue City) from other populations. Therefore, according to these genetic analyses, Hue’s ginger is markedly different from other ginger types. Based on our results, future studies could be conducted with more Vietnamese ginger DNA samples to provide stronger evidence about the unique genomic features of Hue’s ginger.

Keywords: genetic diversity, Hue’s ginger, Retrotransposon Microsatellite Amplification Polymorphisms, *Zingiber officinale* Roscoe
Abbreviations: %P (percentage of polymorphic band), AMOVA (Analysis of molecular variances), BSA (bovine serum albumin), df (degree of freedom), EP (Eppendorf), Fis (inbreeding coefficient), H_e (expected heterozygosity), I (Shanon’s diversity index), IRAP (inter-retrotransposon amplified polymorphism), ISSR (Inter-Simple Sequence Repeat), LTR (Long Terminal Repeat), MI (Marker Index), MS (Mean of Squares), N (number of bands), N_a (observed number of allele), N_e (effective number of allele), N_p (number of polymorphic bands), PCI (phenol, chloroform, isoamyl alcohol), PCoA (Principal Coordinates Analysis), PCR (Polymerase Chain Reaction), PIC (Polymorphism Information Content), RAPD (Randomly amplified polymorphic DNA), REMAP (Retrotransposon Microsatellite Amplification Polymorphisms), R_p (Resolving power), SM (simple matching), SS (Sum of Squares), S-SAP (Sequence-Specific Amplified Polymorphism), SSR (Simple Sequence Repeat), UPGMA (Unweighted Pair Group Method with Arithmetic mean)

1. Introduction

Ginger (*Zingiber officinale* Roscoe, Zingiberaceae) has many important bioactive compounds (gingerol, paradol, shogaol, zingerone, zerumbone, terpenoids, and ginger flavonoids) proved to have remarkable medical effects, including antioxidant activity, antiemetic action, reducing inflammation, antimicrobial activity, hepato-protection, and antitumor activity (Alqasoumi *et al.*, 2011; Chung *et al.*, 2009; Chung *et al.*, 2001; Galal, 1996; Kim *et al.*, 2011; Kirana *et al.*, 2003; Ling *et al.*, 2010; Liu *et al.*, 2012; Manjunatha *et al.*, 2013; Masuda *et al.*, 2004; Park *et al.*, 2008; Rahmani *et al.*, 2014; Shin *et al.*, 2005).

People in Thua Thien Hue (central Vietnam) have long believed that the ginger population in this province (“Hue’s ginger” for short) is a unique chemotype. This belief is in line with the study results of Hien *et al.* (2018) and Stoyanova *et al.* (2006). In all nine comparable substance concentrations, six substances in Hue’s ginger have higher amounts than the ones in the unknown ginger

type. Specifically, the concentrations of α -pinene, camphene, α -zingiberene, copaene, β -bisabolene, and β -sesquiphellandrene in Hue’s ginger and the ginger with unknown origin are 3.81 % - 0.70 %, 11.52 % - 2.50 %, 32.52 % - 10.30 %, 2.10 % - 0.80 %, 5.54 % - 4.10 %, and 11.37 % - 7.40 %, respectively (Hien *et al.*, 2018; Stoyanova *et al.*, 2006). However, Hue’s ginger identification is widely based on the rhizome size. This morphological marker and the mentioned chemical markers make selecting the chemotype for cultivation and oil extraction extremely confusing since they depend on environmental factors (Beleke and Beleke, 2014; Liu *et al.*, 2016). Therefore, today, only the people in Thuy Bieu Ward (Hue City) can declare that their ginger rhizomes are Hue’s ginger. Molecular markers can reliably point out an individual’s genomic features (Paterson *et al.*, 1991). Thus, they can overcome the mentioned detrimental drawback of morphological and chemical markers and can be used for correctly selecting the ginger chemotype. Unfortunately, there has been no research on determining Hue’s ginger at the molecular scale.

* Corresponding author e-mail: • ttbphuong@hueuni.edu.vn, ttbphuongdt@gmail.com.

Retrotransposon microsatellite amplification polymorphism (REMAP) is an efficient technique involving the polymerase chain reaction (PCR) amplification, with a long terminal repeat (LTR) primer and a simple sequence repeat (SSR) or inter-simple sequence repeat (ISSR) primer (Kalendar and Schulman, 2006; Pandotra *et al.*, 2014). REMAP has been efficiently used for cultivar characterizations of many species, including barley (*Hordeum vulgare*), grapevine (*Vitis vinifera* L.), olive (*Olea europaea* L.), and rice (*Oryza sativa* L.) (Branco *et al.*, 2007; Kalendar *et al.*, 1999; Kaya and Yilmaz-Gokdogan, 2016; Strioto *et al.*, 2019; Šimon *et al.*, 2010). In terms of distinguishing ginger cultivars, REMAP can discriminate all the 92 ginger landraces (with a high variation rate of 96.5 %) in the study of Pandotra *et al.* (2014). The authors also demonstrated that REMAP was one of the best markers in all examined ones (ISSR, randomly amplified polymorphic DNA - RAPD, inter-retrotransposon amplified polymorphism - IRAP, and REMAP) (Pandotra *et al.*, 2015).

Considering the lack of scientific evidence for identifying Hue's ginger and the competence of REMAP, this research was conducted to find whether Hue's ginger

chemotype is genetically different from the kinds of ginger grown in other regions of Vietnam.

2. Materials and methods

2.1. Plant materials

Thirty-eight (38) leaf samples, collected from Thua Thien Hue and other provinces in Vietnam, were plant materials for the research. The inner young leaves of ginger shoots, obtained from ginger fields of local people one month after sprouting time (depending on the regions), were separated for DNA extraction. Of all the samples, the local people only consider ginger samples from Thuy Bieu ward as Hue's ginger. The samples were divided into three subpopulations based on the places of sample collection (Table 1), namely P1 (samples in Thuy Bieu), P2 (samples in other regions of Thua Thien Hue), and P3 (samples in several other provinces in Vietnam). The subpopulations were only for genetic diversity analyses to find if P1 could be separated from P2 and P3. P1, P2, and P3 were not real subpopulations in population genetics. The regions of collecting samples are illustrated in Figure 1.

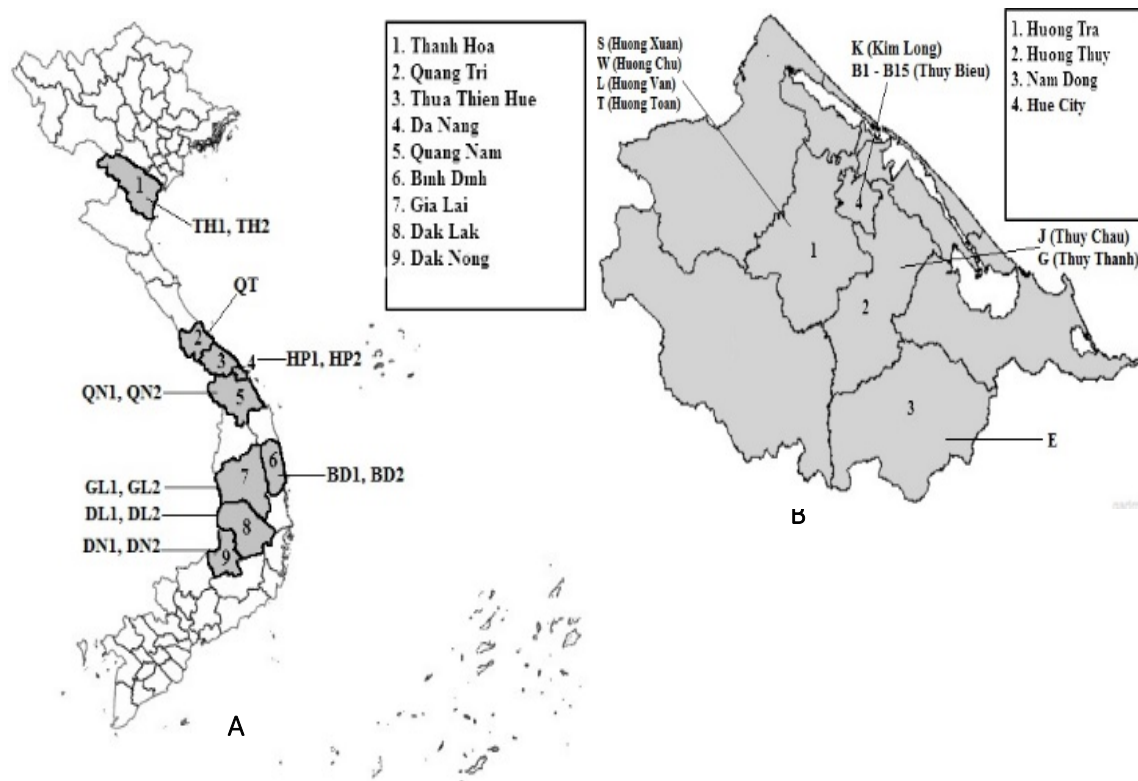


Figure 1. Provinces in Vietnam - Thanh Hoa, Quang Tri, Thua Thien Hue, Da Nang, Quang Nam, Binh Dinh, Gia Lai, Dak Lak, and Dak Nong (A) and regions in Thua Thien Hue - Huong Tra, Huong Thuy, Nam Dong, and Hue City (B) from which ginger samples were collected (the number of samples and sample codes are illustrated in the figure).

Table 1. The list of ginger leaf samples (only the samples from Thuy Bieu were the unique chemotype of Thua Thien Hue)

Province	District/City	Ward	Number of sample(s)	Sample codes	Sub-population	Coordinates
Thua Thien Hue	Hue City	Thuy Bieu	15	From B1 to B15	P1	16.4446° N, 107.5511° E
		Kim Long	1	K		16.4652° N, 107.5605° E
	Huong Tra	Huong Xuan	1	S	P2	16.4770° N, 107.4766° E
		Huong Van	1	L		16.4972° N, 107.4736° E
		Huong Toan	1	T		16.5128° N, 107.5348° E
		Huong Chu	1	W		16.4931° N, 107.5209° E
	Huong Thuy	Thuy Chau	1	J	16.4355° N, 107.6630° E	
		Thuy Thanh	1	G	16.4652° N, 107.6416° E	
	Nam Dong	Thuong Long	1	E	16.0755° N, 107.6275° E	
	Gia Lai	Mang Yang	Lo Pang	2	GL1, GL2	
Thanh Hoa	Thuong Xuan	Luan Thanh	2	TH1, TH2		19.8015° N, 105.4127° E
Quang Nam	Tien Phuoc	Tien Son	2	QN1, QN2		15.5804° N, 108.2674° E
Dak Lak	Krong Nang	Tam Giang	2	DL1, DL2	P3	12.9749° N, 108.3920° E
Dak Nong	Dak Song	Dak N'Drung	2	DN1, DN2		12.2160° N, 107.5624° E
Da Nang	Cam Le	Hoa Phat	2	HP1, HP2		16.0287° N, 108.1725° E
Quang Tri	Cam Lo	Cam Tuyen	1	QT		16.8229° N, 106.9241° E
Binh Dinh	An Lao	An Tan	2	BD1, BD2		14.5748° N, 108.8849° E

2.2. Genomic DNA extraction

Total genomic DNA of the samples was extracted by using the protocol of Doyle and Doyle (1987) (modified). RNA in the genomic DNA solutions was digested by 1 μ L of RNase (100 μ g/ μ L).

200 mg of washed and cut ginger leaves was homogenized by using liquid nitrogen. Then, the leaf powder was transferred into a 1.5 mL Eppendorf (EP) tube.

Next, 1 mL of extraction buffer (200 nM Tris-HCl, pH 8.0; 50 mM ethylenediaminetetraacetic acid; 2 % hexadecyltrimethylammonium bromide, 2.5 % polyvinylpyrrolidone; 1.4 M NaCl) and 20 μ L of 100 % 2-mercaptoethanol were added into each EP tube. After that, tubes were vortexed for two minutes before being incubated at 65°C for 3 hours.

After the incubation, 700 μ L of the supernatant liquid, obtained by centrifugation (13000 rpm, 4°C, 15 minutes), was mixed with an equal volume of PCI (25 phenol : 24 chloroform : 1 isoamyl alcohol). The mixture was then centrifuged under the same condition. 500 μ L of the transparent top liquid was collected after the centrifugation.

The DNA precipitation process was then done by mixing 500 μ L of 100 % isopropanol with the above-mentioned transparent liquid. After that, the mixture was incubated overnight at -40°C.

The precipitated total genomic DNA would be collected on the next day by centrifugation (13000 rpm, 4°C, 15 minutes). DNA pellets were then washed two times by using 500 μ L of cold 70% ethanol.

30 μ L of autoclaved double distilled water was used to dissolve the DNA, which had been dried at ambient temperature.

2.3. Primer selection

Ten REMAP primer pairs (Baruah *et al.*, 2019; Pandotra *et al.*, 2014) were screened (**Table 2**). Each tested primer pair was used to amplify seven randomly chosen DNA samples from distinct regions. The PCR steps were as follows:

Initial denaturation at 94°C for two minutes,

Forty-four (44) amplification cycles: one minute at 94°C, one minute at 45 – 64°C (depending on primers' melting points), and two minutes at 72°C,

Final extension at 72°C for ten minutes.

Each PCR tube contained the following compositions:

1 μ L of genomic DNA (35 ng),

1 μ L of RT-6 primer (10 μ M),

1 μ L of ISSR/SSR primer (10 μ M),

12.5 μ L of GoTaq Green Master Mix 2X (Promega, USA),

9.5 μ L of bovine serum albumin (BSA) (0.421 mg/mL).

PCR products were observed on a 1.6 % agarose gel containing SafeView™ DNA stain (Applied Biological Materials Inc., USA). Primer pairs with the highest indices, namely polymorphism information content (*PIC*), resolving power (*Rp*), marker index (*MI*), number of bands (*N*), and number of polymorphic bands (*N_p*) (Chesnokov and Artemyeva, 2015; Kumar *et al.*, 2014), were chosen for REMAP analysis.

Table 2. The list of primers used for the screening process

Primer codes	5' – 3' sequences	References
RT-6/RM-2	GATAGGGTCGCATCTTGGGCGTGAC/ TCAGCTTCTGGCCGGCCTCCTC	
RT-6/RM-3	GATAGGGTCGCATCTTGGGCGTGAC/ GCCTCGAGCATCATCATCAG	
RT-6/RM-4	GATAGGGTCGCATCTTGGGCGTGAC/ ATCAACCTGCACTTGCCCTGG	
RT-6/RM-125	GATAGGGTCGCATCTTGGGCGTGAC/ AGGGGATCATGTGCCGAAGGCC	
RT-6/RM-130	GATAGGGTCGCATCTTGGGCGTGAC/ TTCCTGTAAAGAGAGAATC	Baruah <i>et al.</i> , 2019 ; Pandotra <i>et al.</i> , 2014
RT-6/ISSR-2	GATAGGGTCGCATCTTGGGCGTGAC/(AG) ₈ T	
RT-6/ISSR-4	GATAGGGTCGCATCTTGGGCGTGAC/(GT) ₈ CTC	
RT-6/ISSR-11	GATAGGGTCGCATCTTGGGCGTGAC/AGG(TC) ₇	
RT-6/ISSR-42	GATAGGGTCGCATCTTGGGCGTGAC/(AG) ₈ CA	
RT-6/ISSR-72	GATAGGGTCGCATCTTGGGCGTGAC/(GGAGA) ₃	

2.4. REMAP analysis

The selected primer pairs were utilized for the amplification of all 38 genomic DNA samples, with PCR conducted similarly to the primer screening process. The amplified products were then also be viewed on a 1.6 % agarose gel containing SafeView™ DNA stain.

2.5. Data analysis

2.5.1. Band scoring

Amplified products of 38 samples were scored to create a binary matrix. Obvious bands were considered as “1” while absent bands were scored as “0”.

2.5.2. Analysis of molecular variances (AMOVA)

The AMOVA (999 permutations) was done by using GenAIEX 6.51 software (Peakall and Smouse, 2006), with the binary matrix as input data, to examine genetic diversity within and among the subpopulations.

2.5.3. Parameters Calculation

The indices for primer pair assessments were manually calculated by using the following formulas (Chesnokov and Artemyeva, 2015; Kumar *et al.*, 2014):

$$PIC = \frac{1}{N} \times \sum_{i=1}^N 2f_i \times (1 - f_i) \quad (1)$$

$$Rp = \sum_{i=1}^N J_i; J_i = 1 - 2 \times \left| \frac{1}{2} - f_i \right| \quad (2)$$

$$MI = \frac{N_e}{N} \times PIC \quad (3)$$

Where f_i is the frequency of the i^{th} allele, N_p is the number of polymorphic bands, N is the total number of bands.

The mentioned binary matrix was also used as the input data for POPGENE software (version 1.32) (Yeh *et al.*, 2000) to calculate diversity parameters, namely expected heterozygosity (H_e), Shanon's diversity index (I), the observed number of allele (N_o), and the effective number of allele (N_e). Genetic diversity parameters were calculated on the Hardy-Weinberg disequilibrium assumption, with an inbreeding coefficient of 1 ($F_{is} = 1$) estimated based on the method of Dasmahapatra *et al.* (2008).

2.5.4. Cluster analysis

NTSYS version 2.1 (Rohlf, 2000) and GenAIEX 6.51 (Peakall and Smouse, 2006) software packages were used

for building an UPGMA dendrogram, with simple matching (SM) genetic distance coefficient (Sokal and Michener, 1958), and PCoA graphs from the distance matrix, generated from the raw binary data.

3. Results

3.1. Primer selections

Of all ten REMAP primer pairs, only four pairs (RT-6/RM-2, RT-6/RM-125, RT-6/RM-130, and RT-6/ISSR-2) for which PIC , Rp , MI , N , and N_p were the highest and ranged from 0.35 – 0.43, 2.86 – 5.14, 1.88 – 3.51, 5 – 10, and 5 – 10, respectively, were selected. (Table 3).

Table 3. Indices for primer pair assessments

Primer codes	PIC^a	Rp	MI	N	N_p	Percentage of polymorphic bands (%)
RT-6/RM-2	0.38	2.86	1.88	5	5	100
RT-6/RM-3	0.00	0.00	0.00	3	0	0.00
RT-6/RM-4	0.15	0.67	0.05	3	1	33.33
RT-6/RM-125	0.43	4.86	3.02	7	7	100
RT-6/RM-130	0.35	5.14	3.51	10	10	100
RT-6/ISSR-2	0.40	4.29	2.78	7	7	100
RT-6/ISSR-4	0.33	2.00	0.75	4	3	75.00
RT-6/ISSR-11	0.15	0.67	0.05	3	1	33.33
RT-6/ISSR-42	0.22	1.33	0.22	4	2	50.00
RT-6/ISSR-72	0.33	2.00	0.75	4	3	75.00

^aNote: PIC (Polymorphism Information Content), Rp (Resolving power), MI (Marker Index), N (total number of bands), N_p (number of polymorphic bands).

3.2. REMAP analysis

The total number of amplicons from REMAP analysis was 29. Additionally, the selected REMAP primer pairs produced a high proportion of polymorphic loci (100 %). There were six region-specific bands generated, namely RT-6/ISSR-2-1134 and RT-6/RM-130-238 of Thuy Bieu samples; RT-6/RM-125-621, RT-6/RM-130-889, and RT-6/RM-130-765 of HP2 (Da Nang); and RT-6/RM-130-250 of QT (Quang Tri) (Table 4).

Table 4. Results of REMAP analysis using the four selected primer pairs to amplify 38 samples.

Primers' codes	<i>N</i> ^a	<i>N_p</i>	% <i>P</i>	Amplicon lengths (bp)	Region-specific bands (bp)	Samples containing the region-specific bands
RT-6/ISSR-2	7	7	100	250 – 1134	1134	B1, B3-B6, B10-B14
RT-6/RM-2	5	5	100	409 – 941	-	-
RT-6/RM-125	7	7	100	229 – 1446	621	HP2
RT-6/RM-130	10	10	100	238 – 1461	889	HP2
					765	HP2
					250	QT
					238	B9, B11
Total:	29	29	100			

^aNote: *N* (total number of bands), *N_p* (number of polymorphic bands), %*P* (percentage of polymorphic bands)

3.3. Analysis of molecular variances (AMOVA)

As is highlighted in **Table 5**, the proportion of variance among populations was 35 %, while the diversity within **Table 5.** Analysis of Molecular Variance (AMOVA) of REMAP

populations accounted for 65 % of the total variation (*P* < 0.01).

Source	<i>df</i> ^a	<i>SS</i>	<i>MS</i>	Variance component	Percentage of total variance (%)	<i>PhiPT</i>	<i>P</i>
Among populations	2	57.04	28.52	2.06	35	0.355	0.001**
Within populations	35	131.12	3.75	3.75	65		
Total	37	188.16		5.81	100		

^aNote: *df*: degree of freedom; *SS*: sum of squares; *MS*: mean of squares

3.4. Genetic diversity parameters

It is clarified in **Table 6** that the diversity indices of P1, P2, and P3 were low, with *H_e*, *I*, *N_a*, *N_e*, and %*P* of 0.22 – 0.29, 0.35 – 0.43, 1.76 – 1.79, 1.36 – 1.49, and 75.86 % – 79.31 %, respectively. Moreover, several parameters reached the minimum values when data from P3 were used to calculate them (*H_e* of 0.22, *I* of 0.35, and *N_e* of 1.36).

Table 6. Genetic diversity parameters of the three ginger subpopulations, calculated on the Hardy – Weinberg disequilibrium assumption (*F_{is}* = 1)

Parameters	P1	P2	P3
<i>H_e</i> ^a	0.25 (0.19)	0.29 (0.17)	0.22 (0.18)
<i>I</i>	0.38 (0.26)	0.43 (0.25)	0.35 (0.24)
<i>N_a</i>	1.76 (0.44)	1.79 (0.41)	1.79 (0.41)
<i>N_e</i>	1.42 (0.37)	1.49 (0.33)	1.36 (0.34)
<i>N_p</i>	22	23	23
% <i>P</i>	75.86 %	79.31 %	79.31 %

^aNote: *H_e*: expected heterozygosity; *I*: Shanon's information index; *N_a*: observed number of alleles; *N_e*: effective number of

alleles; *N_p*: number of polymorphic loci; %*P*: percentage of polymorphic loci; The values in the table are mean (standard deviation).

3.5. Cluster analysis

3.5.1. UPGMA dendrogram

There were two clusters (A and B) obtained from building the UPGMA dendrogram. Almost the ginger samples from P1 were clustered in A (B1, B3, B4, B5, B6, B11 in A1-1; B10, B12, B13, B14, B15 in A1-2; and B2, B9 in A2). All samples from P2 and P3 (except K, S, E, and BD1) were grouped in B. The genetic distance between A and B was 47.00 % (**Figure 2**).

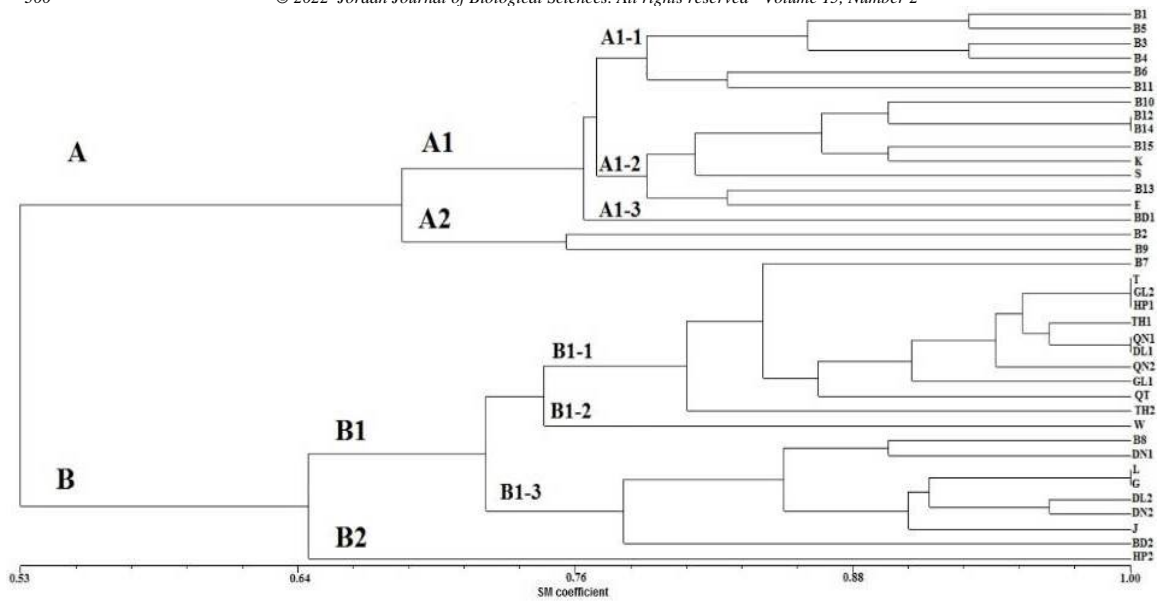


Figure 2. Clusters formed by UPGMA analysis. Cluster A was divided into A1 (containing A1-1, A1-2, and A1-3) and A2. Cluster B also has two groups, namely B1 (with three subclusters – B1-1, B1-2, and B1-3) and B2. Ginger samples from P1 (Hue's ginger) were in cluster A except for B7 and B8

3.5.2. Principal coordinates analysis (PCoA)

Samples in PCoA graphs were divided into three distinct clusters (I, II, and III), with almost P1's samples in cluster I, except B2, B7, and B8. This result demonstrates that the samples from Thuy

Bieu have unique genomic features separating this subpopulation from other clusters. Cluster II contained ten samples from all subpopulations (P1, P2, and P3), while only samples from P3 were grouped in cluster III (**Figure 3**).

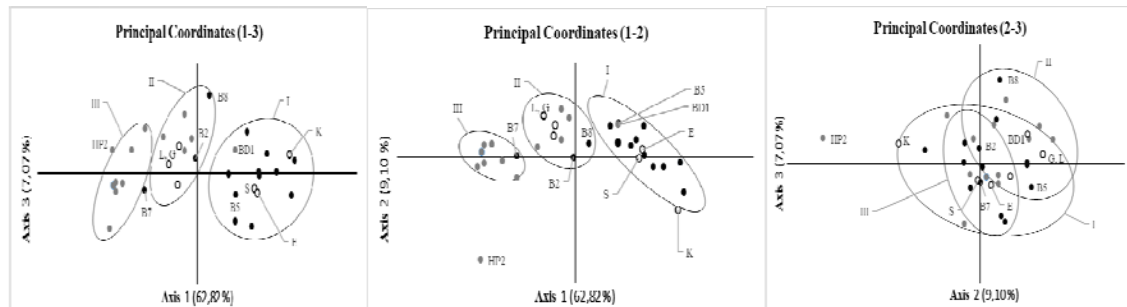


Figure 3. PCoA graphs with three separate clusters (I, II, and III). Samples from P1 were grouped in cluster I. This indicates that ginger from Thuy Bieu was genetically different from ginger grown in other regions. The first three planes of PCoA (1-2, 1-3, and 2-3) reveal 71.92 %, 69.89 %, and 16.17 % of the variations of the three subpopulations, which are P1 (black points), P2 (white points) and P3 (gray points).

4. Discussion

The UPGMA dendrogram supported the conclusion that the ginger samples from P1 were genetically different from the samples of P2 and P3. Specifically, 13 in 15 samples of P1 were grouped in a separated cluster (A), while most of the other samples were in cluster B, with a significant genetic distance between them (47.00 %) (**Figure 2**). The PCoA graphs well supported this result. Samples of P1 formed cluster I separated from cluster II and cluster III, containing other samples (**Figure 3**). However, three P1 samples (B2, B7, and B8) were not in cluster I. Lovell *et al.* (2017) reported that individuals in asexual populations could harbor DNA mutations. Therefore, the mutations accumulated in P1 might cause the difference between those three samples and the other P1 samples.

Choosing the suitable primer pairs played a key role in achieving the above-mentioned positive results.

First, we selected the RT-6 primer (also known as sukkula or sukkula 9900 primer) for our analyses. RT-6 was one of the best retrotransposon primers for producing the highest number of bands in the studies of Leigh *et al.* (2003) and Muhammad and Othman (2005). Muhammad and Othman (2005) observed the maximum number of 13 PCR products when the authors used RT-6 as an IRAP marker in characterizing *Fusarium* wilt-resistant and *Fusarium* wilt-susceptible *Musa* AAB soma clones. Moreover, Leigh *et al.* (2003) obtained one of the highest numbers of PCR products (28) by using RT-6 in the research on sequence-specific amplified polymorphism (S-SAP) markers. The maximum number of bands produced by the primer pairs containing RT-6 in the present study was only ten (**Table 4**). However, all bands generated were polymorphic, proving the prominence of RT-6 primer.

Second, our SSR and ISSR primers, selected from the studies of Pandotra *et al.* (2014) and Baruah *et al.* (2019),

were also proved as efficient primers for ginger genetic diversity analysis. Specifically, Pandotra *et al.* (2014) concluded that RT-6/RM-2, RT-6/RM-3, RT-6/RM-4, RT-6/RM-125, and RT-6/RM-130 were among the best primer pairs, with *PIC*, *Rp*, *MI*, *Np*, and %*P* of 0.17 – 0.31, 7.84 – 10.92, 3.06 – 4.14, 17 – 23, and 89.47 – 100 %, respectively. Additionally, ISSR-2, ISSR-4, ISSR-11, ISSR-42, and ISSR-72 were also the optimal ISSR primers in the study of Baruah *et al.* (2019), with the *Np*, %*P*, *MI*, *Rp*, and *PIC* values ranging from 5 – 9, 81.8 – 100 %, 2.56 – 4.15, 3.57 – 4.9, and 0.51 – 0.68, respectively. However, our primer screening process revealed only four primer pairs (RT-6/ISSR-2, RT-6/RM-2, RT-6/RM-125, and RT-6/RM-130), which were efficient enough for genetic analyses of Vietnamese ginger (Table 3). Additionally, using the same primers/primer pairs, the number of polymorphic bands in our study (29) was lower than in the studies of Baruah *et al.* (2019) (32) and Pandotra *et al.* (2014) (61). The genetic variations between the Vietnamese ginger samples and the ginger samples used in the mentioned authors' studies might cause those differences in the results. Though the number of bands in our study was low, all the four selected primer pairs produced the absolute polymorphic rate (100 %). Moreover, the region-specific band (1134 bp), produced by the primer pair RT-6/ISSR-2, was one of the main factors discriminating Thuy Bieu samples from other samples (Table 4). Thus, the selected primer pairs satisfactorily fulfilled the expectations of our study.

Because of using the effective primer pairs, our AMOVA results could clearly show the genetic variations among the three subpopulations (Table 5). This suggests that REMAP is appropriate for distinguishing the three ginger subpopulations. Specifically, 35 % of the total variations occurred among subpopulations. However, REMAP's ability to reveal differences among populations depends on the species. Noormohammadi *et al.* (2016) found that 33 % of the variations took place among *Gossypium* spp. populations. In contrast, Tanhuanpaa *et al.* (2016) reported that REMAP could only point out a low proportion of variation arising among *Phleum pratense* L. populations (10 %).

From the supportive results of PCR amplification and AMOVA, we conducted the cluster analyses (UPGMA and PCoA) and came to the expected conclusion as described at the beginning of the section.

In parallel, genetic diversity parameters (H_e , I , N_a , N_e) of the subpopulations were also calculated. The values in our study were low. Ginger's asexual reproduction might be the cause of the low diversity indices. Barrett *et al.* (2008) and Qiu *et al.* (2005) proved the effect of lowering diversity parameters of this kind of reproduction in studies on other species, namely *Melampsora lini* and *Dysosma versipellis* (Berberidaceae) (Table 6).

The diversity parameters observed in P1 and P2 were higher than in P3. This finding demonstrates that REMAP might be effective for genetic variation assessments of samples collected from regions adjacent to one another (Table 6). In contrast, Das *et al.* (2017), Kavyashree (2008), and Kizhakkayil and Sasikumar (2010) concluded that there was a correlation between geographical distance and genetic diversity (populations being geographically far from one another would have high genetic diversity among them).

5. Conclusions

Using REMAP markers, we concluded that the ginger population grown in Thuy Bieu, which has long been known as the special ginger chemotype of Thua Thien Hue, is genetically different from populations in other regions of Thua Thien Hue and Vietnam.

The positive results of our research are precursors for future studies, with more ginger DNA samples. Specifically, samples should be collected from a higher number of regions in Thua Thien Hue and other Vietnamese provinces. Moreover, the number of leaf samples in each region should also be increased. Those increments will provide stronger evidence about the unique genomic features of Hue's ginger in Thuy Bieu after a genetic diversity analysis.

Acknowledgements

This study was financially supported by the Department of Science and Technology, Thua Thien Hue Province, Vietnam, under Grant TTH.2018-KC.03.

References

- Alqasoumi S, Yusufoglu H, Farraj A and Alam A. 2011. Effect of 6-shogaol and 6-gingerol on Diclofenac Sodium Induced Liver Injury. *Int J Pharmacol.*, **7(8)**: 868 – 873.
- Barrett LG, Thrall PH, Burdon JJ, Nicotra AB and Linde CC. 2008. Population structure and diversity in sexual and asexual populations of the pathogenic fungus *Melampsora lini*. *Mol Ecol.*, **17(14)**: 3401 – 3415.
- Baruah J, Pandey SK, Begum T, Sarma N, Paw M and Lal M. 2019. Molecular diversity assessed amongst high dry rhizome recovery Ginger germplasm (*Zingiber officinale* Roscoe) from NE-India using RAPD and ISSR markers. *Ind Crop Prod.*, **129**: 463–471.
- Beleke A and Beleke E. 2014. Overview: Morphological and Molecular Markers role in Crop Improvement Programs. *International Journal of Current Research in Life Sciences*, **3(3)**: 35 – 42.
- Branco CJS, Vieira EA, Malone G, Kopp MM, Malone E, Bernardes A, Mistura CC, Carvalho FIF and Oliveira CA. 2007. IRAP and REMAP assessments of genetic similarity in rice. *J Appl Genet.*, **48(2)**: 107 – 113.
- Chesnokov YV and Artemyeva AM. 2015. Evaluation of the measure of polymorphism information of genetic diversity. *Agric Biol.*, **50(5)**: 571–578.
- Chung SW, Kim MK, Chung JH, Kim DH, Choi JS, Anton S, Seo AY, Park KY, Yokozawa T, Rhee SH, Yu BP and Chung HY. 2009. Peroxisome proliferator-activated receptor activation by a short-term feeding of zingerone in aged rats. *J Med Food.*, **12(2)**: 345 – 350.
- Chung WY, Jung YJ, Surh YJ, Lee SS and Park KK. 2001. Antioxidative and antitumor promoting effects of [6]-paradol and its homologs. *Mutat Res.*, **496(1-2)**: 199 – 206.
- Das A, Gaur M, Barik DP and Subudhi E. 2017. Genetic diversity analysis of 60 ginger germplasm core accessions using ISSR and SSR markers. *Plant Biosyst.*, **151(5)**: 822 – 832.
- Dasmahapatra KK, Lacy RC and Amos W. 2008. Estimating levels of inbreeding using AFLP markers. *Heredity*, **100(3)**: 286 – 295.
- Doyle JJ and Doyle JL. 1987. A rapid isolation procedure for small quantities of fresh leaf tissue. *Phytochemical Bulletin*, **19(1)**: 11–15.

- Galal AM. 1996. Antimicrobial Activity of 6-Paradol and Related Compounds. *Inter J Pharmacog.*, **34(1)**: 64 – 69.
- Hien LTB, Quy LTM, Thuy NLL and Hoai NT. 2018. Study on extraction process, chemical composition and antibacterial activity of ginger oil in Thua Thien Hue. *Journal of Medicine and Pharmacy*, **8(3)**: 24 – 30.
- Kalendar R and Schulman AH. 2006. IRAP and REMAP for retrotransposon-based genotyping and fingerprinting. *Nat Protoc.*, **1(5)**: 2478–2484.
- Kalendar R, Grob T, Regina M, Suoniemi A and Schulman A. 1999. IRAP and REMAP: two new retrotransposon-based DNA fingerprinting techniques. *Theor Appl Genet.*, **98(5)**: 704 – 711.
- Kavyashree R. 2008. Molecular and morphological characterization of seven varieties of *Zingiber officinale*. *J Cyto Genet.*, **9**: 101–107.
- Kaya E and Yilmaz-Gokdogan E. 2016. Using Two Retrotransposon Based Marker Systems (IRAP and REMAP) for Molecular Characterization of Olive (*Olea europaea* L.) Cultivars. *Cluj-Napoca.*, **44**: 167 – 174.
- Kim HW, Oh DH, Jung C, Kwon DD and Lim YC. 2011. Apoptotic Effects of 6-Gingerol in LNCaP Human Prostate Cancer Cells. *Soonchungyang Med Sci.*, **17(2)**: 75 – 79.
- Kirana C, McIntosh GH, Record IR and Jones GP. 2003. Antitumor activity of extract of *Zingiber aromaticum* and its bioactive sesquiterpenoid zerumbone. *Nutr Cancer.*, **45(2)**: 218 – 225.
- Kizhakkayil J and Sasikumar B. 2010. Genetic diversity analysis of ginger (*Zingiber officinale* Rosc.) germplasm based on RAPD and ISSR markers. *Sci Hort.*, **125(1)**: 73–76.
- Kumar A, Mishra P, Singh SC and Sundaresan V. 2014. Efficiency of ISSR and RAPD markers in genetic divergence analysis and conservation management of *Justicia adhatoda* L., a medicinal plant. *Plant Syst Evol.*, **300(6)**: 1409–1420.
- Leigh F, Kalendar R, Lea V, Lee D, Domini P and Schulman AH. 2003. Comparison of the utility of barley retrotransposon families for genetic analysis by molecular marker techniques. *Mol Genet Genomics*, **269(4)**: 464–474.
- Ling H, Yang H, Tan SH, Chui WK and Chew EH. 2010. 6-Shogaol, an active constituent of ginger, inhibits breast cancer cell invasion by reducing matrix metalloproteinase-9 expression via blockade of nuclear factor- κ B activation. *Br J Pharmacol.*, **161(8)**: 1763 – 1777.
- Liu W, Yin D, Li N, Hou X, Wang D, Li D and Liu J. 2016. Influence of Environmental Factors on the Active Substance Production and Antioxidant Activity in *Potentilla fruticosa* L. and Its Quality Assessment. *Sci Rep.*, **6(1)**: 28591.
- Liu Y, Whelan RJ, Pattanaik BR, Ludwig K, Subudhi E, Rowland H, Claussen N, Zucker N, Uppal S, Kushner DM, Felder M, Patankar MS and Kapur A. 2012. Terpenoids from *Zingiber officinale* (Ginger) induce apoptosis in endometrial cancer cells through the activation of p53. *PLoS One*, **7(12)**: e53178.
- Lovell JT, Williamson RJ, Wright SI, McKay JK and Sharbel TF. 2017. Mutation Accumulation in an Asexual Relative of *Arabidopsis*. *PLoS Genet.*, **13(1)**: e1006550.
- Manjunatha JR, Bettadaiah BK, Negi PS and Srinivas P. 2013. Synthesis of quinoline derivatives of tetrahydrocurcumin and zingerone and evaluation of their antioxidant and antibacterial attributes. *Food Chem.*, **136(2)**: 650 – 658.
- Masuda Y, Kikuzaki H, Hisamoto M and Nakatani N. 2004. Antioxidant properties of gingerol related compounds from ginger. *Biofactors*, **21(1-4)**: 293 – 296.
- Muhammad AJ and Othman FY. 2005. Characterization of Fusarium Wilt-Resistant and Fusarium Wilt-Susceptible Somaclones of Banana Cultivar Rastali (*Musa AAB*) by Random Amplified Polymorphic DNA and Retrotransposon Markers. *Plant Mol Biol Rep.*, **23(3)**: 241–249.
- Noormohammadi Z, Ibrahim-Khalili N, Ghasemzadeh-Baraki S, Sheidai M and Alishah O. 2016. Genetic screening of diploid and tetraploid cotton cultivars based on retrotransposon microsatellite amplified polymorphism markers (REMAP). *An Biol.*, **38**: 123–132.
- Pandotra P, Gupta AP, Khan S, Ram G and Gupta S. 2015. A comparative assessment of ISSR, RAPD, IRAP, & REMAP molecular markers in *Zingiber officinale* germplasm characterization. *Sci Hort.*, **194**: 201 – 207.
- Pandotra P, Husain MK, Ram G, Gupta S and Gupta AP. 2014. Retrotransposon based genetic status of North-West Himalayan *Zingiber officinale* revealed high heterogeneity. *J Plant Biochem Biotechnol.*, **23(2)**: 211–216.
- Park M, Bae J and Lee DS. 2008. Antibacterial activity of [10]-gingerol and [12]-gingerol isolated from ginger rhizome against periodontal bacteria. *Phytother Res.*, **22(11)**: 1446 – 1449.
- Paterson AH, Tanksley SD and Sorrells ME. 1991. DNA markers in plant improvement. *Adv Agron.*, **46**: 39–90.
- Peakall ROD and Smouse PE. 2006. GenAlEx 6: genetic analysis in excel. Population genetic software for teaching and research. *Mol Ecol Notes.*, **6(1)**: 288–295.
- Qiu YX, Zhou XW, Fu CX and Chan YSG. 2005. A preliminary study of genetic variation in the endangered, Chinese endemic species *Dyosma versipellis* (Berberidaceae). *Bot Bull Acad Sinica.*, **46(1)**: 61 – 69.
- Rahmani AH, Al shabrmi FM and Aly SM. 2014. Active ingredients of ginger as potential candidates in the prevention and treatment of diseases via modulation of biological activities. *Int J Physiol Pathophysiol Pharmacol.*, **6(2)**: 125-136.
- Rohlf FJ. 2000. **NTSYS-pc: numerical taxonomy and multivariate analysis system version 2.1**, Exeter Publishing Setauket, New York.
- Shin SG, Kim JY, Chung HY and Jeong JC. 2005. Zingerone as an Antioxidant against Peroxynitrite. *J Agric Food Chem.*, **53(19)**: 7617 – 7622.
- Šimon S, Zulj M, Preiner D, Pejić I, Gaši F, Malenica N and Zdunic G. 2010. REMAP as a tool for preliminary grapevine accession screening. *Acta Hort.*, **859**: 155-159.
- Sokal RR and Michener CD. 1958. A statistical method for evaluating systematic relationships. *Univ Kansas, Sci Bull.*, **38**: 1409-1438.
- Stoyanova A , Konakchiev A, Damyanova S, Stoilova I and Suu PT. 2006. Composition and Antimicrobial Activity of Ginger Essential Oil from Vietnam . *J Essent Oil-Bear Plants.*, **9(1)**: 93 – 98.
- Striato DK, Kuhn BC, Nagata WSL, Marinelli G, Oliveira-Collet SA, Mangolin CA and Machado M. 2019. Development and use of retrotransposons-based markers (IRAP/REMAP) to assess genetic divergence among table grape cultivars. *Plant Genet Resour.*, **17(3)**: 272-279.
- Suresh K, Manoharan S, Vijayaanand MA and Sugunadevi G. 2010. Chemopreventive and antioxidant efficacy of (6)-paradol in 7,12-dimethylbenz(a)anthracene induced hamster buccal pouch carcinogenesis. *Pharmacol Rep.*, **62(6)**: 1178 – 1185.
- Tanhuanpää P, Erkkilä M, Kalendar R, Schulman AH and Manninen O. 2016. Assessment of genetic diversity in Nordic timothy (*Phleum pratense* L.). *Hereditas*, **153(1)**: 5.
- Yeh FC, Yang RC and Boyle T. 2000. **POPGENE 1.32: A Free Program for the Analysis of Genetic Variation among and Within Populations Using Co-Dominant and Dominant Markers**, Dept of Ren. Res., Uni. Alberta, Canada.
- Young HY, Luo YL, Cheng HY, Hsieh WC, Liao JC and Peng WH. 2005. Analgesic and anti-inflammatory activities of [6]-gingerol. *J Ethnopharmacol.*, **96(1-2)**: 207 – 210.

GC-MS Chemical Profile, Antioxidant Ability, Antibacterial Effect, α -Glucosidase, α -Amylase and Acetylcholinesterase Inhibitory Activity of Algerian Fir Essential Oil

Djamila Benouchene^{1,2}, Ines Bellil¹, Chawki Bensouici³, Mustafa Abdullah Yilmaz⁴, Salah Akkal⁵, Hatice Banu Keskinaya⁶, Douadi Khelifi^{1,7}

¹Laboratoire de Génétique Biochimie et Biotechnologies Végétales, Faculté des Sciences de la Nature et de la Vie, Université Frères

Mentouri Constantine 1, 25000 Constantine, Algeria. ²Centre de Recherche en Sciences Pharmaceutiques, 25000 Constantine, Algeria.

³Laboratoire de Biochimie, Biotechnologie et Division Santé, Centre de Recherche en Biotechnologie, 25000 Constantine, Algeria. ⁴Dicle University Science and Technology Research and Application Center (DUBTAM), Dicle University, 21280 Diyarbakir, Turkey. ⁵Laboratoire de Phytochimie et Analyses Physico-chimiques et Biologiques, Faculté des Sciences Exactes, Université Frères Mentouri Constantine 1, 25000 Constantine, Algeria. ⁶Selcuk University, Faculty of Science, Department of Biology 42130/Keykubat Campüs, Konya, Turkey. ⁷Ecole Nationale Supérieure de Biotechnologie, 25000 Constantine, Algeria.

Received: April 16, 2021; Revised: July 19, 2021; Accepted: August 17, 2021

Abstract

The aims of the current research were to determine the chemical profile of essential oil obtained from Algerian fir leaves as well as to evaluate its biological activities *in-vitro*. Essential oil (EO) was extracted by hydro-distillation from needles. The EO was subjected to gas-chromatography coupled with mass spectrometry (GC-MS). Likewise, the antioxidant ability was examined using different assays including DPPH free radicals scavenging, phenanthroline (Phen assay), and sun protection factor (SPF). Enzymes inhibitory activity was tested on α -glucosidase, α -amylase, and acetylcholinesterase (AChE). The antibacterial effect was analyzed using the disc diffusion method against 6 pathogenic bacterial strains. Twenty-nine compounds representing 93.89% of the oil were identified, Caryophyllene (17.31%), α -pinene (10.58%), 2, 2, 6, 10-Tetramethylbicyclo [5.4.0] undeca-9, 11-diene (8.65%), linalyl acetate (7.41%), β -silinene (7.28%), and sabinene (6.88%) were the major constituents. The results disclosed that the oil has weak antioxidant ability in different tests at the concentration (4mg/ml). The essential oil exerted a strong α -glucosidase inhibitory activity, while it showed a weak α -amylase and AChE enzymes inhibitory ability. The essential oil displayed no effect against all the bacterial strains tested excepting *Staphylococcus aureus* with moderate effect. The results disclosed the potential effect of an Algerian endemic tree, and it is very important to explore it in different domains uses.

Keywords: Algerian fir leaves, essential oil, antioxidant power, enzymes inhibition, antibacterial effect, GC-MS analysis.

1. Introduction

The genus *Abies* is an important and complex genus of *Pinaceae* family, presented by 50 species, distributed through the world, in temperate and boreal regions of the northern hemisphere, North America, Asia (Yang *et al.* 2009). It has been reported that *Abies* species has exhibited several biological activities; it is used in traditional medicine against cold, vascular diseases, as an antimicrobial agent (Seo *et al.* 2016; Noreikaitė *et al.* 2017).

An incredible interest was directed to the use of bioactive molecules extracted from plants to cure illnesses such as cancer, Alzheimer's, and diabetes, either by inhibition of key enzymes implicated in such metabolic disorders, or scavenging of free radicals. Bacterial strains infections and their resistance to several antibiotics is another concern confronting human health. On the other side, a lot of studies have been done to discover therapeutic drugs from plants. Our attention was guided to *Abies numidica* de LANNOY ex CARRIÈRE, which is an Algerian endemic plant, found in Babors mounts, Setif. The cones of this species were used in popular medicine to heal stomach-ache, cataplasms, cold, inflammation, and respiration problems (Tlili Ait-Kaki *et al.* 2013). Despite

these beneficial biological effects on human health, this important species is still unknown and few papers have been published (Tlili Ait-Kaki *et al.* 2013; Ghabane *et al.* 2016). The gum from this fir is one of the essential remedies of folk medicine; it is used as an anti-scorbutic, an antiseptic in wounds and burns. Various preparations were made from this gum, including turpentine oil. A study conducted by Tlili-Ait Kaki *et al.* (2013) revealed that EO extracted from *A. numidica* needles (collected from Seraidi, Annaba), contained bornyl acetate (29.62%), camphene (23.97%) and α -pinene (13.17%) as the abundant constituents, while Ramdani *et al.* 2014 stated that essential oil from *A. numidica* needles harvested from Babors mounts was rich in α -pinene (22.6%), limonene (19.7%), β -pinene (12.3%), camphene (11.2%) and β -phellandrene (7.8%). Yu *et al.* (2004) reported that essential oil extracted from *A. nephrolepis* needles contained sesquiterpenes hydrocarbons and monoterpenes hydrocarbons, where α -Pinene (23.2%), limonene (12.7%), bornyl acetate (9.9%), and β -caryophyllene (10.8%) were noticed as major volatile constituents in this plant. Benouchene *et al.* (2020) reported that ethyl acetate fraction obtained from *Abies numidica* needles was rich in total phenolic compounds and total flavonoids, and the LC-MS/MS confirmed the obtained results, where this fraction was wealthy in astragalins, hyperosides and

quercetrine. In 2021, Benoucheche *et al.* disclosed that n-butanol fraction from this plant contained a high amount of phenolic compounds and flavonoids, as well as LC-MS/MS findings showed that major found molecules were hyperoside, astragalol, and rutin.

The current study aims were the determination of chemical profile and the evaluation of biological activities of the essential oil picked up from Algerian fir needles. Therefore, the present research investigated, for the first time the sun protection factor, phenanthroline assay, and enzymes inhibitory activities of essential oil extracted from this endemic plant.

2. Material and Methods

2.1. Reagents and Chemicals

Bioactivity measurements and calculations were accomplished on a 96-well microplate reader (Perkin Elmer Multimode Plate Reader EnSpire) at the National Center of Biotechnology Research. The chemicals used were: 1,1-diphenyl-2-picrylhydrazyl (DPPH), butylated hydroxyanisole (BHA), butylated hydroxytoluene (BHT), α -tocopherol, Dimethyl sulfoxide (DMSO), acetylcholinesterase from electric eel (AChE, Type-VI-S, EC 3.1.1.7, 827,84 U/mg, Sigma), acetylthiocholine iodide, 5,5'-dithiobis (2-nitrobenzoic) acid (DTNB), galantamine, 4-nitrophenyl- α -D-glucopyranoside ($\geq 99\%$), α -Glucosidase from *Saccharomyces cerevisiae* (Type I, ≥ 10 units/mg protein), acarbose ($\geq 95\%$); they were obtained from Sigma Chemical Co. (Sigma-Aldrich GmbH, Stern-Heim, Germany). Iron (III) chloride (FeCl_3) and phenanthroline were obtained from Biochem Chemopharma. All other chemicals and solvents were of analytical grade.

2.2. Essential oil extraction

2.2.1. Sample preparation

The sample leaves of Algerian fir (*Abies numidica* de Lannoy) were gathered from Constantine in September 2018, Algeria, and dried at room temperature under the shadow. This sample was ground with an electric mill IKIa 10 type, and stored until they were used.

2.2.2. Hydro-distillation method

The EO was tacked out by hydro-distillation using a Clevenger apparatus according to the modified method of Minteguiaga *et al.* (2018). A quantity of 228g of dried powdered leaves was immersed with 1L of distilled water and was left for 4 hours in Clevenger apparatus. The obtained oil was kept in obscure at 4°C until the use.

2.3. Chemical constituent's analysis by Gas Chromatography-Mass Spectrometry (GC-MS)

The chemical constituents of essential oil were determined by GC-MS analysis according to the assay of Ertas *et al.* (2015). Gas Chromatography equipped with Flame Ionisation Detector (GC-FID) was used in this analysis. The extracted *A. numidica* essential oil was analyzed by using a Shimadzu Model GC-2010 GC equipped with flame ionization detector (FID) and an autosampler injector AOC-20I (Shimadzu). The Separation was achieved using a middle polar capillary column RTX-5MS with 30 m length, 0.25 mm in diameter and film thickness of 0.25 μm . The injector and detector temperatures were conditioned at 250°C and 280°C, respectively. The oven temperature program started from 60°C to 300°C at a rate of 3°C min^{-1} with isothermal

temperature constant at 300°C for 2 minutes. Hydrogen gas was used as the carrier gas with a flow rate of 30 $\text{ml} \cdot \text{min}^{-1}$. The mode of injection used was split mode with a ratio of 1:50.

2.4. Antioxidant tests

2.4.1. 2,2-diphenyl-picrylhydrazyl (DPPH) scavenging assay

The DPPH free radical scavenging test was assessed as the method of Tel *et al.* (2012) with slight changes. The sample dilutions were dissolved in methanol. BHT, BHA, and α -tocopherol were used as standards. The reduction of DPPH radical was determined in percentages, and was calculated as following:

$$\% \text{ Inhibition} = \left[\frac{A_{\text{blank}} - A_{\text{sample}}}{A_{\text{blank}}} \right] \times 100$$

A_{blank} : absorbance of control reaction. A_{sample} : absorbance of the test sample.

Tests were approved in triplicates. The inhibition concentration (IC_{50}) is the half of free radicals (50%) was esteemed from the graph of DPPH radical scavenging effect percent against extract concentration.

2.4.2. Phenanthroline assay (Phen assay)

The phenanthroline antioxidant ability was performed as the test defined by Szydłowska-Czeraniak *et al.* (2008). Fifty microliters (50 μl) of FeCl_3 (0.2%), 30 μl of phenanthroline (0.5%) and 110 μl of methanol were added to 10 μl of essential oil at different dilutions in a 96-well microplate. The lecture of the sample and BHT standard was measured at 510 nm after 20 min incubation at 30°C. The results were given as $A_{0.50}$ ($\mu\text{g}/\text{mL}$) corresponding the concentration indicating 0.50 absorbance intensity.

2.4.3. Photoprotective activity (Sun protection factor assay SPF)

SPF assay was determined following the protocol of Mansur *et al.* (1986). Each 5nm, the absorbances were measured, from 290 nm to 320nm. The SPF was calculated by using the following mathematic equation:

$$\text{SPF}_{\text{spectrophotometric}} = \text{CF} * \sum_{290}^{320} \text{EE}(\lambda) \times \text{I}(\lambda) \times \text{Abs}(\lambda)$$

EE: erythemal effect spectrum; **I**: solar intensity spectrum; **Abs**: absorbance of sunscreen product; **CF**: correction factor (= 10). **EE** x **I**: is a constant determined by Sayre *et al.* (1979).

2.5. Essential oil's antidiabetic activity

2.5.1. α -amylase inhibitory test

α -amylase inhibitory assay was assessed according to the modified protocol of Zengin *et al.* (2014). Twenty-five microliters (25 μl) of essential oil at various concentrations were mixed with 50 μl of α -amylase solution (1U) prepared in phosphate buffer (pH 6.9 with 6 mM sodium chloride); the mixture was incubated for 10min at 37°C. Afterward, 50 μL of starch (0.1%) was added and then incubated again for 10min at 37°C. After incubation, 25 μl of HCl and 100 μl of iodine potassium iodide (IKI) were added. A blank solution was prepared using the plant extract without the enzyme. Acarbose was used as a standard. The absorbance was measured at 630nm using a microplate reader. The inhibition percentage of α -amylase was determined using the following formula:

$$\% \text{Inhibition} = 1 - \left[\frac{(A_c - A_e) - (A_s - A_b)}{(A_c - A_e)} \right]$$

A_c =Absorbance [Starch+ IKI + HCl+ solvent of extraction+ Volume of Enzyme buffer].

A_e =Absorbance [Enzyme+ Starch+ IKI+ HCl+ solvent of extraction].

A_s =Absorbance [Enzyme+ Extract+ Starch+ IKI+ HCl].

A_b =Absorbance [Extract+ IKI+125 μ l of buffer].

2.5.2. α -glucosidase inhibitory assay

The α -glucosidase inhibitory ability of essential oil was assessed according to the chromogenic test reported by Lordan *et al.* (2013). Fifty microliters (50 μ l) of the sample at different concentrations were mixed with 100 μ l of α -glucosidase enzyme and 50 μ l of p-nitrophenyl α -D-glucopyranoside (p-NPG) as substrate; the mixture was incubated for 10min at 37°C. Acarbose was used as standards. The absorbance was read spectrophotometrically at 405nm every 10min. The reaction mixture α -glucosidase enzyme and substrate were used as control. Substrate and essential oil were used as blank. The inhibition rate was determined as follows:

$$\text{Inhibition \%} = \left[\frac{(\text{Abs}_{\text{Extract}} - \text{Abs}_{\text{Blanc}})}{\text{Abs}_{\text{control}}} \right] \times 100$$

2.6. Acetylcholinesterase (AChE) inhibitory activity

AChE inhibitory activity was measured using the method of Ellman *et al.* (1961). The reaction mixture contained 150 μ L of 100 mM sodium phosphate buffer (pH 8.0), 10 μ L extract at different concentrations, and 20 μ L of AChE solution. The mixture was incubated at 25°C for 15min, 10 μ L of DTNB (0.5 mM), and 10 μ L of acetylthiocholine iodide (0.71 mM) were added. The absorbance was determined at 0 min and 15 min, at 412 nm. The reference standard used was Galantamine.

The inhibition percentage of AChE enzyme was determined according to the blank (methanol + phosphate buffer pH8), using the following formula:

$$\frac{(E - S)}{E} \times 100$$

E: AChE enzyme activity without extract

S: AChE enzyme activity in the presence of extract.

2.7. Antibacterial activity

The method of agar disc diffusion was used to determine the antibacterial activity of the essential oil

extracted from *A. numidica* leaves (Biondi *et al.* 1993), against 6 pathogenic bacterial strains; obtained from Pasteur institute, Algiers, Algeria; Gram-negative bacteria: *Proteus vulgaris* (ATCC 29905), *Morganella morganii* (ATCC 25830) *Pseudomonas aeruginosa* (ATCC 27853), and *Escherichia coli* (ATCC 25922), and Gram-positive bacteria: *Staphylococcus aureus* (ATCC 43300) and *Bacillus subtilis* (ATCC 6633). Bacteria strains suspension was distributed on Mueller Hinton (MH) agar. 10 μ l of essential oil diluted with dimethylsulfoxide (DMSO) were added to the discs (diameter of 6mm) which were placed on the inoculated agar. Cefepime (FEP) served as a positive reference standard to determine the sensitivity of each bacterial strain tested. The incubation was done at 37°C for 24h. Antibacterial activity was evaluated by measuring the zone of growth inhibition against the test organisms. Each test was done in triplicate.

3. Statistical analysis and

Linear regression analysis was used to calculate the IC_{50} and $A_{0.50}$ values, and one-way ANOVA to detect significant differences ($P < 0.05$) using XLSTAT. Results are reported as the mean value \pm SD of three measurements.

4. Results

4.1. The yield of extraction and the chemical constituents of essential oil

The essential oil (EO) obtained by hydro-distillation from dried, milled needles of *A. numidica* was colorless and possessed an aromatic odor with a yield of 0.592%, based on the dry plant material utilized.

The chromatogram obtained by GC/MS analysis was presented in figure 1. The chemical composition findings of the essential oil extracted from *A. numidica* leaves are shown in table 1, where the percentage of the diverse components and their retention times are given.

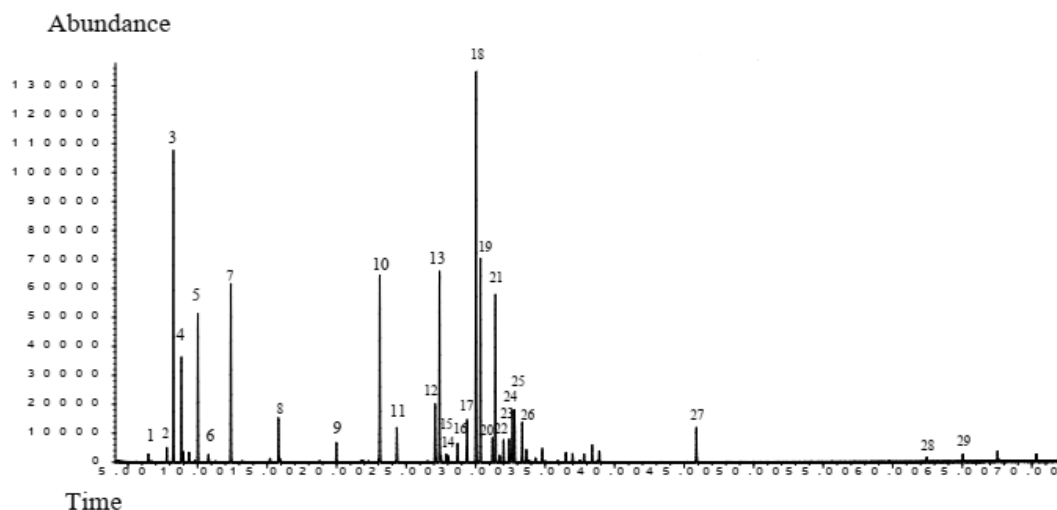


Figure 1. Gas chromatogram of *A. numidica* needles essential oil. The numbers refer to those in Table 1.

A total of 29 compounds representing 93.89% of the essential oil were determined. The main volatile constituents were Caryophyllene (17.31%), α -pinene (10.58%), 2, 2, 6, 10-Tetramethylbicyclo [5.4.0] undeca-9, 11-diene (8.65%), linalyl acetate (7.41%), β -sillinene (7.28%), and sabinene (6.88%). Other compounds were found in traces as α -ylangene (0.18%), santene, and β -myrcene (0.23%). The studied essential oil comprised sesquiterpene hydrocarbons (44.23%) in major, followed by monoterpene hydrocarbons (27.52%).

Table 1. Main components (%) detected by GC-MS in the Algerian fir leaves essential oil.

Peak	Compound	RT (min)	(%)
1	Santene	6.46	0.23
2	Delta3-Carene	7.7871	0.42
3	Alpha-pinene	8.2631	10.59
4	Camphene	8.8401	3.72
5	Beta-pinene	10.0245	5.45
6	Beta-Myrcene	10.7952	0.23
7	Sabinene	12.3945	6.88
8	L-linalool	15.8212	1.55
9	Beta fenchylalcohol	19.9831	0.73
10	Linalylacetate	23.1084	7.42
11	Exobornylacetate	24.3386	1.35
12	Alpha-Longipinene	27.0882	2.54
13	2,6-Octadiene, 2,6-dimethyl	27.4035	7.63
14	Geranylacetate	27.8823	0.33
15	Alpha ylangene	28.0458	0.18
16	4-Hexen-1-ol, 5-methyl-2-(1-methylethenyl)-, acetate	28.7012	0.72

17	Longifolene	29.3869	1.96
18	Caryophyllene	30.0272	17.31
19	2,2,6,10-Tetramethylbicyclo [5.4.0] undeca-9,11-diene	30.345	8.65
20	1H-Benzocycloheptene, 2,4a,5,6,7,8,9,9a-octahydro-3,5,5-trimethyl-9-methylene	31.215	0.85
21	Beta-Selinene	31.4217	7.28
22	Gamma-himachalene	32.4158	0.78
23	Presilphiperfol-1(8)-ene	32.5545	0.31
24	1-ethynyl-2-methyl-1(e)-cyclododecene	32.6476	2.13
25	10s,11s-Himachala-3(12),4-diene	32.8054	2.10
26	Delta-Cardinene	33.6489	0.45
27	1,6,10-Dodecatrien-3-ol, 3,7,11-trimethyl	45.8788	1.34
28	Hentriacontane	65.0468	0.31
29	n-Hentriacontane	67.5444	0.45

Classes compound (%)	
Sesquiterpenhydrocarbons	44.23
Monoterpenhydrocarbons	27.52
Oxygenatedmonoterpens	17.45
Monoterpenalcohols	2.28
Sesquiterpenalcohols	1.65
Others	0.76
Total identified (%)	93.89

4.2. Antioxidant activity

The results of antioxidant capacity of EO extracted from *A. numidica* needles are shown in figure 2 and 3 for DPPH· Free radicals scavenging and phen assays. The EO antioxidant effect findings disclosed no significant activity against free radicals, at the concentrations (800 μ g/ml and 200 μ g/ml, respectively) when compared with standards used. From the results, it is necessary to increase the concentration of the sample in different assays in order to get the inhibition concentration at 50%.

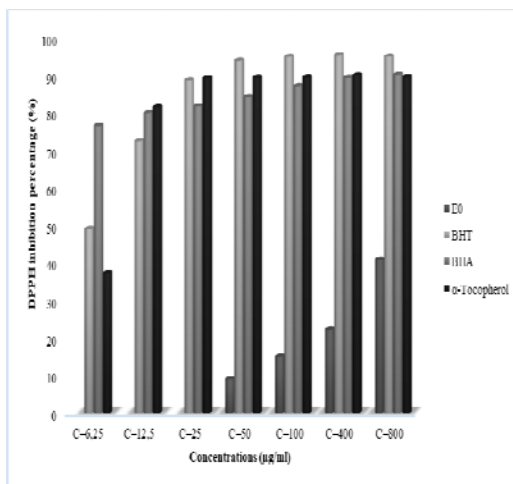


Figure 2. Inhibition percentage of DPPH free radical by *A. numidica* needles EO and standards at different concentrations ($P < 0.05$).

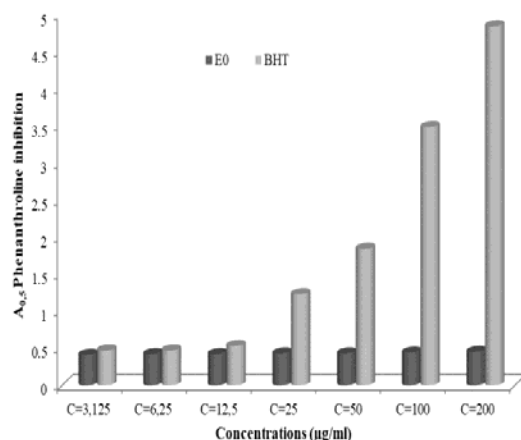


Figure 3. Inhibition percentage of phenanthroline by *A. numidica* needles EO and BHT standard at different concentrations ($P < 0.05$).

Sun protection factor is an indicator for the protection level classification of plant extracts, the data in figure 4 indicated that EO represented a weak protective influence, referring to the different protection categories demanded by the European Commission, 2006, where $SPF = 5.48 \pm 0.17$.

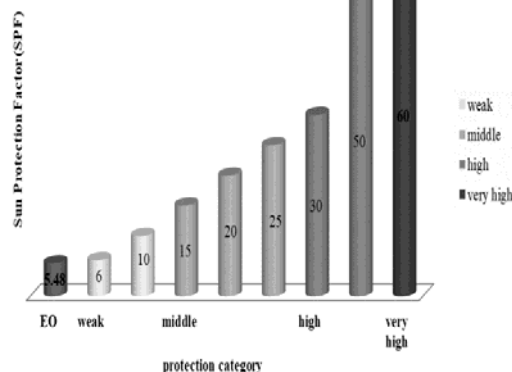


Figure 4. Sun Protection Factor and protection category determination of *A. numidica* needles EO.

4.3. Enzymes inhibitory activities

The enzymes inhibitory activities of the EO on α -glucosidase, α -amylase, and Acetylcholinesterase (AChE) were investigated and the results are shown in table 2.

In this study, the anti-diabetic effect of *A. numidica* needles EO was investigated by testing the α -glucosidase and α -amylase inhibitory assays, *in-vitro*, whereas the neuroprotective effect was examined by AChE inhibition. As presented in table 2, the action of essential oil on the activity of α -glucosidase revealed a powerful inhibition, compared with acarbose standard used, where EO's $IC_{50} = 59.23 \pm 1.55 \mu\text{g/ml}$, and acarbose's $IC_{50} = 275.43 \pm 1.59 \mu\text{g/ml}$. From the results, it is remarkable that the inhibition concentration of the essential oil obtained from *A. numidica* needles was less 5 times than the results obtained for acarbose standard.

For α -amylase findings, as represented in table 2, the EO exerted no α -amylase inhibitory effect, it was not active at the concentration 1600 $\mu\text{g/ml}$, compared with acarbose standard [$IC_{50} = 3650.93 \pm 10.70 \mu\text{g/ml}$], and did not achieve the 50% of the enzyme inhibition level.

The results of the AChE inhibitory activity of the tested EO extracted from *A. numidica* leaves as well as the positive control, galantamine are provided in table 2. The findings showed that EO has a weak AChE inhibition activity compared with standard used, where EO's $IC_{50} = 153.92 \pm 1.94 \mu\text{g/ml}$ and galantamine's $IC_{50} = 6.27 \pm 1.15 \mu\text{g/ml}$. It has been reported that the extract which has a lower IC_{50} , presented a strong and powerful inhibitory activity.

Table 2. Percentage enzyme inhibition and IC_{50} ($\mu\text{g/ml}$) of essential oil extracted from Algerian fir needles.

Samples	α -glucosidase		α -amylase		AChE	
	% inhibition at 1000 $\mu\text{g/ml}$	IC_{50} ($\mu\text{g/ml}$)	%inhibition at 1600 $\mu\text{g/ml}$	IC_{50} ($\mu\text{g/ml}$)	%inhibition at 200 $\mu\text{g/ml}$	IC_{50} ($\mu\text{g/ml}$)
EO	nt	59.23 ± 1.55	34.39 ± 0.00	na	61.85 ± 1.75	153.92 ± 1.94
Acarbose ^a	91.05 ± 0.72	275.43 ± 1.59	53.05 ± 1.59	3650.93 ± 10.70	nt	nt
Galantamine ^a	nt	nt	nt	nt	94.77 ± 0.34	6.27 ± 1.15

Values are expressed as means \pm S.D of three parallel measurements. The results are statistically considered significantly different at ($P < 0.05$). na: not active. nt: not tested. ^aReference compounds. Galantamine is a control for Acetylcholinesterase (AChE). Acarbose for α -glucosidase and α -amylase.

4.4. Antibacterial activity

The results are shown in figure 5. Inhibition zones diameters are summarized in table 3. The essential oil exerted no antibacterial activity against all bacterial strains tested, excluding *S. aureus*, where the inhibition diameter was esteemed by (17±0.1mm, at 10µl/disc), which is lower than Cefepime inhibition diameter (30mm).

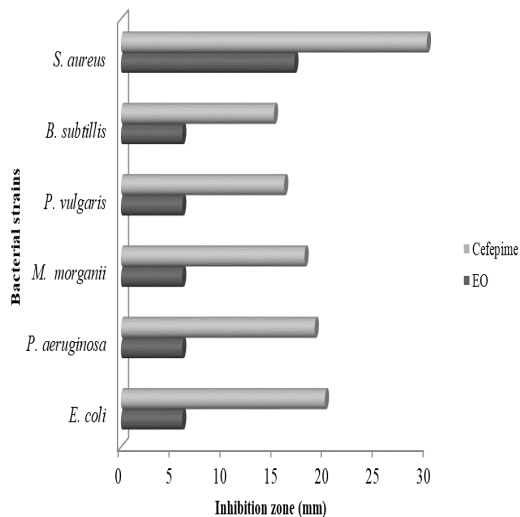


Figure 5. Antibacterial activity of *A. numidica* leaves essential oil and Cefepime antibiotic.

Table 3. Antibacterial effect of Algerian fir needles essential oil using disc diffusion method against bacterial strains.

Strains	Inhibition zone (mm)	
	Algerian fir oil ¹⁾	FEP ²⁾
Gram⁻		
<i>E. coli</i>	6±0.0 ³⁾	20
<i>P. aeruginosa</i>	6±0.0	19
<i>M. morgani</i>	6±0.0	18
<i>P. vulgaris</i>	6±0.0	16
Gram⁺		
<i>subtillis</i>	6±0.0	15
<i>S. aureus</i>	17±0.1	30

¹⁾ Algerian fir oil tested at a concentration of 10µg/disc. ²⁾ Cefepime tested at a concentration of 30µg/disc. ³⁾ Values are diameters of clear zone of inhibition (mm) including disc diameter of 6 mm.

5. Discussion

Secondary metabolites extracted from plants showed a beneficial effect for human health, as flavonoids, phenolic compounds and essential oil. Our attention was directed to *A. numidica* De Lannoy needles. The EO extracted from leaves yielded 0.592% using 228 g of dried powdered sample, and it was in the line with the findings described by Ghadbane *et al.* (2016) that reported a yield of 0.260% using 100g of dried leaves, but the yield was less than those results disclosed by Ramdani *et al.* (2014) and Tlili-Ait Kaki *et al.* (2013), which stated a yield of 0.4% and 0.37% for 100g of dried needles; respectively. We proposed that the variation in the yield of extraction might be the result of different involved factors like genetic

factors, the environment, the methods, and time of extraction (Figueredo *et al.* 2008; Tlili Ait-Kaki *et al.* 2013). A previous study done by Tlili-Ait Kaki *et al.* (2013) revealed that EO extracted from *A. numidica* needles (collected from Seraidi, Annaba) contained bornyl acetate (29.62%), camphene (23.97%) and α -pinene (13.17%) as the major constituents. Ramdani *et al.* (2014) reported that the EO extracted from aerial parts of *A. numidica* (obtained from Babors region, Setif) principally contained α -pinene (22.6%), limonene (19.7%), β -pinene (12.3%), camphene (11.2%) and β -phellandrene (7.8%) in high amounts. The differences in the results might be due to bioclimatic conditions, the characteristics of each region, as well as the period of plant collection.

The antioxidant power is broadly used as a parameter for medicinal biomolecules. The antioxidant activity of *A. numidica* needles EO was examined using three complementary *in vitro* tests: DPPH[•] scavenging, phen assays, and SPF. The potential antioxidant activity of EO was evaluated based on its ability to quench free radicals, by donating an electron. The inhibition percentage increased with the increase of the sample concentration.

The results of antioxidant activity showed that the EO has a weak antioxidant ability, while Ghadbane *et al.* (2016) reported that *A. numidica* leaves EO has a strong DPPH[•] Free radical scavenging capacity. Furthermore, a study reported by Sobrinho *et al.* (2020) revealed that β -caryophyllene exerted a mild antioxidant power in DPPH[•] scavenging assay. Yang *et al.* (2008) demonstrated that α -pinene possessed a very low scavenging capacity for DPPH[•] free radicals. To the best of our knowledge, phen and photoprotective assays for EO extracted from *A. numidica* needles have not previously been reported. The data presented in this research could be the first report for the literature.

To the best of our knowledge and according to the literature, there are no papers about the enzymes inhibitory activities of essential oil extracted from *A. numidica* needles.

Diabetes mellitus and Alzheimer's diseases are two chronic public ailments for human health, and many attempts have been done to look for alternatives from medicinal plants that have minimal adverse effects compared with a synthetic one. A modern therapeutic strategy to cure those pathologies was investigated, based on the inhibition of key metabolic enzymes to conduct such disorders.

α -glucosidase and α -amylase are two main enzymes, catalyze starches (Sharifi-rad *et al.* 2017). α -amylase is present in saliva and pancreas; it is responsible for splitting long-chain carbohydrates (starch) into maltose, which is a substrate for α -glucosidase in the small intestine, to facilitate its absorption leading to hyperglycemia (Hichri *et al.* 2017). Inhibitors of these enzymes delay the cleaving of oligosaccharides that leads to a decrease in the level of postprandial blood glucose in diabetic persons (Kazeem *et al.* 2013).

As can be seen, the inhibition concentration for EO was four-time lower than acarbose standard. It might refer to the several compounds present in the EO, especially sesquiterpene hydrocarbons, that compete with the substrate for binding to the enzyme active site, thus blocking the breaking down of carbohydrates. Our data corroborated with those revealed by Nakagawa *et al.* (2019), which reported that the resin extracted from the Sakhalin fir tree (*Abies sachalinensis*) showed a high α -glucosidase inhibitory activity with [IC₅₀=17. 3µg/ml].

Basha and Sankaranarayanan, (2015) concluded that β -caryophyllene improved glycoprotein levels in STZ-induced diabetic rats.

AChE is an enzyme responsible for the hydrolysis of acetylcholine in the neurons (Owokotomo *et al.* 2015). Acetylcholine has an important role in the nervous system, especially in improving memory state; the inhibition of this enzyme increases the level of acetylcholine in the nervous system and prevents the human body from a large variety of pathologies related to the brain as Alzheimer and dementia (Bonesi *et al.* 2010). A lot of trends showed that plant extracts have a potential AChE inhibitory activity (Ertas *et al.* 2015; Jeong *et al.* 2007); however, little studies have been done on *Abies* genus.

Zengin *et al.* (2016) disclosed that α -pinene has very low activity against cholinesterase enzyme, while, Kim *et al.* (2006) reported that *A. Koreana* EO improved age-related brain problems. These differences in the two results might be due to the difference in the chemical structure of the bioactive components present, for that other analysis is needed as RMN analysis.

Algerian fir's essential oil was examined for its antibacterial effect using a disc diffusion method against six Gram-negative and Gram-positive bacterial strains.

Our results are in accordance with the data reported by Ghadbane *et al.* (2016), which disclosed that essential oil extracted from *A. numidica* needles (collected from Babors region, Setif) has a strong antimicrobial activity, especially against *S. aureus* and *M. luteus*. Also, Yang *et al.* (2008) results revealed that silver fir essential oil revealed no effect against different bacterial strains used, while it was more effective against only *S. aureus*. Ramdani *et al.* (2014) reported that essential oil extracted from Algerian fir leaves, collected from Seraidi, Annaba, has a strong antimicrobial effect against Gram negative bacteria (*E. coli*), and it has a mild growth inhibition against positive bacteria (*S. aureus*). Although *A. numidica* needles essential oil exerts a mild antibacterial ability. It has been reported that β -caryophyllene and α -pinene have a powerful antimicrobial effect (Dahham *et al.* 2015). From the obtained findings, to make it clear, it is very important to test the antibacterial effect of Algerian fir needles essential oil using the main compounds.

There are no recent studies that have been reported about the essential oil extracted from *Abies* genus. But there are two papers published about the extracts obtained from *A. numidica* needles. Benouchenne *et al.* (2020) demonstrated the chemical composition of ethyl acetate fraction and investigated the biological activities (antibacterial and antioxidant), while Benouchenne *et al.* (2021) published the antibacterial and antioxidant ability of n-butanol extract, as well as the chemical constituents of this fraction.

6. Conclusion

In summary, from the above results, we conclude that essential oil extracted from *A. numidica* needles contained Caryophyllene as a major constituent. It presented a weak antioxidant power. It exhibited a strong α -glucosidase inhibitory activity, while it has no effect on α -amylase and AChE. It exerted no antibacterial inhibition growth of bacterial strains tested, excepting *S. aureus*. This EO can be used for pharmaceutical and therapeutic applications in the future; furthermore, more biological assays are needed to go in depth of this little studied endemic plant. This plant can be used as a source of natural antioxidant compounds, to replace the synthetic drugs in different

domains, in industry, pharmaceutical and food fields. Furthermore, this species could be utilized as bioactive molecules for the treatment of diabetes and infection pathologies.

References

- Basha RH and Sankaranarayanan C. 2015. Protective role of β -caryophyllene, a sesquiterpene lactone on plasma and tissue glycoprotein components in streptozotocin-induced hyperglycemic rats. *J. Acute Med.*, **5**: 9–14.
- Benouchenne D, Bellil I, Akkal S, Bensouici Ch and Khelifi D. 2020. LC-MS/MS analysis, antioxidant and antibacterial activities of Algerian fir (*Abies numidica* de LANNROY ex CARRIÈRE) ethyl acetate fraction extracted from needles. *J King Saud Univ Sci.*, **32**: 3321-3327.
- Benouchenne D, Bellil I, Akkal S and Khelifi D. 2021. Investigation of phytochemical and evaluation of antioxidant and antibacterial activities from *abies* extract. *Sci. J. King Faisal Univ: Basic and Applied Sciences.*, **22**(2): 26–32.
- Biondi D, Cianci P, Geraci C, Rubertof G and Piattelli M.1993. Antimicrobial activity and chemical composition of essential oils from Sicilian aromatic plants. *Flavour Fragr J.*, **8**: 331–337.
- Bonesi M, Menichini F, Tundis R, Loizzo MR, Conforti F, Passalacqua NG, Statti GA and Menichini F. 2010. Acetylcholinesterase and butyrylcholinesterase inhibitory activity of Pinus species essential oils and their constituents. *J Enzyme Inhib Med Chem.*, **25**: 622–628.
- Commission of European Communities. Recommendation of 22 September 2006. On sunscreen products and manufacturers' claims. <https://eur-lex.europa.eu>.
- Dahham SS, Tabana YM, Iqbal MA, Ahamed MBK, Ezzat MO, Majid ASA and Majid AMSA. 2015. The anticancer, antioxidant and antimicrobial properties of the sesquiterpene β -Caryophyllene from the essential oil of *Aquilaria crassna*. *Molecules.*, **20**:11808–11829.
- Ellman GL, Courtney KD, Andres V and Featherstone RM. 1961. A new and rapid colorimetric determination of acetylcholinesterase activity. *Biochem. Pharmacol.*, **7**: 88–95.
- Ertas A, Bogab M, Yilmaz MA, Yesild Y, Tel G, Temel H, Hasimi N, Gazioglu I, Ozturk M and Ugurlu P. 2015. A detailed study on the chemical and biological profiles of essential oil and methanol extract of *Thymus nummularius* (Anzer tea): Rosmarinic acid. *Ind Crops Prod.*, **67**: 336–345.
- Figueiredo AC, Barroso JG, Pedro LG and Scheffer JJC. 2008. Factors affecting secondary metabolite production in plants:volatile components and essential oils. *Flavour Fragr J.*, **23**: 213–226.
- Ghadbane M, Bounar R, Khellaf R, Medjekal S, Belhadj H, Benderradji L, Smali T and Harzallah D. 2016. Antioxidant and antimicrobial activities of endemic tree *abies numidica* growing in babor mountains from algeria. *Global Journal of Research on Medicinal Plants and Indigenous Medicine.*, **5**:19-28.
- Hichri F, Omri A, Hossan ASM and Ben Jannet H. 2019. Alpha-glucosidase and amylase inhibitory effects of *Eruca vesicaria* subsp. *longirostris* essential oils: synthesis of new 1,2,4-triazole-thiol derivatives and 1,3,4-thiadiazole with potential inhibitory activity. *Pharm Biol.*, **57**(1): 564–570.
- Jeong SI, Lim JP and Jeon H. Chemical composition activities of the essential oil from *Abies koreana*. 2007. *Phytother Res.*, **21**:1246–1250.
- Kazeem MI, Adamson JO and Ogunwande IA. 2013. Modes of inhibition of α -Amylase and α -Glucosidase by aqueous extract of *Morinda lucida* Benth Leaf. *BioMed Res. Int.*, **2013**: 1-6.
- Kim K, Bu Y, Jeong S, Lim J, Kwon Y, Cha DS, Kim J, Jeon S, Eun J and Jeon H. 2006. Memory-enhancing effect of a supercritical carbon dioxide fluid extract of the needles of *Abies koreana* on scopolamine-induced amnesia in mice. *Biosci. Biotechnol. Biochem.*, **70**: 1821–1826.

- Lordan S, Smyth TJ, Soler-Vila A, Stantonand C and Paul Ross R. 2013. The α -amylase and α -glucosidase inhibitory effects of Irish seaweed extracts. *Food Chem.*, **141**: 2170-2176.
- Mansur JS, Breder MNR and Mansur MCA. 1986. Determination of the factor of solar protection by spectrophotometry. *An Bras Dermatol Rio Janeiro.*, **61**: 121-124.
- Minteguiaga M, Mercado MI, Ponessa GI, Catalán CAN and Dellacassa E. 2018. Morphoanatomy and essential oil analysis of *Baccharis trimera* (Less.) DC. (Asteraceae) from Uruguay. *Ind Crops Prod.*, **112** : 488-498.
- Nakagawa T, Ashour A, Amen Y, Koba Y, Ohnukiand K and Shimizu K. 2019. α -Glucosidase inhibitory activity of resin from Sakhalin fir tree (*Abies sachalinensis*) and its bioactive compounds. *Nat Prod Commun.*, **2019**: 1-4.
- Noreikaitė A, Ayupova R, Satbayeva E, Seitilyeva A, Amirkulova M, Pichkhadze G, Datkhayev U and Stankevicius E. 2017. General Toxicity and Antifungal Activity of a New Dental Gel with Essential Oil from *Abies*. *Med Sci Monit.*, **23**:521-527.
- Owokotomo IA, Ekundayo O, Abayomi TG and Chukwuka AV. 2015. In-vitro anti-cholinesterase activity of essential oil from four tropical medicinal plants. *Toxicol. Rep.*, **2**: 850-857.
- Ramdani M, Lograda T, Chalard P and Figueredo G. 2014. Chemical and antimicrobial properties of essential of *Abies numidica*, endemic species of Algeria. *International Journal of Phytopharmacy.*, **5**: 432-440.
- Sayre RM, Agin PP, Levee GJ and Marlowe EA. 1979. comparison of in vivo and in vitro testing of sun screening formulas. *J. Photochem. Photobiol.*, **29**: 559-566.
- Sharifi-rad J, Sureda A, Tenore GC, Daglia M, Sharifi-Rad M, Valussi M, Tundis R, Sharifi-Ra M, Loizzo MR, Ademiluyi AO, Sharifi-Rad R, Ayatollahi SV and Iriti M. 2017. Biological activities of essential oils: from plant chemocoology to traditional healing systems. *Molecules.*, **22**:1-55.
- Seo M, Sowndhararajan K and Kim S. 2016. Influence of binasal and uninasal inhalations of essential oil of *Abies Koreana* Twigs on electroencephalographic activity of human. *Behav Neurol.*, **2016**: 1-11.
- Sobrinho ACN, de Morais SM, Albuquerque MRJR, dos Santos HS, de Paula Cavalcante CS and de Sousaand HA. 2020. Antifungal and antioxidant activities of *Vernonia Chalybaea* Mart. ex DC. essential oil and their major constituent β -caryophyllene. *Braz Arch Biol Technol.*, **63**:1-11.
- Szydłowska-Czerniak A, Dianoczki C, Recseg K, Karlovits G and Szyk E. 2008. Determination of antioxidant capacities of vegetable oils by ferric-ion spectrophotometric methods. *Talanta.*, **76**: 899-905.
- Tel G, Apaydın M, Duru ME and Öztürk M. 2012. Antioxidant and cholinesterase inhibition activities of three *Tricholoma* species with total phenolic and flavonoid contents: the edible Mushrooms from Anatolia. *Food Anal Methods.*, **5**: 495-504.
- Tlili-Ait Kaki Y, Bennadja S and Chefrou A. 2013. Revalorisation d'une essence endémique: Le sapin de Numidie (*Abies numidica*). *Flora Mediterr.*, **23**: 123-129.
- Yang SA, Jeon SK, Lee EJ, Im NK, Jhee KH and Lee SP. 2009. Radical scavenging activity of the essential oil of silver fir (*Abies alba*). *J Clin Biochem Nutr.*, **44**: 253-259.
- Yu EJ, Kim TH, Kim KH and Lee HJ. 2004. Characterization of aroma-active compounds of *Abies nephrolepis* (Khingang fir) needles using aroma extract dilution analysis. *Flavour Frag J.*, **19**: 74-79.
- Zengin G, Sarikurkcü C, Aktümsek A, Ceylan R and Ceylan O. 2014. A comprehensive study on phytochemical characterization of *Haplophyllum myrtifolium* Boiss. endemic to Turkey and its inhibitory potential against key enzymes involved in Alzheimer, skin diseases and type II diabetes. *Ind Crops Prod.*, **53**: 244-251.
- Zengin G, Sarikürkcü C, Aktümsek A and Ceylan R. 2016. Antioxidant potential and inhibition of key enzymes linked to Alzheimer's diseases and diabetes mellitus by monoterpene-rich essential oil from *Sideritis galatica* Bornm. Endemic to Turkey. *Rec. Nat. Prod.*, **10**:195-206.

Structural and Catalytical Features of Different Amylases and their Potential Applications

Saptadip Samanta*

Department of Physiology, Midnapore College, Midnapore, Paschim Medinipur, 721101, West Bengal, India.

Received: April 29, 2021; Revised: July 8, 2021; Accepted: August 17, 2021

Abstract

Amylases can hydrolyze the O-glycosyl linkage of starch and related polymers. They are ubiquitously present in all living systems. However, microbial amylases meet the demands of industrial applications. Amylase and related enzymes are classified in different glycosyl hydrolases (GH) families. The GH13 is the largest family in the carbohydrate-active enzyme (CAZy) database, which comprises α -amylase, α -glucosidase, maltogenic amylase, debranching enzymes, CGTase, pullulanase, neopullulanase, and others. Despite GH13, some other families also contain α -amylase and related enzymes. Most of the starch-degrading enzymes have a common $(\beta/\alpha)_8$ barrel structure and four or five conserved sequences containing catalytic residues. α -Amylase and related enzymes follow the α -retaining double displacement mechanism during catalysis. The enzymes of the α -amylase family are potentially applied in food, pharmaceutical, textile, paper, detergent, biofuel, and animal feed producing industries. α -Amylase-mediated liquefaction and saccharification of starch is the essential step for the production of glucose, maltose, high fructose-containing syrups, maltooligosaccharides, cyclodextrins. These products are potentially used for the preparation of geriatric and infant foods. In conclusion, starch degrading enzymes bear a common structural arrangement and catalytic activity, and are broadly exploited in different sectors ranging from food, pharmaceutical industries to wastewater treatment.

Keywords: Amylases, starch, glycosyl hydrolases, catalytic properties, maltooligosaccharides

1. Introduction

Starch is the major storage polysaccharide in plant products and is an important source of energy for human and other monogastric animals. Starch is also widely used in different industries. About 75 million tons of starch was utilized in the year 2012; the expected annual growth rate will be continued by 2-3%. Amylolytic enzymes are essential in starch-based industries for the preparation of commercial products. The physicochemical properties of natural starch do not meet the requirements of industrial use (Park *et al.*, 2018). Previously, various physical methods (heat-moisture treatments, freezing, and ultrahigh-pressure treatments) and chemical modification were applied for starch processing (Chung *et al.*, 2010; Park *et al.*, 2018). To overcome the hazards of these treatments, enzymatic modification is the best as the process is safe, healthier, and eco-friendly. The enzymatic processing is mostly mediated by a group of amylolytic enzymes.

Varieties of starch degrading enzymes such as α -amylase, isoamylase, α -glucosidase, CGTase (cyclodextrin glycosyltransferase), branching enzymes, pullulanase, amylopullulanase, and neopullulanase commonly belong to the α -amylase family. Earlier, Kuriki and Imanaka (1999) had classified the amylases into α -amylase (EC 3.2.1.1), debranching enzymes such as pullulanase (EC 3.2.1.41), isoamylase (EC 3.2.1.68), CGTase (EC

2.4.1.19), and branching enzyme (EC 2.4.1.18). The carbohydrate-active enzyme (CAZy) database is the tool for the classification of carbohydrases. This database carries 168 glycosyl hydrolase (GH) families (GH1–GH168) having 18 clans (A–R). CAZy database was constructed for the distribution of all carbohydrate-splitting enzymes (Lombard *et al.*, 2014; <https://www.cazy.org/>). GH13, GH31, GH57, and GH119 are the most important family concerning amylolytic enzymes. Almost all the common amylolytic enzymes (family GH13, GH31, GH57, GH77, and GH119) have multiple domains and similar internal structures containing $(\beta/\alpha)_8$ barrel topology. The molecular structure of amylases, mechanism of catalysis, and mutational effects can improve overall strategies of applications of amylases.

The progression of biotechnology tremendously increases the applications of amylases and other industrial enzymes like cellulase, xylanase, pectinase, and proteases. The global market of industrial enzymes is growing exponentially from the last decade and is projected to be continued in the future. According to the global industrial enzymes market report, the annual growth had started with a value of 5.8% from the year 2017; the estimated values had touched the level of US\$ 5.9 billion in the previous year (2020). The expected estimated values will reach up to US\$ 8.7 billion in 2026 (Industrial Enzymes Market 2016;

<https://www.businesswire.com/news/home/20161219005619/en/Global-Industrial-Enzymes-Market-Analysis-2016-->

* Corresponding author. e-mail: saptadip174@gmail.com.

). The enzymes of the amylase family are potentially used in the brewing process, food and pharmaceutical industry, animal feed preparation, paper recycling, biofuel production, desizing process, detergent preparation, and waste management (Yan and Wu, 2016). Amylases themselves have a 25% share in the world's enzyme market (Rajagopalan and Krishnan, 2008; John, 2017) and more specifically used in different purposes (detergents-37%, textiles-12%, starch processing-11%, baking-8%, and animal feed production-6%) (Deb *et al.*, 2013).

The commercial production of amylase was started in 1894 when Jökichi Takamine isolated "Takadiastase" from a wheat bran culture of *Aspergillus oryzae*. Numerous bacteria (e.g. *Bacillus licheniformis*, *B. amyloliquefaciens*, *B. subtilis*, *B. stearothermophilus*) and fungi (e.g. *Aspergillus oryzae*, *A. niger*, *A. awamori*, *Rhizopus* sp.) were exploited for the large scale production of amylases (Gupta *et al.*, 2003; Mehta and Satyanarayana, 2016; Samanta, 2020a). In the commercial sectors, different multinational companies (Novozymes, DuPont Danisco, AB Enzymes, Dyadic, BASF, DSM, and others) are involved in the production of amylases; they cover more than 70% of the total enzyme market. Indian biotech sector has achieved a vital position in manufacturing and research services in the enzyme sector (Li *et al.*, 2012; Chandel *et al.*, 2007; Kumar *et al.*, 2014; Industrial Enzymes Market, 2016). The enzyme-based preparation of infant and geriatric foods, confectionery products, digestive aids, animal feed, detergents, biofuel, and many other products depend on the supply of amylases and other industrial enzymes from these multinational companies. The present review has focused on the amylases of GH13 and associated families, their sources, production, catalytic properties, primary structure. Special emphasis has been given to the applications of α -amylase, α -glucosidase, maltogenic amylase, debranching enzymes, CGTase, pullulanase, and neopullulanase.

2. Methodology

The CAZy database (Lombard *et al.*, 2014) was thoroughly reviewed for the study of the classification of amylases. Then the literature survey had been done for the collection of information related to molecular structure, catalytic strategies, mechanism of action, and applications of amylolytic enzymes in different sectors. For this purpose, several databases such as NCBI website database PubMed, Springer Nature, Science Direct (Elsevier), Google Scholar, ResearchGate, and others were viewed for searching the relevant articles. Different keywords like classification of amylases, glycosyl hydrolase families, the molecular structure of amylases, mechanism of catalysis by amylases, and applications of amylases were used during the literature survey. Then, this review has been prepared on the basis of the searching content.

3. Starch and some important saccharides

Starch is the major component of the human diet and comprises half of the ingested carbohydrates. Several starch-based products like glucose syrups, high fructose-containing syrup, malto-oligosaccharides, cyclodextrins, anomalously linked oligosaccharides mixture (Alo mixture), branched dextrin are produced through

enzymatic treatment for the formulation of geriatric and infants' foods. Moreover, starch has other industrial applications such as thickener, colloidal stabilizer, gelling, bulking, and water holding agent due to its molecular properties (Singh *et al.*, 2007). Amylases are used for the removal of starch during cloth making, production of finished paper, biofuel production, and wastewater treatment of the sugar and paper industries. Another important use of amylases is in the brewing industry where starchy products are the initial components for making wine. Several digestive medicines are formulated by fungal α -amylase. Recently amylase is used in the diagnostic kit.

Starch is regarded as a biopolymer of glucose. It is usually present inside the plant cells as compact insoluble granules, which may be spherical, lens-shaped, or ovoid. The major sources of starch are maize, rice, tapioca, potato, wheat, and cassava. Natural starches consist of an unbranched amylose chain (15–20%) and branched amylopectin (80–85%). Amylose is a polymer of D-glucopyranosyl units, consists of 300-3000 glucose residues joined by α -1 \rightarrow 4 glycosidic linkages. Amylose can form inclusion complexes with iodine (Zobel, 1988) and generate a colored complex. A minimum of 18 glucose units containing an oligosaccharide chain is required to form a starch iodine color complex (Bailey and Whelan, 1961). However, the intensity of color increases linearly with chain length to about 70 glucose units. The structure of amylopectin is more complex. It is the largest polymer in nature with a DP (degree of polymerization) ranging from 3×10^5 to 3×10^6 D-glucopyranosyl units; however, the individual chains vary between 10 and 100 glucose units (Bijttebier *et al.*, 2008). The backbone of amylopectin is much longer than that of amylose. It contains up to 10^5 glucose residues joined by α -1,4 glycosidic linkages with glucan sidechains having 20-25 residues linked by α -1,4 linkages. Sidechains are attached to the backbone by α -1,6 glycosidic bonds (Fig. 1A). The detailed structure of amylopectin is still speculative; it is composed of 3 types of chains, A, B, and C with the degree of polymerization (DP) in the range of 12–75 glucose residues. A-chains (DP 12-16) are linked to B-chains. These B-chains are further linked to other B-chains and to the C-chain, which carries the only reducing glucose residue. The B-chains can be further divided into B1- (DP 20-24), B2- (DP 42-48), B3- (DP 69-75) and B4-chains (Hizukuri, 1986, 1996) (Fig. 1B). In consideration of general properties, starch appears as polymeric glucan, osmotically inactive, stable, white soft amorphous powder, lacks sweetness, and is insoluble in water, alcohol, and ether at room temperature. It is highly hydrated since it contains many exposed hydroxyl groups.

Pullulan is a fungal polysaccharide (extracellular) that was initially isolated from *Pullularia pullulans*. It comprises maltotriose units linked by α -1,6-glycosidic bonds (Fig. 1C). The other important molecules are isopanose and panose. They are trisaccharides, contain α -1,4- and α -1,6-glycosidic bonds. (Fig. 1D). Another component is isomaltose, which contains only α -1, 6-glycosidic linkage. Although the α -1, 6-glycosidic linkages are similar to amylopectin, starch-debranching enzymes can cleave the pullulan polysaccharide. Pullulan is a water-soluble polysaccharide, produces a colorless

visco-adhesive solution. The food, pharmaceutical, and biomedical industries are the major user of pullulan.

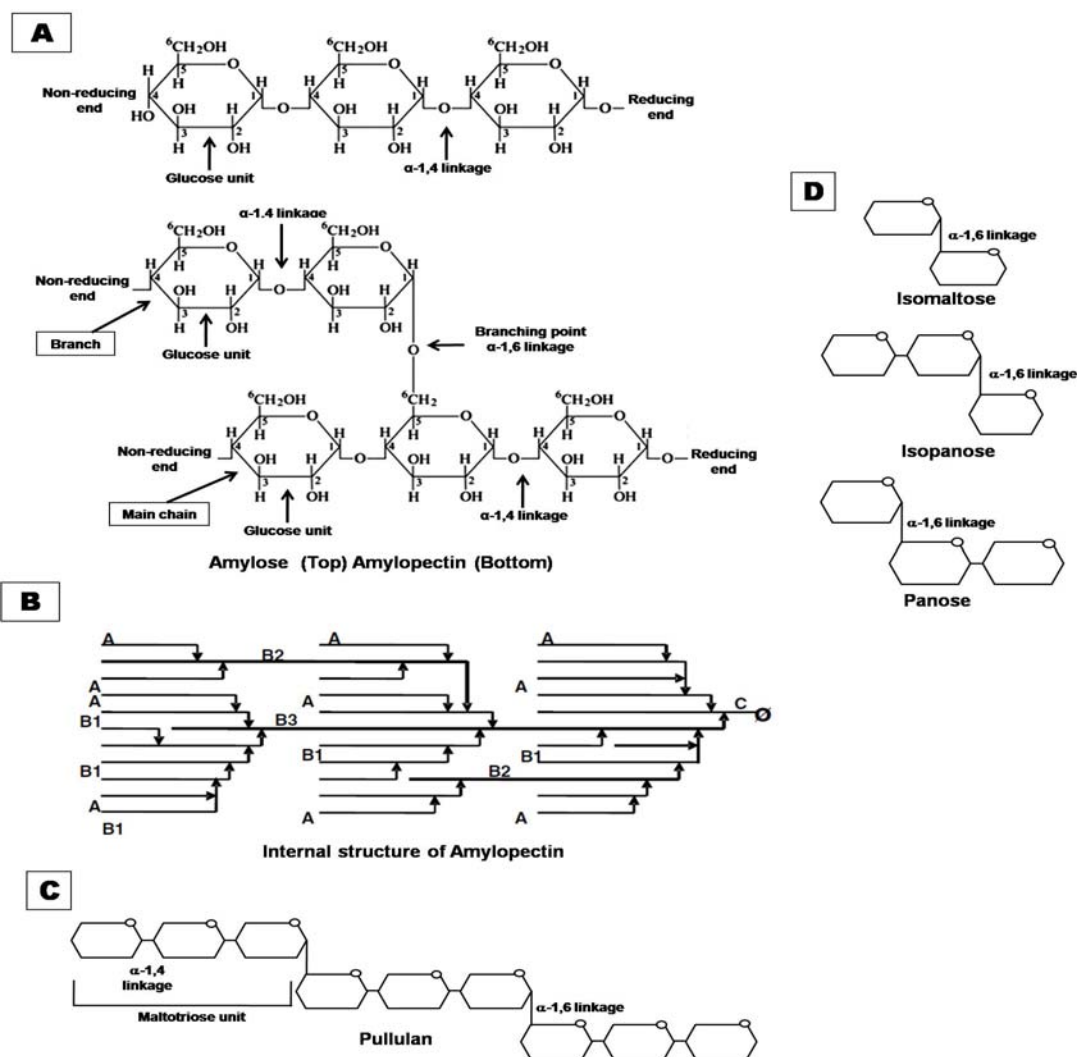


Figure 1. A: Schematic representation of amylose and amylopectin. Amylose molecule has repeating α -1, 4 linkages. Amylopectin molecule showing the α -1, 4, and α -1,6 chain linkages. B: Molecular arrangement of amylopectin, composed by A, B, and C chains. Solid line: α -1,4 bound glucose units; arrow: α -1,6 linkage; σ : reducing glucose residue. (details are given in the text). (Adapted from Hizukuri 1986, 1996). C: Schematic representation of the structure of pullulan. D: Diagrammatic representation of isomaltose, isopanose, and panose.

4. An overview on glycosyl hydrolase family and classification of amylolytic enzymes

Different starch degrading enzymes are most abundant in nature and responsible for metabolism as well as industrial applications. Earlier, R. Kuhn (1925) and later E. Ohlsson (1930) observed the contrastive differences of the enzymatic-hydrolytic products of starch and then classified the starch degrading enzymes in α - and β -amylases according to the anomeric type of sugar products. The classification of amylases had not completed properly at the initial stage of categorization because several starch-degrading enzymes had shown the activity of transfer or condensation reaction in addition to the hydrolytic reaction. Initially, these enzymes had not classified as amylases. The molecular study of these enzymes (cyclodextrin glycosyltransferase, pullulanase isopullulanase, etc.) had shown that they had four

conserved regions of sequence in their primary structure for substrate binding and catalytic activity, which is similar to Taka amylase. These four conserved sequences were not present in β -amylase (EC 3.2.1.2) and glucoamylase (EC 3.2.1.3).

Based on the action pattern, K. Myrback and G. Neumuller (1950) classified amylases into endo-amylases and exo-amylases. Endoamylases cleave internal α -1,4 bonds that are present in the inner part (endo) of the amylose or amylopectin chain. The hydrolytic reaction occurs randomly in the interior of the starch molecule. The end products are α -anomeric oligosaccharides with varying chain lengths and α -limit dextrins, which constitute branched oligosaccharides. The term "alpha" relates to the initial anomeric configuration of the reducing groups of the liberated product and is not related to the configuration of the hydrolyzable linkage. Exoamylases start hydrolysis from the non-reducing end; the subsequent result is the production of short end-products. These

enzymes cleave α -1,4 or α -1,6 bonds of the external glucose residues of amylose or amylopectin resulting, in the formation of α - or β -anomeric products. There are several types of exoamylases. Amylogucosidase (glucoamylase/ γ -amylase, EC 3.2.1.3) and α -glucosidase (EC 3.2.1.20) produce glucose as the sole end product from starch and related polymers. β -amylase produces maltose from amylose, maltose, and β -limit dextrin from amylopectin and glycogen. Maltogenic α -amylase (EC 3.2.1.133), maltotetraose forming amylase (EC 3.2.1.60), maltohexaose forming amylase (EC 3.2.1.98) are also the example of exoamylases. The cyclodextrin producing enzyme cyclodextrin glycosyltransferase (CGTase, EC 2.4.1.19) and branching enzyme (EC 2.4.1.18) have an additional activity of transglycosylation. They belong to the transferase group. CGTase hydrolyzes starch to a homologous series of cyclic, non-reducing D-glucosyl polymers, called cyclodextrins. Besides these, debranching enzymes hydrolyze only α -1,6 bonds exclusively, producing long linear polysaccharides. Enzyme transferases cleave α -1,4 glycosidic bond of the donor molecule, transfer the part of the donor molecule to a glycosidic acceptor, forming a new glycosidic bond. Thus, the classifications of amylolytic enzymes of microbial origin are based on action pattern and end-product formation.

From the year 1991, the α -amylase family belonged to the glycosyl hydrolases family 13 after the establishment of sequence-based classification of all glycoside hydrolases, transferases (Henrissat, 1991). Finally, the concept of the α -amylase family was proposed by Takata (1992). Currently, carbohydrate-splitting all the enzymes are distributed in different glycosyl hydrolase families

(GH family). According to the carbohydrate-active enzymes (CAZy) database, there are 168 glycosyl hydrolases families (GH1–GH168) with 18 clans (A–R). The starch degrading or modifying enzymes are distributed in GH families 3, 13, 14, 15, 31, 57, 63, 77, 97, 119, 122, 126, and 133 (Table 1). Mostly useful amylolytic enzymes are commonly found in GH13, GH57, GH119, and GH126 family (Lombard *et al.*, 2014; Janeček *et al.*, 2014; Kerényiová and Janeček, 2020a). The family GH57 was established more than twenty years ago when the three-dimensional structure of some α -amylases and related enzymes were elucidated that contained a (β/α)₇-barrel (an irregular TIM-barrel domain) in their configuration (Sarian *et al.*, 2017). Later, family GH119 also was established (Janeček and Kuchtová, 2012; Blesák and Janeček, 2013). Initially, there were some disputes about the members of GH126 that were resolved after the crucial contribution of Koseoglu *et al.* (2015), Wu *et al.* (2019), and Janeček *et al.* (2019). The family GH126 was created by Ficko-Blean in the year 2011 (Ficko-Blean *et al.*, 2011). Up to July 2020, this family counts more than 1000 sequences exclusively from the bacteria under the phylum Firmicutes (Kerényiová and Janeček, 2020a). The *in silico* study had revealed that this family has relationships with other GH families. The members of this family bear seven conserved sequence regions; they comprise catalytic (α/α)₆-barrel structure in their three-dimensional configuration (Kerényiová and Janeček, 2020b). Moreover, α -glucosidase (EC 3.2.1.20) belongs to the families GH31, GH63, GH97, and GH122 along with GH13 and glucoamylase (EC 3.2.1.3) is present in the separate family GH15 and GH97.

Table 1. Selected glycosyl hydrolases family (GH family) and their fundamental characteristics (Lombard *et al.*, 2014).

Family	Enzyme name and EC No.	Structure	Mechanism of
GH13	α -Amylase (3.2.1.1); oligo-1,6-glucosidase (3.2.1.10); α -glucosidase (3.2.1.20); pullulanase (3.2.1.41); cyclomaltodextrinase (3.2.1.54); maltotetraose-forming α -amylase (3.2.1.60); isoamylase (3.2.1.68); dextran glucosidase (3.2.1.70); trehalose-6-phosphate hydrolase (3.2.1.93); maltohexaose-forming α -amylase (3.2.1.98); maltotriose-forming α -amylase (3.2.1.116); maltogenic amylase (3.2.1.133); neopullulanase (3.2.1.135); malto-oligosyltrehalose trehalohydrolase (3.2.1.141); limit dextrinase (3.2.1.142); maltopentaose-forming α -amylase (3.2.1.-); amylosucrase (2.4.1.4); sucrose phosphorylase (2.4.1.7); branching enzyme (2.4.1.18); cyclomaltodextrin glucanotransferase (CGTase) (2.4.1.19); 4- α -glucanotransferase (2.4.1.25); isomaltulose synthase (5.4.99.11); trehalose synthase (5.4.99.16).	Number of domains : 3 (A, B, C). Types of fold: (β/α) ₈ -barrel. Catalytic site: (β/α) ₈ -barrel in domain A.	Retaining Some enzymes have transglycosylation activity. Proton donor: Glu Nucleophile: Asp
GH14	β -Amylase (3.2.1.2)	Single domain (β/α) ₈	Inverting Proton donor: Glu Nucleophile: Glu
GH15	Glucoamylase (3.2.1.3); glucodextranase (3.2.1.70); α , α -trehalase (3.2.1.28); dextran dextrinase (2.4.1.2)	Types of fold: (α/α) ₆ barrel Some have super- β -sandwich.	Inverting Proton donor: Glu Nucleophile: Glu
GH31	α -Glucosidase (3.2.1.20); α -galactosidase (3.2.1.22); α -mannosidase (3.2.1.24); α -1,3-glucosidase (3.2.1.84); sucrase-isomaltase (3.2.1.48) (3.2.1.10); α -xylosidase (3.2.1.177); α -glucan lyase (4.2.2.13); isomaltosyltransferase (2.4.1.-); oligosaccharide α -1,4-glucosyltransferase (2.4.1.161); sulfoquinovosidase (3.2.1.-).	Types of the fold: (β/α) ₈ -barrel. N-terminal β -sandwich also present. β -folded proximal and distal C-terminal domain is present in the structure.	Retaining Proton donor: Asp Nucleophile: Asp.
GH57	α -Amylase (3.2.1.1); α -G ^l galactosidase (3.2.1.22); amylopullulanase (3.2.1.41); cyclomaltodextrinase (3.2.1.54); branching enzyme (2.4.1.18); 4- α -glucanotransferase (2.4.1.25).	Number of domains: 3 (A, B, C). Types of fold: (β/α) ₈ -barrel. Catalytic site: (β/α) ₈ -barrel in domain A. Some cases (β/α) ₇ irregular (β/α) ₈ -barrel / pseudo TIM-barre may be present.	Retaining Proton donor: Asp Nucleophile: Glu.
GH77	Amylomaltase or 4- α -glucanotransferase (2.4.1.25)	4-7 conserved sequences are present, but domain C is absent. The TIM-barrel structure is disrupted in the sub-domains B1, B2 and B3 by insertions. Subdomain B1 consists of a highly twisted four-stranded antiparallel β -sheet with two α -helices.	Trans-glycosylation Proton donor: Glu Nucleophile: Asp.
GH97	Glucoamylase (EC 3.2.1.3); α -glucosidase (EC 3.2.1.20); α -galactosidase (EC 3.2.1.22)	Number of domain: 3 N-terminal β -super-sandwich domain, followed by (α/β) ₈ barrel containing central domain, carries catalytic site and a C-terminal β -sheet domain.	Inverting and retaining Proton donor: Glu Nucleophile: Glu for inverting; Asp for retaining.
GH119	α -Amylase (EC 3.2.1.1) Created after Watanabe <i>et al.</i> (2006).	Distantly related to family GH57;	Retaining
GH122	α -glucosidase (EC 3.2.1.20) Created after Confort <i>et al.</i> (2008).	-	-

Among the glycosyl hydrolase families, GH13 is the largest family in the CAZy database having more than 30 types of amylolytic enzymes with different characteristics (Lombard *et al.*, 2014). At present, the GH13 family counts more than 80,000 sequences (Janeček and Zámocká, 2020). The GH13 has 42 subfamilies (Janeček and Gabriško, 2016; Valk *et al.*, 2016; Janeček and Zámocká, 2020). However, the number of subfamilies is still emerging. Currently, another novel GH13 subfamily is proposed after the bioinformatics study of the α -amylase

from the halophilic archaeon *Haloarcula hispanica* (Janeček and Zámocká, 2020). Considering the different subfamilies, only eleven subfamilies contain α -amylases activity: GH13_1 (fungi), GH13_5 (bacterial liquefying enzymes that produce short-chain dextrin from starch and reduce the viscosity of starch suspension), GH13_6 (plants), GH13_7 (archaea), GH13_15 (insects), GH13_24 (animals), GH13_27 (proteobacteria), GH13_28 (bacterial saccharifying enzymes, mostly exoamylases and produce glucose, maltose, maltotetraose, etc.), GH13_32 (bacteria), GH13_36 (intermediary α -amylase), and GH13_37

(marine bacteria) (Janeček and Gabriško, 2016; Møller and Svensson, 2016). Neopullulanase, cyclomaltodextrinase, and maltogenic amylases are classified in the subfamily GH13_20 (Lombard *et al.*, 2014; Kuchtová and Janeček, 2016). These enzymes have the N-terminal starch-binding domain (SBD) that specifically belongs to the carbohydrate-binding modules (CBMs) family 34 (CBM34) (Machovic and Janeček 2006; Kuchtová and Janeček 2016). Additionally, pullulan hydrolase type III enzymes had been included in the subfamily GH13_20 (Lombard *et al.*, 2014). Valk *et al.* (2016) reported that about 10% of enzymes of the GH13 family carried SBDs. Fundamentally, SBDs are the subgroup of CBMs. Several authors observed that raw starch degrading α -amylases had additional CBM at their C-terminal ends (Boraston *et al.*, 2006; Machovič and Janeček, 2006; Lombard *et al.*, 2014). The SBDs are more important for the breakdown of thermally-untreated granular starch. SBD is the independent protein module within the raw starch digesting enzymes. SBD does not exhibit catalytic activity but holding the substrate in a proper position and represents it to the active site. The SBDs along with other CBMs are an integral part of the CAZy database. Currently, there are 85 CBM families; among them CBM20, 21, 25, 26, 34, 41, 45, 48, 53, 58, 68, 69, 74, 82 and 83 exhibit SBD functional characteristics. However, CBM74 is recognized as an extra-long module having a β -sandwich with 100 residues and carrying at least one substrate binding site (Janeček *et al.*, 2019).

The classification of the GH13 family is based on the amino acid sequence homology. Three main groups of enzymes like glycosyl hydrolases (endoamylases, exoamylases), transferases, and isomerases are the member of this family (Møller and Svensson, 2016). GH13 family was further classified based on a larger unit called clan, which is the three-dimensional structure of the catalytic region. A clan consists of two or more families having the same three-dimensional structure of the catalytic domain but with limited sequence similarities. Among the eighteen clans (A–R) of glycosidases and transglycosidases, GH-13 belongs to the clan eighth (GH-H) (MacGregor *et al.*, 2001; MacGregor 2005). Initially, Takata *et al.* (1992) gave the common features of the enzymes of this family: (i) they cleave α -glycosidic bonds and hydrolytic products are α -anomeric mono- or oligosaccharides, transglycosylation activity forms α -1-4 or 1-6 glycosidic linkages or a combination of both; (ii) TIM (triose phosphate isomerase) barrel or $(\beta/\alpha)_8$ barrel structure is the common features, which bears the amino acid residues at the catalytic site; (iii) four highly conserved sequence regions are present in their primary sequence, these hold catalytic residues and stabilize TIM barrel topology; (iv) Asp, Glu, and Asp residues form a triad at the catalytic site to exert hydrolytic cleavage by acid/base retaining mechanism. These three amino acid residues are also present in the catalytic sites of α -amylase, pullulanase, cyclodextrin glycosyltransferase (CGTases), isoamylase, and the branching enzymes (Kuriki and Imanaka, 1999). However, some additional features are also included in the α -amylase family, which cover hydrolases, transferases, and isomerases (Svensson *et al.*, 2002). The enzymes of this family can cleave not only α -1,4- and α -1,6-bonds but also α -1,1-, α -1,2-, α -1,3- and α -1,5-glycosidic linkages (Mac Gregor *et al.*, 2001). Later, three additional

conserved sequence regions were also established along with the previous four conserved regions (Janeček, 2002).

5. Production and purification of amylases

The application of biocatalysts in different industrial sectors is a great success towards the clean and green world. Several biotech companies produce varieties of useful enzymes like amylases, cellulase, pectinases invertase, pullulanase, protease, lipase, lysozyme, and others, which are mostly obtained from microbial sources. Among the industrially important enzymes, amylases constitute a class of enzymes having approximately a quarter shares in the world's enzyme market (John, 2017). Amylases are ubiquitously present in all living organisms. However, in the commercial sectors, different bacteria, fungi, and recombinant microbes are used for amylase production.

Several studies had revealed that various bacteria under the genus *Bacillus* (*B. licheniformis*, *B. stearothermophilus*, *B. amyloliquefaciens*, *B. subtilis*, and others), non-*Bacillus* (*Pseudomonas stutzeri*, *Streptococcus brevis*, *Rhodothermus marinus*, *Corynebacterium gigantea*, *Clostridium acetobutylicum*, *Caldimonas taiwanensis*), and halophilic organisms (*Haloarcula hispanica*, *Halobacillus* sp., *Chromohalobacter* sp., *Bacillus dipsosauri*, *Halomonas meridian*) are the good sources of extracellular amylase production. Not only bacteria, but fungi have also shown good results in this purpose. Different species of *Aspergillus* (*A. oryzae*, *A. niger*, *A. awamori*, *A. fumigates* and others), *Penicillium* (*P. brunneum*, *P. fellutanum*, *P. expansum*, *P. chrysogenum*, etc.), and others (*Streptomyces rimosus*, *Thermomyces lanuginosus*, *Pycnoporus sanguineus*, *Thermomonospora curvata*) are regarded as efficient amylase producer (Samanta, 2020b). Additionally, the genus *Aspergillus* and *Bacillus* are the major contributors of amylases in the industrial sectors, and they are constantly exploited for enzyme preparation. A short-list of amylase producers and their optimized conditions for enzyme production has been furnished in Table 2. To improve the characteristics (pH profile, thermostability, oxidant resistance, metal ion independency, and others) of amylase, recombinant organisms (Table 3) were developed for better purposes.

Production of microbial enzymes mostly depends upon the environmental and nutritional conditions of the culture medium (Table 2). The growth of microorganisms is determined by the organism's ability to utilize the essential nutrients from its surroundings as well as its physiological activities. Several physicochemical parameters, including nutrient supplementation (carbon, nitrogen, and phosphate), pH of the medium, water activity, oxygen supply, temperature, and level of contamination are the crucial factors for optimum growth of the microorganism as well as enzyme production. Fermentation is the process for the production of useful products through the mass culture of certain microorganisms. Production of amylases has been carried out in both solid-state fermentation (SSF) and submerged fermentation (SmF). Traditionally, SmF was used for enzyme production; later SSF is being more popular for large-scale production of amylases due to its cost-benefit and ease of handling. Biotechnological progress makes the SSF more fashionable to the industrial

sectors for the production of enzymes, food and pharmaceutical components, bio-bleaching agents, and others (Soccol *et al.*, 2017). To achieve the maximum yield, several parameters like surface area, porosity, moisture content, particle size, and nutrient supplementation are considered during culture (Farinas, 2015; Singhania *et al.*, 2009). The potential use of moist agricultural polymeric substrates such as wheat bran, rice bran, rice husk, cassava, sunflower meal, cottonseed meal, soybean meal, pearl millet, and others make the process more convenient and eco-friendly. Agricultural residues provide solid support and nutrients as they contain cellulose, hemicellulose, lignin, starch, pectin, protein, minerals, and others (Farinas, 2015). Supplementation of macro (protein) and micro-nutrients (vitamins and minerals) enhance many folds of enzyme synthesis.

The extracellular enzyme is present with other proteins and cell debris in the culture medium; so, it is essential to purify the enzyme up to its homogeneity. Most of the enzymes are purified from other proteins and non-protein contaminants based on their inherent properties like shape, size, charge, hydrophobicity, solubility, and biological activity. Traditionally, a multi-step purification system was the common process of purification. In this technique, centrifugation, or filtration of the culture medium, salting out, ion-exchange chromatography followed by gel filtration were performed in the purification process. High performance liquid chromatography (HPLC) is applied to increase the homogeneity of protein.

The conventional multi-step purification process is cost expensive, time-consuming, and always has a chance of loss of the desired product with low yield (Arauzo *et al.*, 2009). The large scale cost-effective purification of the bulk enzyme for commercial purposes had been developed after the evolution of purification techniques, which are fast, efficient, and economically viable with fewer processing steps (Amritkar *et al.*, 2004). Forced affinity

chromatography, expanded bed / fluidized bed chromatography, high-speed counter-current chromatography (HSCCC), and magnetic affinity adsorption chromatography are the single-step purification process. Forced affinity chromatography provides effective results for the purification of amylase on an industrial scale. Soluble starch, raw potato starch, carboxymethyl-starch, and guar gum are used for the preparation of the gel matrix by cross-linking the polysaccharides with epichlorohydrin. Pectin gel may also be prepared by using carbodiimide (EDC, 1-ethyl-3-(3-dimethyl aminopropyl). Ammonium sulfate acts as a stimulator (forced affinity) for the binding of the enzyme to the gel. The features of single-step purification techniques are given in Table 4.

Molecular weights of α -amylases vary from about 10-148 kD (Nguyen *et al.*, 2000; Valk *et al.*, 2016). The optimum pH value of α -amylase from various sources differs from 2-11 (Sivaramakrishnan *et al.*, 2006). Temperature optima for α -amylase activity vary from 25 °C to 100 °C (Mehta and Satyanarayana, 2016). Most of the α -amylases are calcium-dependent; however, calcium-independent amylase is equally important (Mehta and Satyanarayana, 2014; Samanta *et al.*, 2014; Xian *et al.*, 2015). The major characteristics of microbial α -amylases are presented in Table 5. Variations in the characteristics make them useful for their industrial applications. Despite α -amylase, del Moral *et al.* (2018) reported that fungal α -glucosidases were optimally active in 50 to 65 °C temperatures and pH 4.5-6. The molecular mass of the enzymes was observed in between 50 to 145 kD. Generally, they showed metal ion-independent activity. The molecular weight of isoamylase varied in the range of 60 to 120 kD. The pH and temperature optima were observed between 5-8 and 30 to 80 °C, respectively. The catalytic activity did not depend on metal ions (Ray, 2011).

Table 2: Sources and production of microbial α -amylase.

Source	Fermentation	Substrate	Enzyme production	pH for optimum enzyme production	Tempt. (°C) for optimum enzyme synthesis	Incuba-tion period (hours)	Ref.
Fungi							
<i>Aspergillus oryzae</i> (IFO 30103)	SSF	Spent-brewing grains	11296 U/ gds		30	48	Patel <i>et al.</i> , 2005
<i>Aspergillus oryzae</i>	SSF	Wheat bran	15095 U/gds	5.0	30	72	Sivaramakrishnan <i>et al.</i> , 2007
<i>Aspergillus oryzae</i> IFO 30103	SSF	Wheat bran		6.0	32	48	Dey and Banerjee, 2012
<i>Aspergillus oryzae</i>	SmF	Synthetic media	2.685 U/ml	7.0	45	72	Shah <i>et al.</i> , 2014
<i>Aspergillus niger</i>	SmF	Synthetic medium		5.0	30	120	Gupta <i>et al.</i> , 2008
<i>Aspergillus niger</i> BAN 3E	SSF	Black gram bran	8 U/mg	5.5	37	120-144	Suganthi <i>et al.</i> , 2011
<i>Aspergillus niger</i> WLB42	SmF	Synthetic medium	2189 U/ml	7.0	30	48	Wang <i>et al.</i> , 2016
<i>A. fumigatus</i> NTCC1222	SSF	Wheat bran	341.7 U/mL	6.0	35	144	Singh <i>et al.</i> , 2014
<i>Aspergillus terreus</i> NCFT4269.10	SSF and liquid static surface (LSSF)	Pearl millet		7.0	30	96	Sethi <i>et al.</i> , 2016a and 2016b
<i>Penicillium janthinellum</i> (NCIM)	SSF	Wheat bran	275 U/gds	5.0	35	96	Sindhu <i>et al.</i> , 2011
Bacteria							
<i>Bacillus subtilis</i>	SmF	Soluble starch	3790 U/ml		37	24	Özdemir <i>et al.</i> , 2011
<i>B. amyloliquifaciens</i> TSWK1-1	SmF	Synthetic medium	250 U	7.0	50	48	Kikani and Singh, 2011
<i>B. amyloliquifaciens</i> ATCC23842	SSF	Ground nut oil cake and wheat bran	1671 U/gm	5.0	37	72	Gangadharan <i>et al.</i> , 2011
<i>B. amyloliquefaciens</i> P-001	SmF	Synthetic medium with soluble starch	35.0 4 U/ml	9.0	42	48	Deb <i>et al.</i> , 2013
<i>B. methylotrophicus</i> P11-2	SmF	Soluble starch	144 U/ml	7.2	37	70	Xie <i>et al.</i> , 2014
<i>B. licheniformis</i> AI20	SmF	Soluble starch	166.5 U/ml	7.0	45	40	Abdel-Fattah <i>et al.</i> , 2013
<i>B. licheniformis</i> SKB4	SmF	Soluble starch	3.8 U/ml	6.5	42	24	Samanta <i>et al.</i> , 2014
<i>B. acidicola</i> TSAS1	SmF	Starch	8300 IU/l	4.5	33	36	Sharma and Satyanarayana, 2011
<i>B. cereus</i>	SmF	Potato starch		6.5	35	48	Madhavi <i>et al.</i> , 2010
<i>Bacillus</i> sp. GHA 1	SmF	Potato starch		6.5-8.0	37	72	Ahmadi <i>et al.</i> , 2010
<i>Geobacillus</i> sp. IIPTN 3	SmF	Soyameal Starch	135 U/ ml	6.5	60	14	Dheeran <i>et al.</i> , 2010
<i>Geobacillus stearothermophilus</i> HP 3	SmF	Maltose supplement	80 U/ml	9.0	55	24	Selim, 2012
<i>Cronobacter sakazakii</i> Jor 52	SmF	Soluble starch	2.2 U/ml	7.0	37	24	Samanta <i>et al.</i> , 2013
Recombinant <i>B. licheniformis</i> CBBD302 (PHY-amyl)	SmF	Soybean meal, cotton seed meal, corn steep liquor, lactose	17.6 mg/ml	6.0	42	120	Niu <i>et al.</i> , 2009

Tempt.: Temperature; Ref.: References

Table 3. Sources of recombinant organisms as α -amylase producer and some fundamental features of the enzyme

Organism	Host	Key features of α -amylase from recombinant organism	References
<i>Bacillus licheniformis</i> NH1	<i>Escherichia coli</i> BL21 Vector: pDEST17	MW: 58 kDa pH optima: 6.5 (pH range 5.0 to 10.0) Temperature optima: 90 °C Others: Show better thermostability and maximum stability towards surfactants (SDS, Tween 20 and Triton X-100)	Hmidet <i>et al.</i> , 2008
<i>B. subtilis</i> WB800	<i>E. coli</i> DH5 α Vector: pMD18-T	ORF sequence: 1545 bp encoding 514 amino acid residues Rate of production: 1.48-fold higher than wild type MW: 58.4 kDa (predicted) pH optima: 6.0 Temperature optima: 60 °C Others: sensitive to detergents/surfactants.	Chen <i>et al.</i> , 2015
<i>B. acidicola</i>	<i>E. coli</i> BL21 (DE3) Vector: pET28a(+)	Rate of production: 15-fold higher than wild type MW: 62 kDa pH optima: 4.0 (pH range 3.0 to 7.0) Tempt. optima: 60 °C (tempt. range 30 to 100 °C) Others: Ca ²⁺ -independent, acidstable, and high maltose forming	Sharma and Satyanarayana, 2012
<i>B. subtilis</i> DR8806	<i>E. coli</i> BL21 (DE3) Vector: pET28a(+)	MW: 76 kDa pH optima: 5.0 (pH range 4.0 to 9.0) Tempt. optima: 70 °C (tempt. range 45 to 75 °C) Others: Show high stability towards ionic detergents SDS, CTAB, and maltotriose and maltose forming	Emtenani <i>et al.</i> , 2015
<i>Geobacillus thermoleovorans</i>	<i>E. coli</i>	ORF sequence: 1650 bp encoding 515 amino acid residues MW: 59 kDa pH optima: 5.0 Tempt. optima: 80 °C Others: Ca ²⁺ -independent, highly thermostable and raw starch digesting	Mehta and Satyanarayana, 2013a
<i>Halomonas meridiana</i> DSM 5425	<i>E. coli</i>	α -Amylase gene <i>AmyH</i> is the first extracellular-amylase-encoding gene isolated from halophiles and cloned into <i>E. coli</i>	Coronado <i>et al.</i> , 2000b
<i>Pseudoalteromonas</i> sp.MY-1	<i>E. coli</i>	ORF sequence: 2007 bp encoding 669 amino acid residues MW: 73.77 kDa (predicted) pH optima: 7.0 Tempt. optima: 40 °C Others: oligosaccharides, and maltose forming	Tao <i>et al.</i> , 2008
<i>Staphylothermus marinus</i>	<i>E. coli</i>	Amino acid residues: 696 MW: 82.5 kDa (predicted) pH optima: 5.0 (pH range 3.5 to 5.0) Tempt. optima: 100 °C Others: extremely thermostable; active against linear malto-oligosaccharides, starch, cyclodextrins, and cycloamylose; hydrolyze acarbose and pullulan to acarviosine-glucose and panose, respectively	Li <i>et al.</i> , 2010
<i>Thermobifida fusca</i> NTU22	<i>Pichia pastoris</i> X-33 Vector: pGAPZalphaA	Rate of production: very high MW: 65 kDa pH optima: 7.0 Tempt. optima: 60 °C Others: highly thermostable; raw sago starch digesting	Yang <i>et al.</i> , 2010
<i>Thermoplasma volcanicum</i> GSS1	<i>E. coli</i>	pH optima: 7.0 Tempt. optima: 75 °C and 80 °C Others: highly thermostable; longer subsite structure, highly maltogenic	Kim <i>et al.</i> , 2007

Tempt.: temperature; MW: molecular weight; ORF: open reading frame; SDS: Sodium dodecyl sulphate; CTAB: cetyl trimethylammonium bromide

Table 4: Methods of one-step purification process of α -amylases.

Method	Chromatographic substances	Basis	Advantages
Affinity adsorption chromatography	Cross-linked starch, Epichlorohydrin or bifunctional epoxides activated agarose gel, α -, β -, and γ Cyclodextrin (CD) coupled with sepharose, divinyl sulphone.	Reversible interaction occurs between enzymes and specific ligand attached to chromatographic matrix.	High selectivity, high resolution, high capacity
	Immobilized metal ion affinity chromatography (IMAC): Cyclodextrin is treated by iminodiacetic acid (IDA) or nitrilotriacetic acid (NTA) and then the material is being further charged with cations (Ag^+ , Cu^{2+} , Mg^{2+} , Ni^{2+} , Hg^{2+} , Fe^{2+} and Zn^{2+}).	Enzyme binds with ligand by non-covalent interaction The amino acid residues, such as aspartic acid (carboxyl group), glutamic acid (carboxyl group), histidine (imidazole group), cysteine (thiol group), tryptophan (indoyl group) or lysine (amino group) on the protein surface can specifically interact with different metal ions.	
	Desorption agent -elution buffer with different pH, salt solution, imidazole, N-protected histidines and tryptophan		
Expanded bed chromatography / Fluidized bed chromatography	Alginic acid-cellulose cell beads Cross-linking cellulose with other OH containing polymers like starch, dextrans, sodium alginate, alginic acid, cellulose, DEAE cellulose, carboxymethyl cellulose and microcrystalline cellulose (MCC).	Sample feeding flow and elution flow regulate the entire process	Simple process, low downstream processing cost, reduced number of purification steps, high downstream efficiencies, industrially applicable; enzyme is eluted in increased concentration.
High speed counter current chromatography (HSCCC)	The combinations of aqueous polymer with high water content and low interfacial tension (two phase system) are applicable. Aqueous two phase polymer is made by PEG4000-phosphate aqueous polymer or PEG4000-citrate aqueous polymer.	It is a continuous liquid-liquid partition chromatography without solid support matrix	No interaction between samples with solid support, little chance of denaturation of target products, high recovery, high efficiency, easy to scale-up, industrially compatible, reduces initial downstream steps.
Magnetic affinity adsorption	Magnetic alginate beads (microparticles) is prepared by using sodium alginate and ferromagnetic material (magnetic fluid - citrate-based ferrofluid). Other substances are used for magnetic biopolymers synthesis are agarose, chitosan, and kappa carrageenan.	Magnetic component carries magnetic biopolymer particles which have affinity to the enzyme	Applicable for separation of alpha amylase and other starch degrading enzymes, simple process, very few steps are necessary, all the steps of purification are done in a single vessel, less expensive, no needs of major equipments, time saving, high efficacy value for large scale separation

Table 5: Physico-chemical characteristics of α -amylases.

Source	Purification levels	MW (kD)	pH optima for enzyme activity	Temp. ($^{\circ}\text{C}$) optima for enzyme activity	Kinetic properties	Effects of metal ions	Ref.
Fungi							
<i>Aspergillus oryzae</i> IFO 30103	Sp. Act. (U/mg)- 627 Pur. Fd.- 7.1 Yld. (%) - 40	51.3	5.5	50	K_m - 0.5% V_{max} - 1000 U/mg	$\uparrow \text{Co}^{2+}$, Ca^{2+} , Mg^{2+} $\downarrow \text{Zn}^{2+}$, Cu^{2+}	Dey and Banerjee, 2015
<i>A. oryzae</i> (IFO 30103)	Sp. Act. (U/mg)- 51.08 Pur. Fd.- 7.14 (Up to $(\text{NH}_4)_2\text{SO}_4$ ppt.)	66	5.0	50		$\uparrow \text{Mn}^{2+}$, Fe^{2+} $\downarrow \text{Hg}^{2+}$, Cu^{2+}	Patel <i>et al.</i> , 2005
<i>A. niger</i> WLB42		50	7.0	45		$\uparrow \text{Co}^{2+}$, $\downarrow \text{Zn}^{2+}$, Cu^{2+} , Mg^{2+}	Wang <i>et al.</i> , 2016
<i>A. niger</i>	Sp. Act. (U/mg)- 0.982 Pur. Fd.- 81.83		4.5	45		$\uparrow \text{K}^+$, Ca^{2+} , Mg^{2+} $\downarrow \text{Hg}^{2+}$, Pb^{2+} ,	Aisien and Igbinosa, 2019

		Yld. (%) - 60.227					
<i>A. flavus</i> F ₂ Mbb	Sp. Act. (U/mg)- 4348	52.5	6.4	30	K _m - 0.5 mg/ml		Sidkey <i>et al.</i> , 2011
	Pur. Fd.- 161				V _{max} - 17.78 mg/ml/mi n		
	Yld. (%) - 15.74						
<i>A. flavus</i> NSH9	Sp. Act. (U/mg)- 48.1	54	5.0	50	K _m - 4.22 mg/ml	↑ Ca ²⁺ , ↓ Zn ²⁺ , Cu ²⁺ , Mg ²⁺	Karim <i>et al.</i> , 2018
	Pur. Fd.- 2.55				V _{max} - 65.52 U/mg		
	Yld. (%) - 11.73						
<i>Penicillium camemberti</i> PL21	Sp. Act. (U/mg)- 154.2	60.5	5-6.0	30	K _m - 0.92 mg/ml	↑ Ca ²⁺ ↓ Hg ²⁺ , Ag ⁺	Nouadri <i>et al.</i> , 2010
	Pur. Fd.- 38.5				V _{max} - 38.5 μmole/mi n		
	Yld. (%) - 23						
<i>P. citrinum</i> HBF62	Sp. Act. (U/mg)- 1451	65	5.5	55	K _m - 0.2 mg/ml	↑ Mn ²⁺ , Ca ²⁺ , Co ²⁺ , Fe ³⁺ , Ba ²⁺	Metin <i>et al.</i> , 2010
	Pur. Fd.- 18				V _{max} - 5000 U/mg	↓ K ⁺ , Zn ²⁺ , Hg ²⁺	
	Yld. (%) - 82						
<i>P. janthinellum</i> NCIM)	Sp. Act. (U/mg)- 696.66	42.7	5.0	50		↓ Hg ²⁺ , Zn ²⁺ , Cu ²⁺ , Ag ⁺ , Pb ²⁺ , Fe ²⁺ , Fe ³⁺	Sindhu <i>et al.</i> , 2011
	Pur. Fd.- 44.06						
	Yld. (%) - 30.73						
<i>P. olsonii</i>	Sp. Act. (U/mg)- 23.45		5.6	30	K _m - 0.556 mg/ml	↑ Mn ²⁺ , Mg ²⁺	Afifi <i>et al.</i> , 2008
	Pur. Fd.- 25.14						
	Yld. (%) - 36.5						
Bacteria							
<i>Bacillus cereus</i>	Sp. Act. (U/mg)- 50.0	56	6.0	50	K _m - 1.43 mg/ml	↓ Zn ²⁺	Mahdavi <i>et al.</i> , 2010
					V _{max} - 0.27 μmol /min		
<i>B. subtilis</i> ITBCCB148	Sp. Act. (U/mg)- 40000	67	6.5	60	K _m - 2.5 mg/ml		Yandri <i>et al.</i> , 2010
	Pur. Fd.- 148				V _{max} - 192.3 μmol/ml/ min		
	Yld. (%) - 8.8						
<i>B. amyloliquifaciens</i> TSWK1-1	Sp. Act. (U/mg)- 8000	43	7.0	70	K _m - 0.6 mg/ml	Metal ion independent	Kikani and Singh, 2011
	Pur. Fd.- 13.3				V _{max} - 2632 μmol/ml/ min		
	Yld. (%) - 45.71						
<i>B. methylophilicus</i> P11-2	Sp. Act. (U/mg)- 330.7	44	7.0	70		↑ Mg ²⁺ , Ba ²⁺ , Al ³⁺ ↓ Hg ²⁺ , Cu ²⁺ , Zn ²⁺ , Co ²⁺	Xie <i>et al.</i> , 2014
	Pur. Fd.- 13.1						
	Yld. (%) - 7.0						
<i>B. megaterium</i> VUMB109.	Sp. Act. (U/mg)- 240.19	150	7.75	93	K _m - 1.5 μM	↑ Ag ²⁺ , Cu ²⁺ , Sn ²⁺ , K ⁺ , Mg ²⁺	Jana <i>et al.</i> , 2013
	Pur. Fd.- 27.39				V _{max} - 0.56 μmol/mg/ min	↓ Hg ²⁺ , Pb ²⁺ , Zn ²⁺	
	Yld. (%) - 38.43						
<i>B. licheniformis</i> AI20	Sp. Act. (U/mg)- 748.9	55	6-7.5	60-80	K _m - 0.709 mg/ml	↑ Ca ²⁺ , Co ²⁺ ↓ Hg ²⁺	Abdel-Fattah <i>et al.</i> , 2013
	Pur. Fd.- 59.34				V _{max} - 454		
	Yld. (%) - 12.6						

<i>B. licheniformis</i>	Sp. Act. (U/mg)- 339.5 Pur. Fd.- 203.29 Yld. (%) - 23.62	7.5	90	mU/mg K _m – 1.097% V _{max} - 44.54 U/min	↑ Ca ²⁺ , Mg ²⁺ , Co ²⁺ , Fe ²⁺ ↓ Zn ²⁺ , Ba ²⁺	Adeyanju <i>et al.</i> , 2007	
<i>B. licheniformis</i> SKB4	Sp. Act. (U/mg)- 827 Pur. Fd.- 214 Yld. (%) - 64.8	60	6.5	90	K _m – 6.2 mg/ml V _{max} – 1.04 μmol/mg/ min	↑ K ⁺ , Mg ²⁺	Samanta <i>et al.</i> , 2014; Samanta <i>et al.</i> , 2017
<i>Bacillus</i> sp. GHA1	Sp. Act. (U/mg)- 250 Pur. Fd.- 131.6 Yld. (%) - 28	66	5.5-8		↑ Ca ²⁺	Ahmadi <i>et al.</i> , 2010	
<i>Bacillus</i> sp. SI-136	Sp. Act. (U/mg)- 1193.07 Pur. Fd.- 2.93 Yld. (%) - 84.3 (Up to (NH ₄) ₂ SO ₄ ppt.)	26	10	70-80	↑ Mn ²⁺ ↓ Fe ²⁺ , Mg ²⁺ , Hg ²⁺ , Zn ²⁺	Sarethy <i>et al.</i> , 2012	
<i>Geobacillus</i> <i>stearothermophilus</i> HP 3	Sp. Act. (U/mg)- 1.45 Pur. Fd.- 0.35 Yld. (%) - 13.9	64	9.0		↑ K ⁺ , Mg ²⁺ , Fe ²⁺ ↓ Hg ²⁺ , Zn ²⁺ , Co ²⁺ , Ni ²⁺	Selim, 2012	
<i>Geobacillus</i> sp. IIPTN	Sp. Act. (U/mg)- 1200 Pur. Fd.- 82 Yld. (%) - 31	97	5.0	80	K _m – 36 mg/ml V _{max} – 222 μmol/mg/ min	↑ Mn ²⁺ , Co ²⁺ , Ca ²⁺ , Ba ²⁺ , Na ⁺ , Fe ³⁺ ↓ Cu ²⁺ , Zn ²⁺ , Mg ²⁺	Dheeran <i>et al.</i> , 2010
<i>Anoxybacillus</i> <i>beppuensis</i> TSSC- 1	Sp. Act. (U/mg)- 10,000.00 Pur. Fd.- 19.51 Yld. (%) - 58.53	43	7.0	80	K _m – 0.5 mg/ml V _{max} – 3571.42 μmol/ml/ min	Metal ion independent	Kikani and Singh, 2012

MW: Molecular weight; Temp.: Temperature; Ref.: References; Sp. Act.: Specific activity; Pur. Fd.: Purification fold; Yld.: Yield; ppt.: Precipitation

6. The pattern of the domain structure of different amylases of GH13 and related families

The crystallographic structure of amylases revealed that they consist of a single polypeptide chain folded in three distinct domains A, B, and C (Fig. 2). The A domain is the most conserved structure in the amylase family. The N-terminal part of the A-domain consists of eight parallel β -strands, arranged in a barrel configuration, surrounded by eight α -helices — (β/α)₈ barrel also called TIM barrel (Prakash and Jaiswal, 2010). This (β/α)₈ barrel structure was first observed in the triosephosphate isomerase (TIM) of chicken muscle. Domain B and C are located on the opposite side of the TIM-barrel structure. Domain B is a β -strand rich structure. It is a projection part between β -strand 3 and α -helix 3 of the TIM-barrel (Janecek *et al.*, 1997). Both the domains A and B jointly form the substrate-binding cleft. There are seven other domains (C to I) in this family (Table 6) that are distributed either in front or behind the A domain. Domain C (β -sandwich domain) is present at the C terminal end of the enzyme (Nielsen *et al.*, 2004). The activity of CGTase is influenced by C-domain. E-domain has a role in the raw

starch binding activity. N-terminal F-, H-, or G-domains are involved in the hydrolysis of α -1,6 glycosidic linkages (van der Maarel *et al.*, 2002). Most of the time, calcium ion is associated with amylase structure. It is present at the interface between domains A and B. Calcium ion increases the stability and activity of the enzyme. However, several reports support the calcium independence of amylase activity (Asoodeh *et al.*, 2010; Mehta and Satyanarayana, 2014; Samanta *et al.*, 2014; Xian *et al.*, 2015).

There are slight differences in the domain structure in different amylases. α -Amylase (EC 3.2.1.1) and its related enzymes have A, B, and C domains. Features of these domains are already described. The (β/α)₈ barrel topology is also observed in the structure of α -glucosidase (EC 3.2.1.20); although, the (β/α)₈ structure of GH31 is quite different from GH13 (Mohan and Satyanarayana, 2018). The catalytic domain of all debranching enzymes (oligo-1,6-glucosidase, isoamylase, and pullulanase) is present in (β/α)₈ barrel structure. CTGase (EC 3.2.1.19) consists of five domains (A–E). The A domain is present at the N-terminal site, comprised (β/α)₈ barrel, and appeared as the major functional site. The B and C domains are involved in substrate binding and stability of the catalytic site (Knegtel *et al.*, 1996). Additionally, the C domain helps in

maltose-binding (Strokopytov *et al.*, 1995). The D domain is specifically present in CGTases, but its function is still unknown. E domain is also present in CGTase and other amylases (Table 6). E domain is associated with maltose-binding as well as raw starch binding (Qi and

Zimmermann, 2005). Maltotetraose forming amylase (EC 3.2.1.60) has $(\beta/\alpha)_8$ barrel containing A domain; domain B has five standard anti-parallel β -sheets. At the molecular level, branching enzyme (EC 2.4.1.18) bears $(\beta/\alpha)_8$ barrel structure in their internal topology.

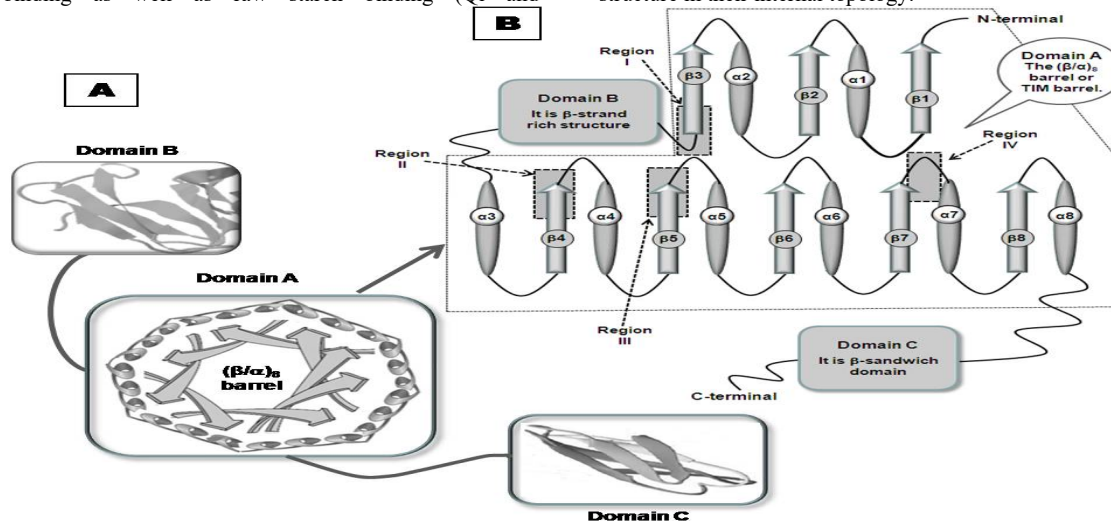


Figure 2. A: Schematic representation of the molecular structure of amylase. Three distinct domains are shown with a different configuration. $(\beta/\alpha)_8$ barrel structure is present in domain A. B: Topology of $(\beta/\alpha)_8$ barrel. The positions of four conserved sequence (I–IV) are indicated with shaded boxes.

Table 6: Different domains present in the enzymes of α -amylase family (van der Maarel *et al.*, 2002).

Common name	EC. No.	Domain	Features of domain
α -amylase	3.2.1.1	A, B, C	The A domain contains $(\alpha/\beta)_8$ barrel structure and catalytic site. The B domain (eight-stranded antiparallel β -sandwich structure) is a short loop structure closely associated with $(\alpha/\beta)_8$ barrel. It forms the wall of the catalytic cleft and few residues of substrate fit within the B domain during catalysis. Some times, Ca^{2+} can bind with B domain. The C domain is made by antiparallel β sandwich structure, folded in a Greek-key motif.
Oligo-1,6-glucosidase	3.2.1.10	A, B	Features are already given.
Isoamylase	3.2.1.68	A, B, F, 7	The domain F (α/β -barrel structure), located at the N-terminal part of $(\alpha/\beta)_8$ barrel
Pullulanase	3.2.1.41	A, B, H, G, I	The domain G and H (both α/β -barrel structure) located at the N-terminal part of $(\alpha/\beta)_8$ barrel
Neopullulanase	3.2.1.135	A, B, G	Features already are given.
Cyclodextrin glycosyltransferase	2.4.1.19	A, B, C, D, E	The β strand of D domain forms immunoglobulin-like fold and E domain has separate β strand motif and also has starch binding capacity.
Branching enzyme	2.4.1.18	A, B, F	Features already are given.
Maltogenic -amylase.	3.2.1.133	A, B, C, D, E	Features already are given.
Maltotetraose forming amylase	3.2.1.60	A, B, C, E	Features already are given.

Isoamylase (EC 3.2.1.68) from *Pseudomonas amyloclavata* contains 750 amino acid residues. Like other GH13 enzymes, it also contains $(\beta/\alpha)_8$ barrel fold, which is not fully completed. An extra domain is present at the N-terminal part of the enzyme. A long region between the third β -strand and third α -helix of $(\beta/\alpha)_8$ barrel form a globular cluster in association with the loop between the fourth β -strand and fourth α -helix of $(\beta/\alpha)_8$ structure. Ca^{2+} is also attached to the internal structure of the enzyme; however, the position of calcium is different from the α -amylase (EC 3.2.1.1) (Ray, 2011).

Pullulanases are the important debranching enzyme. They have been classified into Type I pullulanase and Type II pullulanase, also known as amylopullulanases. Type I pullulanase exclusively hydrolyzes α -1,6-glycosidic bonds in pullulan and other branched oligosaccharides resulting in the formation of maltotriose and linear oligosaccharides. Amylopullulanases (Type II pullulanase) can cleave both α -1,6-glycosidic and α -1,4-glycosidic linkages in branched and linear oligosaccharides (Bertoldo and Antranikian, 2002). Type I pullulanase belongs to GH13 while Type II pullulanase is distributed in GH13 and GH57 based on their structure and

catalytic residues (Nisha and Satyanarayana, 2013). All the pullulanases carry $(\beta/\alpha)_8$ barrel structure, the catalytic triad is composed of aspartate, glutamate, and aspartate residues at the β_4 , β_5 , and β_7 strands, respectively. However, the amylopullulanases of the GH57 family contain $(\beta/\alpha)_7$ barrel structure where catalytic residues glutamate and aspartate are situated in β_4 and β_7 strands, respectively. Moreover, it has five conserved sequences (Nisha and Satyanarayana, 2013; Xu *et al.*, 2013). Previously, Zona *et al.* (2004) first reported that the families GH57 had five conserved sequence regions. GH119 also had five conserved sequence regions (Sarian *et al.*, 2017). Mikami *et al.* (2006) reported that the crystal structures of the pullulanase of *Klebsiella pneumoniae* had five domains (N1, N2, N3, A, and C). N1 domain could bind with maltotriose, maltotetraose and one calcium ion also. The N1 and N2 domains were the exclusive features of pullulanases, while the other three domains (N3, A, and C) had some similarities with *Pseudomonas* isoamylase. Moreover, isoamylase and pullulanase are the debranching enzymes, but the substrate specificities are not similar due to their separate organization of domains and active site. Later, it was revealed that type I pullulanase from *Anoxybacillus* sp. LM18-11 consists of four domains (N1, N2, A, and C). The catalytic amino acids Asp413, Glu442, and Asp526 are arranged in domain A. The N1 domain is recognized as a carbohydrate-binding motif. Interestingly, four molecules of oligosaccharides were associated with the active configuration of pullulanase. In this concern, two molecules of oligosaccharides were present in domain A; another two molecules were located in the N1 domain and the loop between the third β -strand and the third α -helix of domain A (Xu *et al.*, 2013).

Neopullulanase has a close similarity with maltogenic amylase (EC 3.2.1.133) and cyclomaltodextrinase (EC 3.2.1.54) (Hondoh *et al.*, 2003). Neopullulanase, cyclomaltodextrinase, and maltogenic amylase exclusively exhibit the fifth conserved sequence region (CSR V) (Janeček, 2002). Neopullulanases are closely associated with Type I pullulanase (Nisha and Satyanarayana, 2016). The Crystal structures of neopullulanase from *Bacillus stearothermophilus* TRS40 had revealed that the active enzyme forms a dimer. The monomeric configuration possesses four domains (N, A, B, and C). Like other amylases, $(\beta/\alpha)_8$ barrel is present in domain A. However, Hondoh *et al.* (2003) reported that the α -helix 5 and β -strand of the $(\beta/\alpha)_8$ barrel of A domain were incomplete in comparison to the ideal A domain structure. The active site of the neopullulanase lies between the domain of two monomers, located in between domain A and domain N of the other monomer. This type of arrangement makes active-site cleft narrower in comparison to α -amylase and helps to exert hydrolytic activity for both α -1,4 and α -1,6-glucosidic bonds (Hondoh *et al.*, 2003).

β -amylase (EC 3.2.1.2) is organized in a single domain structure that contains a large $(\beta/\alpha)_8$ barrel core, which is similar to α -amylase. A small lobe made by three loops from the β -strand adjacent to the β barrel with a long C-terminal loop is also observed. Glucoamylase (EC 3.2.1.3) has three functional domains. The catalytic domain consists of $(\alpha/\alpha)_6$ barrel structure; O-glycosylated linked domain comprises multiple O-glycosylated sites and two N-glycosylated sites; another domain is the starch binding domain. Besides these, other features of some amylases are presented in Table 7.

Table 7: Structural and functional comparison of different amylases

Parameters	α -amylase	CTGase	Maltotetraose forming amylase	β -amylase	Glucoamylase (γ -amylase)
E.C. number	3.2.1.1	2.4.1.19	3.2.1.60	3.2.1.2	3.2.1.3
	Endo-acting	Transglycosylation	Exo-acting	Exo-acting	Exo-acting
Sources	<i>Bacillus licheniformis</i> (BLA) <i>Aspergillus oryzae</i> (TAKA amylase),	<i>Bacillus stearothermophilus</i>	<i>Pseudomonas stutzeri</i>	<i>Bacillus cereus</i>	<i>Aspergillus awamori</i>
Amino acids residues	512 (BLA) 549 (TAKA amylase)	680	429	516	471
Active site	In domain A at conserved sequence region II, III and IV.	In domain A, another substrate binding site is present in domain D	In domain A	C-terminal end of β -barrel	N-terminal end of α -helix bundle
Catalytic residues	BLA: Asp231, Glu261, TAKA amylase Asp206, Glu230	Asp225, Glu253, and Asp324	Asp193, Glu219, and Asp294	Glu172 and Glu367	Glu179 and Glu400
Calcium ion	2/3	02	02	01	-
Disulfide bond	01 Cys30:38	01 Cys40:47	02 Cys140:150, 216:251	Cys91:99	03 Cys210:213, 266:270, 222:449

7. Conserved region and distribution pattern of catalytic residues in the amylases of GH13 and related families

The enzymes of the α -amylase family have four (I–IV) highly conserved sequence regions in their TIM barrel structure. Despite these four conserved regions, there are three additional conserved sequences in the enzymes of the α -amylase family. The seven conserved sequence regions of different enzymes of the α -amylase family are given in Table 8. The four primary conserved sequence regions are present in the terminal end of β -strand 3, β -strands 4, 5, and in the loop connecting β -strand 7 to α -helix 7 (MacGregor *et al.*, 2001; Janeček, 2002) (Fig. 2). These regions form the substrate-binding site and catalytic center (Kuriki and Imanaka, 1999). Asp residue of the second region and Glu residue of the third region acts as nucleophile and proton donors, respectively in α -amylase and related enzymes. His residue of the first region and

His and Asp residue of the fourth region helps to hold the substrate in the proper position (Prakash and Jaiswal, 2010). The amino acids of the catalytic triad are always present in the conserved sequence region II, III, and IV, but their position number is different among the amylases. The conserved residues exhibit similar functional activity, also contribute to the substrate and calcium-binding capacity (Kumari *et al.*, 2012). The additional three conserved sequence regions are present in the different enzymes (glycoside hydrolases, transferases, isomerases, and others) of clan H. Among the three regions, two regions (VI and VII) are located in the area of β -strand 2 and β -strand 8 of the $(\beta/\alpha)_8$ scaffold. The third region (V) is present near the C-terminus of domain B at the connecting region of β -strand 3 and α -helix 3 in the vicinity of calcium-binding aspartate (Janeček, 2002). Qi and Zimmermann (2005) reported that CGTase had 51 conserved amino acid residues that were distributed in the conserved sequence region of the α -amylase family.

Table 8: Four highly conserved sequence regions and amino acid residues of enzymes of amylase family.

Enzymes	Origin	CSRI	CSR II *	CSRIII *	CSR IV *
α -Amylase	<i>Aspergillus oryzae</i>	117D V VAN H	202GLR I D T V K H	230E V L D	292F V EN H D
Cyclodextrin Glucosyl transferase (CGTase)	<i>Bacillus macerans</i> ; <i>Bacillus circulans</i> 251	135D F AP N H	225G I R F D A V K H	258E W F L	324F I D N H D
Isoamylase	<i>Pseudomonas amyloclavata</i>	292D V VY N H	371G F R F D L AS V	435E P WA	505F I D V H D
Branching enzyme	<i>Escherichia coli</i> ; <i>Bacillus stearothermophilus</i>	335D W VP G H	401AL R V D AVAS	458E E EST	521L P L S H D
Pullulanase	<i>Bacillus flaocaldarius</i> KP 1228	600D G V F N H	671G W R L D V P N E	704E I W H	827L L G S H D
Neopullulanase	<i>Bacillus stearothermophilus</i>	242D A V F N H	324G W R L D V AN E	357E I W H	419L L G S H D
α -Glucosidase	<i>Saccharomyces carlsbergensis</i>	106D L V I N H	210G F R I D T AG L	276E V AH	344Y I EN H D
Oligo-1,6-glucosidase	<i>Bacillus cereus</i>	98D L V V N H	195G F R M D V IN F	255E M PG	324Y W N N H D

Numbering of the amino acid sequences starts from N-terminal. Highlighted parts are the conserved amino acids. * marked indicates the catalytic amino acids.

The additional three conserved regions are not furnished in this table. Here, only the major regions involved in substrate binding and catalysis are presented. Actually, the region VI is located before the region I, region V is placed in between region I and II, and VII is present after region IV (for details see review Janeček, 2002).

All the members of the GH13 family bear Glu as a proton donor and Asp as a nucleophile in their catalytic site (Table 1), but the respective position of the Glu and Asp differs according to their total number of amino acid residues (Table 7). Sarian *et al.* (2017) reported that an atypical α -amylase (BmaN1) from *Bacillus megaterium* NL3 contained only two invariant catalytic residues in place of three residues. The third residue of BmaN1 was histidine, which acts as the transition-state stabilizer instead of aspartate. Typically, this amylase produces glucose and maltose from soluble starch. However, most of the α -amylase gives maltooligomers and branched dextrans as enzyme-catalyzed end products. This specific α -amylase belongs to the group of α -amylases containing aspartate, glutamate, and histidine in their catalytic triad. After phylogenetic analysis, this group of α -amylases is branched into a separate subfamily under GH13 (Sarian *et al.*, 2017). Alternatively, in family GH57, Asp acts as a proton donor, and Glu is a nucleophile. The three-

dimensional structure of 4- α -glucanotransferase of *Thermococcus litoralis* was determined first in the family GH57. Unlike the catalytic triad of the enzymes of the GH13 family, the members of GH57 carried two catalytic residues Glu and Asp in their active site as the nucleophile and the proton donor, respectively (Imamura *et al.*, 2003). The *In Silico* study of Janeček and Kuchtová (2012) had revealed that α -amylase from family GH119 showed the same catalytic residues Glu231 and Asp373 with GH57 family as nucleophile and proton donor, respectively (Table 1). However, in family GH31, both proton donor and nucleophile is Asp (Table 1). Oligo-1,6-glucosidase (EC 3.2.1.10) bears $(\beta/\alpha)_8$ barrel fold in domain A. β -strands 4, 5, and 7 of $(\beta/\alpha)_8$ barrel contain nucleophile (Asp198), proton donor (Glu240), and transition state stabilizer (Asp316), respectively. Domain B involves in substrate recognition. Domain C consists of antiparallel β -sheet, forms a β -sandwich structure. Ca^{2+} forms an octahedral coordination shell, linked with 3 Asp, Asn, and

Ile residues of domain A (Møller *et al.*, 2012). However, Ca^{2+} independent structure was also reported by Watanabe *et al.* (1997).

8. Strategies of catalysis of glycosidic bonds

α -Amylase randomly hydrolyzes α -1,4 glycosidic linkages in polysaccharides containing three or more α -1,4 linked D-glucose units. It cannot hydrolyze α -1,6 linkages and always produce α -anomeric products. The initial products are high molecular weight dextrans, as the reaction proceeds large amounts of maltose, maltotriose, and oligosaccharides (α -limit dextrin) have appeared (Fig. 3). The reaction shows a rapid loss of viscosity and blue loss property (loss of intensity of the blue color of the starch-iodine complex).

α -Glucosidase (EC 3.2.1.20) is an exo-acting enzyme, hydrolyzes terminal non-reducing α -1,4 glycosidic linkage. The hydrolytic product is a single glucose molecule in α -configuration. However, glucoamylase gives the same type of reaction, but the product is in β -configuration (Fig. 3). A recent report indicated that α -glucosidase can cleave not only the α -1,4 linkage but also the α -1,6-, α -1,2-, and α -1,3-glycosidic linkages. Besides these, this enzyme has a transglycosylation activity (Mohan and Satyanarayana 2018). At the catalytic site, both proton donor and nucleophile is Asp.

Debranching enzymes like oligo-1,6-glucosidase (EC 3.2.1.10), isoamylase (EC 3.2.1.68), and pullulanase (EC 3.2.1.41) attack only α -1,6 glycosidic linkages in an endo-acting fashion. They produce a variety of products like maltooligosaccharides (G3, G4, G6) and maltose (Fig. 3). Another debranching enzyme, amylo-1,6-glucosidase (EC 3.2.1.33) mainly found in the animal system; however, few bacterial species produce this enzyme. It is a bifunctional enzyme. It shows 4- α -glucanotransferase (EC 2.4.1.25) activity when the substrate is digested with phosphorylase (EC 2.4.1.1). Isoamylase acts on amylopectin and glycogen but bypasses pullulan. However, pullulanase can break amylopectin, pullulan, and a lesser extent of glycogen. In the industrial sector, pullulanase, in combination with β -amylase is applied for the production of maltose.

Maltohexaose forming amylase (EC 3.2.1.98), maltotetraose forming amylase (EC 3.2.1.60), maltotriose forming amylase (EC 3.2.1.116), and maltogenic amylase (EC 3.2.1.133) specifically produce different maltooligosaccharides and maltose (Fig. 3). All these enzymes are exo-acting, generating the products in α -configuration. Except maltogenic amylase (EC 3.2.1.133), the other three enzymes attack definite α -1,4 glycosidic linkages from the non-reducing end, produce maltohexaose, maltotetraose, and maltotriose, respectively. The maltogenic amylase (EC 3.2.1.133) cleaves α -1,4 glycosidic linkages of the substrates containing only two glucose units at the non-reducing end; the end product appears as maltose.

Cyclodextrin glycosyltransferase (CGTase) catalyzes different reactions: cyclization, coupling, and hydrolysis. These enzymes generate different types of cyclodextrins [(CDs) cyclomaltohexaose (α -CD), cyclomaltoheptaose (β -CD), and cyclomaltooctaose (γ -CD)] (Feng *et al.*, 2011), and few maltooligomers. The cyclization reaction produces CDs. In this reaction, the enzyme incises the α -1,4 glycosidic bond of the glucan chain at a distance of 6, 7, or 8 oligosaccharide units from the non-reducing end. Later, the C-4 hydroxyl group of non-reducing glucose end of the existing glucan chain reacts with newly formed reducing end glucose to complete the cyclization reaction. A coupling reaction occurs in the presence of glucose and CDs, resulting in the formation of maltooligosaccharides. CGTase hydrolyzes α -1,4 glycosidic bond and forms α -1,4 glycosidic bond in their reaction system.

Neopullulanases (EC 3.2.1.135) is a specific class of enzyme, which hydrolyzes α -1,4-glycosidic linkages of pullulan and releases a particular class of trisaccharides called panose, isopanose as well as isomaltose (Fig. 3). Neopullulanases can cleave α -1,4- and α -1,6-bonds of starch and related polysaccharides with poor efficacy. Several authors indicated that this enzyme is polyspecific, exhibits transglycosylation reaction, can hydrolyze cyclomalto-dextrins, starch, and pullulan (Park *et al.*, 2000).

The branching enzyme (2.4.1.18) is a different class of enzymes responsible for starch synthesis and is abundantly present in plants. The branching enzyme forms α -1,6 glycosidic bonds by chopping and transferring the growing α -glucan chains to the C-6 hydroxyl group of another glucan chain. Microbial sources of this enzyme are also available. *Bacillus* Sp., *B. stearothermophilus*, and *Pseudomonas* sp. can produce branching enzymes (Mohan and Satyanarayana, 2018).

Both plant and microbial β -amylases are placed in the GH14 family. It is an exo-acting enzyme, cleaves α -1-4 glycosidic bond from the non-reducing end and successively releases maltose in β -configuration as well as β -limit dextrin (Fig. 3). It cannot cleave α -1,6 linkages. In comparison to the mechanism of action, β -amylase exhibits inverting instead of retaining, in which the hydrolytic product is converted to β -configuration from an α -anomeric structure (Fig. 4). β -Amylase is organized in a single domain structure; both proton donor and nucleophile activity are mediated by glutamate (Glu).

Glucoamylase / γ -amylase / amyloglucosidase (EC 3.2.1.3) was initially isolated from fungi after the identification of α -amylase and β -amylase in Japan. It is an exo-acting enzyme, hydrolyzes terminal α -1-4 glycosidic linkages from the non-reducing end and also enables to hydrolyze α -1-6 bonds at a slower rate than cleavage of α -1-4 glycosidic linkages. The final product is exclusively β -D-glucose (Fig 3). Thus this enzyme completely hydrolyzes starch to glucose. Unlike (β/α)₈ barrel structure of α -amylase and β -amylase, glucoamylase has an (α/α)₆ structure. Both the proton donor and the nucleophile are Glu.

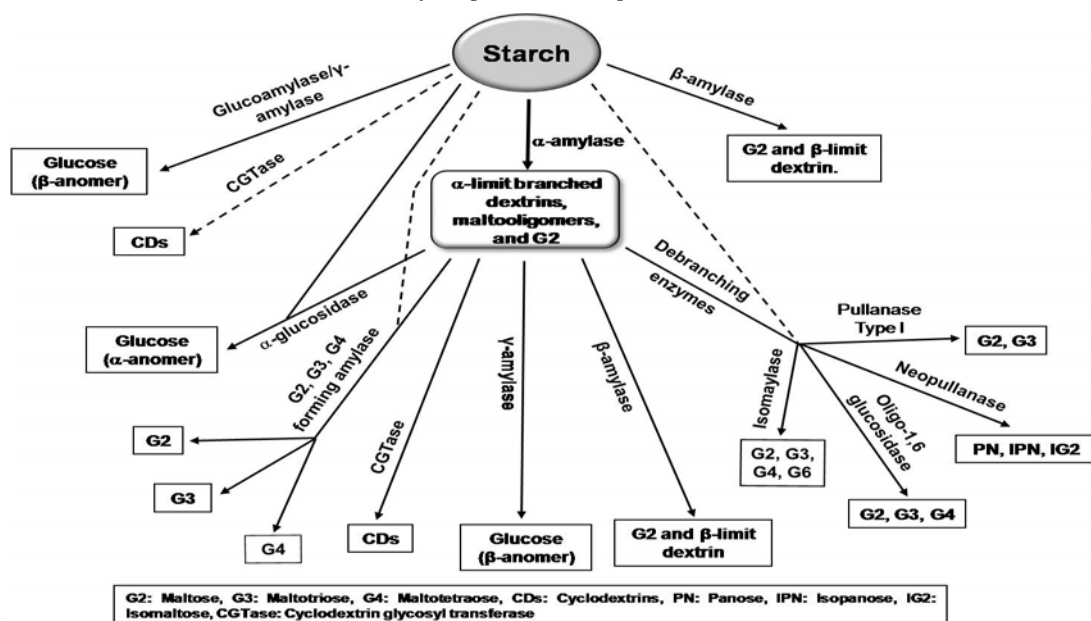


Figure 3. The pattern of product formation from starch and partially hydrolyzed substrate by different types of amylases.

9. Mechanism of catalytic activity

The hydrolytic activity of amylases is mediated through the α -retaining double displacement mechanism (Fig 4) (van der Maarel *et al.*, 2002). Four to ten glucose units of starch are fitted in the substrate-binding cleft. A particular subsite nomenclature is accepted for amylase activity. The nonreducing end of the substrate binds at the minus subsites; while, plus subsites hold the reducing end. The catalysis occurs in between +1 and -1 subsites (Fig 4a) (Davies *et al.*, 1997). Two aspartic acids (Asp) and one glutamic acid (Glu) involve in catalytic activity. Glutamic acid acts as a proton donor and aspartic acid acts nucleophile. During the reaction, Glu donates the proton to the glucosidic oxygen of the starch substrate, while

aspartate starts nucleophilic attack to the C1 of glucose at subsite -1. The proton donation and nucleophilic attack finally cleave the glycosidic bond (Fig 4b). Later, water involves in the reaction system, re-protonates the glutamate and hydroxyl group of water attached to the C1 of the remaining substrate (Fig. 4b,c). The second aspartate residue plays an indirect role in catalysis by holding the substrate in the proper position (Uitdehaag *et al.*, 1999). Agirre *et al.* (2019) reported that α -amylase from *Alicyclobacillus* sp. can give the space to accommodate the branching point of starch. In the inverting reaction mechanism, the α -configuration products are formed after the reaction, which is converted to β -configuration (Fig 4c).

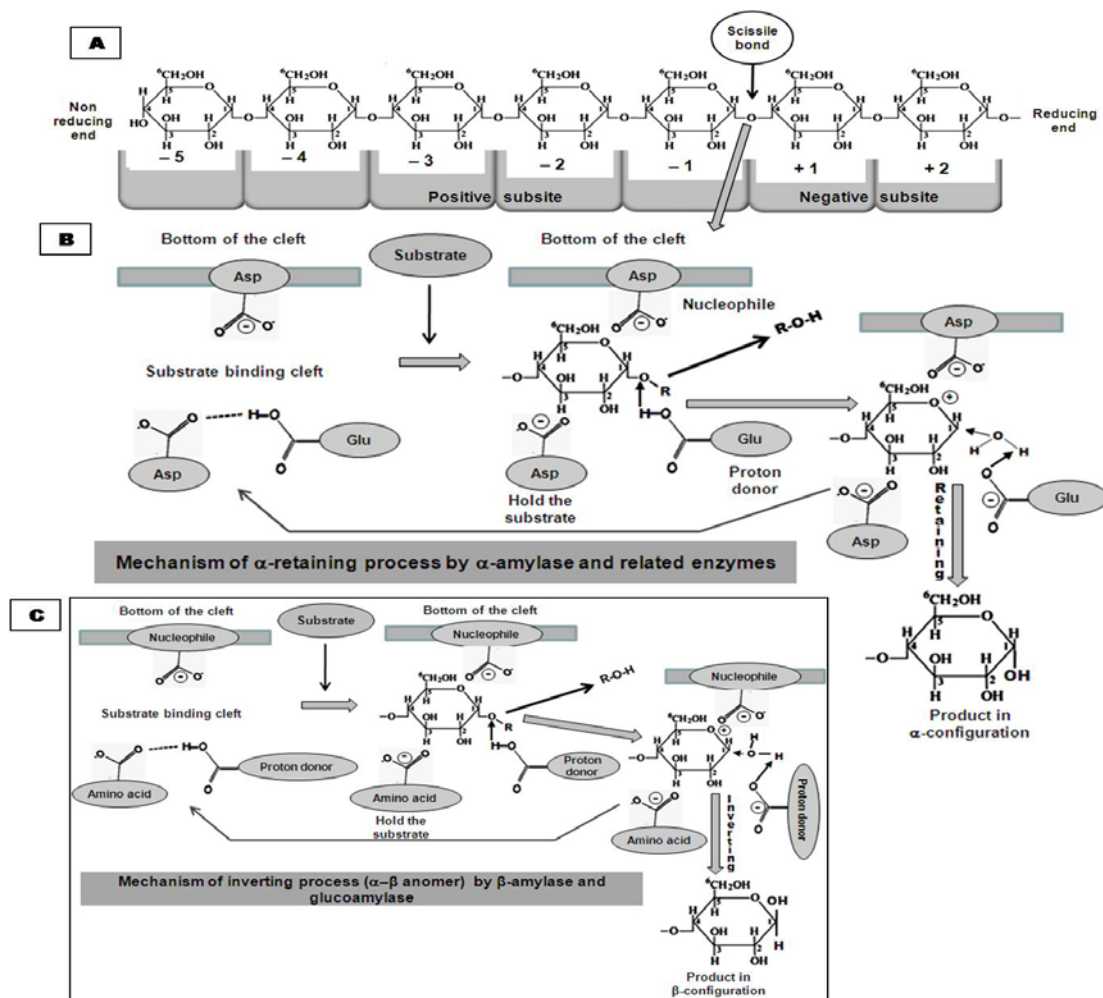


Figure 4: A: The pattern of subsite position, nomenclature, and presentation of a scissible bond. B: The α -retaining mechanism of the catalytic reaction. C: The inverting reaction and formation of β -anomeric product.

10. Application of α -amylase

The journey of applications of amylases was started from the early days of the nineteenth century when the Russian chemist Kirchoff first discovered a starch degrading enzyme in wheat in the year 1811. Later, Payen and Persoz (1833) isolated a catalytic substance 'diastase', which converted gelatinized starch into sugars in experimental conditions. Magendie (1846) showed the diastatic properties of blood and proposed that blood was able to split starch into dextrin and glucose. The commercialization and industrial use of amylase were started after the isolation of fungal α -amylase 'Takadiastase' from *Aspergillus oryzae* by the Japanese scientist Jökichi Takamine in 1894. In 1917, the French scientists, Boidin and Effront initiated the application of bacterial amylase (isolated from *Bacillus subtilis*) as a desizing agent.

10.1. Starch liquefaction, saccharification, and applications of hydrolyzed products

Starch is abundantly present in our environment. Different cereals like barley (50-60%), wheat (65-70%), sorghum (65-75%), rice (75-87%), corn (75-80%) contain

large amount of starch. These ingredients are used in the starch processing industry for the production of different food ingredients, animal feed, biofuel, and therapeutic agents. Enzymatic hydrolysis of starch is a crucial part of the production of various commercially important products like glucose, fructose, high-fructose containing syrup (HFCS), maltose, maltooligosaccharides, dextrin, and cyclodextrins (Fig. 3). For this purpose, about 15%–20% of industrial enzymes are used in the starch industry. The endo- and exo-acting amylolytic enzymes (α -amylase, pullulanase, glucoamylase, glucose isomerase, and others) are potentially used for hydrolysis of starch at the industrial scale. Corn starch is mostly used for hydrolysis due to its huge availability.

Thermostable microbial α -amylase is added in the starch slurry for the production of low-molecular-weight dextrans after hydrolysis. The dextrans (DP3-25) are used for further applications in the preparation of commercial products. Debranching enzymes [oligo-1,6-glucosidase (EC 3.2.1.10), isoamylase (EC 3.2.1.68), and pullulanase (EC 3.2.1.41)] cleave the dextrin to DP2-5 products. The saccharification process is a vital step for starch processing. For this purpose, different enzymes such as α -glucosidase, maltogenic enzyme, maltooligosaccharide forming enzymes, β -amylase (microbial/plant), and γ -amylase are applied for the production of glucose,

fructose, HFCS, maltose, maltotriose, maltotetraose, and others. Pullulanases are widely used in the starch industries for the process of saccharification and preparation of maltose, maltotriose, and other oligosaccharides. This enzyme decreases the application of glucoamylase up to 50% and also reduces the reaction time. The mixture of glucoamylase and pullulanase is commercially available in the brand name of OPTIMAX from Genencor. Application of acid-stable, calcium-independent, thermostable amylopullulanase in the saccharification process makes reaction more convenient to produce different sugar syrups; this step is time-saving, and cost-effective (Nisha and Satyanarayana, 2013a, 2014). The neopullulanase breaks starch, CDs, and maltooligosaccharides, synthesizes large amounts of maltose and little amounts of glucose (α -anomer) during the reaction.

10.1.1. Production of maltose and maltooligosaccharides and their potential applications

Starch slurry is initially treated with the thermostable α -amylase for liquefaction; then saccharification is done with isoamylase, pullulanase, and β -amylase. The final product is prepared after downstream processing. Food grade maltose has several applications in bakery and confectionery products, preparation of infant and geriatric foods. Maltose is also used as a sweetener, quality improver and the preparative of foods. Moreover, highly purified medical-grade maltose is provided in intravenous infusion as it prevents a sudden increase in glucose levels (Samanta, 2020a).

Maltooligosaccharides have different gradations like maltotriose rich maltooligosaccharides, maltotetraose syrup (G4 syrup), and anomalously linked oligosaccharides mixture (Alo-mixture). Specifically, the maltotriose-rich maltooligosaccharides mixture contains glucose (2%), maltose (37.5%), maltotriose (46.5%), and other oligosaccharides (14.0%). The initial step of production is similar to maltose. β -amylase and pullulanase are used for the synthesis of the maltotriose-rich maltooligosaccharides mixture (Maltooligomer Mix). Maltotetraose syrup (G4 Syrup) is formed when saccharification is mediated by G4 amylase and isoamylase. Application β -amylase and fungal α -glucosidase at the saccharification level produces anomalously linked oligosaccharides mixture (Alo Mixture).

Linear maltooligosaccharides contain 3-10 monosaccharide units linked by α -1,4 linkages. Maltooligosaccharides have several beneficial properties and are widely used in the food industry. They have several unique characteristics, including high solubility, less sweet than sucrose, low calorogenic, less hygroscopic, high moisture retention capacity, and anti-retrogradation activity (Mohanan and Satyanarayana, 2018; Samanta, 2020a). Maltooligosaccharides are potentially used for the preparation of infant and geriatric foods, candies, ice creams, and beverages. In the bakery industry, maltooligosaccharides act as an antistaling agent as they interfere with starch–gluten interaction (Nagarajan *et al.*, 2006; Plácido Moore *et al.*, 2005).

Maltotriose-rich maltooligosaccharides mixture exhibits only 30% sweetness as compared to sucrose, low viscosity, low freezing point, less color formation than

corn syrup, better hygroscopic properties. It is used as a sucrose substitution and maintains the hardness and texture of the frozen foods. At the commercial levels, this mixture is essential for the preparation of confectionery products (jams, jelly, cake, chewing gum, butter cream, custard cream), bakery products, frozen foods, canned coffee, cocoa, fruit drinks, and alcoholic beverages (Jana *et al.*, 2013; Samanta, 2014, 2020a).

Enzymatic preparation of maltooligosaccharides is enormously increasing in the last few decades. Two government agencies [Foods for Specified Health Use (FOSHU) and Foods with Nutrient Function Claims (FNFC)] of Japan enlisted 223 items as functional components of foods; among them, 50% are oligosaccharides (Jana *et al.*, 2013). Maltooligosaccharides are commercially available as Fuji Oligosyrups, a product of Nihon Shokuhin Kako Kogyo Kabushiki Kasha (Tokyo, Japan) (US9730464B2, US20130210764A1). G4 syrup contains about 50% maltotetraose, whereas Alo-mixture contains more glucose (40%) and isomaltose (17%). Properties of these two ingredients have some similarities with the maltotriose-rich maltooligosaccharides mixture, and the application fields are also similar. Maltooligosaccharides have health-beneficial effects. They are treated as a prebiotic agent and influence the growth of bifidobacteria in the colon and prevent dysbiosis. This property increases its value as bio preservatives and functional foods (Barreteau *et al.*, 2006). Maltooligosaccharides are poorly absorbed; they are low calorogenic agents. These properties are beneficial to prevent diabetogenic effects, cardiovascular diseases, and obesity (Kayode *et al.*, 2009).

10.1.2. High fructose containing syrup (HFCS) preparation and uses

Treatment of starch by thermostable α -amylase followed by saccharification with the fungal glucoamylase and debranching enzyme produces glucose. The conversion of glucose to fructose is mediated by the action of glucose isomerase (xylose isomerase; EC 5.3.1.5), which converts glucose to fructose as a common product. This conversion is essential for HFCS production, but the enzyme does not belong to the amylase family (Bhosale *et al.*, 1996). Recently, Mohanan and Satyanarayana (2018) had reported that every year, Japan produced 3 million tons of starch from which more than 60% are utilized for glucose and high fructose-containing syrup (HFCS) preparation. Annually, Japan and the United States produce one million tons and 8 million tons of HFCS, respectively. HFCS is the useful ingredients for the preparation of beverages, dairy products, bakery and confectionery products, canned foods, and frozen candies.

10.1.3. Applications amylases in the bakery industry

Amylopectin in wheat flour acts as a staling agent due to its retrogradation activity. Applications of plant β -amylase and maltogenic amylase (EC 3.2.1.133) along with α -amylase degrade the starch into dextrin as well as maltose, which improves the quality of bread by increasing loaf volume. Additionally, the application of amylopullulanase in dough hydrolyzes branched maltodextrins that decrease the stickiness of bread and

bakery foods, improves shelf-life, texture, crispiness, and loaf volume of the products. Moreover, the presence of maltooligosaccharides in bread acts as prebiotics for health benefits (Nisha and Satyanarayana, 2014).

10.1.4. Production of cyclodextrin and its applications

About 2000 tons of cyclodextrins are produced per year for industrial purposes. Cyclodextrins are prepared from gelatinized starch, which is made through boiling of starch in hydrated conditions. This treatment irreversibly changes the intermolecular bonding structure of starch. The production of cyclodextrins is done by the use of cyclodextrin glycosyltransferase (CGTase) enzyme for the treatment of gelatinized starch. Cyclodextrins (CDs) are cyclic-oligosaccharides having 6-8 glucose units linked through the α -1,4-glucosidic bond. Six, seven, and eight glucose units containing cyclodextrins are named as α , β , and γ cyclodextrin, respectively. The types of cyclodextrin production depend on the nature of the enzyme from which it is isolated. Branched cyclodextrin contains maltose or glucose through α -1,6-glucosidic linkage. In the industrial sectors, these types of cyclodextrins are made through a reverse reaction by using a thermostable pullulanase in the presence of high concentration of maltose and cyclodextrins. CDs and branched-cyclodextrin are mostly used in food, pharmaceutical, cosmetic, and plastic industries as emulsifiers. CDs have a hydrophobic cavity for their unique structure, which makes them unable to form inclusion complexes with different hydrophobic agents related to flavor and taste enhancement. The hydrophobic volatile compounds from herbs and spices were packed with CDs. The formation of these inclusion complexes increases the solubility, stability, and bioavailability of hydrophobic components. Thus, CDs are applied as food additives. This conjugation retains the flavor of the foods and also acts as an antioxidant to preserve the foods and other commercial products (Qi and Zimmermann, 2005; Ray, 2011; Mohanan and Satyanarayana, 2018). Volatile flavoring agents were trapped within the hydrophobic cavity of CDs and mixed with different cooking spices. Administration of these conjugate spices in delicious preparation enhances the flavor and taste of served foods.

10.1.5. Production of isomaltooligosaccharides, resistant starch, and their health benefits

Break down of starch by α -amylase followed by treatment of various enzymes like α -glucosidase, oligo-1,6-glucosidase (EC 3.2.1.10), isoamylase (EC 3.2.1.68), pullulanase (EC 3.2.1.41), and neopullulanase (EC 3.2.1.135) produces maltooligosaccharides, isomaltooligosaccharides (IMO), panose, isopanose as well as resistant starch (RS) (Zhang *et al.*, 2012; Møller *et al.*, 2012; Li *et al.*, 2017; del Moral *et al.*, 2018). Recently, these ingredients are used as functional foods as well as dietary supplements for the preparation of therapeutic and healthy diet. IMO, panose and RS have prebiotic activity (Chen *et al.*, 2010; Møller *et al.*, 2012; Li *et al.*, 2017). IMO is poorly absorbed in the human gut and reaches the colon. It influences the growth of bifidobacteria and lactobacillus (Goffin *et al.*, 2011; Ketabi *et al.*, 2011). IMO is metabolized by the human colonic microbiota due

to the presence of oligo 1,6- α -glucosidase (EC 3.2.1.10) and α -glucosidase (EC 3.2.1.20). Additionally, panose and isopanose also have bifidogenic activity. Thus, IMO and panose selectively stimulate the growth of beneficial bacteria; alternatively, they inhibit the growth of other harmful microbes that can synthesize amines and other toxicants. Thus, they maintain the health of the colon and prevent carcinogenic activity.

Another important component is RS. Enzymatic treatment (name already is given) produces RS that is used as dietary supplements. The application of RS as a functional food ingredient improves several properties of foods like color, flavor, gel formation, viscosity texture, and moisture-retaining capacity (Sajilat *et al.*, 2006; Simsek *et al.*, 2012). RS is called high-amylose starches, which is being resistant to hydrolysis by intestinal α -amylase. This effect is beneficial to regulate blood glucose concentrations. Though RS is not digested in the small intestine, the colonic microbiota starts fermentation of RS, resulting in the production of high amounts of short-chain fatty acid (butyrate, acetate). Decrease of blood glucose levels and production of short-chain fatty acids are beneficial to control diabetes and obesity and consequently lowers the risk of cardiovascular diseases (Fuentes-Zaragoza *et al.*, 2010; Zhang *et al.*, 2012). Moreover, short-chain fatty acids preserve colon health (Hii *et al.*, 2012).

10.1.6. Applications of maltitol, trehalose

Isoamylase is used for the preparation of glucose syrup, maltose, maltitol, trehalose, CDs, and RS from the starch substrate. Glucose and maltose are commonly used in the food and pharmaceutical industry. Maltitol is utilized as a sugar substitute in the production of non-calorigenic candies, chewing gum, and other confectionery products (Ray, 2011). Supplementation of trehalose in food enhances stability, controls humidity, and maintains the texture of the food (Olempska-Beer, 2007).

10.2. Preparation of animal feed

Animal feed is produced by using food grains like wheat, barley, maize, cassava, sorghum, rice hush, etc. Starch is the reserve food material in all types of food grains. In the cereals, starch has arranged in concentric layers. Application of un-boiled animal feed lowers the digestibility of the foods and decreases nutrition level. α -Amylases are applied for the preparation of animal feed, which partially cleaves the starch of the grains resulting in enhancement of quality improvement of feed as well as digestive capacity (de Souza and Magalhaes, 2010). Thus, pre-treatment of starchy material with amylases enhances the nutritional value of the feed. Isoamylase is also exploited for the preparation of animal feed. Resistant starch is present in cereal meal-based animal feed, which is partially digested in the gut of monogastric animals. Puspita *et al.* (2019) reported that isoamylase-treated cassava root meal starch can be used for poultry feed.

10.3. Application in desizing (Removal of starch sizer from textile)

Starch paste is applied as a sizer agent in the textile industry during weaving. The starch sizer increases the softness of the strings and protects them from friction, cutting, and generation of static electricity. After making the cloth, starch has removed (desizing) from the cloth. There are different processes of desizing, including enzymatic treatment, oxidative breakdown, acid wash, and fermentative removal. Among these, enzymatic treatment is the best process concerning the quality and safety of the cloth as well as the prevention of the use of harmful chemicals. Application of thermostable α -amylase in the desizing process eliminates the starch paste without affecting the fabric quality.

10.4. Application in papermaking

The application of starch paste during paper making protects the paper against mechanical damage and reduces the tendency of liquid absorption during drying. Removal of starch paste by α -amylase and pullulanase enhances the quality, texture, strength, smoothness, writing, and erasability capacity of the finished paper (Sundarram and Murthy, 2014). Pullulanase-treated high-amylase containing starches are blended in adhesive products and used in the manufacturing of papermaking agents and corrugated boards (Jobling, 2004).

10.5. Production of biofuel

Biofuel is the best choice to control pollution levels. Starch is the initial ingredient of biofuel production due to its low cost and abundant availability. There are three main stages for the production of ethanol from starch. Stage 1: thermostable α -amylase mediated starch liquefaction (Pervez *et al.*, 2014). This step reduces the viscosity of the starch slurry and increases dextrins and oligosaccharide contents. Stage 2: saccharification of liquefied starch by α -glucosidase, isoamylase, pullulanase, β -amylase, and glucoamylase that produce simple sugars and smaller oligosaccharides for alcoholic fermentation. Stage 3: fermentable sugars are then fermented by yeast to produce ethanol (Mohiuddin *et al.*, 2016; Saini *et al.*, 2017).

10.6. Application in detergent preparation

Enzyme-based liquid detergent is environmentally safe. α -Amylase along with protease, lipase, and cellulase are used in the preparation of enzyme-based high-quality detergent. Starch holds the dust particle on the surface of the cloth. Similarly, the residues of starchy food ingredients and some oily substances are present as a remnant over the used food-dishes. α -Amylase and other enzymes degrade the starchy and oily substances to clean the content properly. Alkalophilic amylases having a broad range of temperature profile, chelator insensitivity, and oxidant resistant capacity are potentially used in detergent formulation (Kumari *et al.*, 2012; Sundarram and Murthy, 2014).

10.7. Degradation of extracellular polymeric substances and inhibition of biofilm formation

Biofilm is a syntrophic association that makes the adherence of microbial cells on the biotic and abiotic surfaces. About 80% of microbial pathogenesis is directly associated with the formation of biofilm (Donlan and Costerton, 2002; Lahiri *et al.*, 2021b). Extracellular polymeric substances (EPS) are most important in the formation of biofilm. The biofilm contains proteins and nucleic acids; it stabilizes the microbial association and contributes nutrients to the sessile microbial communities (Lahiri *et al.* 2021c). EPS contains various types of cationic and anionic molecules, such as glycoproteins, glycolipids, and proteins that provide protection from invasion of the motile cells into the biofilm interior. (Nadell *et al.*, 2015). Another important component of EPS is polysaccharides. EPS acts as a protective shield to prevent the penetration of antibiotics into the growing microbial cells. Collectively, biofilm contributes to generating resistance capacity against antimicrobial drugs that creates a crisis in the healthcare system (Jana *et al.*, 2017). Enzymes, particularly amylases (α -amylase, β -amylase, glucoamylase, and α -glucosidase) play important roles in the degradation of biofilm. The breakdown of carbohydrate residues in the biofilm weakens the association between microbes and the host surface. Amylases can be used as antimicrobial components to denature the biofilm and restriction of pathogenesis (Lahiri *et al.* 2021c).

Several microbes like *Candida albicans*, *C. glabrata*, *Enterococcus faecalis*, *Streptococcus mutans*, *Veillonella dispar*, and *Fusobacterium nucleatum* (Berger *et al.*, 2018) are present in the oral cavity. Another important pathogen is *S. aureus*, causal agent of Skin infections, cellulitis, folliculitis, and others. α -Amylase from *Bacillus subtilis* degrades the EPS and is effective against biofilm formation of *S. aureus*, *P. aeruginosa*, and *V. cholerae* (Kalpana *et al.*, 2012). In vitro studies had revealed that α -amylase blocks the biofilm formation of *S. aureus* and *P. aeruginosa* (Lahiri *et al.*, 2021a). Bradford (2011) critically studied the role of amylase on biofilm formation by *S. aureus* and had reported that amylase reduced biofilm formation capacity up to 90%. Moreover, Watters *et al.* (2016) indicated that α -amylase is the potent inhibitor of biofilm formation in drug resistance *S. aureus*. From these observations, it has been stated that amylases can potentially be used in the ointment, mouth gel, and digestive medicine. Application of amylases in these medicines may block the pathogenesis by exerting anti-biofilm activity which will be helpful for the treatment of dermal infection, oral infection, and intestinal pathogenesis.

10.8. Clinical applications

α -Amylase from *Aspergillus oryzae* (diastase) is used for the preparation of digestive medicines, which are formulated in liquid (common composition α -amylase 100 mg; papain 50 mg/5ml) and capsule form. Many companies produce digestive medicines that are available in the market. Digestive medicines are commonly used for the treatment of indigestion, acute pancreatitis, and related diseases. A high level of serum α -amylase has been

observed in pancreatic fistula, acute stress, gastric aspiration, etc. (Yan and Wu, 2016). Ultrasensitive amylase biosensor has been developed for the detection of hyperamylasemia (Gibbs *et al.*, 2015; Wang *et al.*, 2015). This biosensor-mediated amylase detection tool can be used in the diagnostic field.

10.9. Other applications

α -Amylase, α -glucosidase, isoamylase, and pullulanase make the brewing process easier and cost-effective. These enzymes are applied for the production of low-calorie beer. These enzymes in association with pectinase and cellulase are used for making fruit juice and beverages. Commercially available amylase mixture is used for the treatment of starchy wastes containing effluent of starch-based industry. This process is eco-friendly and economically viable as the technique is sometimes associated with microbial biomass or bio-fuel production.

11. Conclusion

All the carbohydrate-splitting enzymes have been classified in different glycosyl hydrolase families based on their sequences, molecular structure, catalytic activity, and product formation. Among the carbohydrate splitting enzymes, amylases (hydrolases and transglycosylases) have multipurpose applications in the industrial sectors ranging from the food industry to waste management. Applications of amylases for the production of food ingredients, garments, paper, detergent, biofuel, and others are the eco-friendly process. To achieve this process, several novel characteristics, including thermostability, catalytic efficacy, pH profile, oxidation resistance capacity, chelator insensitivity are the essential factors in the point of industrial uses. Elucidation of molecular structure, amino acid sequences, and catalytic strategies have made the new arena to improve these profiles through protein engineering techniques. Multinational companies (Novozymes, DuPont Danisco, AB enzymes, Genencor, Calzyme, and others) are also involved in the production of advanced quality amylases by establishing their Research and Development wings. Thus, the multidimensional research in protein structure and protein engineering, and biotechnological progression will open many avenues to achieve the high quality of amylases that will change the scenario of their applications in the near future and will be a forward step towards a clean world. Finally, in conclusion, applications of amylases in various industries (food, pharmaceutical, brewing, textile, detergent) and the clinical system will be beneficial in all aspects, including our health, socio-economic development, and environmental protection in the upcoming days.

Conflict of interest

The author has no conflict of interests.

Funding

No financial grant was available. This review article was self-supported by the author.

Acknowledgment

The author is grateful to Midnapore College, Midnapore, West Bengal, India, for providing all kinds of facilities to prepare this manuscript. The author expresses his sincere thanks to Dr. Amal Kanti Chakraborty, Ex-Associate Professor of English, Midnapore College, Midnapore, for his kind help during the language correction of the manuscript.

References

- Abdel-Fattah YR, Soliman NA, El-Toukhy NM, et al. 2013. Production, Purification, and characterization of thermostable alpha amylase produced by *Bacillus licheniformis* isolate AI20. *J Chem.*, **2013**: Article ID 673173, 11 pages.
- Adeyanju MM, Agboola FK, Omfuvbe BO, et al. 2007. A thermostable extracellular α -amylase from *Bacillus licheniformis* isolated from cassava steep water. *Biotechnol.*, **6**: 473-480.
- Affif AF, Kamel EM, Khalil AA, Fouaad E, Fazzi M, Housery M. 2008. Purification and characterization of α -amylase from *Penicillium olsonii* under the effect some Antioxidant Vitamins. *Global J Biotechnol Biochem.*, **3(1)**: 14-21.
- Agirre J, Moroz O, Meier S, Brask J, Munch, A, Hoff T, Andersen C, Wilson KS, Davies GJ. 2019. The structure of the AliC GH13 α -amylase from *Alicyclobacillus* sp. reveals the accommodation of starch branching points in the α -amylase family. *Acta Crystallography.* **D75**: 1-7. <https://doi.org/10.1107/S2059798318014900>
- Ahmadi A, Ghobadi S, Khajeh K, Nomanpour B, Dalfard AB. 2010. Purification of α -amylase from *Bacillus* sp. GHA1 and its partial characterization. *J Iran Chem Soc.*, **7**: 432-440.
- Aisien ET, Igbinosa IH. 2019. Production, purification, and characterization of α -amylase from *Aspergillus niger*, *Aspergillus flavus* and *Penicillium expansum* using cassava peels as substrate. *Nig J Biotech.*, **36(2)**: 114-126. <https://dx.doi.org/10.4314/njb.v36i2.12>
- Amritkar N, Kamat M, Lali A. 2004. Expanded bed affinity purification of bacterial α -amylase and cellulase on composite substrate analogue-cellulose matrices. *Process Biochem.*, **39**: 565-570.
- Arauz LJ, Jozalaa AF, Mazzolab PG, Penna TCV. 2009. Nisinbiotechnological production and application: a review. *Trends Food Sci Technol.*, **20**: 146-154
- Asoodeh A, Chamanic J, Lagzian M. 2010. A novel thermostable, acidophilic α -amylase from a new thermophilic *Bacillus* sp. *Ferdowsicous* isolated from Ferdows hot mineral spring Iran: Purification and biochemical characterization. *Int J Biol Macromol.*, **46**: 289-297. <https://doi.org/10.1016/j.ijbiomac.2010.01.013>
- Bailey JM, Whelan WJ. 1961. Physical properties of starch I. Relationship between iodine stain and chain length. *J Biol Chem.*, **236**: 969-972.
- Barreteau H, Delattre C, Michaud P. 2006. Production of oligosaccharides as promising new food additive generation. *Food Technol Biotechnol.*, **44**: 323-333.
- Bertoldo C, Antranikian G. 2002. Starch-hydrolyzing enzymes from thermophilic archaea and bacteria. *Curr Opin Chem Biol.*, **6**: 151-160.
- Bhosale SH, Rao MB, Deshpande VV. 1996. Molecular and industrial aspects of glucose isomerase. *Microbiol Rev.*, **60**: 280-300.
- Bijttebier A, Goesart H, Delcour JA. 2008. Amylase action pattern on starch polymers. *Biologia*, **63**: 989-999.

- Blesák K, Janeček Š. 2013. Two potentially novel amylolytic enzyme specificities in the prokaryotic glycoside hydrolase α -amylase family GH57. *Microbiol.*, **159**: 2584–2593.
- Boraston AB, Healey M, Klassen J, Ficko-Blean E, Lammerts van Bueren A, Law V. 2006. A structural and functional analysis of α -glucan recognition by family 25 and 26 carbohydrate-binding modules reveals a conserved mode of starch recognition. *J Biol Chem.*, **281**(1): 587–598. <https://doi.org/10.1074/jbc.M509958200>
- Bradford C. 2011. The use of commercially available alpha-amylase compounds to inhibit and remove *Staphylococcus Aureus* biofilms. *Open Microbiol J.*, **5**: 21–31. <https://doi.org/10.2174/1874285801105010021>
- Chandel AK, Rudravaram R, Rao LV, Ravindra P, Narasu, ML. 2007. Industrial enzymes in bioindustrial sector development: An Indian perspective. *J Commercial Biotechnol.*, **13**: 283–291.
- Chen DL, Tong X, Chen SW et al. 2010. Heterologous expression and biochemical characterization of alpha-glucosidase from *Aspergillus niger* by pichia pastoris. *J Agric Food Chem.*, **58**: 4819–4824. <https://doi.org/10.1021/jf1000502>
- Chen J, Chen X, Dai J, Xie G, Yan L, Lu L, et al. 2015. Cloning, enhanced expression and characterization of an alpha-amylase gene from a wild strain in *B. subtilis* WB800. *Int J Biol Macromol.*, **80**: 200–207. <https://doi.org/10.1016/j.ijbiomac.2015.06.018>
- Chung HJ, Liu Q, Hoover R. 2010. Effect of single and dual hydrothermal treatments on the crystalline structure, thermal properties and nutritional fractions of pea, lentil and navy starches. *Food Res Int.*, **43**: 501–508.
- Comfort DA, Chou C-J, Connors SB, VanFossen AL, Kelly RM. 2008. Functional-genomics-based identification and characterization of open reading frames encoding α -glucosidase processing enzymes in the hyperthermophilic archaeon *Pyrococcus furiosus*. *Appl Environ Microbiol.*, **74**(4): 1281–283. <https://doi.org/10.1128/AEM.01920-07>
- Coronado MJ, Vargas C, Mellado E, Tegos G, Drains C, Nieto JJ, et al. 2000b. The alpha-amylase gene amyH of the moderate halophile *Halomonas meridiana*: cloning and molecular characterization. *Microbiology*, **146**: 861–868. <https://doi.org/10.1099/00221287-146-4-861>
- Davies G, Wilson K, Henrissat B. 1997. Nomenclature for sugar-binding subsites in glycosyl hydrolases. *Biochem J.*, **321**: 557–59.
- de Souza PM, Magalhaes POE. 2010. Application of microbial-amylase in industry—a review. *Braz J Microbiol.*, **41**: 850–861.
- Deb P, Talukdar SA, Mohsinar K, Sarke PK, Sayem SMA. 2013. Production and partial characterization of extracellular amylase enzyme from *Bacillus amyloliquefaciens* P-001, *Springer Plus*, **2**: 154. <http://www.springerplus.com/content/2/1/154>
- del Moral S, Barradas-Dermitz DM, Aguilar-Uscanga MG. 2018. Production and biochemical characterization of α -glucosidase from *Aspergillus niger* ITV-01 isolated from sugar cane bagasse. *3 Biotechnol.*, **8**: 7. <https://doi.org/10.1007/s13205-017-1029-6>
- Dey TB, Banerjee R. 2012. Hyperactive α -amylase production by *Aspergillus oryzae* IFO 30103 in a new bioreactor. *Lett Appl Microbiol.*, **54**(2): 102–7. <https://doi.org/10.1111/j.1472-765X.2011.03177.x>
- Dey TB, Banerjee R. 2015. Purification, biochemical characterization and application of α -amylase produced by *Aspergillus oryzae* IFO-30103. *Biocatalysis and Agricultural Biotechnology*, **4**(1): 83–90 <https://doi.org/10.1016/j.bcab.2014.10.002>
- Dheeran P, Kumar S, Jaiswal YK, Adhikari DK. 2010. Characterization of hyperthermostable α -amylase from *Geobacillus sp.* IPTN. *Appl Microbiol Biotechnol.*, **86**: 1857–1866. <https://doi.org/10.1007/s00253-009-2430-9>
- Donlan RM, Costerton JW. 2002. Biofilms: Survival mechanisms of clinically relevant microorganisms. *Clin Microbiol Rev.*, **15**: 167–193. <https://doi.org/10.1128/CMR.15.2.167-193.2002>
- Emtenani S, Asoodeh A, Emtenei S. 2015. Gene cloning and characterization of a thermostable organic-tolerant alpha-amylase from *Bacillus subtilis* DR8806. *Int J Biol Macromol.*, **72**: 290–298. <https://doi.org/10.1016/j.ijbiomac.2014.08.023>
- Farinas CS. 2015. Developments in solid-state fermentation for the production of biomass degrading enzymes for the bioenergy sector. *Renewable and Sustainable Energy Rev.*, **52**: 179–188.
- Feng T, Zhuang H, Ran Y. 2011. The application of cyclodextrin glycosyl transferase in biological science. *J Bioequivalence Availability*, **3**: 9. <https://doi.org/10.4172/jbb.1000086>
- Ficko-Blean E, Stuart CP, Boraston AB. 2011. Structural analysis of CPF_2247, a novel α -amylase from *Clostridium perfringens*. *Proteins*, **79**: 2771–2777. <https://doi.org/10.1002/prot.23116>
- Fuentes-Zaragoza E, Riquelme-Navarrete MJ, Sánchez-Zapata E, Pérez-Álvarez JA. 2010. Resistant starch as functional ingredient: a review. *Food Res Int.*, **43**(4): 931–42. <https://doi.org/10.1016/j.foodres.2010.02.004>
- Gangadharan D, Sivaramkrishnan S, Nampoothiri KM, Sukumaran RK, Pandey A. 2008. Response surface methodology for the optimization of alpha amylase production by *Bacillus amyloliquefaciens*. *Bioresour Technol.*, **99**(11): 4597–602. <https://doi.org/10.1016/j.biortech.2007.07.028>
- Gibbs MJ, Biela A, Krause S. 2015. α -amylase sensor based on the degradation of oligosaccharide hydrogel films monitored with a quartz crystal sensor. *Biosens Bioelectron.*, **15**(67): 540–545.
- Goffin D, et al. 2011. Will isomaltoligosaccharides, a well-established functional food in Asia, break through the European and American market? The status of knowledge on these prebiotics. *Critical Rev Food Sci Nutri.*, **51**:394–409.
- Gupta A, Gupta VK, Modi DR, Yadava LP. 2008. Production and Characterization of α -Amylase from *Aspergillus niger*. *Biotechnology*, **7**: 551–556. <https://doi.org/10.3923/biotech.2008.551.556>
- Gupta R, Gigras P, Mohapatra H, Goswami VK, Chauhan B. 2003. Microbial α -amylases: a biotechnological perspective. *Process Biochem.*, **38**: 1599–1616.
- Henrissat B. 1991. A classification of glycosyl hydrolases based on amino acid sequence similarities. *Biochem J.*, **280**(2): 309–316. <https://doi.org/10.1042/bj2800309>
- Hii SL, Tan JS, Ling TC, Ariff AB. 2012. Pullulanase: role in starch hydrolysis and potential industrial applications. *Enz Res.*, Article ID 921362. <https://doi.org/10.1155/2012/921362>
- Hizukuri S. 1986. Polymodal distribution of the chain lengths of amylopectin and its significance. *Carbohydrate Res.*, **147**: 342–347.
- Hizukuri S. 1996. Starch: analytical aspects. In: **Carbohydrates in Food**, ed. A. C. Eliasson. New York, Marcel Dekker, pp 347–429.
- Hmidet N, Bayouh A, Berrin JG, Kanoun S, Juge N, Nasri M. 2008. Purification and biochemical characterization of a novel α -amylase from *Bacilluslicheniformis* NH1 Cloning, nucleotide sequence and expression of amy N gene in *Escherichia coli*. *Process Biochem.*, **43**: 499–510. <https://doi.org/10.1016/j.procbio.2008.01.017>
- Hondoh H, Kuriki T, Matsuura Y. 2003. Three-dimensional structure and substrate binding of *Bacillus stearothermophilus* neopullulanase. *J Mol Biol.*, **326**: 177–188.
- Imamura H, et al. 2003. Crystal structures of 4- α -glucanotransferase from *Thermococcus litoralis* and its complex with an inhibitor. *J Biol Chem.*, **278**: 19378–19386.

- Industrial Enzymes Market by Type (carbohydrases, proteases, lipases, polymerases & nucleases, other types), source, application (food & beverages, feed, bioethanol, detergents, pulp & paper, textiles & leather, wastewater treatment, other applications), form, and region - Global Forecast to 2026. <https://www.businesswire.com/news/home/20161219005619/en/Global-Industrial-Enzymes-Market-Analysis-2016-->
- Jana B, Cain AK, Doerrler WT, Boinett CJ, Fookes MC, Parkhill J, et al. 2017. The secondary resistome of multidrug-resistant *Klebsiella pneumoniae*. *Sci Rep.*, **7**: 42483. <https://doi.org/10.1038/srep42483>
- Jana M, Maity C, Samanta S, Pati BR, Islam SS, Mohapatra PKD, Mondal KC. 2013. Salt-independent thermophilic α -amylase from *Bacillus megaterium* VUMB109: An efficacy testing for preparation of maltooligosaccharides. *Industrial Crops and Products*, **41**: 386–391. <http://dx.doi.org/10.1016/j.indcrop.2012.04.048>
- Janeček Š, Gabriško M. 2016. Remarkable evolutionary relatedness among the enzymes and proteins from the α -amylase family. *Cell Mol Life Sci.*, **73**: 2707–2725.
- Janeček Š, Kuchtová A. 2012. *In silico* identification of catalytic residues and domain fold of the family GH119 sharing the catalytic machinery with the α -amylase family GH57. *FEBS Lett.*, **586**: 3360–3366. <http://dx.doi.org/10.1016/j.febslet.2012.07.020>
- Janecek S, Marecek F, MacGregor EA, Svensson B. 2019. Starchbinding domains as CBM families: history, occurrence, structure, function and evolution. *Biotechnol Advan.*, **37**(8): 107451. <https://doi.org/10.1016/j.biotechadv.2019.107451>
- Janeček S, Svensson B, Henriessat B. 1997. Protein engineering in the amylases family. *J Mol Evol.*, **45**: 322–331.
- Janeček Š, Svensson B, MacGregor EA. 2014. α -Amylase: an enzyme specificity found in various families of glycoside hydrolases. *Cell Mol Life Sci.*, **71**: 1149–1170.
- Janeček Š, Zámocká B. 2020. A new GH13 subfamily represented by the α -amylase from the halophilic archaeon *Haloarcula hispanica*. *Extremophiles*, **24**(2): 207–217. <https://doi.org/10.1007/s00792-019-01147-y>
- Janeček Š. 2002. How many conserved sequence regions are there in the α -amylase family? *Biologia*, **57**: 29–41.
- Jobling S. 2004. Improving starch for food and industrial applications. *Curr Opin Plant Biol.*, **7**(2): 210–218.
- John J. 2017. Amylases- bioprocess and potential applications: A review. *Intl. J Bioinform Biol Sci.*, **5**(2): 41–50. <https://doi.org/10.5958/2321-7111.2017.00006.3>
- Kalpana B, Aarthy S, Karutha S. 2012. Antibiofilm Activity of α -Amylase From *Bacillus Subtilis* S8-18 Against Biofilm Forming Human Bacterial Pathogens. *Appl Biochem Biotechnol.*, **167**: 1778–1794. <https://doi.org/10.1007/s12010-011-9526-2>
- Karim KMR, Husaini A, Sing NN, Sinang FM, Roslan HA, Hussain H. 2018. Purification of an alpha amylase from *Aspergillus favus* NSH9 and molecular characterization of its nucleotide gene sequence. *3 Biotech.*, **8**:204. <https://doi.org/10.1007/s13205-018-1225-z>
- Kayode J, Sola A, Adelani A, et al. 2009. The role of carbohydrate in diabetic nutrition: A review. *Internet J Lab Med.*, **3**: 2.
- Kerényiová L, Janeček S. 2020a. Extension of the taxonomic coverage of the family GH126 outside Firmicutes and *in silico* characterization of its non-catalytic terminal domains. *3 Biotechnol.*, **10**: 420. <https://doi.org/10.1007/s13205-020-02415-x>
- Kerényiová L, Janecek S. 2020b. A detailed *in silico* analysis of the amylolytic family GH126 and its possible relatedness to family GH76. *Carbohydrate Res.*, **495**: 108082. <https://doi.org/10.1016/j.carres.2020.108082>
- Ketabi A, Dieleman LA, Gaenzle MG. 2011. Influence of isomaltooligosaccharides on intestinal microbiota in rats. *J Appl Microbiol.*, **110**: 1297–1306.
- Kikani BA, Singh SP. 2011. Single step purification and characterization of a thermostable and calcium independent α -amylase from *Bacillus amyloliquifaciens* TSWK1-1 isolated from Tulsī Shyam hot spring reservoir, Gujarat (India). *Int J Biol Macromol.*, **48**: 676–681.
- Kikani BA, Singh SP. 2012. The stability and thermodynamic parameters of a very thermostable and calcium independent α -amylase from a newly isolated bacterium, *Anoxybacillus beppuensis* TSSC-1. *Process Biochem.*, **47**: 1791–1798.
- Kim JW, Kim YH, Lee HS, Yang SJ, Kim YW, Lee MH, et al. 2007. Molecular cloning and biochemical characterization of the first archaeal maltogenic amylase from the hyper thermophilic archaeon *Thermoplasma volcanium* GSS1. *Biochem Biophys Acta*, **1774**: 661–669. <https://doi.org/10.1016/j.bbapap.2007.03.010>
- Knegtel RM, Wind RD, Rozeboom HJ, Kalk KH, Buitelaar RM, Dijkhuizen L, Dijkstra BW. 1996. Crystal structure at 2.3 Å resolution and revised nucleotide sequence of the thermostable cyclodextrin glycosyltransferase from *Thermonaerobacterium thermosulfurigenes* EM1. *J Mol Biol.*, **256**: 611–622.
- Koseoglu VK, Heiss C, Azadi P, Topchiy E, Guvener ZT, Lehmann TE, Miller KW, Gomelsky M. 2015. *Listeria monocytogenes* exopolysaccharide: origin, structure, biosynthetic machinery and c-di-GMP-dependent regulation. *Mol Microbiol.*, **96**: 728–743. <https://doi.org/10.1111/mmi.12966>
- Kuchtová A, Janeček Š. 2016. Domain evolution in enzymes of the neopullulanase subfamily. *Microbiol.*, **162**: 2099–2115. <https://doi.org/10.1099/mic.0.000390>
- Kumar P, Pant DC, Mehariya S, Sharma R, Kansal A, Kalia VC. 2014. Ecobiotechnological strategy to enhance efficiency of bioconversion of wastes into hydrogen and methane. *Ind J Microbiol.*, **54**: 262–267.
- Kumari A, Singh K, Kayastha AM. 2012. α -Amylase: General properties, mechanism and biotechnological applications – A Review. *Curr Biotechnol.*, **1**: 98–107.
- Kuriki T, Imanaka T. 1999. The concept of α -amylase family: Structural similarity and common catalytic mechanism. *J Biosci Bioeng.*, **87**: 557–565.
- Lahiri D, Nag M, Banerjee R, Mukherjee D, Garai S, Sarkar T, Dey A, Sheikh HI, Pathak SK, Edinur HA, Pati S, Ray RR. 2021c. Amylases: biofilm inducer or biofilm inhibitor? *Front Cell Infect Microbiol.*, **11**: Article ID 660048. <https://doi.org/10.3389/fcimb.2021.660048>
- Lahiri D, Nag M, Sarkar T, Dutta B, Ray RR. 2021a. Antibiofilm activity of α -amylase from *Bacillus Subtilis* and prediction of the optimized conditions for biofilm removal by response surface methodology (RSM) and artificial neural network (ANN). *Appl Biochem Biotechnol.*, **193**: 1–20. <https://doi.org/10.1007/s12010-021-03509-9>
- Lahiri D, Nag M, Sheikh HI, Sarkar T, Edinur H, Siddhartha P, et al. 2021b. Microbiologically synthesized nanoparticles and their role in silencing the biofilm signaling cascade. *Front Microbiol.*, **12**: 636588. <https://doi.org/10.3389/fmicb.2021.636588>
- Li D, Park JT, Li X, Kim S, Lee S, Shim JH, et al. 2010. Over expression and characterization of an extremely thermostable maltogenic amylase, with an optimal temperature of 100 degrees C, from the hyper thermophilic archaeon *Staphylothermus marinus*. *New Biotechnol.*, **27**: 300–307. <https://doi.org/10.1016/j.nbt.2010.04.001>
- Li S, Yang X, Yang S, Zhu M, Wang X. 2012. Technology prospecting on enzymes: application, marketing and engineering. *Computat Structural Biotechnol J.*, **2**: 1–11.

- Li Y, Xu J, Zhang L, Ding Z, Gu Z, Shi G. 2017. Investigation of debranching pattern of a thermostable isoamylase and its application for the production of resistant starch. *Carbohydrate Res.*, **446-447**: 93–100. <http://dx.doi.org/10.1016/j.carres.2017.05.016>
- Lombard V, Golaconda RH, Drula E, Coutinho PM, Henrissat B. 2014. The Carbohydrate-Active enZymes database (CAZy) in 2013. *Nucleic Acids Res.*, **42**: D490–D495. <https://doi.org/10.1093/nar/gkt1178>; CAZy database: <https://www.cazy.org/>
- MacGregor EA, Janeček Š, Svensson B. 2001. Relationship of sequence and structure to specificity in the alpha-amylase family of enzymes. *Biochimica et Biophysica Acta.*, **1546(1)**: 1-20. [https://doi.org/10.1016/s0167-4838\(00\)00302-2](https://doi.org/10.1016/s0167-4838(00)00302-2)
- MacGregor EA. 2005. An overview of clan GH-H and distantly related families. *Biologia*, **60**: 5–12.
- Machovič M, Janeček Š. 2006. Starch-binding domains in the post-genome era. *Cell Molecular Life Sci.*, **63**: 2710–2724.
- Mahdavi A, Sajedi RH, Rassa M, Jafarian V. 2010. Characterization of an α -amylase with broad temperature activity from an acid-neutralizing *Bacillus cereus* strain. *Iran J Biotechnol.*, **8**: 103-111.
- Mehta D, Satyanarayana T. 2013a. Biochemical and molecular characterization of recombinant acidic and thermostable raw starch hydrolysing α -amylase from an extreme thermophile *Geobacillus thermoleovorans*. *J Mol Catal B Enzym.*, **85-86**: 229–238. <https://doi.org/10.1016/j.molcatb.2012.08.017>
- Mehta D, Satyanarayana T. 2014. Domain C of thermostable alpha-amylase of *Geobacillus thermoleovorans* mediates raw starch adsorption. *Appl Microbiol Biotechnol.*, **98**: 4503–4519. <https://doi.org/10.1007/s00253-013-5459-8>
- Mehta D, Satyanarayana T. 2016. Bacterial and archaeal α -Amylases: diversity and amelioration of the desirable characteristics for industrial applications. *Front Microbiol.*, **7**: 1129. <https://doi.org/10.3389/fmicb.2016.01129>
- Metin K, Koç Ö, Atelir ZBB, Bıyık HH. 2010. Purification and characterization of α -amylase produced by *Penicillium citrinum* HBF62. *Afr J Biotechnol.*, **9(45)**: 7692-7701.
- Mikami B, Iwamoto H, Malle D, Yoon HJ, Demirkan-Sarikaya E, Mezaki Y, Katsuya Y. 2006. Crystal structure of pullulanase: evidence for parallel binding of oligosaccharides in the active site. *J Mol Biol.*, **359**: 690–707.
- Mohan N, Satyanarayana T. 2019. Amylases. In **Encyclopedia of Microbiology** (Fourth Edition). Elsevier Pub, pp. 107–126. <https://doi.org/10.1016/B978-0-12-809633-8.13003-1>
- Mohiuddin M, Arbain D, Islam AK, Ahmad MS, Ahmad MN. 2016. Alpha-glucosidase enzyme biosensor for the electrochemical measurement of antidiabetic potential of medicinal plants. *Nanoscale Res Lett.*, **11**: 95. <https://doi.org/10.1186/s1161-016-1292-1>
- Møller MS, Fredslund F, Majumder A, Nakai H, Poulsen J-CN, Leggio LL, Svensson B, Hachema MA. 2012. Enzymology and structure of the GH13_31 Glucan 1,6- β -glucosidase that confers isomaltooligosaccharide utilization in the probiotic *Lactobacillus acidophilus* NCFM. *J Bacteriol.*, **194(16)**: 4249–4259. <https://doi.org/10.1128/JB.00622-12>
- Møller MS, Svensson B. 2016. Structural biology of starch-degrading enzymes and their regulation. *Curr Opin Structural Biol.*, **40**: 33–42. <https://doi.org/10.1016/j.sbi.2016.07.006>
- Nadell CD, Drescher K, Wingreen NS, Bassler BL. 2015. Extracellular matrix structure governs invasion resistance in bacterial biofilms. *ISME J.*, **9**: 1700–1709. <https://doi.org/10.1038/ismej.2014.246>
- Nagarajan DR, Rajagopalan G, Krishnan C. 2006. Purification and characterization of a maltooligosaccharide-forming α -amylase from a new *Bacillus subtilis* KCC103. *Appl Microbiol Biotechnol.*, **73**:591.
- Nguyen QD, Rezessy-Szabo JM, Hoschke A. 2000. Optimisation of composition of media for the production of amylolytic enzymes by *Thermomyces lanuginosus* ATCC 34626. *Food Technol Biotechnol.*, **38**: 229–234.
- Nielsen PK, Bonsager BC, Fukuda K, Svensson B. 2004. Barley α -amylase/subtilisin inhibitor: Structure, biophysics and protein engineering. *Biochim Biophys Acta*, **1696**: 1557–564.
- Nisha M, Satyanarayana T. 2013. Characterization of recombinant amylopullulanase (gt-apu) and truncated amylopullulanase (gtapuT) of the extreme thermophile *Geobacillus thermoleovorans* NP33 and their action in starch saccharification. *Appl. Microbiol Biotechnol.*, **97**: 6279–6292
- Nisha M, Satyanarayana T. 2013. Recombinant bacterial amylopullulanases: developments and perspectives. *Bioengineered*, **4**: 388–400.
- Nisha M, Satyanarayana T. 2014. Characterization and multiple applications of a highly thermostable and Ca^{2+} -independent amylopullulanase of the extreme thermophile *Geobacillus thermoleovorans*. *Appl. Microbiol Biotechnol.*, **174**: 2594–2615.
- Nisha M, Satyanarayana T. 2016. Characteristics, protein engineering and applications of microbial thermostable pullulanases and pullulan hydrolases. *Appl Microbiol Biotechnol.*, **100**:5661–5679.
- Niu D, Zuo Z, Shi GY, *et al.* 2009. High yield recombinant thermostable α -amylase production using an improved *Bacillus licheniformis* system. *Microb Cell Fact.*, **8**, 58. <https://doi.org/10.1186/1475-2859-8-58>
- Nouadri T, Meraihi Z, Shahrazed D, Leila B. 2010. Purification and characterization of the α -amylase isolated from *Penicillium camemberti* PL21. *Afr J Biochem Res.*, **4(6)**: 155-162.
- Olempska-Bier Z. 2007. Isoamylase from *Pseudomonas amyloclavata*. *Chemical Technol Assessment*, 1- 6.
- Özdemir S, Matpan F, Güven K, Baysal Z. 2011. Production and characterization of partially purified extracellular thermostable α -amylase by *Bacillus subtilis* in submerged fermentation (SmF). *Prep Biochem Biotechnol.*, **41(4)**: 365-381 <https://doi.org/10.1080/10826068.2011.552142>
- Park KH, Kim TJ, Cheong TK, Kim W, Oh BH, Svensson B. 2000. Structure, specificity and function of cyclomaltodextrinase, a multispecific enzyme of the alpha-amylase family. *Biochimica Biophysica Acta*, **1478**: 165–185.
- Park SH, Na Y, Kim J, Kang SD, Park, K-H. 2018. Properties and applications of starch modifying enzymes for use in the baking industry. *Food Sci Biotechnol.*, **27(2)**: 299–312. <https://doi.org/10.1007/s10068-017-0261-5>
- Patel AK, Nampoothiri KM, Ramachandran S, *et al.* 2005. Partial purification and characterization of α -amylase produced by *Aspergillus oryzae* using Spent-brewing grains. *Ind J Biotechnol.*, **4**: 336-341.
- Pervez S, Aman A, Iqbal S, Siddiqui NN, Ul Qader SA. 2014. Saccharification and liquefaction of cassava starch: an alternative source for the production of bio-ethanol using amylolytic enzymes by double fermentation process. *BMC Biotechnol.*, **14**: 49.
- Plácido Moore GR, Rodríguez do Canto L, Amante ER. 2005. Cassava and corn starch in maltodextrin production. *Quim Nova*, **28**: 596.
- Prakash O, Jaiswal N. 2010. α -Amylase: an ideal representative of thermostable enzymes. *Appl Biochem Biotechnol.*, **160**: 2401–2414.

- Puspita PS, Hermawan W, Nahrowi. 2019. Effect of isoamylase application on chemical characteristic of cassava root meal starch. IOP Conf. Series: *Earth and Environmental Science*, **251**: 012058. <https://doi.org/10.1088/1755-1315/251/1/012058>
- Qi Q, Zimmermann W. 2005. Cyclodextrin glucanotransferase: from gene to applications. *Appl Microbiol Biotechnol.*, **66**: 475–85 <https://doi.org/10.1007/s00253-004-1781-5>
- Rajagopalan G, Krishnan C. 2008. Alpha-amylase production from catabolite derepressed *Bacillus subtilis* KCC103 utilizing sugarcane bagasse hydrolysate. *Bioresource Technol.*, **99**: 3044–3050.
- Ray RR. 2011. Microbial isoamylase: an over view. *American J Food Technol.*, **6**(1): 1–18. <https://doi.org/10.3923/ajft.2011.1.18>
- Saini R, Saini HS, Dahiya A. 2017. Amylases: characteristics and industrial applications. *J Pharmacog Phytochem.*, **6**(4): 1865–1871.
- Sajilata MG, Singhal RS, Kulkarni PR. 2006. Resistant Starch—A Review. *Com Rev Food Sci Food Safety*, **5**: 1–17. <https://doi.org/10.1111/j.1541-4337.2006.tb00076.x>
- Samanta A, Mitra D, Roy S, Sinha C, Pal P, 2013. characterization and optimization of amylase producing bacteria isolated from solid waste, *Journal of Environmental Protection*, **4**(6): 647-652. <https://doi.org/10.4236/jep.2013.46074>
- Samanta S, Das A, Halder SK, Jana A, Kar S, Mahapatra PKD, Pati BR, Mondal KC. 2014. Thermodynamic and kinetic characteristics of an α -amylase from *Bacillus licheniformis* SKB4. *Acta Biologica Szegediensis*, **58**(2): 147–156.
- Samanta S, Jana M, Kar S, Parua S, Mohapatra PKD, Pati BR, Mondal KC. 2017. Purification and biochemical characterization of a maltooligosaccharide producing α -amylase from *Bacillus licheniformis* SKB 4. *Ind J Appl Microbiol.*, **20**(2): 55-71.
- Samanta S. 2020b. Enhancement of characteristics and potential applications of amylases: A Brief Review. *Am J Pure Appl Sci.*, **2**(2), 24-35. <https://doi.org/10.34104/ajpab.020.24035>
- Samanta, S. 2020a. α -Amylases: An Overview on molecular structure and biotechnological perspectives. In: **Microbial Fermentation and Enzyme Technology**. CRC Press, pp 13–39.
- Sarethy I, Saxena Y, Kapoor A, Sharma M, Seth R, Sharma H, Sharma S, Gupta S. 2012. Amylase produced by *Bacillus* sp. SI-136 isolated from sodic-alkaline soil for efficient starch desizing. *J Biochem Technol.*, **4**(2): 604-609.
- Sarian FD, Janeček Š, Pijning T, Ihsanawati, Nurachman Z, et al. 2017. A new group of glycoside hydrolase family 13 α -amylases with an aberrant catalytic triad. *Sci Rep.*, **7**: 44230. <https://doi.org/10.1038/srep44230>
- Selim SA. 2012. Novel thermostable and alkalitolerant amylase production by *Geobacillus stearothermophilus* HP 3. *Natural Product Research*, **26**(17): 1626–1630
- Sethi BK, Nanda PK, Sahoo S, Sena S. 2016b. Characterization of purified α -amylase produced by *Aspergillus terreus* NCF 4269.10 using pearl millet as substrate. *Cogent Food and Agriculture*, **2**: 1. <https://doi.org/10.1080/23311932.2016.1158902>
- Sethi BK, Jana A, Nanda PK, DasMohapatra PK, Sahoo SL, Patra JK. 2016a. Production of α -amylase by *Aspergillus terreus* NCF 4269.10 using pearl millet and its structural characterization. *Front Plant Sci.*, **7**:639. <https://doi.org/10.3389/fpls.2016.00639>
- Shah IJ, Gami PN, Shukla RM, Acharya DK. 2014. Optimization for α -amylase production by *Aspergillus oryzae* using submerged fermentation technology. *Basic Res J Microbiol.*, **1**(4): 01-10
- Sharma A, Satyanarayana T. 2011. Optimization of medium components and cultural variables for enhanced production of acidic high maltose-forming and Ca-independent α -amylase by *Bacillus acidicola*. *J Biosci Bioeng.*, **111** (5): 550-553. <https://doi.org/10.1016/j.jbiosc.2011.01.004>
- Sharma A, Satyanarayana T. 2012. Cloning and expression of acid stable, high maltose-forming, Ca²⁺-independent α -amylase from an acidophile *Bacillus acidicola* and its applicability in starch hydrolysis. *Extremophiles*, **16**: 515–522. <https://doi.org/10.1007/s00792-012-0451-2>
- Shivaramakrishnam S, Ganghadharan D, Nampoothiri KM, Soccol CR, Pandey A. 2007. Alpha amylase production by *Aspergillus oryzae* employing solid-state fermentation *J Sci and Ind Res.*, **66**: 621-626.
- Sidkey NM, Abo-Shadi MA, Balahmar R, Sabry R, Badrany G. 2011. Purification and characterization of α -amylase from a newly isolated *Aspergillus flavus* F₂Mbb. *Int Res J Microbiol.*, **2**(3): 096-103
- Simsek S, El SN. 2012. Production of resistant starch from taro (*Colocasia esculenta* L. Schott) corm and determination of its effects on health by in vitro methods, *Carbohydr Polymer*, **90**: 1204-09. <https://doi.org/10.1016/j.carbpol.2012.06.039>
- Sindhu R, Suprabha GN, Shashidhar S. 2011. Purification and characterization of α -amylase from *Penicillium janthinellum* (NCIM 4960) and its application in detergent industry. *Biotechnol Bioinf Bioeng.*, **1**(1): 25-32.
- Singh J, Kaur L, McCarthy OJ. 2007. Factors influencing the physico-chemical, morphological, thermal and rheological properties of some chemically modified starches for food applications—A review. *Food Hydrocolloids*, **21**(1): 1–22 <https://doi.org/10.1016/j.foodhyd.2006.02.006>
- Singh S, Singh S, Bali V, Sharma L, Mangla J. 2014. Production of fungal amylases using cheap, readily available agriresidues, for potential application in textile industry, BioMed Research International, **2014**: Article ID 215748. <https://doi.org/10.1155/2014/215748>
- Singhania RR, Patel AK, Soccol CR, Pandey A. 2009. Recent advances in solid-state fermentation. *Biochem Engineering J.*, **44**: 13–18.
- Sivaramakrishnan S, Gangadharan D, Nampoothiri KM, Soccol CR, Pandey, A. 2006. α -Amylases from microbial sources – An overview on recent developments. *Food Technol Biotechnol.*, **44**: 173–184.
- Soccol CR, da Costa ESF, Letti LAJ, Karp SG, Woiciechowski AL, Vandenberghe L PD-S. 2017. Recent developments and innovations in solid state fermentation. *Biotechnol Res Innov.*, **1**: 52–71 <https://doi.org/10.1016/j.biori.2017.01.002>
- Strokopytov B, Penninga D, Rozeboom HJ. 1995. X-ray structure of cyclodextrin glycosyltransferase complexed with acarbose. Implications for the catalytic mechanism of glycosidases. *Biochem.*, **34**: 2234–2240
- Suganthi R, Benazir JF, Santhi R, Ramesh KV, Anjana H, Nitya M, Nidhiya KA, Kavitha G, Lakshmi R. 2011. Amylase production by *Aspergillus niger* under solid state fermentation using agroindustrial wastes. *Int J Eng Sci Technol.*, **3**(2): 1756-1763.
- Sundaram A, Murthy TPK. 2014. α -Amylase production and applications: a review. *J Appl Environ Microbiol.*, **2**(4): 166–175.
- Svensson B, Jensen MT, Mori H, Bak-Jensen KS, et al. 2002. Fascinating facets of function and structure of amylolytic enzymes of glycoside hydrolase family 13. *Biologia*, **57**(Suppl. 11): 5–19.
- Takata H, Kuriki T, Okada S, Takesada Y, Iizuka M, Minamiura N, Imanaka T. 1992. Action of neopullulanase: Neopullulanase catalyzes both hydrolysis and transglycosylation at α -(1–4)- and α -(1–6)-glucosidic linkages. *J Biol Chem.*, **267**: 18447–18452.
- Tao X, Jang MS, Kim KS, Yu Z, Lee YC. 2008. Molecular cloning, expression and characterization of alpha-amylase gene

- from a marine bacterium *Pseudoalteromonas* sp. MY-1. *Indian J Biochem Biophys*, **45**: 305–309.
- Uitdehaag JCM, Mosi R, Kalk KH, Van der Veen BA, Dijkhuizen L, Withers SG, Dijkstra B W. 1999. X-ray structures along the reaction pathway of cyclodextrin glycosyltransferase elucidate catalysis in the α -amylase family. *Nature Structural Biol.*, **6**: 432–436.
- Valk V, van der Kaaij R M, Dijkhuizen L. 2016. Characterization of the starch-acting MaAmyB enzyme from *Microbacterium aurum* B8.A representing the novel subfamily GH13_42 with an enlarged catalytic region and an unusual and multidomain organization. *Sci Rep.*, **6**: 36100. <https://doi.org/10.1038/srep36100>
- van der Maarel MJEC, van der Veen B, Uitdehaag JCM, Leemhuis H, Dijkhuizen L. 2002. Properties and applications of starch-converting enzymes of the α -amylase family. *J Biotechnol.*, **94**: 137–155.
- Wang Q, Wang ., Yang X, *et al.* 2015. A sensitive one-step method for quantitative detection of α -amylase in serum and urine using a personal glucose meter. *Analyst*, **140**(4): 1161–1165.
- Wang S, Lin C, Liu Y, Shen Z, Jeyaseelan J, Qin W. 2016. Characterization of a starch-hydrolyzing α -amylase produced by *Aspergillus niger* WLB42 mutated by ethyl methanesulfonate treatment. *Int J Biochem Mol Biol.*, **7**(1): 1-10.
- Watanabe H, Nishimoto T, Kubota M, Chaen H, Fukuda S. 2006. Cloning, sequencing, and expression of the genes encoding an isocyclomaltooligosaccharide glucanotransferase and an alpha-amylase from a *Bacillus circulans* strain. *Biosci Biotechnol Biochem.*, **70**(11): 2690–2702. <https://doi.org/10.1271/bbb.60294>
- Watanabe K, Hata Y, Kizaki H, Katsube Y, Suzuki Y. 1997. The refined crystal structure of *Bacillus cereus* oligo-1,6-glucosidase at 2.0 angstrom resolution: Structural characterization of proline-substitution sites for protein thermostabilization. *J Mol Biol.*, **269**: 142–153.
- Watters CM, Burton T, Kirui DK, Millenbaugh NJ. 2016. Enzymatic Degradation of In Vitro *Staphylococcus Aureus* Biofilms Supplemented With Human Plasma. *Infect Drug Resist.*, **9**: 71–78. <https://doi.org/10.2147/IDR.S103101>
- Wu H, Qiao S, Li D, Guo L, Zhu M, Ma LZ. 2019. Crystal structure of the glycoside hydrolase PssZ from *Listeria monocytogenes*. *Acta Crystallography F Structural Biology Communication*, **75**: 501–506. <https://doi.org/10.1107/S2053230X19008100>
- Xian L, Wang F, Luo X, Feng Y-L, Feng J-X. 2015. Purification and characterization of a highly efficient calcium-independent α -amylase from *Talaromyces pinophilus* 1-95. *PLoS ONE*, **10**(3): e0121531. <https://doi.org/10.1371/journal.pone.0121531>
- Xie F, Quan S, Liu D, *et al.* 2014. Purification and characterization of a novel α -amylase from a newly isolated *Bacillus methylotrophicus* strain P11-2. *Process Biochem.*, **49**: 47–53.
- Xu J, Ren F, Huang C-H, Zheng Y, Zhen J, *et al.* 2013. Functional and structural studies of pullulanase from *Anoxybacillus* sp. LM18-11. *Protein*, 1685–1693. <https://doi.org/10.1002/prot.24498>
- Yan S, Wu G. 2016. Analysis on evolutionary relationship of amylases from archaea, bacteria and eukaryota. *World J Microbiol Biotechnol.*, **32**(24): 16 pages. <https://doi.org/10.1007/s11274-015-1979-y>
- Yandri, Suhartati T, Hadi S. 2010. Purification and characterization of extracellular α -amylase enzyme from locale bacteria isolate *Bacillus subtilis* ITBCCB148. *Eur J Sci Res.*, **39**(1): 64-74.
- Yang CH, Huang YC, Chen CY, Wen CY. 2010. Expression of *Thermobifida fusca* thermostable raw starch digesting alpha-amylase in *Pichia pastoris* and its application in raw sago starch hydrolysis. *J Ind Microbiol Biotechnol.*, **37**(4): 401–406. <https://doi.org/10.1007/s10295-009-0686-9>
- Zhang H, Xu X, Jin Z. 2012. Fermentation characteristics of resistant starch from maize prepared by the enzymatic method in vitro. *Int J Biol Macromol.*, **51**: 1185–1188. <https://doi.org/10.1016/j.ijbiomac.2012.08.031>
- Zobel HF. 1988. Molecules to granules: a comprehensive review. *Starch*, **40**(2): 44–50. <https://doi.org/10.1002/star.19880400203>
- Zona R, Chang-Pi-Hin F, O'Donohue MJ, Janeček Š. 2004. Bioinformatics of the glycoside hydrolase family 57 and identification of catalytic residues in amylopullulanase from *Thermococcus hydrothermalis*. *Eur J Biochem* **271**(14): 2863–2872. <https://doi.org/10.1111/j.1432-033.2004.04144.x>

Molecular Docking and TLC Analysis of Candidate Compounds from Lesser used Medicinal Plants Against Diabetes Mellitus Targets

Bhavika Batra¹, Sukhvinder Singh Sudan¹, Manu Pant^{2,*}, Kumud Pant¹, Ankita Lal¹, Tushar Gusain¹

¹ Department of Biotechnology, Graphic Era (Deemed to be University), 566/6, Bell Road, Clement Town, Dehradun, India.;

² Department of Life Sciences, Graphic Era (Deemed to be University), 566/6, Bell Road, Clement Town, Dehradun, India.

Received: May 15, 2021; Revised: July 6, 2021; Accepted: August 22, 2021

Abstract

The present work intends to investigate the potential of phytochemicals from less commonly used medicinal plants as possible candidates for Type 2 Diabetes (T2D) treatment using an *in silico* method. Plant ligands with T2D targets were studied using molecular docking techniques. The total binding energies of the targets and commonly used allopathic drugs were assessed and compared. The docking studies demonstrated very high binding energies between phytochemicals and diabetes targets as compared to the allopathic drugs. The presence of pharmacologically active components of the genus in the selected raw material of the plant species was also established. The study suggests that phytochemicals from the three species, *Silybum marianum*, *Eriobotrya japonica*, and *Withania coagulans*, can be effective therapeutic products for the treatment of T2D, calling for focused research on pharmacological investigations and product formulation.

Keywords: Diabetes mellitus, *Silybum marianum*, *Eriobotrya japonica*, *Withania coagulans* Molecular Docking

1. Introduction

Diabetes mellitus is a metabolic disorder where either the pancreas is unable to produce enough insulin (Type 1 diabetes) or is unable to utilize the insulin produced (Type 2 diabetes or NIDMM-Non-insulin dependent diabetes mellitus), or both. It can also occur during pregnancy (Gestational diabetes). Type 2 diabetes (T2D) is the most common of the three types (American Diabetes Association, 2009). Diabetes aggravates the chances of cardiovascular, neurological, and immunological failures and is known to affect around 463 million people worldwide (Saeedi *et al.*, 2019). Different treatments for diabetes have been prescribed in Ayurveda, Unani, Allopathy, Homeopathy, etc. Sulfonylureas, GLP-1 agonists, DPP4 inhibitors, PPAR-gamma agonists, GPR119 agonists, bariatric surgeries, and therapies like SGLT2 are all common medications available in today's allopathic medicine and surgery system (Kaladhar *et al.*, 2012). They do, however, have drawbacks, such as limited efficacy with hyperglycemic individuals and potential adverse effects such as low blood sugar, liver, kidney, and other organ damage (Feingold, 2020). Plant-based medications are highly suggested for diabetes therapy in this scenario (Al Jamal, 2009). The use of many plants for the treatment of diabetes is mentioned in Ayurveda (one of the oldest therapeutic sciences) (Pandey *et al.*, 2013). Despite the fact that more than 400 plants have been found to have anti-hyperglycemic properties, only a few are consistently used in the production of herbal drugs (Verma *et al.*, 2018). As a result, there is a need to investigate

different medicinal plants for the production of herbal drugs.

In bioinformatics, molecular docking has been useful in predicting the orientation of targets and ligands to create a stable complex, which is then used for drug discovery and drug designing (Ahmad *et al.*, 2016). The efficacy of a therapeutic molecule is anticipated in these studies based on the interaction and 'best-fit' between a ligand and the target (Abuhamdah *et al.*, 2020). The aim of this study was to apply these methodologies to forecast the anti-diabetic potential of less widely used medicinal plants for the treatment of T2D and to compare their efficacy to that of commonly used allopathic diabetes medicines.

2. Materials and Methods

2.1. Survey of Literature

An extensive literature survey was done to identify plants with anti-diabetic properties but rarely used in diabetes treatment. Following that, a list of potential plants was compiled by studying the ingredients of commercially available ayurvedic formulations. Simultaneously, a study was conducted on the various types of allopathic drugs used to treat diabetes (Gandhi *et al.*, 2017; Narhe *et al.*, 2018).

2.2. Ligand and Target Preparation

For docking experiments, the active components of chosen plants with anti-diabetic potential were employed as ligands. Commonly used allopathic drugs served as a control ligands. Docking was performed on 20 probable T2D targets. The Protein Data Bank (PDB) file format of

* Corresponding author. e-mail: manupant@geu.ac.in.

selected ligands and targets was acquired from the Research Collaboratory for Structural Bioinformatics PDB (<https://www.rcsb.org/>) (Natarajan *et al.*, 2015) and canonical or isomeric smiles from Pubchem database (<https://pubchem.ncbi.nlm.nih.gov/>) (Ahmad *et al.*, 2016) (later converted into PDB format) (<https://cactus.nci.nih.gov/translate/>) (Renuka and Berla 2013).

2.3. Molecular Docking

For molecular docking, the iGemdock software was employed. All of the targets were docked with each ligand. Default settings such as population size of 200, generation size of 70, and number of solutions 2 were used to predict docking locations. The interaction of ligands and targets was investigated.

2.4. Thin layer chromatography (TLC) analysis

To identify the active components in the plant extracts, TLC was used with a variety of aqueous media and solvent solutions.

2.4.1. Sample and Solvent preparation

2.4.1.1. Silymarin from *Silybum marianum* (*S. marianum*)

The starting material was defatted *S. marianum* seeds obtained from Sorich Organics (New Delhi, India) (Figure 1a), from which two samples were made. Seeds were weighed, macerated, and dissolved in 70 % ethanol (v/v) in a 1:3 (w/v) ratio for the first sample, which was stored at room temperature for 24 hours. 70 % ethanol (v/v) was added to this extract (1:10 v/v). After repeating the process four times, 1 ml of the extract was collected and kept for future use (Natarajan *et al.*, 2015). For the second sample, the crushed seeds were treated in 100% methanol. The solution was incubated at room temperature for 24 hours before being processed in the same way as sample 1.

The solvent systems used were chloroform: acetone: formic acid (75:16.5:8.5), ethyl acetate: n-hexane (40:60), benzene: ethyl acetate (70:30), methanol: water (9:1) and 100% methanol (Suha and Khadeem, 2007; Abouzid, 2012).

2.4.1.2. Ursolic Acid from *Eriobotrya japonica* (*E. japonica*)

E. japonica leaves were collected from the mother plant growing at Laxman Chowk (Dehradun, Uttarakhand, India) (Figure 1b), oven-dried (40°C for 24 hours), crushed and used as an extracting material for two samples. The first sample was prepared by dissolving extracted material in 100% methanol (1:1 ratio w/v) and incubating it at room temperature for 24 hours with intermittent shaking (Khatik *et al.*, 2019). Crushed leaves were dissolved in 100% ethanol (1:5 w/v) and kept at room temperature for 24 hours with intermittent shaking for the second sample (Delfanian *et al.*, 2016). The samples were evaporated in a water bath at 64°C for methanol and 78°C for ethanol until thick concentrated samples were obtained. Toluene: ethyl acetate: formic acid (8:2:0.1), acetonitrile: water (3:2) and butanol: acetic acid: water (4:1:5) were utilized as mobile phases (Gupta *et al.*, 2011).

2.4.1.3. Withanolide A and Withaniferin A from *Withania coagulans* (*W. coagulans*)

Seeds of *W. coagulans* were procured from a local Ayurvedic medicinal store in Dehradun, Uttarakhand,

India (Figure 1c). Seeds were dried, crushed, dissolved in 100% methanol (1:4 ratio w/v) and kept at room temperature for 24 hours with intermittent shaking for sample preparation (Peerzade *et al.*, 2018). The solution was evaporated at 64°C in a water bath until a concentrated solution was obtained. For the second sample, 15-20 seeds of *W. coagulans* were soaked in 50 ml water. The solution was incubated at room temperature for 24 hours before being evaporated in a water bath at 100°C until a concentrated solution of 1ml was produced.

The solvent systems used were butanol: water: acetic acid (7:1:2), toluene: ethyl acetate: formic acid (5:5:1), chloroform: methanol (9:1) and benzene: ethyl acetate (2:1) (Sudhanshu *et al.*, 2012, Preethi and Senthil, 2014; Poorani, 2014;).

2.4.2. Solvent application, development of chromatogram and visualization

The chromatographic analysis was performed on a heat activated aluminium, pre-coated silica gel 60 F₂₅₄ TLC plate (E. Merck) of uniform thickness (0.2mm). A 100 µl syringe was used and a 10 µl sample was loaded. The component separation was carried out at room temperature in a twin trough glass chamber (20 x 10 cm) filled with 20 ml of the solvent system. The TLC plates were then visualized at 256 nm and 366 nm and the R_f value was evaluated.



Figure 1 Plant material for sample preparation for chromatographic analysis
1a: Seeds of *Silybum marianum* 1b: Leaves of *Eriobotrya japonica* 1c: Seeds of *Withania coagulans*

3. Results

The aim of this research was to find medicinal herbs that have excellent anti-diabetic properties but are underutilized in commercial pharmaceutical compositions. Besides the existing literature, the Ayurvedic medicines available in Indian marketplaces for diabetes management were investigated. Diabecon Tablets 60, Diabecon (DS) Tablets 60, Dabur Madhu Rakshak Tablets, and Dabur Vasant Kusumakar Ras Tablets, Dia-beta plus 60 veggi capsules, are a few examples. Based on above findings, eight plants were identified with strong anti-diabetic properties. Chemically active ingredients of these plants were also identified to be used as ligands for docking studies (Table 1). The 20 powerful targets were chosen based on their functions in the human body (Table 2). A total of 400 ligand-target combinations were examined. The efficiency of medicinal plant ligands for diabetes treatment was also compared to commercially accessible

and commonly used allopathic drugs. Control ligands Metformin, Glimepiride, Pioglitazone, and Gliclazide were used docked with 20 potential targets, making a total of 80 combinations of control treatments.

Table 1. Medicinal plants with antidiabetic potential and their active components.

S.N	Scientific name	Active component
1.	<i>Commiphora wightii</i> (Sarup <i>et al.</i> , 2015)	E-guggulsterone Guggulsterol2 Guggulsterol3 Guggulsterol4 Guggulsterone Z- guggulsterone
2.	<i>Swertia chirayita</i> (Kumar and Staden, 2016)	Mangiferin Swerchirin Amarogentin
3.	<i>Withania coagulans</i> (Maurya, 2010)	Coagulin C Coagulin L Withanferin A 17 β Withanolide K
4.	<i>Eriobotrya japonica</i> (Liu <i>et al.</i> , 2016; Zhou <i>et al.</i> , 2007)	Ursolic Acid Triterpenoid
5.	<i>Berberis vulgaris</i> (Rahimi-Madiseh <i>et al.</i> , 2017)	Berberine
6.	<i>Silybum marianum</i> (Kazazis <i>et al.</i> , 2014)	Silymarin
7.	<i>Myrica esculenta</i> (Sood and Shri <i>et al.</i> , 2018)	Myricetin Quercetin
8.	<i>Tinospora cordifolia</i> (Saha and Ghosh, 2012)	Tinosporin Quercetin Berberine

Table 2. Protein targets and their role in Type 2 Diabetes (T2D) regulation.

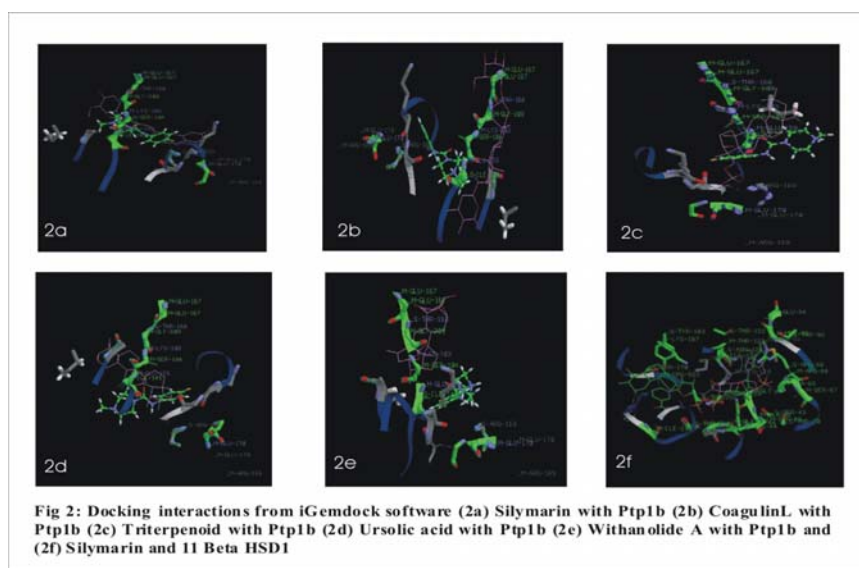
S.N.	Target name	Role
1.	T-cell protein tyrosine phosphatase (TCPTP) (Dodd <i>et al.</i> , 2019)	Regulates insulin receptor signalling and gluconeogenesis in the liver.
2.	PTP1B (Kumar and Staden, 2016; Dodd <i>et al.</i> , 2019; Thareja <i>et al.</i> , 2012)	Dephosphorylates the insulin receptor in liver and muscle to regulate glucose homeostasis.
3.	α amylase (Kumar <i>et al.</i> , 2016)	Responsible for postprandial glucose levels
4.	α galactosidase	Increases blood glucose levels.
5.	11 β -Hydroxysteroid-dehydrogenase type 1 (Kumar and Staden, 2016)	Inhibition of this helps in reducing tissue-specific gluconeogenesis and fatty acid metabolism.
6.	Aldose Reductase (Natarajan <i>et al.</i> , 2015; Oates, 2008)	Catalyzes the reduction of glucose to sorbitol in the polyol pathway.
7.	Fructose 1,6 biphosphatase (Poelje <i>et al.</i> , 2006)	Fructose 1,6-bisphosphatase (FBPase) is a key enzyme in gluconeogenesis. It is a potential drug target in the treatment of type II diabetes
8.	AMPK subunit beta-1 (Zhang <i>et al.</i> , 2009)	Maintains glucose homeostasis
9.	α 2 subunit	Helps in proper β -cell Ca^{2+} influx through multiple HVCC isoforms. Its absence lowers insulin secretion and results in impaired glucose tolerance.
10.	Sodium glucose cotransporter inhibitor (Kumar and Staden, 2016)	Helps kidneys in lowering blood glucose levels.
11.	Glycogen synthase kinase 3 (Natarajan <i>et al.</i> , 2015; Ring <i>et al.</i> , 2003)	Regulates glycogen synthesis
12.	Gpr40 (Kumar and Staden, 2016)	It is highly expressed in pancreatic β cells and is involved in insulin secretion.
13.	Sulfonyl ureas (Del Prato and Pulizzi, 2006)	Stimulates insulin secretion from pancreatic β cells
14.	Glucokinase (Natarajan <i>et al.</i> , 2015; Ferre <i>et al.</i> , 2003)	Functions as a glucose sensor in the β cells by controlling the rate of glucose entry into the glycolytic pathway
15.	PPAR- γ (Natarajan <i>et al.</i> , 2015; Kumar and Staden, 2016)	Regulates insulin sensitivity.
16.	Glucagon-like peptide 1 (Glp 1) (Kumar and Staden, 2016)	Stimulates insulin secretion and inhibits glucagon secretion.
17.	Cytochrome P450 (Eid <i>et al.</i> , 2009)	Increases the drug response in different disease
18.	DGAT0 1 (Kumar and Staden, 2016)	Catalyzes triglycerides synthesis
19.	Pyruvate dehydrogenase kinase isoform 2 (Lee, 2014)	Helps in glucose disposal
20.	17 β -Hydroxysteroid-dehydrogenase type 1 (Kumar and Staden, 2016)	Activates functionally inert glucocorticoid precursors (cortisone) to active glucocorticoids (cortisol) within insulin target tissues, such as adipose tissue, thereby regulating local glucocorticoid action.

3.1. Docking results

The aim of molecular docking is to achieve an optimal orientation and conformation of the ligand-receptor binding complex, demonstrated by less free energy of the binding. The energy levels obtained from the plant ligand-target combinations and allopathic medicine ligand-target combinations showed better docking results between plants' active ingredients and the targets as compared to the docking combination of allopathic medicines with their specific targets. Out of the different combinations, good energy levels were obtained with chemical constituents of *S. marianum*, *E. japonica*, and *W. coagulans* with targets Ptp1b and 11 Beta HSD1 (Table 3, Figure 2).

Table 3. Docking results of active components of *Silybum marianum*, *Eriobotrya japonica* and *Withania coagulans* with various targets of Type 2 Diabetes.

S.N.	Target- ligand	Plant used for extraction	Total energy of binding (kcal/mol)
1	ptp1b-silymarin	<i>S.marianum</i>	-323.716
2	ptp1b-coagulinL	<i>W.coagulans</i>	-301.848
3	ptp1b-triterpenoid	<i>E.japonica</i>	-285.77
4	ptp1b-coagulinC	<i>W.coagulans</i>	-284.116
5	ptp1b-ursolicacid	<i>E.japonica</i>	-262.094
6	ptp1b-withanolide A	<i>W.coagulans</i>	-251.823
7	DGAT1-triterpenoid	<i>E.japonica</i>	-151.823
8	11 beta HSD1-silymarin	<i>S.marianum</i>	-150.736
9	17beta HSD1-silymarin	<i>S.marianum</i>	-139.748



For target PPAR γ , the best results were obtained with Coagulin L from *W. coagulans*. The total binding energy was observed at -115.16 kcal/mol, which is comparatively higher than the energy observed with other plant ligands, Silymarin (-103.886 kcal/mol), Ursolic acid (-106.6196 kcal/mol), all of which were much higher than the binding energy of Pioglitazone (-93.79 kcal/mol) with the target (Figure 3). For Cytochrome P450, the best docking results were observed with withanolide A (active component of *W. coagulans*) showing binding energy of -120.897 kcal/mol, which was higher than that obtained with allopathic medicines, gliclazide and glimepiride (-97.93 kcal/mol and -100.9 kcal/mol, respectively) (Figure 4). For target AMPK subunit beta-1, the best results were obtained with silymarin (*S. marianum*), the total binding energy being -113.586 kcal/mol, higher than the energy observed with commonly used metformin (-52.7833 kcal/mol) (Figure 5).

Docking studies revealed that *S. marianum* (common name: Milk Thistle), *E. japonica* (common name: Loquat), and *W. coagulans* (common name: Indian rennet) have

chemical components with substantially strong anti-diabetic potential.

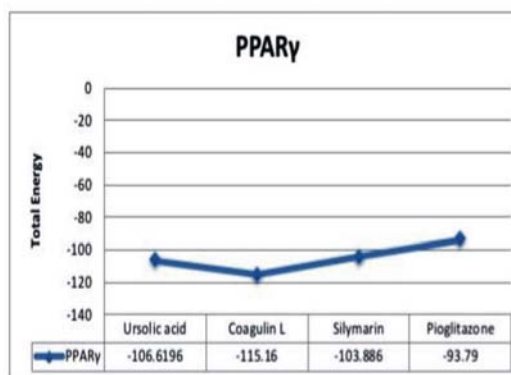


Figure 3: Comparison of total binding energies of Pioglitazone (an allopathic medicine) and other plant ligands with PPAR γ

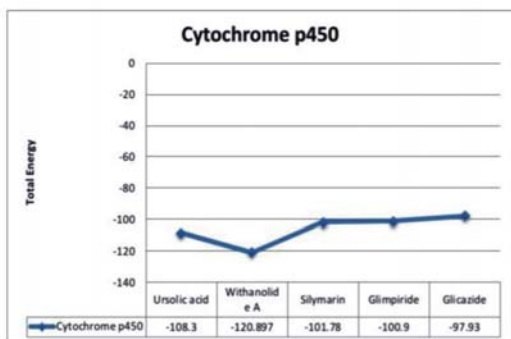


Figure 4: Comparison of total binding energies of allopathic medicines Glimpiride and Glicazide and other plant ligands with Cytochrome p450

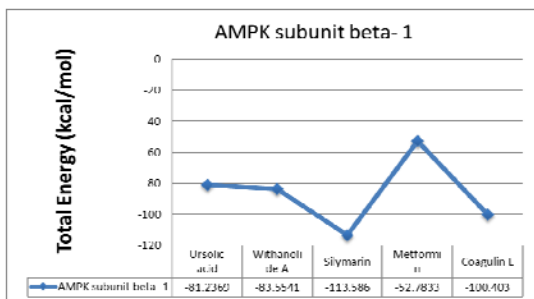


Figure 5: Comparison of binding total energies of allopathic medicine Metformin and other plant ligands with AMPK subunit beta-1.

3.2. Thin layer chromatography (TLC analysis)

Silymarin from *S. marianum*, ursolic acid from *E. japonica*, withaniferin A and withanolide A from *W. coagulans* were the four active components identified based on their binding energies. TLC in different solvent systems was used to confirm their existence in the readily accessible plant source material.

3.2.1. Silymarin

Identification was done on the basis of the standard R_f value, 0.57 in the various solvent systems (Suha and Khadeem, 2007). Of the different combinations tried, the best results were obtained in the ethanolic and 100% methanolic extracts in the benzene: ethyl acetate (70:30) solvent system (Table 4). The ethanolic extract had a dark wide band while a narrow band was observed in the 100% methanolic extract with an R_f value of silymarin, confirming that the seeds contain silymarin (Figure 6).

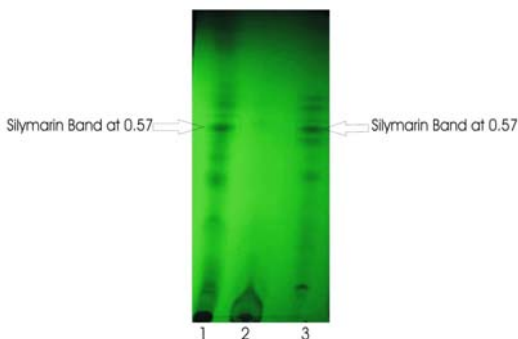


Figure 6: TLC plate developed in benzene:ethyl acetate (70:30) solvent system (Lane 1-Ethanol, lane 2- Ethyl acetate, Lane 3- 100%

Table 4: TLC observations of Silymarin in benzene: ethyl acetate (70:30) solvent system.

100% Methanol		Ethanol		Ethyl acetate	
Distance moved (cms)	R_f	Distance moved (cms)	R_f	Distance moved (cms)	R_f
6.3	0.41	3.5	0.23	5.7	0.37
6.8	0.45	5.8	0.38	7.0	0.46
7.2	0.47	6.8	0.45	7.3	0.48
8.7	0.57	7.2	0.47	7.5	0.49
10	0.66	8.7	0.57		
		11.8	0.78		

3.2.2. Ursolic Acid

On the basis of a standard R_f value of 0.42, the presence of ursolic acid in the leaf extract of *E. japonica* was confirmed (Naumoska et al., 2013). The best results were obtained using the solvent system toluene: ethyl acetate: formic acid (8:2:0.1) (Table 5). At the standard R_f value, a green colour band was detected in the 100% methanolic extract (Figure 7).

Table 5: TLC observation of Ursolic Acid in toluene: ethyl acetate: 0.1% formic acid (8:2:0.1) solvent system.

100% Methanol		Ethanol		Ethyl acetate		Chloroform	
Distance moved (cms)	R_f	Distance moved (cms)	R_f	Distance moved (cms)	R_f	Distance moved (cms)	R_f
4.3	0.29	5.4	0.36	4.6	0.31	4.6	0.61
5.1	0.34	6	0.4	7.9	0.53		
5.8	0.39	6.7	0.45	8.1	0.54		
6	0.40	12.1	0.80	12.1	0.80		
6.3	0.42						



Figure 7: TLC plate developed in toluene: ethyl acetate:0.1% formic acid (8:2:0.1) solvent system (E-Ethanol extract, M-100% Methanol extract, CM-Chloroform methanol extract, EA-Ethyl acetate extract),Methanol)

3.2.3. Withanolide A and Withaniferin A

Standard R_f values of 0.932 and 0.81 in different solvent systems were used to determine the presence of withanolide A and withaniferin A in the seed extract (Peerzade et al., 2018). Of the different combinations tried, the best results were obtained in the Butanol: Water: Acetic acid (7:1:2) solvent system (Table 6). As per the R_f value of withanolide A and withaniferin A, bands were observed in the 100% methanolic extract (Figure 8).

Table 6. TLC observations of Withanolide A and Withaniferin A in butanol: water: acetic (7:1:2) solvent system.

100% Methanol		Acetone	
Distance moved (cms)	R _f	Distance moved (cms)	R _f
3.6	0.24	2.5	0.16
4.5	0.25	3.7	0.24
6.4	0.42	4.6	0.30
7.7	0.50	6.4	0.42
9.2	0.60	7.8	0.51
12.4	0.81	9.2	0.60
14.3	0.93	11.3	0.74
		14	0.91

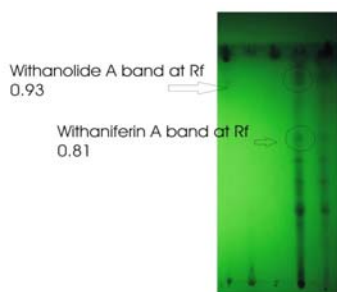


Figure 8: TLC plate developed in butanol: water: acetic (7:1:2) solvent system (C-Chloroform, W- water, P- Petroleum ether, M- 100% Methanol, A-Acetone)

4. Discussion

In our study, molecular docking studies were performed on plants that have been reported to be known in the traditional systems of medicine for diabetes treatment (Modak *et al.*, 2007; Mondal *et al.*, 2012). iGemdock is a graphical-automatic drug design system for docking, virtual screening, and identifying pharmacological interactions between ligand molecules and receptors (Kaladhar *et al.*, 2012; Dar and Mir, 2017). In this study on molecular docking, three plants *S. marianum*, *E. japonica*, and *W. coagulans* outperformed other plants and commonly used allopathic drugs such as metformin, glimepiride, pioglitazone, and gliclazide. Metformin is reported to have a strong affinity for AMPK receptors (Leclerc *et al.*, 2004; Leverve *et al.*, 2003). Out of the different ligands tested, including metformin, the best docking results were observed between the AMPK subunit beta1 receptor and the silymarin ligand. The contributing bonds between target and ligand were hydrogen bonds with a -25.1233 kcal/mol and vander waals bonds with a -88.66 kcal/mol contribution to the total binding energy level. The major amino acids involved in this binding were arginine at 63, 138 and 171, serine at 173, leucine at 170, methionine at 163 and asparagine at 162. In the present investigation, Withanolide A was found to be a better ligand than allopathic drugs gliclazide and glimepiride, since it had the highest total binding energy with cytochrome P450. Hydrogen bonds (contribution-21.117 kcal/mol) and vander waals bonds (contribution-99.78 kcal/mol) were the most prominent bonds during this binding. The amino acids lysine (391), phenylalanine (393), glycine (396), and asparagine (395) contributed to this binding.

Similarly, thiazolidinediones are reported to be highly effective ligands for PPAR γ receptors (Wilson *et al.*, 1996). According to this study, Coagulin L from *W. coagulans* is more successful as a ligand in binding to the target than Pioglitazone, a thiazolidinedione. The major contributors to binding between Coagulin L and the PPAR γ receptor were hydrogen bonds and vander waals bonds. Hydrogen bonds contributed- 104.77 kcal/mol energy whereas vander waals bonds contributed-10.39 kcal/mol energy to the total binding energy level, which is- 115.16 kcal/mol. The amino acids that took part in the binding were serine at 370, phenylalanine at 315, isoleucine at 369, arginine at 316 and glutamic acid at 371.

Our results are in consonance with prior research that found active compounds in the selected plants to be promising candidates for diabetic treatment. Silymarin (from *S. marianum*) has been reported to be a complex of 7 active molecules that can be utilized for various therapeutic targets of T2D (Gupta *et al.*, 2011; Ahmad *et al.*, 2019). Wu *et al.*, 2015 reported that ursolic acid and its triterpene analogues could be a potential ligand for treating T2D because of its high binding energy levels with the targets. Likewise, anti-diabetic properties have been reported for *W. coagulans* constituents (Guzman *et al.*, 2018; Subburaya *et al.*, 2020).

A chromatographic analysis of readily accessible raw materials of target plants was also performed as part of our research to establish the presence of active compounds. Solvents such as chloroform: acetone: formic acid (75:16.5:8.5) (Abouzid *et al.*, 2012), ethyl acetate: n-hexane (40:60), benzene: ethyl acetate (70:30) (Suha and Khadeem, 2007), methanol: water (9:1), and 100% methanol were previously used to detect silymarin in *S. marianum*. Ursolic acid in *E. japonica* leaves has been determined using toluene: ethyl acetate: formic acid (8:2:0.1) (Gupta *et al.*, 2011), acetonitrile: water (3:2) and butanol: acetic acid: water (4:1:5) (Khatik *et al.*, 2019). For withanolide A and withaniferin A in *W.coagulans*, different reports have suggested the use of solvent systems including benzene: ethyl acetate (2:1) (Sudhanshu *et al.*, 2012), toluene: ethyl acetate: formic acid (5:5:1) (Preethi *et al.*, 2014), chloroform: methanol (9:1) (Poorani, 2014) and butanol: acetic acid (7:1:2) (Peerzade *et al.*, 2018).

Our results confirm prior research that identified silymarin, ursolic acid, withanolide A and withaniferin A in the plant raw material.

5. Conclusion

Diabetes mellitus is a rapidly spreading threat to public health, healthcare, and the economy. Long-term use of allopathic drugs has been linked to debilitating side effects as well as potentially significant metabolic diseases. As a result, there is a growing demand for herbal remedies for diabetes therapy, which has resulted in overexploitation of several medicinal plants. There is a need to explore different phytochemical-target protein interactions to facilitate judicious drug development. Docking is a simple and effective method for predicting a phytochemical's efficiency by modelling plant ligand and protein receptor interaction. According to the findings of this study, Silymarin, Ursolic acid, Withanolide A, and Withaniferin A are prospective medication candidates that might be employed to build a successful therapeutic product.

Furthermore, TLC research has revealed that these compounds are present in commonly available plant materials. More concentrated efforts on these plants should be made for extensive phytochemical characterization, genotype-based active ingredient analysis, and subsequent herbal medicine development.

References

- Abouzid S. 2012. Silymarin, natural flavolignans from milk thistle. In: Rao V (Ed.), **Phytochemicals-A Global Perspective of Their Role in Nutrition and Health**. InTech, Egypt, pp. 255-272.
- Abuhamdah S, Abuhamdah R, Howes MJ, Uttley G and Chazot PL. 2020. A molecular docking study of *Aloysia citrodora* Palau. Leaf essential oil constituents towards human acetylcholinesterase: implications for Alzheimer's disease. *Jordan Journal of Biological Sciences.*, **13**: 575-580.
- Ahmad H, Gupta P, Tufchi N, Pant K and Kumar N. 2016. In silico modeling and docking of cch1 protein of *Candida glabrata* with FDA-approved drugs: a drug repurposing approach. *Asian J Pharma Clin Res.*, **9**: 148-153.
- Ahmad Z, Prashantha CN, D Visaga P and Zahra M. 2019. In silico analysis of active constituents of silymarin as alpha-glucosidase enzyme inhibitors in type 2 diabetes mellitus. *Asian J Pharma Clin Res.*, **12**: 225-229.
- Al Jamal AR. 2009. Effects of cinnamon on blood glucose and lipids levels in diabetic patients (type2). *Jordan Journal of Biological Sciences.*, **2(3)**: 135-138.
- American Diabetes Association. 2009. Diagnosis and classification of diabetes mellitus. *Diabetes Care.*, **32(1)**: S62-7.
- Dar AM and Mir S. 2017. Molecular docking: approaches, types, applications and basic challenges. *J Anal Bioanal Tech.*, **8**: 356.
- Del Prato S and Pulizzi N. 2006. The place of sulfonylureas in the therapy for type 2 diabetes mellitus. *Metabolism.*, **55(5)**: S20-S27.
- Delfanian M, Kenari RE and Sahari MA. 2016. Effect of natural extracted antioxidants from *Eriobotrya japonica* (Lindl.) fruit skin on thermo oxidative stability of soyabean oil during deep frying. *Int J Food Prop.*, **19**: 958-973.
- Dodd GT, Xirouchaki CE, Eramo M, Henry BA, Cowley MA and Tiganis T. 2019. Intranasal targeting of hypothalamic PTP1B and TCPTP reinstates leptin and insulin sensitivity and promotes weight loss in obesity. *Cell Rep.*, **28(11)**: 2905-2922.
- Eid AA, Gorin Y, Fagg BM, Maalouf R, Barnes JL, Block K and Abboud HE. 2009. Mechanisms of podocyte injury in diabetes: role of cytochrome P450 and NADPH oxidases. *Diabetes.*, **58(5)**: 1201-1211.
- Feingold KR. 2020. **Oral and injectable (non-insulin) pharmacological agents for type 2 diabetes**. In: Feingold KR, Anawalt B, Boyce A, Chrousos G, de Herder WW, Dhatariya K, Dungan K, Grossman A, Hershman JM, Hofland J, Kalra S, Kalsas G, Koch C, Kopp P, Korbonits M, Kovacs CS, Kuohung W, Laferrère B, McGee EA, McLachlan R, Morley JE, New M, Purnell J, Sahay R, Singer F, Stratakis CA, Trencle DL, Wilson DP (eds.). Endotext [Internet]. South Dartmouth (MA): MDText.com, Inc.
- Ferre T, Riu E, Franckhauser S, Agudo J and Bosch F. 2003. Long-term overexpression of glucokinase in the liver of transgenic mice leads to insulin resistance. *Diabetologia.*, **46(12)**: 1662-1668.
- Gandhi AJ, Maji JK and Shukla VJ. 2017. Ayurvedic and allopathic formulations for diabetes mellitus: a pharmacoeconomic study. *World J Pharm Sci Tech.*, **(1)**: 49-68.
- Gupta M, Bisht D, Khatoon S, Srivastava S and Kumar A. 2011. Determination of ursolic acid a biomarker in different swertia species through high performance thin layer chromatography. *Chinese Med.*, **2**: 121-124.
- Guzmán-Ávila R, Flores-Morales V, Paoli P, Camici G, Ramírez-Espinosa JJ, Cerón-Romero L, Navarrete-Vázquez G, Hidalgo-Figueroa S, Yolanda Rios M, Villalobos-Molina R and Estrada-Soto S. 2018. Ursolic acid derivatives as potential antidiabetic agents: In vitro, in vivo, and in silico studies. *Drug Dev Res.*, **79**: 70-80.
- <https://cactus.nci.nih.gov/translate/>
- <https://pubchem.ncbi.nlm.nih.gov/>
- <https://www.rcsb.org/>
- Kaladhar DS, Anusha N, VarahalaRao V, Surekha C and Meesala S. 2012. Regulation of Metabolic Syndromes by means of controlling diseased ache and bche with multitarget inhibitors through in silico techniques. *J Comput Methods Mol Des.*, **2**: 122-129.
- Kazakis CE, Evangelopoulos AA, Kollas A and Vallianou NG. 2014. The therapeutic potential of Milk Thistle in diabetes. *Rev Diabet Stud.*, **11(2)**: 167-174.
- Khatik GL, Singh A, Khurana N, Sharma N, Tomar B, Yadav P, Vyas M and Satija S. 2019. Physicochemical analysis of leaves of *Eriobotrya japonica* and antioxidant and antidiabetic evaluation of its methanolic extract. *Int J Green Pharm.*, **13**: 306-311.
- Kumar SP, Prasad P and Roy A. 2016. Screening of in vitro antidiabetic activity of herbal formulation meshashringi. *UK Journal of Pharmaceutical and Biosciences.*, **4(6)**: 75-79.
- Kumar V and Staden JV. 2016. A review of *Swertia chirayita* (Gentianaceae) as a traditional medicinal plant. *Front Pharmacol.*, **6**: 308
- Leclerc I, Woltersdorf WW, da Silva Xavier G, Rowe RL, Cross SE, Korbitt GS, Rajotte RV, Smith R, Rutter GA. 2004. Metformin, but not leptin, regulates AMP-activated protein kinase in pancreatic islets: impact on glucose-stimulated insulin secretion. *Am J Physiol Endocrinol Metab.*, **286(6)**: E1023-31.
- Lee IK. 2014. The role of pyruvate dehydrogenase kinase in diabetes and obesity. *Diabetes Metab J.*, **38(3)**: 181-186.
- Leverve XM, Guigas B, Demaille D, Batandier C, Kocwir EA, Chauvin C, Fontaine E and Wiernsperger NF. 2003. Mitochondrial metabolism and type-2 diabetes: a specific target of metformin. *Diabetes Metab.*, **29(4 Pt 2)**: 6S88-94.
- Liu Y, Zhang W, Xu C and Li X. 2016. Biological activities of extracts from loquat (*Eriobotrya japonica* Lindl.): A review. *Int J Mol Sci.*, **17(12)**.
- Maurya R. 2010. Chemistry and pharmacology of *Withania coagulans*: An ayurvedic remedy. *J Pharm Pharmacol.*, **62(2)**: 153-160.
- Miyazaki Y, Mahankali A, Wajcberg E, Bajaj M, Mandarino LJ and DeFronzo RA. 2004. Effect of pioglitazone on circulating adipocytokine levels and insulin sensitivity in type 2 diabetic patients. *J Clin Endocrinol Metab.*, **89(9)**: 4312-9.
- Modak M, Dixit P, Londhe J, Ghaskadbi S and Devasagayam TPA. 2007. Indian herbs and herbal drugs used for the treatment of diabetes. *J Clin Biochem Nutr.*, **40**: 163-173.
- Mondal P, Bhuyan N, Das S, Kumar M, Borah S and Mahato K. 2012. Herbal medicines useful for the treatment of diabetes in North-East India. *Int J Pharm Biol Sci.*, **3**: 575-589.

- Narhe S, Kshirsagar SS and Patil VS. 2018. Review on medicinal herbs used for diabetes. *Int J Pharm Clin Res.*, **10**: 224-228.
- Natarajan A, Sugumar S, Bitragunta S and Balasubramanyan N. 2015. Molecular docking studies of (4z, 12z)- cyclopentadeca-4, 12-dienone from *Grewia hirsute* with some targets related to type 2 diabetes. *BMC Complement Altern Med.*, **15**(1):1-8.
- Naumoska K, Simonovsla B, Albreit A and Vovk I. 2013. TLC and TLC-MS screening of ursolic, oleanolic, betulinic acids in plant extracts. *J Planar Chromat.*, **2**: 125-131.
- Oates PJ. 2008. Aldose reductase, still a compelling target for diabetic neuropathy. *Curr Drug Targets.*, **9**(1): 14-36.
- Pandey MM, Rastogi S and Rawat AKS. 2013. Indian Traditional Ayurvedic System of Medicine and Nutritional Supplementation. *Evid-Based Compl Alt.* doi: 10.1155/2013/376327.
- Peerzade N, Sayed N and Dr. Das N. 2018. Antimicrobial and phytochemical screening of methanolic fruit extract of *Withania coagulans* L. Dunal for evaluating the anti diabetic properties. *Pharma Innov J.*, **7**: 197-204.
- Poelje PD, Potter SC, Chandramouli VC, Landau BR, Dang Q and Erion MD. 2006. Inhibition of fructose 1,6-bisphosphatase reduces excessive endogenous glucose production and attenuates hyperglycemia in Zucker diabetic fatty rats. *Diabetes.*, **55**(6): 1747-1754.
- Poorani R. 2014. Comparative evaluation of phytochemicals, method development and karyotyping in in-vitro and in-vivo tissues of *Withania* species. MSc dissertation, Avinashilingam Institute for Home Science and Higher Education for Women, Coimbatore, India.
- Preethi MP and Senthil K. 2014. Principal component analysis and HPTLC fingerprint of in vitro and field grown root extracts of *Withania coagulans*. *Int J Pharm Pharm Sci.*, **6**: 480-488.
- Rahimi-Madiseh M, Lorigoini Z, Zamani-Gharaghoshi H and Rafieian-Kopaei M. 2017. *Berberis vulgaris*: Specifications and traditional uses. *Iran J Basic Med Sci.*, **20**(5): 569-587.
- Renuka DJ and Berla TE. 2013. Prediction of interaction of various apoptotic proteins with Sulforaphane (SFN) isolated from *Brassica oleraceae* using docking studies. *Int J Res Pharm Sci.*, **4**: 65-69.
- Ring DB, Johnson KW, Henriksen EJ, Nuss JM, Goff D, Kinnick TR, Ma ST, Reeder JW, Samuels I, Slabiak T, Wagman AS, Hammond ME and Harrison SD. 2003. Selective glycogen synthase kinase 3 inhibitors potentiate insulin activation of glucose transport and utilization in vitro and in vivo. *Diabetes.*, **52**(3): 588-595.
- Saeedi P, Petersohn I, Salpea P, Malanda B, Karuranga S, Unwin N, Colagiuri S, Guariguata L, Motala AA, Ogurtsova K, Shaw JE, Bright D and Williams R; IDF Diabetes Atlas Committee. 2019. Global and regional Diabetes prevalence estimates for 2019 and projection for 2030 and 2045: Results from the International Diabetes Federation Diabetes Atlas, 9th edition. *Diabetes Res Clin Pract.*, **157**.
- Saha S and Ghosh S. 2012. *Tinospora Cordifolia*: One plant, many roles. *Anc Sci Life.*, **31**(1): 151-159.
- Sarup P, Bala S and Kamboj S. 2015. Pharmacology and Phytochemistry of Oleo-Gum Resin of Commiphora wightii (Guggulu). *Scientifica (Cairo)*. doi: 10.1155/2015/138039.
- Sood P and Shri R. 2018. A review on ethnomedicinal, phytochemical and pharmacological aspects of *Myrica esculenta*. *Indian J Pharm Sci.*, **80**(1): 02-13.
- Subburaya U, Meeran SB and Narasimhan G. 2020. In Silico and in vitro screening of ethanolic extract of fruits of *Withania coagulans* against Diabetes. *Res J Pharm and Tech.*, **13**: 631-635.
- Sudhanshu, Mittal S, Rao N and Menghani E. 2012. Phytochemical and antimicrobial activity of *Withania coagulans* (stocks) Dunal (fruit). *Int. J. Pharm. Pharm. Sci.*, **4**: 387-389.
- Suha H Al-M and Khadeem JE. 2007. Identification of silymarin in *Echinopus tenuisectus* Family Compositae. *J Biotech Res Centre.*, **1**: 27-43.
- Thareja S, Aggarwal S, Bhardwaj TR and Kumar M. 2012. Protein tyrosine phosphatase 1B inhibitors: A molecular level legitimate approach for the management of diabetes mellitus. *Med Res Rev.*, **32**(3): 459-517.
- Verma S, Aggarwal G, Gupta M and Popli H. 2018. Diabetes mellitus treatment using herbal drugs. *Int J Phytomed.*, **10**: 1-10.
- Willson TM, Cobb JE, Cowan DJ, Wiethe RW, Correa ID, Prakash SR, Beck KD, Moore LB, Kliever SA and Lehmann JM. 1996. The structure-activity relationship between peroxisome proliferator-activated receptor gamma agonism and the antihyperglycemic activity of thiazolidinediones. *J Med Chem.*, **39**(3): 665-8.
- Wu P, Zheng J, Huang T, Li D, Hu Q, Cheng A, Jiang Z, Jiao L, Zhao S and Zhang K. 2015. Synthesis and evaluation of novel triterpene analogues of ursolic acid as potential antidiabetic agent. *PLoS One.*, **10**(9): e0138767. <https://doi.org/10.1371/journal.pone.0138767>.
- Zhang BB, Zhou G and Li C. 2009. AMPK: An emerging drug target for diabetes and the metabolic syndrome. *Cell Metab.*, **9**(5): 407-416.
- Zhou C, Chen K, Sun C, Chen Q, Zhang W and Li X. 2007. Determination of oleanolic acid, ursolic acid and amygdalin in the flower of *Eriobotrya japonica* Lindl. by HPLC. *Biomed Chromatogr.*, **21**(7): 755-61.

Jordan Journal of Biological Sciences

An International Peer – Reviewed Research Journal

Published by the Deanship of Scientific Research, The Hashemite University, Zarqa, Jordan



Name: الاسم:

Specialty: التخصص:

Address: العنوان:

P.O. Box: صندوق البريد:

City & Postal Code: المدينة: الرمز البريدي:

Country: الدولة:

Phone: رقم الهاتف:

Fax No.: رقم الفاكس:

E-mail: البريد الإلكتروني:

Method of payment: طريقة الدفع:

Amount Enclosed: المبلغ المرفق:

Signature: التوقيع:

Cheque should be paid to Deanship of Research and Graduate Studies – The Hashemite University.

I would like to subscribe to the Journal

For

- One year
 Two years
 Three years

One Year Subscription Rates

	Inside Jordan	Outside Jordan
Individuals	JD10	\$70
Students	JD5	\$35
Institutions	JD 20	\$90

Correspondence

Subscriptions and sales:

The Hashemite University
P.O. Box 330127-Zarqa 13115 – Jordan
Telephone: 00 962 5 3903333
Fax no. : 0096253903349
E. mail: jjbs@hu.edu.jo

المجلة الأردنية للعلوم الحياتية
Jordan Journal of Biological Sciences (JJBS)

<http://jjbs.hu.edu.jo>

المجلة الأردنية للعلوم الحياتية: مجلة علمية عالمية محكمة ومفهرسة ومصنفة، تصدر عن الجامعة الهاشمية وبدعم من صندوق دعم البحث العلمي والإبتكار – وزارة التعليم العالي والبحث العلمي.

هيئة التحرير

رئيس التحرير

الأستاذ الدكتورة منار فايز عتوم
الجامعة الهاشمية، الزرقاء، الأردن

مساعد رئيس التحرير

الدكتور مهند عليان مساعدة
الجامعة الهاشمية، الزرقاء، الأردن

الأعضاء:

الأستاذ الدكتور خالد محمد خليفات
جامعة مؤتة

الأستاذ الدكتور أيث ناصر العيطان
جامعة العلوم و التكنولوجيا الأردنية

الأستاذ الدكتورة طارق حسن النجار
الجامعة الأردنية / العقبة

الأستاذ الدكتور وسام محمد هادي الخطيب
الجامعة اليرموك

الأستاذ الدكتور عبد اللطيف علي الغزاوي
الجامعة الهاشمية

الأستاذ الدكتور نضال احمد عودات
جامعة البلقاء التطبيقية

فريق الدعم:

المحرر اللغوي

الدكتور شادي نعامنة

تنفيذ وإخراج

م. مهند عقده

ترسل البحوث الى العنوان التالي:

رئيس تحرير المجلة الأردنية للعلوم الحياتية
الجامعة الهاشمية

ص.ب , 330127 , الزرقاء, 13115 , الأردن

هاتف: 0096253903333

E-mail: jjbs@hu.edu.jo, Website: www.jjbs.hu.edu.jo



المملكة الأردنية الهاشمية



المجلة الأردنية



للعلوم الحياتية

مجلة علمية عالمية محكمة

تصدر بدعم من صندوق دعم البحث العلمي و الابتكار



<http://jjbs.hu.edu.jo/>